



Improving the calculation of fisheries reference points

Influences of density dependence and size selectivity

van Gemert, Rob

Publication date:
2019

Document Version
Publisher's PDF, also known as Version of record

[Link back to DTU Orbit](#)

Citation (APA):

van Gemert, R. (2019). *Improving the calculation of fisheries reference points: Influences of density dependence and size selectivity*. DTU Aqua.

General rights

Copyright and moral rights for the publications made accessible in the public portal are retained by the authors and/or other copyright owners and it is a condition of accessing publications that users recognise and abide by the legal requirements associated with these rights.

- Users may download and print one copy of any publication from the public portal for the purpose of private study or research.
- You may not further distribute the material or use it for any profit-making activity or commercial gain
- You may freely distribute the URL identifying the publication in the public portal

If you believe that this document breaches copyright please contact us providing details, and we will remove access to the work immediately and investigate your claim.

Ph.D. Thesis
Doctor in Philosophy

DTU Aqua
National Institute of Aquatic Resources

Improving the calculation of fisheries reference points

Influences of density dependence and size selectivity

Rob van Gemert

Supervisor:
Ken Haste Andersen
Co-supervisor(s):
Martin Lindegren

Kgs. Lyngby 2019



MARmaED

DTU Aqua
National Institute of Aquatic Resources
Technical University of Denmark

Kemitorvet, Building 202
2800 Kgs. Lyngby
Denmark
www.aqua.dtu.dk/english

Summary

Fisheries reference points are an important tool used by fisheries scientists to give advice on the management of fish stocks. Thus, it is important that fisheries reference points are calculated as accurately as possible. The value of fisheries reference points is strongly affected by density-dependent processes of the fish stock, which determine how vital rates such as growth, mortality, and reproduction change with a change in stock abundance. On top of that, because fish of different sizes often experience different forms of density-dependent regulation, the size-selectivity of a fishery also impacts the density-dependent regulation experienced by the fish stock. Therefore, to accurately calculate the value of fisheries reference points, it is important that the processes of density dependence and size-selectivity are properly incorporated.

In spite of the importance of density dependence in regulating fish stocks, most fisheries models disregard the existence of density-dependent growth. However, density-dependent growth is increasingly observed in marine fish stocks. Furthermore, density-dependent growth may also influence the size-selectivity at which maximum sustainable yield (MSY) is obtained. The central aim of this thesis therefore is to contribute to the maximum sustainable exploitation of fish stocks by investigating how density-dependent regulation and size-selectivity, as well as their interplay, affect fisheries reference points, with a particular focus on density-dependent growth. This aim is addressed in three separate papers which are outlined in this thesis.

Paper I shows how signs of recovery are appearing among previously overfished large-bodied fish stocks, and raises the question of whether current fisheries advice and management procedures are also well-suited for the management of recovered stocks. The paper shows that recovered stocks are more likely to experience density-dependent growth, which will make reference points calculated with current procedures inaccurate. Furthermore, this paper shows how a biomass increase of large-bodied piscivorous fish can trigger a reverse trophic cascade, where their increased predation mortality on forage fish reduces forage fish productivity and abundance. The resulting decrease in sustainable yield from forage fish stocks could lead to conflicts between forage and large-piscivore fisheries.

Paper II examines whether the observed strength of density-dependent growth in actual fish stocks is sufficiently strong to reduce optimal fishery size-at-entry to below size-at-maturity. For this, a size-structured model is fitted to three stocks that have shown indications of late-in-life density-dependent growth: North Sea plaice (*Pleuronectes platessa*), Northeast Atlantic mackerel (*Scomber scombrus*), and Baltic sprat (*Sprattus sprattus balticus*). The results show that for all examined stocks,

MSY exploitation takes place when only adults are targeted, indicating that density-dependent growth in fish stocks is generally not strong enough to warrant the targeting of juveniles.

Paper III examines the relationship between fecundity and female size, and uses a simple population model to test whether differences in this relationship have a meaningful impact on density-dependent recruitment to the stock. The results indicate that the relationship between fecundity and female size appears to be stock-specific, where some stocks show a power law relationship and others do not. This raises questions on the origin of the relationship between fecundity and female size. However, this study also shows that early-life density dependence often ensures that the type of relationship between fecundity and female size has little to no effect on actual recruitment to the stock. For the MSY management of fish stocks, it therefore matters little whether fecundity scales with female size according to a power law or not.

In conclusion, this thesis makes it clear that the calculation of accurate fisheries reference points requires accounting for all relevant density-dependent processes that the stock is subject to, including density-dependent growth. Furthermore, for an accurate calculation of MSY, it is necessary to consider the interplay between size-selectivity and density-dependent growth, and in rare cases the relationship between fecundity and female size. With the recent recovery of many large-bodied fish stocks, it can be expected that density-dependent growth will become a more important process in the regulation of fish stocks, and it should be further studied how density-dependent growth can best be incorporated in the calculation of fisheries reference points.

Dansk Resumé

Forvaltningen af fiskebestande et bygget op omkring såkaldte referencepunkter. Det er derfor vigtigt, at referencepunkterne for fiskeriet beregnes på et et så præcist grundlag som muligt. Fiskerireferencepunkterne er stærkt påvirket af fiskebestandens tæthedsaflængige processer, som bestemmer, hvordan vitale satser som vækst, dødelighed og reproduction ændrer sig med bestandenes størrelse. Fordi fisk af forskellig storrelse ofte oplever forskellige former for tæthedsaflængig regulering, påvirker størrelsesselektiviteten af et fiskeri ogsåden tæthedsaflængige regulering i fiskebestanden. For at præcist beregne værdien af referencepunkterne for fiskeriet er det derfor vigtigt, at processerne af tæthedsaflængighed og størrelsesselektivitet er korrekt indarbejdet.

På trods af vigtigheden af tæthedsaflængighed i reguleringen af fiskebestande ignorerer de fleste fiskerimodeller eksistensen af tæthedsaflængig vækst. Tæthedsaflængig vækst er dog i stigende grad observeret i marine fiskebestande. Desuden kan densitetsaflængig vækst ogsåpåvirke størrelsesselektiviteten, hvorved der opnås maksimalt bæredygtigt udbytte (MSY). Det centrale formål med denne afhandling er derfor at bidrage til den maksimale bæredygtige udnyttelse af fiskebestandene ved at undersøge, hvordan tæthedsaflængig regulering og størrelsesselektivitet samt deres samspil påvirker referencepunkterne for fiskeriet, med særlig fokus på tæthedsaflængig vækst. Dette mål er behandlet i tre separate artikler:

Artikel I viser at der er tegn på genopretning blandt tidligere overfiskede fiskebestande. Derfra rejses spørgsmålet om, hvorvidt de nuværende forvaltningsprocedurer ogsåer velegnede til forvaltning af genvundne bestande. Artiklen viser, at genopbyggede bestande er mere tilbøjelige til at opleve tæthedsaflængig vækst, hvilket kan gøre referencepunkter beregnet med de nuværende procedurer unøjagtige. Desuden viser artiklen, hvordan en biomasseforøgelse af store fisk kan udløse en omvendt trofisk kaskade, hvor deres øgede prædationsdødelighed påsmå industrifisk reducerer produktionen af industrifisk. Det resulterende fald i bæredygtigt udbytte fra fiskebestandene kan føre til konflikter mellem fiskerier på industrifisk og konsumfisk.

Artikel II undersøger, om den observerede styrke af densitetsaflængig vækst i faktiske fiskebestande er tilstrækkelig stærk til at reducere optimal fiskestørrelse ved indgang til under størrelse. Til dette er der udviklet en størrelsесesstruktureret model af tre fiskebestande, der har vist tegn på tæthedsaflængig vækst: Nordsøspætte (*Pleuronectes platessa*), Nordøstatlantisk makrel (*Scomber scombrus*) og Baltisk brisling (*Sprattus sprattus balticus*). Resultaterne viser, at MSY-udnyttelsen for alle undersøgte bestande finder sted, når kun fiskeriet kun er rettet mod voksne individer, hvilket

tyder på, at tæthedsafhængig vækst i fiskebestande generelt ikke er stærk nok til at berettige et målrettet fiskeri på juvenile individer.

Artikel III undersøger forholdet mellem ægproduktion og størrelse af hunner og bruger en simpel population model til at teste om forskelle om dette forhold har en meningsfuld indvirkning på tæthedsafhængig rekruttering til bestanden. Resultaterne viser, at forholdet mellem ægproduktion og størrelse af hunner ser ud til at være bestandsspecifik, hvor nogle bestande viser en potenslovssammenhæng, og andre ikke gør det. Dette rejser spørgsmål om oprindelsen af forholdet mellem ægproduktion og størrelsen af hunner. Denne undersøgelse viser imidlertid også, at afhængighed af tidlig livstæthed ofte sikrer, at typen af forhold mellem ægproduktion og størrelsen af hunner har ringe eller ingen effekt på den faktiske rekruttering til bestanden. Til MSY-forvaltning af fiskebestandene betyder det derfor ikke noget om hvorvidt sammenhængen mellem ægproduktion og størrelsen af hunner er en potensfunktion eller blot linær.

Afslutningsvis gør denne afhandling det klart, at beregningen af nøjagtige referencepunkter for fiskeriet kræver regnskab for alle relevante tæthedsafhængige processer, som bestanden er underlagt, herunder tæthedsafhængig vækst. For en nøjagtig beregning af MSY er det desuden nødvendigt at overveje samspillet mellem størrelseselekтивitet og tæthedsafhængig vækst og i sjældne tilfælde forholdet mellem ægproduktion og størrelse af hunner. Med den nylige genopretning af mange store fiskebestande kan det forventes, at tæthedsafhængig vækst vil blive en mere vigtig proces i reguleringen af fiskebestande, og det bør undersøges nærmere, hvordan tæthedsafhængig vækst bedst kan indarbejdes i beregning af referencepunkter for fiskeriet i fremtiden.

Preface

This thesis is the product of three years of research, and is submitted as part of the requirements for obtaining the Doctor of Philosophy degree (Ph.D.) at the Technical University of Denmark (DTU). The research was carried out from November 2015 until February 2019 at the Centre for Ocean Life, a Villum Foundation Centre of Excellence, at the National Institute of Aquatic Resources (DTU Aqua) in Charlottenlund and Kongens Lyngby, Denmark. During these three years, I was supervised by Ken Haste Andersen and Martin Lindegren.

Additionally, two external research stays were performed during the course of the research presented in this thesis. These were performed at the Danish Pelagic Producers Organization (DPPO) in Copenhagen, Denmark, and at the Centre for Ecological and Evolutionary Synthesis (CEES) at the University of Oslo, in Oslo, Norway, under supervision of Claus Reedz Sparrevohn and Joël Durant, respectively.

This PhD has been a part of the MARmaED innovative training network. The MARmaED project has received funding from the European Union's Horizon 2020 research and innovation programme under the Marie Skłodowska-Curie grant agreement No 675997. The results of this thesis reflect only the author's view and the Commission is not responsible for any use that may be made of the information it contains.

Furthermore, a travel grant from the Otto Mønsted Foundation supported conference participation in Riga, Latvia.

Kgs. Lyngby, 14th February 2019



Rob van Gemert

Acknowledgements

This PhD Thesis could not have been made without the help of a great number of people. First of all, I would like to thank my main supervisor Ken Haste Andersen. In 2015 I came to Denmark to do my MSc Thesis under your supervision. Because of your guidance and faith in me, this five-month stay turned into a four-year stay, as I got accepted for this PhD position. You have truly been an amazing supervisor to have, enabling a great deal of independent work whilst always being supportive and full of great ideas. Moreover, I would like to thank Martin Lindegren for co-supervising my PhD, your never-ending optimism and encouragement provided welcome relieve to the more tiresome times that come with being a PhD student.

I would also like to thank my colleagues in the Centre for Ocean Life and DTU Aqua. You have all made these past years a truly amazing experience, and you have set the bar very high for any of my future places of employment. I will look back very fondly upon my time with you all, and I am sure I will meet most of you again somewhere down the path of life. Additionally, I would like to thank the Villum Foundation for enabling the creation of the Centre for Ocean Life, which has allowed for such a diverse group of excellent scientists to gather together and work toward understanding the mysteries of life in the oceans.

Furthermore, I would like to thank all the partners and young researchers in the MARmaED Marie Skłodowska-Curie innovative training network, which my PhD has been a part of. It has been great getting to know all of you and working together with you. I would like to give special mention to Joël Durant for making this network a reality, and also for hosting me at the CEES institute at Oslo University. To everybody in the MARmaED network, this PhD wouldn't have been the same without you. My gratitude also goes out the European Commission for setting up the Horizon 2020 programme and the Marie Skłodowska-Curie actions, which has enabled the training of a tremendous amount of talented young scientists in the European Union, enabling the advancements of numerous scientific fields for decades to come.

I would also like to thank the Danish Pelagic Producers Organization, especially Claus Reedz Sparrevohn, for hosting me at their organization and allowing me the opportunity to learn more about the workings of the Danish fishing industry. I would look forward to working again with you some time in the future.

Lastly, I would like to thank my friends and family for their support. My parents have made sure that my brothers and I have never wanted for anything, and I am eternally grateful for that. Especially, I would like to thank my wife Michelle. Without hesitation you followed me in our great Danish adventure, and I cannot imagine how

the past years would have been without you. I cannot express how grateful I am for your constant love and support, and I would not be where I am today, nor be the man I am today, without you by my side. I look forward to the exciting times that are ahead of us, and I am sure that our adventure is far from over.

Contents

Summary	i
Dansk Resumé	iii
Preface	v
Acknowledgements	vii
1 Introduction	1
1.1 Aim	3
1.2 Fisheries reference points	4
1.2.1 The MSY concept	4
1.2.2 The calculation of fisheries reference points	6
2 A size-structured model	11
2.1 Size-spectrum theory	11
2.2 Consumption	12
2.3 Growth & Maturity	17
2.4 Reproduction	19
2.5 Mortality & Fishing	19
2.6 Population structure	22
2.7 Resource dynamics	24
2.8 Reference points	26
3 Density dependence	29
3.1 Density-dependent growth	30
3.2 Density-dependent mortality	33
3.3 Density-dependent reproduction	36
3.4 Density-dependent recruitment	36
3.5 Timing	38
3.6 Interactions	39
3.7 Density dependence & reference points	42

4 Size-selectivity	47
4.1 Balanced harvesting	48
4.2 Density-dependent growth	49
4.3 Fisheries-induced evolution	50
5 The ability of a surplus production model to capture different forms of density dependence	53
5.1 Methods	54
5.2 Results & Discussion	56
6 Filling in the gaps	61
7 Conclusion and future perspectives	65
8 References	69
9 Paper I	77
10 Paper II	85
11 Paper III	97
A Appendices Paper I	117
B Appendices Paper II	123
C Appendices Paper III	155

CHAPTER 1

Introduction

The world's oceans are large, covering over two-thirds of our planet. To many, therefore, it seems an impossible-to-grasp concept that anything we do could have a lasting impact on the oceans. Be it plastic pollution, TBT antifoulants, or oil spills, there are always those who believe that in the grand scheme of things, we are too insignificant to cause any lasting damage to the world's oceans or its ecosystems. So too with fishing. Thomas Henry Huxley, for instance, delivered these memorable lines in his opening address to the 1883 International Fisheries Exhibition in London:

I believe, then, that the cod fishery, the herring fishery, the pilchard fishery, the mackerel fishery, and probably all the great sea fisheries, are inexhaustible; that is to say, that nothing we do seriously affects the number of the fish. And any attempt to regulate these fisheries seems consequently, from the nature of the case, to be useless.

The idea that mankind is unable to deplete marine stocks continued to exist well into the 20th century (see, e.g., McIntosh, 1919), and undoubtedly continues to persist among uninformed individuals today.

Unfortunately, fish stocks are not inexhaustible resources. Contrary to what many believed in the not-so-distant past, mankind most certainly does have the ability to drive just about any fish stock on this planet to extinction. Even more so, in an unregulated fishery where all fishers have equal and open access to the resource, the only realistic outcome is usually that of the depletion of the stock. This is called the tragedy of the commons (Hardin, 1968), and it is the result of individuals seeking to maximize their gain, to the detriment of the community as a whole. Put into the context of fisheries, the tragedy of the commons can be described as such: Imagine a sea with an abundance of fish. The first few fishers making use of this resource will find it to be very profitable. This will attract new fishers, and prompt the existing fishers to perhaps increase the size of their fleet by adding new boats. This influx of new consumers of the resource will decrease the returns that each individual receives from the stock. However, fishers will continue to increase the size of their fleet, because

for the individual, adding one new boat will still increase their returns, while the loss on returns that results from the addition of a single new boat is shared among all the resource users. Thus, to maximize their individual gain, fishers will continue adding new boats, until the stock is completely depleted.

Assuming that fish stocks are inexhaustible resources, which need no regulation, will almost inevitably lead to a tragedy of the commons, resulting in stock depletion and possibly even extinction (Berkes, 1985). Thankfully though, most of us have come to realize that fish stocks are not inexhaustible resources, and therefore acknowledge that active management of fish stocks is needed if we are to make sure that future generations can still make use of them. There are multiple ways in which the tragedy of the commons can be averted, most of which involve taking away the 'commons' aspect, for instance by restricting the number of days at which fishing is allowed, giving out a limited number of fishing licenses, or by the use of fishing quotas. Some of these methods have been more successful than others, and the active management of fish stocks has not been able to prevent some high-profile collapses, such as that of the northern cod (*Gadus morhua*) off the coast of Newfoundland in 1992, which resulted in an estimated loss of almost 40,000 jobs and 400,000 tons of annual yield (Steele et al., 1992). Faulty fisheries management has taken place as a result of inaccurate advice calculations and poor management strategies, among others, and the field of fisheries advice and management is continuously being improved upon to try and overcome these faults.

The primary aim of fisheries management is usually to avoid complete stock collapse. However, often another important target is to maximize the yield that can be sustainably harvested from the stock, referred to as the maximum sustainable yield (MSY). After all, fish provides an important source of protein for a large portion of the global population, making up almost 20% of the animal protein in the diets of roughly 3.2 billion people in 2015 (FAO, 2018). Maximizing the sustainable output of global fisheries will therefore play an important role in the future food security of many nations (Godfray et al., 2010). In recent times, one of the paramount questions in fisheries science has therefore been: how can a fish stock best be exploited so that its yield approaches MSY (Punt and Smith, 2001)?

To this end, fisheries scientists have devised a wide range of management strategies, as well as a great variety of methods for calculating fisheries advice. Usually, a key component therein is the calculation of fisheries reference points. Fisheries reference points are used to quantify the goals of a fishery, and thereby allow managers to assess the performance of the fishery. In the end, the assessed state of the fish stock and its fishery, when compared with the values of the fisheries reference points of the stock, will often shape the decisions made by the stock's regulatory body. Thus, it is important that reference points are calculated correctly.

1.1 Aim

The central aim of this thesis is to contribute to the pursuit of achieving the maximum sustainable exploitation of fish stocks. For this, the predominant focus is on how to improve upon the calculation of fisheries reference points, so that they will aid better in approaching a fishing mortality that yields MSY.

The value of fisheries reference points are mainly determined by the traits and ecological dynamics of the stock (Andersen and Beyer, 2015). Here, density-dependent dynamics play a key role, as they are one of the main processes that regulate fish stocks. However, the various density-dependent processes that a stock is subject to are not always properly incorporated in the calculation of fisheries reference points, and density-dependent growth in particular is usually disregarded (Hilborn and Walters, 1992; Rochet, 2000). Therefore, the main question this thesis will try to answer is:

How can the inclusion of density-dependent processes, with density-dependent growth in particular, improve upon the calculation of fisheries reference points?

Furthermore, fisheries reference points can also be affected by management actions such as minimum-size regulations, as these change the size-specific catchability of fish. On top of this, size regulations also influence the regulation by density dependence, as different modes of density dependence are prevalent at different individual sizes (see, e.g., Andersen et al., 2017). Thus, a secondary question this thesis aims to answer is:

At which minimum catch size can MSY be obtained, and how does this vary with different forms of density-dependent regulation?

In this thesis, the concepts of fisheries reference points, density dependence, and size-selectivity will first be explained in more detail. Then, an overview is presented on how this thesis helps to fill in some of the knowledge gaps in how best to calculate fisheries reference points taking into account various forms of density dependence and size regulations, and the implications this has for future work. Lastly, the main body is presented, containing 3 papers that together aim to improve upon the calculation of fisheries reference points and the maximum sustainable exploitation of fish stocks.

1.2 Fisheries reference points

There exists a great variety in strategies and approaches to fisheries management, but the thing they have in common is that all have one or multiple objectives. For instance, the Common Fisheries Policy (CFP) of the European Union (EU) aims to "ensure that exploitation of living marine biological resources restores and maintains populations of harvested species above levels which can produce the maximum sustainable yield" (European Commission, 2013). To be able to achieve such an objective, quantifiable reference points are needed. For instance, regarding the aim of the CFP, what is the maximum sustainable yield of the population? What will be the population level that can produce this yield? What will be the exploitation level that will allow the population to remain above that level? Thus, for any management strategy, quantifiable fisheries reference points are a crucial component.

Generally speaking, fisheries reference points come in two forms: target reference points and limit reference points. A target reference point represents the general management goal for the fishery. Examples could be, among others, the maximum yield that can be reliably obtained indefinitely from a stock year after year, usually referred to as the maximum sustainable yield (MSY), the fishing mortality at which MSY is obtained (F_{MSY}), and the stock biomass that produces MSY (B_{MSY}). Limit reference points, on the other hand, represent a state that should be avoided. Examples are, among others, the stock biomass at which stock recruitment is impaired (B_{lim}), and the fishing mortality that is expected to result in B_{lim} (F_{lim}). Alternatively, F_{MSY} and B_{MSY} could also be considered limit reference points, if for instance the main management objective would be to avoid overfishing and preserve biomass/biodiversity.

1.2.1 The MSY concept

So far, all aforementioned reference point examples have been related to the concept of MSY. This idea that fish stocks could be exploited for a maximum sustainable yield is not a new concept. In the 1930s, Russell (1931) and Graham (1935) laid the foundation for the MSY concept with their dynamic pool models, in the 1950s Schaefer (1954) further developed these models into what we now know as the surplus production model which was actually capable of calculating MSY, and in 1957, Beverton and Holt solidified the concept of MSY in their groundbreaking work which is still used to this day. Clearly though, not everything went according to plan when applying the MSY concept to fisheries management. The period between the 1970s and 1990s saw rampant overfishing and massive declines in fish stocks, and in 2003 Myers and Worm estimated that global large predatory fish biomass was at only 10% of pre-industrial levels. Fishing for MSY clearly appeared to not be the answer to sustainable fisheries

M. S. Y.
1930s–1970s

Here lies the concept, MSY.
It advocated yields too high,
And didn't spell out how to slice the pie.
We bury it with the best of wishes,
Especially on behalf of fishes.
We don't know yet what will take its place,
But hope it's as good for the human race.

R. I. P.

Figure 1.1: The well-known epitaph for the MSY concept, by Larkin (1977).

management, and in 1977 already, Larkin wrote their now-famous epitaph for the concept of MSY (Figure 1.1), and assumed that that would lay it to rest. Nowadays however, the MSY concept is still deeply ingrained into fisheries management practices. For instance, the CFP stipulates that all EU fisheries should have achieved the MSY exploitation rate by no later than the year 2020 (European Commission, 2013). What changed?

Punt and Smith (2001) attribute the initial failure of the MSY concept, as perceived by Larkin (1977), to three elements: problems with correctly estimating MSY, the appropriateness of MSY as a management goal, and issues with getting fishers to comply with fishing for MSY. However, since the time that Larkin (1977) wrote their epitaph, major improvements have taken place on all three of these issues. New management strategies have been able to make fishers comply better with fishing for MSY: buyout programs have reduced fleet overcapacity (Engelhard et al., 2015; European Commission, 2016), individual transferable quotas have given fishers a long-term stake in their resource (Chu, 2009), monitoring systems have become more advanced (e.g., the Vessel Monitoring System; European Commission, 2003), and stakeholder involvement in management decisions has been increased (Pastoors, 2016), to name a few. Furthermore, fishing for MSY is now less seen as a target, and more as a limit for the exploitation of the fishery. For instance, the CFP lists that it aims to keep fish stocks not at, but "above levels which can produce the maximum sustainable yield" (European Commission, 2013). Lastly, research in fisheries science has not been at a standstill, and problems with correctly estimating MSY and its associated reference points are slowly being overcome. For instance, the proliferation of scientific surveys has improved the quality of data we have on many stocks, and advancements in computation have allowed for the development of more advanced models. Due to improvements in reference point calculation, better management goals, and better compliance among fishers, fishing effort in EU waters has been greatly reduced. In

2011, over 50% of ICES-assessed stocks were being exploited at a rate consistent with obtaining MSY (Fernandes and Cook, 2013).

1.2.2 The calculation of fisheries reference points

A detailed explanation of how to calculate fisheries reference points could probably fill an entire book, given the wide range of models that have been developed. For this, I refer to such works as Beverton and Holt (1957) and Hilborn and Walters (1992). Here, I stick to a small summary of the most widely-used models for calculating fisheries reference points.

The basic principle of calculating MSY reference points is fairly straightforward. Ideally, you would have a model capable of calculating the biomass of a stock, and how this responds to a given fishing mortality over time. Then, you simply run the model to equilibrium a number of times, each time applying a different fishing mortality. After that, it is simply a matter of seeing which fishing mortality results in the highest equilibrium yield. This yield is then MSY, the associated fishing mortality is F_{MSY} , and the associated stock biomass is B_{MSY} . However, it is not always this simple, often due to data limitations, and in the past also due to computational limitations. Thus, there exists a great variety in methods for calculating reference points, the most common of which are probably the surplus production models, yield-per-recruit models, and full population models.

Surplus production models

Surplus production models (also known as biomass dynamic models) are one of the simplest models used for calculating MSY reference points. They were introduced by Graham (1935), and further developed by Schaefer (1954), Pella and Tomlinson (1969), and Fox Jr (1970), among others. These models rely on the assumption that, for any given stock size, there is a certain level of yield (or surplus production) that can be harvested so that the stock size remains unchanged in the following year. The only required input to this type of model are two time-series: one of fisheries catch, and one of an associated stock biomass index. Then, a so-called surplus production curve is fitted to this data, which is a parabolic curve describing surplus production as a function of stock biomass. The peak of this curve then indicates MSY and B_{MSY} , and F_{MSY} can be subsequently calculated. The advantage of using surplus production models for estimating fisheries reference points is that they do not require a lot of data, implicitly incorporating many otherwise intricate stock dynamics by simply assuming that the stock will respond to fishing according to the surplus production curve. One of the downsides of this type of model, therefore, is that it is poorly able to handle

environmental variation that impacts stock productivity (Walters, 1987), or changes in the catchability of fish (e.g., due to changes in fishing gear) (Pella and Tomlinson, 1969). Furthermore, for a reliable fit of a production curve, good contrast is usually required in the time-series data (data from both an over- and underfished state), which is not always the case (Ludwig and Walters, 1985).

Yield-per-recruit models

The shortcomings of surplus production models encouraged the development of new models, better able to describe the population dynamics of a stock. One model that became particularly popular and continues to see widespread use is the yield-per-recruit model, introduced by Beverton and Holt (1957). The yield-per-recruit model, as the name implies, focuses on investigating how to maximize the mean yield produced by an average recruit entering the fished population. For this, an age-structured model is used that includes information on individual growth, natural mortality, and size/age selectivity by the fishery. Yield-per-recruit models focus on the trade-off between growth and mortality. At low fishing mortality many individuals are able to grow to a large size, resulting in a high stock biomass, but also in a low catch (and thus yield-per-recruit) due to the low level of fishing. As fishing mortality is increased, yield-per-recruit increases as well, but the greater mortality means that less fish grow to large sizes, and the biomass of older cohorts is reduced. Thus, as fishing mortality continues to increase, the rate of increase of yield-per-recruit starts to reduce, until a maximum yield-per-recruit is reached (Figure 1.2). The fishing mortality at which yield-per-recruit is maximized is usually referred to as F_{\max} . A further increase in fishing mortality would lead to a reduction in yield-per-recruit, as too many individuals are fished out of the stock at small sizes, given no chance to grow larger. This form of overfishing is therefore often referred to as growth overfishing (Cushing, 1973).

One of the main advantages of yield-per-recruit models over surplus production models is that they allow for the incorporation of multiple fleets with varying size-selectivities, and that they are useful for determining minimum catch sizes. Furthermore, yield-per-recruit models do not rely on recruitment data, as they assume constant recruitment. This means that, in the absence of long time-series data or recruitment data, the yield-per-recruit model is often the model of choice (Punt, 1993). However, the assumption of constant recruitment, independent of spawning stock biomass (SSB), is also one of the main drawbacks of yield-per-recruit models, as this also results in the assumption that recruitment is unaffected by fishing mortality. However, recruitment is rarely unaffected by fishing mortality, as even stocks that produce millions of eggs per individual will suffer a reduction in recruitment if fishing mortality is high enough, especially when environmental variability can cause years with very bad recruitment. As such, F_{\max} is almost always higher than F_{MSY} (Deriso, 1982), and is therefore more likely to push a stock toward depletion. For this reason, yield-per-recruit models

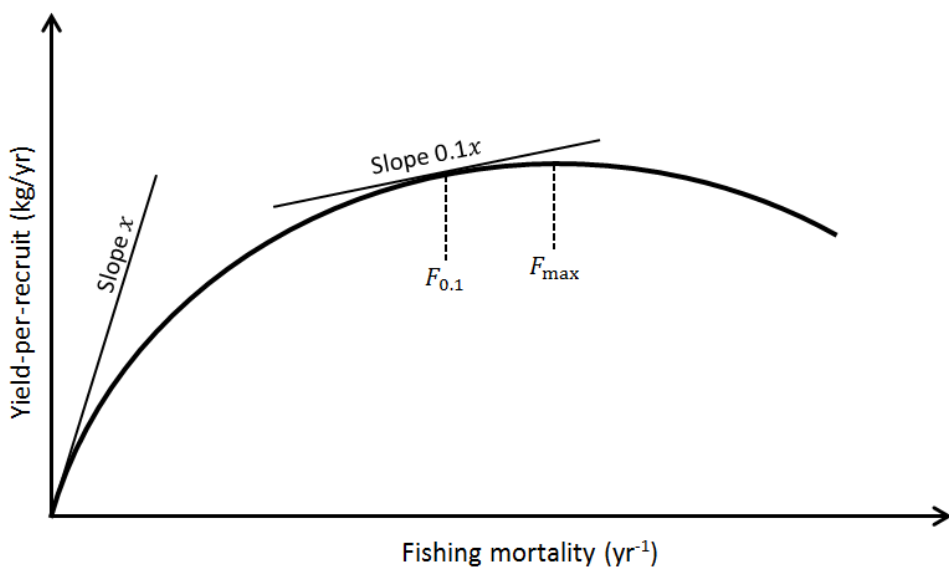


Figure 1.2: An example of a yield-per-recruit model, showing the relationship between fishing mortality and yield-per-recruit, including its associated reference points.

are often used to calculate a reference point called $F_{0.1}$ instead, which is the fishing mortality at which the slope of the relationship between fishing mortality and yield-per-recruit is equal to 10% of the initial slope through the origin, when $F = 0$ (Figure 1.2). Alternatively, reference points such as $F_{SB40\%}$ are used (e.g., Mace, 1994), which is the fishing mortality at which the spawning stock per recruit is 40% that of an unfished stock.

Population models incorporating recruitment

Contrary to the assumptions of yield-per-recruit models, recruitment is rarely constant. There often is a relationship between SSB and recruitment, and knowing this relationship is an important part of calculating reference points. Such stock-recruitment relationships are discussed in more detail further below, in section 3.7. Suffice to say, when calculating fisheries advice, a large part of time is usually devoted to making estimations of recruitment depending on the size of the spawning stock. Alternatively, instead of being strongly dependent on SSB, recruitment can exhibit strong interannual fluctuations, usually due to some form of environmental variability, as is for instance the case with sandeel (*Ammodytes marinus*) in the North Sea (Arnott and Ruxton, 2002) and sprat (*Sprattus sprattus*) in the Baltic Sea (Baumann et al., 2006; MacKenzie

and Köster, 2004). To estimate recruitment for such stocks, large-scale egg/larvae surveys are often undertaken periodically, such as the multiannual International Bottom Trawl Survey (IBTS, which initially started as a survey meant to estimate herring recruitment), or the tri-annual (once every three years) mackerel and horse mackerel egg survey in the Northeast Atlantic (MEGS). These estimates of recruitment are subsequently used in population models.

There can be large variability in the specifications of population models used for calculating fisheries reference points, but usually they are age-structured, and the calculated reference points depend on the interplay between growth, recruitment, and mortality. Furthermore, advances in computing have allowed for these models to make extensive stochastic projections into the future for any given model setup, allowing for risk assessments of the effects of environmental variability and uncertainty in the model parameters. Thus, the percentage chance that a stock crosses a given biomass limit reference point for a given level of fishing mortality can be estimated. This allows for the development of precautionary reference points, where F_{MSY} for instance is defined as the fishing mortality that results in the highest long-term sustainable yield, so long as the chance to reduce stock biomass to below B_{lim} is less than 5%. An example of such a type of model is Eqsim, which is used by ICES to calculate reference points for a wide number of data-rich stocks (ICES, 2015).

Descriptive or mechanistic

All ecological models attempt to simulate reality in some way. Some models, such as the surplus production models described earlier, do this in a descriptive manner: they do not attempt to incorporate the actual mechanisms responsible for the processes they simulate, but they merely use the correlations that have been observed between certain variables to predict the outcome of certain processes. More advanced models are often somewhat more mechanistic in nature, actually making an attempt at incorporating some of the underlying mechanisms that are responsible for the observed processes. For instance, the aforementioned Eqsim population model incorporates an underlying age structure into the population, assuming that vital rates such as growth, mortality, and reproduction are largely determined by the age of a fish or cohort.

A large amount of population models used to calculate management advice for marine fish are age-structured. For instance, a brief look at the latest stock assessment of the North Sea cod stock shows how landings, maturity, natural mortality, and fishing mortality are all reported or estimated per age group (ICES, 2018). However, from a mechanistic point of view, age can be considered as an unsuitable estimator of individual-level processes. After all, it is not the age of a fish that determines whether or not it is retained by fishing gear, or eaten by some other predator. Instead, it is the size of the fish that determines whether or not it can fit through the mesh of the

fishing net, or through the mouth of a larger fish. Thus, using an age-structured model is actually more descriptive than it is mechanistic.

The aim of this thesis was to contribute to the question of how to achieve the maximum sustainable exploitation of fish stocks, with a particular focus on reference points and density-dependent processes. The mechanisms through which density dependence operates can be very intricate, and can lead to counter-intuitive outcomes. For instance, in some scenarios of strong density dependence, it is possible to increase population biomass by increasing fishing effort (de Roos et al., 2007). Thus, to be able to capture these density-dependent dynamics, a population model is needed that is more mechanistic than a standard age-structured model.

In this thesis, a size-structured population model is used that is trait-based, and incorporates elements from metabolic and size-spectrum theory. This mechanistic model uses an energy budget to describe individual-level processes, which then shape the population structure. This bioenergetic approach enables the model to incorporate a variety of density-dependent processes, making it a suitable tool to use in this thesis. The following chapter explains the details of this size-structured model, after which it is shown how the model can be used to investigate how various density-dependent processes and size-selectivities of fisheries can influence the reference points of fish stocks.

CHAPTER 2

A size-structured model

Body size influences virtually all processes of an organism. As individuals grow in size, the amount of energy they take in changes, and the amount of energy they expend changes as well, through a number of size-specific processes. As a result, the energy that individuals have available for growth and reproduction also changes with size. Here, a population model is described that takes into account many of these size-specific processes, and how they change with body size w . For this, individual size w is described in grams of wet weight, but alternative measures such as dry weight, carbon weight, or energetic content could also be used, albeit with different parameter values. A key trait is the asymptotic size W_∞ , which is the maximum size that an average individual of the population can be expected to grow to if it were never eaten. The model can be constructed as a community model, incorporating a number of fish stocks which differ only in their value for W_∞ . Here, however, I mainly use this model in its single-stock form, where a single stock is modeled which feeds upon a dynamic resource spectrum.

The model described here is based upon those described by Andersen and Beyer (2015); Hartvig et al. (2011), and Andersen et al. (2017). The model equations and parameters are listed in Tables 2.1 and 2.2, respectively, and the model is described in detail below.

2.1 Size-spectrum theory

The model described in this chapter is for a large part a product of size-spectrum theory. One of the cornerstones of size-spectrum theory is that species should not be looked at separately, but that all individuals of all species in the community together make up the size spectrum of the community. In 1972, Sheldon et al. showed that, on a log-log scale, cumulative biomass of all individuals within a certain size range $w + \delta w$ remains almost constant as individual size w increases. In other words, from

the smallest microbes to the largest whales, Sheldon et al. (1972) found that the biomass in logarithmically-equal size bins hardly changes, laying the foundation for size-spectrum theory.

In general, the size spectrum of a community can be displayed in three different ways. The first is as a number spectrum, where individual abundance N is shown as a function of individual size w , which follows a power law:

$$N(w) = \kappa w^\lambda \quad (2.1)$$

where κ is the coefficient and λ the exponent of the power law. The value of κ will be system-specific, and can be considered as an indication of the biomass or abundance richness of the ecosystem. Multiplying the abundance spectrum with individual size w gives the biomass B spectrum:

$$B(w) = \kappa w^{1+\lambda} \quad (2.2)$$

Lastly, the Sheldon spectrum as observed by Sheldon et al. (1972) is obtained by multiplying the biomass spectrum with bin width, where the bin width is proportional to w . The Sheldon spectrum is therefore proportional to the biomass spectrum multiplied with body size:

$$B(w)w = \kappa w^{2+\lambda} \quad (2.3)$$

If the slope of the Sheldon spectrum is 0, this means that $2 + \lambda = 0$, so that $\lambda = -2$. However, the value of λ also emerges from predator-relationships. Below, a detailed overview is given of the size-specific processes regulating prey consumption in this model, and it is also shown how the value λ can be derived from these processes.

2.2 Consumption

Individuals need energy to maintain their basic metabolism, to grow, and to reproduce. They obtain this energy by consuming other individuals, a process also known as predation. Before the predator can consume a prey, however, the predator first needs to actually encounter the prey. Then, the size of the prey item should also be of a preferred size, relative to the size of the predator. Lastly, even if a prey of the right size is encountered, it cannot be eaten if the predator's digestive tract is at its limit, or in other words, if the predator is still full from a previous meal. Thus, consumption is shaped by encounter rate, prey-size preferences, and a maximum consumption rate. Below, I show how these processes are incorporated in the size-structured model, and how they are all influenced by w .

Clearance rate

The rate at which a predator encounters prey items is, to a large extent, determined by the predator's clearance rate. This clearance rate represents the volume of water that the predator is able to process within a given time period. For a filter feeder, this volume is equal to the surface area of the filter multiplied with the velocity at which water is passed through the filter. For a cruise-feeding visual predator, it is equal to the surface of the area searched, multiplied with the cruising velocity of the fish. Both filter area and search area scale allometrically, and clearance rate V therefore scales with individual size w according to a power law:

$$V(w) = \gamma w^q \quad (2.4)$$

Where γ is the coefficient and q the exponent of the power law. For fish, the average value of the exponent q has been estimated to be around 0.8 (Andersen and Beyer, 2006).

The rate at which a predator encounters prey does not only depend on the predator's clearance rate, but also on the concentration of prey items in the water. Thus, encounter rate can be calculated by multiplying the clearance rate of the predator with the integral of the biomass spectrum as $\gamma w^q \int_0^\infty w N(w) dw$. However, the predator cannot consume all encountered individuals. The prey items need to be of a size that the predator is able, or willing, to handle and consume. Thus, to properly describe the rate at which a predator encounters prey, the predator's size preference for prey needs to be described first.

Size preference for prey

The size of prey that a predator prefers, depends on the size of the predator. If the prey is too small, the predator may not be able to detect it, or the predator may not think it worth the effort. If the prey is too large, the predator could be unable to catch it, or the prey may simply be unable to fit through the predator's mouth. Thus, a predator's size preference for prey ϕ is a function of both predator size w and prey size w_p , and can be described according to a dome-shaped relationship:

$$\phi\left(\frac{w}{w_p}\right) = \exp\left[-\left(\ln\left(\frac{w}{w_p\beta}\right)\right)^2/(2\sigma^2)\right] \quad (2.5)$$

where β is the predator-prey mass ratio preferred by the predator, and σ helps determine the width of the dome. An example of this dome-shaped preference curve is shown in Figure 2.1.

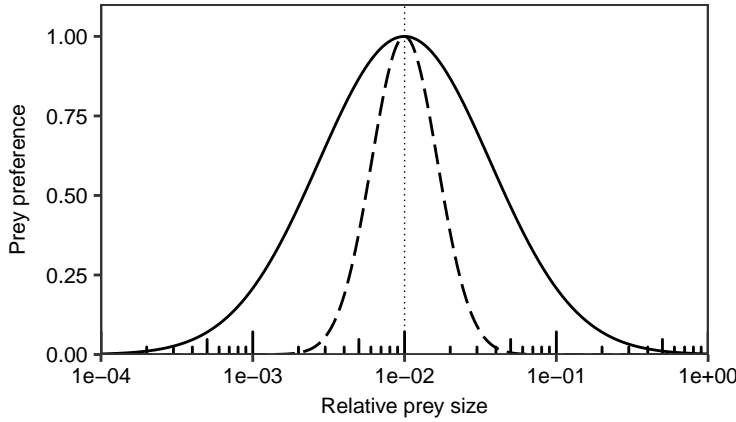


Figure 2.1: Preference for prey ϕ (Equation 2.5), as determined by the prey size relative to the size of the individual. Shown for a σ of 1.3 (solid), and 0.5 (dashed). The thin vertical dotted line shows w/β , indicating the highest preferred size of prey for the individual.

Using Equations 2.4 and 2.5, the rate at which an individual of size w encounters suitable prey items of size w_p out of the entire community can be described as:

$$E_e(w) = \gamma w^q \int_0^\infty \phi\left(\frac{w}{w_p}\right) w_p N(w_p) dw_p \quad (2.6)$$

Here, no distinction is made between conspecifics and heterospecifics within the community. Later on, however, it will become important to make this distinction and be able to change the stock's tendency toward cannibalism (see Section 3.2). Therefore, a distinction is made between the abundance of conspecific individuals N , and the abundance of heterospecific individuals N_r . Equation 2.6 can then be rewritten as:

$$E_e(w) = \gamma w^q \int_0^\infty \phi\left(\frac{w}{w_p}\right) w_p (cN(w_p) + N_r(w_p)) dw_p \quad (2.7)$$

where w_p indicates the prey size (which can be both con- and heterospecific), and c is a parameter that indicates the stock's tendency toward cannibalism. The value of c can range between 0 and 1.

Maximum consumption & feeding level

Consumption is equal to E_e at very low prey abundances. However, as the abundance of prey increases, predators generally become saturated, and consume less. This process, often called a type II functional response (Holling, 1959b), can be the result of a predator simply no longer having the gut capacity to process more prey. The

capacity of the gut is limited by its surface area through which nutrients and carbon are taken in. Surface area is proportional to length squared, or, assuming a length-weight relationship of $w \propto l^3$, proportional to weight to the power of 2/3. Thus, the surface area of the gut could be expected to scale with w according to a power law with an exponent of 2/3. However, the surface area of the gut is often fractal, meaning that the scaling exponent n can be expected to be higher than 2/3. Here, I follow West et al. (1997) in assuming an exponent of 3/4. Maximum consumption can then be described as:

$$C_{\max}(w) = hw^n \quad (2.8)$$

where $n = 3/4$ is the scaling exponent and h the coefficient for maximum consumption.

Food intake is not limited solely by maximum consumption, as most fish are captured with an unfull stomach (Armstrong and Schindler, 2011). Thus, consumption by the fish remains below maximum consumption C_{\max} when $E_e = C_{\max}$. Here, actual consumption is therefore calculated by multiplying maximum consumption C_{\max} with a feeding level f , where the value of f is determined by the encounter rate E_e :

$$f(w) = \frac{E_e(w)}{E_e(w) + C_{\max}(w)} \quad (2.9)$$

The predator's consumption C can now be calculated as:

$$C(w) = f(w)C_{\max}(w) \quad (2.10)$$

When food is plentiful, the feeding level is smaller than 1, but large enough to give the individual sufficient energy to maintain its metabolism, activity, growth, and reproduction. Therefore, I assume that the standard feeding level under conditions of plentiful food f_0 is equal to 0.6 (Hartvig et al., 2011). The values of the coefficients γ and h can then be set so that an individual feeding in an environment with plentiful food will have a feeding level $f(w) = 0.6$, giving a γ value of $6.57/\kappa \text{ g}^{-q} \text{ yr}^{-1}$ and an h value of $18.6 \text{ g}^{1-n} \text{ yr}^{-1}$ (Andersen et al., 2017).

Multiple hypotheses have been proposed to explain that fish consumption is often lower than their maximum consumption. Armstrong and Schindler (2011) propose that fish maintain a digestive overcapacity to be able to make full use of rare periods of plentiful food. (Walters and Juanes, 1993) propose that foraging for food comes with an increased risk of predation, and that many fish are therefore faced with a trade-off between either increasing food intake or decreasing predation mortality. Thus, (Walters and Juanes, 1993) predict that fish often decide to stop foraging once they have obtained sufficient energy to fuel most of their energetic needs (Walters and Juanes, 1993). At some point, the extra energy intake that results from additional time spent foraging simply does not weigh up against the increased risk of mortality. Here, I do not explicitly incorporate the mechanism behind this reduced consumption among fish, but merely describe it with the feeding level as described in Equation 2.9.

Available energy

Now that individual consumption has been described, an individual energy budget can be constructed to which the energy obtained from consumption can be allocated. The energy that a predator uses can be roughly subdivided into four different categories: standard metabolism, activity, growth, and reproduction. However, a predator cannot assimilate all of the energy contained within a prey item. Firstly, the predator does not digest the full mass of the prey into its body. Some energy is lost through egestion of undigested material (e.g., defecation or regurgitation). Furthermore, energy is needed to convert digested material into usable substances, a process known as specific dynamic action. Lastly, excretion of digested waste products results in a further loss of energy. Kitchell et al. (1977) estimated that egestion, specific dynamic action, and excretion respectively use up 15%, 15%, and 10% of the total energetic content of consumed food. Thus, to find the total amount of energy available to an individual, consumed food is multiplied with an assimilation efficiency α equal to 0.6.

Any individual needs to pay the energetic costs of upkeep of the body's tissues and functions, also referred to as the standard metabolism. The energy used for standard metabolism scales with individual size w according to a power law $k_s w^n$, where the exponent n is the same as the exponent for maximum consumption and is equal to 3/4 (Kleiber, 1932; West et al., 1997). This is because metabolism is effectively limited by the transport of oxygen through the surface of the lungs or gills, which, just like the gut, are also fractal. Thus, n can be considered as both the metabolic exponent as well as the maximum consumption exponent. The standard metabolism coefficient k_s is proportional to the coefficient for maximum consumption h , and is given by $f_c \alpha h$ (Hartvig et al., 2011). Here, f_c is the minimum feeding level required to obtain sufficient energy to maintain the standard metabolism, also known as the critical feeding level. If $f(w)$ were to be smaller than f_c , the individual would not be able to sustain its standard metabolism and it would starve to death. 0.2 can be considered as a reasonable value for f_c (Hartvig et al., 2011). The energy that is used to maintain standard metabolism scales with individual size w in a very straightforward way. This scaling is less obvious for the energy that is used for activity, as it depends on the activity pattern which may be highly species-specific. For now, I follow the description of Andersen and Beyer (2015) and Andersen et al. (2017) for the energy used for activity, who describe the energy invested into activity as $k_a w$. Here, k_a is equal to $\epsilon_a \alpha h (f_0 - f_c) W_\infty^{n-1}$ (Andersen and Beyer, 2015), where ϵ_a indicates the fraction of energy invested into activity and is equal to 0.8 (Andersen and Beyer, 2015), and W_∞ is the asymptotic size of the fish stock.

Using the equations described above, I can now describe how much energy an individual obtains from consumption, and how much of this energy the individual will have left over after having paid the energetic costs of standard metabolism and activity:

$$E_a(w) = \alpha f(w) h w^n - k_s w^n - k_a w \quad (2.11)$$

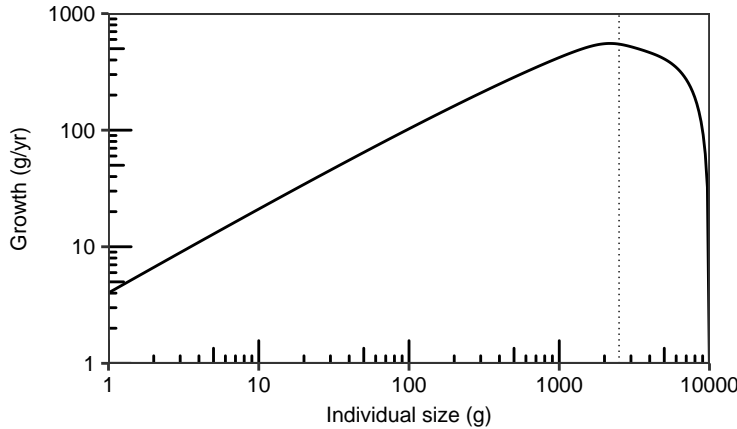


Figure 2.2: Growth g as a function of size w (Equation 2.12), shown for a W_∞ value of 10 kg. The vertical dotted line shows size at 50% maturity.

where E_a thus represents the energy available for growth and reproduction.

2.3 Growth & Maturity

Available energy E_a is allocated between growth and reproduction. Thus, individual growth rate g can be described as:

$$g(w) = (1 - \psi(w))E_a(w) \quad (2.12)$$

where $\psi(w)$ refers to the fraction of available energy $E_a(w)$ that is invested into reproduction. $\psi(w)$ thus determines the allocation of energy between growth and reproduction, and its value is a function of two different functions, namely maturation and size of the gonads.

Maturity ψ_m is a function of size. As an individual grows from egg size w_{egg} to asymptotic size W_∞ , maturation smoothly increases from 0 to 1 according to a sigmoidal function:

$$\psi_m(w) = \left(1 + \left(\frac{w}{\eta_m W_\infty} \right)^{-u_m} \right)^{-1} \quad (2.13)$$

where u_m determines the steepness of the maturation curve, and η_m is the size at 50% maturity relative to asymptotic size W_∞ . Relative size at 50% maturity can vary between species, and may also be dependent on environmental conditions, but here I

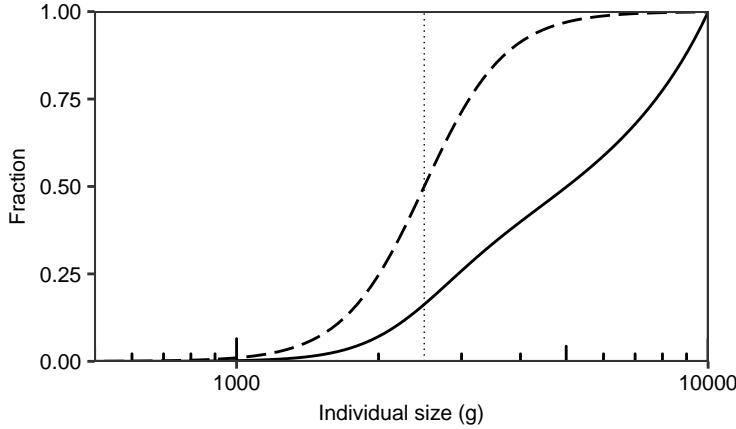


Figure 2.3: Fraction of individuals mature ψ_m (dashed), and fraction of energy invested into reproduction ψ (solid), both as a function of individual size w . Shown for a W_∞ value of 10 kg. The vertical dotted line shows size at 50% maturity.

use an average value of $\eta_m = 0.25$ as reported by Andersen and Beyer (2015), who used data from Gunderson (1997).

Next, I assume that mature individuals have a constant gonadosomatic index (GSI), or in other words, I assume that the size of the gonads is directly proportional to mature body mass $w\psi_m(w)$. Thus, the total amount of energy invested into reproduction by an individual of size w can be described as:

$$\psi(w)E_a(w) = k_r\psi_m(w)w \quad (2.14)$$

where k_r represents fraction of investment in reproduction as determined by the GSI. When an individual has reached size W_∞ , all available energy $E_a(W_\infty)$ is invested in reproduction, and both $\psi(W_\infty)$ and $\psi_m(W_\infty)$ are equal to 1. Thus, $k_r = E_a(W_\infty)/W_\infty$, and Equation 2.14 can be rewritten as $\psi(w) = \psi_m(w)\frac{E_a(W_\infty)}{E_a(w)}\frac{w}{W_\infty}$. By inserting Equation 2.11 and 2.13, considering that $k_s = f_c\alpha h$ and $k_a = \epsilon_a\alpha h(f_0 - f_c)W_\infty^{n-1}$, and assuming a constant feeding level of $f(w) = f_0$, the equation for $\psi(w)$ can be rewritten as:

$$\psi(w) = \left(1 + \left(\frac{w}{\eta_m W_\infty}\right)^{-u_m}\right)^{-1} \frac{1 - \epsilon_a}{(w/W_\infty)^{n-1} - \epsilon_a} \quad (2.15)$$

How maturity ψ_m and the fraction of energy invested into reproduction ψ change with size w can be seen in Figure 2.3.

2.4 Reproduction

The available energy that an individual of size w invests into reproduction can now be given as $\psi(w)E_a(w)$. Not all of this energy is actually transferred to eggs. Some is lost through metabolic inefficiencies involved in egg production, whilst other energy is lost through reproduction-related activity such as a spawning migration or an active search for mates. Thus, energy available for reproduction is multiplied with a reproduction efficiency ϵ_R . The value of ϵ_R will be stock-specific, but as a generalization it is here assumed that $\epsilon_R = 0.1$. Dividing the remaining available energy with the size of the egg w_{egg} gives the amount off eggs produced by an individual as $\epsilon_R\psi(w)E_a(w)/w_{\text{egg}}$. Integrating over the abundance size-spectrum of the stock then gives total egg production R_p of individuals in the stock as:

$$R_p = \int_{w_{\text{egg}}}^{W_{\infty}} \frac{\epsilon_R\psi(w)E_a(w)}{2w_{\text{egg}}} N(w) dw \quad (2.16)$$

where the term inside the integral has been multiplied with 1/2 to take into account that only females produce eggs.

In fisheries models, reproduction is often calculated in the form of recruitment R , which usually refers to the number of fish that enter the fished component of the population. Recruitment size then depends on the size-selectivity of the fishing gear, and a mortality term needs to be introduced to represent the mortality from egg size w_{egg} to recruitment size w_R . For now, however, I maintain a recruitment size $w_R = w_{\text{egg}}$. A Beverton-Holt stock-recruitment relationship is added in the model to describe the density dependence that takes place early-in-life. This is explained in greater detail later on, in Section 3.4. For now, it is only important to note that recruitment R is described as:

$$R = R_{\max} \frac{R_p}{R_{\max} + R_p} \quad (2.17)$$

where R_{\max} is the maximum recruitment of the stock.

2.5 Mortality & Fishing

In this model, mortality can come from three different sources, namely natural mortality, cannibalistic predation mortality, and fishing mortality.

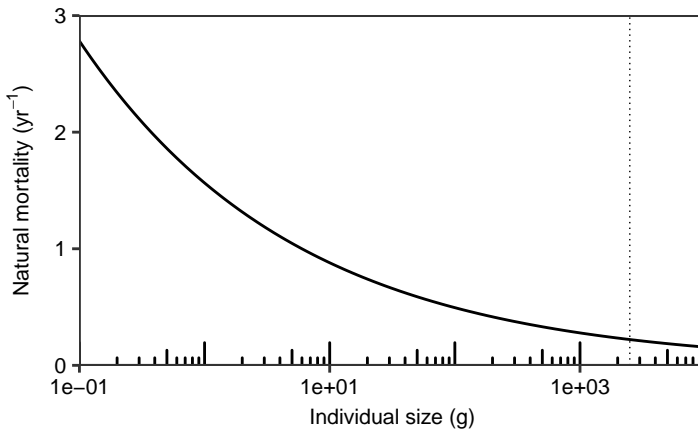


Figure 2.4: Natural mortality μ_0 as a function of individual size w . Shown for a W_∞ value of 10 kg. The vertical dotted line shows size at 50% maturity.

Natural mortality

In the single-stock notation of this model, natural mortality represents mortality inflicted by predation of heterospecific organisms, as well mortality arising from disease and parasitism. Natural mortality μ_0 scales with individual size according to a power law with an exponent of $n - 1$ (Brown et al., 2004):

$$\mu_0(w) = \alpha_p w^{n-1} \quad (2.18)$$

where the coefficient α_p is roughly equal to $1.56 \text{ g}^{1-n} \text{ yr}^{-1}$ (Andersen et al., 2017). The exponent of $-1/4$ means that natural mortality rate decreases with an increase in individual size (Figure 2.4).

Cannibalistic mortality

The rate of cannibalistic mortality μ_c by other conspecifics of size w_P can be derived from Equation 2.7 as:

$$\mu_c(w) = \int_0^\infty \phi\left(\frac{w_P}{w}\right) (1 - f(w_P)) \gamma w_P^q c N(w_P) dw_P \quad (2.19)$$

taking into account the feeding level $f(w_P)$ of the predator. Cannibalism is described in greater detail later on, in Section 3.2.

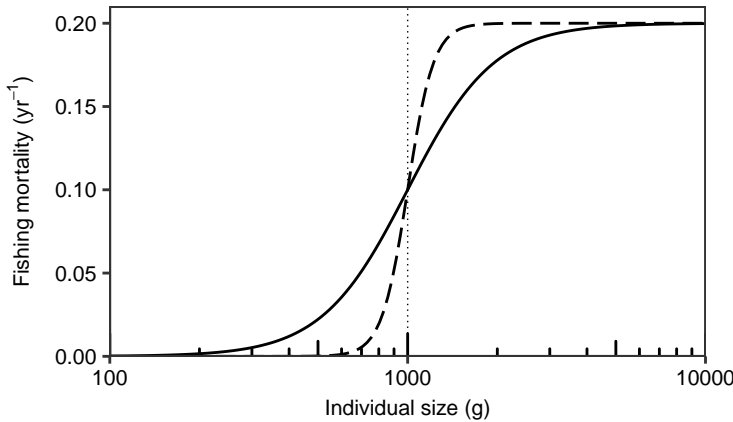


Figure 2.5: Fishing mortality μ_F as a function of individual size w , shown for $u_F = 3$ (solid) and $u_F = 10$ (dashed). Shown for a W_∞ value of 10 kg, and a maximum fishing mortality F of 0.2 yr^{-1} . The vertical dotted line shows mean size-at-entry into the fishery w_F .

Fishing mortality

If fishing takes place, a fishing mortality rate F is applied to the stock by the fishing gear. However, this mortality only applies to individuals that are targeted by the gear. As most fishing gear are size-selective, this means that the individual fishing mortality rate μ_F is a function of size w . Selectivity patterns change depending on the gear used. Here, I assume a trawl fishing gear, which increasingly targets all individuals above a mean size-at-entry w_F , which is determined by the mesh size of the net. Thus, the selectivity pattern of the gear can be described by a sigmoidal relationship with w_F as the inflection point, and individual fishing mortality rate thus becomes:

$$\mu_F(w) = F \left(1 + \left(\frac{w}{w_F} \right)^{-u_F} \right)^{-1} \quad (2.20)$$

where u_F determines the steepness of the sigmoidal relationship (Figure 2.5). Multiplying the size-specific individual fishing mortality rate with the biomass in each size bin, and integrating over all size bins, gives yield Y as:

$$Y = \int_{w_{\text{egg}}}^{W_\infty} \mu_F(w) w N(w) dw \quad (2.21)$$

Taking the above equations, the total mortality rate μ of an individual of size w can be described as:

$$\mu(w) = \mu_0(w) + \mu_c(w) + \mu_F(w) \quad (2.22)$$

2.6 Population structure

The above equations on growth, mortality, and reproduction can be used to describe how individuals move through successive size bins, which allows for dynamic modelling of the population structure. Individuals enter a size bin by growing into it, and can leave it by growing out of it or by dying. In a continuous notation, this can be represented by the McKendrick-von Foerster conservation equation:

$$\frac{\partial N(w)}{\partial t} + \frac{\partial g(w)N(w)}{\partial w} = -\mu(w)N(w) \quad (2.23)$$

with $g(w_{\text{egg}})N(w_{\text{egg}}) = R$ as a boundary condition that represents that individual moving into the smallest size bin do so through the process of recruitment.

To be able to use Equation 2.23 in discrete calculations, a numerical solution to the model is needed. To numerically solve the model, it first needs to be converted to a discrete notation. For this, a range of m logarithmically-distributed size bins is created for the stock, ranging from $w_1 = w_{\text{egg}}$ to $w_m = W_\infty$. The i th weight bin can be described as $w_i = \exp[\ln(w_{\text{egg}}) + (i-1)\delta]$, with δ describing the logarithmic spacing between weight bins as:

$$\delta = \frac{\ln(W_\infty) - \ln(w_{\text{egg}})}{m-1} \quad (2.24)$$

Now, the McKendrick-von Foerster conservation equation (Eq. 2.23) can be rewritten in a discrete form, following the description by Andersen et al. (2016):

$$\frac{N_i^{t+\Delta t} - N_i^t}{\Delta t} + \frac{g(w_i)N_i^{t+\Delta t} - g(w_{i-1})N_{i-1}^{t+\Delta t}}{w_i - w_{i-1}} = -\mu(w_i)N_i^{t+\Delta t} \quad (2.25)$$

This can be rearranged as:

$$N_{i-1}^{t+\Delta t} \left(-\frac{\Delta t}{\Delta w_i} g(w_{i-1}) \right) + N_i^{t+\Delta t} \left(1 + \frac{\Delta t}{\Delta w_i} g(w_i) + \Delta t \mu(w_i) \right) = N_i^t \quad (2.26)$$

where $\Delta w_i = w_i - w_{i-1}$. When defining the two terms within brackets as $X(w_i) = -\frac{\Delta t}{\Delta w_i} g(w_{i-1})$ and $Z(w_i) = 1 + \frac{\Delta t}{\Delta w_i} g(w_i) + \Delta t \mu(w_i)$, Equation 2.26 can be rewritten as

$$N_{i-1}^{t+\Delta t} X(w_i) + N_i^{t+\Delta t} Z(w_i) = N_i^t \quad (2.27)$$

which in turn can be rewritten as

$$N_i^{t+\Delta t} = \frac{N_i^t - X(w_i)N_{i-1}^{t+\Delta t}}{Z(w_i)} \quad (2.28)$$

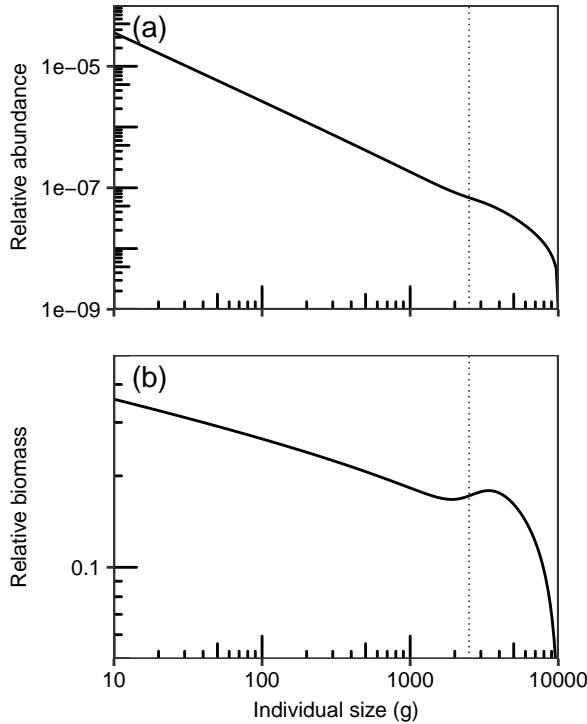


Figure 2.6: The abundance N spectrum (a) and biomass B spectrum (b) as a function of individual size w . The abundance and biomass spectrum are shown relative to their maximum (outside of the plot range). Shown for a W_∞ value of 10 kg. The vertical dotted line shows size at 50% maturity.

with $N_m^{t+\Delta t} = 0$ to make sure that no pooling of individuals will occur in the last size bin.

In this notation, to be able to calculate the new abundance of individuals in a given weight bin $N_i^{t+\Delta t}$, the abundance of individuals in the weight bin before it ($N_{i-1}^{t+\Delta t}$) needs to be known. The abundance within the first size bin, $N_1^{t+\Delta t}$, can be found with the boundary condition to Eq. 2.23, and is given by Andersen et al. (2016) as

$$N_1^{t+\Delta t} = \frac{N_1^t + R\Delta t/(w_2 - w_1)}{Z(w_1)} \quad (2.29)$$

Equations 2.28 and 2.29 can subsequently be used to calculate the abundance spectrum over time, reaching a stable state if iterated to equilibrium. Figure 2.6 shows the shape of the abundance and biomass spectra the stock in a steady state.

2.7 Resource dynamics

The above equations can be used to construct a community of any given number of fish stocks, where the asymptotic size W_∞ is the main governing trait of each stock. This is for instance shown by Andersen et al. (2016). The plankton community, upon which the smallest fish feed, is then represented with a separate resource size-spectrum. I, however, mainly use this model in its single-stock notation. Thus, a resource size spectrum is needed for the single stock to feed upon, ranging in particle size w_r from well below w_{egg} up to W_∞ . At carrying capacity, the abundance size-spectrum of the resource then follows Equation 2.1 as $N_r(w_r) = \kappa w_r^\lambda$, where λ is the exponent of the community size-spectrum. Using the above equations on predator-prey dynamics, the value of the size-spectrum exponent λ can now be calculated.

Resource size-spectrum exponent

To calculate the value of λ the available resource biomass B_r for a given predator of size w is first defined using consumption C and clearance rate V as:

$$B_r(w) = C(w)/V(w) \quad (2.30)$$

assuming that the predator consumes all suitable resource particles in the volume of water that it clears. Alternatively, using Equation 2.6 and 2.3, $B_r(w)$ can also be written as the resource biomass portion from the Sheldon spectrum $\kappa w_r^{2+\lambda}$ that is available as prey to a predator of size w :

$$B_r(w) = \int_0^\infty \phi\left(\frac{w}{w_r}\right) w_r N(w_r) dw_r = \Phi \kappa w_r^{2+\lambda} \quad (2.31)$$

where Φ is a constant that is related to the predator's prey preference. The value of Φ can be found by solving the integral in Equation 2.31 (see Andersen and Beyer, 2006). Here, the value of Φ is not relevant for calculating the value of λ , so I will not get into it further.

Combining equations 2.30 and 2.31, and inserting $C(w) = f_0 h w^n$ (Eq. 2.8 & 2.10) and $V(w) = \gamma w^q$ (Eq. 2.4) gives

$$\Phi \kappa w_r^{2+\lambda} = f_0 \frac{h}{\gamma} w^{-q+n} \quad (2.32)$$

which can be rearranged to the resource abundance size-spectrum of Equation 2.1 as:

$$N_r(w_r) = \kappa w_r^\lambda = \frac{f_0}{\Phi} \frac{h}{\gamma} w^{-2-q+n} \quad (2.33)$$

Thus, by looking at the exponents on both sides of the equation, $\lambda = -2 - q + n$, and is thus roughly equal to -2.05. This means that the resource biomass spectrum declines slightly with an increasing w , which is also what Sheldon et al. (1972) observed for what we now refer to as the Sheldon spectrum.

Resource growth and mortality

The resource carrying capacity is given as $N_r(w_r) = \kappa w_r^\lambda$. However, when the model is run in continuous time, the resource abundance N_r need not always be at carrying capacity. This is determined by the growth and mortality of the resource.

The resource is consumed by individuals from the stock, as shown in Equation 2.7. Following Equation 2.19, the predation mortality μ_p of resource particles of size w_r can be described as:

$$\mu_p(w_r) = \int_{w_{\text{egg}}}^{W_\infty} \phi\left(\frac{w}{w_r}\right) (1 - f(w)) \gamma w^q N(w) dw \quad (2.34)$$

To keep the resource dynamics simple, and avoid the need to introduce recruitment dynamics to the resource, growth in each resource size bin is described according to a semi-chemostat. The chemostat's dilution rate, which in this case can be better interpreted as a maximum regeneration rate, scales with resource particle size w_r according to a power law $r_0 w_r^{n-1}$, with exponent $n-1$ (Fenchel, 1974) and a coefficient r_0 . The size-specific rate of change of resource abundance N_r can now be described as:

$$\frac{dN_r(w_r)}{dt} = r_0 w_r^{n-1} [\kappa w_r^\lambda - N_r(w_r)] - \mu_p(w_r) N_r(w_r) \quad (2.35)$$

For the discrete notation of the model, a series of m_r size bins with index j are created for the resource particles, ranging from $w_{r,1} = w_{r0}$ to $w_{r,m_r} = W_\infty$, using the same logarithmic spacing between weight bins as was used to create the weight bins for the stock. Here, w_{r0} should be smaller than $0.01w_{\text{egg}}$, to ensure sufficient food for smallest individuals. Next, Equation 2.35 can be solved analytically, as shown by Hartvig et al. (2011):

$$N_{r,j}^{t+\Delta t} = K_e(w_{r,j}) - [K_e(w_{r,j}) - N_{r,j}^t] e^{-[r_0 w_{r,j}^{n-1} + \mu_p(w_{r,j})] \Delta t} \quad (2.36)$$

where $K_e(w_{r,j}) = \frac{r_0 w_{r,j}^{n-1} \kappa w_{r,j}^\lambda}{r_0 w_{r,j}^{n-1} + \mu_p(w_{r,j})}$ is the size-specific effective carrying capacity of the resource.

2.8 Reference points

MSY reference points for the stock that is simulated with the model can be calculated by making use of the discrete model notation. To find MSY, as well as the fishing mortality and stock biomass that yields MSY (F_{MSY} and B_{MSY}), the model should simply be run for a range of different fishing mortality F values. For each F value, the model should be iterated through a sufficient number of time steps so that a steady state is reached. Then, one of the model runs will have a yield Y output that is higher than that of the other runs. This maximum yield represents MSY, the associated F value represents F_{MSY} , and the associated stock biomass represents B_{MSY} .

The model as outlined above can be used to describe the dynamics of a single fish stock that feeds upon a dynamic resource spectrum. In its current notation, the population abundance is regulated by two different emergent density-dependent mechanisms: density-dependent growth through resource competition, and density-dependent mortality through cannibalism. The following chapter will explain more about how the population abundance of fish stocks is regulated through density dependence, and how this density dependence is usually incorporated in fisheries models. Furthermore, I will show how density-dependent recruitment can be added to the model. Lastly, I will show how the strength of density-dependent regulation in recruitment, mortality, and growth can be changed in the model, and what the effect of this is on the MSY reference points of the stock.

Table 2.1: Model equations

<i>Consumption</i>		
Size preference for prey	$\phi\left(\frac{w}{w_r}\right) = \exp\left[-\left(\ln\left(\frac{w}{w_r\beta}\right)\right)^2/(2\sigma^2)\right]$	M1
Encountered food	$E_e(w) = \gamma w^q \int_0^\infty \phi\left(\frac{w}{w_r}\right) w_r [cN(w_r) + N_r(w_r)] dw_r$	M2
Feeding level	$f(w) = \frac{E_e(w)}{E_e(w) + hw^n}$	M3
<i>Growth</i>		
Available energy	$E_a(w) = \alpha f(w)hw^n - k_s w^n - k_a w$	M4
Maturation	$\psi(w) = \left(1 + \left(\frac{w}{\eta_m W_\infty}\right)^{-u_m}\right)^{-1} \frac{1 - \epsilon_a}{(w/W_\infty)^{n-1} - \epsilon_a}$	M5
Growth rate	$g(w) = (1 - \psi(w))E_a(w)$	M6
<i>Mortality</i>		
Background predation	$\mu_0(w) = \alpha_p w^{n-1}$	M7
Cannibalism	$\mu_c(w) = \int_{w_{\text{egg}}}^{W_\infty} \phi\left(\frac{w_P}{w}\right) (1 - f(w_P)) \gamma w_P^q cN(w_P) dw_P$	M8
Fishing, trawl selectivity	$\mu_F(w) = F \left(1 + \left(\frac{w}{w_F}\right)^{-u_F}\right)^{-1}$	M9
Total mortality	$\mu(w) = \mu_0(w) + \mu_c(w) + \mu_F(w)$	M10
<i>Reproduction</i>		
Egg production	$R_p = \int_{w_{\text{egg}}}^{W_\infty} \frac{\epsilon_R \psi(w) E_a(w)}{2w_{\text{egg}}} N(w) dw$	M11
Recruitment	$R = R_{\max} \frac{R_p}{R_{\max} + R_p}$	M12
<i>Population structure</i>		
Abundance spectrum	$\frac{\partial N(w)}{\partial t} + \frac{\partial g(w)N(w)}{\partial w} = -\mu(w)N(w)$	M13
Boundary condition	$g(w_{\text{egg}})N(w_{\text{egg}}) = R$	M14
<i>Fishery performance</i>		
Yield	$Y = \int_{w_{\text{egg}}}^{W_\infty} \mu_F(w) w N(w) dw$	M15
<i>Resource</i>		
Predation on resource	$\mu_p(w_r) = \int_{w_{\text{egg}}}^{W_\infty} \phi\left(\frac{w}{w_r}\right) (1 - f(w)) \gamma w^q N(w) dw$	M16
Resource spectrum	$\frac{\partial N_r(w_r)}{\partial t} = r_0 w_r^{n-1} [\kappa w_r^\lambda - N_r(w_r)] - \mu_p(w_r) N_r(w_r)$	M17

Table 2.2: Model parameters

Symbol	Description	Value	Unit	Source(s)
<i>Body size</i>				
W_∞	Asymptotic size (weight)	variable	g	
w_{egg}	Egg weight	0.001	g	1
<i>Consumption</i>				
n	Metabolic exponent	3/4	-	2
β	Preferred pred.-prey mass ratio	100	-	3
σ	Range of preferred prey size	1.3	-	4
q	Clearance rate exponent	0.8	-	5
γ	Clearance rate coefficient	$6.57/\kappa$	$\text{g}^{-q} \text{ yr}^{-1}$	4
f_0	Standard feeding level	0.6	-	6
f_c	Critical feeding level	0.2	-	6
h	Maximum consumption	18.6	$\text{g}^{1-n} \text{ yr}^{-1}$	4
<i>Growth</i>				
α	Assimilation efficiency	0.6	-	7
η_m	Size at maturation rel. to W_∞	0.25	-	8, 9
ϵ_a	Fraction of energy for activity	0.8	-	9
k_s	Standard metabolism coefficient	$f_c \alpha h$	$\text{g}^{1-n} \text{ yr}^{-1}$	6
k_a	Activity coefficient	$\epsilon_a \alpha h (f_0 - f_c) W_\infty^{n-1}$	yr^{-1}	9
u_m	Maturity ogive steepness	5	-	10
<i>Mortality</i>				
α_p	Mortality level	1.56	$\text{g}^{1-n} \text{ yr}^{-1}$	4
c	Cannibalism coefficient	variable	-	
<i>Reproduction</i>				
R_{\max}	Maximum recruitment	variable	yr^{-1}	
ϵ_R	Recruitment efficiency	0.1	-	
<i>Fishery performance</i>				
w_F	Mean size-at-entry into the fishery	variable	g	
F	Fishing mortality	variable	yr^{-1}	
u_F	Trawl selectivity steepness	3	-	10
<i>Resource</i>				
κ	Carrying capacity coefficient	variable	$\text{g}^{-1-\lambda}$	
λ	Carrying capacity exponent	$-2 - q + n$	-	
r_0	Resource growth rate coefficient	4	$\text{g}^{1-n} \text{ yr}^{-1}$	6, 11

¹ Neuheimer et al. (2015). ² West et al. (1997). ³ Jennings et al. (2002). ⁴ Andersen et al. (2017). ⁵ Andersen and Beyer (2006). ⁶ Hartvig et al. (2011). ⁷ Kitchell et al. (1977). ⁸ Gunderson (1997). ⁹ Andersen and Beyer (2015). ¹⁰ Andersen (2019). ¹¹ Savage et al. (2004).

CHAPTER 3

Density dependence

All populations of organisms experience some form of regulation, which prevents their population size from exponentially growing to infinity. Usually, this regulation comes in the form of density dependence. Density dependence takes place when vital rates (e.g. growth, reproduction, and mortality) of individuals are affected by population density. As such, when the abundance of individuals N in the population increases, the overall growth rate of the population decreases. In theory, this continues until the population size has reached its carrying capacity K , at which point the population growth rate is 0, and population size has reached an equilibrium. A simple mathematical representation of this process can be given by

$$\frac{dN}{dt} = rN\left(1 - \frac{N}{K}\right) \quad (3.1)$$

where r is the intrinsic growth rate of the population. Figure 3.1 gives an overview of the associated population dynamics, and shows how population growth becomes negative if N were to overshoot K for some reason. Thus, density-dependent regulation keeps the population at a steady state around its carrying capacity.

This above description of density dependence, where population growth rate is negatively affected by an increase in population density, is often referred to as compensation or compensatory density dependence (see, e.g., Rose et al., 2001). A loss of individuals will then be *compensated* by an increased population growth, keeping the population density more or less the same. However, population growth rate can also be positively affected by an increase in population density. This is often referred to as depensation or depensatory density dependence (see, e.g., Liermann and Hilborn, 1997), where population growth rate *depends* on the presence of sufficient individuals to sustain the population. An alternative term is the Allee effect, so named after the groundbreaking work of W.C. Allee (e.g., 1931, 1938). Under strong depensatory density dependence, if population density declines to a critical threshold, the population growth becomes negative, and the population will become extinct.

Although density dependence ultimately changes population growth rate, it usually does this by acting on individual-level processes, which can be both positively and

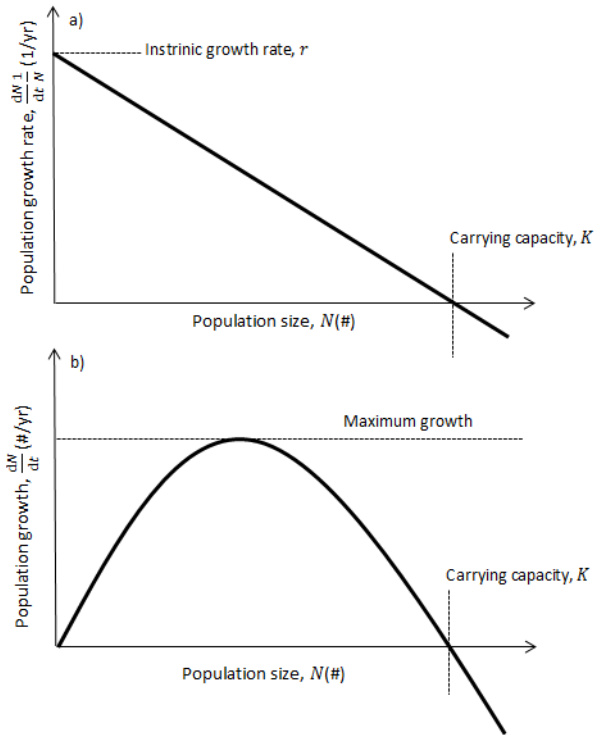


Figure 3.1: Population growth rate as a function of population size (a), and the resulting population growth curve (b), showing the basic functioning of density dependence in population regulation.

negatively influenced by population density. Individuals can be affected by density dependence throughout their lives, and density dependence often acts upon more than just one individual-level process. For instance, North Sea plaice experience at least three separate periods of density-dependent mortality during their first 16 months of life (Beverton and Iles, 1992). Which processes density dependence acts upon can vary greatly, but in the end it affects at least one of three different vital rates: growth, reproduction, or mortality.

3.1 Density-dependent growth

Growth is influenced by density dependence mainly through competition for resources. As population size increases, more individuals are competing for the same resources. If

there is only a limited amount of said resource, this will cause the resource to become depleted, and as a result most individuals will suffer from a reduced energy intake. This reduced energy intake subsequently causes a reduction in growth.

Density-dependent growth is a widespread phenomenon among fish, especially among those living in freshwater (Ylikarjula et al., 1999). However, many marine fishes are also susceptible to density-dependent growth (Lorenzen and Enberg, 2002; Zimmermann et al., 2018). For instance, the temporary halt of fishing in the North Sea during the Second World War (WWII) resulted in an abundance increase of North Sea plaice, who subsequently suffered from a reduced growth rate (Margetts and Holt, 1948; Rijnsdorp and Van Leeuwen, 1992). Nowadays, with the recent increase in North Sea plaice SSB, individual growth rate of plaice is once again starting to decline (van der Sleen et al., 2018). Another example would be Baltic sprat. After the collapse of the eastern Baltic cod in the 1980s, Baltic sprat experienced a great increase in SSB due to a reduced predation mortality from cod (Köster et al., 2003). This increase in SSB was followed by a strong decline in individual growth rate (Eero, 2012), likely the result of density-dependent growth. A last example is haddock (*Melanogrammus aeglefinus*) in the southwestern Scotian Shelf, where mean length of age-1 individuals appears to be negatively correlated to the abundance of age-4+ adults (Marshall and Frank, 1999).

Resource intake is not always negatively affected by population density. For instance, although schooling or shoaling is generally associated with increased resource competition due to higher densities of individuals (Grand and Dill, 1999), for several species schooling or shoaling has been demonstrated to result in locating food more rapidly and an increased feeding success (Pitcher et al., 1982; Ranta and Kaitala, 1991).

Density-dependent growth in the size-structured model

In the model described in Chapter 2, density-dependent growth takes place when individuals are able to graze down the abundance of a resource size-bin to below its carrying capacity. This happens when the predation mortality exerted on the resource exceeds its growth rate, thereby reducing resource abundance within the given size bin. This decreased resource abundance subsequently reduces the feeding level of the individuals that prefer to feed on resource particles from that size bin. This reduced feeding level reduces individual consumption, which in turn reduces individual growth (Figure 3.2).

Individuals of the stock feed on the resource following a certain size-preference, meaning that individuals mostly compete with other individuals that are around the same size. Thus, the strength of density-dependent growth experienced by the modelled individuals depends on the biomass of individuals in a given size bin relative to the biomass of the resource that they are competing for. Because the resource spectrum

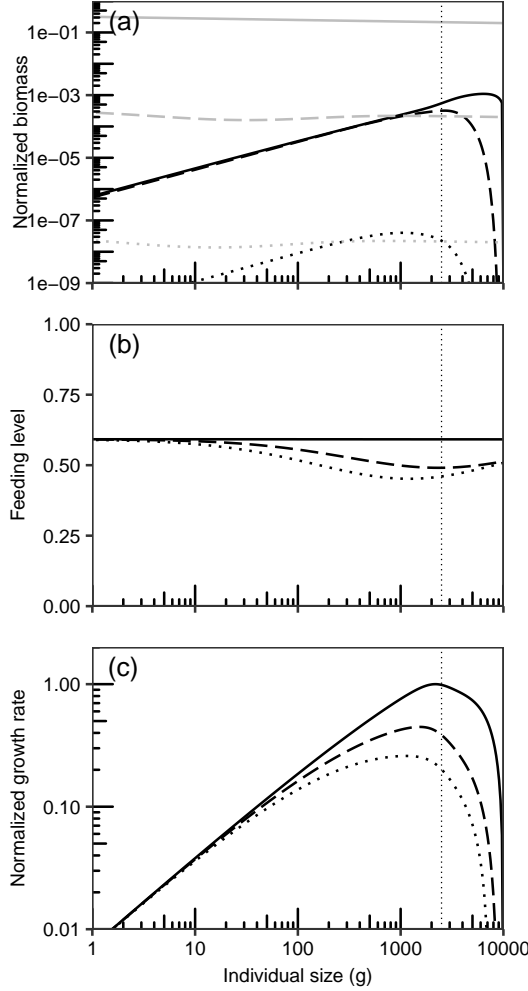


Figure 3.2: The emergence of density-dependent growth in a stock (black) that feeds on a dynamic resource (grey), brought about by different values of the resource carrying capacity coefficient κ , assuming a constant maximum recruitment R_{\max} . Here, it is the ratio between R_{\max} and κ that determines the strength of density-dependent growth, and the values of R_{\max}/κ are given as 0.0001 (solid), 0.1 (dashed), and 1000 (dotted). Shown are the biomass of the stock and resource (a), the associated feeding level of the stock (b), and the resulting growth of the stock (c). Here, biomass and growth are normalized to their maximum, and the thin vertical dotted line shows size at 50% maturity. As the value of κ decreases relative to the value of R_{\max} , competition for food increases, resulting in a lower feeding level and a lower growth. If the value of κ is sufficiently decreased, recruitment will decrease as well, and is no longer limited by R_{\max} .

follows an almost-flat Sheldon spectrum, it can therefore be expected that the strength of density-dependent growth is highest around the peak of the biomass spectrum of the stock. This peak is located around size-at-maturity (Figure 3.2a). The reason for this is that, in early life, biomass in successive size bins increases because the growth of biomass exceeds the loss of biomass due to mortality. After maturation however, an increasing amount of energy is invested into reproduction instead of growth, and the stock biomass spectrum starts to decrease with increasing size instead.

In a sense, the carrying capacity coefficient κ of the resource spectrum can be considered to regulate the strength of density-dependent growth, relative to other density-dependent processes. If recruitment to the stock R is kept limited to a certain maximum recruitment R_{\max} , different values of κ influence whether or not individuals from the stock are able to graze down on the resource (Figure 3.2). A higher κ value increases the abundance of the resource, thereby decreasing the depletion of the resource. This keeps individual feeding level closer to the standard feeding level, preventing the emergence of density-dependent growth. The use of κ in regulating the strength of density-dependent growth is described in more detail in Section 3.6.

In the absence of any other form of density dependence, recruitment R depends on the value of κ . The stock is then completely regulated by density-dependent growth, emerging as a reduction in growth rate of individuals in a broad size range around size-at-maturity (Figure 3.2, dotted lines). This reduced growth in turn limits reproduction through a number of mechanisms. Firstly, individuals simply take longer to mature, and thereby experience a greater risk of mortality before being able to reproduce. Second, even if individuals mature, their slower growth means that it is less likely that they will survive to a larger size, where fecundity is higher. Lastly, the same low energy intake that reduces energy available for growth also reduces the energy available for reproduction. Thus, through density-dependent growth, the population size spectrum will stabilize at a level where the same number of individuals are recruited to the stock as the number of individuals that are removed from the stock through mortality.

3.2 Density-dependent mortality

The most straightforward way in which mortality is affected by population density is through cannibalism, where a high abundance of larger individuals will result in increased predation mortality for smaller individuals (or eggs) of the same stock. For instance, cannibalism plays a major role in the population dynamics of sandeel (Eigaard et al., 2014), Peruvian anchovy (*Engraulis ringens*; Alheit, 1987), and cod (Bogstad et al., 1994) stocks.

Additionally, increased population density can increase mortality through a process known as 'prey switching', where predators will choose to disproportionately feed on a certain type of prey if it is abundant enough. This process is also known as a type III functional response (Holling, 1959b).

Furthermore, similar to growth, mortality can also be affected by the increased resource competition that results from an increased population density. If increased resource competition depletes resources to a sufficiently-low level, individuals will start starving, increasing mortality rate (Myers and Cadigan, 1993). On top of this, some species have shown a tendency to actively avoid a reduced energy intake (and thus a reduced growth rate) when resources are depleted. Instead, individuals of those species will increase their foraging rate (Walters and Juanes, 1993; Wyatt, 1972), or take greater risks during foraging (Damsgird and Dill, 1998), increasing their susceptibility to predation and thereby their mortality rate. Aside from food limitation, density-dependent mortality can also arise from other limiting factors, such as habitat size available for larval settlement (Ursin, 1982).

However, mortality can also be reduced due to increased population density. Schooling behaviour, for instance, is generally understood to mainly be employed to reduce predation (Grand and Dill, 1999). Schooling is a strategy used by many species of fish, and it becomes more effective at reducing mortality rate as the school becomes larger (Grand and Dill, 1999). Furthermore, if a species becomes very abundant, predators may become saturated, thereby reducing the individual predation rate (Type II functional response; Holling, 1959a). Additionally, in some stocks, a high abundance of large adults will reduce the predation mortality experienced by juveniles of that stock, because the adults predate on the predators of the juveniles (Walters and Kitchell, 2001).

Density-dependent mortality in the size-structured model

In the model described in Chapter 2, density-dependent mortality arises through cannibalism: larger individuals from the stock feed upon smaller individuals, as described in Equation 2.7. Thus, the strength of density-dependent mortality is highest for individuals that are targeted by the greatest biomass of predators. Because the biomass of the stock peaks around size-at-maturity, this means that density-dependent mortality is strongest for those individuals that are predominantly targeted by old juveniles and young adults (Figure 3.3).

In this model, the strength of density-dependent mortality can be altered by changing the value of c in Equations 2.7 and 2.19. This parameter has been introduced to be able to manually change a stock's tendency toward cannibalism, from no cannibalism ($c = 0$) to no discrimination between conspecifics and heterospecifics ($c = 1$). The

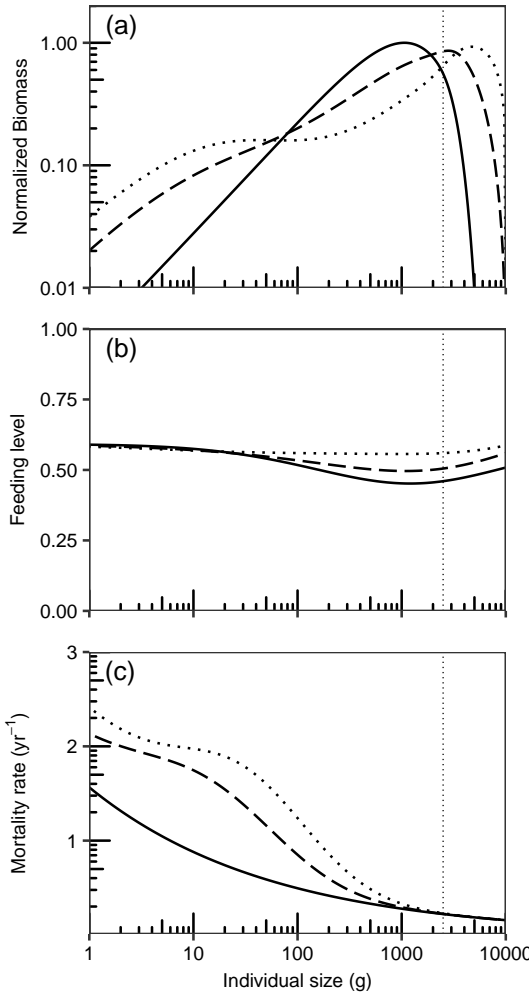


Figure 3.3: The emergence of density-dependent mortality, brought about by a stock's tendency toward cannibalism, as determined by the parameter c . Here, the values of c are given as 0 (solid, no cannibalism), 0.5 (dashed, some cannibalism but a greater preference for heterospecifics), and 1 (dotted, no difference in preference between heterospecifics and conspecifics). Shown are the biomass (a), the feeding level (b), and the mortality rate (c) of the stock. Here, biomass is normalized to its maximum, and the thin vertical dotted line shows size at 50% maturity. Furthermore, no limit is set on recruitment ($R_{\max} = \infty$), so when $c = 0$ the stock is completely regulated by density-dependent growth, as shown in Figure 3.2. However, as the value of c increases, individuals are increasingly cannibalized by larger individuals. This raises the feeding level of the cannibalizing individuals, increasing their growth. However, increased cannibalism also increases the mortality rate, particularly for individuals targeted by the size bins with the largest biomass. Thus, as the value of c increases, the stock becomes more regulated by density-dependent mortality.

effect of different values of c on cannibalistic mortality can be seen in Figure 3.3. The use of c in regulating the strength of density-dependent mortality is described in more detail in Section 3.6.

3.3 Density-dependent reproduction

Reproduction can be influenced by density dependence in a similar way as growth. After all, fish not only use energy for growth, but also need energy to invest in e.g. the development of gonads and eggs. Thus, if an increased population density results in increased resource competition, the resulting reduced energy intake can cause a reduction in individual reproductive output (Henderson et al., 1996). Additionally, reduced individual growth will also mean that individuals will either take longer to reach size-at-maturity (Colby and Nepszy, 1981), or instead will mature at a smaller size (De Leo and Gatto, 1996), both of which reduce reproductive output. Furthermore, if there is only a limited area of suitable spawning habitat available, this can also reduce mean individual reproductive output at high population densities, when all available spawning habitat is occupied (Fukushima et al., 1998).

Density-dependent reproduction in the size-structured model

In the absence of a stock-recruitment relationship, when $R = R_p$, the stock is mainly regulated through density-dependent growth and density-dependent mortality (Figure 3.3). Both processes limit the size of the spawning stock, thereby limiting reproduction as well. Furthermore, the resource mechanism that leads to the emergence of density-dependent growth also leads to the emergence of density-dependent reproduction: competition for resources results in a reduced feeding level, which results in a reduced consumption, which results in less energy available for reproduction.

3.4 Density-dependent recruitment

In standard fisheries models, the predominant form of density-dependent regulation is density-dependent recruitment to the stock. Usually, density-dependent recruitment is incorporated by making use of a stock-recruitment relationship. This relationship, as the name suggests, is used to approximate the number of recruits R produced for a given spawning stock size S . Thus, the stock-recruitment relationship represents a

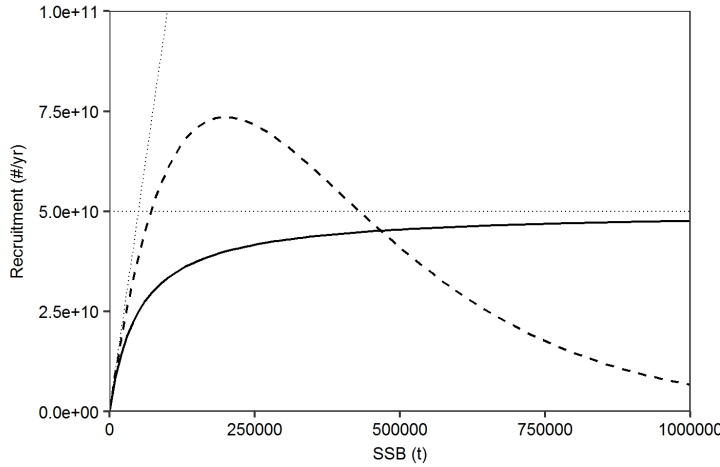


Figure 3.4: The Beverton-Holt (solid) and Ricker (dashed) stock-recruitment relationships, showing R_{\max} (horizontal dotted line) and R_1 (sloped dotted line).

descriptive method for incorporating all density dependence that takes place in the pre-recruit environment.

The most well-known stock-recruitment relationships are the Beverton-Holt (Beverton and Holt, 1957) and Ricker (Ricker, 1954) relationships (Figure 3.4), which can be described as

$$R = \frac{R_{\max}S}{S_{0.5} + S} \quad (3.2)$$

and

$$R = R_1 S e^{-R_2 S} \quad (3.3)$$

respectively, where R_{\max} is the maximum recruitment of the stock at high biomass, $S_{0.5}$ is the size of the spawning stock that would produce $R = 0.5R_{\max}$, R_1 is the productivity (R/S) of the stock at low stock size ($S \approx 0$), and R_2 determines the rate of decline in R/S as S increases.

Figure 3.4 illustrates the main difference between the Beverton-Holt and Ricker stock-recruitment relationships. The Beverton-Holt relationship assumes a carrying capacity in the pre-recruit environment, caused for instance by a shortage of food or shelter. Thus, recruitment does not increase linearly with spawning stock size, but instead levels off toward a maximum recruitment at high spawning stock sizes. Initially, the Ricker relationships shows a similar leveling off in recruitment as spawning stock size increases. However, as the spawning stock continues to increase in size, recruitment actually starts to decrease. Therefore, the Ricker relationship is mainly used when cannibalism is an important process in the pre-recruit environment. Note that in this

case, therefore, cannibalism falls under the category of density-dependent recruitment, and not density-dependent mortality.

Density-dependent recruitment in the size-structured model

So far, the model has included density dependence in a mechanistic way: density dependence emerges late-in-life due to resource competition and cannibalistic mortality. To incorporate early-life density-dependent recruitment into the model, a Beverton-Holt stock-recruitment relationship is added to describe recruitment R :

$$R = R_{\max} \frac{R_p}{R_{\max} + R_p} \quad (3.4)$$

This notation may seem different from the one described in Equation 3.2, but this is because the R_p term already includes parameters that affect reproduction. For instance, if I were to move the ϵ_R term out of the equation for egg production R_p (Eq. 2.16) and into the stock-recruitment relationship instead, I could write:

$$R = R_{\max} \frac{\epsilon_R R_p}{R_{\max} + \epsilon_R R_p} = \frac{R_{\max} R_p}{R_{\max}/\epsilon_R + R_p} \quad (3.5)$$

which clearly resembles Equation 3.2.

By changing the value of R_{\max} , the strength of density-dependent recruitment, relative to other forms of density dependence, can be changed. This is described in more detail in Section 3.6.

3.5 Timing

The overall strength of density dependence experienced by an individual often changes with individual size. For instance, high rates of juvenile density-dependent mortality are reported for many stocks (Myers and Cadigan, 1993). On the other hand, strong adult density density-dependent growth for example can be prevalent as well, especially among freshwater lake fish (Ylikarjula et al., 1999). Thus, the precise time in life when an individual experiences the majority of density-dependent regulation appears to be variable, and is likely dependent on stock-specific bottlenecks.

In the generalized environment that the model described in Chapter 2 simulates, both density-dependent growth and mortality emerge late-in-life, around size-at-maturity. These processes have a mechanistic basis in the model, emerging due to predator-prey

relationships and energetic requirements. The stock-recruitment relationship, on the other hand, has been introduced into the model as a descriptive way of incorporating early-in-life density dependence, without providing a clear mechanism behind the relationship.

A mechanistic way to incorporate early-in-life density dependence in a size-structured model, such as the one I have outlined, has been described by Andersen et al. (2017). In their model, Andersen et al. (2017) introduce a term that describes the spatial spreading of juveniles through their habitat. For small habitats, where juveniles have spread throughout shortly after hatching, the model resembles the one I have outlined in Chapter 2, where there is no density-dependent recruitment and density-dependent regulation happens late-in-life. In larger habitats however, it takes longer for the newly-hatched larvae to spread throughout the habitat. Thus, in early life, the density of individuals and biomass is actually higher than later-in-life, as individuals are condensed in a smaller area early-in-life. In such a case, the spectrum of biomass density actually peaks early-in-life. As a result, density-dependent regulation takes place early in life, through density-dependent growth emerging through resource competition and density-dependent mortality emerging through cannibalism.

The model variation applied by Andersen et al. (2017) shows how density-dependent regulation can emerge early-in-life in a mechanistic way, preventing the need to use a stock-recruitment relationship. However, in this thesis, I will continue using the descriptive stock-recruitment relationship instead to describe early-in-life density dependence. This is the predominant way that the model has been applied in this thesis. Also, this simply makes the model more relatable to standard fisheries models, which predominantly use a stock-recruitment relationship.

3.6 Interactions

Density dependence can originate from a variety of sources, which can often interact with each other. For instance, increased population density can increase the competition for resources among individuals, which in turn reduces energy intake, which subsequently can result in reduced growth, while at the same time decreasing individual reproductive output and increasing starvation mortality. Thus, disentangling and then quantifying the strength of the various sources of density dependence is less straightforward than it sounds. In this thesis therefore, for the sake of simplicity, I distinguish between three main sources of density dependence: density-dependent growth stemming from resource competition, density-dependent mortality stemming from cannibalism, and density-dependent recruitment stemming from all sources of

density dependence taking place before individuals reach a size where they are targeted by the fishery (size at recruitment).

In the size-structured model, the regime of density-dependent regulation can be changed by changing the relative strengths of density-dependent growth, mortality, and recruitment. It should be expected that regulation through density-dependent growth can be changed through the parameter κ , regulation through density-dependent mortality can be changed through the parameter c , and regulation through density-dependent recruitment can be changed through the parameter R_{\max} . However, it is not the absolute values of κ , c , and R_{\max} that determine the regime of density-dependent regulation. Rather, it is the ratio between them, particularly between R_{\max} and κ .

R_{\max} and κ

The ratio between R_{\max} and κ determines the relative strength of density-dependent recruitment and density-dependent growth. Simply put, when $c = 0$, changing the value of R_{\max} relative to that of κ changes the size-specific biomass of the stock relative to that of the resource, which in turn changes the relative magnitude of the predation that the stock exerts on the resource. For instance, if the value of R_{\max}/κ is very small, recruitment is completely limited by the stock-recruitment relationship so that $R = R_{\max}$, and at no size w does the stock even come close to depressing the biomass of the resource (Figure 3.5, solid line).

If the value of R_{\max}/κ is increased, the biomass spectrum of the stock increases relative that of the resource. If R_{\max}/κ is increased sufficiently, the stock biomass within certain size bins (around the peak of the biomass spectrum) will become high enough to be able to graze down part of the resource spectrum to below carrying capacity (Figure 3.5). This in turn decreases the feeding level of those individuals, decreasing individual growth, which in turn reduces egg production R_p through the processes described at the end of Section 3.1. Thus, recruitment R is decreased somewhat, but is also still heavily influenced by R_{\max} through the stock-recruitment relationship.

This influence of the stock-recruitment relationship ends if the value of R_{\max}/κ is increased sufficiently further. Then, stock biomass increases even further relative to the biomass of the resource, and a broad size-range of individuals will be able to graze down the resource to below its carrying capacity (Figure 3.5). The subsequent reduction in individual growth is strong enough to reduce recruitment to such an extent that $R = R_p$, completely removing the influence of the stock-recruitment relationship.

For the functioning of the model, the absolute values of R_{\max} and κ are of no consequence. It is only their ratio that matters. For instance, the model will produce the same dynamics when R_{\max} is set to 1 yr^{-1} and κ is set to $10 \text{ g}^{-1-\lambda}$, as when

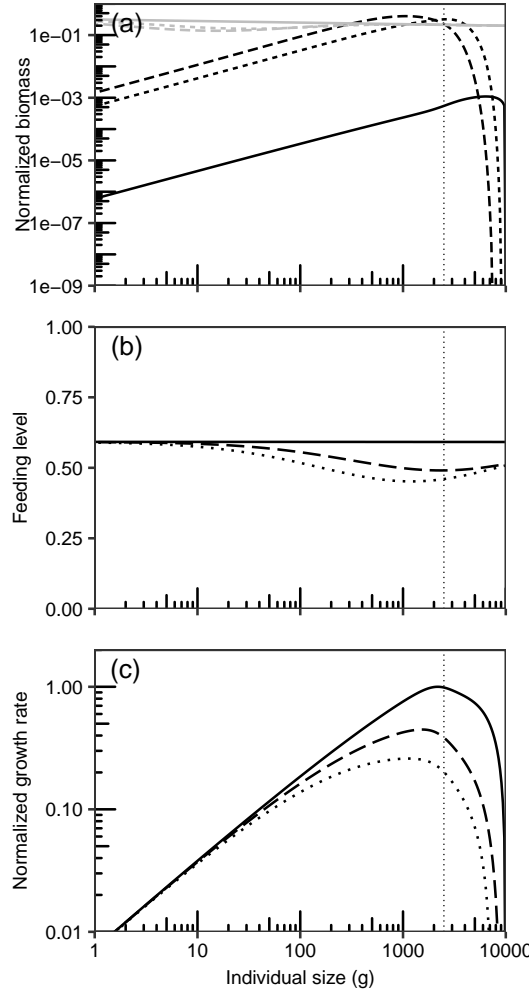


Figure 3.5: The effect of R_{\max}/κ on the emergence of density-dependent growth in a stock (black) that feeds on a dynamic resource (grey), with the values of R_{\max}/κ given as 0.0001 (solid), 0.1 (dashed), and 1000 (dotted). Shown are the biomass of the stock and resource (a), the associated feeding level of the stock (b), and the resulting growth of the stock (c). Here, biomass and growth are normalized to their maximum, and the thin vertical dotted line shows size at 50% maturity. It may be obvious that this figure is largely identical to Figure 3.2. Indeed, the only difference is that Figure 3.2 is displayed with a constant R_{\max} value, whereas this figure is displayed with a constant κ value. Thereby, I hope to have made it clear that the absolute values of R_{\max} and κ are of not important for the density-dependent dynamics of the stock. Rather, it is only their ratio that matters.

R_{\max} is set to 1,000,000 yr^{-1} and κ is set to 10,000,000 $\text{g}^{-1-lambda}$. Only the absolute values of abundance and biomass in the system will be different.

R_{\max}/κ and c

Now, by changing the value of c relative to that of R_{\max}/κ , the relative strengths of density dependence in growth, mortality, and recruitment can be set, which together shape the regime of density dependence that the stock is subject to. Thus, by changing the values of two parameters, the strengths of three different forms of density dependence can be regulated in the model.

A very low or very high value of R_{\max}/κ (when $c = 0$) has the stock regulated completely by density-dependent recruitment or growth (Figure 3.5). However, as long as the value of c does not exceed 1 (signifying an equal preference of stock individuals for conspecifics and heterospecifics), the stock will never be completely regulated by density-dependent mortality, no matter the value of R_{\max}/κ . Instead, when the value of c approaches 1, the effects of density-dependent growth in recruitment and/or growth will be somewhat mediated, but not completely eliminated. Theoretically, the value of c could of course be increased beyond 1, all the way up to infinity. However, this will simply cause the stock to collapse, as at some point individuals from the stock will only consume other individuals from the stock.

Usually, when calculating fisheries advice, an important step is to properly incorporate the stock's various density-dependent dynamics into the calculations. MSY reference points, for instance, are related to the biomass that produces the highest population growth. In a simplified case such as that presented in Figure 3.1, the peak of the curve would be at biomass B_{MSY} , for example. The position of this peak will be influenced by the density-dependent processes outlined above. Thus, properly incorporating density-dependent recruitment, mortality, and growth is crucial for correctly estimating fisheries reference points.

3.7 Density dependence & reference points

Fishing changes the population density of the fish stock, and any given level of fishing mortality will therefore influence the density-dependent processes a stock is normally regulated by. If density dependence were then to be incorrectly incorporated

in reference point calculations, both targets and limits to the fishery would be set incorrectly, resulting in either over- or underfishing of the stock. Therefore, when fisheries advice is calculated, a good portion of time and energy is usually devoted to figuring out how best to incorporate density dependence in the calculations.

When it comes to incorporating density-dependent processes into the calculation of fisheries reference points, the greatest effort, by far, has been invested in correctly trying to estimate the density dependence in recruitment. For this, stock-recruitment relationships are generally the tool-of-choice (Section 3.4). Alternatively, for stocks with a high commercial importance such as North Sea herring (*Clupea harengus*) and cod, extensive survey programs (in this case, the IBTS) are used to directly estimate recruitment through empirical observations.

By making use of a Ricker stock-recruitment relationship (Section 3.4), cannibalism can also be incorporated in the calculation of fisheries reference points. However, this will only incorporate cannibalism in the pre-recruit environment, while recruits can experience cannibalism as well. To incorporating cannibalism of recruits in the calculation of fisheries reference points, the natural mortality of the ages that are vulnerable to cannibalism are usually set to depend in part on the biomass or abundance of larger individuals of the stock. This is, for instance, done with Arctic cod (ICES, 2016).

Density dependence in both recruitment and mortality has been widely incorporated into stock assessments and fisheries reference points calculations. Density-dependent growth, on the other hand, has virtually always been disregarded (Hilborn and Walters, 1992; Rochet, 2000). The most likely reason for this is simple: for as long as we have been actively trying to manage stocks, we have at the same time been overfishing most of them. And since density-dependent growth is expected to predominantly occur among mature (and therefore fished) individuals (Section 3.1), we can make the preliminary conclusion that, in recent history, stocks have been overfished to such an extent that density-dependent growth quite simply has never been a very prominent process. However, with the recent decline in fishing effort in the Northeast Atlantic (Fernandes and Cook, 2013), we can expect to see a biomass recovery of many stocks in these waters. As a result, we can also expect density-dependent growth to become a more prominent process in the regulation of stocks, making it increasingly important to incorporate into the calculation of fisheries reference points.

There are various methods for incorporating density-dependent growth into the calculation of fisheries reference points. Often, a von Bertalanffy growth equation is used to describe individual growth, of which one or more parameter values are made dependent on stock biomass. This is done for instance by Lorenzen and Enberg (2002) and Pastoors et al. (2015), who make the value of asymptotic length L_∞ dependent on total stock biomass, reducing individual growth when stock biomass is high. Such models, however, incorporate density dependence in a descriptive manner, without

incorporating the actual mechanisms behind it. Instead, it can be worthwhile to incorporate density dependence in a mechanistic manner, as the functioning of density-dependent growth can give counter-intuitive results (such as that an increase in fishing mortality increases stock biomass; de Roos et al., 2007), and because the strength of density-dependent growth can vary with individual size.

MSY reference points in the size-structured model

As explained in Section 2.8, MSY reference points in the size-structured model are found by seeing which F value gives the highest long-term sustainable yield. Furthermore, the regime of density-dependent regulation can be set by changing the values of R_{\max}/κ and c (Section 3.6). Thus, how various strengths of density-dependent growth, mortality, and recruitment influence fisheries reference points can be studied by calculating fisheries reference points for a number of different R_{\max}/κ and c values.

Here, using a stock with an asymptotic size W_∞ of 10 kg and setting fishery size-at-entry w_F to 10% of W_∞ , four different MSY reference points are calculated, namely MSY , F_{MSY} , B_{MSY} , and B_{\max} , where B_{\max} is the maximum SSB value of the stock (usually reached when $F = 0$) and thus represents the carrying capacity of the stock. These reference points were calculated for an R_{\max}/κ value ranging from 0.0001 to 1000, and a c value ranging from 0 to 1.

The results show that different regimes of density-dependent regulation result in different values for the analyzed reference points (Figure 3.6). When looking at the reference points related to biomass (MSY , B_{MSY} , and B_{\max}), these appear to decrease in value with an increasing strength of density dependence in growth and mortality. This is to be expected, as both a reduction in growth as well as an increase in mortality will take away from the productivity of the fish stock. However, the really interesting plot is that of F_{MSY} .

The value of F_{MSY} is lowest when there is no density dependence in mortality or growth, and the stock is completely regulated by density-dependent recruitment (Figure 3.6). If the strength of density-dependent growth is increased, through an increase in R_{\max}/κ , the value of F_{MSY} increases as well. This is because, when density-dependent growth is strong, a higher fishing mortality will decrease population density, and thereby increase individual growth, which in turn increases the productivity of the stock. Thus, fish stocks subject to strong density-dependent growth will be able to tolerate higher F values, and will also have a higher F_{MSY} , than fish stocks that are fully regulated by density-dependent recruitment.

In the absence of density-dependent growth, an increase in the strength of density-dependent mortality (a higher c value) also results in a higher F_{MSY} value (Figure

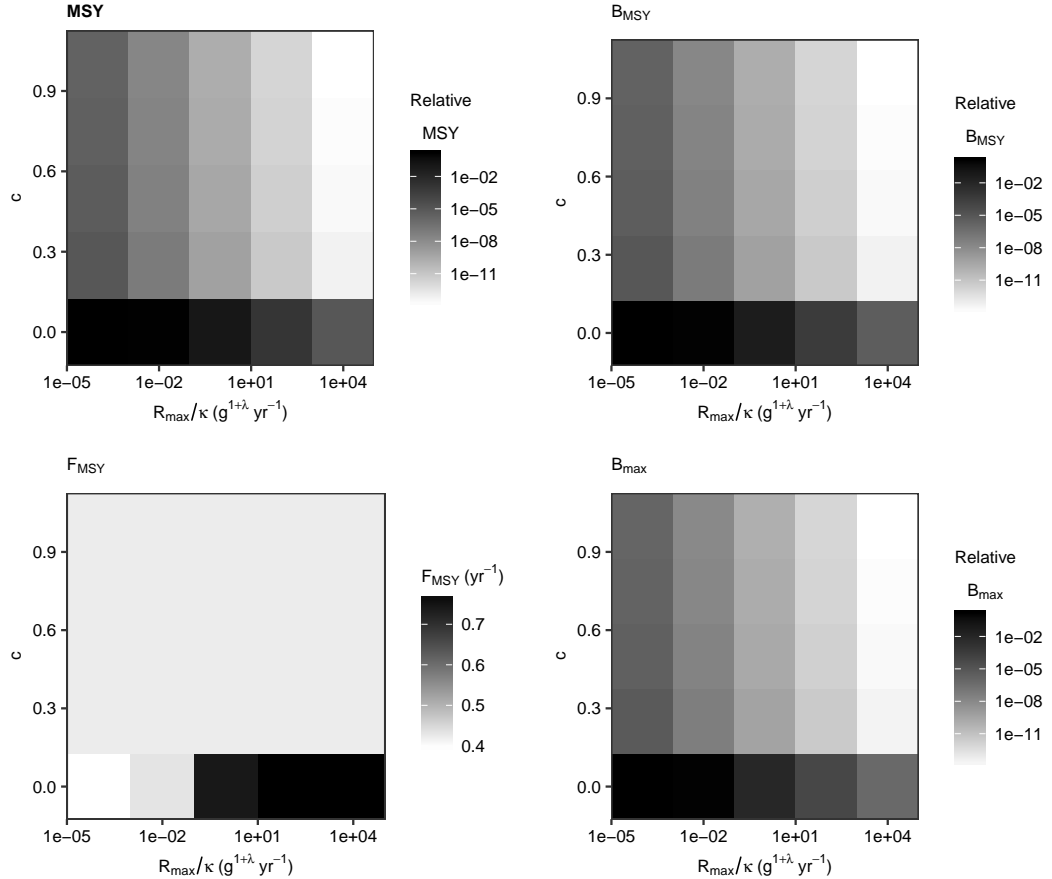


Figure 3.6: MSY reference point values as a function of R_{\max}/κ and c , illustrating how different regimes of density dependence result in different reference point values. Here, B_{MSY} is given in terms of biomass of fish available to the fishery, as determined by the trawl selectivity curve (Eq. 2.20). B_{\max} represents the carrying capacity of the stock, given as the SSB when $F = 0$. Here, the values of MSY, B_{MSY} , and B_{\max} are given relative to their maximum value among all combinations of R_{\max}/κ and c . Shown for a W_{∞} of 10 kg and a w_F of $0.10W_{\infty}$.

3.6). This is because, in the presence of cannibalism, an increased fishing mortality will decrease population density, which in turn decreases predation mortality on the stock. Similar to density-dependent growth therefore, fish stocks subject to strong density-dependent mortality will be able to tolerate somewhat higher F values, and will also have a higher F_{MSY} , than fish stocks that are fully regulated by density-dependent recruitment.

When looking at F_{MSY} , it is also evident that, when density-dependent mortality becomes stronger, this counteracts some of the effects of density-dependent growth (Figure 3.6). This is because an increased predation mortality through cannibalism will decrease population density, thereby decreasing the strength of density-dependent growth. This, in turn, will decrease the capacity of the stock to buffer an increase in fishing mortality, meaning that F_{MSY} will not be as high as when the stock is completely regulated by density-dependent growth.

When a stock's regime of density-dependent regulation is not properly incorporated in the calculation of fisheries reference points, this will lead to an inaccurate estimation of reference points (Figure 3.6). For instance, density-dependent growth is usually disregarded in the calculation of fisheries reference points (Hilborn and Walters, 1992; Rochet, 2000). From Figure 3.6, it is clear that incorrectly disregarding density-dependent growth will lead to an underestimation of F_{MSY} , when the stock is not subject to cannibalism. This underestimation of F_{MSY} will, in turn, lead to an under-exploitation of the stock, where potential yield will be left unharvested. Furthermore, incorrectly disregarding density-dependent growth will also lead to unrealistically-high expectations of yield and stock biomass (see MSY, B_{MSY} , and B_{max} in Figure 3.6). Similar, incorrectly disregarding cannibalism, in the absence of density-dependent growth, will also result in an underestimation of F_{MSY} and overestimation of MSY, B_{MSY} , and B_{max} .

Different sources of density dependence can occur during different life stages. Selectively removing certain life stages from the stock, through size-selective fishing, can therefore also change the dynamics of density-dependent regulation. Thus, when fisheries managers decide on length regulations, such as a minimum landing size, it is important to properly incorporate the effect that this will have on the various forms of density-dependent regulation. The following chapter will discuss the size-selectivity in fisheries, including how density dependence can influence the optimal size at which fish should start to be targeted.

CHAPTER 4

Size-selectivity

All of the world's fisheries harvest with a certain degree of size-selectivity, meaning that fish within a certain size range are more likely to be caught by the fishing gear than fish outside of that size range. This size-selectivity is usually the result of the type of fishing gear used. A trawl gear, for instance, retains all fish above a certain size, with its selectivity curve being described by a sigmoidal relationship (Millar, 1992). The model described in Chapter 2, for instance, makes use of such a trawl selectivity curve (Eq. 2.20). A gillnet, on the other hand, only retains fish around a certain size, and usually results in a bell-shaped selectivity curve (Millar, 1992). In both of these examples, changing the mesh size of the net will result in fish of a different size being caught. Aside from fishing gear, the size-selectivity of a fishery can also be affected by the area fishers choose to fish in, as for many fish stocks different life stages are abundant in different areas. For instance, in the hundreds of years before the 1930s, the Northeast Arctic cod stock could only be fished in Norwegian coastal waters, where only the adults of the stock were present (Law and Grey, 1989). Size-selectivity can also be affected by the time of year at which fishing takes place, both because fish have a different size in different times of the year, but also because many fish migrate resulting that many areas have different size assemblages of fish at different times in the year (Jansen et al., 2012).

The size-selectivity of the fishery will have an impact on the yield obtained from the stock, and on the value of the stock's fisheries reference points. A very straightforward example of this would be that, if every year a fishery were to fish out all fish from an immature year-class, the stock would go extinct in a couple of years, when all juveniles have been fished out and all adults have died due to natural mortality. If, however, every year a fishery were to fish out all fish from a mature year-class that has already spawned once, the stock would be exploited sustainably, and there would be no danger of stock depletion. In such a case, the stock would always be guaranteed of recruitment into the next year.

Only targeting fish that have already spawned once is a fool-proof way of ensuring sustainable exploitation of a fish stock. Furthermore, because cohort biomass often peaks around or after maturity (Figure 3.5), MSY is usually also highest when the

fishery targets only mature fish. As such, most management strategies concerning size-selectivity therefore focus on enforcing regulations that limit the fishing mortality on juvenile fish, such as fishing bans on nursery habitats that mainly contain immature fish (e.g., the plaice box; Beare et al., 2013), or a minimum landing size, among others.

For a long time, the idea that sustainable catch is maximized by fishing only mature individuals has remained a fixed and dominant paradigm, so much so that it is usually considered to be standard fisheries wisdom, and "only a shrinking minority of fools think that increasing fishing pressure on juveniles is smart or sustainable" (Borrell, 2013). English citizens appear to have already been concerned about the effects of overfishing juvenile fish in the 14th century, as evidenced by a petition presented to Parliament in 1376-1377 (Pet. 51, Edw. III, A. D. 1376-'77, Petition No. 50.), in which complaints were made about an early form of the beam trawl:

By means of which instruments called 'wondy chouns' in many places aforesaid, the fishermen aforesaid take so great abundance of small fish aforesaid, that they know not what to do with them, to the great damage of the commons of the kingdom, and the destruction of the fisheries in like places. - Collins (1889)

By 1716, minimum mesh sizes and minimum landing sizes had been imposed for multiple fish stocks in England, to avoid the capture of small fish (Policansky, 1993), and to this day they remain an effective management tool for regulating the size-selectivity of a fishery.

It seems clear that the avoid-catching-juveniles concept is set in stone in fisheries science. However, some cracks have slowly started to appear in this dogma, and several theories have been recently put forth that build a case for why it is not always best to only catch adult fish. Here I discuss two of these theories: balanced harvesting, and strong density-dependent growth.

4.1 Balanced harvesting

The theory of balanced harvesting was proposed by Zhou et al. (2010) and Garcia et al. (2012), stimulated by the increasing call for a more ecosystem-based approach to fisheries management. Advocates of balanced harvesting argue that fishing should be made less selective, both on a species level and on an ecosystem level. Instead of only targeting large fish, balanced harvesting suggests that fish should be targeted proportional to their productivity. Because smaller fish generally have a higher

productivity than larger fish (Brown et al., 2004; Law et al., 2012), this should therefore be achieved with a theoretical selectivity curve that is highest for the youngest and smallest fish, and slopes downward as fish grow in size. It has been proposed that, by implementing balanced harvesting, fisheries yields could be increased (Garcia et al., 2012; Jacobsen et al., 2014; Law et al., 2012), the size-structure within an ecosystem would be better preserved (Jacobsen et al., 2014; Zhou et al., 2010), and ecosystem resilience to overfishing would be increased (Law et al., 2012). However, advocating an increased capture of juvenile fish has not remained without criticism. Froese et al. (2015), for instance, lay out an extensive critique of balanced harvesting, stressing a number of unrealistic assumptions, poor economic returns resulting from increased catches of small low-value fish, and practical difficulties of implementation. It is clear that, as of yet, there is not yet a consensus on the concept of balanced harvesting, and many questions still remain (Burgess et al., 2016). Nevertheless, balanced harvesting has certainly opened up the debate about whether catching juvenile fish is a good thing or not.

4.2 Density-dependent growth

A second theory for why it could be beneficial to start catching fish before they mature is if the population is experiencing strong regulation by density-dependent growth. This can be illustrated using the model described in Chapter 2, and its modes of density-dependent regulation as described in Chapter 3. In the absence of cannibalism, and when the value of R_{\max}/κ is low, density-dependent recruitment dominates over density-dependent growth (Figure 3.5), and MSY is highest when only adult fish are targeted by the fishing gear (Figure 4.1). This result is in line with standard fisheries wisdom, which dictates that yield is maximized when only adults are targeted by the fishery. However, if the value of R_{\max}/κ is increased, density-dependent growth will become stronger (Figure 3.5), reducing the growth rate of adults as well as of juveniles close to maturation. Reducing fishery size-at-entry to below size-at-maturity would then reduce competition for food, increasing the growth rate of older juveniles and adults, and subsequently increasing yield. Thus, when the strength of density-dependent growth is very high, the highest MSY will be obtained by catching juveniles.

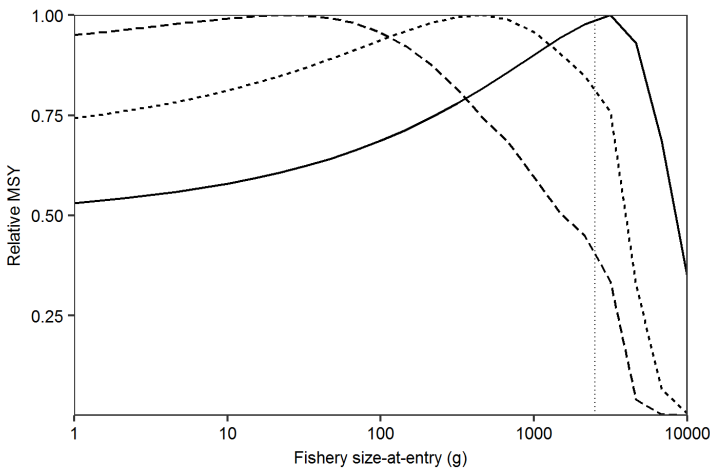


Figure 4.1: MSY as a function of fishery size-at-entry. Shown for a scenario where density-dependent recruitment is dominant (solid, $R_{\max}/\kappa = 0.0001$), a scenario where density-dependent recruitment and density-dependent growth both regulate the stock (dotted, $R_{\max}/\kappa = 0.1$), and a scenario where density-dependent growth dominates (dashed, $R_{\max}/\kappa = 1000$). Each curve is shown relative to its own maximum. $W_\infty = 10000$ g, and $c = 0$.

4.3 Fisheries-induced evolution

Lastly, when the topic of size-selective fisheries is brought up, the topic of fisheries-induced evolution cannot be avoided. The theory of fisheries-induced evolution posits that the act of fishing functions as a selection pressure akin to natural selection. Size-selective fishing distributes this selection pressure over the population in a non-random manner, giving certain phenotypes a higher reproductive output than others, and thus a higher fitness. If parts of those phenotypes are genetically transferred to offspring, then the act of fishing will result in genetic changes to the stock (Law, 2000), and evolution is thus fisheries-induced. The knowledge that fishing applies a selective pressure that can change the traits of a stock has existed for a while already (e.g., Nelson, 1987; Rijnsdorp, 1993; Stokes et al., 1993), and the implications are slowly being made clear.

If both juvenile and adult sizes would be targeted by a fishery, then the risk of mortality would be very high throughout life, and the chances that an individual makes it to a mature size would be low. Thus, mean reproductive output, and therefore fitness, would be highest for individuals that mature as fast as possible, thereby making sure to have reproduced at least once before they are fished out of the population. Targeting both juveniles and adults would therefore result in a selection pressure that favours individuals that mature at an earlier age and at smaller sizes (Ernande et al., 2004;

Jørgensen et al., 2009). This would lower the overall productivity of the stock, as smaller fish produce fewer eggs, making the stock more vulnerable to the effects of fishing. Borrell (2013), for instance, links the collapse of the northern cod stock off the coast of Newfoundland in 1992 to these trait changes.

If only mature sizes would be targeted by a fishery, one of two reactions to this selection pressure can happen, depending on the source of the size-selectivity. If a fishery is only active in a stock's spawning ground, such a spawner fishery will only capture mature fish, irrespective of size. In such a case, it is likely that mature fish will not live longer than a few years, and the odds of reproducing more than once are slim. Thus, lifetime reproductive output would be maximized by waiting as long as possible to mature, reaching as large a size as possible at maturation, and thereby producing as much eggs as possible in the first spawning event. A spawner fishery will therefore favourably select for traits such as a late age- and large size-at-maturity (Jørgensen et al., 2009; Law, 2000). On the other hand, this picture could be different if selectivity is strictly driven by size, for instance in a trawl fishery with mesh size regulations. Then, regardless of maturity, fish above a certain size would be exposed to a high degree of fishing mortality. Even if, initially, this size-selectivity would only target mature fish, the reaction norm can be expected to be the same as if both juvenile and adult sizes would be targeted: lifetime reproductive output would be higher if the fished size would be avoided, and traits such as an earlier age- and smaller size-at-maturation would be selected for (Jørgensen et al., 2009).

If only juvenile sizes were to be targeted by a fishery, for instance through the use of a gillnet, again two reactions to this selection pressure can happen, depending on the intensity of the fishing effort. When fishing effort is very high, it is unlikely that a fish will be able to survive to the size no longer targeted by the fishing gear. Thus, again, the reaction norm can be expected to be the same as for when both juvenile and adult sizes are targeted, and traits such as an earlier age- and smaller size-at-maturation would be selected for (Jørgensen et al., 2009). If, on the other hand, fishing mortality remains below a certain threshold, there is a decent-enough chance for an individual to survive to a size no longer targeted by the fishery. Thus, individual fitness would be highest by maturing late, at a large size with a high fecundity, and traits such as a late age- and large size-at-maturity would be positively selected for (Jørgensen et al., 2009).

By changing the traits of individuals within a stock, fisheries-induced evolution can also slowly change a stock's fisheries reference points (Heino et al., 2013). However, the exact speed at which fisheries-induced evolution acts is expected to be slow, estimated to result at most in a reduction of fisheries yield of 0.7% per year (Andersen and Brander, 2009). Thus, although certainly a concern for the long term, in the short term preventing the collapse of fish stocks from overfishing seems to be a more pressing matter for fisheries management.

CHAPTER 5

The ability of a surplus production model to capture different forms of density dependence

In Chapter 2, I have outlined a size-structured model in which density-dependent growth and mortality emerge due to predator-prey and resource dynamics, and density-dependent recruitment takes place through a stock-recruitment relationship. This is a relatively complex method to describe the density-dependent processes within a stock, but makes sure to capture most of the underlying mechanisms responsible for the emergence of density-dependent regulation. As such, an informative analysis can be made to see how different regimes of density-dependent regulation will influence the fisheries reference points of a stock (Section 3.7).

However, there are also much simpler models that aim to capture all density-dependent processes that a fish stock is subject to. One of these is the surplus production class of models (see Section 1.2.2). Surplus production models use data on catch and biomass to create a so-called surplus production curve, which describes yield that can be sustainably harvested (also called the surplus production of the stock) as a function of stock biomass. This curve looks somewhat like Figure 3.1b, although it need not be symmetric. It is assumed that all density-dependent processes that the stock is subject to are implicitly incorporated in the surplus production curve. Thus, surplus production models implicitly incorporate all forms of density dependence.

One of the major disadvantages of surplus production models is that they need contrast in the catch and biomass data to be able to create a reliable surplus production curve (Ludwig and Walters, 1985). Thus, data is needed from both an underexploited and overexploited state. However, data from a virgin fish stock is rarely available, and most commercially-important stocks have been heavily exploited since before we actively

started collected high-quality data on them. Thus, little data is usually available on the underexploited state of a stock. Furthermore, another disadvantage of surplus production models is that they require long time-series of data for a reliable fit, which is also rarely available.

These two disadvantages, a lack of data from an underexploited state and a lack of sufficiently-long time-series, are slowly being overcome however. In the Northeast Atlantic, fishing mortality on many stocks is being decreased (Fernandes and Cook, 2013), meaning that these stocks can be expected to recover in biomass and thus give us more information on their underexploited state. Furthermore, as monitoring programs such as the IBTS keep collecting data, and as landings of fishers keep being recorded, the length of data time-series continues to increase. Thus, as these disadvantages are being overcome, it can be expected that surplus production models are becoming increasingly attractive to use when calculating reference points and advice for fish stocks.

A biomass recovery due to reduced fishing mortality should result in an increased strength of density-dependent regulation of recruitment, mortality, and growth. Because surplus production models implicitly incorporate all forms of density-dependent regulation, this therefore makes them even more attractive to use in the calculation of fisheries reference points and exploitation advice.

However, even though surplus production models should implicitly incorporate all forms of density-dependent regulation, the question is how well they are actually able to do this. This chapter aims to shed some light on this question. This is done by comparing the reference points predicted by the size-structured model from Chapter 2 with the reference points predicted by the SPiCT surplus production model (Pedersen and Berg, 2017), for a number of different regimes of density dependence. The following represents a work in progress, which may eventually be collected in a separate manuscript and submitted for publication in a scientific journal.

5.1 Methods

Using the size-structured model from Chapter 2, a range of catch and biomass time-series were created for a stock with an asymptotic size W_∞ of 25 kg. These time-series were created with a number of different R_{\max}/κ (3.33E-05, 3.33E-02, and 3.33E+1 $\text{g}^{-1-\lambda} \text{ yr}^{-1}$) and c (0, 0.5, and 1) combinations, representing different strengths of density-dependent growth, mortality, and recruitment (see Section 3.6). Each time-series was created by running the model for 50 years. To ensure good contrast in the data, the model was started in an overexploited steady state ($F = 1.5F_{\text{MSY}}$) and

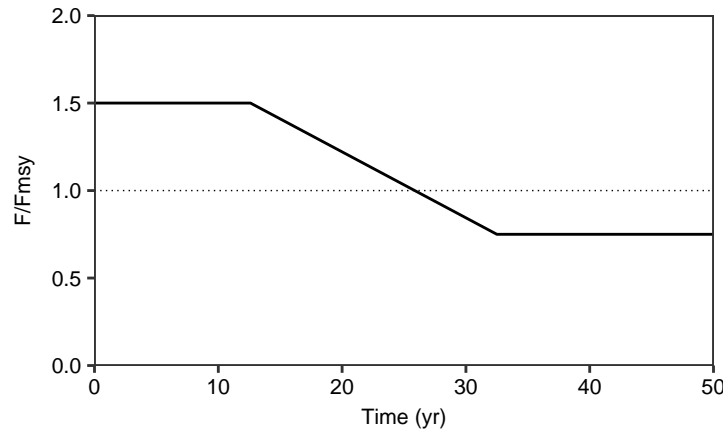


Figure 5.1: Exploitation pattern of the created time-series, where fishing mortality was set relative to the F_{MSY} value of each respective regime of density dependence, to ensure consistency among time-series. The horizontal dotted line indicates F_{MSY} .

run for 13 years, then fishing mortality F was linearly reduced to $0.75F_{MSY}$ over the course of 20 years, and then the model was run with $F = 0.75F_{MSY}$ for the remaining 17 years (Figure 5.1). Here, the mean fishery size-at-entry was set at $0.1W_\infty$. In each year the yield and exploitable biomass of the stock was calculated, together making up the catch and biomass time-series of the stock. Here, exploitable biomass is calculated as biomass that is available to exploitation by the fishery, as determined by the trawl selectivity curve (Eq. 2.20, Chapter 2).

For each combination of R_{max}/κ and c values, MSY reference points were calculated with the size-structured model. To be able to better compare the reference points between the size-structured model and the surplus production model, all reference points are given relative to either the value of F or B in the last data point of the time-series. The calculated reference points were B/B_{MSY} , B/B_{max} , B_{MSY}/B_{max} , and F/F_{MSY} . Here, all biomass terms are given in terms of biomass exploitable by the fishery. B_{max} is the maximum exploitable biomass of the stock at $F = 0$, representing the carrying capacity of the stock.

Then, for each regime of density dependence, the SPiCT surplus production model (Pedersen and Berg, 2017) was fitted to the time-series of catch and biomass. SPiCT is a stochastic surplus production model in continuous time, which is able to include both the error in the catch time-series as well as the error in the biomass time-series in uncertainty estimates. Here, however, I provide it with data without error, because I would first like to see if the model is able to calculate correct reference points using flawless data.

Lastly, for each regime of density dependence, the reference points as predicted by the model are compared to the reference points as predicted by SPiCT. This is done by dividing each reference point predicted by SPiCT, including its 95% confidence interval, by the reference point as calculated by the size-structured model.

5.2 Results & Discussion

In general, Figure 5.2 shows that SPiCT was properly able to fit surplus production curves to the various time-series. As the strength of density-dependent growth increases (left-to-right direction of plots), the peak of the surplus production curve appears to move to a higher B value, relative to the value of B_{max} . This effect is especially pronounced when the stock is fully regulated by density-dependent growth (Figure 5.2, bottom-right).

The results show that the accuracy of biomass reference points predicted by SPiCT varies depending on the regime of density dependence (Figure 5.3). B/B_{MSY} is most accurately calculated, only deviating from the value calculated by the size-structured model when there is no cannibalism and the stock is completely regulated by density-dependent growth (Figure 5.3, bottom-right). Then, B/B_{MSY} is underestimated, meaning that B_{MSY} is likely overestimated. Nevertheless, it appears that SPiCT is able to approximate the value of B_{MSY} fairly well.

The reference points involving B_{max} are almost always overestimated (at most with a factor 6), except when there is no cannibalism and the stock is completely regulated by density-dependent growth (Figure 5.3, bottom-right), and they are underestimated instead. Thus, it appears that SPiCT has difficulty estimating the value of B_{max} here, usually underestimating it (as B/B_{max} and $B_{\text{MSY}}/B_{\text{max}}$ are mostly overestimated). The value of F/F_{MSY} appears to be universally underestimated by SPiCT with about the same degree of error, regardless of mode of density dependence (Figure 5.3). This likely suggests that SPiCT consistently overestimates the value of F_{MSY} .

These results suggest that the accuracy of reference points calculated by SPiCT changes with differences in density-dependent regulation, meaning that surplus production models do not always implicitly incorporate all forms of density dependence equally well. This is important to consider when using surplus production models to calculate fisheries reference points. Furthermore, the apparent consistent overestimation of F_{MSY} is also important to take into consideration, as setting the F_{MSY} of a stock too high will lead to an increased risk of overexploitation and stock collapse.

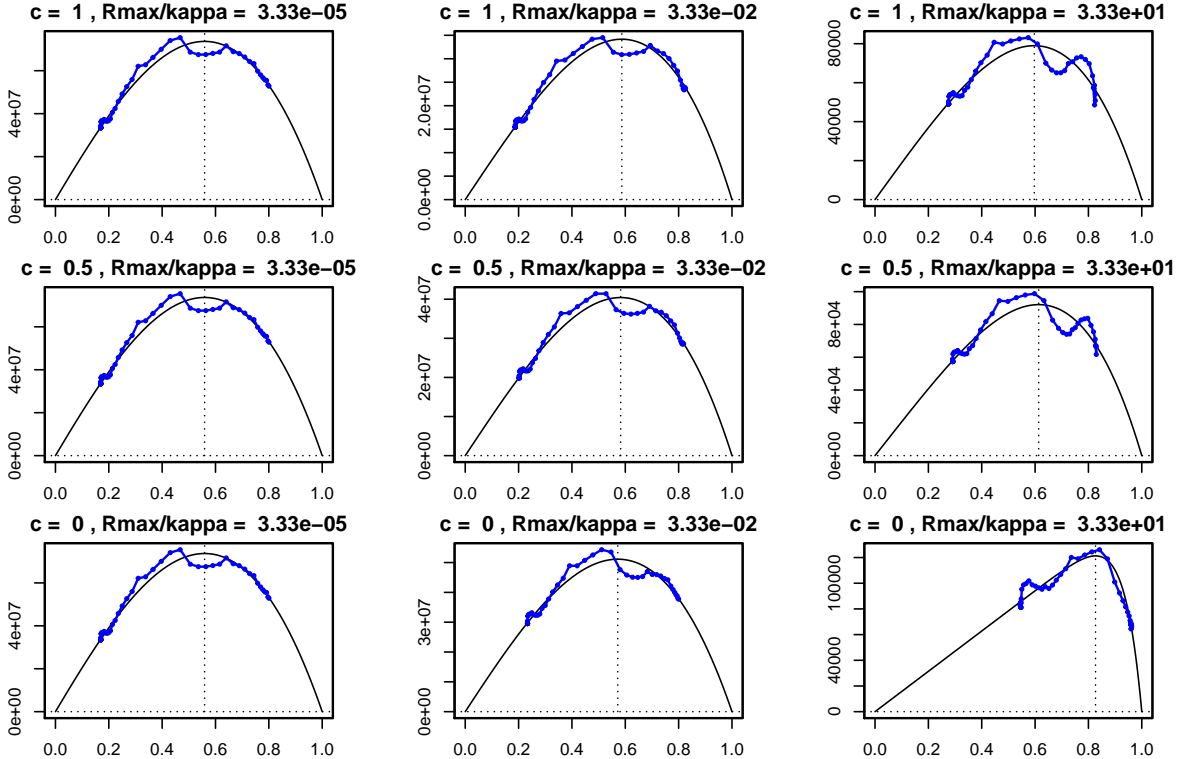


Figure 5.2: Surplus-production curves (black), as fitted by SPiCT to the data from the various regimes of density dependence (blue). The x-axes shows B relative to B_{\max} , as estimated by SPiCT, and the y-axes shows surplus production. The value of R_{\max}/κ , and thereby the strength of density-dependent growth, increases from left to right. The value of c , and thereby the strength of density-dependent mortality, increases from bottom to top. The thin vertical dotted line indicates at which B/B_{\max} value SPiCT estimates the peak of the surplus production curve to be.

These differences in the accuracy of calculated reference points appear to emerge more clearly when the strength of density-dependent growth increases, compared to when the strength of density-dependent mortality increases. This appears to result from density-dependent growth having a greater influence than density-dependent mortality on the shape of the fitted surplus production curve (Figure 5.2).

The recent reduction in fishing mortality for many previously-overfished stocks in the Northeast Atlantic ((Fernandes and Cook, 2013)) means that a recovery of adult biomass can be expected for those stocks. This recovery will likely create more contrast in the biomass time-series of many stocks, which should make surplus production models increasingly attractive for calculating the reference points of these stocks. However, this recovery could also make density-dependent growth and mortality more

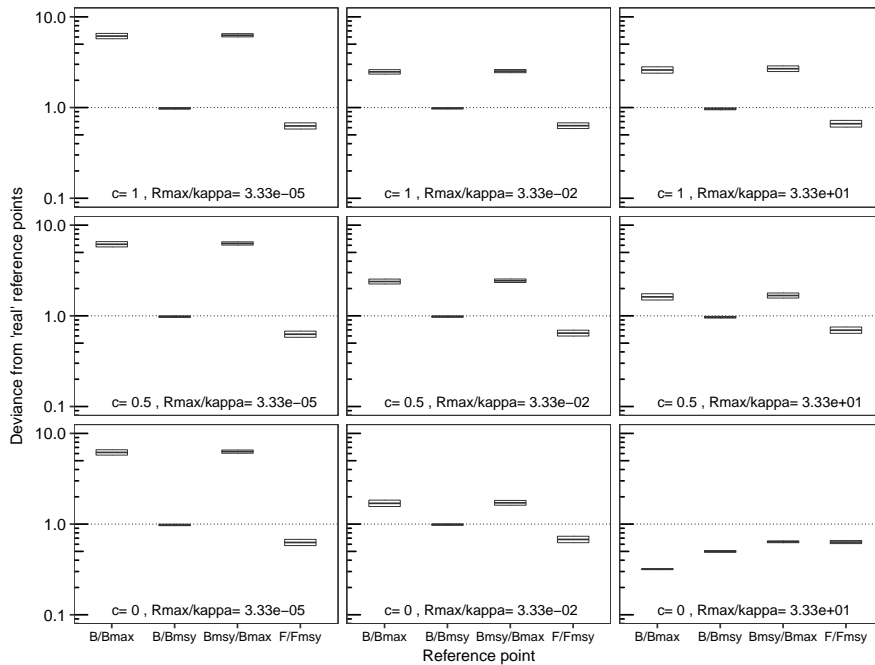


Figure 5.3: Fisheries reference point values as predicted by SPiCT, divided by their 'real' values as calculated by the size-structured model. Shown for different regimes of density dependence, as determined by the values of R_{\max}/κ and c . The value of R_{\max}/κ , and thereby the strength of density-dependent growth, increases from left to right. The value of c , and thereby the strength of density-dependent mortality, increases from bottom to top. The displayed reference points are B/B_{\max} , B/B_{MSY} , B_{MSY}/B_{\max} , and F/F_{MSY} , where the value of F and B are given by their last data point in the time-series, and all biomass terms are given as biomass available to the fishery as determined by a trawl selectivity curve with a mean size-at-entry of $0.1W_{\infty}$.

prominent processes. Based on the results of this study, it appears that reference points predicted by surplus production models could be different in their accuracy, depending on the regime of density-dependent regulation. Thus, surplus production models are not always equally capable at implicitly incorporating all density-dependent processes in the stock, which should be kept in mind when considering their use for calculating fisheries reference points.

The results of this study were generated from a single F exploitation pattern. This exploitation pattern was set to move from a pattern of overfishing to a pattern of underfishing (Figure 5.1), so that the resulting time-series would have a good contrast in the data. Nevertheless, it is likely that the accuracy of the calculated reference points will change if a different exploitation pattern is used. Thus, the consistent overestimation of F_{MSY} and underestimation of B_{\max} that was found here may not

appear when other exploitation patterns are used. Furthermore, the results of this study are specific to the SPiCT surplus production model, and using a different surplus production model may change the accuracy of the predicted reference points.

In this study, it was decided to apply no process noise nor observation noise to the data, to observe how the surplus production model would perform with perfectly clean data. However, the SPiCT surplus production model was specifically designed to be able to incorporate process and observation noise in both catch and biomass data. Thus, a next step would be to see how these results compare to a model setup which includes process and observation noise in the catch and biomass time-series.

CHAPTER 6

Filling in the gaps

There remain many gaps in the knowledge of how to achieve a maximum sustainable exploitation of fish stocks. The aim of this thesis is to contribute to this issue, particularly by focusing on density-dependent growth and size-selectivity. Here, I illustrate how the main body of this thesis, consisting of 3 papers, contributes to this issue.

Paper I

Challenges to fisheries advice and management due to stock recovery

In spite of the recent decline in fishing effort on many Northeast Atlantic fish stocks (Fernandes and Cook, 2013), little to no biomass recovery has been noticed, especially among stocks of larger-bodied fish such as cod (Hutchings, 2000). A recovery in biomass of large-bodied fish would have multiple consequences for the ecological dynamics of both the stock and ecosystem. On top of this, because almost all advice calculations and management approaches have been devised and optimized during a period of overexploitation, a biomass recovery of large-bodied stocks will raise the question of whether these advice calculations and management approaches will still be optimal for the maximum sustainable management of recovered stocks. This paper therefore aims to examine whether or not stocks of large-bodied fish are recovering in the Northeast Atlantic, and what the consequences of such a recovery would be for the advice calculations and management of those stocks.

Stock recovery is examined by extracting SSB time series data as well as the MSY B_{trigger} reference point of 25 stocks, each with a maximum length > 1 metre, from the ICES database. For each stock, the annual ratio of SSB to MSY B_{trigger} is calculated, where MSY B_{trigger} is a reference points that indicates the lower bound of the biomass range in which the stock is expected to fluctuate when exploited at F_{MSY} . Averaging this annual ratio over all 25 stocks shows that average SSB to MSY B_{trigger} ratio is increasing in recent years. Additionally, summed-up SSB of the 25 examined stocks is increasing as well in recent years. Thus, there are clear indications that large-bodied fish stocks are recovering in the Northeast Atlantic.

A recovery of large-bodied stock biomass means that the strength of density-dependent regulation will increase for those stocks. Density-dependent recruitment and mortality are usually fairly well-incorporated into the calculation of fisheries advice, but the same cannot be said for density-dependent growth. Thus, next, this paper aims to investigate the consequences of ignoring density-dependent growth when calculating fisheries advice, when in actuality it is an important process regulating a recovered stock. For this, an adaptation of the model used by Lorenzen and Enberg (2002) is used. The results show that ignoring density-dependent growth could lead to an overestimation of yield and SSB from a recovered stock, leading to unrealistic recovery expectations, and to an underestimation of F_{MSY} , resulting in underexploitation of the stock.

Aside from single-stock consequences, a recovery of large-bodied fish stocks will also have consequences for the community those stocks are part of. To examine this, a community size-spectrum model is used to compare a scenario of overfishing of large-bodied stocks to a scenario where those stocks are recovered. The results show that while large-bodied stocks are overfished, smaller forage fish stocks experience a great increase in biomass, following typical trophic cascade dynamics. Consequently, a recovery in large-bodied fish stocks results in a decrease in SSB of forage fish stocks, reversing the trophic cascade. The implications of this are twofold. Firstly, reference points of stocks should be frequently recalculated, also referred to as the dynamic calculation of reference points. After all, the increased natural mortality of forage fish stocks will their F_{MSY} reference point. If exploitation advice for the forage fish stocks were set with the older and higher F_{MSY} values, those stocks would risk overexploitation and collapse. Secondly, there exists a conflict between the fishers of forage fish and the fishers of large-bodied fish. The latter are obviously happy with the recovery of large-bodied stocks, but the former should prefer to see a state of depleted large-bodied stocks, as this increases the productivity of forage fish stocks. Thus, this conflict should be acknowledged, and a desired ecosystem exploitation state should be decided upon. It is important that this involves stakeholder participation, to prevent non-compliance.

Paper II

Implications of late-in-life density-dependent growth for fishery size-at-entry leading to maximum sustainable yield

When the strength of density-dependent growth increases compared to the strength of density-dependent recruitment, the fishery size-at-entry at which MSY is highest will decrease. However, the question remains whether, in practice, density-dependent growth in marine fish stocks can actually be strong enough to reduce optimal fishery size-at-entry to below size-at-maturity. To examine this, a single-stock size-structured model such as that developed in Chapter 2 is fitted to growth data of three separate

marine stocks that have shown signs of density-dependent growth in the past: Baltic sprat, Northeast Atlantic mackerel, and North Sea plaice. By varying the ratio of R_{\max} to κ , the relative strength of density dependence in recruitment and growth is changed, allowing for the closest match of the growth curve, SSB, and yield data to be identified. Thus, an approximation is made of the strength of density-dependent growth that is regulating each stock. Subsequently, for each stock, the fishery size-at-entry that will yield the highest MSY is identified. The results show that, for none of the three examined stocks, density-dependent growth appears to be strong enough to justify a fishery size-at-entry smaller than the stock's respective size-at-maturity. Moreover, for Northeast Atlantic mackerel, the model appears to suggest the observed change in growth was not due to density-dependent growth at all, or at least not the form of density-dependent growth incorporated in the model. Thus, the results of this study give support to the idea that minimum catch sizes should be set so that only adults are targeted by the fishery, even in the presence of density-dependent growth.

Paper III

Density dependence dampens the impact of a non-constant gonado-somatic index

Female fecundity, which is the number of eggs produced by a female fish, is generally assumed to scale isometrically with female size, for instance by the assumption of a constant gonadosomatic index (Gunderson, 1997; Roff, 1983). In other words, the number of eggs produced per unit of female weight is usually assumed to remain constant. However, this may not always be the case, and a recent meta-analysis suggests that fecundity predominantly scales hyperallometrically with female size, or in other words, that the number of eggs produced per unit of female weight increases with female size (Barneche et al., 2018). This could have major implications for the calculation of fisheries advice, including reference points. However, Andersen et al. (2019) contest the findings of Barneche et al. (2018), but use an analysis for this which is limited in scope to a single stock. Therefore, the aim of this paper is to investigate the relationship between female size and fecundity in more detail, and see whether it truly matters for the reproductive output of the stock.

Using the data provided by Barneche et al. (2018), this article fits both an isometric and power law relationship to stock-specific data on size-specific fecundity. The results show variation in the type of relationship that best fits the data. For some stocks an isometric relationship best describes the data, for others a hyperallometric relationship fits best, and for a few stocks a hypoallometric relationship (fecundity decreases with an increase in individual weight) fits best. Furthermore, there is also variability among stocks of the same species. For some species, there was little difference among stocks in the fit to size-specific fecundity (e.g., the different stocks of sole), whereas other species displayed noticeable variability among their stocks in the fitted relationship between fecundity and size (e.g., cod). This raises questions on the origin of the relationship

between size and fecundity. A consistent relationship among stocks of the same species would suggest some kind of life-history adaptation as the responsible mechanism, emerging through an individual's physiology. On the other hand, variation in the relationship between size and fecundity among stocks of the same species would suggest that this relationship likely originates due to variability in the feeding environment of the stock, emerging through an individual's available energy for reproduction. More research is needed to reach a clear consensus on this, and it is possible that both mechanisms play a role. Regardless, the results of this study suggest that there is no clear dominant relationship between size and female fecundity, but rather that the type of relationship is variable both among species as well as between stocks of some species.

Next, to find out what the impact of either an isometric or power law relationship would be on stock reproductive output, a simple age-structured population model was built and run for each stock. Stock-specific parameter values were obtained from Thorson et al. (2017), and for each stock the model was run with the fitted isometric as well as with the fitted power law relationship between fecundity and female size. Subsequently, for both fits, the cumulative egg production, as well as recruitment to the stock, was compared. This was done both for a fished and unfished scenario. What was found was that, in an unfished scenario, stock egg production generally differed little between the isometric and power law relationship between fecundity and female size. On the other hand, for the fished scenario, the egg production of the stock was often markedly lower for the power law relationship than for the isometric relationship. However, when accounting for early-life density dependence through the use of a stock-recruitment relationship, there was no difference in stock recruitment between the isometric and power law relationship, neither for the unfished nor the fished scenario.

Thus, the conclusions of this paper are two-fold. Firstly, whether or not fecundity scales isometrically or according to a power law with female size appears to be stock-specific, without a clear general preference for one of the two. Secondly, the relationship between size and fecundity generally matters little for recruitment to the stock, except when overfishing results in a weakening of early-life density dependence. Thus, for a stock that is being exploited at a level consistent with obtaining MSY, not incorporating a hyperallometric relationship between fecundity and female size when in fact there is a significant relationship should have little implications for the exploitation of the stock.

CHAPTER 7

Conclusion and future perspectives

Density-dependent growth is rarely incorporated into the calculation of fisheries reference points, possibly because overfishing resulted in few stocks having an adult biomass high enough to result in an emergence of density-dependent growth. However, there are now signs of recovery among previously-overfished large-bodied stocks (van Gemert and Andersen, 2018a), likely making density-dependent growth a more prominent process in the future. By outlining how density-dependent growth may affect fisheries reference points, this thesis provides an important contribution to the pursuit of achieving a maximum sustainable exploitation of fish stocks.

In this thesis, I asked how the inclusion of density-dependent processes, with density-dependent growth in particular, can improve upon the calculation of fisheries reference points. Therefore, my co-authors and I examined how density-dependent growth can influence the value of fisheries reference points (van Gemert and Andersen, 2018a), we studied how early-life density dependence influences the importance of the relationship between female size and fecundity, and we looked at the performance of a surplus production model under various regimes of density dependence. Additionally, I asked at which minimum catch size MSY can be obtained, and how this varies with different forms of density-dependent regulation. We therefore estimated the strength of density-dependent growth for a number of fish stocks, and explored whether it is strong enough to reduce optimal fishery size-at-entry to a juvenile size (van Gemert and Andersen, 2018b).

We showed that failing to account for density-dependent growth when it is an important process will result in a misestimation of fisheries reference points, overestimating MSY and B_{MSY} while underestimating F_{MSY} (van Gemert and Andersen, 2018a). Additionally, we showed how a recovery of large-bodied stocks results in community changes, and outlined the possible consequences for fisheries advice and management (van Gemert and Andersen, 2018a). Furthermore, we showed that the strength of density-dependent growth currently observed in several fish stocks is not high enough

to warrant the capture of juveniles, and MSY is obtained when a fishery only targets adults (van Gemert and Andersen, 2018b). We also showed that the type of relationship between fecundity and female size may affect stock egg production, but that density-dependent recruitment usually ensures that it matters little for recruitment to the stock, and therefore probably does not affect the value of target reference points. Lastly, we show how a surplus production model may not always implicitly incorporate all density-dependent processes equally well when calculating reference points.

Based on the findings of this thesis, several points of advice can be given to improve upon the calculation of fisheries reference points. First of all, given the apparent potential for density-dependent growth to influence fisheries reference points, a greater focus should be put on trying to identify cases of density-dependent growth in marine fish. Next, when a stock is suspected to experience density-dependent growth, the potential effects of this on the stock's reference points should be calculated. Furthermore, when the strength of density-dependent growth is found to be very high, it may be worthwhile to examine how this influences the optimal size-selectivity of the stock, especially for a large-bodied stock. Lastly, when a surplus production model is used to incorporate density-dependent growth into the calculation of fisheries reference points, it should be kept in mind that such a model does not always implicitly incorporate all forms of density dependence equally well, and that therefore the estimated reference points may not be entirely accurate.

This thesis illustrates the importance of incorporating all forms of density dependence, with density-dependent growth in particular, into the calculation of fisheries reference points and size-selectivity regulations. How this can best be done, however, should be further investigated. Efforts of including density-dependent growth in the calculation of fisheries advice have already been undertaken by Pastoors et al. (2015), for instance, but better methods may be found. Furthermore, it is difficult to predict exactly how widespread the presence of density-dependent growth will become in recovered fish stocks. Likely, this will simply become a matter of waiting to see for which stocks density-dependent growth will emerge as an important regulatory process. If stock recovery leads to more stocks being regulated by density-dependent growth, this will also yield more data with which the effect of density-dependent growth on optimal fishery size-at-entry can be re-evaluated.

This thesis has largely examined density dependence from a single-stock perspective. Thus, a next step would be to see how the results of this thesis hold up in a multi-species model setting. For this, the size-structured model that has mainly been used in this thesis can be expanded to a community model, as is for instance shown by Andersen et al. (2016). Furthermore, such a community model can also be used to examine density-dependent dynamics between different populations in the community. We have already briefly examined such interspecific density dependence, and highlighted some of its implications for the management of fish stocks (van Gemert and Andersen, 2018a). However, much work can still be done on this subject, and new insights in the

functioning of interspecific density dependence could greatly improve community-based management approaches, such as ecosystem-based fisheries management (Pikitch et al., 2004).

It is my hope that this thesis will be able to contribute to achieving a maximum sustainable exploitation of fish stocks, thereby helping to feed a growing world population, while preventing fish stock collapse. Much work remains to be done in the pursuit of this goal, but I am confident that, slowly but surely, we are moving in the right direction.

CHAPTER 8

References

- Alheit, J. (1987). Egg cannibalism versus egg predation: their significance in anchovies. *South African Journal of Marine Science*, 5(1):467–470.
- Allee, W. C. (1931). *Animal aggregations*. University of Chicago Press, Chicago.
- Allee, W. C. (1938). *The social life of animals*. William Heinemann, London.
- Andersen, K. H. (2019). *Fish ecology, evolution, and exploitation: The size- and trait-based approach*. Manuscript in preparation.
- Andersen, K. H. and Beyer, J. E. (2006). Asymptotic size determines species abundance in the marine size spectrum. *The American Naturalist*, 168(1):54–61.
- Andersen, K. H. and Beyer, J. E. (2015). Size structure, not metabolic scaling rules, determines fisheries reference points. *Fish and Fisheries*, 16(1):1–22.
- Andersen, K. H. and Brander, K. (2009). Expected rate of fisheries-induced evolution is slow. *Proceedings of the National Academy of Sciences*, <https://doi.org/10.1073/pnas.0901690106>.
- Andersen, K. H., Jacobsen, N. S., and Farnsworth, K. D. (2016). The theoretical foundations for size spectrum models of fish communities. *Canadian Journal of Fisheries and Aquatic Sciences*, 73(4):575–588.
- Andersen, K. H., Jacobsen, N. S., Jansen, T., and Beyer, J. E. (2017). When in life does density dependence occur in fish populations? *Fish and Fisheries*, 18(4):656–667.
- Andersen, K. H., Jacobsen, N. S., and van Denderen, P. D. (2019). Limited impact of big fish mothers for population replenishment. *Canadian Journal of Fisheries and Aquatic Sciences*, <https://doi.org/10.1139/cjfas-2018-0354>.
- Armstrong, J. B. and Schindler, D. E. (2011). Excess digestive capacity in predators reflects a life of feast and famine. *Nature*, 476(7358):84.
- Arnott, S. A. and Ruxton, G. D. (2002). Sandeel recruitment in the North Sea: demographic, climatic and trophic effects. *Marine Ecology Progress Series*, 238:199–210.
- Barneche, D. R., Robertson, D. R., White, C. R., and Marshall, D. J. (2018). Fish reproductive-energy output increases disproportionately with body size. *Science*, 360(6389):642–645.

- Baumann, H., Hinrichsen, H. H., Möllmann, C., Köster, F. W., Malzahn, A. M., and Temming, A. (2006). Recruitment variability in Baltic Sea sprat (*Sprattus sprattus*) is tightly coupled to temperature and transport patterns affecting the larval and early juvenile stages. *Canadian Journal of Fisheries and Aquatic Sciences*, 63(10):2191–2201.
- Beare, D., Rijnsdorp, A. D., Blaesberg, M., Damm, U., Egekvist, J., Fock, H., Kloppmann, M., Röckmann, C., Schroeder, A., and Schulze, T. (2013). Evaluating the effect of fishery closures: lessons learnt from the Plaice Box. *Journal of Sea Research*, 84:49–60.
- Berkes, F. (1985). Fishermen and ‘the tragedy of the commons’. *Environmental conservation*, 12(3):199–206.
- Beverton, R. J. H. and Holt, S. J. (1957). *On the Dynamics of Exploited Fish Populations*. Her Majesty’s Stationery Office, London.
- Beverton, R. J. H. and Iles, T. C. (1992). Mortality rates of 0-group plaice (*Platessa platessa* L.), dab (*Limanda limanda* L.) and turbot (*Scophthalmus maximus* L.) in European waters: III. Density dependence of mortality rates of 0-group plaice and some demographic implications. *Netherlands Journal of Sea Research*, 29(1-3):61–79.
- Bogstad, B., Lilly, G. R., Mehl, S., Palsson, O. K., and Stefánsson, G. (1994). Cannibalism and year-class strength in Atlantic cod (*Gadus morhua* L.) in Arcto-boreal ecosystems (Barents Sea, Iceland, and eastern Newfoundland). *ICES Marine Science Symposia*, 198:576–599.
- Borrell, B. (2013). A big fight over little fish. *Nature*, 493(7434):597.
- Brown, J. H., Gillooly, J. F., Allen, A. P., Savage, V. M., and West, G. B. (2004). Toward a metabolic theory of ecology. *Ecology*, 85(7):1771–1789.
- Burgess, M. G., Diekert, F. K., Jacobsen, N. S., Andersen, K. H., and Gaines, S. D. (2016). Remaining questions in the case for balanced harvesting. *Fish and Fisheries*, 17(4):1216–1226.
- Chu, C. (2009). Thirty years later: the global growth of ITQs and their influence on stock status in marine fisheries. *Fish and Fisheries*, 10(2):217–230.
- Colby, P. J. and Nepszy, S. J. (1981). Variation among stocks of walleye (*Stizostedion vitreum vitreum*): management implications. *Canadian Journal of Fisheries and Aquatic Sciences*, 38(12):1814–1831.
- Collins, J. W. (1889). *The beam-trawl fishery of Great Britain: with notes on beam-trawling in other European countries*. US Government Printing Office, Washington DC.
- Cushing, D. H. (1973). Dependence of recruitment on parent stock. *Journal of the Fisheries Board of Canada*, 30(12):1965–1976.
- Damsgird, B. and Dill, L. M. (1998). Risk-taking behavior in weight-compensating coho salmon, *Oncorhynchus kisutch*. *Behavioral Ecology*, 9(1):26–32.
- De Leo, G. A. and Gatto, M. (1996). Trends in vital rates of the European eel: evidence for density dependence? *Ecological Applications*, 6(4):1281–1294.

- de Roos, A. M., Schellekens, T., van Kooten, T., van de Wolfshaar, K., Claessen, D., and Persson, L. (2007). Food-dependent growth leads to overcompensation in stage-specific biomass when mortality increases: the influence of maturation versus reproduction regulation. *The American Naturalist*, 170(3):E59–E76.
- Deriso, R. B. (1982). Relationship of fishing mortality to natural mortality and growth at the level of maximum sustainable yield. *Canadian Journal of Fisheries and Aquatic Sciences*, 39(7):1054–1058.
- Eero, M. (2012). Reconstructing the population dynamics of sprat (*Sprattus sprattus balticus*) in the Baltic Sea in the 20th century. *ICES Journal of Marine Science*, 69(6):1010–1018.
- Eigaard, O. R., van Deurs, M., Behrens, J. W., Bekkevold, D., Brander, K., Plambech, M., Plet-Hansen, K. S., and Mosegaard, H. (2014). Prey or predator—expanding the food web role of sandeel *Ammodytes marinus*. *Marine Ecology Progress Series*, 516:267–273.
- Engelhard, G. H., Lynam, C. P., Garcia-Carreras, B., Dolder, P. J., and Mackinson, S. (2015). Effort reduction and the large fish indicator: spatial trends reveal positive impacts of recent European fleet reduction schemes. *Environmental Conservation*, 42(3):227–236.
- Ernande, B., Dieckmann, U., and Heino, M. (2004). Adaptive changes in harvested populations: plasticity and evolution of age and size at maturation. *Proceedings of the Royal Society of London B: Biological Sciences*, 271(1537):415–423.
- European Commission (2003). Commission Regulation (EC) No. 2244/2003 of 18 December 2003 laying down detailed provisions regarding satellite-based Vessel Monitoring Systems. *Official Journal of the European Union*, 333:17–27.
- European Commission (2013). Regulation (EU) No 1380/2013 of the European Parliament and of the Council of 11 December 2013 on the Common Fisheries Policy, amending Council Regulations (EC) No 1954/2003 and (EC) No 1224/2009 and repealing Council Regulations (EC) No 2371/2002. *Official Journal of the European Union*, 354:22–61.
- European Commission (2016). Report from the Commission to the European Parliament and the Council on Member States' efforts during 2014 to achieve a sustainable balance between fishing capacity and fishing opportunities, 10 June 2016, Brussels, Belgium. 52016DC0380.
- FAO (2018). *The State of World Fisheries and Aquaculture 2018 - Meeting the sustainable development goals*. Food & Agriculture Organization of the United Nations, Rome.
- Fenchel, T. (1974). Intrinsic rate of natural increase: the relationship with body size. *Oecologia*, 14(4):317–326.
- Fernandes, P. G. and Cook, R. M. (2013). Reversal of fish stock decline in the Northeast Atlantic. *Current Biology*, 23(15):1432–1437.
- Fox Jr, W. W. (1970). An exponential surplus-yield model for optimizing exploited fish populations. *Transactions of the American Fisheries Society*, 99(1):80–88.
- Froese, R., Walters, C., Pauly, D., Winker, H., Weyl, O. L. F., Demirel, N., Tsikliras, A. C., and Holt, S. J. (2015). A critique of the balanced harvesting approach to fishing. *ICES Journal of Marine Science*, 73(6):1640–1650.

- Fukushima, M., Quinn, T. J., and Smoker, W. W. (1998). Estimation of eggs lost from superimposed pink salmon (*Oncorhynchus gorbuscha*) redds. *Canadian Journal of Fisheries and Aquatic Sciences*, 55(3):618–625.
- Garcia, S. M., Kolding, J., Rice, J., Rochet, M.-J., Zhou, S., Arimoto, T., Beyer, J. E., Borges, L., Bundy, A., and Dunn, D. (2012). Reconsidering the consequences of selective fisheries. *Science*, 335(6072):1045–1047.
- Godfray, H. C. J., Beddington, J. R., Crute, I. R., Haddad, L., Lawrence, D., Muir, J. F., Pretty, J., Robinson, S., Thomas, S. M., and Toulmin, C. (2010). Food security: the challenge of feeding 9 billion people. *science*, 327(5967):812–818.
- Graham, M. (1935). Modern theory of exploiting a fishery, and application to North Sea trawling. *ICES Journal of Marine Science*, 10(3):264–274.
- Grand, T. C. and Dill, L. M. (1999). The effect of group size on the foraging behaviour of juvenile coho salmon: reduction of predation risk or increased competition? *Animal Behaviour*, 58(2):443–451.
- Gunderson, D. R. (1997). Trade-off between reproductive effort and adult survival in oviparous and viviparous fishes. *Canadian Journal of Fisheries and Aquatic Sciences*, 54(5):990–998.
- Hardin, G. (1968). The tragedy of the commons. *Science*, 162(3859):1243–1248.
- Hartvig, M., Andersen, K. H., and Beyer, J. E. (2011). Food web framework for size-structured populations. *Journal of Theoretical Biology*, 272(1):113–122.
- Heino, M., Baulier, L., Boukal, D. S., Ernande, B., Johnston, F. D., Mollet, F. M., Pardoe, H., Therkildsen, N. O., Uusi-Heikkilä, S., and Vainikka, A. (2013). Can fisheries-induced evolution shift reference points for fisheries management? *ICES Journal of Marine Science*, 70(4):707–721.
- Henderson, B. A., Wong, J. L., and Nepszy, S. J. (1996). Reproduction of walleye in Lake Erie: allocation of energy. *Canadian Journal of Fisheries and Aquatic Sciences*, 53(1):127–133.
- Hilborn, R. and Walters, C. J. (1992). *Quantitative fisheries stock assessment: choice, dynamics and uncertainty*. Chapman and Hall, New York, USA.
- Holling, C. S. (1959a). Some characteristics of simple types of predation and parasitism. *The Canadian Entomologist*, 91(7):385–398.
- Holling, C. S. (1959b). The Components of Predation as Revealed by a Study of Small-Mammal Predation of the European Pine Sawfly. *The Canadian Entomologist*, 91(5):293–320.
- Hutchings, J. A. (2000). Collapse and recovery of marine fishes. *Nature*, 406(6798):882–885.
- ICES (2015). Report of the Workshop to consider FMSY ranges for stocks in ICES categories 1 and 2 in Western Waters (WKMSYREF4), 13–16 October 2015, Brest, France. ICES CM 2015/ACOM:58. 185 pp.
- ICES (2016). Report of the Arctic Fisheries Working Group (AFWG), 19–25 April 2017, Copenhagen, Denmark. ICES CM 2017/ACOM:06. 493 pp.

- ICES (2018). Report of the Working Group on the Assessment of Demersal Stocks in the North Sea and Skagerrak (WGNSSK), 24 April - 3 May 2018, Oostende, Belgium. ICES CM 2018/ACOM:22. 1250 pp.
- Jacobsen, N. S., Gislason, H., and Andersen, K. H. (2014). The consequences of balanced harvesting of fish communities. *Proceedings of the Royal Society of London B: Biological Sciences*, 281(1775):20132701.
- Jansen, T., Campbell, A., Kelly, C., Hatun, H., and Payne, M. R. (2012). Migration and fisheries of North East Atlantic Mackerel (*Scomber scombrus*) in autumn and winter. *PLoS One*, 7(12):e51541.
- Jennings, S., Warr, K. J., and Mackinson, S. (2002). Use of size-based production and stable isotope analyses to predict trophic transfer efficiencies and predator-prey body mass ratios in food webs. *Marine Ecology Progress Series*, 240:11–20.
- Jørgensen, C., Ernande, B., and Fiksen, Ø. (2009). Size-selective fishing gear and life history evolution in the Northeast Arctic cod. *Evolutionary applications*, 2(3):356–370.
- Kitchell, J. F., Stewart, D. J., and Weininger, D. (1977). Applications of a bioenergetics model to yellow perch (*Perca flavescens*) and walleye (*Stizostedion vitreum vitreum*). *Journal of the Fisheries Board of Canada*, 34(10):1922–1935.
- Kleiber, M. (1932). Body size and metabolism. *Hilgardia*, 6(11):315–353.
- Köster, F. W., Möllmann, C., Neuenfeldt, S., Vinther, M., St John, M. A., Tomkiewicz, J., Voss, R., Hinrichsen, H.-H., Kraus, G., and Schnack, D. (2003). Fish stock development in the Central Baltic Sea (1976-2000) in relation to variability in the environment. In *ICES Marine Science Symposia*, volume 219, pages 294–306. ICES.
- Larkin, P. A. (1977). An epitaph for the concept of maximum sustained yield. *Transactions of the American fisheries society*, 106(1):1–11.
- Law, R. (2000). Fishing, selection, and phenotypic evolution. *ICES Journal of Marine Science*, 57(3):659–668.
- Law, R. and Grey, D. R. (1989). Evolution of yields from populations with age-specific cropping. *Evolutionary Ecology*, 3(4):343–359.
- Law, R., Plank, M. J., and Kolding, J. (2012). On balanced exploitation of marine ecosystems: results from dynamic size spectra. *ICES Journal of Marine Science*, 69(4):602–614.
- Liermann, M. and Hilborn, R. (1997). Depensation in fish stocks: a hierachic Bayesian meta-analysis. *Canadian Journal of Fisheries and Aquatic Sciences*, 54(9):1976–1984.
- Lorenzen, K. and Enberg, K. (2002). Density-dependent growth as a key mechanism in the regulation of fish populations: evidence from among-population comparisons. *Proceedings of the Royal Society of London B: Biological Sciences*, 269(1486):49–54.
- Ludwig, D. and Walters, C. J. (1985). Are age-structured models appropriate for catch-effort data? *Canadian Journal of Fisheries and Aquatic Sciences*, 42(6):1066–1072.

- Mace, P. M. (1994). Relationships between common biological reference points used as thresholds and targets of fisheries management strategies. *Canadian Journal of Fisheries and Aquatic Sciences*, 51(1):110–122.
- MacKenzie, B. R. and Köster, F. W. (2004). Fish production and climate: sprat in the Baltic Sea. *Ecology*, 85(3):784–794.
- Margetts, A. R. and Holt, S. J. (1948). The effect of the 1939–1945 war on the English North Sea trawl fisheries. *Rapports et procès-verbaux des réunions: Conseil permanent international pour l'exploration de la mer.*, 122:26–46.
- Marshall, C. T. and Frank, K. T. (1999). Implications of density-dependent juvenile growth for compensatory recruitment regulation of haddock. *Canadian Journal of Fisheries and Aquatic Sciences*, 56(3):356–363.
- McIntosh, W. C. (1919). The Fisheries and the International Council. *Nature*, 103:355–358.
- Millar, R. B. (1992). Estimating the size-selectivity of fishing gear by conditioning on the total catch. *Journal of the American Statistical Association*, 87(420):962–968.
- Myers, R. A. and Cadigan, N. G. (1993). Density-dependent juvenile mortality in marine demersal fish. *Canadian Journal of Fisheries and Aquatic Sciences*, 50(8):1576–1590.
- Myers, R. A. and Worm, B. (2003). Rapid worldwide depletion of predatory fish communities. *Nature*, 423(6937):280.
- Nelson, K. (1987). Genetical conservation of exploited fishes. *Population genetics and fishery management*, pages 345–368.
- Neuheimer, A. B., Hartvig, M., Heuschele, J., Hylander, S., Kiørboe, T., Olsson, K. H., Sainmont, J., and Andersen, K. H. (2015). Adult and offspring size in the ocean over 17 orders of magnitude follows two life history strategies. *Ecology*, 96(12):3303–3311.
- Pastoors, M., Brunel, T., Skagen, D., Utne, K. R., Enberg, K., and Sparrevohn, C. R. (2015). Mackerel growth, the density dependent hypothesis and implications for the configuration of MSE simulations: Results of an ad-hoc workshop in Bergen, 13–14 August 2015. *Working Document to ICES Working Group on Widely Distributed Stocks (WGWHITE), 25–31 August 2015, AZTI-Tecnalia, Pasaia, Spain*.
- Pastoors, M. A. (2016). Stakeholder participation in the development of management strategies. In Edwards, C. T. T. and Dankel, D. J., editors, *Management Science in Fisheries: An Introduction to Simulation-based Methods*, chapter 20, pages 409–422. Routledge.
- Pedersen, M. W. and Berg, C. W. (2017). A stochastic surplus production model in continuous time. *Fish and Fisheries*, 18(2):226–243.
- Pella, J. J. and Tomlinson, P. K. (1969). A generalized stock production model. *Inter-American Tropical Tuna Commission Bulletin*, 13(3):416–497.
- Pikitch, E., Santora, C., Babcock, E. A., Bakun, A., Bonfil, R., Conover, D. O., Dayton, P., Doukakis, P., Fluharty, D., Heneman, B., Houde, E. D., Link, J., Livingston, P. A., Mangel, M., McAllister, M. K., Pope, J., and Sainsbury, K. J. (2004). Ecosystem-based fishery management. *Science*, 305(5682):346–347.

- Pitcher, T. J., Magurran, A. E., and Winfield, I. J. (1982). Fish in larger shoals find food faster. *Behavioral Ecology and Sociobiology*, 10(2):149–151.
- Policansky, D. (1993). Fishing as a cause of evolution in fishes. In *The exploitation of evolving resources*, pages 1–18. Springer-Verlag, Berlin.
- Punt, A. E. (1993). The use of spawner-biomass-per-recruit in the management of linefisheries. *Special Publication of the Oceanographic Research Institute, Durban*, 2:80–89.
- Punt, A. E. and Smith, T. (2001). The gospel of maximum sustainable yield in fisheries management: birth, crucifixion and reincarnation. In Reynolds, J., Mace, G., Redford, K., and Robinson, J., editors, *Conservation of exploited species*, pages 41–66. Cambridge University Press, Cambridge, UK.
- Ranta, E. and Kaitala, V. (1991). School size affects individual feeding success in three-spined sticklebacks (*Gasterosteus aculeatus* L.). *Journal of Fish Biology*, 39(5):733–737.
- Ricker, W. E. (1954). Stock and Recruitment. *Journal of the Fisheries Research Board of Canada*, 11(5):559–623.
- Rijnsdorp, A. D. (1993). Fisheries as a large-scale experiment on life-history evolution: disentangling phenotypic and genetic effects in changes in maturation and reproduction of North Sea plaice, *Pleuronectes platessa* L. *Oecologia*, 96(3):391–401.
- Rijnsdorp, A. D. and Van Leeuwen, P. I. (1992). Density-dependent and independent changes in somatic growth of female North Sea plaice *Pleuronectes platessa* between 1930 and 1985 as revealed by back-calculation of otoliths. *Marine Ecology Progress Series*, 88(1):19–32.
- Rochet, M.-J. (2000). Does the concept of spawning per recruit make sense? *ICES Journal of Marine Science*, 57(4):1160–1174.
- Roff, D. A. (1983). An allocation model of growth and reproduction in fish. *Canadian Journal of Fisheries and Aquatic Sciences*, 40(9):1395–1404.
- Rose, K. a., Cowan, J. H., Winemiller, K. O., Myers, R. a., and Hilborn, R. (2001). Compensatory density dependence in fish populations: Importance, controversy, understanding and prognosis. *Fish and Fisheries*, 2(4):293–327.
- Russell, E. S. (1931). Some theoretical considerations on the “overfishing” problem. *ICES Journal of Marine Science*, 6(1):3–20.
- Savage, V. M., Gillooly, J. F., Brown, J. H., West, G. B., and Charnov, E. L. (2004). Effects of body size and temperature on population growth. *The American Naturalist*, 163(3):429–441.
- Schaefer, M. (1954). Some aspects of the dynamics of populations important to the management of the commercial marine fisheries. *Bulletin of Inter-American Tropical Tuna Commission*, 53(1):25–56.
- Sheldon, R. W., Prakash, A., and Sutcliffe Jr, W. (1972). The size distribution of particles in the ocean. *Limnology and oceanography*, 17(3):327–340.

- Steele, D. H., Andersen, R., and Green, J. M. (1992). The managed commercial annihilation of northern cod. *Newfoundland and Labrador Studies*, 8(1).
- Stokes, T. K., McGlade, J. M., and Law, R. (1993). *The Exploitation of Evolving Resources: Proceedings of an International Conference, Held at Jülich, Germany, September 3–5, 1991*, volume 99. Springer-Verslag, Berlin.
- Thorson, J. T., Munch, S. B., Cope, J. M., and Gao, J. (2017). Predicting life history parameters for all fishes worldwide. *Ecological Applications*, 27(8):2262–2276.
- Ursin, E. (1982). Stability and variability in the marine ecosystem. *Dana*, 2:51–67.
- van der Sleen, P., Stransky, C., Morrongiello, J. R., Haslob, H., Peharda, M., and Black, B. A. (2018). Otolith increments in European plaice (*Pleuronectes platessa*) reveal temperature and density-dependent effects on growth. *ICES Journal of Marine Science*, 75(5):1655–1663.
- van Gemert, R. and Andersen, K. H. (2018a). Challenges to fisheries advice and management due to stock recovery. *ICES Journal of Marine Science*, 75(6):1864–1870.
- van Gemert, R. and Andersen, K. H. (2018b). Implications of late-in-life density-dependent growth for fishery size-at-entry leading to maximum sustainable yield. *ICES Journal of Marine Science*, 75(4):1296–1305.
- Walters, C. and Kitchell, J. F. (2001). Cultivation/depensation effects on juvenile survival and recruitment: implications for the theory of fishing. *Canadian Journal of Fisheries and Aquatic Sciences*, 58(1):39–50.
- Walters, C. J. (1987). Nonstationarity of production relationships in exploited populations. *Canadian Journal of Fisheries and Aquatic Sciences*, 44(S2):s156–s165.
- Walters, C. J. and Juanes, F. (1993). Recruitment limitation as a consequence of natural selection for use of restricted feeding habitats and predation risk taking by juvenile fishes. *Canadian Journal of Fisheries and Aquatic Sciences*, 50(10):2058–2070.
- West, G. B., Brown, J. H., and Enquist, B. J. (1997). A general model for the origin of allometric scaling laws in biology. *Science*, 276(5309):122–126.
- Wyatt, T. (1972). Some effects of food density on the growth and behaviour of plaice larvae. *Marine Biology*, 14(3):210–216.
- Ylikarjula, J., Heino, M., and Dieckmann, U. (1999). Ecology and adaptation of stunted growth in fish. *Evolutionary Ecology*, 13(5):433–453.
- Zhou, S., Smith, A. D. M., Punt, A. E., Richardson, A. J., Gibbs, M., Fulton, E. A., Pascoe, S., Bulman, C., Bayliss, P., and Sainsbury, K. (2010). Ecosystem-based fisheries management requires a change to the selective fishing philosophy. *Proceedings of the National Academy of Sciences*, <https://doi.org/10.1073/pnas.0912771107>.
- Zimmermann, F., Ricard, D., and Heino, M. (2018). Density regulation in Northeast Atlantic fish populations: Density dependence is stronger in recruitment than in somatic growth. *Journal of Animal Ecology*, 87(3):672–681.

CHAPTER 9

Paper I

Challenges to fisheries advice and
management due to stock recovery

van Gemert, R. and Andersen, K. H.

ICES Journal of Marine Science

2018

75(6), 1864–1870

ICES Journal of Marine Science (2018), 75(6), 1864–1870. doi:10.1093/icesjms/fsy084

Food for Thought

Challenges to fisheries advice and management due to stock recovery

Rob van Gemert^{1,*} and Ken H. Andersen¹

¹Centre for Ocean Life, National Institute of Aquatic Resources (DTU-Aqua), Technical University of Denmark, Kemitorvet, Building 202, 2800 Kgs. Lyngby, Denmark

*Corresponding author: e-mail: rvge@aqua.dtu.dk.

van Gemert, R. and Andersen, K. H. Challenges to fisheries advice and management due to stock recovery. – ICES Journal of Marine Science, 75: 1864–1870.

Received 5 January 2018; revised 25 April 2018; accepted 7 June 2018; advance access publication 8 August 2018.

During the 20th century, many large-bodied fish stocks suffered from unsustainable fishing pressure. Now, signs of recovery are appearing among previously overfished large-bodied fish stocks. This new situation raises the question of whether current fisheries advice and management procedures, which were devised and optimized for depleted stocks, are well-suited for the management of recovered stocks. We highlight two challenges for fisheries advice and management: First, recovered stocks are more likely to show density-dependent growth. We show how the appearance of density-dependent growth will make reference points calculated with current procedures inaccurate. Optimal exploitation of recovered large-bodied fish stocks will therefore require accounting for density-dependent growth. Second, we show how a biomass increase of large-bodied piscivorous fish will lead to a reverse trophic cascade, where their increased predation mortality on forage fish reduces forage fish productivity and abundance. The resulting decrease in maximum sustainable yield of forage fish stocks could lead to conflicts between forage and large-piscivore fisheries. Avoiding such conflicts requires that choices are made between the exploitation of interacting fish stocks. Failure to account for the changed ecological state of recovered stocks risks creating new obstacles to sustainable fisheries management.

Keywords: density dependence, ecosystem-based management, fisheries management, stock recovery

Introduction

The 20th century saw the decline of many fish stocks due to the effects of overfishing. In an attempt to counteract this decline, a great number of measures have since been taken to make fishing more sustainable and prevent future stock collapse. Widespread survey programmes have been set up that provide a wealth of data for scientific advice (e.g. the European Union's Data Collection Framework), there is an increasing focus on sustainable exploitation in management tools (e.g. harvest control rules) and strategies (e.g. landing obligations), and there is an increasing cooperation between science and industry (e.g. [Pastoors, 2016](#)) meant to build trust and integrate the knowledge of fishers and scientists to the benefit of fisheries science and management ([Kaplan and McCay, 2004](#); [Hartley and Robertson, 2008](#)). Due to

these and other factors, an increasing percentage of ICES-assessed stocks have had their exploitation rate reduced to a more sustainable level ([Fernandes and Cook, 2013](#)). This decrease in exploitation rate should result in the recovery of many previously overfished stocks.

For stocks of small forage fish, a biomass recovery would be expected to occur rapidly after fishing mortality is reduced, due to their short generation time. Especially clupeids adhere to this expectation ([Hutchings, 2000](#)), aided by them being often targeted by pelagic gear that leaves their habitat intact ([Hutchings and Reynolds, 2004](#)).

It takes a longer time for large-bodied fish stocks to recover. We here define large-bodied fish as those whose adult life stages do not rely mainly on planktivory. Large-bodied fish generally

have a longer generation time, slowing their recovery. Furthermore, they may be caught up by changes in the ecosystem that impede recovery, either through competition (Bundy and Fanning, 2005; Van Leeuwen *et al.*, 2008) or predation (Trzcinski *et al.*, 2006; Cook *et al.*, 2015), with gadoid stocks as a notable example (Hutchings, 2000; Shelton *et al.*, 2006). Despite these challenges, we will provide an indication that large-bodied fish stocks are starting to recover, at least in the Northeast Atlantic waters.

Almost all advice calculations and management approaches have been devised while large-bodied fish stocks were overexploited, begging the question of whether they will still work optimally when those stocks are recovered. Density-dependent growth, for instance, is almost always disregarded when calculating target reference points (e.g. Hilborn and Walters, 1992; Rochet, 2000), but an increase in stock biomass may well make density-dependent reductions in growth more common among large-bodied fish stocks. For example, the absence of fishing during the Second World War led to recovery of several North Sea fish stocks, which resulted in slower growth rates (Margetts and Holt, 1948; Rijnsdorp and Van Leeuwen, 1992). Furthermore, a recovery of large-bodied stocks could trigger far-reaching community responses in the form of reverse trophic cascades, where an increased predator biomass leads to lower prey biomass. This may be especially problematic if it affects commercially valuable prey species such as forage fish.

Against this background we ask whether fisheries management, and its advisory bodies, are fully prepared for a recovery of large-bodied fish stocks. We address this question in three separate sections, each with its own methodology, results, and discussion. In the first section, we show that stocks of large-bodied fish in the Northeast Atlantic are starting to recover. In the second section, we argue how an increase in stock biomass will make these stocks more susceptible to density-dependent adult growth and show what this will mean for the calculation of target reference points. In the third section, we show how a recovery of large-bodied piscivorous fish stocks can affect the marine community, and what this would mean for the fisheries that exploit this community. We conclude by summarizing the challenges that stock recovery presents to current fisheries advice and management and suggesting preparatory measures.

Stock recovery

In 2000, Hutchings offered a grim prospect of little to no recovery amongst stocks of large marine fish. Myers and Worm (2003) followed up by concluding that the biomass of large predatory fish stocks had been reduced with 90% when compared with pre-industrial levels. More recently, Fernandes and Cook (2013) provided us with more positive outlook for stock recovery in the Northeast Atlantic, although they mainly looked at levels of exploitation rather than biomass. Here we use spawning stock biomass (SSB) data from ICES assessments, to look for signs of recovery among stocks of large-bodied fish in the Northeast Atlantic.

To compare recovery between stocks, each stock's SSB data needs to be normalized to a suitable biomass reference. We use the maximum sustainable yield (MSY) B_{trigger} reference point as a reference. MSY B_{trigger} is used by ICES to indicate the lower bound of the biomass range within which a stock exploited at F_{MSY} naturally fluctuates (ICES, 2016a). Ideally, MSY B_{trigger} would be calculated based on an SSB time-series during which the stock was consistently exploited at F_{MSY} . However, because many stocks have not been exploited at F_{MSY} long enough for such a time-series to exist, MSY B_{trigger} is often simply set equal

to the B_{pa} reference point (e.g. cod in the North Sea, eastern English Channel, and Skagerrak: ICES, 2017b). Nevertheless, the MSY B_{trigger} reference point is a useful baseline to compare stock recovery to. We used SSB data from all stocks where ICES has determined the MSY B_{trigger} reference point (as used in the year 2016), which have an SSB time-series that goes back to the year 1995, and which have a maximum length of 100 cm or greater according to Fishbase (Froese and Pauly, 2000; Boettiger *et al.*, 2012). This left us with 25 time-series of SSB/ B_{trigger} (Supplementary Appendix S1). For each year from 1995 to 2016, we then took the mean across all 25 stocks. The trend of this mean indicates whether, on average, large-bodied fish stocks are recovering in the Northeast Atlantic.

Stocks of large-bodied fish have indeed begun to recover in the Northeast Atlantic (Figure 1). The mean SSB/ B_{trigger} of the 25 stocks we examined shows an upward trend, after having reached its lowest levels around the year 2000 (Figure 1a). The same can be said for the summed-up SSB of all stocks (Figure 1b), illustrating that it is not just the scarcer stocks that are recovering. Examples of recovery are North Sea cod (*Gadus morhua*), North Sea plaice (*Pleuronectes platessa*), and Northern hake *Merluccius merluccius* (Figure 1c–e). Note that excluding these three stocks from the overall mean does not change the pattern in Figure 1a and b (Supplementary Appendix S1).

Reduced fishing pressure is not necessarily the sole cause of the observed biomass recoveries of large-bodied stocks. Examining in detail how different processes have affected stock recovery is, however, outside of the scope of this work. Suffice it to say, there are clear signs that both the mean and summed-up SSB of large-bodied fish stocks within the Northeast Atlantic waters have increased in recent years. This increase in large predator biomass will have consequences for the recovering stocks themselves, the marine ecosystems containing these stocks, and the fisheries exploiting those marine ecosystems.

Density dependence

Increased stock biomass will lead to stronger density-dependent processes. Generally speaking, density dependence influences three vital rates: reproduction, growth, and mortality. Density dependence within reproduction is usually incorporated in fisheries advice through the use of stock–recruitment relationships. Similarly, density-dependent mortality can also be incorporated in stock–recruitment relationships, if it takes place in the pre-recruit life stage. Cannibalism can for instance be incorporated by a Ricker stock–recruitment relationship, or by changing natural mortality according to stock size, which is for example done for Arctic cod (ICES, 2016b). We can therefore expect that, in future advice, density-dependent changes in recruitment and mortality that arise due to changes in stock biomass will be described fairly well. The same cannot be said about density dependence in growth.

In the past decades, most large-bodied commercial stocks had a biomass that was too low for a noticeable density-dependent growth effect. Nevertheless, increasing evidence shows that marine fish can experience density-dependent growth not only in the pre-recruit phase but also as older juveniles and adults (e.g. Lorenzen and Enberg, 2002; Cormon *et al.*, 2016; Zimmermann *et al.*, in press). In adult North Sea plaice for instance, van der Sleen *et al.* (in press) observed both a significant effect of density on growth, and a growth decrease overlapping with the biomass recovery in Figure 1d. Similarly, ICES (2018) finds a negative relationship between biomass and weight-at-age not only for adult

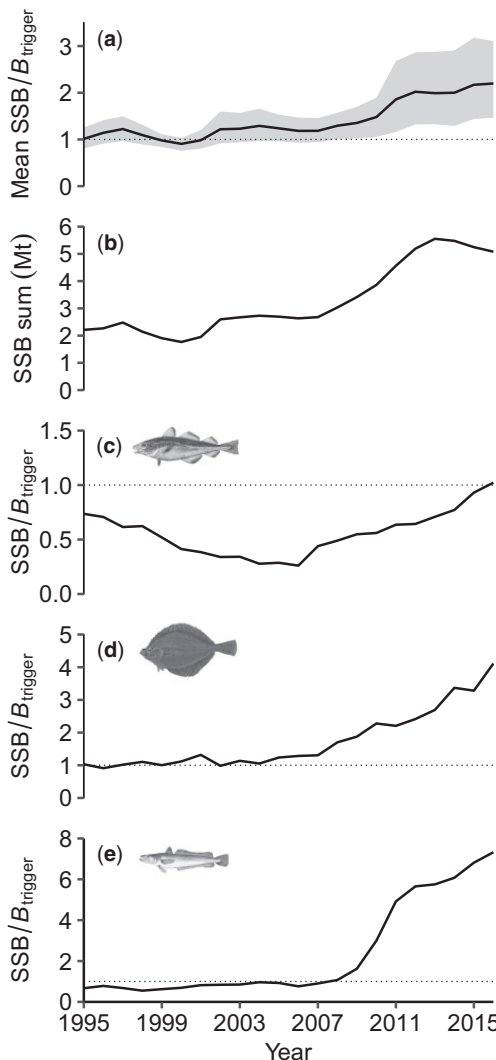


Figure 1. Recovery of large-bodied stocks in the Northeast Atlantic. The thin dotted lines show the MSY B_{trigger} reference point, as determined by ICES in 2016. Note that the scales on the y-axes vary. (a) Mean $\text{SSB}/B_{\text{trigger}}$ of all 25 examined stocks. The grey area shows the 95% confidence interval of the mean, as calculated by a non-parametric bootstrap with 1000 samples. (b) Summed-up SSB of all 25 examined stocks. (c) $\text{SSB}/B_{\text{trigger}}$ of cod (*G. morhua*) in the North Sea, Eastern English Channel, and Skagerrak. (d) $\text{SSB}/B_{\text{trigger}}$ of plaice (*P. platessa*) in the North Sea. (e) $\text{SSB}/B_{\text{trigger}}$ of hake (*M. merluccius*), Northern stock.

North Sea plaice, but also for adult North Sea dab (*Limanda limanda*) and adult Georges Bank haddock (*Melanogrammus aeglefinus*). With stocks of large-bodied fish starting to recover, it is therefore likely that density-dependent growth will become a more prominent process within large-bodied fish stocks, and it

should thus be considered when calculating fisheries advice. Density-dependent growth is partly covered by current advice when changes in observed weight-at-age are used to update reference points. However, the process of density-dependent growth is rarely included directly in the calculation of reference points.

We illustrate how density-dependent growth can influence an exploited stock's yield, biomass, and asymptotic length, by using a population model that is based on Lorenzen and Enberg (2002). The model introduces density-dependent growth into the von Bertalanffy growth equation through a dependency of asymptotic length $L_{\infty B}$ on the total stock biomass B :

$$L_{\infty B} = L_{\infty L} - gB \quad (1)$$

where $L_{\infty L}$ is asymptotic length for $B = 0$ (i.e. without density dependence), and g is a coefficient that determines the reduction in asymptotic length per unit of population biomass (Lorenzen and Enberg, 2002). The other model equations are standard: recruitment is described with a Beverton-Holt stock-recruitment relationship, natural mortality decreases with individual size, and fishing mortality F follows a trawl-selectivity curve (Supplementary Appendix S2). For the coefficient $g = 0$, no density-dependent growth takes place and the model therefore corresponds to a standard age-based fish demographic model.

We show how density-dependent growth can affect the way a fish stock recovers from overfishing, and how this influences both MSY and the fishing mortality and stock biomass at which MSY is obtained (F_{MSY} and B_{MSY} , respectively). We do this by running the model with a range of F values for four stocks with identical parameter settings (Supplementary Appendix S2), except for their value of g .

Density-dependent growth can influence how a stock recovers from overfishing. After fishing mortality is lowered, stocks that experience stronger density-dependent growth (higher value of g) will not have as great of an increase in yield and stock biomass as stocks that experience weaker density-dependent growth (Figure 2a and b). This is because the increased stock biomass reduces $L_{\infty B}$ (Figure 2c), which in turn slows individual growth, impairing a further increase of stock biomass.

Furthermore, stocks that experience stronger density-dependent growth will have a higher F_{MSY} , while MSY and B_{MSY} will be lower. This increase in F_{MSY} is not an unexpected result. An increase in fishing mortality will reduce stock biomass, thereby increasing $L_{\infty B}$ which in turn will increase individual growth, which increases biomass productivity.

Based on the results from Figure 2, two important consequences of ignoring density-dependent growth in recovering stocks can be identified. First of all, the expected increase in yield and stock biomass that results from reducing fishing mortality may be overestimated. This will lead to unrealistic expectations of recovery and could prevent recognition of when a stock has fully recovered from overfishing. Second, F_{MSY} may be underestimated. If F_{MSY} is set too low, the yield of the fishery will be below MSY, and the fishery will therefore lose out on potential yield. Such an underestimation of F_{MSY} has for instance already been reported for Baltic sprat (Horbowy and Luzeńczyk, 2017).

Figure 2 also provides insight into why, up until now, density-dependent growth has been little observed in marine stocks. The differences among stock B , yield, and $L_{\infty B}$ are small while stocks are overexploited, even though the value of g greatly varies between the modelled stocks. This shows that observations from a

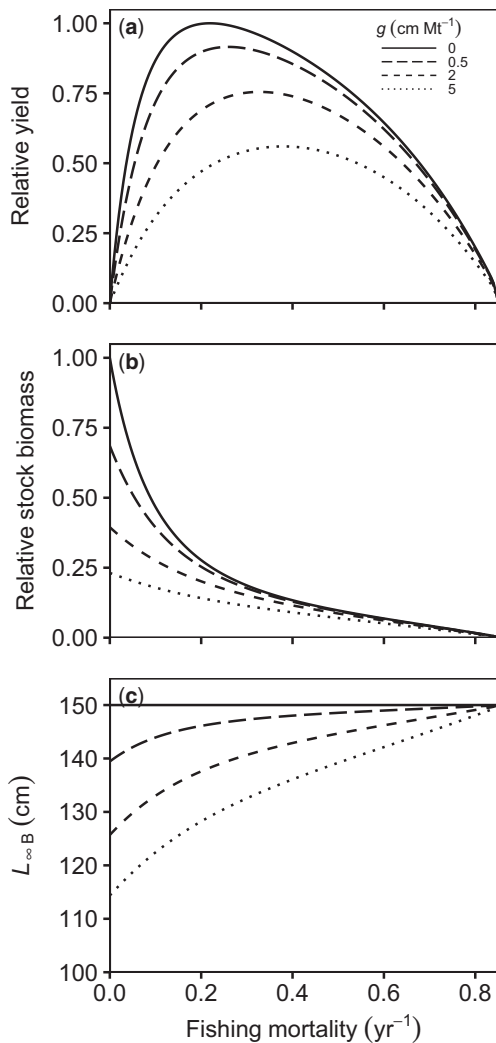


Figure 2. The influence of density-dependent growth strength g on yield (a), total stock biomass (b), and asymptotic length (c), as a function of fishing mortality F . Yield and stock biomass are displayed relative to their maximum. Four stocks are shown that experience different strengths of density-dependent growth g but are identical in all other parameters. It is clear that a higher strength of density-dependent growth results in a higher F_{MSY} , while resulting in a lower MSY and B_{MSY} . This is because density-dependent growth slows individual growth at a high stock biomass, which impedes the recovery of stock biomass as fishing mortality is decreased.

past overfished state are a poor basis for making assumptions on whether or not recovered stocks will experience density-dependent growth.

How, then, can we identify which stocks are susceptible to density-dependent growth, and to what extent? The magnitude of density-dependent growth will likely be highly stock-specific (see,

e.g. Lorenzen and Enberg, 2002; van Gemert and Andersen, 2018; Zimmermann *et al.*, in press). Therefore, for most stocks we will simply have to wait for recovery to see whether density-dependent growth is observed. Nevertheless, we can expect that stocks with a larger asymptotic size will be more susceptible to density-dependent growth than those with a small asymptotic size, due to the former's higher degree of density-dependent regulation in total (Andersen and Beyer, 2015; Andersen *et al.*, 2017). This does not mean that the occurrence of density-dependent growth is limited to only large-bodied stocks, as indicated by, e.g. Northeast Atlantic mackerel (Olafsdottir *et al.*, 2016) and Baltic sprat (Eero, 2012). The existence of density-dependent growth should be taken into account in the advice of both large- and small-bodied fish.

Another consequence of density-dependent growth is how it influences the size-at-entry into the fishery that maximises sustainable yield. Without density-dependent growth, fishery size-at-entry should be at a large size, above size of maturation (Froese *et al.*, 2008), which is the logic supporting most mesh size regulations. However, recent theoretic developments have shown that if there is sufficiently strong density-dependent growth, yield may be maximised by fishing juveniles (Svedäng and Hornborg, 2014; Andersen *et al.*, 2017; van Gemert and Andersen, 2018). Nevertheless, an analysis of three stocks by van Gemert and Andersen (2018) showed that for these stocks the levels of density-dependent growth were not strong enough to make fishing juveniles advantageous for yield maximisation.

The challenge to advisory bodies is to devise a widely-accepted method to estimate and incorporate density-dependent growth into calculations for target reference points. Some advisory bodies, such as ICES, do use updated weight-at-age data in their stock assessments and subsequent reference point estimations. However, this approach still disregards the density-dependent mechanism, and would assess stock productivity according to the most recent growth data. A reduction in individual growth would then be seen as reducing stock productivity, which would result in a reduction of the estimated F_{MSY} . However, if that growth reduction were due to density dependence, our results demonstrate that F_{MSY} should be increased instead to relieve part of the density dependence and thereby increase stock productivity. Only updating weight-at-age data is therefore not enough to account for density-dependent growth in stock assessments. Recently an effort to incorporate density-dependent growth in reference point calculations has already been made for Northeast Atlantic mackerel (*Scomber scombrus*) (ICES, 2015; Pastoors *et al.*, 2015), but more approaches should be developed.

Reverse trophic cascades

Fisheries advice is predominantly given from a single-stock perspective. There are a few notable exceptions to this, such as the calculation of natural mortality of most stocks in the North Sea, which takes changes in predator biomass into account (ICES, 2017a). Generally, though, reference points are calculated independently from the exploitation regimes and biomasses of other stocks. In reality however, the changes in exploitation of one stock will influence the vital rates of other stocks, and thereby their reference points, through predation and interspecific density dependence. Food availability of a stock may decrease if exploitation increases on the stock's main prey, or it might increase instead if exploitation is increased on its main competitor. The main effect, though, is that exploitation changes of a given stock's

main predator change the predation mortality that the stock is subject to. These dynamics are not limited to the interactions between a few stocks, but can reverberate throughout the ecosystem as trophic cascades (e.g. Daskalov, 2002; Daan *et al.*, 2005; Frank *et al.*, 2005).

Trophic cascades are often described as resulting from a removal of large-predator biomass (e.g. Schmitz *et al.*, 2000; Myers *et al.*, 2007), and there are well-documented examples where the overexploitation of large-bodied predatory fish stocks has resulted in such trophic cascades (e.g. Frank *et al.*, 2005; Casini *et al.*, 2008; Altieri *et al.*, 2012). However, now that the stocks of large-bodied fish appear to be recovering in the Northeast Atlantic, we can expect to see a reversal of this process in the form of reverse trophic cascades.

We illustrate a reverse trophic cascade with an existing community size spectrum model (Andersen *et al.*, 2016). The model has previously been used to simulate direct trophic cascades (Andersen and Pedersen, 2009) and interactions between fisheries of different components of the fish community (Houle *et al.*, 2013; Andersen *et al.*, 2015). The model resolves all species in a community with asymptotic weights (W_∞) in the range of 4 g–100 kg. Both inter- and intraspecific density dependence are incorporated in the form of predation/cannibalism and competition for food, according to the mechanism of “big eats small”. We applied two different types of exploitation regimes to the community (Figure 3a) and observed how fishing impacted the SSB and natural mortality of each stock. The first exploitation regime is one of “high F ”, where fishing mortality is 0.3 year⁻¹ for stocks of small-bodied species (arbitrarily set as asymptotic sizes smaller than 2.5 kg) and 0.6 year⁻¹ for larger-bodied stocks. The second exploitation regime is one of “low F ”, where fishing mortality on stocks of large-bodied species is reduced to 0.2 year⁻¹, whereas it is still 0.3 year⁻¹ for small-bodied species. For each stock, fishing mortality is allocated according to a trawl selectivity curve, with a mean fishery size-at-entry of 0.05 W_∞ (Andersen *et al.*, 2016). A third exploitation regime, without fishing, was used as a baseline for comparison.

The “high F ” exploitation regime results in a clear trophic cascade when compared with an unfished system (compare dashed and dotted lines in Figure 3), as would be expected. Large-bodied fish stocks with a high trophic level become severely depleted, causing the small-bodied fish stocks at a lower trophic level to increase in SSB substantially above their unfished SSB due to reduced predation (panel b). Changing from “high F ” to “low F ” in turn triggers the expected reverse trophic cascade in the community (solid lines). Large-bodied fish stocks become more abundant, which increases predation mortality on the smaller-bodied prey species. As a result, these small-bodied stocks decrease in SSB.

The simulations reflect the typical development in fully exploited marine ecosystems: when large-bodied piscivorous fish stocks are overfished, forage fish stocks will have a higher productivity due to a reduced predation mortality. This higher productivity facilitates the development of highly profitable forage fisheries. An extreme example of this effect occurred in the East China Sea, where the near-obliviation of larger-bodied fish stocks lead to a large increase in biomass yield of small-bodied fish (Szuwalski *et al.*, 2017).

When large-bodied stocks have recovered, the higher predation mortality on forage fish stocks will also reduce the F_{MSY} reference point of forage fish stocks. If this reduction in F_{MSY} is not

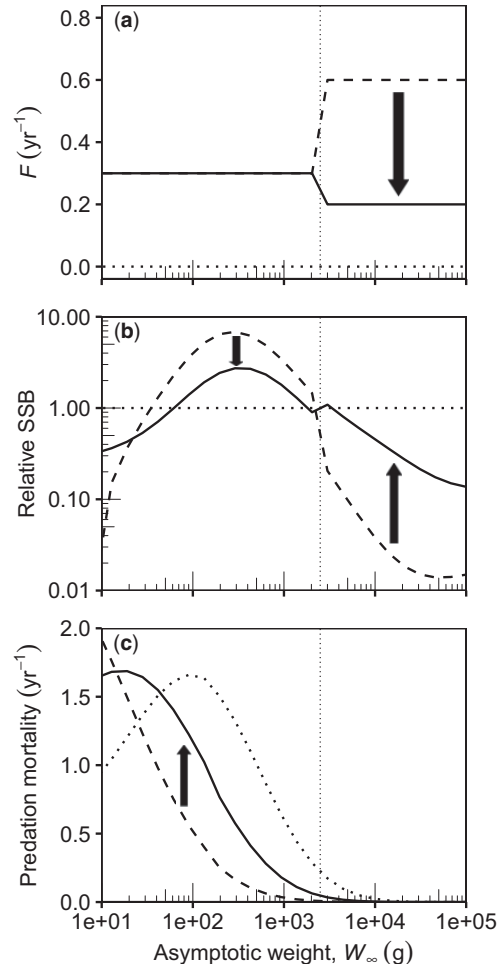


Figure 3. Community cascade due to recovery of large-bodied piscivorous fish stocks, illustrated by two scenarios: collapsed large-bodied stocks ($W_\infty > 2.5$ kg) due to heavy fishing (dashed lines), and recovery of large-bodied stocks effectuated by lowering their fishing mortality F from 0.6 to 0.2 year⁻¹ (solid lines). The thick dotted lines show an unfished community. The thin vertical dotted lines indicate $W_\infty = 2.5$ kg. (a) Level of fishing mortality F depending on stock W_∞ . (b) SSB, relative to when $F = 0$. (c) Predation mortality.

recognized by the advice, the stocks of forage fish will become overexploited. Therefore, a situation with recovering large-bodied piscivorous stocks requires that reference points of their prey species are frequently updated to reflect the continuous changes in predation mortality. Failure to take a more dynamic approach to calculating the reference points of forage fish stocks will lead to increased risk of their overexploitation and collapse.

A continued recovery of large piscivorous fish stocks may also lead to conflicts between fisheries. Whereas fleets that target large piscivorous fish will welcome the recovery of these stocks, fleets

targeting forage fish should ideally like to see a return to a situation with depleted large piscivorous fish stocks and the associated higher productivity of their forage fish stocks. Forage fish fleets may see a lesser return, or no return at all, on their investments if forage fish productivity were to decrease. A reverse trophic cascade as a result of large-piscivore stock recovery may therefore lead to conflicts between the fisheries of forage fish and large piscivorous fish.

The potential conflict between fisheries needs to be addressed by regulatory bodies. A first step is simply to acknowledge the conflict. The next step is to set a desired exploitation state for the ecosystem. Formulating such a desired exploitation state will require quantifying the magnitude of interdependence of the system's fish stocks, both in terms of biomass production and economic rent (Ravn-Jonsen *et al.*, 2016). This will require a fair degree of biological knowledge on the ecological interactions within the given ecosystem and how these are affected by exploitation, as well as economic knowledge on how different exploitation regimes translate into financial returns. If such knowledge is available, the regulatory body can then start to define their desired ecosystem state and the associated exploitation regimes.

Setting a desired exploitation state should include stakeholder participation. However, as previously shown, not all stakeholders will be affected positively by such a new exploitation state. The concept of fairness plays a large role in determining fisher compliance with regulations (Jentoft, 1989), and negatively-affected fishers will be unlikely to voluntarily agree with new regulations without some form of compensation for their reduced revenue, for instance in the form of subsidies. Obtaining compliance using enforcement is possible, but carries its own economic cost. More importantly, the punitive measures associated with stronger enforcement could come at the cost of a reduced perception of legitimacy of the regulatory body, especially if the regulations are perceived as unfair.

Conclusion

Undoing the consequences of decades of unsustainable fishing has been one of the major goals of fisheries management in recent years. As a result, signs are now appearing that large-bodied stocks are recovering from overfishing. We have identified three actions needed to prepare for a future with recovered stocks of large-bodied fish: (i) Density-dependent growth must be explicitly considered in stock assessments, reference point calculations, and management strategy evaluations. (ii) Reference points must be dynamically updated, to include the community changes that result from a reverse trophic cascade. (iii) The possible conflict between fisheries of forage fish and those of large piscivorous fish resulting from a reverse trophic cascade should be addressed: decision makers need to be aware that management actions can favour some fisheries whilst hurting others, and make appropriate decisions based on this information. Ignoring the challenges that arise due to the recovery of large-bodied stocks could jeopardize one of the major success stories of recent fisheries management.

Supplementary data

Supplementary material is available at the ICESJMS online version of the manuscript.

Acknowledgements

We thank K. Enberg, J. J. Poos, and an anonymous reviewer for their valuable input. This work was supported by the MARmaED

project, which has received funding from the European Union's Horizon 2020 research and innovation programme under the Marie Skłodowska-Curie grant agreement No 675997. This work was further supported by the Centre for Ocean Life, a VKR Centre of Excellence supported by the Villum Foundation. KHA was supported by the EU H2020 project under grant agreement no 773713 (Pandora). The results of this work reflect only the authors' views and the Commission is not responsible for any use that may be made of the information it contains.

References

- Altieri, A. H., Bertness, M. D., Coverdale, T. C., Herrmann, N. C., and Angelini, C. 2012. A trophic cascade triggers collapse of a salt-marsh ecosystem with intensive recreational fishing. *Ecology*, 93: 1402–1410.
- Andersen, K. H., and Beyer, J. E. 2015. Size structure, not metabolic scaling rules, determines fisheries reference points. *Fish and Fisheries*, 16: 1–22.
- Andersen, K. H., Brander, K., and Ravn-Jonsen, L. 2015. Tradeoffs between objectives for ecosystem management of fisheries. *Ecological Applications*, 25: 1390–1396.
- Andersen, K. H., Jacobsen, N. S., and Farnsworth, K. D. 2016. The theoretical foundations for size spectrum models of fish communities. *Canadian Journal of Fisheries and Aquatic Sciences*, 73: 575–588.
- Andersen, K. H., Jacobsen, N. S., Jansen, T., and Beyer, J. E. 2017. When in life does density dependence occur in fish populations? *Fish and Fisheries*, 18: 656–667.
- Andersen, K. H., and Pedersen, M. 2009. Damped trophic cascades driven by fishing in model marine ecosystems. *Proceedings of the Royal Society of London B: Biological Sciences*. doi: 10.1098/rspb.2009.1512.
- Boettiger, C., Lang, D. T., and Wainwright, P. C. 2012. rfishbase: exploring, manipulating and visualizing FishBase data from R. *Journal of Fish Biology*, 81: 2030–2039.
- Bundy, A., and Fanning, L. P. 2005. Can Atlantic cod (*Gadus morhua*) recover? Exploring trophic explanations for the non-recovery of the cod stock on the eastern Scotian Shelf, Canada. *Canadian Journal of Fisheries and Aquatic Sciences*, 62: 1474–1489.
- Casini, M., Lövgren, J., Hjelm, J., Cardinale, M., Molinero, J.-C., and Kornilovs, G. 2008. Multi-level trophic cascades in a heavily exploited open marine ecosystem. *Proceedings of the Royal Society of London B: Biological Sciences*, 275: 1793–1801.
- Cook, R. M., Holmes, S. J., and Fryer, R. J. 2015. Grey seal predation impairs recovery of an overexploited fish stock. *Journal of Applied Ecology*, 52: 969–979.
- Cormon, X., Ernande, B., Kempf, A., Vermaud, Y., and Marchal, P. 2016. North Sea saithe *Pollachius virens* growth in relation to food availability, density dependence and temperature. *Marine Ecology Progress Series*, 542: 141–151.
- Daan, N., Gislason, H. G., Pope, J. C., and Rice, J. 2005. Changes in the North Sea fish community: evidence of indirect effects of fishing? *ICES Journal of Marine Science*, 62: 177–188.
- Daskalov, G. M. 2002. Overfishing drives a trophic cascade in the Black Sea. *Marine Ecology Progress Series*, 225: 53–63.
- Eero, M. 2012. Reconstructing the population dynamics of sprat (*Sprattus sprattus balticus*) in the Baltic Sea in the 20th century. *ICES Journal of Marine Science*, 69: 1010–1018.
- Fernandes, P. G., and Cook, R. M. 2013. Reversal of fish stock decline in the Northeast Atlantic. *Current Biology*, 23: 1432–1437.
- Frank, K. T., Petrie, B., Choi, J. S., and Leggett, W. C. 2005. Trophic cascades in a formerly cod-dominated ecosystem. *Science*, 308: 1621–1623.
- Froese, R., and Pauly, D. 2000. FishBase 2000: Concepts, Design and Data Sources. ICLARM, Los Baños, Laguna, Philippines, 344 pp.

- Froese, R., Stern-Pirlot, A., Winker, H., and Gascuel, D. 2008. Size matters: how single-species management can contribute to ecosystem-based fisheries management. *Fisheries Research*, 92: 231–241.
- Hartley, T. W., and Robertson, R. A. 2008. Stakeholder collaboration in fisheries research: integrating knowledge among fishing leaders and science partners in northern New England. *Society and Natural Resources*, 22: 42–55.
- Hilborn, R., and Walters, C. J. 1992. Quantitative Fisheries Stock Assessment: Choice, Dynamics and Uncertainty. Chapman and Hall, New York, USA.
- Horbowy, J., and Luceńczyk, A. 2017. Effects of multispecies and density-dependent factors on MSY reference points: example of the Baltic Sea sprat. *Canadian Journal of Fisheries and Aquatic Sciences*, 74: 864–870.
- Houle, J. E., Andersen, K. H., Farnsworth, K. D., and Reid, D. G. 2013. Emerging asymmetric interactions between forage and predator fisheries impose management tradeoffs. *Journal of Fish Biology*, 83: 890–904.
- Hutchings, J. A. 2000. Collapse and recovery of marine fishes. *Nature*, 406: 882–885.
- Hutchings, J. A., and Reynolds, J. D. 2004. Marine fish population collapses: consequences for recovery and extinction risk. *AIBS Bulletin*, 54: 297–309.
- ICES. 2015. EU, Norway, and the Faroe Islands request to ICES on the management of mackerel (*Scomber scombrus*) in the Northeast Atlantic. *In Report of the ICES Advisory Committee*, 2015. ICES Advice 2015, Book 9, Section 9.2.3.1. 11 pp.
- ICES. 2016a. Advice basis. *In Report of the ICES Advisory Committee*, 2016. ICES Advice 2016, Book 1, Section 1.2. 15 pp.
- ICES. 2016b. Report of the Arctic Fisheries Working Group (AFWG), Dates 19–25 April 2016, ICES HQ, Copenhagen, Denmark. ICES CM 2016/ACOM:06. 621 pp.
- ICES. 2017a. Greater North Sea Ecoregion - Fisheries overview. *In Report of the ICES Advisory Committee*, 2017. ICES Advice 2017, Book 7, Section 7.2. 29 pp. doi: 10.17895/ices.pub.3116
- ICES. 2017b. Report of the Working Group on Assessment of Demersal Stocks in the North Sea and Skagerrak (2017), 26 April–5 May 2017, ICES HQ, Copenhagen, Denmark. ICES CM 2017/ACOM:21. 1248 pp.
- ICES. 2018. Report of the Working Group on Ecosystem Effects of Fishing Activities (WGECO), 12–19 April 2018, San Pedro del Pinatar, Spain. ICES CM 2018/ACOM:27. 69 pp.
- Jentoft, S. 1989. Fisheries co-management: delegating government responsibility to fishermen's organizations. *Marine Policy*, 13: 137–154.
- Kaplan, I. M., and McCay, B. J. 2004. Cooperative research, co-management and the social dimension of fisheries science and management. *Marine Policy*, 28: 257–258.
- Lorenzen, K., and Enberg, K. 2002. Density-dependent growth as a key mechanism in the regulation of fish populations: evidence from among-population comparisons. *Proceedings of the Royal Society of London B: Biological Sciences*, 269: 49–54.
- Margetts, A. R., and Holt, S. J. 1948. The effect of the 1939–1945 war on the English North Sea trawl fisheries. *Rapports et procès-verbaux des réunions: conseil permanent international pour l'exploitation de la mer*. 122: 26–46.
- Myers, R. A., Baum, J. K., Shepherd, T. D., Powers, S. P., and Peterson, C. H. 2007. Cascading effects of the loss of apex predatory sharks from a coastal ocean. *Science*, 315: 1846–1850.
- Myers, R. A., and Worm, B. 2003. Rapid worldwide depletion of predatory fish communities. *Nature*, 423: 280.
- Olafsdottir, A. H., Slotte, A., Jacobsen, J. A., Oskarsson, G. J., Utne, K. R., and Nøttstad, L. 2016. Changes in weight-at-length and size-at-age of mature Northeast Atlantic mackerel (*Scomber scombrus*) from 1984 to 2013: effects of mackerel stock size and herring (*Clupea harengus*) stock size. *ICES Journal of Marine Science*, 73: 1255–1265.
- Pastoors, M., Brunel, T., Skagen, D., Utne, K. R., Enberg, K., and Sparrevoorn, C. R. 2015. Mackerel growth, the density dependent hypothesis and implications for the configuration of MSE simulations: results of an ad-hoc workshop in bergen, 13–14 August 2015. Working Document to ICES Working Group on Widely Distributed Stocks (WGWHITE), 25–31 August 2015, AZTI-Tecnalia, Pasai, Spain.
- Pastoors, M. A. 2016. Stakeholder participation in the development of management strategies. *In Management Science in Fisheries: An Introduction to Simulation-Based Methods*, pp. 409–422, Chap. 20. Ed. by C. T. T. Edwards and D. J. Dankel. Routledge, New York, NY.
- Ravn-Jonsen, L., Andersen, K. H., and Vestergaard, N. 2016. An indicator for ecosystem externalities in fishing. *Natural Resource Modeling*, 29: 400–425.
- Rijnsdorp, A. D., and Van Leeuwen, P. I. 1992. Density-dependent and independent changes in somatic growth of female North Sea plaice *Pleuronectes platessa* between 1930 and 1985 as revealed by back-calculation of otoliths. *Marine Ecology Progress Series*, 88: 19–32.
- Rochet, M.-J. 2000. Does the concept of spawning per recruit make sense? *ICES Journal of Marine Science*, 57: 1160–1174.
- Schmitz, O. J., Hambäck, P. A., and Beckerman, A. P. 2000. Trophic cascades in terrestrial systems: a review of the effects of carnivore removals on plants. *The American Naturalist*, 155: 141–153.
- Shelton, P. A., Sinclair, A. F., Chouinard, G. A., Mohn, R., and Duplisea, D. E. 2006. Fishing under low productivity conditions is further delaying recovery of Northwest Atlantic cod (*Gadus morhua*). *Canadian Journal of Fisheries and Aquatic Sciences*, 63: 235–238.
- Svedäng, H., and Hornborg, S. 2014. Selective fishing induces density-dependent growth. *Nature Communications*, 5: 4152.
- Szuwalski, C. S., Burgess, M. G., Costello, C., and Gaines, S. D. 2017. High fishery catches through trophic cascades in China. *Proceedings of the National Academy of Sciences of the United States of America*, 114: 717–721.
- Trzcinski, M. K., Mohn, R., and Bowen, W. D. 2006. Continued decline of an Atlantic cod population: how important is gray seal predation? *Ecological Applications*, 16: 2276–2292.
- van der Sleen, P., Stransky, C., Morrongiello, J. R., Haslob, H., Peherda, M., and Black, B. A. in press. Otolith increments in European plaice (*Pleuronectes platessa*) reveal temperature and density-dependent effects on growth. *ICES Journal of Marine Science*. doi: 10.1093/icesjms/fsy011.
- van Gemert, R., and Andersen, K. H. 2018. Implications of late-in-life density-dependent growth for fishery size-at-entry leading to maximum sustainable yield. *ICES Journal of Marine Science*, 75: 1296–1305.
- Van Leeuwen, A., De Roos, A. M., and Persson, L. 2008. How cod shapes its world. *Journal of Sea Research*, 60: 89–104.
- Zimmermann, F., Ricard, D., and Heino, M. in press. Density regulation in Northeast Atlantic fish populations: density dependence is stronger in recruitment than in somatic growth. *Journal of Animal Ecology*. doi: 10.1111/1365–2656.12800.

CHAPTER 10

Paper II

Implications of late-in-life
density-dependent growth for fishery
size-at-entry leading to maximum
sustainable yield

van Gemert, R. and Andersen, K. H.

ICES Journal of Marine Science

2018

75(4), 1296–1305

ICES Journal of Marine Science (2018), 75(4), 1296–1305. doi:10.1093/icesjms/fsx236

Original Article

Implications of late-in-life density-dependent growth for fishery size-at-entry leading to maximum sustainable yield

Rob van Gemert* and Ken H. Andersen

Centre for Ocean Life, National Institute of Aquatic Resources (DTU-Aqua), Technical University of Denmark, Kemitorvet, Building 202, 2800 Kgs. Lyngby, Denmark

*Corresponding author: tel: +45 35 88 33 00; fax: +45 35 88 33 33; e-mail: rvge@aqua.dtu.dk

van Gemert, R. and Andersen, K. H. Implications of late-in-life density-dependent growth for fishery size-at-entry leading to maximum sustainable yield. – ICES Journal of Marine Science, 75: 1296–1305.

Received 15 February 2017; revised 5 December 2017; accepted 7 December 2017; advance access publication 18 January 2018.

Currently applied fisheries models and stock assessments rely on the assumption that density-dependent regulation only affects processes early in life, as described by stock-recruitment relationships. However, many fish stocks also experience density-dependent processes late in life, such as density-dependent adult growth. Theoretical studies have found that, for stocks which experience strong late-in-life density dependence, maximum sustainable yield (MSY) is obtained with a small fishery size-at-entry that also targets juveniles. This goes against common fisheries advice, which dictates that primarily adults should be fished. This study aims to examine whether the strength of density-dependent growth in actual fish stocks is sufficiently strong to reduce optimal fishery size-at-entry to below size-at-maturity. A size-structured model is fitted to three stocks that have shown indications of late-in-life density-dependent growth: North Sea plaice (*Pleuronectes platessa*), Northeast Atlantic (NEA) mackerel (*Scomber scombrus*), and Baltic sprat (*Sprattus sprattus balticus*). For all stocks, the model predicts exploitation at MSY with a large size-at-entry into the fishery, indicating that late-in-life density dependence in fish stocks is generally not strong enough to warrant the targeting of juveniles. This result lends credibility to the practise of predominantly targeting adults in spite of the presence of late-in-life density-dependent growth.

Keywords: density dependence, maximum sustainable yield, selective fishing, size spectrum

Introduction

Density dependence is a key process in population ecology. Negative (or compensatory) density dependence takes place when an increase in population size results in a decrease in individual growth, reproduction, or survival, usually due to increased intra-specific competition or increased predation mortality. Density dependence due to intraspecific competition can, for instance, stem from competition for food (Hassell, 1975) or spawning sites (Reichard *et al.*, 2004). Likewise, density dependence as a result of predation mortality can stem from cannibalism (Ricker, 1954), or from the predator switching to the most abundant prey (type III functional response; Holling, 1959). Because population density is changed by exploitation, it is essential to understand how density dependence operates within a population when predicting how that population may respond to exploitation.

The strength of density dependence varies with the size of the individual. Here we distinguish between two mechanisms of density dependence: early-in-life density-dependent recruitment and late-in-life density-dependent growth. In many stocks, individuals experience strong density dependence during the larval and early-juvenile stage. In spite of the wide prevalence of this early-in-life density dependence, its causal mechanisms are usually poorly understood. Therefore, it is sometimes referred to as density-dependent recruitment, as it takes place before the individual enters the “recruited” component of the stock. Whereas density-dependent recruitment takes place early in life, density-dependent growth can be assumed to be strongest later in life, after an individual reaches size-at-maturity. This is because density-dependent growth emerges due to resource competition, at the adult size where biomass of a cohort (and therefore its

consumption) is usually the largest (e.g. Munch *et al.*, 2005; Jennings *et al.*, 2007). However, in spite of its potentially significant role in population regulation, late-in-life density-dependent growth is rarely incorporated in the calculation of fisheries reference points.

Instead, current fisheries advice is generally given under the assumption that all density dependence occurs early in life, in the form of density-dependent recruitment (e.g. Beverton and Holt, 1957; Myers and Cadigan, 1993). This early-in-life density dependence is either described as a constant recruitment (yield-per-recruit models), or through a stock-recruitment relationship. This assumption of only early-in-life density dependence is likely acceptable for fish stocks that experience heavy fishing pressure, where fishing mortality relieves the exploited population component from late-in-life density dependence. However, during the last decade, improved fisheries management has led to many fish stocks in the NEA gradually showing signs of recovery from overfishing (Fernandes and Cook, 2013). For some species, this recovery coincided with reduced individual growth of older juveniles and adults, possibly as a result of late-in-life density-dependent resource competition (e.g. Cormon *et al.*, 2016; Olafsdottir *et al.*, 2016). Therefore, it may be problematic that late-in-life density-dependent growth is rarely taken into account in fisheries management.

Optimal management strategies could differ substantially for stocks that experience late-in-life density-dependent growth. For example, a model study by Andersen *et al.* (2017) showed that if density-dependent regulation mainly happens late in life, maximum sustainable yield (MSY) is obtained by fishing on juvenile fish. This relieves the remaining juveniles from density dependence, thereby increasing the productivity of the entire stock. This prediction challenges reigning fisheries management procedures, which enforce minimum landing size regulations to avoid excessive fishing mortality on juveniles. The study of Andersen *et al.* (2017) only compared scenarios for hypothetical stocks, where density dependence either occurred mainly early in life or mainly late in life. However, density-dependent population regulation need not necessarily occur at only a single bottleneck.

Given the widespread nature of density-dependent processes, it is likely that many fish stocks experience some form of density-dependent regulation at multiple life stages. For instance, Dover sole (*Solea solea*) recruitment appears to follow a classic Beverton-Holt stock-recruitment relationship (Lorenzen, 2005). This is indicative of strong early-in-life density dependence, but the stock also shows significant density-dependent growth in the recruited phase (Lorenzen and Enberg, 2002). Another example is North Sea plaice (*P. platessa*), which shows strong early-in-life density dependence when larvae settle in their nursery grounds (Van der Veer, 1986), but has also shown significant late-in-life density-dependent growth (Rijnsdorp and Van Leeuwen, 1992). Based on the findings of Andersen *et al.* (2017), fishery size-at-entry at which MSY is obtained should gradually decrease when the strength of late-in-life density-dependent growth increases (relative to that of early-in-life density dependence). However, it is unknown whether the late-in-life density-dependent growth that is experienced by marine fish stocks is actually strong enough to trigger a reduction in optimal fishery size-at-entry.

We aim to explore whether marine fish stocks can actually experience late-in-life density-dependent growth that is strong

enough to reduce optimal fishery size-at-entry (i.e. size-at-entry at which MSY is obtained). To this end we estimated the relative strengths of early- and late-in-life density dependence in three fish stocks, by fitting a dynamic single-stock size-structured model to empirical stock data. The three examined fish stocks, North Sea plaice (*P. platessa*) (Rijnsdorp and Van Leeuwen, 1992), NEA mackerel (*S. scombrus*) (Olafsdottir *et al.*, 2016), and Baltic sprat (*S. s. balticus*) (Eero, 2012), have shown indications of experiencing some late-in-life density-dependent resource competition and only show little cannibalism.

We focus on density-dependent resource competition as the primary mechanism behind late-in-life density-dependent regulation, to avoid any confounding effects of cannibalism. In our model, early-in-life density dependence is described by a stock-recruitment relationship. Late-in-life density dependence is not described with a single equation, but emerges through feeding on a dynamic resource spectrum. Varying the relative strengths of early- and late-in-life density dependence was possible by varying the stock-recruitment relationship's maximum recruitment relative to the resource spectrum's carrying capacity. This allowed us to examine whether the strength of density-dependent growth experienced by the stock is high enough so that optimal fishery size-at-entry is below size-at-maturity.

Methods

We apply a standard size-spectrum model (Andersen *et al.*, 2015), adapted to represent only a single stock (Andersen *et al.*, 2017). The model describes the population dynamics of a single fish stock feeding on a dynamic resource spectrum and incorporates early-in-life density dependence through a Beverton-Holt stock-recruitment relationship, and late-in-life density dependence emerges through size-based resource competition. Here we describe the main assumptions and principles of the model. Detailed descriptions of the assumptions and equations used in size-spectrum models such as this one can also be found e.g. in Hartwig *et al.* (2011), Andersen and Beyer (2015), and Andersen *et al.* (2015). All model equations and parameters are listed in Tables 1 and 2, and the numerical implementation of our model is given in Supplementary Appendix A. Throughout, size refers to body weight, w .

Growth, mortality, and demography

We assume that individuals feed on a resource $N_R(w_R)$ that represents food of all sizes in the ecosystem. Individuals prefer food a factor $\beta = 100$ smaller than themselves (Jennings *et al.*, 2002). Multiplying an individual's size-preference with the biomass of that resource size, and integrating over all resource sizes, gives the total amount of food available to the individual. When multiplied with clearance rate γw^n , this then gives the food actually encountered by the individual $E_c(w)$ (M2). Consumption is described by a functional response type II (M3), with maximum consumption hw^n and $n = 3/4$, giving the feeding level $f(w)$ as consumed food relative to maximum consumption. From consumption we calculate the energy available for somatic growth and reproduction from an energy budget (M4). Energy is assimilated from consumed food with efficiency α and costs of standard metabolism ($k_t w^n$) and activity ($k_a w$) are paid. The remaining available

Table 1. Governing model equations.

Consumption	
Size preference for prey	$\varphi\left(\frac{w}{w_R}\right) = \exp[-\left(\ln\left(\frac{w}{w_R\beta}\right)\right)^2/(2\sigma^2)]$ M1
Encountered food	$E_e(w) = \gamma w^q \int_0^\infty \varphi\left(\frac{w}{w_R}\right) w_R N_R(w_R) dw_R$ M2
Feeding level	$f(w) = \frac{E_e(w)}{E_e(w) + h w^n}$ M3
Growth	
Available energy	$E_a(w) = af(w)hw^n - k_r w^n - k_a w$ M4
Switching function	$H(x) = (1+x^{-10})^{-1}$ M5
Maturation	$\psi(w) = H\left(\frac{w}{\eta_m W_\infty}\right) \frac{1-c_3}{(w/W_\infty)^{n-1}-c_2}$ M6
Growth rate	$g(w) = (1-\psi(w))E_a(w)$ M7
Mortality	
Background predation	$\mu_0(w) = a_p w^{n-1}$ M8
Fishing, trawl selectivity	$\mu_F(w) = FH\left(\frac{w}{w_F}\right)$ M9
Reproduction	
Egg production	$R_p = \int_{w_{egg}}^{W_\infty} \frac{\psi(w)E_a(w)}{2w^{n-1}} N(w) dw$ M10
Recruitment	$R = R_{max} \frac{c_p R_p}{R_{max} + c_p R_p}$ M11
Mortality	
Background predation	$\mu_0(w) = a_p w^{n-1}$ M12
Fishing, trawl selectivity	$\mu_F(w) = FH\left(\frac{w}{w_F}\right)$ M13
Population structure	
Abundance spectrum	$\frac{\partial N(w)}{\partial t} + \frac{\partial g(w)N(w)}{\partial w} = -[\mu_0(w) + \mu_F(w)]N(w)$ M14
Boundary condition	$g(w_{egg})N(w_{egg}) = R$ M15
SSB	$B_{SSB} = \int_{w_{egg}}^{W_\infty} H\left(\frac{w}{\eta_m W_\infty}\right) w N(w) dw$ M16
Fishery performance	
Yield	$Y = \int_{w_{egg}}^{W_\infty} \mu_F(w) w N(w) dw$ M17
Resource	
Predation on resource	$\mu_p(w_R) = \int_{w_{egg}}^{W_\infty} \varphi\left(\frac{w}{w_R}\right) (1-f(w)) \gamma w^q N(w) dw$ M18
Resource spectrum	$\frac{\partial N_R(w_R)}{\partial t} = r_0 w_R^{n-1} [\kappa w_R^{\lambda} - N_R(w_R)] - \mu_p(w_R) N_R(w_R)$ M19

energy $E_a(w)$ is divided between somatic growth and reproduction, with individual growth rate $g(w)$:

$$g(w) = [1 - \psi(w)][af(w)hw^n - k_r w^n - k_a w] \quad (1)$$

Here $\psi(w)$ represents the fraction of available energy invested into reproduction. The remaining available energy, $(1 - \psi(w))$, is invested into growth. $\psi(w)$ approaches 0 so long as individual size w remains well below size at 50% maturation $\eta_m W_\infty$. The switch to maturity is described by a sigmoid function that smoothly varies between 0 and 1 around size at 50% maturation (M5). Mature individuals still invest energy in growth, but this investment decreases as their size approaches W_∞ , until at size W_∞ all energy is invested into egg production (M6). This procedure results in a von Bertalanffy-like weight-at-age curve if food is plentiful, $f(w) = f_0$, but reduces growth if the resource has become depleted, $f(w) < f_0$.

The energy not used for growth is invested into egg production: $\psi(w)E_a(w)$. Total egg production of the stock R_p emerges by integrating egg production over all individual sizes, taking into account that only females produce eggs (M10).

We assume that natural mortality rate $\mu_0(w)$ is mainly due to predation by other species, and decreases with individual size according to $\mu_0(w) = a_p w^{n-1}$ (M8). We assume that mortality due to cannibalism is negligible.

The fishing mortality rate $\mu_F(w)$ is the product of a level F and a size-specific gear selectivity (M9). We use a sigmoid function

that smoothly switches from 0 to 1 around size-at-entry into the fishery w_F to resemble a trawl selectivity curve.

The density of individuals across all sizes within the population makes up the abundance size-spectrum $N(w)$ as calculated by the McKendrick-von Foerster conservation equation:

$$\frac{\partial N(w)}{\partial t} + \frac{\partial g(w)N(w)}{\partial w} = -[\mu_0(w) + \mu_F(w)]N(w) \quad (2)$$

Spawning stock biomass B_{SSB} can be calculated from the abundance size-spectrum by integrating mature biomass over all sizes (M16). Yield from fishing can be calculated by multiplying stock biomass targeted by the fishing gear with fishing mortality, and integrating over all sizes (M17).

Density dependence

Density dependence emerges from two sources: a stock-recruitment relationship determines the strength of density dependence early in life, and competition for food from the resource spectrum determines the strength of density dependence late in life. The relative importance of the two processes is described by the ratio between the parameters that describe the carrying capacity of the early life environment and the late-life environment. Below we first describe both of these processes individually, and then explain how they interact.

Table 2. Model parameters.

Symbol	Description	Value	Unit	Footnote(s)
<i>Body size</i>				
W_∞	Asymptotic size (weight)*	stock specific	g	
w_{egg}	Egg weight	0.001	g	a
<i>Consumption</i>				
n	Metabolic exponent	3/4	—	b
β	Preferred predator-prey mass ratio	100	—	c
σ	Range of preferred prey size	1.3	—	d
q	Clearance rate exponent	0.8	—	e
γ	Clearance rate coefficient	$6.57/\kappa$	$\text{g}^{-q} \text{ year}^{-1}$	f
f_0	Standard feeding level	0.6	—	f
f_c	Critical feeding level	0.2	—	f
h	Maximum consumption*	$\approx 3KW_\infty^{1/3}/[a(f_0 - f_c)]$	$\text{g}^{1-n} \text{ year}^{-1}$	g
<i>Growth</i>				
α	Assimilation efficiency	0.6	—	f
η_m	Size at maturation rel. to W_∞	0.25	—	h
ϵ_a	Fraction of energy for activity	0.8	—	i
k_r	Standard metabolism coefficient	$f_c ah$	$\text{g}^{1-n} \text{ year}^{-1}$	f
k_a	Activity coefficient	$\epsilon_a ah(f_0 - f_c)W_\infty n - 1$	year^{-1}	i
<i>Mortality</i>				
α_p	Mortality level*	$\approx M(\eta_m W_\infty)^{1-n}$	$\text{g}^{1-n} \text{ year}^{-1}$	j
<i>Reproduction</i>				
R_{\max}	Maximum recruitment*	stock specific	year^{-1}	
ϵ_r	Recruitment efficiency*	stock specific	—	
<i>Fishery performance</i>				
w_F	Mean size-at-entry into the fishery	variable	g	
F	Fishing mortality	variable	year^{-1}	
<i>Resource</i>				
κ	Carrying capacity magnitude*	stock specific	$\text{g}^{-1-\lambda}$	
λ	Carrying capacity exponent	$-2 - q + n$	—	e
r_0	Resource growth rate coefficient	4	$\text{g}^{1-n} \text{ year}^{-1}$	f, k

Parameters marked with an asterisk are specific for each stock, and the relation to standard parameters (K , W_∞ , and M) are provided.

^aNeuheimer *et al.* (2015).

^bWest *et al.* (1997).

^cJennings *et al.* (2002).

^dAndersen *et al.* (2017).

^eAndersen and Beyer (2006).

^fHartwig *et al.* (2011).

^gJuvenile growth rate (g/year) for $w \ll W_\infty$ from (M7) is $\approx ah(f_0 - f_c)w^n$. A von Bertalanffy growth equation gives the growth rate for $w \ll W_\infty$ as $3KW_\infty^{1/3}w^{2/3}$. Ignoring the small difference in exponents gives the approximation in the table.

^hJensen (1996), Froese and Binohlan (2000), and He and Stewart (2001).

ⁱAndersen and Beyer (2015).

^jThe adult mortality from (M8) is $M = \alpha_p(\eta_m W_\infty)^{n-1}$, from which α_p follows as $\alpha_p = M(\eta_m W_\infty)^{1-n}$.

^kSavage *et al.* (2004).

A standard Beverton-Holt stock-recruitment relationship (Beverton and Holt, 1957) is used to describe recruitment R :

$$R = R_{\max} \frac{\epsilon_r R_p}{R_{\max} + \epsilon_r R_p} \quad (3)$$

where R_{\max} is the maximum recruitment, R_p is the number of eggs produced by the spawning stock, and ϵ_r is the stock-specific recruitment efficiency which accounts for costs of reproduction and egg survival.

The recruitment R is used as a boundary condition for the conservation Equation (2): $g(w_{\text{egg}})N(w_{\text{egg}}) = R$. Which specific type of stock-recruitment relationship we use here is of lesser importance; the most important thing is that it describes the density dependence that takes place early in life. We have used a Beverton-Holt stock-recruitment relationship because it is both

simple and well-known. We consider the recruitment efficiency ϵ_r as constant for each stock. The maximum recruitment R_{\max} represents the carrying capacity of the early life environment and we therefore use this parameter to determine the strength of early-in-life density dependence relative to the strength of late-in-life density dependence.

The resource spectrum $N_R(w_R)$ represents all individuals, of all sizes, that do not belong to the focal stock. The change in resource abundance is described with a semi-chemostat:

$$\frac{dN_R(w_R)}{dt} = r_0 w_R^{n-1} [\kappa w_R^\lambda - N_R(w_R)] - \mu_p(w_R)N_R(w_R) \quad (4)$$

where $r_0 w_R^{n-1}$ is the size-specific resource regeneration rate and $\mu_p(w_R)$ (M18) is the size-specific resource mortality due to predation by the focal stock. Food abundance is determined by the

carrying capacity of the resource κw_R^λ . The value of the slope λ has been determined as $-2 - q + n$ (Andersen and Beyer, 2006), meaning that the resource carrying capacity follows a Sheldon spectrum (Sheldon *et al.*, 1977), where biomass is approximately constant in logarithmically-spaced size groups. Food availability is therefore largely independent of size, with the overall level determined by κ . The value of κ then determines the resource availability, and thereby the level of density-dependent competition and growth.

Intraspecific competition for resources emerges when the consumption of any given resource size exceeds the regeneration of that resource size, thereby reducing its abundance (Figure 1a, grey lines). In fish, cohort biomass usually increases until

maturity (and fishing) sets in. As the biomass of the fish stock increases with size (Figure 1a, black lines), the highest competition will be for the resource sizes that are targeted by mature fish. Density-dependent competition for resources therefore mainly takes place late in life, amongst the mature and late juvenile portion of the stock.

In the model, density-dependent population regulation emerges from two sources: early-in-life stock-recruitment, as determined by R_{\max} , and density-dependent growth as determined by the resource carrying capacity κ . Their ratio, R_{\max}/κ , controls the relative importance of the two processes of density dependence: a low value of R_{\max}/κ leads to a dominance of early-in-life density-dependent recruitment, whereas a high value leads to a dominance of late-in-life density-dependent growth (Figure 1).

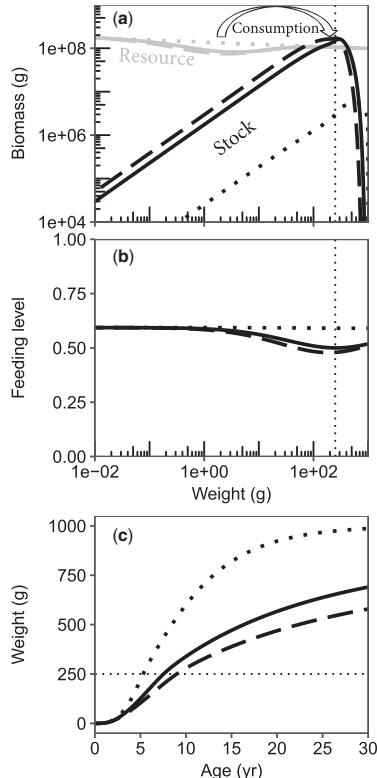


Figure 1. Mechanisms of density dependence in the model, illustrated with three different R_{\max} to κ ratios: 0.01 (dotted), 1 (solid), and 100 (dashed) $\text{g}^{1+\lambda}/\text{year}$. These describe scenarios of only early-in-life, a mix of early- and late-in-life, and only late-in-life density dependence, respectively. The thin dotted lines indicate size-at-maturity. Shown for a W_∞ of 1000 g and no fishing mortality. (a) Stock (black) and resource (grey) biomass as a function of size. Note that the dotted stock line intersects the y-axis outside of the plotted range. (b) Feeding levels (ratio between consumption and maximum consumption) associated with the different R_{\max} to κ ratios, indicating that resource competition peaks around maturation size. (c) Weights-at-age associated with the different R_{\max} to κ ratios, showing how different strengths of early- and late-in-life density dependence affect growth.

Fitting the model to fish stocks

To find realistic R_{\max} to κ ratios for the examined stocks, we fitted the model to empirical data of three fish stocks: North Sea plaice, NEA mackerel, and Baltic sprat. These stocks vary in asymptotic size, show little-to-no cannibalism, and all have shown indications of density-dependent growth beyond the juvenile stage. The dynamics of each stock depend on stock-specific physiological parameters describing: growth (h), asymptotic size (W_∞), recruitment (ϵ_r), and mortality (α_p), and on parameters that influence density dependence: maximum recruitment (R_{\max}) and resource abundance (κ).

The physiological parameters are determined from classical parameters, the von Bertalanffy growth coefficient K , and adult mortality M , with the procedure described in Andersen *et al.* (2009); see Table 2 for relations, and Table 3 for parameters for each stock. For plaice and sprat, W_∞ was calculated from the stock's observed length-at-maturity (L_m) (Supplementary Appendix B). For mackerel, W_∞ was calculated from the L_∞ that was associated with the used value for K . Values for K are taken from empirical studies, and values for M from ICES assessments. Recruitment efficiency (ϵ_r) was set so that the model's F_{MSY} matched the advised F_{MSY} of the stock, having set the size at 50% fisheries selectivity, w_F , according to fisheries data. A more detailed explanation of the parameterization process for each stock can be found in Supplementary Appendix B.

After having parameterized the model with stock-specific parameters, realistic R_{\max} to κ ratios were determined for each stock. For this, the aim was to match simulated density-dependent changes in individual growth and SSB with observed changes in individual growth and SSB, while also matching modelled fishery yield with historical yield data. To observe density-dependent changes in growth, the model was fitted to two historical scenarios between which there were significant differences in both SSB and individual growth (one scenario with low SSB and fast individual growth, and a second scenario with high SSB and slow individual growth).

For North Sea plaice, the two scenarios were before and at the end of the Second World War. No fishing during the war resulted in roughly a tripling of plaice SSB at the end of the war (Margetts and Holt, 1948), and coincided with a reduction in late-juvenile and adult growth (Rijnsdorp and Van Leeuwen, 1992). No actual SSB data is known from this time, with SSB changes instead having been inferred from changes in catch-per-unit-effort. To be able to fit our model to plaice data, we therefore assumed that plaice SSB and yield figures from the 1990s would have been

Table 3. Stock-specific parameters that were used as input for the model, and the resulting SSB and yield predicted by the model.

		Baltic sprat	NEA mackerel	North Sea plaice
Parameters				
Asymptotic size	W_∞ (g)	21	890	1600
Von Bertalanffy growth constant	K (year ⁻¹)	0.68	0.18	0.16
Recruitment efficiency	ϵ_r (-)	0.0055	0.00060	0.10
Size-at-entry into fishery	w_F (g)	3.6	240	120
Maximum recruitment	R_{\max} (year ⁻¹)	$2.5 \cdot 10^{13}$	$4.5 \cdot 10^{10}$	$5.0 \cdot 10^9$
Resource carrying capacity coeff.	κ (g ^{-1-λ})	$2.5 \cdot 10^{12}$	$1.5 \cdot 10^{13}$	$3.3 \cdot 10^{12}$
<i>Low-SSB scenario</i>				
Natural mortality	M (year ⁻¹)	0.50	0.15	0.10
Fishing mortality	F (year ⁻¹)	0.23	0.46	0.60
<i>High-SSB scenario</i>				
Natural mortality	M (year ⁻¹)	0.20	0.15	0.10
Fishing mortality	F (year ⁻¹)	0.39	0.29	0.050
Results				
<i>Low-SSB scenario</i>				
SSB	B_{SSB} (Mt)	0.36	1.7	0.15
Annual yield	Y (Mt/year)	0.094	0.77	0.28
<i>High-SSB scenario</i>				
SSB	B_{SSB} (Mt)	2.1	3.0	2.7
Annual yield	Y (Mt/year)	1.0	0.86	0.18

The input parameters include the R_{\max} and κ values that resulted in the best model fit for each stock. Sources for the parameter values are listed in [Supplementary Appendix B](#).

similar to those of pre-WWII, as for both these times F was around 0.6 year⁻¹ ([Bevertton and Holt, 1957; ICES, 2015b](#)).

The model was fitted to NEA mackerel using scenarios from 2003 and 2013. In 2003 NEA mackerel was heavily fished (F : 0.46 year⁻¹, Y : 680 kt; [ICES, 2015a](#)), SSB was relatively low (1900 kt; [ICES, 2015a](#)) and individual growth was fast ([Olafsdottir et al., 2016](#)). In 2013 fishing mortality had been decreased to 0.29 year⁻¹ ([ICES, 2015a](#)), though yield had increased to 930 kt/year ([ICES, 2015a](#)). At the same time, SSB almost doubled to around 3600 kt ([ICES, 2015a](#)), and individual growth had decreased ([Olafsdottir et al., 2016](#)).

Last, the model was fitted to Baltic sprat using scenarios from 1988 and 1998. The main predator of Baltic sprat, Eastern Baltic cod (*Gadus morhua*), suffered a large decrease in abundance during the mid-1980s ([Köster et al., 2003](#)). The reduction in predators reduced Baltic sprat mortality, and after 1988 sprat SSB started to increase. Whereas Baltic sprat SSB was around 415 kt in 1988, SSB had more than tripled to around 1400 kt in 1998 ([ICES, 2015c](#)) with a concurrent decrease in late-juvenile and adult growth ([Eero, 2012](#)). Furthermore, whereas in 1988 Baltic sprat yield was around 80 kt/year with a fishing mortality of 0.23 year⁻¹, in 1998 yield had increased to 417 kt/year with a fishing mortality of 0.39 year⁻¹ ([ICES, 2015c](#)).

Using the empirical data from the above scenarios, the model was fitted to each of the three stocks. A detailed description of this fitting procedure is given in [Supplementary Appendix B](#). After fitting, the size-at-entry into the fishery w_F which yielded MSY was determined by running the fitted model with a range of w_F and F combinations. For each value of w_F this resulted in a different highest sustainable yield and a different value of F leading to that highest sustainable yield. The w_F with the largest value for highest sustainable yield is the w_F that yields MSY. Furthermore, a sensitivity analysis was performed of the fitted variables ϵ_r and R_{\max}/κ , by varying their values with a factor 2. Those values were subsequently used to recalculate F_{MSY} and optimal fishery size-at-entry respectively. The sensitivity analysis

and its results are presented in more detail in [Supplementary Appendix C](#).

Results

Fitted parameters, including the R_{\max} and κ values, are shown in [Table 3](#). The resulting weight-at-age curves for both the high- and low-SSB scenarios are shown in [Figure 2](#).

Baltic sprat

The modelled growth for Baltic sprat approaches the empirical weight-at-age data points of the high- and low-SSB scenarios ([Figure 2a](#)). In the low-SSB scenario modelled growth is high, and closely follows the reference line for only early-in-life density dependence. In the high-SSB scenario modelled growth is reduced by strong late-in-life density-dependent growth, and closely follows the reference line for only late-in-life density dependence.

Fishery size-at-entry for which MSY is obtained is close to asymptotic size in the low-SSB scenario ([Figure 2d](#)), and closely follows the reference line for only early-in-life density dependence. In the high-SSB scenario, fishery size-at-entry for which MSY is obtained is smaller, but still greater than size-at-maturity. Again, the fitted curve closely follows the reference line for only late-in-life density dependence.

The sensitivity analysis shows that both weight-at-age and optimal fishery size-at-entry are relatively unaffected by changes in the R_{\max} to κ ratio ([Supplementary Appendix C](#)). This indicates that, for Baltic sprat, a change in natural mortality M has a far stronger impact on strength of density-dependent growth than a change in the R_{\max} to κ ratio.

NEA mackerel

The historical change in weight-at-age of NEA mackerel could not be replicated ([Figure 2b](#)). Changing F from 0.46 to 0.29 year⁻¹ resulted in only a minor reduction in growth. However,

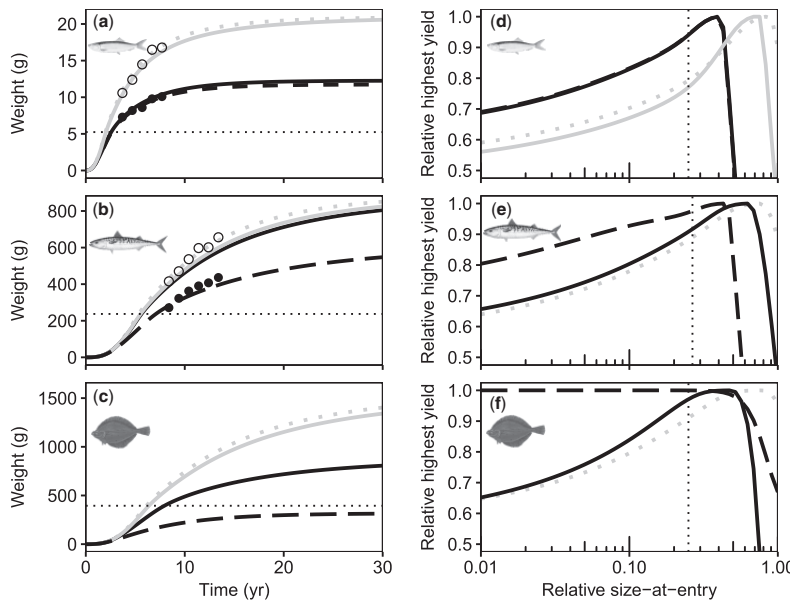


Figure 2. Weight-at-age (a–c) and highest sustainable yield as a function of size-at-entry into the fishery (d–f), modelled for Baltic sprat (a, d), NEA mackerel (b, e), and North Sea plaice (c, f). Highest sustainable yield is calculated separately for each size-at-entry value and, for each scenario, is shown relative to its maximum value among all size-at-entry values (MSY). Size-at-entry into the fishery is shown relative to W_{∞} . Grey lines represent the stock's low-SSB scenario, and black lines represent the stock's high-SSB scenario (Table 3). These lines overlap in (e) and (f), because only fishing mortality changes between scenarios there. The solid lines show the model fit of each stock. The grey dotted lines show the hypothetical model fit of each stock if all density dependence would occur early in life ($R_{\max}/\kappa = 0.00001 \text{ g}^{1+\lambda}/\text{year}$). They are only shown for each stock's low-SSB scenario (Table 3), and act as a reference to that scenario's fitted curve (solid). The black dashed lines show the hypothetical model fit of each stock if all density dependence would occur late in life ($R_{\max}/\kappa = 100 000 \text{ g}^{1+\lambda}/\text{year}$). They are only shown for each stock's high-SSB scenario (Table 3), and act as a reference to that scenario's fitted curve (solid). The thin dotted lines show size-at-maturity. Historical weight-at-age data points are shown for the low-SSB (open points) and high-SSB (filled points) scenarios of sprat and mackerel. They are not shown for plaice, because Rijnsdorp and Van Leeuwen (1992) do not show changes in weight-at-age but in growth-increments of length groups. Supplementary Appendix B contains an overview of how the model fit for plaice overlaps with this data type.

the reference line for only late-in-life density dependence is close to the high-SSB scenario data points. According to these results, it is likely that the observed decrease in NEA mackerel weight-at-age is not solely the result of a decrease in fishing mortality.

For the R_{\max} to κ ratio predicted for NEA mackerel, MSY exploitation occurs with a large size-at-entry into the fishery (Figure 2e). Furthermore, the reference line for only late-in-life density dependence also peaks at a large size-at-entry into the fishery. This suggests that even if NEA mackerel would experience strong late-in-life density-dependent growth, optimal fishery size-at-entry would still be large.

North Sea plaice

For North Sea plaice, the fitted model was able to replicate historical growth data (Figure 2c, Supplementary Appendix B). For a high fishing mortality, growth is fast and almost all density dependence takes place early in life. When fishing mortality drops to nearly zero, late-in-life density dependence becomes stronger due to increased SSB, and growth is decreased. The reference line for only late-in-life density dependence predicts a scenario of severely reduced growth: density-dependent growth would be so

strong that an average individual would not be able to grow to 50% size-at-maturity.

For the R_{\max} to κ ratio predicted for North Sea plaice, MSY exploitation occurs with a large size-at-entry into the fishery (Figure 2f). The sensitivity analysis (Supplementary Appendix C) shows that this would still be the case if the R_{\max} to κ ratio would be a factor 2 higher (stronger density-dependent growth). The dashed reference line shows that, when late-in-life density dependence is very strong, there is a wide range of fishery size-at-entries for which MSY is obtained: from very small to larger than size-at-maturity. This is because throughout this size-at-entry range, the stock remained in a state of severe growth reduction. In this state, the stock had almost no tolerance for fishing mortality, so the yield was very small and almost independent of fishery size-at-entry.

Discussion

For all three analysed stocks the model predicts that fishing at MSY occurs with a large fishery size-at-entry. The optimal fishery size-at-entry can decrease somewhat when the strength of late-in-life density-dependent growth is high, but for the fitted stocks it

always remained above size-at-maturity. Therefore, for the examined stocks this study indicates that the current practice of setting size-at-entry such that predominantly adults are targeted is sound, in spite of the presence of strong late-in-life density-dependent growth. However, this does not mean that late-in-life density-dependent growth should be completely disregarded when calculating fisheries reference points. For other stocks, if late-in-life density dependence is very strong, the optimal size-at-entry could be smaller than size-at-maturity. Further, strong late-in-life density-dependent growth will influence a stock's F_{MSY} reference point. Fishing on a stock that experiences strong late-in-life density-dependent growth will increase individual growth rate by relieving the stock of density dependence, and will thereby increase stock productivity. If this is ignored when calculating fisheries reference points, it is likely that the calculated F_{MSY} will be lower than the actual F_{MSY} . This would cause the fishery to lose out on potential yield. Therefore, it is important to consider density-dependent growth when calculating fisheries reference points.

Previous theoretical work has indicated that stocks with a larger asymptotic size should have a larger density-dependent buffer against population decline, or in other words, they should experience stronger density-dependent regulation (Andersen and Beyer, 2015). Consequently, the issue of density-dependent growth might be most important for stocks of large-bodied species. Our results for North Sea plaice (which in this study is the stock with the greatest asymptotic size) give some confirmation of this. The model predicts that North Sea plaice is at risk of "stunted growth" (Alm, 1946; Ylikarjula *et al.*, 1999) when late-in-life density-dependent growth is very strong, with growth stopping before size-at-maturity. Cases of stunted growth are, however, rarely observed in marine fish populations, possibly due to the large spatial extent of the habitat for adults in marine systems (Andersen *et al.*, 2017). Whether our model is correct in predicting that North Sea plaice could become subject to stunted growth is therefore not completely certain.

Model limitations

We were unable to replicate NEA mackerel's observed reduction in growth by only changing fishing mortality. We therefore assume that the observed reduction in NEA mackerel individual growth (Olafsdottir *et al.*, 2016) is not, or not solely, the result of a reduction in fishing mortality and a subsequent SSB increase. If the observed growth reduction did occur via intraspecific density dependence, some environmental change should then be the cause. A possibility would be increased sea surface temperatures in NEA waters, which have been thought to have extended NEA mackerel's feeding range northwards to Svalbard (Berge *et al.*, 2015), and to have shifted the egg production centre-of-gravity of NEA mackerel's western spawning component northward (Hughes *et al.*, 2014). However, it is also possible that the observed growth reduction of NEA mackerel individuals is rather due to interspecific competition instead of intraspecific competition, as suggested by Olafsdottir *et al.* (2016). They show that the increase in NEA mackerel SSB occurred simultaneously with an increase in SSB of its competitor: Norwegian spring-spawning herring. Thus, increased interspecific competition for resources could also have caused or contributed to the observed growth decrease in NEA mackerel.

Our model assumes a homogeneously distributed resource spectrum with a carrying capacity that follows a Sheldon spectrum (Sheldon *et al.*, 1977). As a result of this, late-in-life resource competition is automatically highest for individuals with a size that is near the size-spectrum's biomass peak (Figure 1). In reality however, marine fish often move through different habitats and resources as they grow. These may differ in a multitude of aspects from each other, with each habitat or resource type being able to contribute to density-dependent effects. It is especially important to consider habitat size, as this can be a major factor in shaping density dependence (Casini *et al.*, 2016), in particular if habitat size changes during ontogeny (Andersen *et al.*, 2017). To truly consider density dependence taking place throughout life requires incorporating this heterogeneity into the resource spectrum. Since this heterogeneity will be highly stock-specific, that can only be properly done when sufficient knowledge is available about it. This is only rarely the case. In the absence of this knowledge, our model offers a simplified method for incorporating dependence both early and late in life.

We have assumed that decreased resource availability reduces the feeding level of the individual, and thereby its growth rate, without affecting size-specific mortality. A reduced growth rate does cause individuals to spend a longer time at a smaller size, where mortality rate is higher (Peterson and Wroblewski, 1984), which decreases their chances of survival. Nevertheless, this does not change the size-specific mortality rate. In an experiment on reef fish, Forrester (1990) shows that density-dependent growth can take place without an associated mortality increase. However, other studies show that decreased resource availability can increase mortality rate, resulting in density-dependent mortality as well as density-dependent growth. For instance, individuals can attempt to prevent their feeding level from decreasing too much by increasing their time spent searching for food (Wyatt, 1972; Walters and Juanes, 1993) or by taking greater risks during foraging (Damsgård and Dill, 1998). An increase in search rate or risk-taking puts the individual at a greater risk of predation (Walters and Juanes, 1993; Biro *et al.*, 2003, 2004), leading to an increased mortality rate. Furthermore, many fish stocks experience a reduction in body condition due to an increased stock density (e.g. Winters and Wheeler, 1994; Schindler *et al.*, 1997; Olafsdottir *et al.*, 2016). A decline in body condition can increase mortality rate. It may for instance decrease an individual's ability to avoid predation (Hoey and McCormick, 2004), or increase mortality risk after spawning (Lambert and Dutil, 2000). We have not incorporated such density-dependent mortality mechanisms in this study. If these above processes have influenced the data to which we have fitted our model, this could therefore influence the interpretation of our results. An additional presence of density-dependent mortality alongside the observed density-dependent growth would indicate that late-in-life density dependence was stronger than what we have found. Optimal size-at-entry for MSY exploitation would then likely be smaller than what we have found.

Interspecific density dependence

We have mainly focussed on intraspecific density dependence, providing a method for analysing density dependence in fish stocks from a single-stock management perspective. For a while now however, an increasing amount of fisheries research has been devoted to ecosystem-based management. When modelling

density dependence from an ecosystem perspective it is important to incorporate that fish stocks do not only experience intraspecific density dependence, but also react to density changes of interspecific prey, competitors, and predators. The model type that we have used can be a useful tool for describing density dependence throughout life from an ecosystem perspective. We have already partly done so in this study, by linking Baltic sprat predation mortality to Eastern Baltic cod stock size. However, we did this in a simplified way, and not for NEA mackerel or North Sea plaice. Fully incorporating interspecific density dependence into the model will require the addition of dynamic prey, competitor, and predator stocks. Unfortunately, the interplay between interspecific and intraspecific density dependence is hard to extract from field observations, and therefore difficult to accurately model. Nevertheless, understanding both of these processes is important for making long-term stock predictions, especially from an ecosystem point-of-view.

Conclusion

It is unlikely that the stocks examined in this study experience late-in-life density-dependent growth strong enough to decrease optimal fishery size-at-entry to below size-at-maturity. However, this could still change on a case-by-case basis, especially now that increased sustainable exploitation is increasingly leading to stock recovery in the NEA. This will likely lead to more available data on late-in-life density-dependent growth, which may change this conclusion. Nevertheless, right now the practice of advising a large fishery size-at-entry seems to be valid for the examined stocks, even in the presence of strong late-in-life density-dependent growth.

Supplementary data

Supplementary material is available at the ICESJMS online version of the article.

Acknowledgements

This work was supported by the Centre for Ocean Life, a VKR Centre of Excellence supported by the Villum Foundation. This work has received funding from the European Union's Horizon 2020 research and innovation programme under the Marie Skłodowska-Curie grant agreement No 675997.

References

- Alm, G. 1946. Reasons for the occurrence of stunted fish populations with special regard to the perch. Report from the Institute of Freshwater Research, Drottningholm, 25: 1–146.
- Andersen, K. H., and Beyer, J. E. 2006. Asymptotic size determines species abundance in the marine size spectrum. *The American Naturalist*, 168: 54–61.
- Andersen, K. H., and Beyer, J. E. 2015. Size structure, not metabolic scaling rules, determines fisheries reference points. *Fish and Fisheries*, 16: 1–22.
- Andersen, K. H., Farnsworth, K. D., Pedersen, M., Gislason, H., and Beyer, J. E. 2009. How community ecology links natural mortality, growth, and production of fish populations. *ICES Journal of Marine Science*, 66: 1978–1984.
- Andersen, K. H., Jacobsen, N. S., and Farnsworth, K. D. 2015. The theoretical foundations for size spectrum models of fish communities. *Canadian Journal of Fisheries and Aquatic Sciences*, 73: 575–588.
- Andersen, K. H., Jacobsen, N. S., Jansen, T., and Beyer, J. E. 2017. When in life does density dependence occur in fish populations? *Fish and Fisheries*, 18: 656–667.
- Berge, J., Heggland, K., Lønne, O. J., Cottier, F., Hop, H., Gabrielsen, G. W., Nøttestad, L. et al. 2015. First records of Atlantic mackerel (*Scomber scombrus*) from the Svalbard Archipelago, Norway, with possible explanations for the extension of its distribution. *Arctic*, 68: 54–61.
- Beverton, R. J. H., and Holt, S. J. 1957. On the Dynamics of Exploited Fish Populations. Her Majesty's Stationery Office, London, 540 pp.
- Biro, P. A., Abrahams, M. V., Post, J. R., and Parkinson, E. A. 2004. Predators select against high growth rates and risk-taking behaviour in domestic trout populations. *Proceedings of the Royal Society of London B: Biological Sciences*, 271: 2233–2237.
- Biro, P. A., Post, J. R., and Parkinson, E. A. 2003. Density-dependent mortality is mediated by foraging activity for prey fish in whole-lake experiments. *Journal of Animal Ecology*, 72: 546–555.
- Casini, M., Käll, F., Hansson, M., Plikhs, M., Baranova, T., Karlsson, O., Lundström, K., et al. 2016. Hypoxic areas, density-dependence and food limitation drive the body condition of a heavily exploited marine fish predator. *Royal Society Open Science*, 3: 160416.
- Cormon, X., Ernande, B., Kempf, A., Vermard, Y., and Marchal, P. 2016. North Sea saithe *Pollachius virens* growth in relation to food availability, density dependence and temperature. *Marine Ecology Progress Series*, 542: 141–151.
- Damsgård, B., and Dill, L. M. 1998. Risk-taking behavior in weight-compensating coho salmon, *Oncorhynchus kisutch*. *Behavioral Ecology*, 9: 26–32.
- Eero, M. 2012. Reconstructing the population dynamics of sprat (*Sprattus sprattus balticus*) in the Baltic Sea in the 20th century. *ICES Journal of Marine Science*, 69: 1010–1018.
- Fernandes, P. G., and Cook, R. M. 2013. Reversal of fish stock decline in the Northeast Atlantic. *Current Biology*, 23: 1432–1437.
- Forrester, G. E. 1990. Factors influencing the juvenile demography of a coral reef fish. *Ecology*, 71: 1666–1681.
- Froese, R., and Binohlan, C. 2000. Empirical relationships to estimate asymptotic length, length at first maturity and length at maximum yield per recruit in fishes, with a simple method to evaluate length frequency data. *Journal of Fish Biology*, 56: 758–773.
- Hartwig, M., Andersen, K. H., and Beyer, J. E. 2011. Food web framework for size-structured populations. *Journal of Theoretical Biology*, 272: 113–122.
- Hassell, M. P. 1975. Density-dependence in single-species populations. *Journal of Animal Ecology*, 44: 283–295.
- He, J. X., and Stewart, D. J. 2001. Age and size at first reproduction of fishes: predictive models based only on growth trajectories. *Ecology*, 82: 784–791.
- Hoey, A. S., and McCormick, M. I. 2004. Selective predation for low body condition at the larval-juvenile transition of a coral reef fish. *Oecologia*, 139: 23–29.
- Holling, C. S. 1959. The components of predation as revealed by a study of small-mammal predation of the European Pine Sawfly. *The Canadian Entomologist*, 91: 293–320.
- Hughes, K. M., Dransfeld, L., and Johnson, M. P. 2014. Changes in the spatial distribution of spawning activity by north-east Atlantic mackerel in warming seas: 1977–2010. *Marine Biology*, 161: 2563–2576.
- ICES. 2015a. Mackerel (*Scomber scombrus*) in Subareas I–VII and XIV and Divisions VIIIA–e and IXA (Northeast Atlantic). In ICES Advice 2015, Book 9.
- ICES. 2015b. Report of the Working Group on Widely Distributed Stocks (WGWHITE). ICES CM 2015/ACOM: 15.
- ICES. 2015c. Sprat (*Sprattus sprattus*) in Subdivisions 22–32 (Baltic Sea). In ICES Advice 2015, Book 8.

- Jennings, S., Oliveira, J. A. A. D. E., and Warr, K. J. 2007. Measurement of body size and abundance in tests of macroecological and food web theory. *Journal of Animal Ecology*, 76: 72–82.
- Jennings, S., Warr, K. J., and Mackinson, S. 2002. Use of size-based production and stable isotope analyses to predict trophic transfer efficiencies and predator-prey body mass ratios in food webs. *Marine Ecology Progress Series*, 240: 11–20.
- Jensen, A. L. 1996. Beverton and Holt life history invariants result from optimal trade-off of reproduction and survival. *Canadian Journal of Fisheries and Aquatic Sciences*, 53: 820–822.
- Köster, F. W., Möllmann, C., Neuenfeldt, S., Vinther, M., St John, M. A., Tomkiewicz, J., Voss, R. et al. 2003. Fish stock development in the central Baltic Sea (1974–1999) in relation to variability in the environment. *ICES Marine Science Symposia*, 219: 294–306.
- Lambert, Y., and Dutil, J.-D. 2000. Energetic consequences of reproduction in Atlantic cod (*Gadus morhua*) in relation to spawning level of somatic energy reserves. *Canadian Journal of Fisheries and Aquatic Sciences*, 57: 815–825.
- Lorenzen, K. 2005. Population dynamics and potential of fisheries stock enhancement: practical theory for assessment and policy analysis. *Philosophical Transactions of the Royal Society of London B: Biological Sciences*, 360: 171–189.
- Lorenzen, K., and Enberg, K. 2002. Density-dependent growth as a key mechanism in the regulation of fish populations: evidence from among-population comparisons. *Proceedings of the Royal Society of London B: Biological Sciences*, 269: 49–54.
- Margetts, A. R., and Holt, S. J. 1948. The effect of the 1939–1945 war on the English North Sea trawl fisheries. *Rapports et Procès-Verbaux des Réunions: Conseil Permanent International pour l'exploration de la mer*, 122: 26–46.
- Munch, S. B., Snover, M. L., Watters, G. M., and Mangel, M. 2005. A unified treatment of top-down and bottom-up control of reproduction in populations. *Ecology Letters*, 8: 691–695.
- Myers, R. A., and Cadigan, N. G. 1993. Density-dependent juvenile mortality in marine demersal fish. *Canadian Journal of Fisheries and Aquatic Sciences*, 50: 1576–1590.
- Neuheimer, A. B., Hartwig, M., Heuschele, J., Hylander, S., Kiørboe, T., Olsson, K. H., Sainmont, J. et al. 2015. Adult and offspring size in the ocean over 17 orders of magnitude follows two life history strategies. *Ecology*, 96: 3303–3311.
- Olafsdottir, A. H., Slotte, A., Jacobsen, J. A., Oskarsson, G. J., Utne, K. R., and Nottestad, L. 2016. Changes in weight-at-length and size-at-age of mature Northeast Atlantic mackerel (*Scomber scombrus*) from 1984 to 2013: effects of mackerel stock size and herring (*Clupea harengus*) stock size. *ICES Journal of Marine Science*, 73: 1255–1265.
- Peterson, I., and Wroblewski, J. S. 1984. Mortality rate of fishes in the pelagic ecosystem. *Canadian Journal of Fisheries and Aquatic Sciences*, 41: 1117–1120.
- Reichard, M., Jurajda, P., and Smith, C. 2004. Male-male interference competition decreases spawning rate in the European bitterling (*Rhodeus sericeus*). *Behavioral Ecology and Socio-Biology*, 56: 34–41.
- Ricker, W. E. 1954. Stock and Recruitment. *Journal of the Fisheries Research Board of Canada*, 11: 559–623.
- Rijnsdorp, A. D., and Van Leeuwen, P. I. 1992. Density-dependent and independent changes in somatic growth of female North Sea plaice *Pleuronectes platessa* between 1930 and 1985 as revealed by back-calculation of otoliths. *Marine Ecology Progress Series*, 88: 19–32.
- Savage, V. M., Gillooly, J. F., Brown, J. H., West, G. B., and Charnov, E. L. 2004. Effects of body size and temperature on population growth. *The American Naturalist*, 163: 429–441.
- Schindler, D. E., Hodgson, J. R., and Kitchell, J. F. 1997. Density-dependent changes in individual foraging specialization of largemouth bass. *Oecologia*, 110: 592–600.
- Sheldon, R. W., Sutcliffe, W. H. Jr., and Paranjape, M. A. 1977. Structure of pelagic food chain and relationship between plankton and fish production. *Journal of the Fisheries Board of Canada*, 34: 2344–2353.
- Van der Veer, H. W. 1986. Immigration, settlement, and density-dependent mortality of a larval and early postlarval 0-group plaice (*Pleuronectes platessa*) population in the western Wadden Sea. *Marine Ecology Progress Series*, 29: 223–236.
- Walters, C. J., and Juanes, F. 1993. Recruitment limitation as a consequence of natural selection for use of restricted feeding habitats and predation risk taking by juvenile fishes. *Canadian Journal of Fisheries and Aquatic Sciences*, 50: 2058–2070.
- West, G. B., Brown, J. H., and Enquist, B. J. 1997. A general model for the origin of allometric scaling laws in biology. *Science*, 276: 122–126.
- Winters, G. H., and Wheeler, J. P. 1994. Length-specific weight as a measure of growth success of adult Atlantic herring (*Clupea harengus*). *Canadian Journal of Fisheries and Aquatic Sciences*, 51: 1169–1179.
- Wyatt, T. 1972. Some effects of food density on the growth and behaviour of plaice larvae. *Marine Biology*, 14: 210–216.
- Ylikarjula, J., Heino, M., and Dieckmann, U. 1999. Ecology and adaptation of stunted growth in fish. *Evolutionary Ecology*, 13: 433–453.

Handling editor: Anna Kuparinen

CHAPTER 11

Paper III

Density dependence dampens the
impact of a non-constant
gonado-somatic index

*van Gemert, R., van Denderen, P. D., Jacobsen, N. S., and Andersen,
K. H.*

In preparation

2019

Density dependence dampens the impact of a non-constant gonado-somatic index

Rob van Gemert

rvge@aqua.dtu.dk

Corresponding author

P. Daniël van Denderen

pdvd@aqua.dtu.dk

Nis Sand Jacobsen

nisjac@uw.edu

Ken Haste Andersen

kha@aqua.dtu.dk

Centre for Ocean Life, National Institute of Aquatic Resources (DTU-Aqua),

Technical University of Denmark, Kemitorvet, Building 202, 2800 Kgs.

Lyngby, Denmark.

February 14, 2019

Abstract

The relationship between size and fecundity in female fish is considered important for stock management, but remains uncertain. Usually, by assuming a constant gonadosomatic index, the relationship is assumed to be isometric, but a recent study suggests a predominantly hyperallometric relationship. In this study, we aim to shed new light on the relationship between size and fecundity, as well as its importance to stock reproductive

output, by examining the size-fecundity data of 107 fish stocks. We fit an isometric and power law relationship to the data of each stock, and use the resulting parameters in an age-structured model with species-specific life-history parameters. We find considerable variability in the type of relationship between size and fecundity, both between species as well as between some stocks of the same species. Furthermore, when under the influence of fishing, the age-structured model predicts that stock egg production is likely lower when fecundity scales with size according to a power law, than when it follows an isometric relationship. However, through the use of a stock-recruitment, we find that early-life density dependence greatly dampens these possible differences in stock egg production, and stock recruitment is largely independent of the type of relationship between size and fecundity. Thus, this study concludes that there does not appear to be a single overarching relationship between fish size and fecundity, but rather that it can vary between stocks. Furthermore, we conclude that this type of relationship is usually of little importance for the management of the stock.

Keywords: Fish, fecundity, size, allometric scaling

Introduction

Knowledge on the reproductive output of a fish stock is important for the stock assessments of numerous stocks. For many fish stocks, reproductive output is not directly measured every year, but instead it is extrapolated based on the number of adult female fish that is estimated to be in the population. Therefore, it is important to know how many eggs a given adult female from the stock produces. In that regard, body size is one of the most important factors affecting the fecundity of a female fish. After all, as a fish grows larger, the amount of energy it can invest into reproduction becomes larger as well. More energy for reproduction presents the fish with two different strategies of increasing its fecundity: spawn more eggs while keeping the individual egg size roughly the same, or spawn larger eggs while keeping the number of spawned eggs roughly the same. Teleost fish follow the first strategy, and produce an increasing number of offspring as they grow larger whilst roughly maintaining the same offspring size throughout life (Neuheimer *et al.*, 2015). Elasmobranchs, for instance, appear to follow the second strategy, maintaining a hatchling size that is directly proportional to the size of the spawner (Neuheimer *et al.*, 2015). Here, we focus on teleost fish, as the majority of the world's fisheries yield comes from teleosts (FAO, 2018).

In marine teleost fish, it is often assumed that the weight of the gonads relative to somatic weight (the gonadosomatic index) is constant (e.g., Roff, 1983; Gunderson, 1997), making the number of eggs that a female fish produces directly proportional to body weight. This assumption of an isometric relationship between female fecundity and body size implies that, as a female fish grows in size, the number of eggs produced per unit body weight stays the same. However, there is also evidence that the relationship between female fecundity and body size

follows a power law instead (Hislop, 1988; Buckley *et al.*, 1991; Hixon *et al.*, 2013; Barneche *et al.*, 2018), meaning that the number of eggs produced per unit body weight changes as a female fish changes in size. If the number of eggs produced per unit body weight increases with female size, this can be called a hyperallometric relationship between fecundity and body size. On the other hand, if the number of eggs produced per unit body weight decreases with female size, this can be called a hypoallometric relationship between fecundity and body size. For a power law $E_a = \alpha w^\beta$, where E_a is individual egg production and w is female body weight, the relationship would be hyperallometric if the value of the exponent β would be greater than 1, whereas it would be hypoallometric if the value of β would be smaller than 1. If $\beta = 1$, the power law reverts back to an isometric relationship.

In a recent paper, Barneche *et al.* (2018) showed that fecundity of female fish generally increases hyperallometrically with body size, by fitting a linear hierarchical model to data of 342 fish species. Barneche *et al.* (2018) state that this hyperallometric relationship is "not the exception but rather the rule for marine fishes". They argue that, due to this hyperallometric relationship between fecundity and body size, large adult female fish are responsible for a disproportionately high portion of the reproductive output of a fish stock, resulting in major implications for population replenishment and stock management. Andersen *et al.* (2019), however, contest the implications suggested by Barneche *et al.* (2018). Using data from the Icelandic cod stock (*Gadus morhua*), Andersen *et al.* (2019) show how the discrepancy in stock reproductive output between an isometric and hyperallometric scaling of size-specific fecundity is only on the order of 10%. Even though Andersen *et al.* (2019) only explored one stock, and their result may just be anecdotal, a hyperallometric relationship between fecundity and body size may not be as prevalent as suggested by Barneche *et al.* (2018).

The question remains, therefore, whether hyperallometry in size-specific fecundity is really the rule, as claimed by Barneche *et al.* (2018). In their study, Barneche *et al.* (2018) included many stocks with 1 or just a few data points, and did not show the raw data. Further, they employed a statistical method that exploited phylogenetic relationships between species. This assumes that hyperallometry in size-specific fecundity is a species-specific phenomena; some species have a hyperallometric relationship between fecundity and size, while others do not. In other words, this assumes that hyperallometry is tied to physiology. However, hyperallometry in size-specific fecundity could also be a result of ecological interactions. As fish grow, they typically go through ontogenetic feeding niche shifts (Persson, 1988; Osenberg *et al.*, 1994), meaning that the feeding environment changes during ontogeny. This may lead to variations in consumption which translate into variations in growth and, for adults, also in reproductive effort. Such changes in the feeding environment and body conditions have, for instance, been documented for Icelandic cod (Marteinsdottir and Begg, 2002) and Baltic cod (Eero *et al.*, 2012; Casini *et al.*, 2016). If hyperallometry is the result of such ecological changes, it will vary between stocks of the same species. In that case, it is inappropriate to use a statistical methodology that exploits the phylogenetic relation between species.

Moreover, when fecundity scales hyperallometrically with female size instead of isometrically, it is unclear what the implications for the stock would be. Firstly, smaller adults are far more abundant in a stock than larger adults. Thus, it is possible that smaller adults are responsible for a far greater egg production than larger adults simply by virtue of this greater abundance, which may decrease the importance of the relationship between size and fecundity for total egg production of the stock. Furthermore, the implications suggested by Barneche *et al.* (2018) depend on the assumption that egg production translates directly into recruitment to the stock. However, recruitment to the stock is often highly density-dependent, especially in stocks with a larger asymptotic size, and therefore larger adults (Andersen and Beyer, 2015). Under the influence of density dependence, recruitment is no longer directly proportional to egg production. Instead, recruitment levels off (Beverton-Holt stock-recruitment relationship; Beverton and Holt, 1957) or even decreases (Ricker stock-recruitment relationship; Ricker, 1954) with increasing egg production. Therefore, even if large adult female fish contribute a disproportionately-large number of eggs to the reproductive output of the stock, it could be possible that this effect is lost through the dampening effect of density-dependent recruitment (Calduch-Verdiell *et al.*, 2014).

In this study, we aim to examine whether the relationship between fecundity and female size in marine fish is predominantly hyperallometric, or whether there is variability among stocks. This could also help shed light on whether hyperallometry in fecundity is determined by physiology or ecology. Furthermore, we aim to examine whether the type of relationship between fecundity and female size has a meaningful impact on recruitment to the stock, or whether it is actually of little importance. To this end, we first make use of the size-fecundity data provided by Barneche *et al.* (2018), and fit a power law and isometric relationship to the data of each separate stock. Then, using the parameters obtained from these fits, we run an age-structured model for each stock to obtain egg production and recruitment figures for both the power law and isometric relationship. Thus, we are able to investigate to what degree the total egg production, as well as recruitment, of a stock is different when fecundity scales either isometrically or according to a power law with female body size.

Methods

We extracted data on female size w (g), length l (cm), and associated fecundity R (number of eggs produced) for 234 stocks (Appendix A, Table A.1), using the raw data provided by Barneche *et al.* (2018). We proceeded to divide individual fecundity by female weight to obtain weight-specific fecundity R_w (#/g). Where possible, we used the data where female size was provided in weight. When female size was provided in length, we used the same method as Barneche *et al.* (2018) to convert this to weight, namely use the highest-scored length-weight conversion parameters from Fishbase (Froese and Pauly, 2000) for that specific species. An overview of the w and R_w data for all stocks, including a moving average of R_w generated by

local regression, is provided in Appendix A.

Here, we have only made use of the size and fecundity data provided by Barneche *et al.* (2018). However, Barneche *et al.* (2018) also provide data on egg volume and energetic content, and use these to find that overall egg-specific energetic content increases with female size, with an exponent of 0.91. This scaling may be hypoallometric, but still implies that the energetic content of an egg increases quite substantially with female size, a relationship that should not be disregarded. Barneche *et al.* (2018) arrive at this exponent of 0.91 from Equation 5 from their material and methods: Egg-energy = $\beta_{0M3}\beta_{0M2}^{\beta_{1M3}}\text{Mass}^{\beta_{1M2}\times\beta_{1M3}}$, with $\beta_{1M2}\times\beta_{1M3} = 0.91$. The values of β_{1M2} and β_{1M3} should be taken from the exponents of the power law fits to the data of female mass and egg volume, and the data of egg volume and egg energy. However, as Barneche *et al.* (2018)'s Figure 2 indicates, these exponent values are $\beta_{1M2} = 0.14$ and $\beta_{1M3} = 0.77$, and their product is 0.11. Here, we consider an exponent of 0.11 small enough to be ignored. Thus, we conclude that the increase in egg energetic content with female size is negligible. Therefore, we use only data on female size and number of eggs.

Next, we fit an isometric and power law relationship to the data. The power law relationship is standard and follows $R_w = \alpha w^\beta$, while the isometric relationship follows $R_w = \mu_{R_w}$, where μ_{R_w} is a mean value derived from the data of R_w . Here, R_w is given in terms of eggs per unit weight. We used linear regression to fit these isometric and power law relationships to the log-transformed data of w and R_w :

$$\ln R_{w,i} = \ln \alpha_i + \beta_i \ln w_i + \varepsilon_i \quad (1)$$

$$\ln R_{w,i} = \alpha_i + \varepsilon_i \quad (2)$$

where ε is the log-normally distributed error. In this regression analysis, we use R_w as the response variable, which has units of number of eggs per unit weight. Thus, for an isometric relationship, β is equal to 0 instead of 1. In Equation 2 therefore, the term βw has been dropped and α_i has been set equal to the mean of all $\ln R_w$ values of the stock, $\mu_{\ln R_w}$. Barneche *et al.* (2018), on the other hand, show regression results with R as the response variable, which has units of number of eggs. Thus, the power law exponent β that we find is comparable to the exponent reported by Barneche *et al.* (2018) plus 1.

The regression analysis calculates a standard error for each power law exponent β , which is used to calculate a 95% confidence interval of the exponent as well as a p -value. This p -value of the β exponent indicates whether or not β significantly differs from 0. If $p > 0.05$, it is assumed that β does not significantly differ from 0, and the power law therefore reverts to an isometric relationship.

Furthermore, for each stock, the quality of the isometric and power law fit was examined by looking at the value of the residual sum of squares (RSS) and the Akaike information criterion (AIC), where a lower RSS indicates a better fit to the data, and a lower AIC indicates which model better represents the data. An example of the output of this fitting procedure is displayed

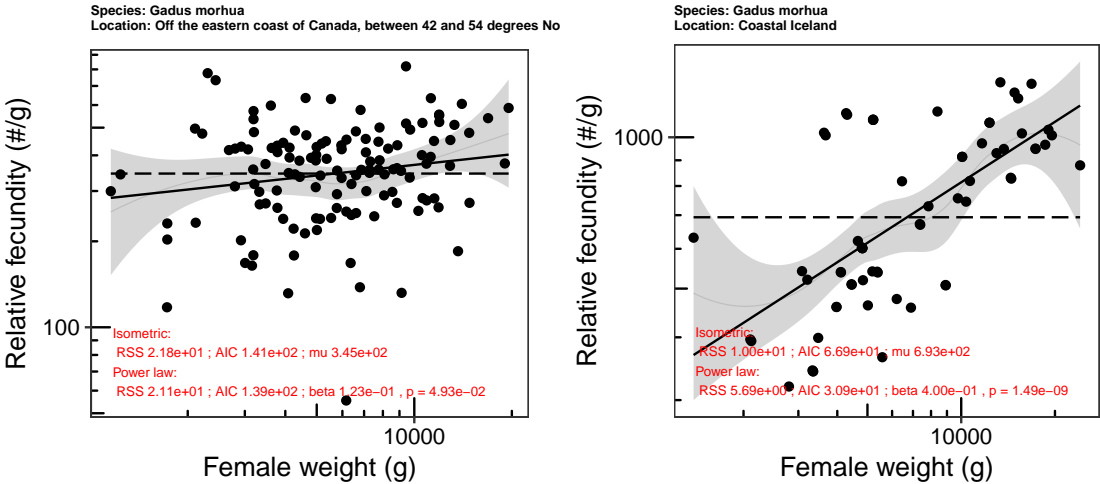


Figure 1: An example of the output of the isometric (dashed) and power law (solid) relationship fits between fecundity and size, for two different cod stocks. The red text shows information on the fit of the isometric and power law relationship. For the isometric fit, the RSS, AIC, and μ_{R_w} values are shown, where $\mu_{R_w} = e^{\mu_{\ln R_w}}$. For the power law fit, the RSS, AIC, β , and β p -values are shown. The grey line and grey area show the smoothed conditional mean of the data points with 95% confidence interval.

in Figure 1, which shows two cod stocks with different qualities of the fitted power law and isometric relationship between fecundity and size.

Many stocks only have a few w and R_w data points available (Appendix A). With so few data points, fits to these stocks will likely return a power law exponent with a very wide confidence interval and an insignificant p -value, rendering the comparison between the power law and isometric relationship rather meaningless. Therefore, to make sure that only meaningful fits to the data were made, this linear regression analysis was only performed for stocks with at least 20 data points. Furthermore, the data of some stocks are clearly not raw data but the output of a model, due to the absence of any variability, as can for instance be seen in the data of *Sebastodes brevispinis* (Appendix A). *Sebastodes brevispinis* was the only stock with at least 20 data points that did clearly not consist of raw data, and was therefore also removed from the subsequent analyses. In total, the number of analyzed stocks was reduced from 234 to 107 (Table A.2, Appendix A).

Stock Model

In order to compare the reproductive output of the fitted isometric and power law relationships for each stock, we created a simple age-structured model (Table 1) where reproductive output was calculated both with the fitted isometric relationship and with the fitted power law relationship of each stock. Weight w_a at age a is described according to a standard von-Bertalanffy growth equation, where asymptotic length L_∞ has been converted to asymptotic weight W_∞ (M1). Maturity-at-age ψ_a follows a sigmoidal curve that increases from 0 to 1 around weight

at 50% maturity w_{mat} (M2 & M3). Similarly, fishing mortality F is also distributed over the stock according to a sigmoidal trawl-selectivity curve, which increases from 0 to 1 around the size-at-entry w_F , describing the fishing mortality a given individual is exposed to as F_a (M4). Here, w_F has been set equal to w_{mat} . Individual fecundity E_a (number of eggs produced per individual of age a per year) is calculated by multiplying maturity-at-age with individual weight-at-age and size-specific individual fecundity, which follows either a power law, or an isometric relationship (M5a & M5b).

Recruitment R is calculated with a Beverton-Holt stock-recruitment relationship. Because the value of R_{\max} is highly stock-specific, difficult to assess, and ultimately irrelevant in this context, the steady state of R was calculated relative to maximum recruitment R_{\max} , as follows: In steady state, abundance-at-age N_a can be described as: $N_a = R e^{-(M+F_a)a}$, where M is natural mortality. Dividing on both sides by maximum recruitment gives

$$\frac{N_a}{R_{\max}} = \frac{R}{R_{\max}} e^{-(M+F_a)a} \quad (3)$$

Similarly, the annual number of eggs produced by the stock E can be written relative to maximum recruitment as

$$\frac{E}{R_{\max}} = \sum_a \varepsilon_R E_a \frac{N_a}{R_{\max}} = \frac{R}{R_{\max}} E' \quad (4)$$

where ε_R is the recruitment efficiency of the stock, representing loss of eggs due to mortality and non-fertilization. Furthermore, $E' = \sum_a \varepsilon_R E_a e^{-(M+F_a)a}$ for notational simplicity. A Beverton-Holt stock-recruitment relationship describes recruitment as

$$R = R_{\max} \frac{P_R E'}{P_R E' + R_{\max}} = R_{\max} \frac{P_R E' / R_{\max}}{P_R E' / R_{\max} + 1} \quad (5)$$

where P_R is the survivorship of an egg to age at recruitment (M6). For simplicity, age at recruitment has been set to 1 here. Inserting E/R_{\max} and isolating R/R_{\max} gives

$$\frac{R}{R_{\max}} = 1 - \frac{1}{P_R E'} \quad (6)$$

Thus, aside from giving us the solutions for the recruitment of the stock (M7) and the abundance-at-age of the stock (M8), this series of equations also gives us both the egg production of a single cohort (M9), as well as the egg production of the entire stock (M10), all relative to R_{\max} .

The parameters used in the model are listed in (Table 2). Stock-specific life-history parameters were used to tune the model to each stock (Appendix A, Table A.2). The value of b was obtained from Fishbase (Froese and Pauly, 2000), and the values of the other life-history parameters were obtained using the R package *FishLife* Thorson *et al.* (2017), which applies a multivariate model that uses life history and taxonomic data to generate predictions for mortality, maturity, size, and growth. However, for several stocks, all w data-points were smaller

than the weight-at-age of 50% maturity as predicted by the FishLife package age-at-maturity parameter. Therefore, instead of using the FishLife package to predict weight-at-maturity, we assumed that the smallest w data-point of a stock would be at a weight-at-age of 25% maturity.

For each stock i , egg production of the stock is compared between the isometric and power law relationship by calculating the percentage relative error δ_E of the power law stock egg production (E_P) as compared to the isometric stock egg production (E_I):

$$\delta_{E,i} = \frac{E_{P,i} - E_{I,i}}{E_{I,i}} 100\% \quad (7)$$

where E_P and E_I have both been calculated using Equation M10. The R_{\max} division from M10 is absent in Equation 7 because it is on both sides of the fraction, and can therefore be removed in the notation. Similarly, for each stock i , recruitment is compared between the isometric and power law relationship by calculating the percentage relative error δ_R of the power law recruitment (R_P) as compared to the isometric recruitment (R_I):

$$\delta_{R,i} = \frac{\sum R_{P,i} - \sum R_{I,i}}{\sum R_{I,i}} 100\% \quad (8)$$

Fishing mortality will influence the values of δ_E and δ_R . Therefore, the model was run for two different scenarios: one with and one with no fishing mortality. When the model was run with fishing mortality, the value of the maximum fishing mortality F was set equal to the stock's natural mortality M .

Results

The parameter values of the isometric and power law relationship fits are shown for each stock in Appendix B, Table B.1. In total, for 57 out of the 107 fitted stocks the power law exponent β was significantly different from 0 ($p < 0.05$). For the remaining 50 fitted stocks, the power law relationship did not significantly differ from an isometric relationship. The frequency distribution for the power law exponent β is shown in Figure 2, and is shown both for only the statistically-significant exponent values as well as for all the exponent values. For each stock, an RSS and AIC value was calculated for the power law and isometric relationship (Appendix B, Table B.1).

Furthermore, Figure 3 shows how the value of β differs among stocks of the same species. There, it can be seen that for some stocks of the same species, there is relatively little variability in the values of β . This can for instance be seen for the various stocks of neon damselfish (*Pomacentrus coelestis*) and sole (*Solea solea*). For several other species there is more variability in the β value of their stocks, as can be seen for grey triggerfish (*Balistes capriscus*), cod (*Gadus morhua*), and boccacio (*Sebastes paucispinis*).

The above results indicate whether a power law relationship between female w and R_w

Table 1: Age-structured model equations.

Von Bertalanffy growth	$w_a = W_\infty(1 - e^{-Ka})^b$	M1
Weight at 50% maturity	$w_{\text{mat}} = w_{\min}(m^{-1} - 1)^{1/u_m}$	M2
Maturity ogive	$\psi_a = (1 + (w_a/w_{\text{mat}})^{u_m})^{-1}$	M3
Fishing mortality	$F_a = F(1 + (w_a/w_F)^{u_F})^{-1}$	M4
Individual fecundity, power law	$E_a = \psi_a w_a \alpha w_a^\beta$	M5a
Individual fecundity, isometric relationship	$E_a = \psi_a w_a \mu_{R_w}$	M5b
Survivorship from egg to age 1	$P_R = (\frac{w_1}{w_{\text{egg}}})^{-a_p}$	M6
Recruitment	$\frac{R}{R_{\max}} = 1 - \frac{1}{P_R \sum_a \varepsilon_R E_a \exp(-(M + F_a)a)}$	M7
Abundance-at-age	$\frac{N_a}{R_{\max}} = \frac{R}{R_{\max}} \exp(-(M + F_a)a)$	M8
Cohort egg production	$\frac{E_{C,a}}{R_{\max}} = E_a \frac{N_a}{R_{\max}}$	M9
Stock egg production	$\frac{E}{R_{\max}} = \sum_a E_a \frac{N_a}{R_{\max}}$	M10

Table 2: Description and values of the parameters used in the age-structured model (Table 1).

Symbol	Description	Value	Unit
W_∞	Asymptotic size	stock-specific	g
K	Von Bertalanffy growth constant	stock-specific	yr^{-1}
b	Length-weight conversion exponent	stock-specific	-
w_{\min}	Smallest w data-point of the stock	stock-specific	g
m	Maturity of w_{\min}	0.25	-
u_m	Maturity ogive steepness	5	-
u_F	Trawl selectivity steepness	3	-
F	Maximum fishing mortality	0 or M	yr^{-1}
w_F	Fishery size-at-entry	w_{mat}	g
M	Natural mortality	stock-specific	yr^{-1}
a_p	Physiological mortality ¹	0.35	-
ε_R	Recruitment efficiency	0.1	-
μ_{R_w}	Mean of weight-specific egg production	$\exp \mu_{\ln R_w}$	# g $^{-1}$

¹ Andersen and Beyer (2015).

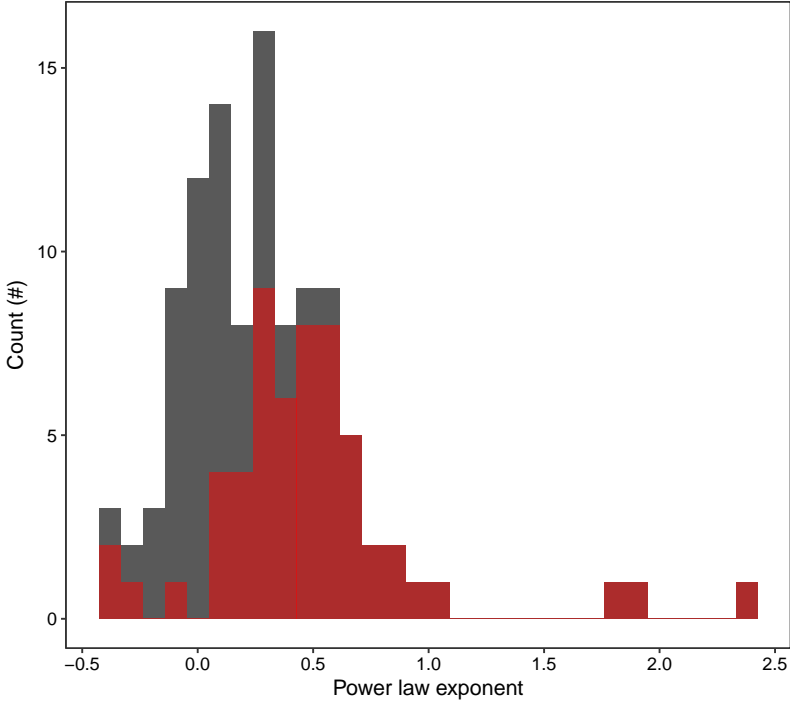


Figure 2: Distribution of the fitted exponent β values of the power law relationship between weight and size-specific reproductive output. Shown for only statistically-significant exponent values (red) and all exponent values (grey), with all red columns therefore contained within the grey columns (also when they overlap). In total, for 57 stocks the power law fit exponent was statistically significant ($p < 0.05$), whereas for 50 exponents it was non-significant.

is prevalent or not. However, the question that remains unanswered is whether this type of relationship actually matters in terms of recruitment to the stock. For this, the population model was used to calculate stock fecundity E and stock recruitment R , for both the power law and isometric relationship between female w and R_w , after which a percentage relative error was calculated (Eq. 7 & 8). The egg production percentage relative error δ_E appears to be evenly distributed around 0% in the absence of fishing (Figure 4a), indicating a roughly equal egg production between the power law and isometric relationship. Furthermore, it is clear that the stock-recruitment relationship greatly reduces the variance observed for δ_E , with the recruitment percentage relative error δ_R being very closely centered around 0% (Figure 4a) with almost no variance.

In the presence of fishing, there is a clear trend toward a negative value for δ_E (Figure 4b), indicating lower egg production when the relationship between female w and R_w follows a power law than if it were to be isometric. However, it is clear that this effect is lost through the stock-recruitment relationship, as δ_R is again centered very closely around 0% with almost no variance.

Lastly, Appendix B Figure B.1 provides a detailed overview of the stock-specific data-

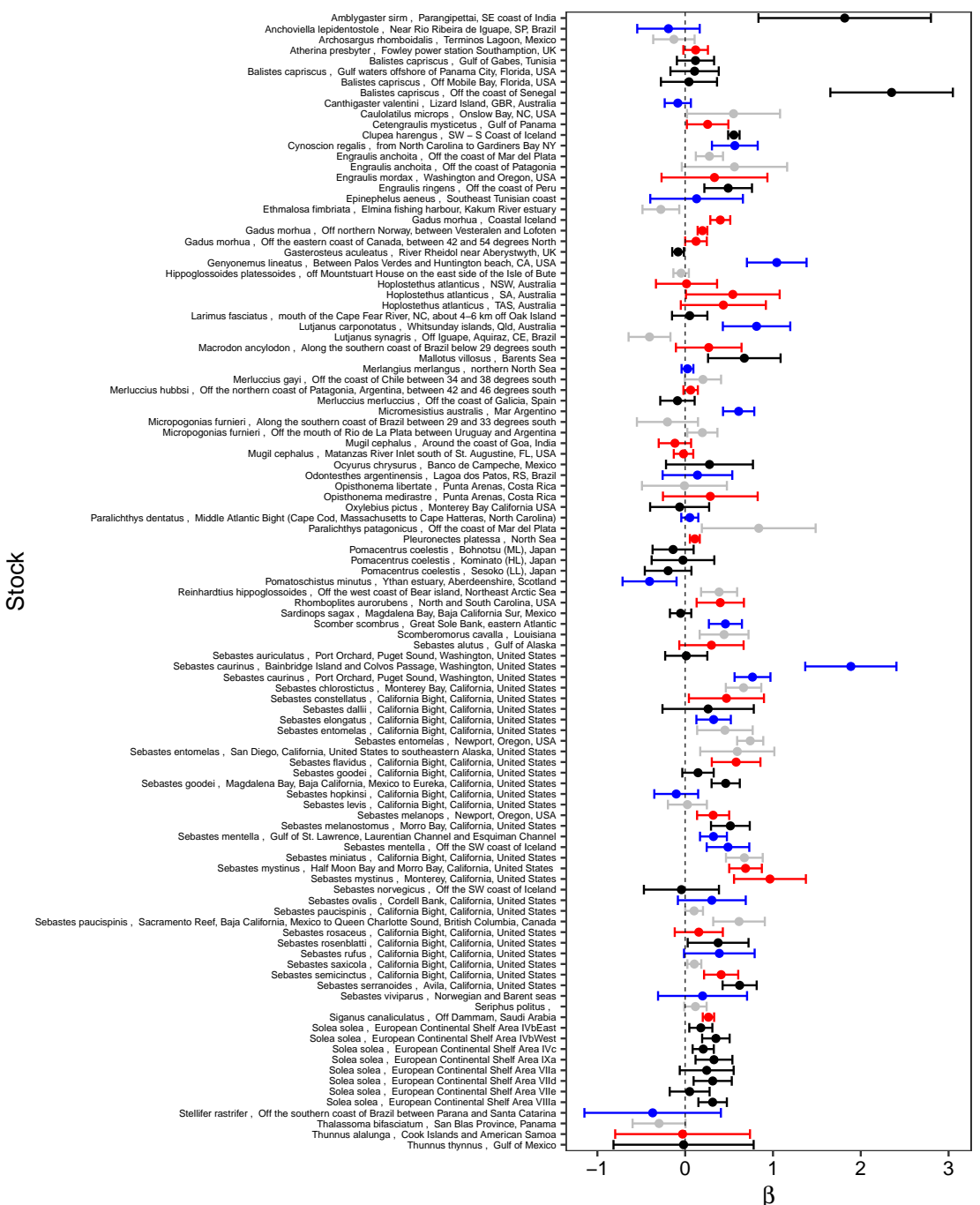


Figure 3: Stock-specific values of the power law exponent β , including the 95% confidence interval. The vertical dashed line shows $\beta = 0$, which would be analogous to an isometric relationship. Species is indicated by colour, with successive data points of the same colour belonging to stocks of the same species. Thereby, the differences in β values between stocks of the same species can be better observed.

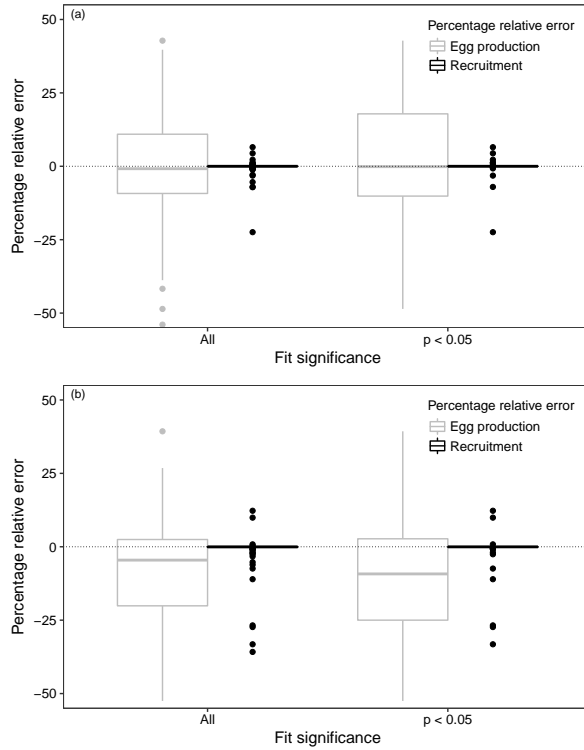


Figure 4: Distribution of percentage relative error of the power law egg production, compared to the isometric egg production (δ_E , grey), as well as of percentage relative error of the power law recruitment, compared to the isometric recruitment (δ_R , black). Shown for all fitted stocks, and only for the stocks with a statistically-significant power law fit. Shown for a scenario of no fishing (a) and for a scenario where $F = M$ (b).

points for w and R_w , the associated isometric and power law relationship fits (including values for RSS and AIC), their respective egg production in both a fished and unfished scenario, and their values of δ_E and δ_R . There, it can also be seen that for several stocks, the applied level of fishing mortality resulted in a non-viable population with zero recruitment. Furthermore, very rarely, the egg mortalities imposed by ϵ_R and P_R also resulted in a non-viable population when $F = 0$, indicating that ϵ_R was set too high for these stocks. These stocks were not incorporated in Figure 4.

Discussion

The results of this study suggest that the relationship between female size and fecundity is not always best described by a hyperallometric relationship. Out of the 107 stocks that had 20 or more data points, only 57 ended up having a power law exponent β with an estimated value that significantly differed from 0. Out of those 57, a further 4 had a negative value estimated for β , suggesting a hypoallometric relationship between female size and fecundity

instead of a hyperallometric one. Thus, the results indicate that there is no clear dominance of hyperallometry in the relationship between fecundity and female size. These findings are similar to those of Barneche *et al.* (2018), in that their results also show quite a number of stocks for which the exponent cannot be said to significantly differ from isometry, due to the breadth of its confidence interval. Contrary to Barneche *et al.* (2018), however, we imply that these results suggest that the presence of a hyperallometric relationship between fecundity and female size is not the norm among marine fish stocks, but that it varies between stocks.

Furthermore, this study shows that there can be considerable variability in the value of the power law exponent, both between species but also between stocks of a single species (Figure 3). Therefore, as can also be seen from the stock-specific plots in Appendix B, whether the relationship between female size and fecundity is hyperallometric or isometric (and sometimes hypoallometric) can vary on a stock-by-stock basis, without a general preference for one or the other.

Although the results show the possibility for variability in exponent values of stocks of the same species, for some species exponent values of stocks were more consistent (Figure 3). This raises questions about the mechanism behind fecundity and female size. Ultimately, two different mechanisms can be hypothesized. First, the relationship between fecundity and female size can be an adaptive response determined through phylogeny and life-history adaptations and emerges as a result of the individual's physiology. In such a case, a consistent power law exponent among stocks of the same species can be expected. Second, the relationship can be a direct response to the food environment and emerges due to the limitations of the individual's metabolic energy. In such a case, the power law exponent among stocks of the same species can be expected to be variable. Since we have observed both variability as well as consistency among the exponent values of stocks of the same species, it remains unclear which mechanism is prevalent, and it is possible that both are involved in determining whether the relationship between fecundity and size follows an isometric or power law relationship. Thus, more research is needed to precisely determine what the origin is of the relationship between fecundity and female size. Until then, we advise to examine the relationship between fecundity and size on the stock level instead of the species level.

The absence of a general trend for hyperallometry in the scaling of fecundity with size could be because many of the studied stocks have been historically exploited, meaning that their size distributions are truncated. The smaller the realized size range in the stock, the harder it is to obtain data to significantly determine a hyperallometric relationship between size and fecundity. The use of exploited species therefore risks under-appreciating the generality of hyperallometric scaling.

Next, the question remains whether the relationship between female size and fecundity actually matters for the recruitment to the stock. Our age-structured population model with species-specific life-history parameters showed that, when a fishing mortality $F = M$ is applied to the stock, egg production is lower for a power law relationship than for an isometric relation-

ship (Figure 4). However, it appears that density dependence in the early pre-recruit life stages largely removes this effect, and that there is little variance in overall stock recruitment when comparing between the two types of relationships between female size and fecundity. Thus, it can be expected that the way in which reproductive output scales with female size has only limited implications for stocks that are harvested at a fishing mortality consistent with obtaining maximum sustainable yield. For instance, the value of the F_{MSY} and B_{MSY} reference points is unlikely to be impacted. The exception to this would be stocks that do not experience strong density-dependent recruitment.

However, if higher levels of fishing mortality were to be applied, the buffering capacity of the pre-recruit density dependence would degrade. In other words, the stock would move further to the left on the stock-recruitment relationship curve. This would increase the effect that the egg production of the stock has on its overall recruitment. Thus, stocks of which fecundity scales with female size according to a power law will sooner be impacted by overfishing than stocks where it scales isometrically, because of the lower egg production from the power law relationship under fished conditions. For instance, it is likely that the value of the F_{lim} and B_{lim} will be higher for stocks where fecundity follows a power law than if an isometric relationship were to be assumed for the same stock.

In this study, we have applied a simple linear regression analysis to the data of each separate stock with more than 20 data points, to obtain stock-specific parameters for the relationship between fecundity-per-unit-weight and female size. Barneche *et al.* (2018), on the other hand, used a more advanced linear hierarchical model on the combined data of all species (including those with only 1 data point), incorporating species uniqueness and phylogenetic relatedness as random effects for the coefficient, and only species uniqueness as a random effect for the exponent of the relationship between fecundity and female size. This advanced analysis of Barneche *et al.* (2018) is able to explain a greater variance in their data, and it is thus possible that their calculated exponent values are more reliable than the ones we have calculated here. Our analysis leaves more variance unexplained, but it still provides a straightforward and robust analysis for the stock-specific relationship between fecundity and female size. Furthermore, for the management of a specific stock, it is more likely that a single-stock data-analysis such as ours will be performed.

The data analyzed in this study does not contain a representative selection of marine fish stocks. Rather, it is biased towards stocks of species for which the relationship between fecundity and female size has been deemed important-enough to study. These will mainly be species which have a high commercial value and which are caught by nations with a long tradition of fisheries management and research (e.g., cod and sole), or stocks which have a high conservation value (*Sebastodes*). For instance, the data includes 8 closely-related stocks of sole, and 35 stocks of the *Sebastodes* genus (which has a range that is largely limited to the US west coast). Thus, the relationships found here between fecundity and female size may not extend to all fish stocks in general.

The prevalence of *Sebastodes* in the data may add further bias in the results because most *Sebastodes* species have a life-history that could be considered inordinary for many species of fish. Compared to similarly-sized fish, *Sebastodes* species generally have a low growth rate (Mangel, 2003) and a very high maximum age (Mangel *et al.*, 2007). This has been hypothesized to be an adaptation to the large degree of environmental variability in their habitat, where conditions can change rapidly between states that can last decades (Mangel, 2003). Additionally, many *Sebastodes* species exhibit viviparity (Wourms, 1991), meaning their eggs are fertilized internally and they give birth to live young. In their analysis Barneche *et al.* (2018) address this over-representation by *Sebastodes* species by showing that there is no significant difference between their model and one where phylogenetic relatedness is introduced as a random effect for the exponent of the relationship between fecundity and female size. Thus, it seems that the potential bias resulting from *Sebastodes*'s inordinary life-history is limited in scope, and can be disregarded.

In our age-structured population model, we obtained species-specific life-history parameter values by making use of the new *FishLife* R package of Thorson *et al.* (2017). However, just like how the relationship between fecundity and female size can differ among stocks of the same species, so too can life-history parameters. Thus, it is possible that there are some inaccuracies in the values of the used life-history parameters. This was made evident, for instance, by the values of the age at 50% maturity parameters predicted by Thorson *et al.* (2017), which resulted in multiple stocks having all of their w data points at a size smaller than the predicted size at 50% maturity, which made us set the size at 50% maturity manually. Thus, our analysis of how egg production translates into recruitment could be made more accurate by the use of stock-specific parameters that are based on empirical observations. However, such parameters are unavailable for many stocks. In the absence of stock-specific parameters, our preliminary conclusion is that density dependence early in life often makes it irrelevant to determine the type of relationship between fecundity and female size.

Even though it appears that the relationship between fecundity and female size is often of little consequence to recruitment to the stock, there could also be other reasons for selectively preserving the larger fish of a stock. For instance, there is evidence to suggest that the migratory behaviour of herring is passed on from older fish to younger ones (Corten, 2002). For stocks that rely on memory and learning for their spawning and feeding migrations, a loss of older fish could then result in the loss of knowledge on migratory pathways. Furthermore, under certain conditions of size selectivity and fishing mortality, the negative effects of fisheries-induced evolution can be counteracted by avoiding the capture of larger adults (Jørgensen *et al.*, 2009). Thus, the relationship between fecundity and female size is one of multiple factors that should be considered when studying the potential benefits of preserving larger fish.

Conclusion

There does not appear to be one overarching relationship between female size and fecundity. Rather, whether the relationship is isometric, hyperallometric, or hypoallometric can be species- or stock-specific, possibly resulting from species-specific life-history adaptions or from stock-specific differences in the food environment. In the presence of strong early-life density-dependent regulation, the relationship between female size and fecundity has little influence on recruitment to the stock, and therefore can be expected to be inconsequential in the calculation of fisheries advice such as MSY target reference points. However, if an isometric relationship is assumed when in actuality the relationship is hyperallometric, there is some risk at calculating inaccurate limit reference points. Thus, we conclude that there does not appear to be major reason for concern that hyperallometry in fecundity is often not incorporated in stock assessment, but that it would be prudent to include if hyperallometry is obviously present. There may, however, be other reasons to selectively protect larger fish, such as preserving spawning migrations, or counteracting the effects of fishing-induced evolution.

References

- Andersen, K. H. and Beyer, J. E. 2015. Size structure, not metabolic scaling rules, determines fisheries reference points. *Fish and Fisheries*, 16: 1–22.
- Andersen, K. H., Jacobsen, N. S., and van Denderen, P. D. 2019. Limited impact of big fish mothers for population replenishment. *Canadian Journal of Fisheries and Aquatic Sciences*.
- Barneche, D. R., Robertson, D. R., White, C. R., and Marshall, D. J. 2018. Fish reproductive-energy output increases disproportionately with body size. *Science*, 360: 642–645.
- Beverton, R. J. H. and Holt, S. J. 1957. On the Dynamics of Exploited Fish Populations. Her Majesty's Stationery Office, London, 540 pp.
- Buckley, L. J., Smigielski, A. S., Halavik, T. A., Calderone, E. M., Burns, B. R., and Laurence, G. C. 1991. Winter flounder *Pseudopleuronectes americanus* reproductive success. II. Effects of spawning time and female size on size, composition and viability of eggs and larvae. *Marine ecology progress series*. Oldendorf, 74: 125–135.
- Calduch-Verdiell, N., MacKenzie, B. R., Vaupel, J. W., and Andersen, K. H. 2014. A life-history evaluation of the impact of maternal effects on recruitment and fisheries reference points. *Canadian journal of fisheries and aquatic sciences*, 71: 1113–1120.
- Casini, M., Käll, F., Hansson, M., Plikshs, M., Baranova, T., Karlsson, O., Lundström, K., *et al.* 2016. Hypoxic areas, density-dependence and food limitation drive the body condition of a heavily exploited marine fish predator. *Royal Society Open Science*, 3: 160416.

- Corten, A. 2002. The role of "conservatism" in herring migrations. *Reviews in Fish Biology and Fisheries*, 11: 339–361.
- Eero, M., Vinther, M., Haslob, H., Huwer, B., Casini, M., StorrPaulsen, M., and Köster, F. W. 2012. Spatial management of marine resources can enhance the recovery of predators and avoid local depletion of forage fish. *Conservation Letters*, 5: 486–492.
- FAO 2018. The State of World Fisheries and Aquaculture 2018 - Meeting the sustainable development goals. Food & Agriculture Organization of the United Nations, Rome.
- Froese, R. and Pauly, D. 2000. FishBase 2000: concepts, design and data sources. ICLARM, Los Baños, Laguna, Philippines, 344 pp.
- Gunderson, D. R. 1997. Trade-off between reproductive effort and adult survival in oviparous and viviparous fishes. *Canadian Journal of Fisheries and Aquatic Sciences*, 54: 990–998.
- Hislop, J. R. G. 1988. The influence of maternal length and age on the size and weight of the eggs and the relative fecundity of the haddock, *Melanogrammus aeglefinus*, in British waters. *Journal of Fish Biology*, 32: 923–930.
- Hixon, M. A., Johnson, D. W., and Sogard, S. M. 2013. BOFFFFs: on the importance of conserving old-growth age structure in fishery populations. *ICES Journal of Marine Science*, 71: 2171–2185.
- Jørgensen, C., Ernande, B., and Fiksen, Ø. 2009. Sizeselective fishing gear and life history evolution in the Northeast Arctic cod. *Evolutionary applications*, 2: 356–370.
- Mangel, M. 2003. Environment and longevity: the demography of the growth rate. *Population and Development Review*, 29: 57–70.
- Mangel, M., Kindvater, H. K., and Bonsall, M. B. 2007. Evolutionary analysis of life span, competition, and adaptive radiation, motivated by the Pacific rockfishes (*Sebastodes*). *Evolution: International Journal of Organic Evolution*, 61: 1208–1224.
- Marteinsdottir, G. and Begg, G. A. 2002. Essential relationships incorporating the influence of age, size and condition on variables required for estimation of reproductive potential in Atlantic cod *Gadus morhua*. *Marine Ecology Progress Series*, 235: 235–256.
- Neuheimer, A. B., Hartvig, M., Heuschele, J., Hylander, S., Kiørboe, T., Olsson, K. H., Sainmont, J., et al. 2015. Adult and offspring size in the ocean over 17 orders of magnitude follows two life history strategies. *Ecology*, 96: 3303–3311.
- Osenberg, C. W., Olson, M. H., and Mittelbach, G. G. 1994. Stage structure in fishes: resource productivity and competition gradients. *Theory and application in fish feeding ecology*, pp. 151–170.

- Persson, L. 1988. Asymmetries in competitive and predatory interactions in fish populations. *In* Size-structured populations, pp. 203–218. Springer.
- Ricker, W. E. 1954. Stock and Recruitment. Journal of the Fisheries Research Board of Canada, 11: 559–623.
- Roff, D. A. 1983. An allocation model of growth and reproduction in fish. Canadian Journal of Fisheries and Aquatic Sciences, 40: 1395–1404.
- Thorson, J. T., Munch, S. B., Cope, J. M., and Gao, J. 2017. Predicting life history parameters for all fishes worldwide. Ecological Applications, 27: 2262–2276.
- Wourms, J. P. 1991. Reproduction and development of *Sebastes* in the context of the evolution of piscine viviparity. Environmental Biology of Fishes, 30: 111–126.

CHAPTER A

Appendices Paper I

Challenges to fisheries advice and management due to stock recovery

Appendices

Appendix S1 Stock Recovery

To see if stocks of large-bodied fish are recovering, we have looked at the spawning stock biomass (SSB) time-series data of all ICES-assessed stocks that have a maximum total length of 1 metre or more, for which an MSY B_{trigger} reference point has been set, and whose SSB time-series goes back to at least the year 1995. This gave us 25 different stocks from 10 different species. These stocks, as well as their MSY B_{trigger} reference point, are listed in Table S1.1. Out of the 10 species in Table S1.1, only plaice does not include fish in its diet.

The observed patterns of stock recovery in Figure S1.1 of the main text are not solely due to the recovery patterns of the figure's three example stocks. To illustrate this, we have here removed from the recovery dataset the SSB data of plaice in Subarea IV (North Sea), cod in Subarea IV and Divisions VIId and IIIa West (North Sea, Eastern English Channel, Skagerrak), and hake in Division IIIa, Subareas IV, VI, and VII and Divisions VIIIa,b,d (Northern stock). We again show the mean SSB/ B_{trigger} , as well as the SSB sum of all stocks (Figure S1.1), which show the same general pattern as Figure 1 from the main text.

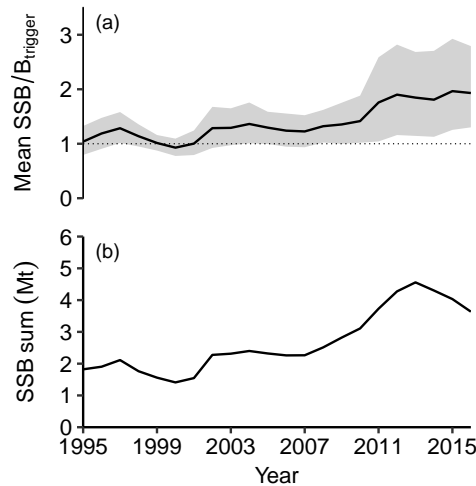


Figure S1.1: Stock recovery pattern of 22 out of the 25 examined stocks (excluding the stock of cod in the North Sea, Eastern English Channel, and Skagerrak, the stock of plaice in the North Sea, and the Northern hake stock). (a) Mean SSB/ B_{trigger} , with the grey area showing the 95% confidence interval of the mean, as calculated by a non-parametric bootstrap with 1000 samples. The thin dotted line shows the standardized MSY B_{trigger} reference point. (b) Summed-up SSB of the 22 stocks.

Table S1.1: A list of the stocks used to test for stock recovery, including their MSY B_{trigger} reference point in the year 2016.

Species	Stock	MSY B_{trigger} (tonnes)
Blue ling (<i>Molva dypterygia</i>)	Subareas VI-VII and Division Vb (Celtic Seas, English Channel, and Faroes Grounds)	75,000
Cod (<i>Gadus morhua</i>)	Division Va (Iceland grounds)	220,000
	Division VIa (West of Scotland)	20,000
	Division VIIa (Irish Sea)	10,000
	Divisions VIIe-k (Western English Channel and Southern Celtic Seas)	10,300
	Subarea IV and Divisions VIId and IIIa West (North Sea, Eastern English Channel, and Skagerrak)	165,000
	Subareas I and II (Northeast Arctic)	460,000
	Subdivision Vb1 (Faroe Plateau)	40,000
	Subdivisions 22-24 (Western Baltic Sea)	38,400
Golden Redfish (<i>Sebastes norvegicus</i>)	Subareas V, VI, XII, and XIV (Iceland and Faroes grounds, West of Scotland, North of Azores, and East of Greenland)	220,000
Haddock (<i>Melanogrammus aeglefinus</i>)	Division Vb	35,000
	Division VIb (Rockall)	10,200
	Divisions VIIb,c,e-k	10,000
	Subarea IV and Divisions IIIa West and VIa (North Sea, Skagerrak, and West of Scotland)	132,000
	Subareas I and II (Northeast Arctic)	80,000
Hake (<i>Merluccius merluccius</i>)	Division IIIa, Subareas IV, VI, and VII and Divisions VI-IIa,b,d (Northern stock)	45,000
	Division VIIIC and IXa (Southern stock)	11,100
Ling (<i>Molva molva</i>)	Division Va	9,500
Plaice (<i>Pleuronectes platessa</i>)	Division VIId (Eastern Channel)	25,826
	Subarea IV (North Sea)	230,000
Saithe (<i>Pollachius virens</i>)	Division Va (Icelandic saithe)	65,000
	Division Vb (Faroe Saithe)	55,000
	Subareas IV and VI, and Division IIIa (North Sea, Rockall and West of Scotland, Skagerrak, and Kattegat)	150,000
Seabass (<i>Dicentrarchus labrax</i>)	Divisions IVb and c, VIIa, and VIIId-h (Central and South North Sea, Irish Sea, English Channel, Bristol Channel, and Celtic Sea)	12,673
White anglerfish (<i>Lophius piscatorius</i>)	Divisions VIIIC and IXa (Cantabrian Sea and Atlantic Iberian Waters)	5,400

Appendix S2 Population model

Here we describe a population model that incorporates density-dependent growth. The model is an adaptation of Lorenzen and Enberg (2002), with natural and fishing mortality being made size-dependent, the maturity ogive being changed from knife-edge to smooth, and the addition of a stock-recruitment relationship. The model equations are shown in Table S2.1, and the model parameters are shown in Table S2.2. The subscripts a and t indicate individual age and time in units of years.

Growth is described with a standard von-Bertalanffy growth equation (S2.1). Density-dependent growth is incorporated into the von-Bertalanffy growth equation by making the asymptotic length $L_{\infty B}$ dependent on stock biomass B (S2.2), according to the method described by Lorenzen and Enberg (2002). A decrease in $L_{\infty B}$ results in a decrease in individual growth. The slope of the relationship between B and $L_{\infty B}$ is determined by the competition coefficient g . A higher value of g means a stronger density-dependent effect on the value of $L_{\infty B}$, and thus a greater growth decrease.

Mortality is size-dependent. Natural mortality decreases with size, following standard size-spectrum theory, and is proportional to L^{-1} (S2.3). Fishing mortality is applied to the population following a trawl selectivity curve (S2.4). This selectivity curve switches smoothly from 0 to 1 around the mean fishery size-at-entry L_F . Total mortality is the sum of natural and fishing mortality (S2.5).

Maturity is size-dependent, and described with a smooth maturity ogive that increases from 0 to 1 around length-at-maturity L_m (S2.6). L_m thus represents the length at which 50% of individuals are mature, which is here assumed to be 0.63 times the maximum asymptotic length ($L_{\infty L}$). Recruitment is described with a standard Beverton-Holt stock-recruitment relationship (S2.7), where α determines the amount of recruits produced per unit of spawning stock biomass.

The population model is age-structured (S2.8). Mortality occurs as individuals grow from one age to the next, with the flow into the first age-group being determined by the recruitment R . Stock biomass is the sum of the weight of each age-group (S2.9), spawning stock biomass is the sum of the mature weight of each age-group (S2.10), and annual yield is the sum of each age group's biomass multiplied with its size-specific mortality to fishing (S2.11).

References

- Lorenzen, K. and Enberg, K. 2002. Density-dependent growth as a key mechanism in the regulation of fish populations: evidence from among-population comparisons. Proceedings of the Royal Society of London B: Biological Sciences, 269: 49–54.

Table S2.1: Governing model equations.

<i>Growth</i>		
Von-Bertalanffy growth	$L_{a,t} = L_{\infty B} - (L_{\infty B} - L_{a-1,t-1})\exp(-K)$	S2.1
Asymptotic length	$L_{\infty B} = L_{\infty L} - g(\frac{B_{t-1} + B_t}{2})$	S2.2
<i>Mortality</i>		
Background predation	$M = \alpha_p L_{a,t}^{-1}$	S2.3
Fishing, trawl selectivity	$F_s = F(1 + [\frac{L_{a,t}}{L_F}]^{-30})^{-1}$	S2.4
Total mortality	$Z = M + F_s$	S2.5
<i>Reproduction</i>		
Maturity	$P_{a,t} = (1 + [\frac{L_{a,t}}{L_m}]^{-30})^{-1}$	S2.6
Recruitment	$R = R_{\max} \frac{\alpha B_{SSB,t}}{R_{\max} + \alpha B_{SSB,t}}$	S2.7
<i>Population</i>		
Population numbers	$N_{a,t} = N_{a-1,t-1}\exp(-Z),$ $N_{1,t} = R$	S2.8
Stock biomass	$B_t = \sum_a c L_{a,t}^b N_{a,t}$	S2.9
Spawning stock biomass	$B_{SSB,t} = \sum_a P_{a,t} c L_{a,t}^b N_{a,t}$	S2.10
<i>Fishery performance</i>		
Yield	$Y_t = \sum_a F c L_{a,t}^b N_{a,t}$	S2.11

Table S2.2: Model parameters with description, value, and units.

Symbol	Description	Value	Unit	Footnote(s)
$L_{\infty L}$	Maximum asymptotic length	150	cm	
c	Length-to-weight conversion factor	0.01	g cm^{-b}	
b	Length-to-weight conversion exponent	3	-	
K	Von Bertalanffy growth constant	0.2	yr^{-1}	
g	Competition coefficient		cm Mt^{-1}	
α_p	Mortality coefficient	19	cm yr^{-1}	1
L_F	Mean fishery size-at-entry	55	cm	
F	Fishing mortality		yr^{-1}	
L_m	Length at maturation	$0.63L_{\infty L}$	cm	
α	Recruitment coefficient	0.015	g^{-1}	2
R_{\max}	Maximum recruitment	5,000,000,000	yr^{-1}	

¹ Set so that natural mortality is around 0.2 yr^{-1} when $L_{a,t} = L_m$.

² Lorenzen and Enberg (2002).

CHAPTER B

Appendices Paper II

Implications of late-in-life
density-dependent growth for fishery
size-at-entry leading to maximum
sustainable yield

Appendices

¹ Appendix A Discrete solution

² To present the model in a discrete form, individual size w is subdivided into a
³ series of logarithmically-distributed weight-bins. In this study we have used $m =$
⁴ 1000 weight bins, where $w_1 = w_{\text{egg}}$ and $w_m = W_\infty$. The precise value for m is
⁵ inconsequential for the results, so long as it is greater than 100 (Andersen *et al.*,
⁶ 2015). The sequence of weight bins can then be set up as $w_i = \exp[\ln(w_{\text{egg}}) +$
⁷ $(i - 1)\delta]$, where the index i ranges from 1 to m and δ describes the logarithmic
⁸ spacing between the weight bins as

$$\delta = \frac{\ln(W_\infty) - \ln(w_{\text{egg}})}{m - 1}$$

⁹ The resource particle size w_R is subdivided into weight bins in a similar way,
¹⁰ substituting m for m_R and w_{egg} for w_{R0} . The size w_{R0} at which the resource weight
¹¹ bin sequence starts is irrelevant, so long as it is far smaller than $0.01w_{\text{egg}}$. This
¹² will ensure that fish of size w_{egg} will not experience a truncation at the lower end
¹³ of their prey-size selection. In this study, we set w_{R0} equal to $2.526 \cdot 10^{-7}$ g and
¹⁴ used $m_R = 1599$, so that $w_{R,599+i} = w_i$ with $w_{R,600} = w_{\text{egg}}$.

¹⁵ [Table A1 about here.]

¹⁶ Having constructed the weight bins, we can now rewrite the continuous equa-
¹⁷ tions from the main text into discrete equations (Table A1). In their Appendix B,
¹⁸ Andersen *et al.* (2015) create a discretization scheme for the numerical solution
¹⁹ to the abundance size-spectrum:

$$\frac{N_i^{t+\Delta t} - N_i^t}{\Delta t} + \frac{g(w_i)N_i^{t+\Delta t} - g(w_{i-1})N_{i-1}^{t+\Delta t}}{w_i - w_{i-1}} = -\mu(w_i)N_i^{t+\Delta t}$$

20 where $\mu(w_i) = \mu_0(w_i) + \mu_F(w_i)$, and $\mu(w_i)$ as well as $g(w_i)$ are calculated from
 21 N_i^t . This can be rewritten as

$$N_{i-1}^{t+\Delta t} \left(-\frac{\Delta t}{w_i - w_{i-1}} g(w_{i-1}) \right) + N_i^{t+\Delta t} \left(1 + \frac{\Delta t}{w_i - w_{i-1}} g(w_i) + \Delta t \mu(w_i) \right) = N_i^t$$

22 which, when defining the two terms within parentheses as $X(w_i)$ and $Z(w_i)$, be-
 23 comes

$$N_{i-1}^{t+\Delta t} X(w_i) + N_i^{t+\Delta t} Z(w_i) = N_i^t$$

24 Thus, the new abundance of individuals within a weight bin $N_i^{t+\Delta t}$ can be written
 25 as

$$N_i^{t+\Delta t} = \frac{N_i^t - X(w_i) N_{i-1}^{t+\Delta t}}{Z(w_i)}$$

26 with $N_m^{t+\Delta t} = 0$. From this equation it is clear that to calculate the new abundance
 27 of individuals within a weight bin $N_i^{t+\Delta t}$ we need to know the new abundance of
 28 individuals in the weight bin before it: $N_{i-1}^{t+\Delta t}$. Thus, we start the discrete calcula-
 29 tion of the size spectrum at $N_1^{t+\Delta t}$, and work up through all the weight bins from
 30 there. The value of $N_1^{t+\Delta t}$ is found with the boundary condition to the abundance
 31 spectrum, and is given by Andersen *et al.* (2015) as

$$N_1^{t+\Delta t} = \frac{N_1^t + R \Delta t / (w_2 - w_1)}{Z(w_1)}$$

32 With the above equations we can calculate the abundance spectrum at stable state
 33 through iteration. For this, we need to specify an initial abundance spectrum for
 34 the first iteration. The size or shape of this spectrum does not matter to the end
 35 result, so long as sufficient time steps are used to allow a stable state to be reached

³⁶ at the end of the iteration process.

³⁷ A discrete analytical solution to the resource particle abundance spectrum is
³⁸ given by Hartvig *et al.* (2011) in their Appendix G:

$$N_{R,j}^{t+\Delta t} = K_e(w_{R,j}) - [K_e(w_{R,j}) - N_{R,j}^t] e^{-[r_0 w_{R,j}^{n-1} + \mu_p(w_{R,j})]\Delta t}$$

³⁹ where $K_e(w_{R,j}) = \frac{r_0 w_{R,j}^{n-1} \kappa w_{R,j} \lambda}{r_0 w_{R,j}^{n-1} + \mu_p(w_{R,j})}$ is the size-specific effective carrying capacity
⁴⁰ of the resource.

⁴¹ **Appendix B Model fitting**

⁴² **North Sea plaice**

⁴³ In the period 1936-1938, North Sea plaice (*Pleuronectes platessa*) fishing mortal-
⁴⁴ ity (F) was close to 0.6 yr^{-1} (Beverton and Holt, 1957). When the Second World
⁴⁵ War (WWII) started in 1938, fishing was severely reduced and largely restricted to
⁴⁶ coasts, resulting in an increase in plaice stock size (Jenssen, 1947). When fishing
⁴⁷ resumed in 1946, the plaice stock had increased by a factor of around 3 when com-
⁴⁸ pared with pre-war levels (Margetts and Holt, 1948). At the same time, growth
⁴⁹ rates of both immature and mature individuals had become smaller (Rijnsdorp
⁵⁰ and Van Leeuwen, 1992). In 1944-1945, before fishing was resumed to pre-war
⁵¹ intensities, growth rates of 25-30 cm individuals were at 70% of pre-war growth
⁵² rates (Rijnsdorp and Van Leeuwen, 1992). A decrease in growth rate together
⁵³ with an increase in stock size is indicative of density-dependent growth, which
⁵⁴ in our model is the result of late-in-life density-dependence. Fitting the model to
⁵⁵ this data will allow for an estimation of the degree to which plaice is regulated by
⁵⁶ late-in-life density-dependence.

⁵⁷ Model fitting is done by changing the values of maximum recruitment (R_{\max})
⁵⁸ and resource carrying capacity (κ) to give the best approximation of the empirical
⁵⁹ data pre-WWII and end-WWII, and by changing the reproductive efficiency (ε_r)
⁶⁰ so that the model's predicted F_{MSY} approximates the scientific consensus. This
⁶¹ means that empirical data is needed for these two times on stock biomass and
⁶² yield. However, although the WWII data shows a threefold increase of plaice
⁶³ biomass when F changed from 0.6 yr^{-1} to almost 0 yr^{-1} , exact biomass figures
⁶⁴ are unknown as biomass changes were inferred from catch-per-unit-effort data

65 (Margetts and Holt, 1948).

66 To be able to make an approximation of North Sea plaice biomass and yield
67 during these times, the assumption is made that mean parameter values for the
68 stock have remained unchanged from the year 1938 to 2000. Under this assump-
69 tion, stock size and yield in 1938 should be close to those of the 1990s, when F
70 also averaged around 0.6 yr^{-1} (ICES, 2015b). During the 1990s, spawning stock
71 biomass (SSB) averaged at 250 kt and yield at 150 kt/yr (ICES, 2015b). Further-
72 more, F_{MSY} of North Sea plaice is considered to be 0.19 yr^{-1} (ICES, 2014b). A
73 proper model fit will therefore result in a SSB of 250 kt and a yield of 150 kt/yr at
74 a F of 0.6 yr^{-1} , as well as a SSB of 750 kt and a 30% reduction in growth rate of
75 25-30 cm individuals at a F of 0.05 yr^{-1} , with F_{MSY} equal to 0.19 yr^{-1} for both
76 of these scenarios. We assume North Sea plaice F to have been around 0.05 yr^{-1}
77 instead of 0 yr^{-1} at the end of WWII, because it was still fished by a small coastal
78 fishery (Jenssen, 1947).

79 Parameterization

80 In order to fit the model to plaice, it will first have to be parameterized to plaice.
81 This means finding the relevant values for asymptotic size (W_∞), mean size-at-
82 entry into the fishery (w_F), natural mortality (M), von Bertalanffy growth constant
83 (K), and ε_r . There is more data available on plaice asymptotic length (L_∞) than
84 on plaice W_∞ . Therefore, it would be more reliable to calculate plaice W_∞ from
85 plaice L_∞ instead of using a recorded W_∞ . However, data on plaice L_∞ vary greatly
86 between studies and between sexes, from as low as 41 cm for males (Bannister,
87 1978) to as high as 70 cm for females (Beverton and Holt, 1959). Therefore,
88 plaice W_∞ will be calculated from length-at-maturity (L_m), which shows a more

consistent value across studies. Female L_m is used, because it is the females that produce the eggs that are described in the model equations. W_∞ will be calculated from L_m by converting L_m to weight-at-maturity (w_{mat}). This is done via the conversion factors $a = 0.009$ and $b = 3.031$ (ICES, 2005), through $w = aL^b$ (where L is total length). W_∞ is then calculated from w_{mat} , assuming that $w_{mat} = 0.25W_\infty$ (Jensen, 1996; Froese and Binohlan, 2000; He and Stewart, 2001) holds true for North Sea plaice. Lastly, L_∞ can be calculated from W_∞ through $L = (wa)^{1/b}$. Female plaice L_m is 34 cm (Rijnsdorp, 1989), meaning that $w_{mat} = 394.60$ g, $W_\infty = 1578.39$ g, and $L_\infty = 53.72$ cm. Female plaice L_∞ ranges between 52 and 57 cm in the North Sea (Bannister, 1978), so we can assume that $w_{mat} = 0.25W_\infty$ holds true.

The minimum landing length for North Sea plaice is 27 cm (ICES, 2005). However, Danish discard data show that individuals of at least 23-24 cm are abundant in discards (Madsen *et al.*, 2013). It is therefore assumed that mean length-at-entry into the fishery L_F (length at which 50% of fish are first exposed to fishing) equals 23 cm, with w_F then equalling 120.68 g.

Because there was only a small coastal fishery targeting plaice during WWII, most plaice mortality in this period was due to natural mortality. This allowed Beverton and Holt (1957) to determine plaice M at 0.1 yr^{-1} . This value is still accepted as the current plaice M by ICES today (ICES, 2016a).

With regard to the von Bertalanffy growth constant, Froese and Sampang (2013) describes a plaice K of 0.16 yr^{-1} .

Lastly, the value of ε_r should be set so that the model's predicted F_{MSY} approximates 0.19 yr^{-1} , given a w_F of 120.68 g. We do this for 100% early-in-life density dependent regulation, because in practice late-in-life density dependence

₁₁₄ is disregarded when setting fisheries reference points. However, for high values
₁₁₅ of ε_r (0.01 to 1), the modelled F_{MSY} value for plaice remained at a constant point
₁₁₆ below 0.19^{-1} and would not increase further. We therefore set ε_r to 0.1 (Figure
₁₁₇ B1).

₁₁₈ [Figure B1 about here.]

₁₁₉ **Model fitting**

₁₂₀ The model was fitted to the empirical data by changing the values of maximum
₁₂₁ recruitment (R_{max}) and resource carrying capacity (κ), so that a fishing mortality
₁₂₂ of 0.6 yr^{-1} results in approaching a SSB and yield of 250 kt and 150 kt/yr re-
₁₂₃ spectively, and a fishing mortality of 0.05 yr^{-1} results in approaching a SSB of
₁₂₄ 750 kt and a 30% reduction in growth rate of 25-30 cm individuals. This was best
₁₂₅ achieved with the model for $R_{max} = 5 \cdot 10^9 \text{ yr}^{-1}$, and $\kappa = 3.33 \cdot 10^{12} \text{ g}^{-1-\lambda}$. For
₁₂₆ $F = 0.6 \text{ yr}^{-1}$, this results in a SSB of 152 kt and a yield of 276 kt/yr. Further-
₁₂₇ more, the von Bertalanffy growth curve ($K = 0.16 \text{ yr}^{-1}$; Froese and Sampang,
₁₂₈ 2013) matches the length-at-age curve produced by the model fairly well (Figure
₁₂₉ B2). For $F = 0.05$, these values of R_{max} and κ result in a SSB of 2650 kt, a yield of
₁₃₀ 179 kt, and a reduction in growth rate of the length group 25-30 cm of around
₁₃₁ 30-40% (Figure B3). The modelled increase in SSB when fishing is restricted rep-
₁₃₂ resents more than a 15-fold increase in biomass, whereas the empirical data only
₁₃₃ indicates a 3-fold increase. However, it is possible that the North Sea plaice SSB
₁₃₄ had not yet finished increasing at the end of WWII, and would have continued to
₁₃₅ increase in biomass if fishing had not resumed. This is further supported by the
₁₃₆ observation that the recent gradual reduction in plaice F from around 0.6 to 0.2

¹³⁷ yr^{-1} has already coincided with a 3.5-fold increase in plaice SSB between 2003
¹³⁸ and 2016, which appears to still be increasing (ICES, 2016a).

¹³⁹ [Figure B2 about here.]

¹⁴⁰ [Figure B3 about here.]

¹⁴¹ **Northeast Atlantic mackerel**

¹⁴² Between 2003 and 2013, the length- and weight-at-age of Northeast Atlantic
¹⁴³ (NEA) mackerel (*Scomber scombrus*) has decreased, as a result of an increase
¹⁴⁴ in both NEA mackerel stock size and Norwegian herring (*Clupea harengus*) stock
¹⁴⁵ size (Olafsdottir *et al.*, 2016). In 2003, weights-at-age of NEA mackerel aged
¹⁴⁶ 3, 4, 5, 6, 7, and 8 were around 416, 471, 537, 598, 602 and 657 g respectively
¹⁴⁷ (Olafsdottir *et al.*, 2016). In 2013 this had decreased to around 272, 323, 363,
¹⁴⁸ 391, 408 and 437 g respectively (Olafsdottir *et al.*, 2016). At the same time, NEA
¹⁴⁹ mackerel spawning stock biomass almost doubled in size. These changes of the
¹⁵⁰ NEA mackerel stock are coinciding with around a 33% reduction in fishing mor-
¹⁵¹ tality, from 0.46 yr^{-1} in 2003 to 0.291 yr^{-1} in 2013 (ICES, 2015a). We fit our
¹⁵² model to these observations and thereby obtain a rough estimation for the values
¹⁵³ of R_{\max} and κ , giving us an indication of when in life most density dependent
¹⁵⁴ regulation of NEA mackerel takes place. Model fitting is done by changing the
¹⁵⁵ values of R_{\max} and κ , to give the best approximation of the empirical data. In
¹⁵⁶ 2003, SSB equalled 1.9 million tonnes, yield plus discards equalled 0.68 million
¹⁵⁷ tonnes, and fishing mortality equalled 0.46 yr^{-1} (ICES, 2015a). In 2013, SSB
¹⁵⁸ equalled 3.6 million tonnes, yield plus discards equalled 0.93 million tonnes, and
¹⁵⁹ fishing mortality equalled 0.291 yr^{-1} (ICES, 2015a).

160 **Parameterization**

161 In order to fit the model to NEA mackerel, it will first have to be parameterized to
162 NEA mackerel. This means finding the relevant values for asymptotic size (W_∞),
163 mean size-at-entry into the fishery (w_F), natural mortality (M), von Bertalanffy
164 growth constant (K), and reproductive efficiency (ε_r). NEA mackerel is a highly
165 migratory species, with a distribution ranging from North-west Africa to northern
166 Norway, and from Greenland to the Baltic Sea (Berge *et al.*, 2015). Although
167 NEA mackerel is a single species, the stock can actually be subdivided into three
168 spawning components: Western, Southern, and North Sea (ICES, 2013). As the
169 data on density-dependent growth of NEA mackerel mainly concerns mackerel
170 from the Western and North Sea spawning component that feed in the northern
171 North Sea and southern Norwegian Sea, the model will be parameterized to data
172 from these components as much as possible.

173 Data on asymptotic weight and length can vary greatly, and we could find no
174 data on either for the mackerel that feed around the northern North Sea and south-
175 ern Norwegian Sea. In fact, the length-at-age that Olafsdottir *et al.* (2016) reported
176 for 8 year-old mackerel was higher (up to 40.5 cm) than the asymptotic length that
177 is reported for NEA mackerel in the North Sea (up to 40.0 cm; Kästner, 1977),
178 even though these 8-year old mackerel are still growing. Because no asymptotic
179 length is known for the stock component that we want to parameterize our model
180 to, we instead use data from the Southern spawning component of NEA mackerel.
181 Using data from Martins (1998) (sampled in ICES division IXa), Villamor *et al.*
182 (2004) calculated mackerel L_∞ to be 45.3 cm. W_∞ is calculated from L_∞ according
183 to $W_\infty = aL_\infty^b$, where $a = 0.00430$ and $b = 3.210$ (Wilhelms, 2013).

184 In the northern North Sea, NEA mackerel L_m equals around 30 cm (ICES,
185 2016b). w_{mat} then equals 237.15 g, using the same length-to-weight conversion
186 that was used for calculating W_∞ .

187 In the northern North Sea, NEA mackerel L_F equals around 30 cm (ICES,
188 2016b), meaning that w_F equals 237.15 g.

189 NEA mackerel M was set at 0.15 yr^{-1} , as used by ICES (ICES, 2016b).

190 We assume NEA mackerel K to be 0.182 yr^{-1} , which Villamor *et al.* (2004)
191 calculated together with the L_∞ value that we have used for NEA mackerel.

192 The value of ε_r should be set so that the model's predicted F_{MSY} approximates
193 0.22 yr^{-1} (ICES, 2015a), given a w_F of 237.15 g. We do this for 100% early-in-
194 life density dependent regulation, because in practice late-in-life density depen-
195 dence is disregarded when setting fisheries reference points. This is achieved for
196 an ε_r value of 0.0006 (Figure B4).

197 Lastly, to be able to compare the empirical mackerel weight-at-age data with
198 the model fit, 8.4 years have been added to all NEA mackerel empirical weight-at-
199 age data points. The reason for this is that the model underestimates larval growth
200 rate, and because recorded weight-at-age is usually rounded down.

201 [Figure B4 about here.]

202 Model fitting

203 The model was fitted to the empirical data by changing the values of maximum
204 recruitment (R_{\max}) and resource carrying capacity (κ), so that a fishing mortality
205 of 0.46 yr^{-1} results in approaching a SSB of 1.9 Mt and a yield of 0.68 Mt/yr,
206 and a fishing mortality of 0.291 yr^{-1} results in approaching a SSB of 3.6 Mt and

207 a yield of 0.93 Mt/yr. Furthermore, this decrease in fishing mortality should lead
208 to a decrease in individual growth similar to the decrease observed by Olafsdottir
209 *et al.* (2016).

210 The above was best achieved with the model for $R_{\max} = 4.5 \cdot 10^{10} \text{ yr}^{-1}$, and
211 $\kappa = 1.5 \cdot 10^{13} \text{ g}^{-1-\lambda}$. This gave a SSB of 1.68 Mt and a yield of 0.77 Mt/yr for a
212 fishing mortality of 0.46 yr^{-1} , and a SSB of 2.97 Mt and a yield of 0.83 Mt/yr for
213 a fishing mortality of 0.291 yr^{-1} .

214 With the values for R_{\max} and κ used above, the model was able to approach
215 the empirical SSB and yield values for the two historical scenarios fairly well.
216 However, the decrease in growth predicted by the model is much smaller than
217 what is shown in the empirical data (Figure 2b, main text). Regardless of which
218 R_{\max} and κ were used, this change in growth remained small. Therefore, it was
219 decided to use values for R_{\max} and κ which best matched the empirical SSB, yield,
220 and weight-at-age data for the low-SSB, high growth scenario.

221 The length-at-age curve produced by the model shows a similar growth to the
222 von Bertalanffy growth curve (Figure B5).

223 [Figure B5 about here.]

224 **Baltic sprat**

225 As a result of a sharp decrease in Eastern Baltic cod (*Gadus morhua callarias*)
226 abundance and due to favourable temperature conditions, Baltic sprat (*Sprattus*
227 *sprattus balticus*) has experienced a strong increase in SSB between the 1980s
228 to the 1990s (Köster *et al.*, 2003). This increase in SSB was accompanied with
229 decreased growth (Eero, 2012) and body condition (Casini *et al.*, 2014), likely

caused by competition for food (Casini *et al.*, 2006). In 1988, weights-at-age of Baltic sprat aged 2, 3, 4, 5, and 6 were around 10.6, 12.4, 14.5, 16.5, and 16.8 g respectively (Eero, 2012). In 1998 this had decreased to around 7.3, 8.2, 8.6, 9.8, and 10.1 g respectively (Eero, 2012). In 1988, Baltic sprat SSB was 415,000 t and total catches numbered 80,000 t, with a fishing mortality of 0.23 yr^{-1} . In 1998, Baltic sprat SSB had increased to 1,406,000 t and total catches had increased to 417,000 t, with fishing mortality increased to 0.386 yr^{-1} (ICES, 2015c). Baltic sprat recruitment shows a high variability, mostly thought to be the result of interannual differences in temperature (which is linked to zooplankton abundance) and drift patterns (MacKenzie and Köster, 2004; Baumann *et al.*, 2006; Ojaveer and Kalejs, 2010), influencing late larval and early juvenile survival. Furthermore, after accounting for temperature, MacKenzie and Köster (2004) also found an influence of SSB on recruitment. Nevertheless, for simplicity and methodological consistency, we used a Beverton-Holt stock-recruitment relationship to describe sprat recruitment.

Parameterization

In order to fit the model to Baltic sprat, it will first have to be parameterized to Baltic sprat. This means finding the relevant values for asymptotic size (W_∞), mean size-at-entry into the fishery (w_F), natural mortality (M), von Bertalanffy growth constant (K), and reproductive efficiency (ε_r). Data on asymptotic weight and length can vary greatly. Therefore, assuming that $w_{mat} = 0.25W_\infty$ holds true for Baltic sprat, W_∞ is calculated from w_{mat} . As more data is available on length than on weight, w_{mat} in turn is calculated from L_m through $w = aL^b$, where $a = 0.00377$ and $b = 3.200$ (Froese and Sampang, 2013). Baltic sprat L_m equals around 9.6 cm

254 (Grygiel and Wyszynski, 2003; Haslob, 2011). w_{mat} then equals 5.2 g, W_∞ equals
255 20.97 g, and L_∞ then equals 14.8 cm. With an empirical study estimating Baltic
256 sprat L_∞ to be around 15.0 cm (Froese and Sampang, 2013), we therefore assume
257 that $w_{mat} = 0.25W_\infty$ holds true for Baltic sprat.

258 There is no minimum catch size for Baltic sprat, with w_F equalling around 3.6
259 g (ICES, 2014a).

260 Sprat M is estimated to have been 0.43 yr^{-1} in 1988, and 0.32 yr^{-1} in 1998
261 (ICES, 2014a). However, to obtain a better model fit on growth, and because
262 natural mortality is notoriously hard to measure accurately, we assumed that Baltic
263 sprat M was 0.5 yr^{-1} in 1988 and 0.2 yr^{-1} in 1998.

264 Baltic sprat K was set at 0.68 yr^{-1} , as reported by Jenkins (1902).

265 The value of ε_r should be set so that the model's predicted F_{MSY} approximates
266 0.26 yr^{-1} (ICES, 2015c), given a w_F of 3.6 g. We do this for 100% early-in-life
267 density dependent regulation, because in practice late-in-life density dependence
268 is disregarded when setting fisheries reference points. This is achieved for an ε_r
269 value of 0.0055 (Figure B6).

270 Lastly, to be able to compare the empirical sprat weight-at-age data with the
271 model fit, 3 years have been added to all sprat empirical weight-at-age data points.
272 The reason for this is that the model underestimates larval growth rate, and be-
273 cause recorded weight-at-age is usually rounded down.

274 [Figure B6 about here.]

275 **Model fitting**

276 The model was fitted to the empirical data by changing the values of maximum
277 recruitment (R_{\max}) and resource carrying capacity (κ), so that a fishing mortality
278 of 0.23 yr^{-1} and a natural mortality of 0.5 yr^{-1} result in approaching a SSB of
279 415 kt and a yield of 80 kt/yr , and a fishing mortality of 0.386 yr^{-1} and a natural
280 mortality of 0.2 yr^{-1} result in approaching a SSB of 1406 kt and a yield of 417
281 kt/yr . Furthermore, this change in F and M should lead to a decrease in individual
282 growth similar to the decrease observed by Eero (2012).

283 The above was best achieved with the model for $R_{\max} = 2.5 \cdot 10^{13} \text{ yr}^{-1}$, and
284 $\kappa = 2.5 \cdot 10^{12} \text{ g}^{-1-\lambda}$. This gave a SSB of 358 kt and a yield of 93.8 kt/yr for
285 the high-growth scenario, and a SSB of 2070 kt and a yield of 1020 kt/yr for the
286 low-growth scenario. This approached the empirical SSB and yield values for the
287 low-SSB scenario fairly well, but slightly overestimated those for the high-SSB
288 scenario. Furthermore, with these R_{\max} and κ values the model also showed a
289 proper fit to the difference in individual growth between the two scenarios (Figure
290 2a).

291 The length-at-age curve produced by the model shows a slightly slower indi-
292 vidual growth than the von Bertalanffy growth curve (Figure B7). This is partly
293 compensated by adding 3.7 years to all sprat empirical weight-at-age data points.

294 [Figure B7 about here.]

295 **Appendix C Sensitivity analysis**

296 A sensitivity test was performed to examine how sensitive the model F_{MSY} output
297 is to changes in the fitted value of ε_r , and how sensitive the model weight-at-age
298 and optimal fishery size-at-entry output is to changes in the fitted value of R_{\max}/κ .
299 For each stock, F_{MSY} values were recalculated (method described in the main
300 text) using the fitted value of ε_r , a factor 2 lower than the fitted value of ε_r , and a
301 factor 2 higher than the fitted value of ε_r . Similarly, for each stock the weight-at-
302 age and optimal fishery size-at-entry were recalculated (method described in the
303 main text) using the fitted value of R_{\max}/κ , a factor 2 lower than the fitted value of
304 R_{\max}/κ , and a factor 2 higher than the fitted value of R_{\max}/κ . The F_{MSY} results
305 are shown in Figure C1, and the weight-at-age and optimal fishery size-at-entry
306 results are shown in Figure C2.

307 [Figure C1 about here.]

308 [Figure C2 about here.]

309 **References**

- 310 Andersen, K. H., Jacobsen, N. S., and Farnsworth, K. D. 2015. The theoretical
311 foundations for size spectrum models of fish communities. Canadian Journal
312 of Fisheries and Aquatic Sciences, 73: 575–588.
- 313 Bannister, R. C. A. 1978. Changes in plaice stocks and plaice fisheries in the
314 North Sea. Rapports et proces-verbaux des reunions du Conseil permanent
315 international pour l'exploration de la mer, 172: 86–101.

- 316 Baumann, H., Hinrichsen, H. H., Möllmann, C., Köster, F. W., Malzahn, A. M.,
317 and Temming, A. 2006. Recruitment variability in Baltic Sea sprat (*Sprattus*
318 *sprattus*) is tightly coupled to temperature and transport patterns affecting the
319 larval and early juvenile stages. Canadian Journal of Fisheries and Aquatic
320 Sciences, 63: 2191–2201.
- 321 Berge, J., Heggland, K., Lønne, O. J., Cottier, F., Hop, H., Gabrielsen, G. W.,
322 Nøttestad, L., *et al.* 2015. First records of Atlantic mackerel (*Scomber scom-*
323 *brus*) from the Svalbard Archipelago, Norway, with possible explanations for
324 the extension of its distribution. Arctic, 68: 54–61.
- 325 Beverton, R. J. H. and Holt, S. J. 1957. On the Dynamics of Exploited Fish
326 Populations. Her Majesty's Stationery Office, London, 540 pp.
- 327 Beverton, R. J. H. and Holt, S. J. 1959. A review of the lifespans and mortal-
328 ity rates of fish in nature, and their relation to growth and other physiological
329 characteristics. In Ciba Foundation Symposium-The Lifespan of Animals (Col-
330 loquia on Ageing), Volume 5, pp. 142–180. Wiley Online Library.
- 331 Casini, M., Cardinale, M., and Hjelm, J. 2006. Inter-annual variation in herring,
332 Clupea harengus, and sprat, *Sprattus sprattus*, condition in the central Baltic
333 Sea: what gives the tune? Oikos, 112: 638–650.
- 334 Casini, M., Rouyer, T., Bartolino, V., Larson, N., and Grygiel, W. 2014. Density-
335 Dependence in Space and Time: Opposite Synchronous Variations in Popula-
336 tion Distribution and Body Condition in the Baltic Sea Sprat (*Sprattus sprattus*)
337 over Three Decades. PLOS ONE, 9: e92278.

- 338 Eero, M. 2012. Reconstructing the population dynamics of sprat (*Sprattus sprattus*
339 *balticus*) in the Baltic Sea in the 20th century. ICES Journal of Marine Science,
340 69: 1010–1018.
- 341 Froese, R. and Binohlan, C. 2000. Empirical relationships to estimate asymptotic length, length at first maturity and length at maximum yield per recruit in
342 fishes, with a simple method to evaluate length frequency data. Journal of Fish
343 Biology, 56: 758–773.
- 344
- 345 Froese, R. and Sampang, A. 2013. Potential indicators and reference points for
346 good environmental status of commercially exploited marine fishes and invertebrates in the German EEZ. World Wide Web electronic publication, available
347 from <http://oceanrep.geomar.de/22079/>.
- 348
- 349 Grygiel, W. and Wyszynski, M. 2003. Temporal (1980-2001) and geographic
350 variation in the sexual maturity at age and length of herring and sprat inhabiting
351 the southern Baltic. Bulletin of the Sea Fisheries Institute, 2: 3–34.
- 352
- 353 Hartvig, M., Andersen, K. H., and Beyer, J. E. 2011. Food web framework for
size-structured populations. Journal of Theoretical Biology, 272: 113–122.
- 354
- 355 Haslob, H. 2011. Reproductive ecology of Baltic sprat and its application in stock
assessment. (Doctoral thesis/PhD), Christian-Albrechts-Universität, Kiel, Ger-
many, 133 pp.
- 356
- 357 He, J. X. and Stewart, D. J. 2001. Age and size at first reproduction of fishes:
358 predictive models based only on growth trajectories. Ecology, 82: 784–791.

359 ICES 2005. ICES-FishMap: plaice (*Pleuronectes platessa*) factsheet. ICES,
360 Copenhagen.

361 ICES 2013. Mackerel in the Northeast Atlantic (combined Southern, Western,
362 and North Sea spawning components). In ICES Advice 2013, Book 9.

363 ICES 2014a. Report of the Baltic Fisheries Assessment Working Group (WGB-
364 FAS). ICES CM 2014/ACOM:10.

365 ICES 2014b. Report of the Joint ICES-MYFISH Workshop to consider the basis
366 for FMSY ranges for all stocks (WKMSYREF3). ICES CM 2014/ACOM:64.

367 ICES 2015a. Mackerel (*Scomber scombrus*) in Subareas I-VII and XIV and
368 Di-visions VIIa-e and IXa (Northeast Atlantic). In ICES Advice 2015, Book 9.

369 ICES 2015b. Report of the Working Group on Widely Distributed Stocks (WG-
370 WIDE). ICES CM 2015/ACOM:15.

371 ICES 2015c. Sprat (*Sprattus sprattus*) in Subdivisions 22-32 (Baltic Sea). In ICES
372 Advice 2015, Book 8.

373 ICES 2016a. Plaice (*Pleuronectes platessa*) in Subarea 4 (North Sea) and Subdi-
374 vision 3.a.20 (Skagerrak). In ICES Advice 2016, Book 6.

375 ICES 2016b. Report of the Working Group on Widely Distributed Stocks (WG-
376 WIDE). ICES CM 2016/ACOM:16.

377 Jenkins, J. T. 1902. Alters-bestimmung durch Otolithen bei den Clupeiden,
378 Inaugural-Dissertation. Druck von Schmidt und Klaunig.

- 379 Jensen, A. L. 1996. Beverton and Holt life history invariants result from opti-
380 mal trade-off of reproduction and survival. Canadian Journal of Fisheries and
381 Aquatic Sciences, 53: 820–822.
- 382 Jenssen, A. J. C. 1947. The stocks of plaice in the North Sea and the Transi-
383 tion area during the war. Rapports et procès-verbaux des réunions du Conseil
384 permanent international pour l’exploration de la mer., 122: 19–25.
- 385 Kästner, D. 1977. Preliminary results of the occurrence of two mackerel groups
386 (*Scomber scombrus* L.) with different growth pattern west of Britain. ICES
387 CM.
- 388 Köster, F. W., Möllmann, C., Neuenfeldt, S., Vinther, M., St John, M. A.,
389 Tomkiewicz, J., Voss, R., *et al.* 2003. Fish stock development in the central
390 Baltic Sea (1974-1999) in relation to variability in the environment. In ICES
391 Marine Science Symposia, vol. 219, pp. 294–306.
- 392 MacKenzie, B. R. and Köster, F. W. 2004. Fish production and climate: sprat in
393 the Baltic Sea. Ecology, 85: 784–794.
- 394 Madsen, N., Feeckings, J., and Lewy, P. 2013. Discarding of plaice (*Pleuronectes*
395 *platessa*) in the Danish North Sea trawl fishery. Journal of sea research, 75:
396 129–134.
- 397 Margetts, A. R. and Holt, S. J. 1948. The effect of the 1939-1945 war on the
398 English North Sea trawl fisheries. Rapports et procès-verbaux des réunions:
399 Conseil permanent international pour l’exploration de la mer., 122: 26–46.
- 400 Martins, M. M. 1998. As populações do gênero Scomber: Sarda (*S. scombrus*

- 401 L., 1758) e Cavala (S. japonicus, H., 1782). Biologia e estado de conservação
402 destes recursos nas áreas de distribuição do Atlântico Nordeste. Instituto Por-
403 tuguês das Pescas e do Mar. Lisboa, Julho 1998.
- 404 Ojaveer, E. and Kalejs, M. 2010. Ecology and long-term forecasting of sprat
405 (*Sprattus sprattus balticus*) stock in the Baltic Sea: a review. Reviews in Fish
406 Biology and Fisheries, 20: 203–217.
- 407 Olafsdottir, A. H., Slotte, A., Jacobsen, J. A., Oskarsson, G. J., Utne, K. R., and
408 Nøttestad, L. 2016. Changes in weight-at-length and size-at-age of mature
409 Northeast Atlantic mackerel (*Scomber scombrus*) from 1984 to 2013: effects
410 of mackerel stock size and herring (*Clupea harengus*) stock size. ICES Journal
411 of Marine Science, 73: 1255–1265.
- 412 Rijnsdorp, A. D. 1989. Maturation of male and female North Sea plaice (*Pleu-*
413 *ronectes platessa* L.). ICES Journal of Marine Science, 46: 35–51.
- 414 Rijnsdorp, A. D. and Van Leeuwen, P. I. 1992. Density-dependent and inde-
415 pendent changes in somatic growth of female North Sea plaice *Pleuronectes*
416 *platessa* between 1930 and 1985 as revealed by back-calculation of otoliths.
417 Marine Ecology Progress Series, 88: 19–32.
- 418 Villamor, B., Abaunza, P., and Celso Fariña, A. 2004. Growth variability of mack-
419 erel (*Scomber scombrus*) off north and northwest Spain and a comparative re-
420 view of the growth patterns in the northeast Atlantic. Fisheries Research, 69:
421 107–121.
- 422 Wilhelms, I. 2013. Atlas of length-weight relationships of 93 fish and crustacean
423 species from the North Sea and the North-East Atlantic. Tech. rep.

Table A1: Model equations in discrete form.

<i>Consumption</i>		
Size preference for prey	$\phi\left(\frac{w_i}{w_{R,j}}\right) = \exp[-(\ln(\frac{w_i}{w_{R,j}\beta}))^2/(2\sigma^2)]$	A1
Encountered food	$E_e(w_i) = \gamma w_i^q \sum_{j=1}^{m_R-1} \phi\left(\frac{w_i}{w_{R,j}}\right) w_{R,j} N_{R,j} (w_{R,j+1} - w_{R,j})$	A2
Feeding level	$f(w_i) = \frac{E_e(w_i)}{E_e(w_i) + h w_i^n}$	A3
<i>Growth</i>		
Available energy	$E_a(w_i) = \alpha f(w_i) h w_i^n - k_r w_i^n - k_a w_i$	A4
Switching function	$H(x) = (1 + x^{-10})^{-1}$	A5
Maturation	$\psi(w_i) = H\left(\frac{w_i}{\eta_m W_\infty}\right) \frac{1 - \varepsilon_a}{(w_i/W_\infty)^{n-1} - \varepsilon_a}$	A6
Growth rate	$g(w_i) = (1 - \psi(w_i)) E_a(w_i)$	A7
<i>Reproduction</i>		
Egg production	$R_p = \sum_{i=1}^{m-1} \frac{\psi(w_i) E_a(w_i)}{2 w_{\text{egg}}} N_i (w_{i+1} - w_i)$	A8
Recruitment	$R = R_{\max} \frac{\varepsilon_r R_p}{R_{\max} + \varepsilon_r R_p}$	A9
<i>Mortality</i>		
Background predation	$\mu_0(w_i) = \alpha_p w_i^{n-1}$	A10
Fishing, trawl selectivity	$\mu_F(w_i) = F H\left(\frac{w_i}{w_F}\right)$	A11
<i>Population structure</i>		
Abundance argument 1	$X(w_i) = -\frac{g(w_{i-1}) \Delta t}{w_{i+1} - w_i}$	A12
Abundance argument 2	$Z(w_i) = 1 + \frac{g(w_i) \Delta t}{w_{i+1} - w_i} + [\mu_0(w_i) + \mu_F(w_i)] \Delta t$	A13
Abundance spectrum	$N_1^{t+\Delta t} = \frac{N_1^t + R \Delta t / (w_2 - w_1)}{Z(w_1)},$ $N_i^{t+\Delta t} = \frac{N_i^t - X(w_i) N_{i-1}^{t+\Delta t}}{Z(w_i)}$ for $i \geq 2 < m$, $N_m^{t+\Delta t} = 0$	A14
Spawning stock biomass	$B_{SSB} = \sum_{i=1}^{m-1} H\left(\frac{w_i}{\eta_m W_\infty}\right) w_i N_i (w_{i+1} - w_i)$	A15
<i>Fishery performance</i>		
Yield	$Y = \sum_{i=1}^{m-1} \mu_F(w_i) w_i N_i (w_{i+1} - w_i)$	A16
<i>Resource</i>		
Predation on resource	$\mu_p(w_{R,j}) = \sum_{i=1}^{m-1} \phi\left(\frac{w_i}{w_{R,j}}\right) (1 - f(w_i)) \gamma w_i^q N_i (w_{i+1} - w_i)$	A17
Effective resource carrying capacity	$K_e(w_{R,j}) = \frac{r_0 w_{R,j}^{n-1} \kappa w_{R,j}^\lambda}{r_0 w_{R,j}^{n-1} + \mu_p(w_{R,j})}$	A18
Resource spectrum	$N_{R,j}^{t+\Delta t} = K_e(w_{R,j}) - [K_e(w_{R,j}) - N_{R,j}^t] e^{-[r_0 w_{R,j}^{n-1} + \mu_p(w_{R,j})] \Delta t}$	A19

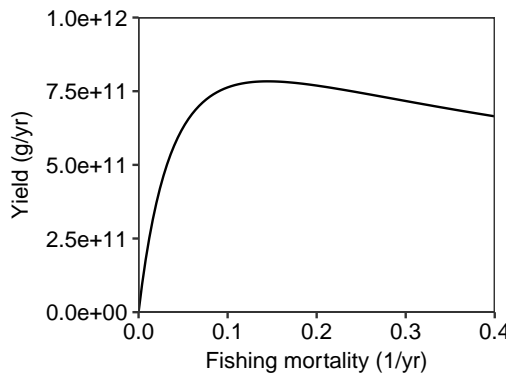


Figure B1: Modelled yield of North Sea plaice as a function of fishing mortality, with the peak indicating F_{MSY} . Shown for $\varepsilon_r = 0.1$. Yield is calculated with $R_{\max} = 1 \cdot 10^{10} \text{ yr}^{-1}$ and $\kappa = 1 \cdot 10^{50} \text{ g}^{-1-\lambda}$.

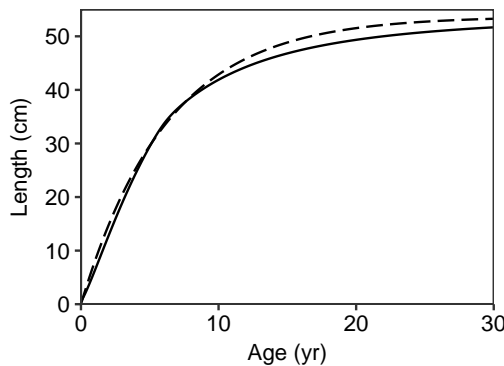


Figure B2: Modelled plaice length-at-age for complete early-in-life density dependent regulation (solid), and plaice length-at-age according to the von Bertalanffy growth equation with $K = 0.16 \text{ yr}^{-1}$ (dashed).

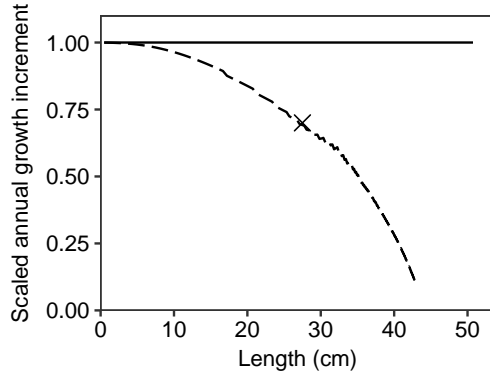


Figure B3: Plaice annual growth increment, scaled to annual growth increments for $F = 0.6 \text{ yr}^{-1}$. Shown for $F = 0.6 \text{ yr}^{-1}$ (solid) and $F = 0.05 \text{ yr}^{-1}$ (dashed). The cross shows the annual growth increment of 25-30 cm individuals in 1944-1945, scaled to their pre-WWII annual growth increment (Rijnsdorp and Van Leeuwen, 1992).

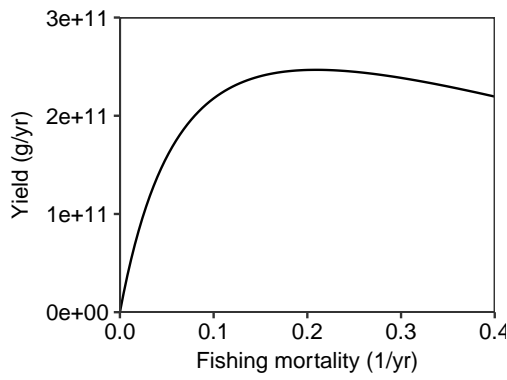


Figure B4: Modelled yield of NEA mackerel as a function of fishing mortality, with the peak indicating F_{MSY} . Shown for $\varepsilon_r = 0.0006$. Yield is calculated with $R_{\max} = 1 \cdot 10^{10} \text{ yr}^{-1}$ and $\kappa = 1 \cdot 10^{50} \text{ g}^{-1-\lambda}$.

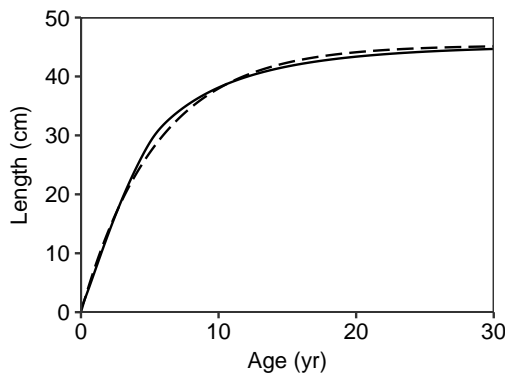


Figure B5: Modelled NEA mackerel length-at-age for complete early-in-life density dependent regulation (solid), and NEA mackerel length-at-age according to the von Bertalanffy growth equation with $K = 0.18 \text{ yr}^{-1}$ (dashed).

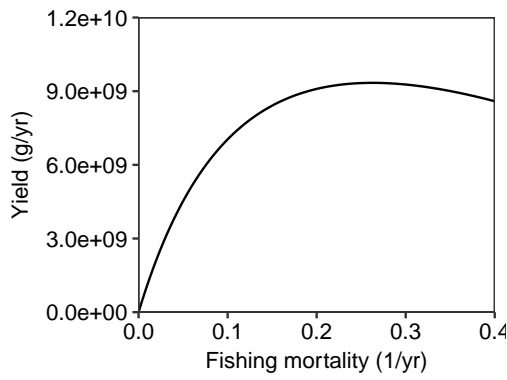


Figure B6: Modelled yield of Baltic sprat as a function of fishing mortality, with the peak indicating F_{MSY} . Shown for $\varepsilon_r = 0.0055$. Yield is calculated with $R_{\max} = 1 \cdot 10^{10} \text{ yr}^{-1}$ and $\kappa = 1 \cdot 10^{50} \text{ g}^{-1-\lambda}$.

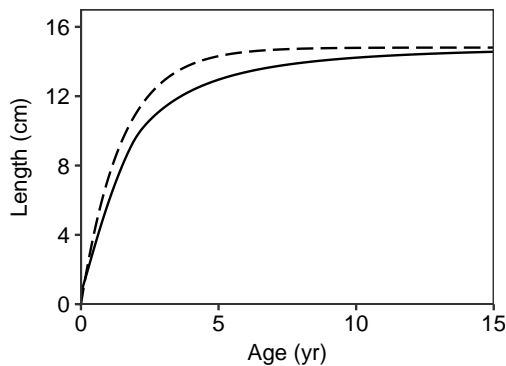


Figure B7: Modelled Baltic sprat length-at-age for complete early-in-life density dependent regulation (solid), and Baltic sprat length-at-age according to the von Bertalanffy growth equation with $K = 0.68 \text{ yr}^{-1}$ (dashed).

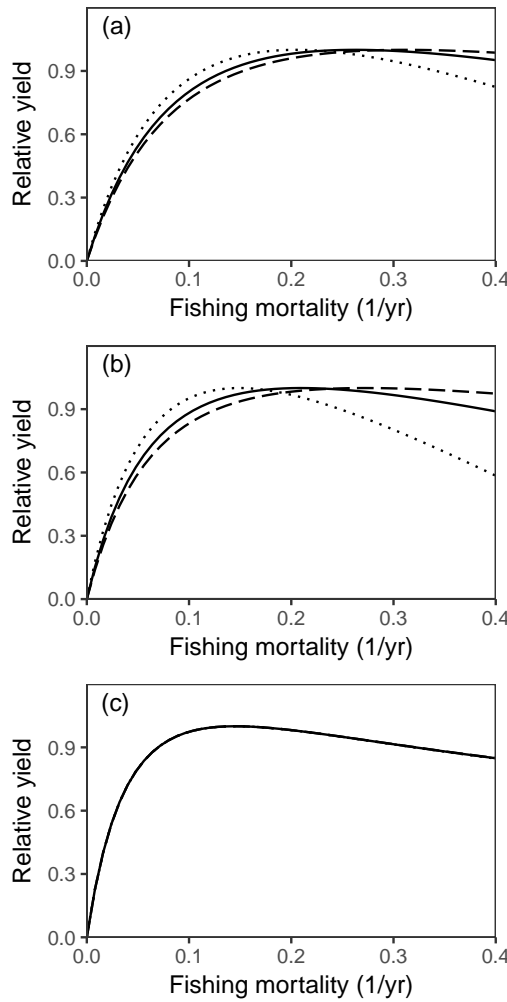


Figure C1: Yield as a function of fishing mortality, and its sensitivity to changes in the value of ε_r . The used values of ε_r are the fitted value (solid), a factor 2 lower than the fitted value (dashed), and a factor 2 higher than the fitted value (dotted). Yield is shown relative to the MSY of each ε_r value. Shown for Baltic sprat (a), NEA mackerel (b), and North Sea plaice (c).

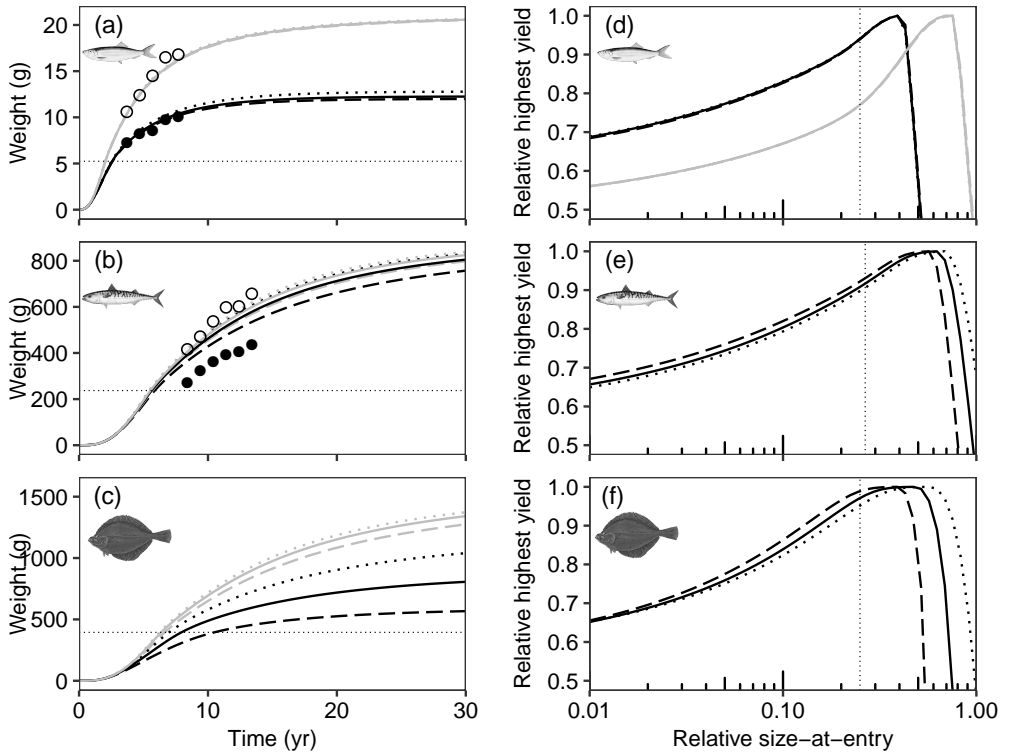


Figure C2: Sensitivity of the model to changes in the value of R_{\max}/κ . The used values of R_{\max}/κ are the fitted value (solid), a factor 2 lower than the fitted value (dotted), and a factor 2 higher than the fitted value (dashed). Shown for weight-at-age (a, b, c) and highest sustainable yield as a function of size-at-entry into the fishery (d, e, f), modelled for Baltic sprat (a, d), NEA mackerel (b, e), and North Sea plaice (c, f). Highest sustainable yield is shown relative to MSY of each scenario. Size-at-entry into the fishery is shown relative to W_∞ . Grey lines represent the stock's low-SSB scenario, and black lines represent the stock's high-SSB scenario. These lines overlap in (e) and (f), because only fishing mortality changes between scenarios there. The thin dotted lines show size-at-maturity. Historical weight-at-age data points are shown for the low-SSB (open points) and high-SSB (filled points) scenarios of sprat and mackerel. They are not shown for plaice, because Rijnsdorp and Van Leeuwen (1992) do not show changes in weight-at-age but in growth-increments of length groups.

CHAPTER C

Appendices Paper III

Density dependence dampens the
impact of a non-constant
gonado-somatic index

Appendices

Appendix A Stock data overview

Table A.1: List of stocks with available data on w and R_w . Stocks with too few data points (< 20), or data that was clearly not raw data, have not been used in the subsequent fits and population model.

Species	Stock	Datapoints (#)	Notes
<i>Abudefduf saxatilis</i>	Bimini Islands, The Bahamas	1	Too few data points
<i>Acanthochromis polyacanthus</i>	Heron island, GBR, Australia	15	Too few data points
<i>Acanthoclinus fuscus</i>	Central California, United States	7	Too few data points
<i>Acanthopagrus latus</i>	Kuwaiti waters	5	Too few data points
<i>Aidablennius sphynx</i>	Marine reserve of Miramare in the Northern Adriatic	1	Too few data points
<i>Amblygaster sirm</i>	Parangipettai, SE coast of India	33	
<i>Anchoviella lepidostole</i>	Near Rio Ribeira de Iguape, SP, Brazil	24	
<i>Aphanopus carbo</i>	Off Funchal, Madeira Is	14	Too few data points
<i>Archosargus rhomboidalis</i>	Terminos Lagoon, Mexico	23	
<i>Arnoglossus laterna</i>	Camas Nathais, in the Lynn of Lorne, Scotland	2	Too few data points
<i>Artediellus atlanticus</i>	Barents Sea	1	Too few data points
<i>Atherina presbyter</i>	Fowley power station Southampton, UK	33	
<i>Auxis rochei</i>	Shimizu Bay, Shimizu Ward, Japan	1	Too few data points
<i>Bairdiella chrysoura</i>	Mouth of Newport River, NC, USA	1	Too few data points
<i>Balistes capriscus</i>	Gulf of Gabes, Tunisia	38	
<i>Balistes capriscus</i>	Off Mobile Bay, Florida, USA	33	
<i>Balistes capriscus</i>	Gulf waters offshore of Panama City, Florida, USA	64	
<i>Balistes capriscus</i>	Off the coast of Senegal	37	
<i>Boreogadus saida</i>	Arctic Ocean	1	Too few data points
<i>Brachaluteres jacksonianus</i>	Terrigal, NSW, Australia	1	Too few data points
<i>Canthigaster valentini</i>	Lizard Island, GBR, Australia	66	
<i>Careproctus reinhardti</i>	Barents Sea	1	Too few data points
<i>Caulolatilus microps</i>	Onslow Bay, NC, USA	43	
<i>Centropomus undecimalis</i>	Between Ciudad del Carmen y Sabancuy, Mexico	15	Too few data points
<i>Cephalopholis cruentata</i>	Curacao island, Caribbean	12	Too few data points
<i>Cetengraulis mysticetus</i>	Gulf of Panama	86	
<i>Cheilodipterus macrodon</i>	Gulf of Aqaba, Red Sea	1	Too few data points
<i>Chelon labrosus</i>	Isles of Scilly, UK	13	Too few data points
<i>Chelon ramada</i>	River Tamar, UK	2	Too few data points
<i>Clupea harengus</i>	SW - S Coast of Iceland	419	
<i>Cyclopteropsis mcalpinii</i>	Arctic Ocean	1	Too few data points
<i>Cynoscion regalis</i>	from North Carolina to Gardiners Bay NY	29	
<i>Cynoscion striatus</i>	Off the southern coast of Brazil between Parana and Santa Catarina	5	Too few data points
<i>Decapterus punctatus</i>	Between Cape Fear, NC and Cape Canaveral, FL, USA	2	Too few data points
<i>Dicentrarchus labrax</i>	Carmarthen Bay, northern Bristol Channel, UK	10	Too few data points
<i>Dicentrarchus labrax</i>	Eddystone Rocks off Plymouth, western English Channel, UK	6	Too few data points
<i>Elacatinus oceanops</i>	Florida Keys, USA	1	Too few data points
<i>Elagatis bipinnulata</i>	Archipelago of Saint Peter and Saint Paul, Brazil	15	Too few data points
<i>Elagatis bipinnulata</i>	Fernando de Noronha Archipelago, Brazil	14	Too few data points
<i>Eleginops nawaga</i>	South Barents Sea	1	Too few data points
<i>Engraulis anchoita</i>	Off the coast of Mar del Plata	134	
<i>Engraulis anchoita</i>	Off the coast of Patagonia	25	
<i>Engraulis mordax</i>	Washington and Oregon, USA	21	
<i>Engraulis ringens</i>	Off the coast of Peru	129	
<i>Engraulis ringens</i>	Southern Chile	5	Too few data points
<i>Engraulis ringens</i>	Central Chile	5	Too few data points
<i>Engraulis ringens</i>	Chimbote, Ancash, Peru	10	Too few data points
<i>Enophryss bison</i>	Puget Sound, WA, USA	2	Too few data points
<i>Epinephelus aeneus</i>	Southeast Tunisian coast	27	
<i>Epinephelus fasciatus</i>	Southeast Tunisian coast	9	Too few data points
<i>Epinephelus marginatus</i>	Southeast Tunisian coast	2	Too few data points

Table A.1: List of stocks with available data on w and R_w . Stocks with too few data points (< 20), or data that was clearly not raw data, have not been used in the subsequent fits and population model.

Species	Stock	Datapoints (#)	Notes
<i>Epinephelus tauvina</i>	Kuwaiti waters	4	Too few data points
<i>Ethmalosa fimbriata</i>	Elmina fishing harbour, Kakum River estuary	32	
<i>Eubalichthys bucephalus</i>	Sutherland Point, situated at the entrance to Botany Bay, Kur nell, NSW, Australia	2	Too few data points
<i>Gadus morhua</i>	Off the eastern coast of Canada, between 42 and 54 degrees North	130	
<i>Gadus morhua</i>	Coastal Iceland	67	
<i>Gadus morhua</i>	Off northern Norway, between Vesteralen and Lofoten	216	
<i>Gadus morhua</i>	Southern Bight, North Sea	15	Too few data points
<i>Gasterosteus aculeatus</i>	River Rheidol near Aberystwyth, UK	108	
<i>Gasterosteus aculeatus</i>	Camargue Park, France	2	Too few data points
<i>Genyonemus lineatus</i>	Between Palos Verdes and Huntington beach, CA, USA	44	
<i>Gobiosoma robustum</i>	Tampa Bay station, St. Petersburg, Florida, United States	1	Too few data points
<i>Gymnelus viridis</i>	Arctic Ocean	1	Too few data points
<i>Haemulopsis corvinaeformis</i>	Mostly off the coast of Natal, RN, Brazil	2	Too few data points
<i>Hemiramphus brasiliensis</i>	Mostly off the coast of Natal, RN, Brazil	2	Too few data points
<i>Hemitripterus americanus</i>	Rhode Island, United States	6	Too few data points
<i>Hippocampus reidi</i>	Maracaípe mangrove, Ipojuca, PE, Brazil	3	Too few data points
<i>Hippoglossoides platessoides</i>	off Mountstuart House on the east side of the Isle of Bute	154	
<i>Hirundichthys affinis</i>	Mostly off the coast of Natal, RN, Brazil	2	Too few data points
<i>Holapogon maximus</i>	Oman	1	Too few data points
<i>Hoplostethus atlanticus</i>	TAS, Australia	55	
<i>Hoplostethus atlanticus</i>	SA, Australia	70	
<i>Hoplostethus atlanticus</i>	NSW, Australia	41	
<i>Icelus bicornis</i>	Barents Sea	1	Too few data points
<i>Ilisha africana</i>	off Lagos Coast, Nigeria	1	Too few data points
<i>Isopisthus parvipinnis</i>	Off the southern coast of Brazil between Parana and Santa Catarina	8	Too few data points
<i>Jaydia hungi</i>	Madagascar	1	Too few data points
<i>Larimus breviceps</i>	Off the southern coast of Brazil between Parana and Santa Catarina	6	Too few data points
<i>Larimus fasciatus</i>	mouth of the Cape Fear River, NC, about 4-6 km off Oak Island	81	
<i>Lates calcarifer</i>	Van Diemen Gulf	7	Too few data points
<i>Lates calcarifer</i>	Gulf of Carpentaria	18	Too few data points
<i>Lepidonotothen nudifrons</i>	Bouvet Island	1	Too few data points
<i>Leptagonus decagonus</i>	North Atlantic	1	Too few data points
<i>Leuresthes tenuis</i>	California, United States	7	Too few data points
<i>Lutjanus campechanus</i>	Off the north-northeastern coast of Brazil	9	Too few data points
<i>Lutjanus carponotatus</i>	Whitsunday Islands, Qld, Australia	55	
<i>Lutjanus synagris</i>	Off Iguape, Aquiraz, CE, Brazil	39	
<i>Lycodes esmarkii</i>	Sub Arctic, Norwegian Sea	1	Too few data points
<i>Lycodes eudipleurostictus</i>	Barents Sea	1	Too few data points
<i>Lycodes frigidus</i>	Barents Sea	1	Too few data points
<i>Lycodes pallidus</i>	Barents Sea	1	Too few data points
<i>Lycodes vahlii</i>	North Atlantic	1	Too few data points
<i>Macrodon ancylodon</i>	Along the southern coast of Brazil below 29 degrees south	21	
<i>Mallotus villosus</i>	Barents Sea	34	
<i>Melanostigma atlanticum</i>	Laurentian Trough off Rimouski, Quebec	3	Too few data points
<i>Merlangius merlangus</i>	northern North Sea	178	
<i>Merluccius gayi</i>	Off the coast of Chile between 34 and 38 degrees south	50	
<i>Merluccius hubbsi</i>	Off the northern coast of Patagonia, Argentina, between 42 and 46 degrees south	251	
<i>Merluccius merluccius</i>	Off the coast of Galicia, Spain	209	
<i>Micrognathus crinitus</i>	Cedar Key, Florida, United States	1	Too few data points
<i>Micromesistius australis</i>	Mar Argentino	96	

Table A.1: List of stocks with available data on w and R_w . Stocks with too few data points (< 20), or data that was clearly not raw data, have not been used in the subsequent fits and population model.

Species	Stock	Datapoints (#)	Notes
<i>Micropogonias furnieri</i>	Along the southern coast of Brazil between 29 and 33 degrees south	54	
<i>Micropogonias furnieri</i>	Off the mouth of Rio de La Plata between Uruguay and Argentina	31	
<i>Mugil cephalus</i>	Matanzas River Inlet south of St. Augustine, FL, USA	71	
<i>Mugil cephalus</i>	Around the coast of Goa, India	22	
<i>Mugil cephalus</i>	Negombo Lagoon, Sri Lanka	2	Too few data points
<i>Mugil curema</i>	Tunas de Zaza, Sancti Spiritus, Cuba	4	Too few data points
<i>Mugil curema</i>	Havana, Cuba	4	Too few data points
<i>Mugil hospes</i>	Tunas de Zaza, Sancti Spiritus, Cuba	1	Too few data points
<i>Mugil liza</i>	Tunas de Zaza, Sancti Spiritus, Cuba	1	Too few data points
<i>Mugil trichodon</i>	Tunas de Zaza, Sancti Spiritus, Cuba	1	Too few data points
<i>Myctoperca tigris</i>	Bajos del Norte Is, Mexico	2	Too few data points
<i>Nematalosa vlaminghi</i>	Swan-Avon river system, Perth WA, Australia	1	Too few data points
<i>Ocyurus chrysurus</i>	Banco de Campeche, Mexico	21	
<i>Odontesthes argentinensis</i>	Lagoa dos Patos, RS, Brazil	24	
<i>Opisthonema libertate</i>	Punta Arenas, Costa Rica	58	
<i>Opisthonema medirastre</i>	Punta Arenas, Costa Rica	46	
<i>Ostorhinus cookii</i>	Gulf of Aqaba, Red Sea	1	Too few data points
<i>Ostorhinus cyanosoma</i>	Gulf of Aqaba, Red Sea	1	Too few data points
<i>Oxylebius pictus</i>	Monterey Bay California USA	22	
<i>Oxymonacanthus longirostris</i>	Enewetak Atoll	3	Too few data points
<i>Pampus chinensis</i>	Chandipur, Odisha, India	8	Too few data points
<i>Paragobiodon echocephalus</i>	Heron island, GBR, Australia	1	Too few data points
<i>Paragobiodon lacunicolus</i>	Heron island, GBR, Australia	1	Too few data points
<i>Paragobiodon xanthosoma</i>	Heron island, GBR, Australia	1	Too few data points
<i>Paralichthys dentatus</i>	Middle Atlantic Bight (Cape Cod, Massachusetts to Cape Hatteras, North Carolina)	134	
<i>Paralichthys patagonicus</i>	Off the coast of Mar del Plata	24	
<i>Paraliparis bathybius</i>	Barents Sea	1	Too few data points
<i>Paralonchurus brasiliensis</i>	Off the southern coast of Brazil between Parana and Santa Catarina	16	Too few data points
<i>Planiliza subviridis</i>	Penang Island, facing the Western Channel of the Straits of Penang	12	Too few data points
<i>Pleuronectes platessa</i>	North Sea	486	
<i>Pomacanthus zonipectus</i>	Off Espiritu Santo Is, Baja California, Mexico	5	Too few data points
<i>Pomacentrus coelestis</i>	Bohnotsu (ML), Japan	27	
<i>Pomacentrus coelestis</i>	Sesoko (LL), Japan	27	
<i>Pomacentrus coelestis</i>	Kominato (HL), Japan	27	
<i>Pomatoschistus minutus</i>	Ythan estuary, Aberdeenshire, Scotland	28	
<i>Pseudopleuronectes americanus</i>	Narragansett Bay, Portsmouth, RI, United States	17	Too few data points
<i>Reinhardtius hippoglossoides</i>	Off the west coast of Bear island, Northeast Arctic Sea	88	
<i>Rhomboplites aurorubens</i>	North and South Carolina, USA	41	
<i>Rudarius ercodes</i>	Rocky reef off Tsuyazaki, northern Kyushu, Japan	3	Too few data points
<i>Sardinops sagax</i>	Magdalena Bay, Baja California Sur, Mexico	185	
<i>Scomber scombrus</i>	Great Sole Bank, eastern Atlantic	27	
<i>Scomberomorus cavalla</i>	Texas	11	Too few data points
<i>Scomberomorus cavalla</i>	Louisiana	24	
<i>Scomberomorus cavalla</i>	NW Florida	17	Too few data points
<i>Scomberomorus cavalla</i>	North Carolina	12	Too few data points
<i>Scomberomorus cavalla</i>	Off Iguape, Aquiraz, CE, Brazil	11	Too few data points
<i>Scomberomorus maculatus</i>	Off Iguape, Aquiraz, CE, Brazil	13	Too few data points
<i>Scomberomorus maculatus</i>	Narragansett Bay, Portsmouth, Rhode Island to South Carolina	1	Too few data points
<i>Sebastes alutus</i>	Washington, United States and southern Vancouver Island, Canada	17	Too few data points

Table A.1: List of stocks with available data on w and R_w . Stocks with too few data points (< 20), or data that was clearly not raw data, have not been used in the subsequent fits and population model.

Species	Stock	Datapoints (#)	Notes
<i>Sebastodes alutus</i>	Gulf of Alaska	43	
<i>Sebastodes alutus</i>	Vancouver Island	7	Too few data points
<i>Sebastodes alutus</i>	Queen Charlotte Sound, New Zealand	14	Too few data points
<i>Sebastodes alutus</i>	Bering Sea	7	Too few data points
<i>Sebastodes atrovirens</i>	Central California, United States	17	Too few data points
<i>Sebastodes auriculatus</i>	Port Orchard, Puget Sound, Washington, United States	35	
<i>Sebastodes brevispinis</i>	Sea Otter Trough, BC, Canada	22	No raw data points
<i>Sebastodes carnatus</i>	Central California, United States	11	Too few data points
<i>Sebastodes caurinus</i>	Port Orchard, Puget Sound, Washington, United States	33	
<i>Sebastodes caurinus</i>	Bainbridge Island and Colvos Passage, Washington, United States	21	
<i>Sebastodes chlorostictus</i>	California Bight, California, United States	16	Too few data points
<i>Sebastodes chlorostictus</i>	Monterey Bay, California, United States	48	
<i>Sebastodes constellatus</i>	California Bight, California, United States	21	
<i>Sebastodes crameri</i>	Santa Monica Bay, California, United States to Bering Sea.	12	Too few data points
<i>Sebastodes dallii</i>	California Bight, California, United States	23	
<i>Sebastodes diploproa</i>	Coronado Islands, Baja California, Mexico to Vancouver, British Columbia, Canada	15	Too few data points
<i>Sebastodes elongatus</i>	California Bight, California, United States	25	
<i>Sebastodes entomelas</i>	Newport, Oregon, USA	63	
<i>Sebastodes entomelas</i>	California Bight, California, United States	27	
<i>Sebastodes entomelas</i>	San Diego, California, United States to southeastern Alaska, United States	20	
<i>Sebastodes flavidus</i>	San Diego, California, United States to Vancouver Island, British Columbia, Canada	15	Too few data points
<i>Sebastodes flavidus</i>	California Bight, California, United States	34	
<i>Sebastodes goodei</i>	California Bight, California, United States	39	
<i>Sebastodes goodei</i>	Magdalena Bay, Baja California, Mexico to Eureka, California, United States	23	
<i>Sebastodes helvomaculatus</i>	Vancouver, Canada to California, United States	5	Too few data points
<i>Sebastodes hopkinsi</i>	California Bight, California, United States	39	
<i>Sebastodes jordani</i>	Ensenada, Baja California, Mexico to Washington, United States	10	Too few data points
<i>Sebastodes levis</i>	California Bight, California, United States	27	
<i>Sebastodes melanops</i>	Newport, Oregon, USA	226	
<i>Sebastodes melanostomus</i>	Morro Bay, California, United States	39	
<i>Sebastodes melanostomus</i>	Santa Barbara, California, United States	3	Too few data points
<i>Sebastodes mentella</i>	Gulf of St. Lawrence, Laurentian Channel and Esquiman Channel	173	
<i>Sebastodes mentella</i>	Off the SW coast of Iceland	54	
<i>Sebastodes miniatus</i>	California Bight, California, United States	47	
<i>Sebastodes miniatus</i>	San Benito Islands, Baja California, Mexico to Vancouver Island, British Columbia, Canada	12	Too few data points
<i>Sebastodes mystinus</i>	Central California, United States	17	Too few data points
<i>Sebastodes mystinus</i>	Monterey, California, United States	50	
<i>Sebastodes mystinus</i>	Half Moon Bay and Morro Bay, California, United States	84	
<i>Sebastodes norvegicus</i>	East Greenland	12	Too few data points
<i>Sebastodes norvegicus</i>	Iceland	14	Too few data points
<i>Sebastodes norvegicus</i>	Off the SW coast of Iceland	26	
<i>Sebastodes norvegicus</i>	Faro Islands	15	Too few data points
<i>Sebastodes ovalis</i>	Cordell Bank, California, United States	35	
<i>Sebastodes ovalis</i>	Santa Barbara, California, United States	4	Too few data points
<i>Sebastodes paucispinis</i>	California Bight, California, United States	51	
<i>Sebastodes paucispinis</i>	Sacramento Reef, Baja California, Mexico to Queen Charlotte Sound, British Columbia, Canada	24	

Table A.1: List of stocks with available data on w and R_w . Stocks with too few data points (< 20), or data that was clearly not raw data, have not been used in the subsequent fits and population model.

Species	Stock	Datapoints (#)	Notes
<i>Sebastes pinniger</i>	Cape Colnett, Baja California, Mexico to Dixon Entrance, British Columbia, Canada	10	Too few data points
<i>Sebastes rastrelliger</i>	southern California, United States	2	Too few data points
<i>Sebastes rosaceus</i>	California Bight, California, United States	23	
<i>Sebastes rosenblatti</i>	California Bight, California, United States	26	
<i>Sebastes rufus</i>	California Bight, California, United States	27	
<i>Sebastes saxicola</i>	California Bight, California, United States	30	
<i>Sebastes saxicola</i>	Sebastian Viscaino Bay, Baja California, Mexico to southeastern Alaska, United States	13	Too few data points
<i>Sebastes semicinctus</i>	California Bight, California, United States	46	
<i>Sebastes serranoides</i>	Avila, California, United States	83	
<i>Sebastes viviparus</i>	Norwegian and Barent seas	32	
<i>Seriphis politus</i>		142	
<i>Seriphis politus</i>	Off the coast between San Clemente and Oceanside, CA, USA	1	Too few data points
<i>Siganus canaliculatus</i>	Off Dammam, Saudi Arabia	27	
<i>Siphonia tubifer</i>	Gulf of Aqaba, Red Sea	1	Too few data points
<i>Solea solea</i>	European Continental Shelf Area IXa	33	
<i>Solea solea</i>	European Continental Shelf Area VIIa	29	
<i>Solea solea</i>	European Continental Shelf Area VIIId	49	
<i>Solea solea</i>	European Continental Shelf Area IVc	55	
<i>Solea solea</i>	European Continental Shelf Area VIIe	33	
<i>Solea solea</i>	European Continental Shelf Area IVbWest	45	
<i>Solea solea</i>	European Continental Shelf Area VIIia	39	
<i>Solea solea</i>	European Continental Shelf Area IVbEast	40	
<i>Sparidentex hasta</i>	Kuwaiti waters	6	Too few data points
<i>Spatelloides gracilis</i>	Ysabel passage, Papua New Guinea	18	Too few data points
<i>Stegastes fuscus</i>	Buzios beach, Nisia Floresta, RN, Brazil	14	Too few data points
<i>Stellifer rastrifer</i>	Off the southern coast of Brazil between Parana and Santa Catarina	44	
<i>Strangomera bentincki</i>	Southern Chile	5	Too few data points
<i>Strangomera bentincki</i>	Central Chile	5	Too few data points
<i>Syngnathus floridae</i>	Cedar Key, Florida, United States	1	Too few data points
<i>Syngnathus louisianae</i>	Cedar Key, Florida, United States	1	Too few data points
<i>Syngnathus scovelli</i>	Cedar Key, Florida, United States	1	Too few data points
<i>Taeniamia lineolata</i>	Gulf of Aqaba, Red Sea	1	Too few data points
<i>Thalassoma bifasciatum</i>	San Blas Province, Panama	66	
<i>Thunnus alalunga</i>	Cook Islands and American Samoa	69	
<i>Thunnus albacares</i>	Gulf of Guinea, Africa	4	Too few data points
<i>Thunnus thynnus</i>	Gulf of Mexico	27	
<i>Trachurus picturatus</i>	Off Mar del Plata, Argentina	8	Too few data points
<i>Triglops pingelii</i>	Arctic Ocean	1	Too few data points

Table A.2: List of stocks for which the population model was run, showing stock-specific parameter values as given by the R package *FishLife* (Thorson *et al.*, 2017), and the value of b as given by Fishbase (Froese and Pauly, 2000).

Species	Stock	W_{∞} (g)	K (yr $^{-1}$)	M (yr $^{-1}$)	b
<i>Amblygaster sirm</i>	Parangipettai, SE coast of India	84.20	1.104	1.706	3.123
<i>Anchoviella lepidostole</i>	Near Rio Ribeira de Iguape, SP, Brazil	31.28	0.768	1.585	2.983
<i>Archosargus rhomboidalis</i>	Terminos Lagoon, Mexico	476.94	0.633	1.204	2.883
<i>Atherina presbyter</i>	Fowley power station Southampton, UK	20.94	0.520	0.978	3.300
<i>Balistes capriscus</i>	Gulf of Gabes, Tunisia	1250.02	0.305	0.937	2.515
<i>Balistes capriscus</i>	Off Mobile Bay, Florida, USA	1250.02	0.305	0.937	2.515
<i>Balistes capriscus</i>	Gulf waters offshore of Panama City, Florida, USA	1250.02	0.305	0.937	2.515
<i>Balistes capriscus</i>	Off the coast of Senegal	1250.02	0.305	0.937	2.515
<i>Canthigaster valentini</i>	Lizard Island, GBR, Australia	525.32	0.480	0.942	2.943
<i>Caulolatilus microps</i>	Onslow Bay, NC, USA	3904.77	0.172	0.313	3.024
<i>Cetengraulis mysticetus</i>	Gulf of Panama	60.08	1.339	2.058	3.404
<i>Clupea harengus</i>	SW - S Coast of Iceland	212.22	0.334	0.250	2.875
<i>Cynoscion regalis</i>	from North Carolina to Gardiners Bay NY	2591.82	0.203	0.351	2.984
<i>Engraulis anchoita</i>	Off the coast of Mar del Plata	43.14	0.387	0.925	3.050
<i>Engraulis anchoita</i>	Off the coast of Patagonia	43.14	0.387	0.925	3.050
<i>Engraulis mordax</i>	Washington and Oregon, USA	45.58	0.383	0.885	2.860
<i>Engraulis ringens</i>	Off the coast of Peru	53.49	0.924	1.181	2.604
<i>Epinephelus aeneus</i>	Southeast Tunisian coast	12216.39	0.140	0.211	2.850
<i>Ethmalosa fimbriata</i>	Elmina fishing harbour, Kakum River estuary	389.62	0.583	0.678	3.210
<i>Gadus morhua</i>	Off the eastern coast of Canada, between 42 and 54 degrees North	12310.02	0.168	0.270	3.035
<i>Gadus morhua</i>	Coastal Iceland	12310.02	0.168	0.270	3.035
<i>Gadus morhua</i>	Off northern Norway, between Vesteralen and Lofoten	12310.02	0.168	0.270	3.035
<i>Gasterosteus aculeatus</i>	River Rheidol near Aberystwyth, UK	2.98	1.746	1.945	3.260
<i>Genyonemus lineatus</i>	Between Palos Verdes and Huntington beach, CA, USA	1320.30	0.345	0.596	2.943
<i>Hippoglossoides platessoides</i>	off Mountstuart House on the east side of the Isle of Bute	2558.35	0.107	0.211	3.285
<i>Hoplostethus atlanticus</i>	TAS, Australia	1875.59	0.069	0.192	2.737
<i>Hoplostethus atlanticus</i>	SA, Australia	1875.59	0.069	0.192	2.737
<i>Hoplostethus atlanticus</i>	NSW, Australia	1875.59	0.069	0.192	2.737
<i>Larimus fasciatus</i>	mouth of the Cape Fear River, NC, about 4-6 km off Oak Island	434.89	0.586	0.961	3.080
<i>Lutjanus carponotatus</i>	Whitsunday islands, Qld, Australia	2368.53	0.369	0.298	2.980
<i>Lutjanus synagris</i>	Off Iguape, Aquiraz, CE, Brazil	1542.65	0.228	0.413	2.917
<i>Macrodon ancylodon</i>	Along the southern coast of Brazil below 29 degrees south	799.76	0.390	0.669	2.737
<i>Mallotus villosus</i>	Barents Sea	49.52	0.461	1.000	2.595
<i>Merlangius merlangus</i>	northern North Sea	800.18	0.292	0.472	3.086
<i>Merluccius gayi gayi</i>	Off the coast of Chile between 34 and 38 degrees south	6074.50	0.213	0.403	3.070
<i>Merluccius hubbsi</i>	Off the northern coast of Patagonia, Argentina, between 42 and 46 degrees south	2486.58	0.221	0.401	3.102
<i>Merluccius merluccius</i>	Off the coast of Galicia, Spain	3684.46	0.140	0.319	3.110
<i>Micromesistius australis</i>	Mar Argentino	1171.04	0.212	0.230	3.265
<i>Micropogonias furnieri</i>	Along the southern coast of Brazil between 29 and 33 degrees south	2462.25	0.176	0.448	3.050
<i>Micropogonias furnieri</i>	Off the mouth of Rio de La Plata between Uruguay and Argentina	2462.25	0.176	0.448	3.050
<i>Mugil cephalus</i>	Matanzas River Inlet south of St. Augustine, FL, USA	2061.67	0.247	0.329	2.979
<i>Mugil cephalus</i>	Around the coast of Goa, India	2061.67	0.247	0.329	2.979
<i>Ocyurus chrysurus</i>	Banco de Campeche, Mexico	2504.05	0.181	0.309	2.793
<i>Odontesthes argentinensis</i>	Lagoa dos Patos, RS, Brazil	247.97	0.548	0.993	3.068
<i>Opisthonema libertate</i>	Punta Arenas, Costa Rica	136.84	0.443	0.636	3.039
<i>Opisthonema medirastre</i>	Punta Arenas, Costa Rica	102.42	0.582	0.836	3.040
<i>Oxylebius pictus</i>	Monterey Bay California USA	231.17	0.332	0.521	3.040
<i>Paralichthys dentatus</i>	Middle Atlantic Bight (Cape Cod, Massachusetts to Cape Hatteras, North Carolina)	5761.81	0.353	0.661	3.246
<i>Paralichthys patagonicus</i>	Off the coast of Mar del Plata	1228.33	0.373	0.710	3.121

Table A.2: List of stocks for which the population model was run, showing stock-specific parameter values as given by the R package *FishLife* (Thorson *et al.*, 2017), and the value of b as given by Fishbase (Froese and Pauly, 2000).

Species	Stock	W_{∞} (g)	K (yr^{-1})	M (yr^{-1})	b
<i>Pleuronectes platessa</i>	North Sea	1752.78	0.138	0.144	3.017
<i>Pomacentrus coelestis</i>	Bohnotsu (ML), Japan	69.94	0.562	0.985	2.630
<i>Pomacentrus coelestis</i>	Sesoko (LL), Japan	69.94	0.562	0.985	2.630
<i>Pomacentrus coelestis</i>	Kominato (HL), Japan	69.94	0.562	0.985	2.630
<i>Pomatoschistus minutus</i>	Ythan estuary, Aberdeenshire, Scotland	3.01	0.853	1.942	3.289
<i>Reinhardtius hippoglossoides</i>	Off the west coast of Bear island, Northeast Arctic Sea	24975.85	0.072	0.095	3.328
<i>Rhomboptilus aurorubens</i>	North and South Carolina, USA	2385.24	0.185	0.258	2.894
<i>Sardinops sagax</i>	Magdalena Bay, Baja California Sur, Mexico	151.47	0.440	0.384	3.230
<i>Scomber scombrus</i>	Great Sole Bank, eastern Atlantic	624.37	0.345	0.288	3.084
<i>Scomberomorus cavalla</i>	Louisiana	13709.06	0.171	0.286	2.893
<i>Sebastes alutus</i>	Gulf of Alaska	1054.28	0.125	0.101	3.220
<i>Sebastes auriculatus</i>	Port Orchard, Puget Sound, Washington, United States	930.76	0.128	0.100	3.070
<i>Sebastes caurinus</i>	Port Orchard, Puget Sound, Washington, United States	1693.28	0.114	0.094	3.000
<i>Sebastes caurinus</i>	Bainbridge Island and Colvos Passage, Washington, United States	1693.28	0.114	0.094	3.000
<i>Sebastes chlorostictus</i>	Monterey Bay, California, United States	930.76	0.128	0.100	3.000
<i>Sebastes constellatus</i>	California Bight, California, United States	1138.84	0.116	0.095	3.000
<i>Sebastes dallii</i>	California Bight, California, United States	930.76	0.128	0.100	3.070
<i>Sebastes elongatus</i>	California Bight, California, United States	671.16	0.132	0.108	3.000
<i>Sebastes entomelas</i>	Newport, Oregon, USA	930.76	0.128	0.100	3.070
<i>Sebastes entomelas</i>	California Bight, California, United States	930.76	0.128	0.100	3.070
<i>Sebastes entomelas</i>	San Diego, California, United States to southeastern Alaska, United States	930.76	0.128	0.100	3.070
<i>Sebastes flavidus</i>	California Bight, California, United States	1781.09	0.124	0.078	3.000
<i>Sebastes goodei</i>	California Bight, California, United States	427.08	0.188	0.151	3.000
<i>Sebastes goodei</i>	Magdalena Bay, Baja California, Mexico to Eureka, California, United States	427.08	0.188	0.151	3.000
<i>Sebastes hopkinsi</i>	California Bight, California, United States	335.66	0.149	0.130	3.070
<i>Sebastes levis</i>	California Bight, California, United States	1870.43	0.105	0.089	3.090
<i>Sebastes melanops</i>	Newport, Oregon, USA	2050.30	0.147	0.109	3.000
<i>Sebastes melanostomus</i>	Morro Bay, California, United States	2318.34	0.069	0.060	3.000
<i>Sebastes mentella</i>	Gulf of St. Lawrence, Laurentian Channel and Esquiman Channel	1444.37	0.090	0.077	2.977
<i>Sebastes mentella</i>	Off the SW coast of Iceland	1444.37	0.090	0.077	2.977
<i>Sebastes miniatus</i>	California Bight, California, United States	930.76	0.128	0.100	3.000
<i>Sebastes mystinus</i>	Monterey, California, United States	791.07	0.155	0.124	3.000
<i>Sebastes mystinus</i>	Half Moon Bay and Morro Bay, California, United States	791.07	0.155	0.124	3.000
<i>Sebastes norvegicus</i>	Off the SW coast of Iceland	1302.26	0.096	0.076	3.180
<i>Sebastes ovalis</i>	Cordell Bank, California, United States	1145.52	0.098	0.084	3.000
<i>Sebastes paucispinis</i>	California Bight, California, United States	1078.48	0.137	0.125	3.000
<i>Sebastes paucispinis</i>	Sacramento Reef, Baja California, Mexico to Queen Charlotte Sound, British Columbia, Canada	1078.48	0.137	0.125	3.000
<i>Sebastes rosaceus</i>	California Bight, California, United States	930.76	0.128	0.100	3.070
<i>Sebastes rosenblatti</i>	California Bight, California, United States	2413.18	0.089	0.075	3.070
<i>Sebastes rufus</i>	California Bight, California, United States	930.76	0.128	0.100	3.000
<i>Sebastes saxicola</i>	California Bight, California, United States	295.38	0.144	0.122	3.070
<i>Sebastes semicinctus</i>	California Bight, California, United States	127.51	0.256	0.194	2.810
<i>Sebastes serranoides</i>	Avila, California, United States	1613.09	0.185	0.131	2.968
<i>Sebastes viviparus</i>	Norwegian and Barent seas	641.80	0.122	0.102	3.212
<i>Seriphis politus</i>		1320.30	0.345	0.596	3.090
<i>Siganus canaliculatus</i>	Off Dammam, Saudi Arabia	197.81	1.339	1.527	3.011
<i>Solea solea</i>	European Continental Shelf Area IXa	443.58	0.324	0.285	3.175
<i>Solea solea</i>	European Continental Shelf Area VIIa	443.58	0.324	0.285	3.175
<i>Solea solea</i>	European Continental Shelf Area VIIId	443.58	0.324	0.285	3.175

Table A.2: List of stocks for which the population model was run, showing stock-specific parameter values as given by the R package *FishLife* (Thorson *et al.*, 2017), and the value of b as given by Fishbase (Froese and Pauly, 2000).

Species	Stock	W_{∞} (g)	K (yr^{-1})	M (yr^{-1})	b
<i>Solea solea</i>	European Continental Shelf Area IVc	443.58	0.324	0.285	3.175
<i>Solea solea</i>	European Continental Shelf Area VIIe	443.58	0.324	0.285	3.175
<i>Solea solea</i>	European Continental Shelf Area IVbWest	443.58	0.324	0.285	3.175
<i>Solea solea</i>	European Continental Shelf Area VIIia	443.58	0.324	0.285	3.175
<i>Solea solea</i>	European Continental Shelf Area IVbEast	443.58	0.324	0.285	3.175
<i>Stellifer brasiliensis</i>	Off the southern coast of Brazil between Paraná and Santa Catarina	1320.30	0.345	0.596	3.270
<i>Thalassoma bifasciatum</i>	San Blas Province, Panama	90.32	0.601	1.187	2.916
<i>Thunnus alalunga</i>	Cook Islands and American Samoa	37677.49	0.180	0.256	2.928
<i>Thunnus thynnus</i>	Gulf of Mexico	660586.73	0.098	0.152	2.800

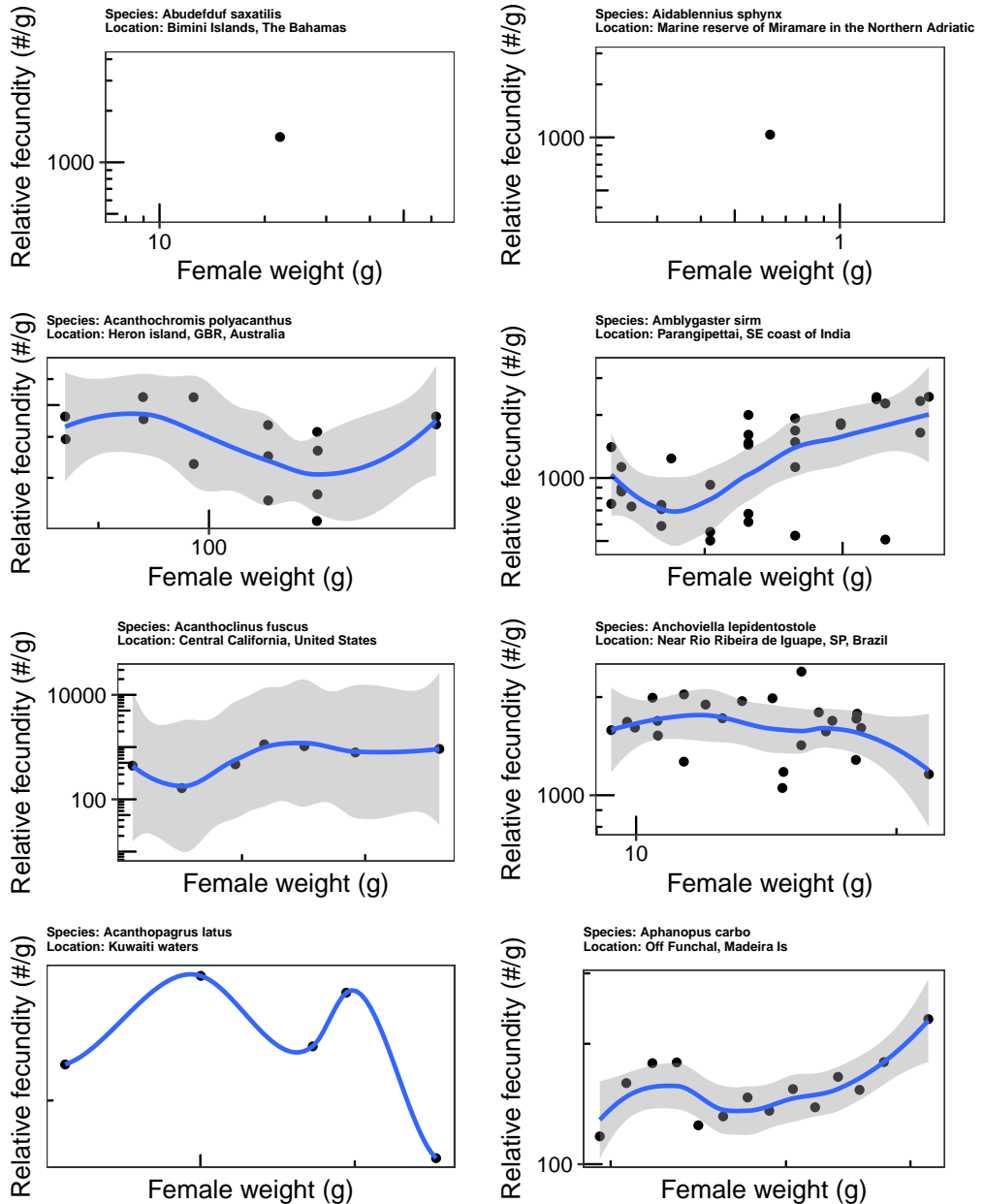
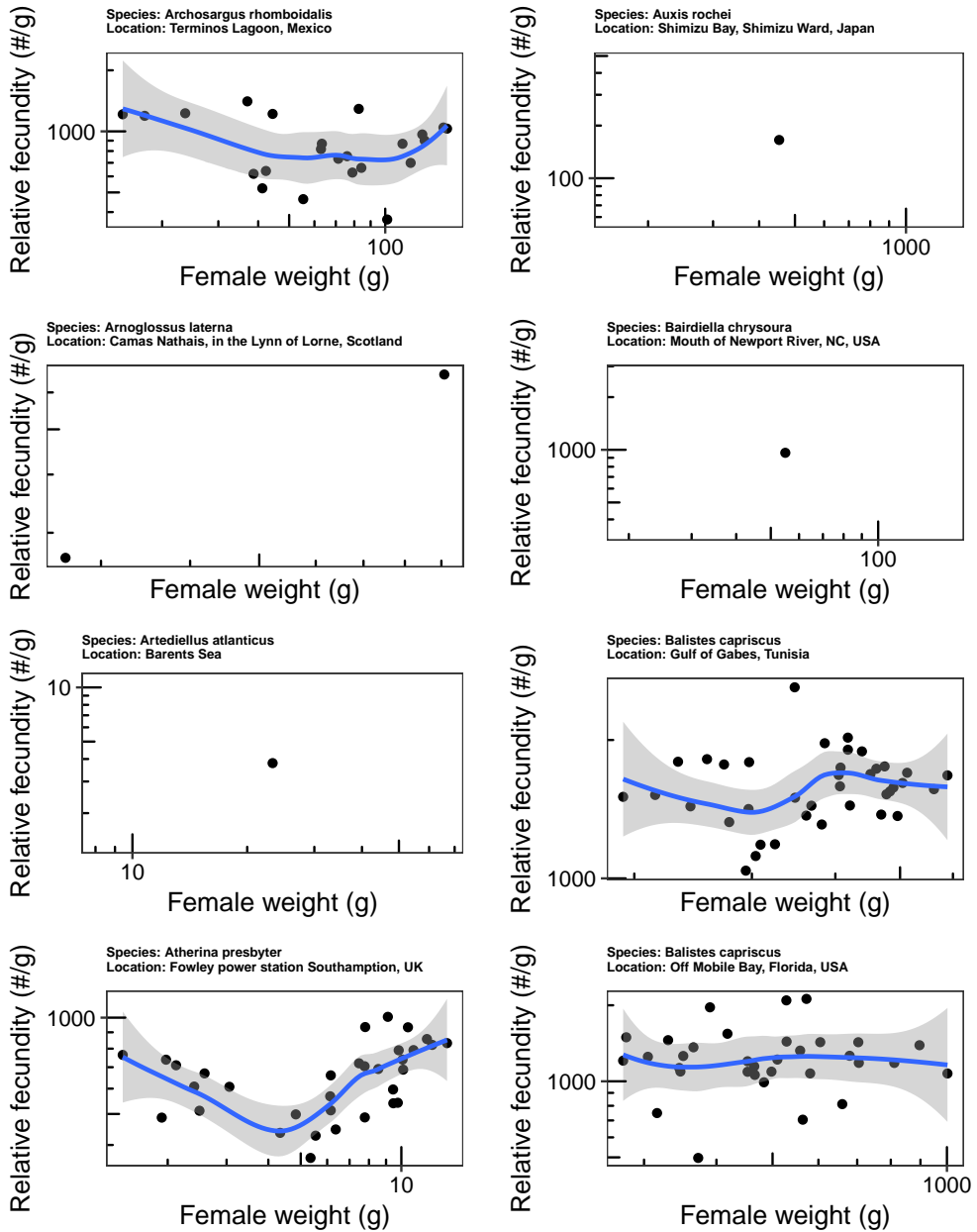
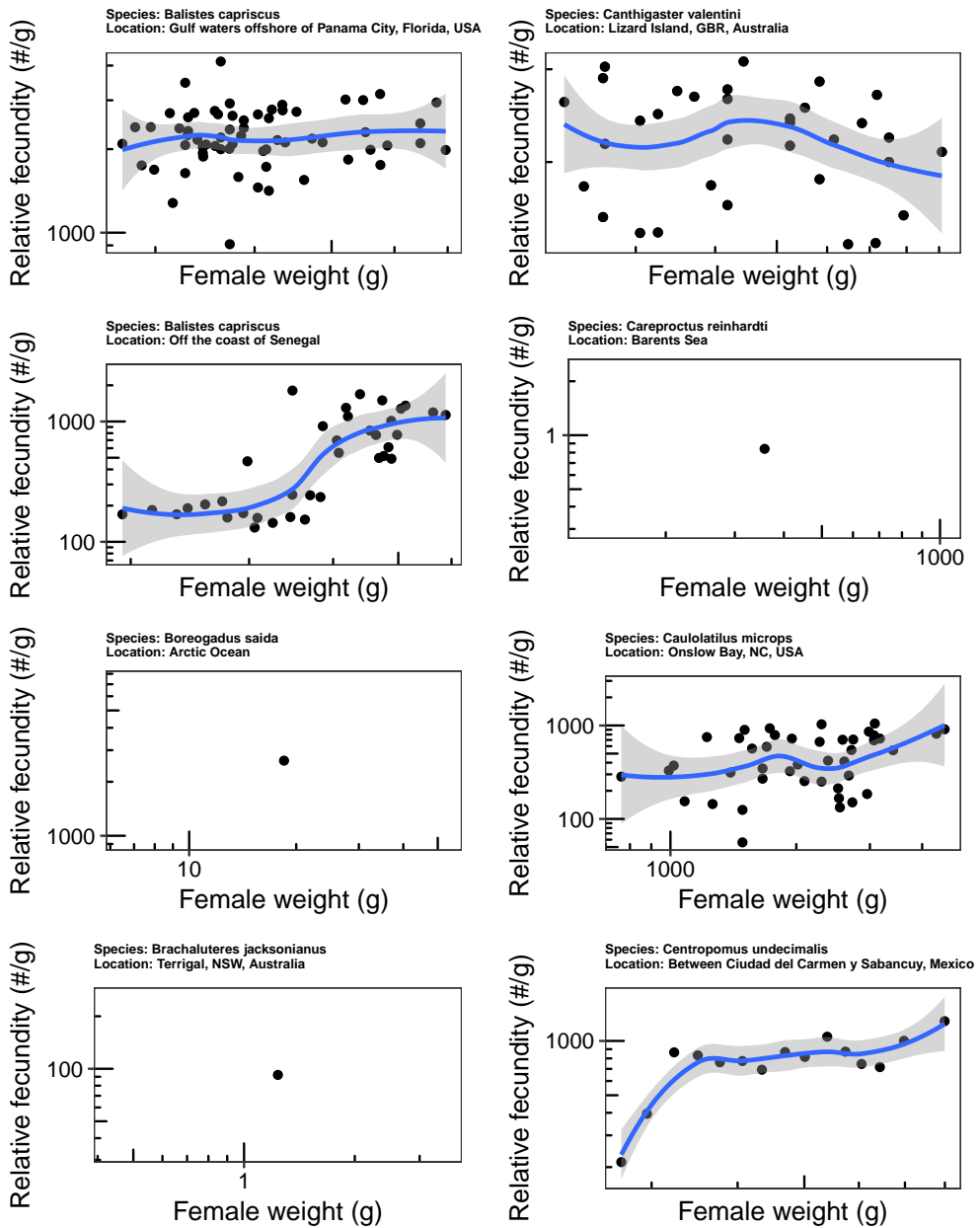
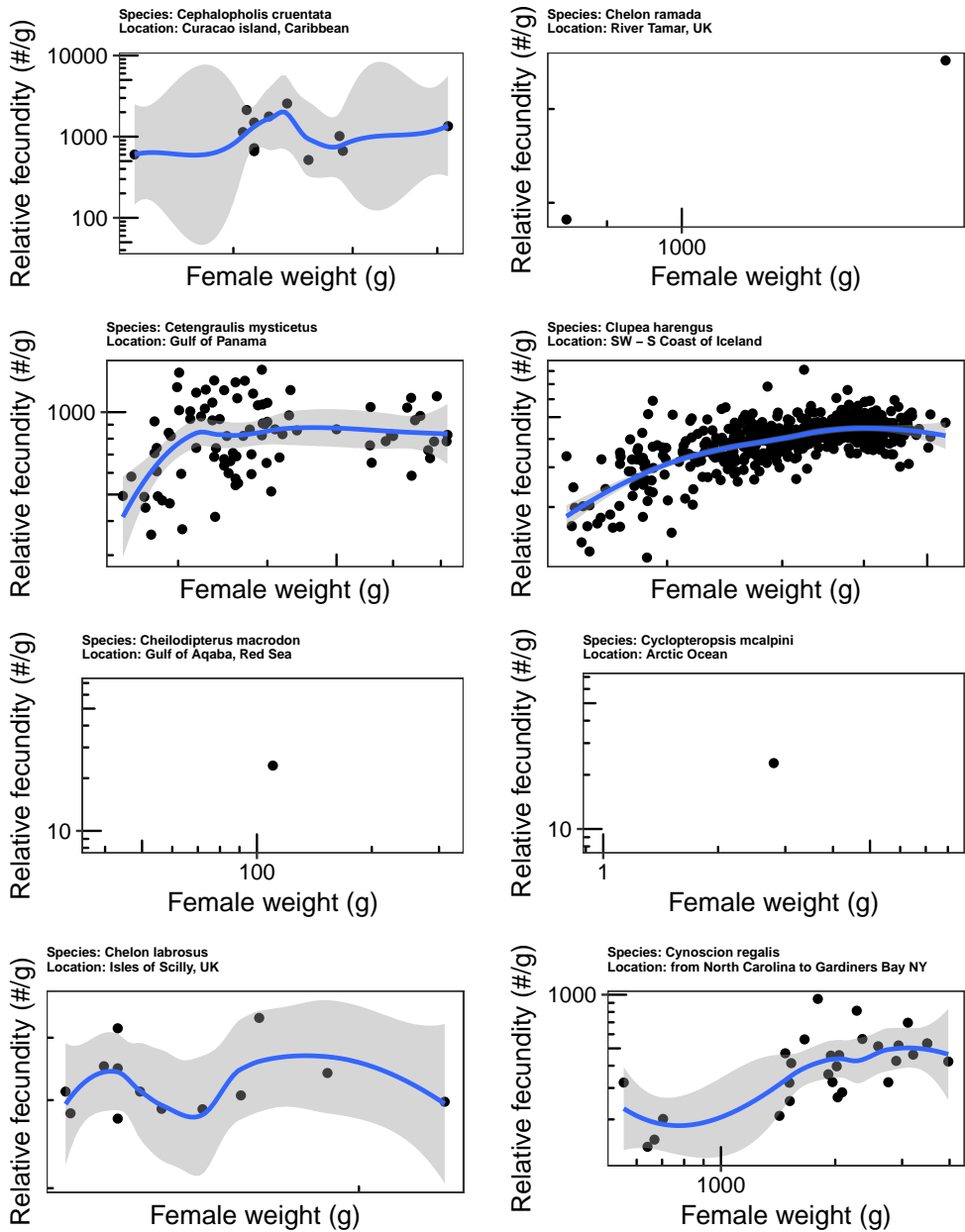
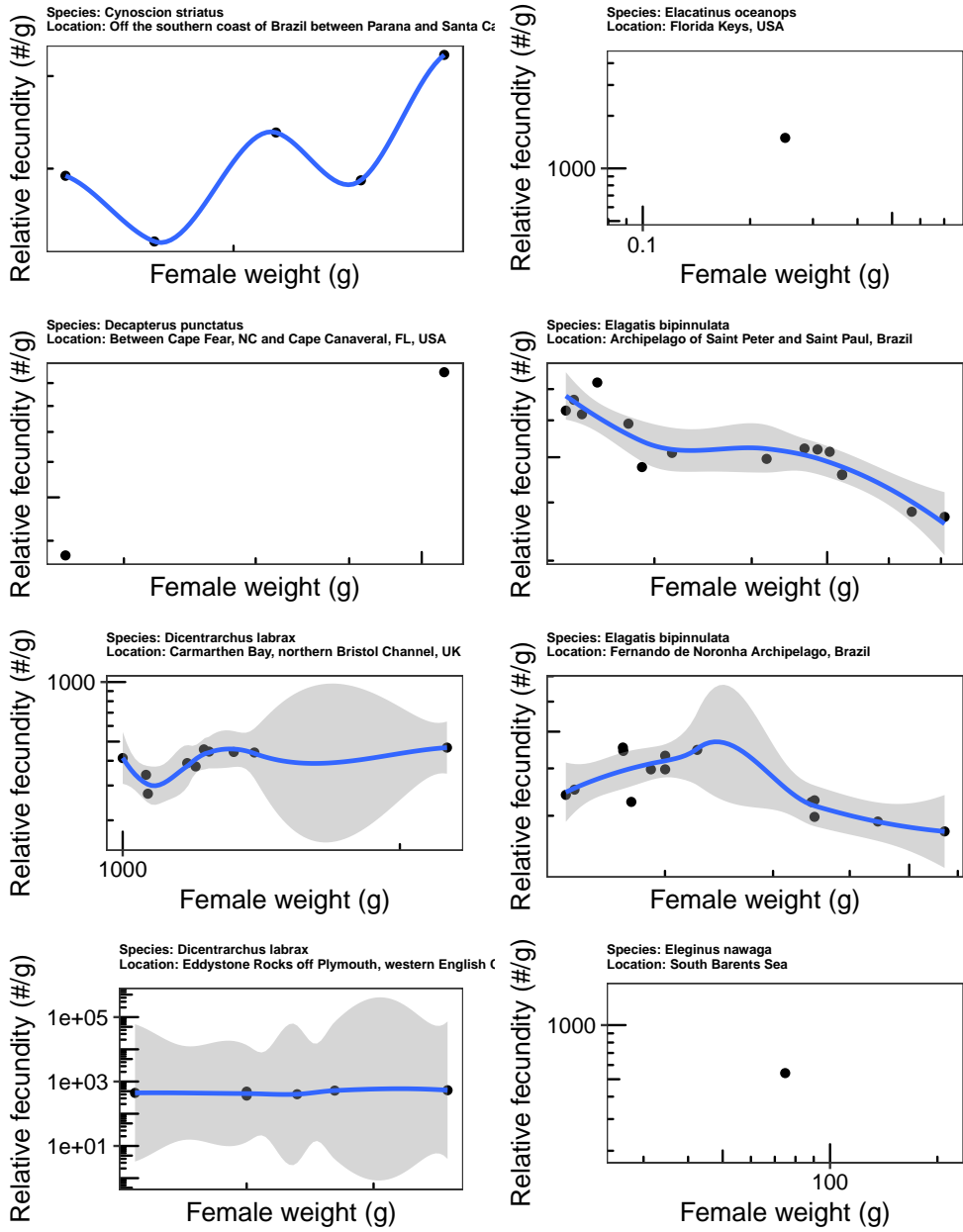


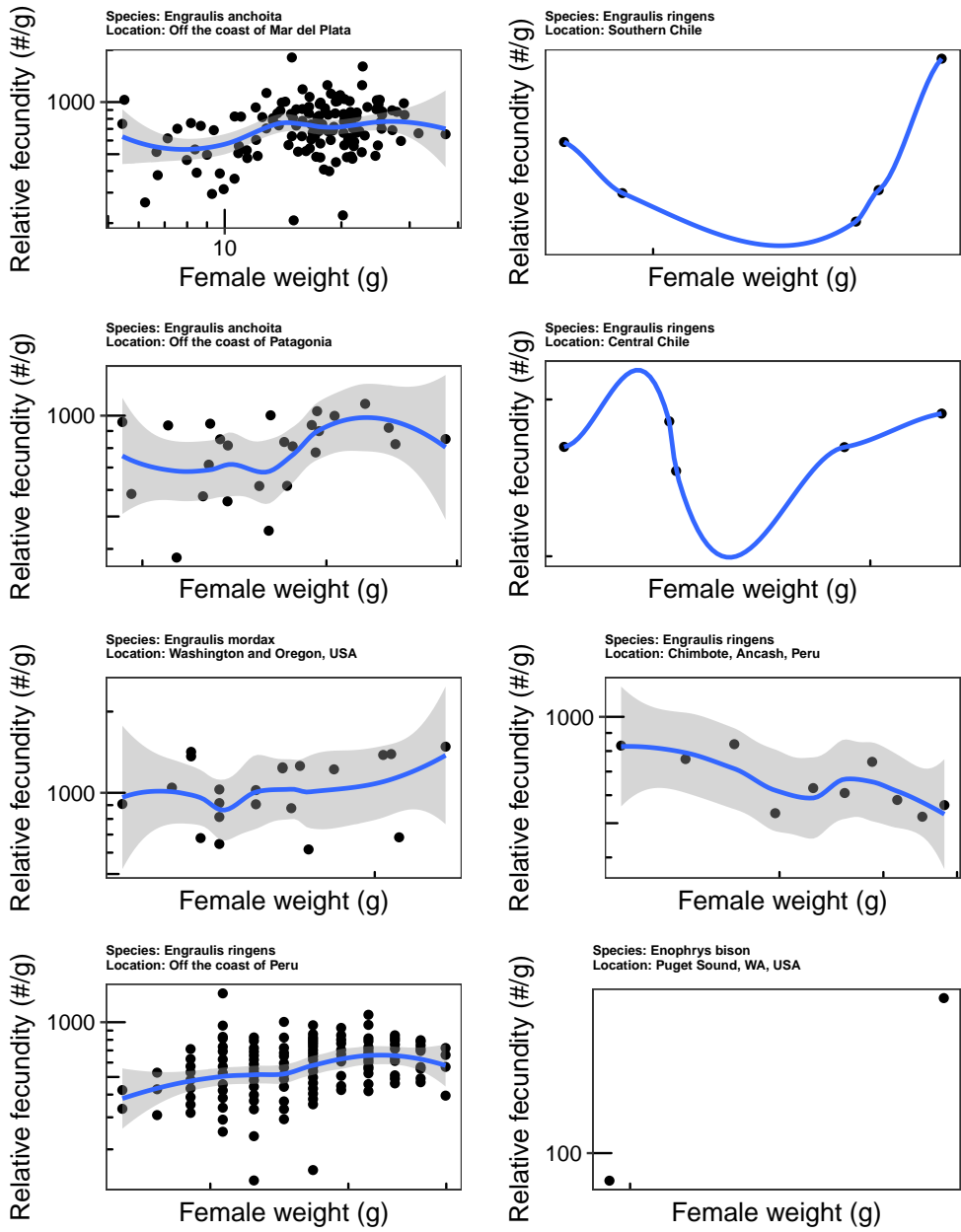
Figure A.1: Stock-specific data points on female weight (g) and relative fecundity (number of eggs per unit weight), including a trendline showing the smoothed conditional mean with 95% confidence interval. Data from Barneche *et al.* (2018).

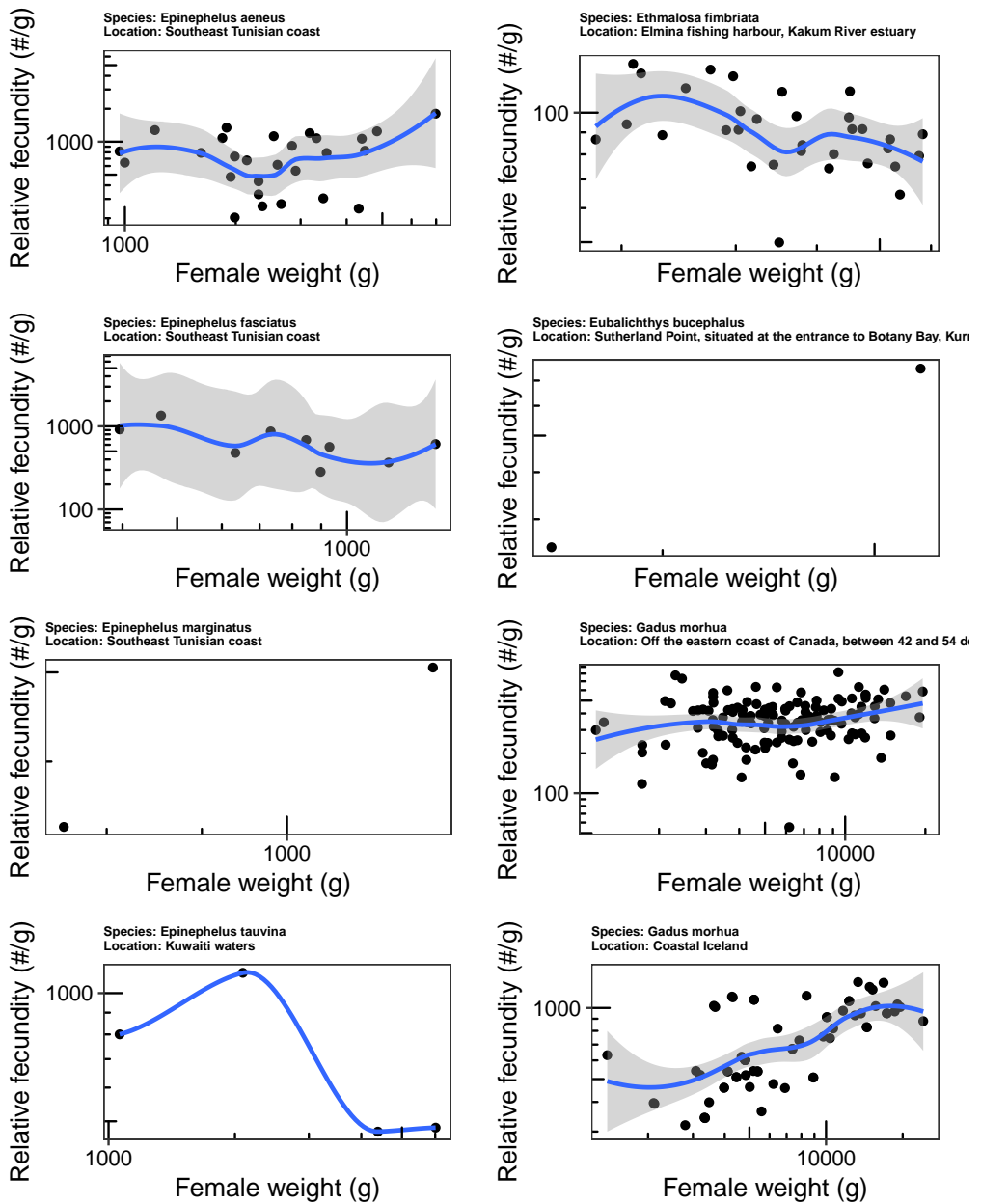


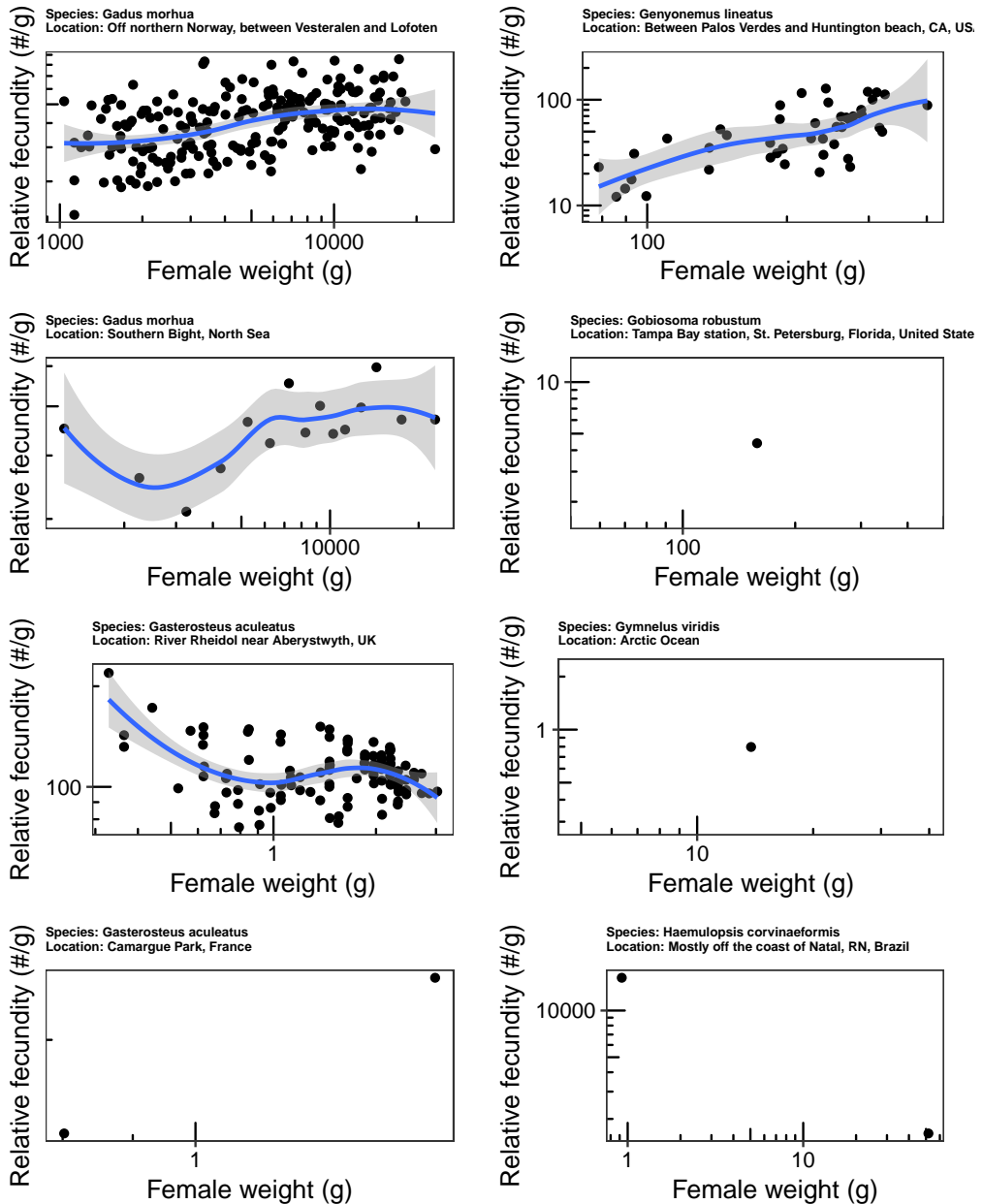


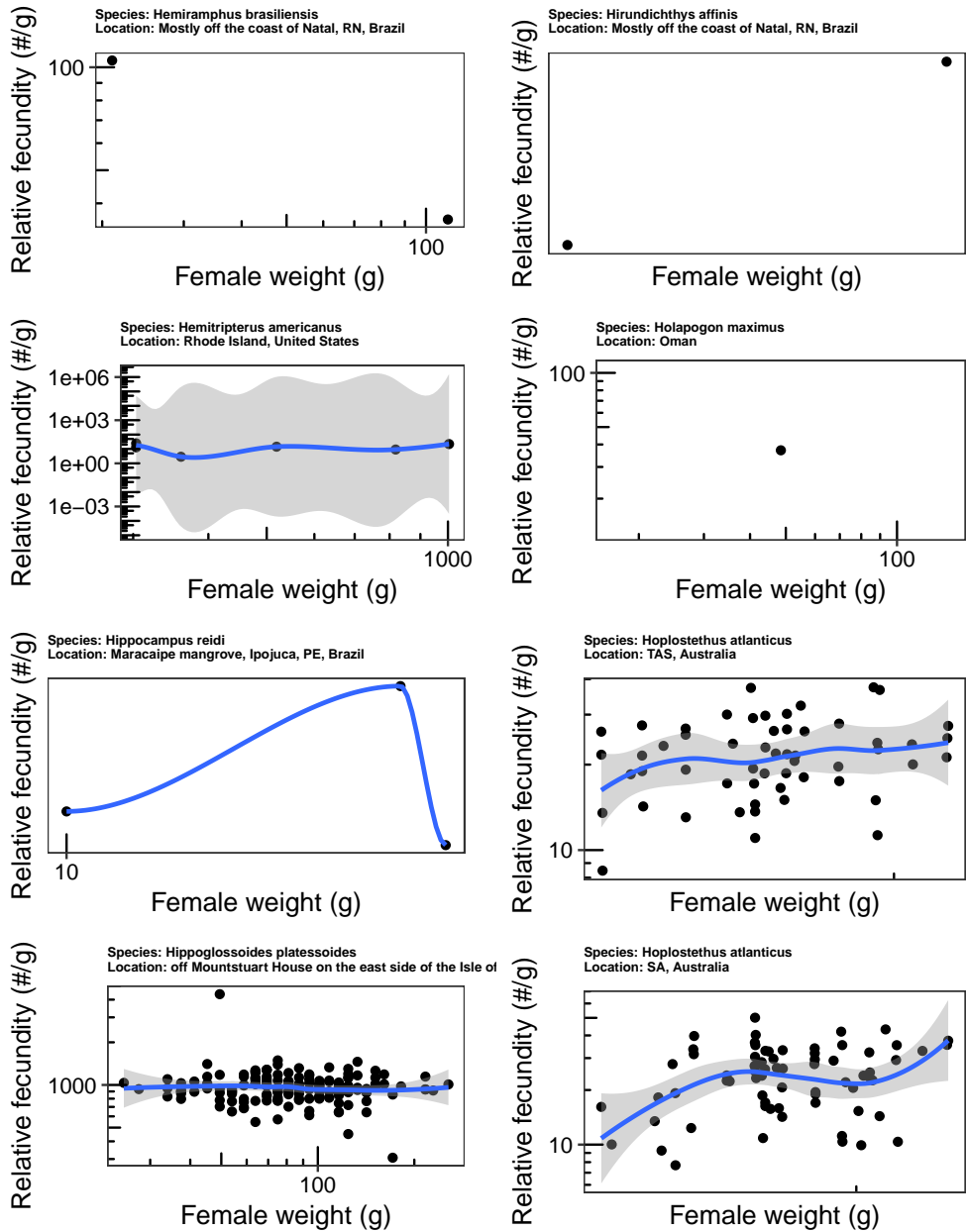


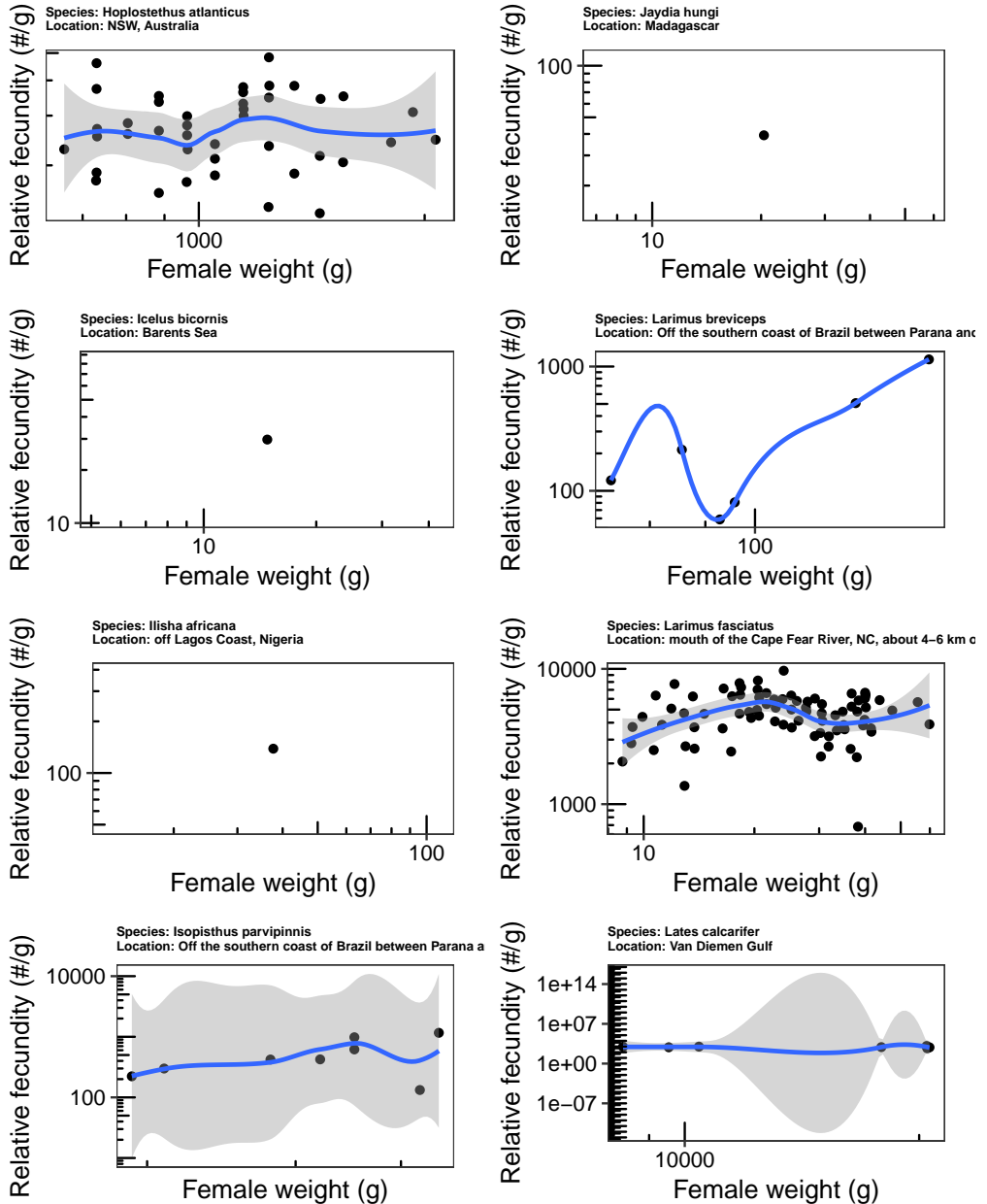


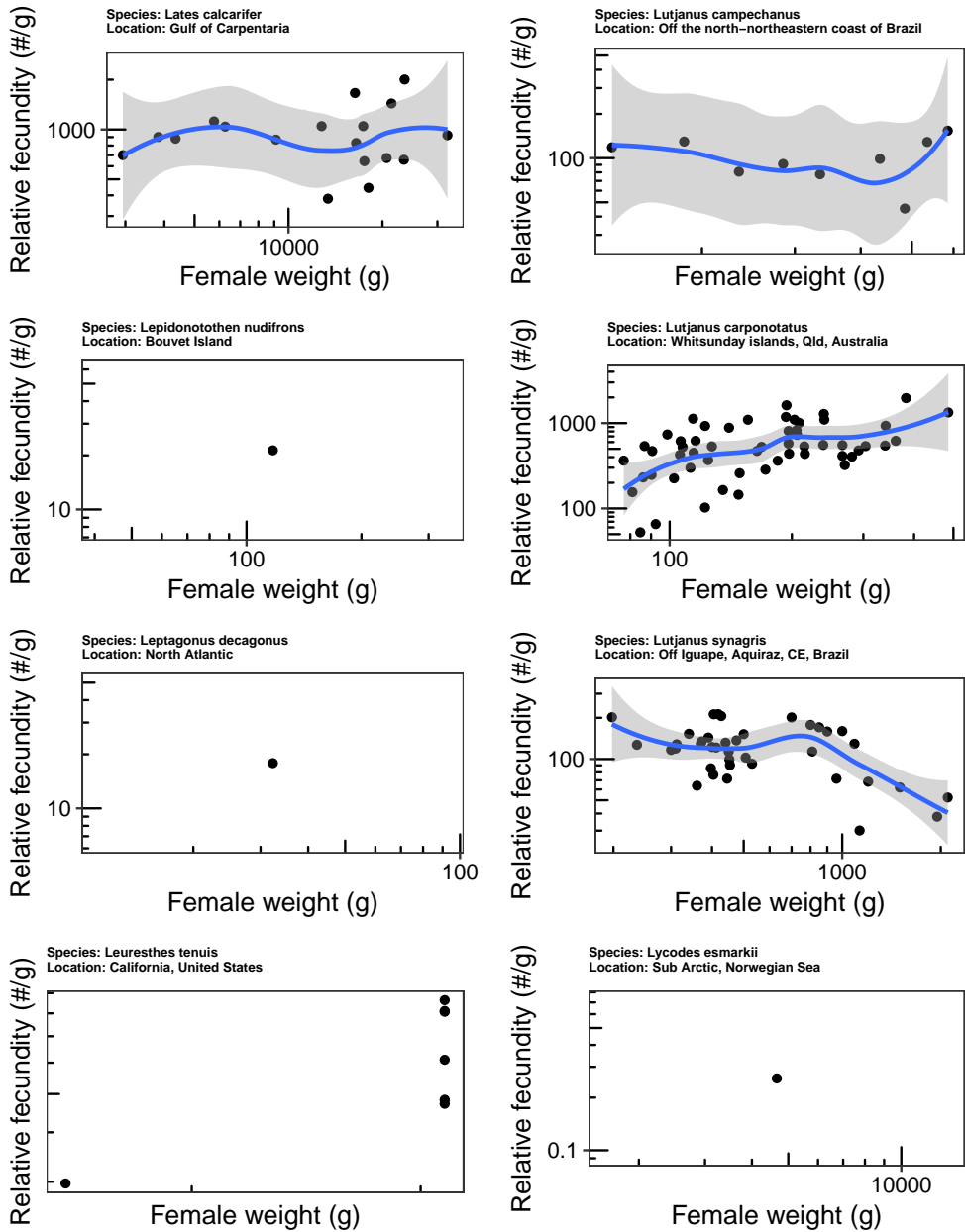


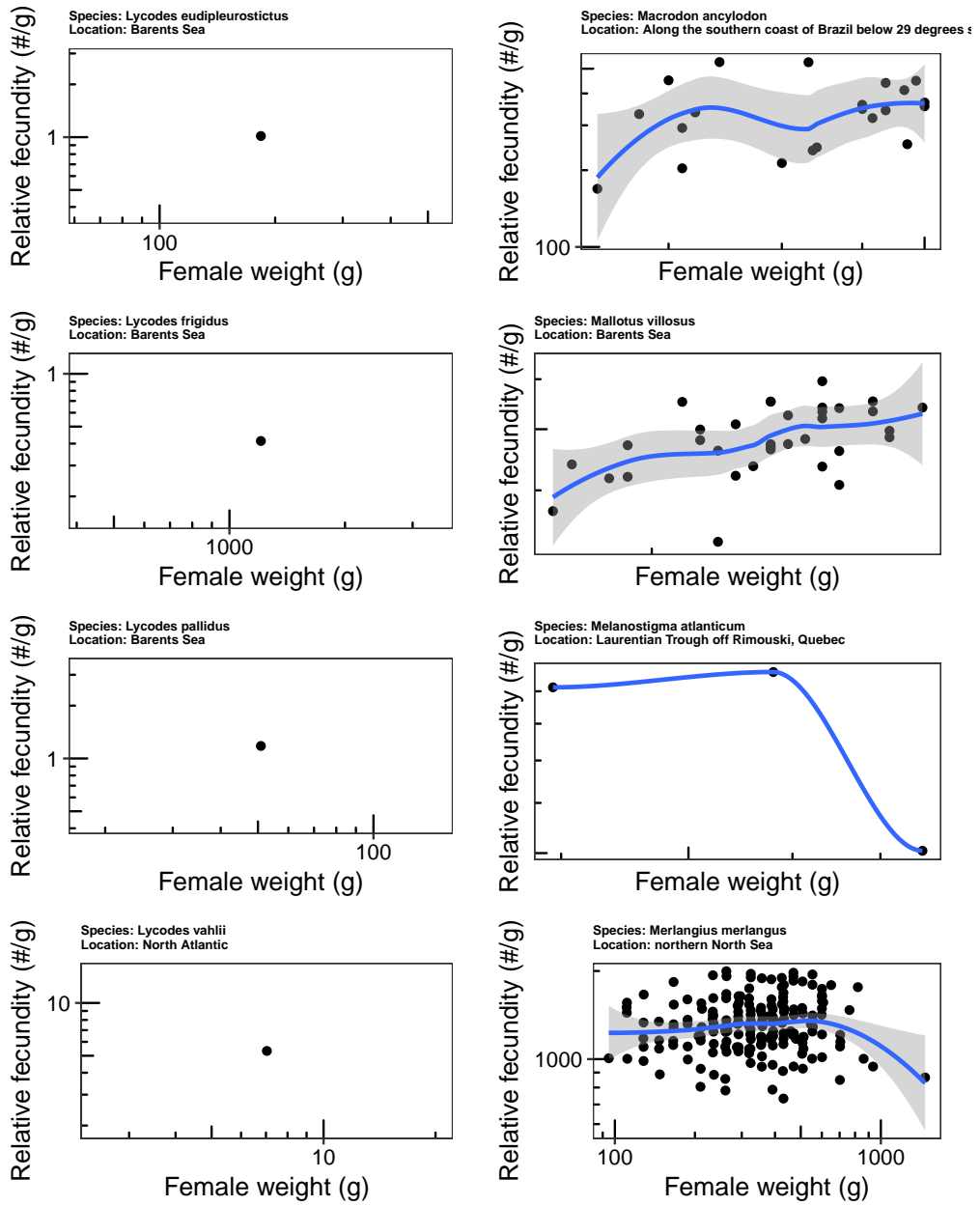


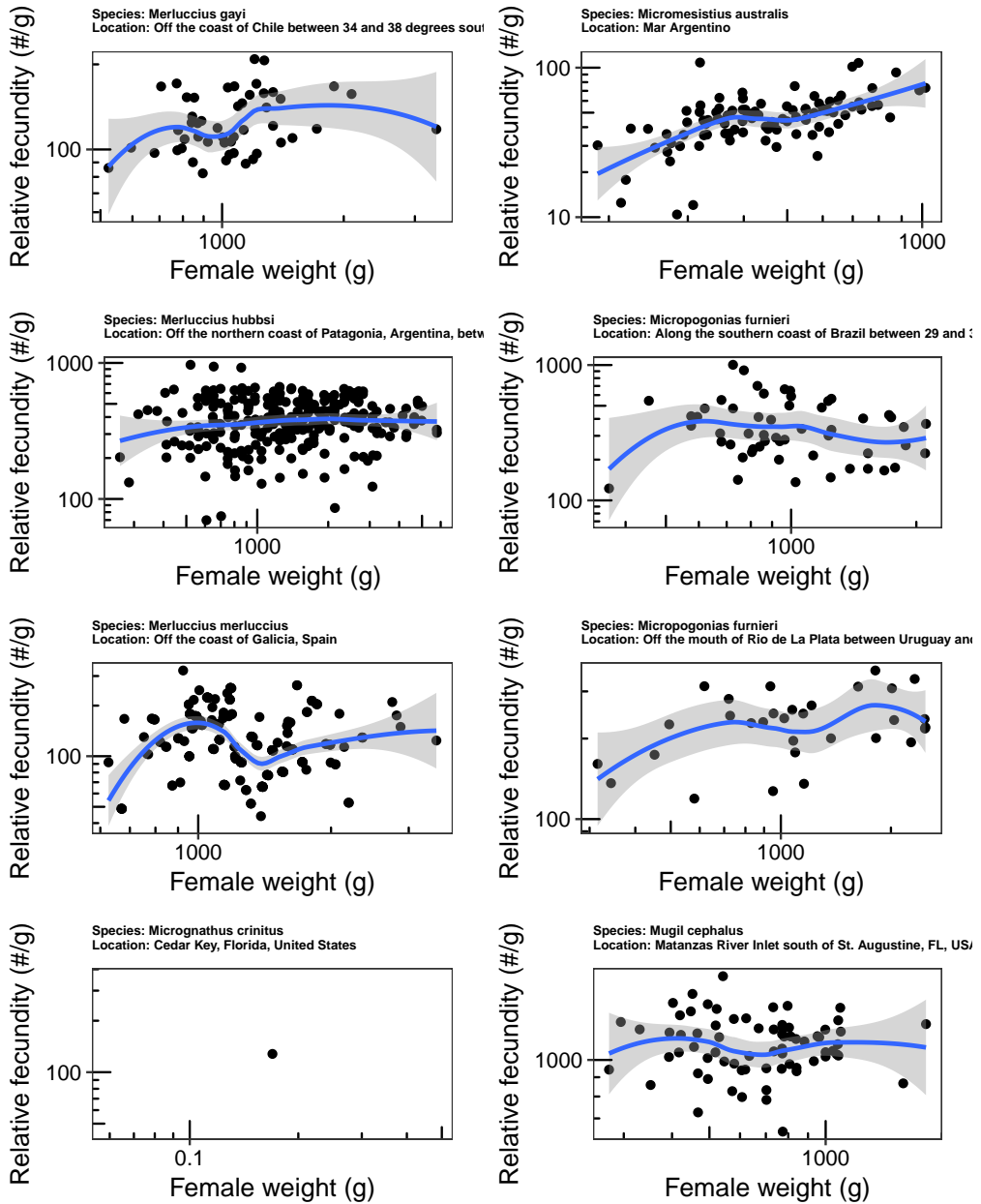


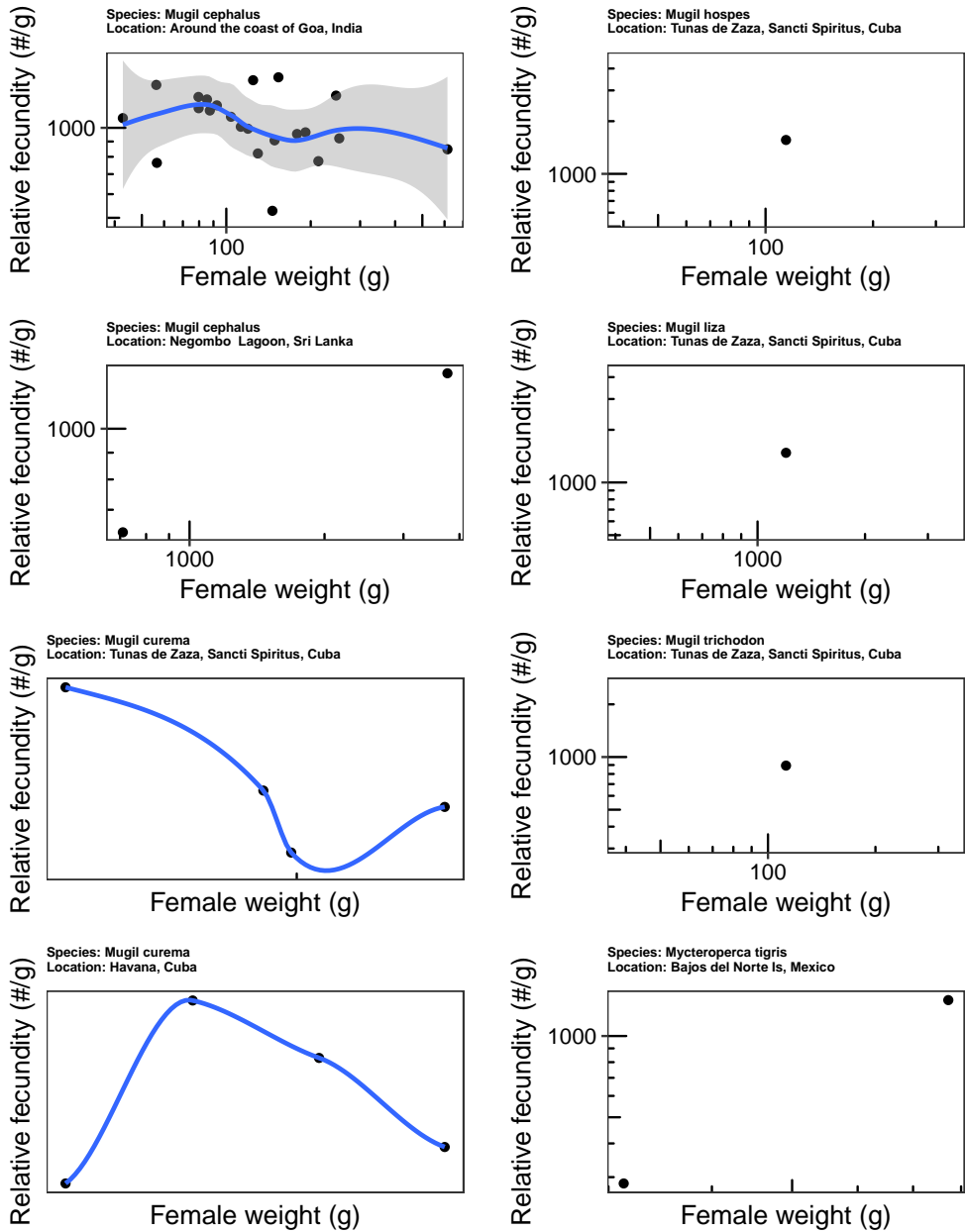


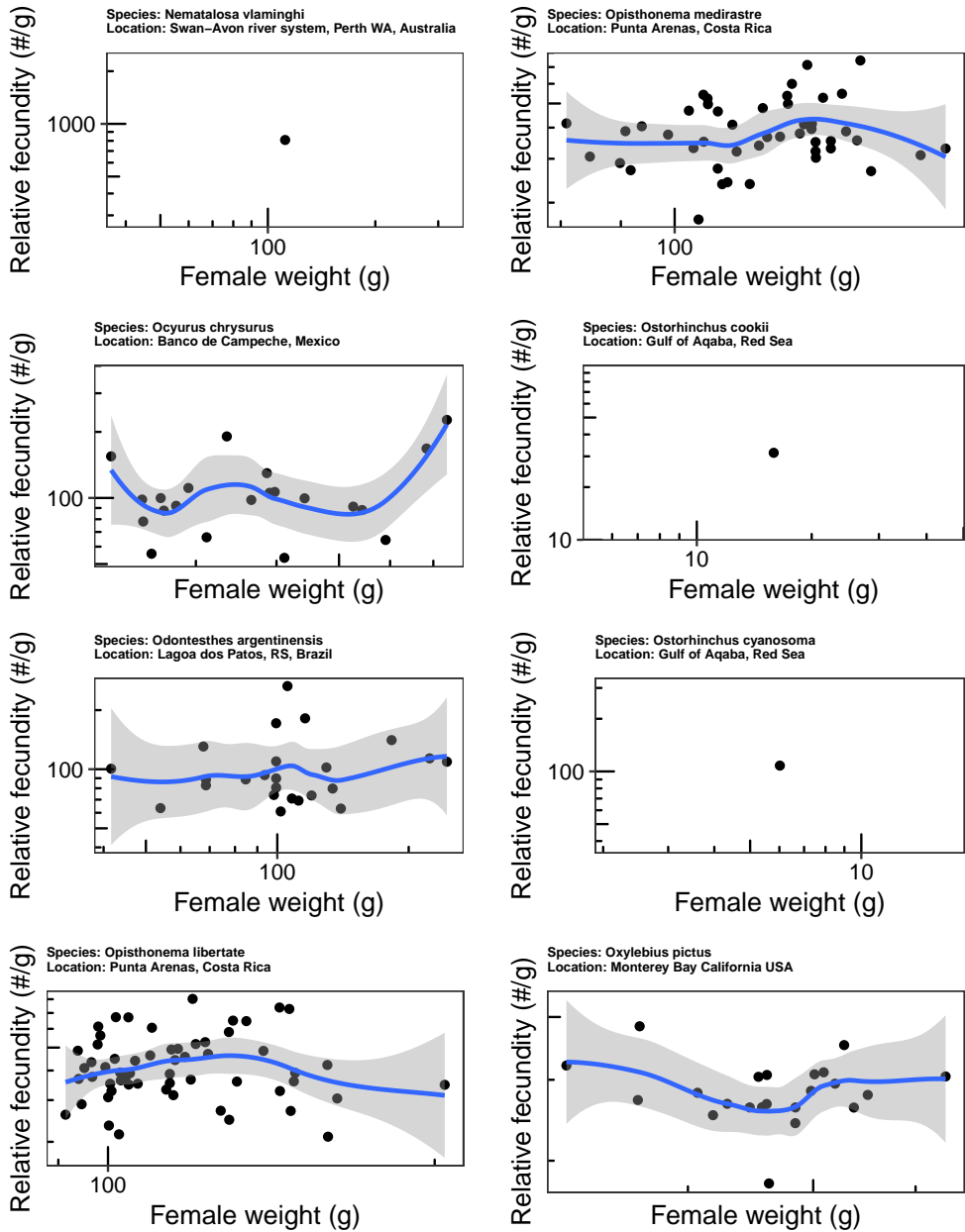


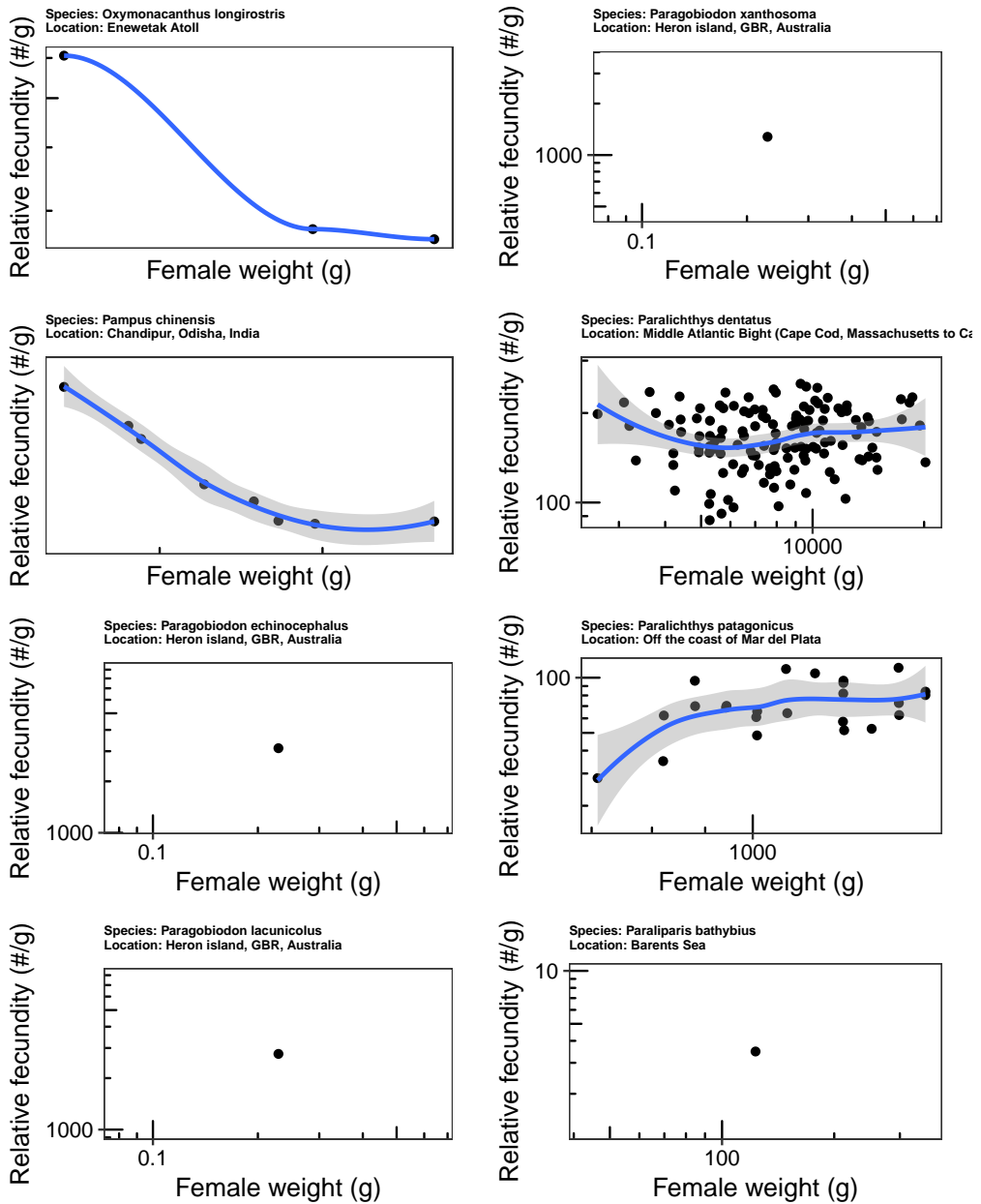


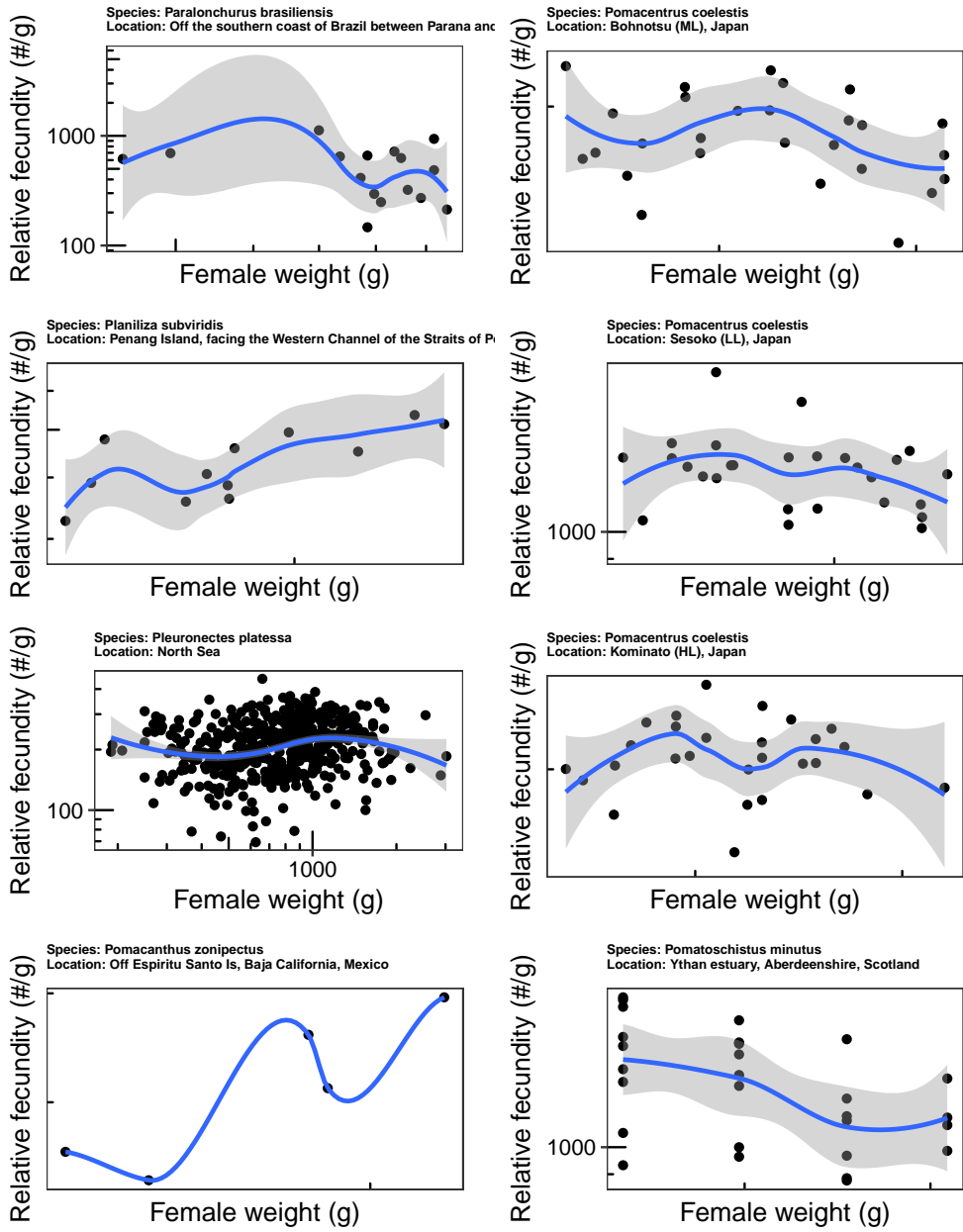


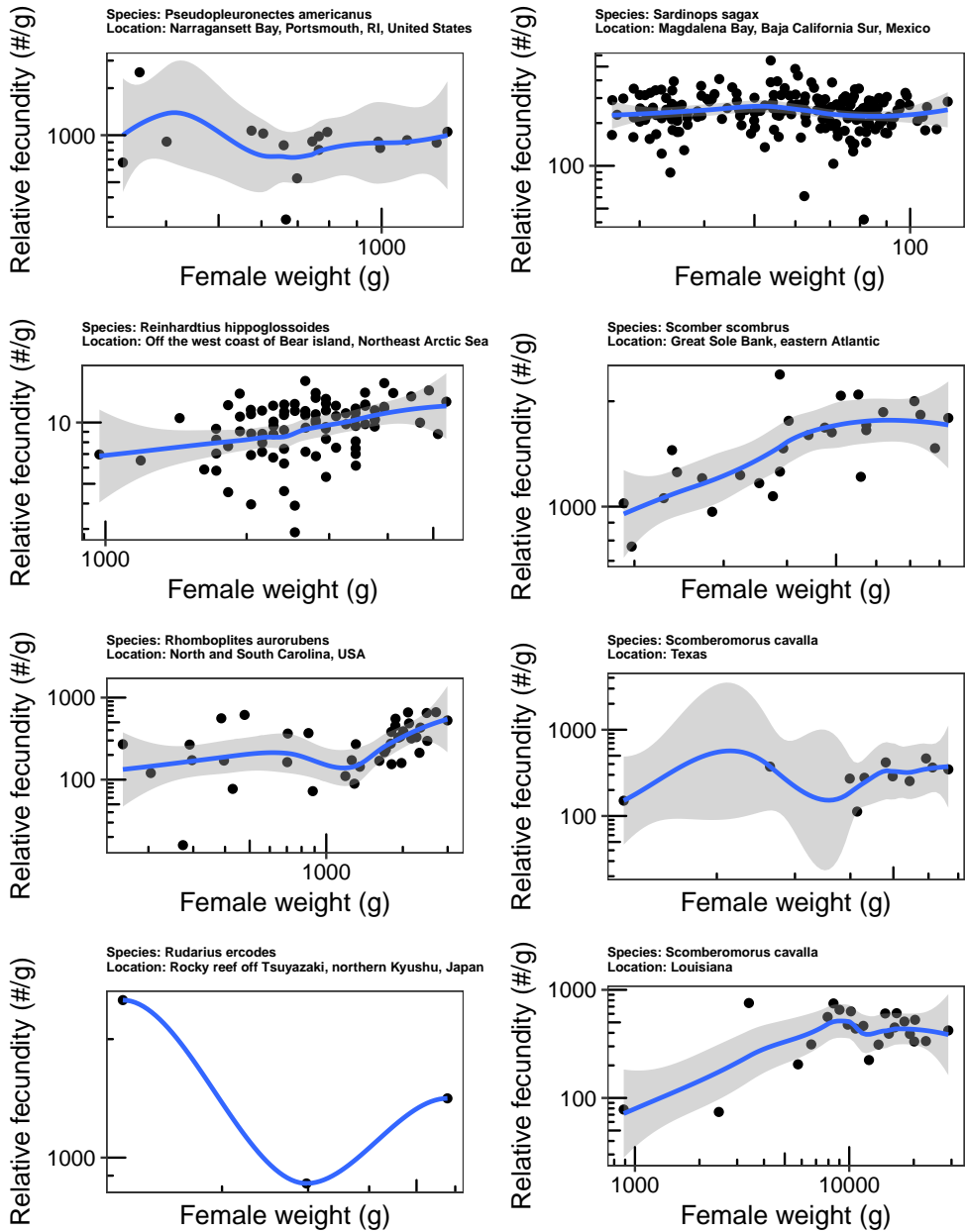


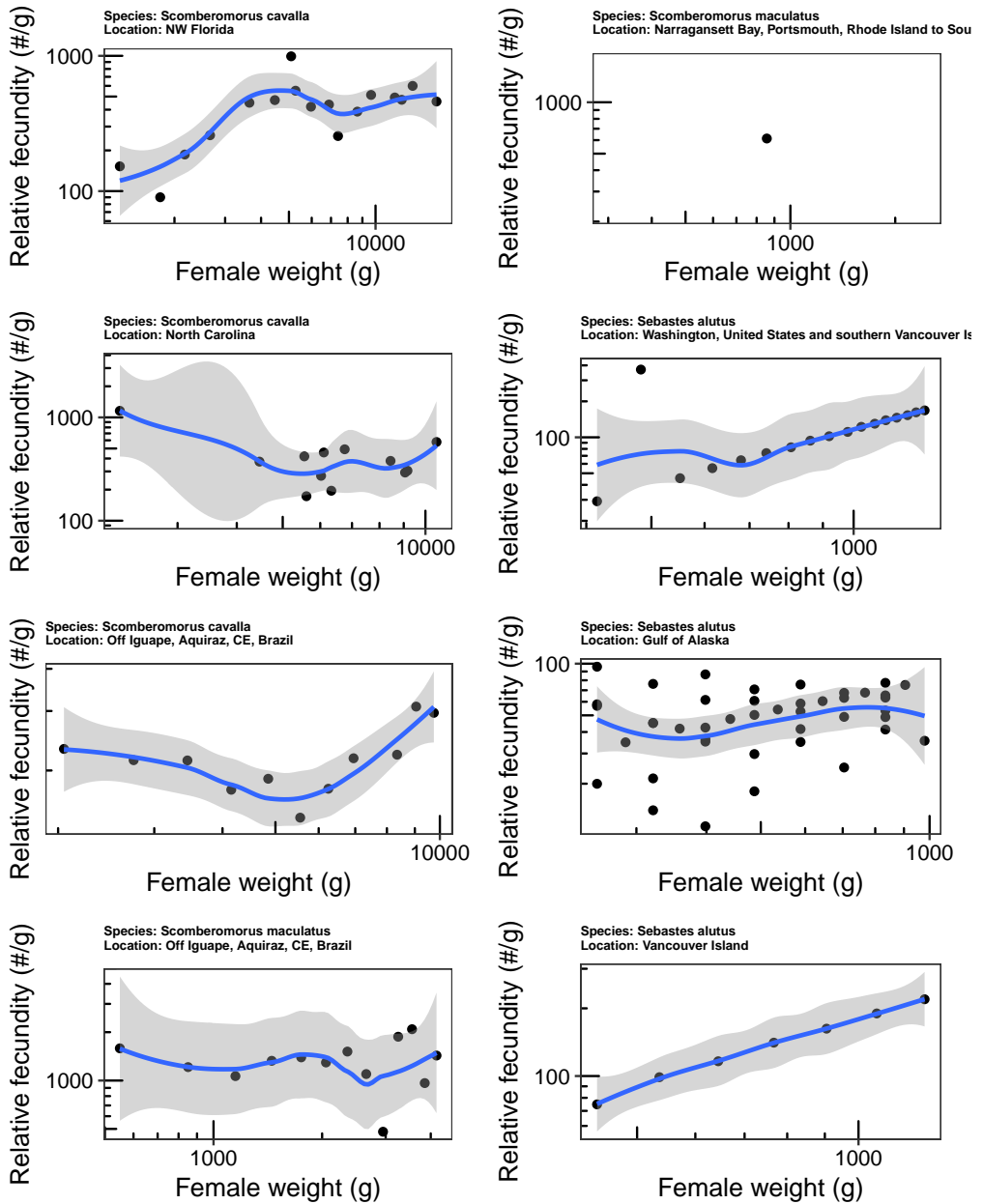


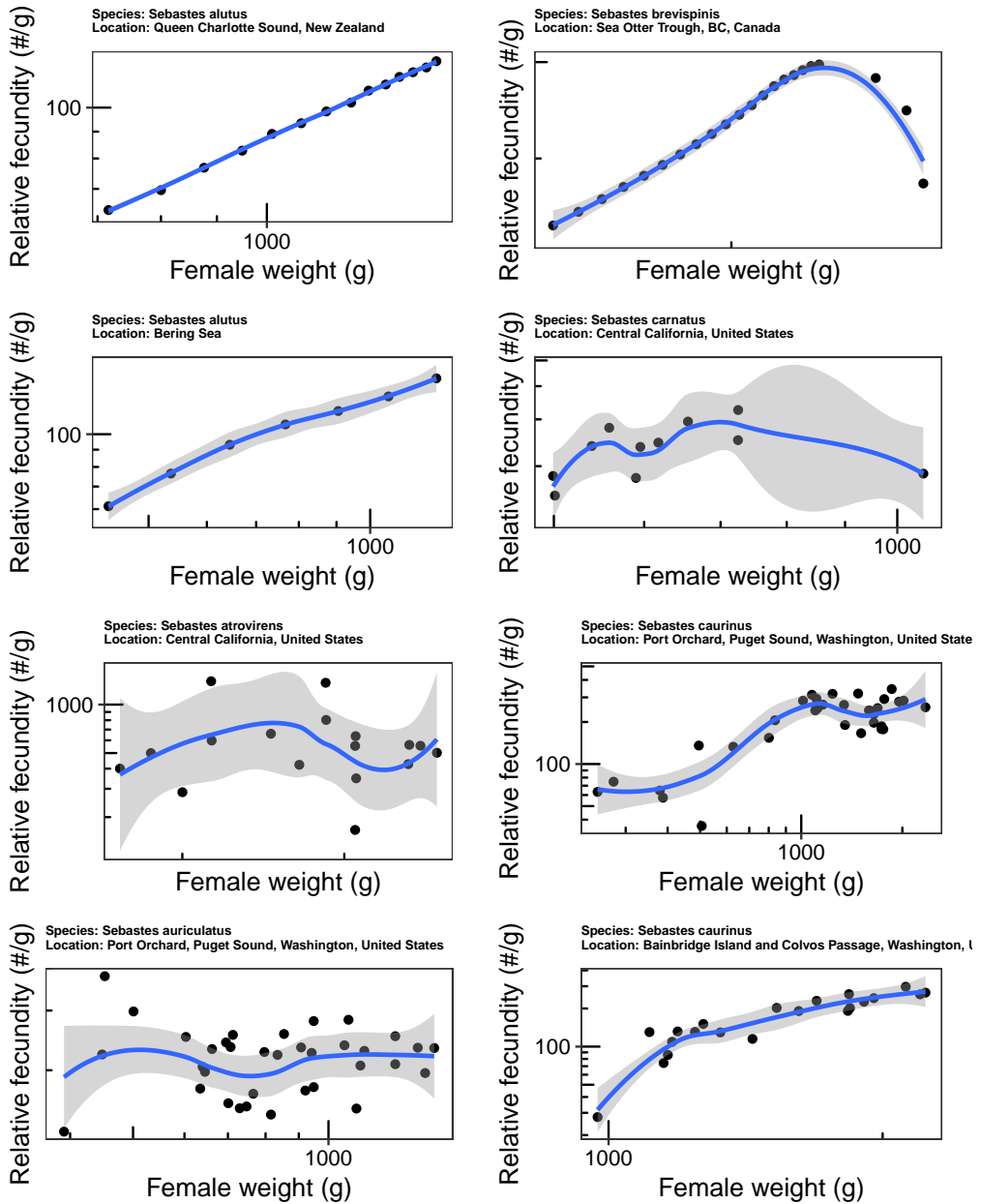


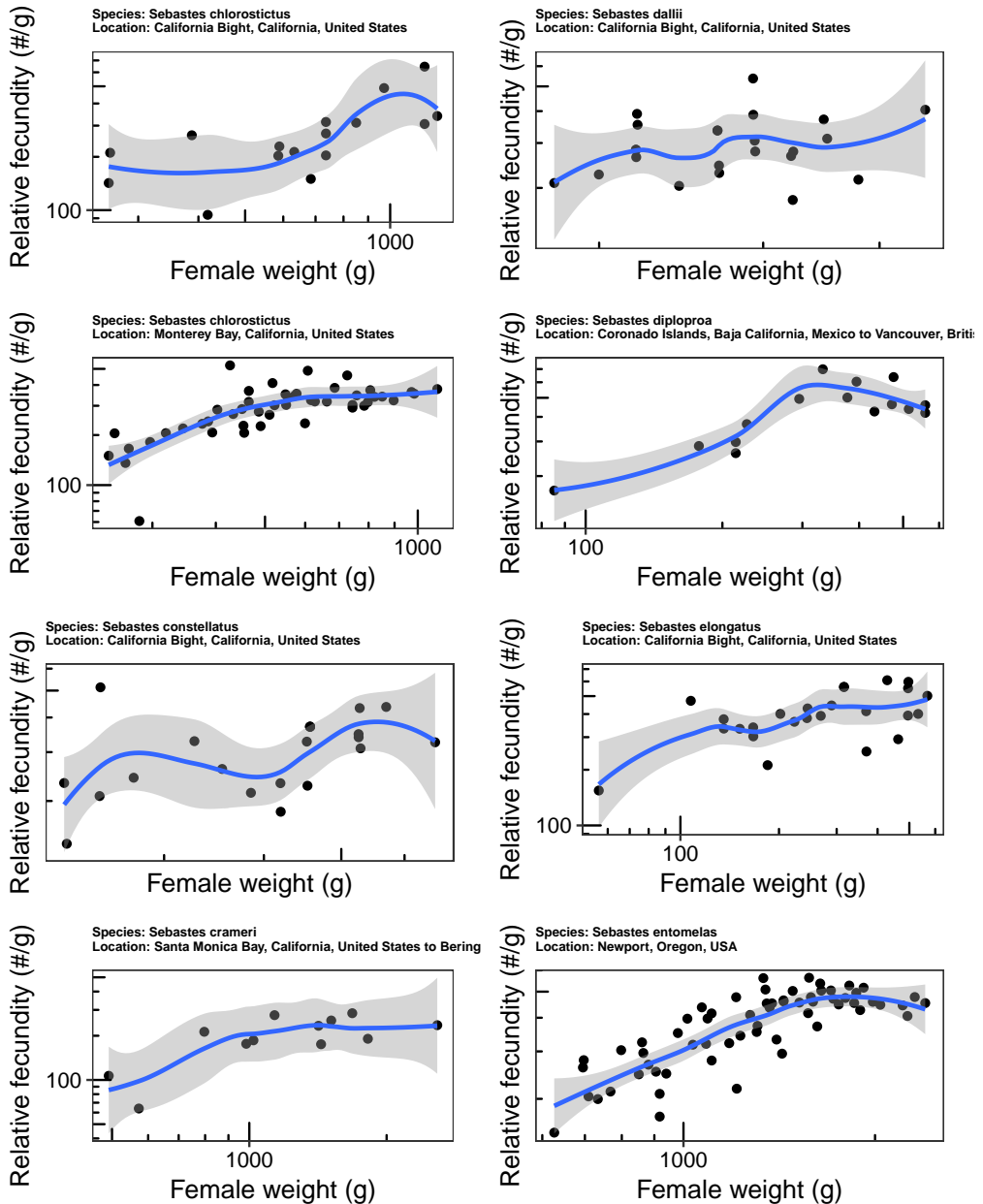


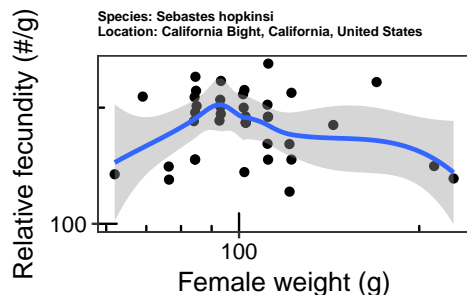
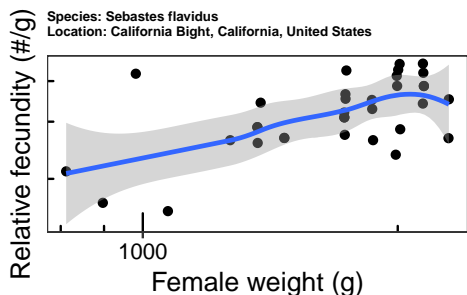
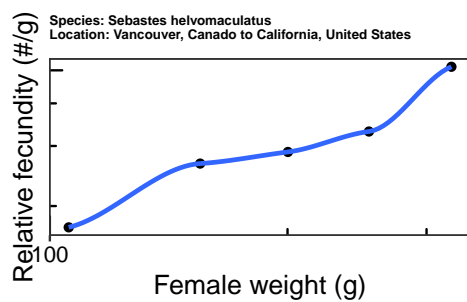
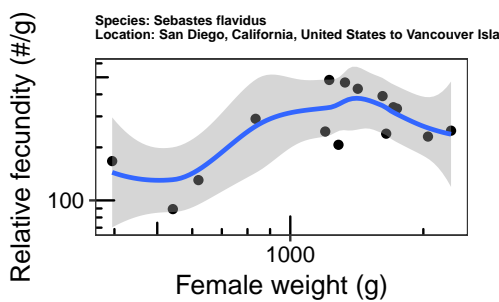
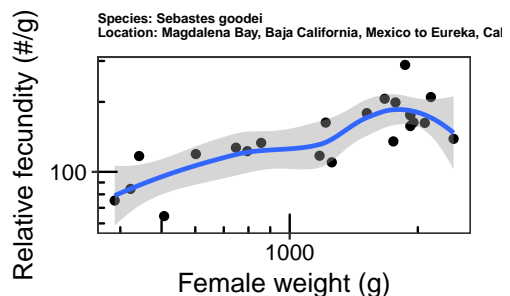
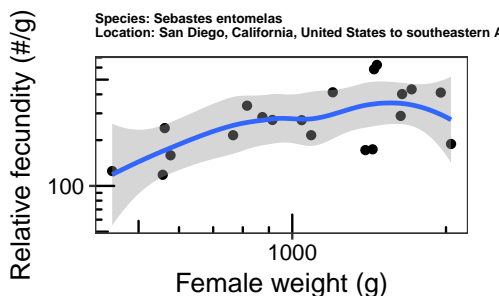
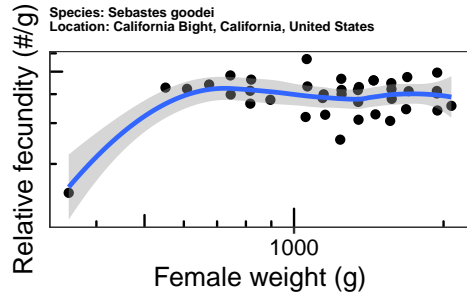
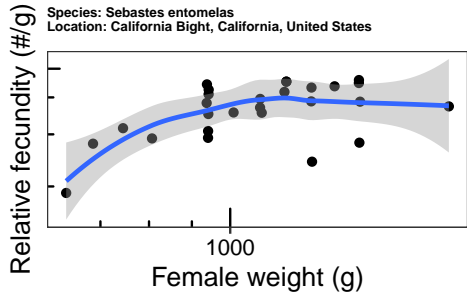


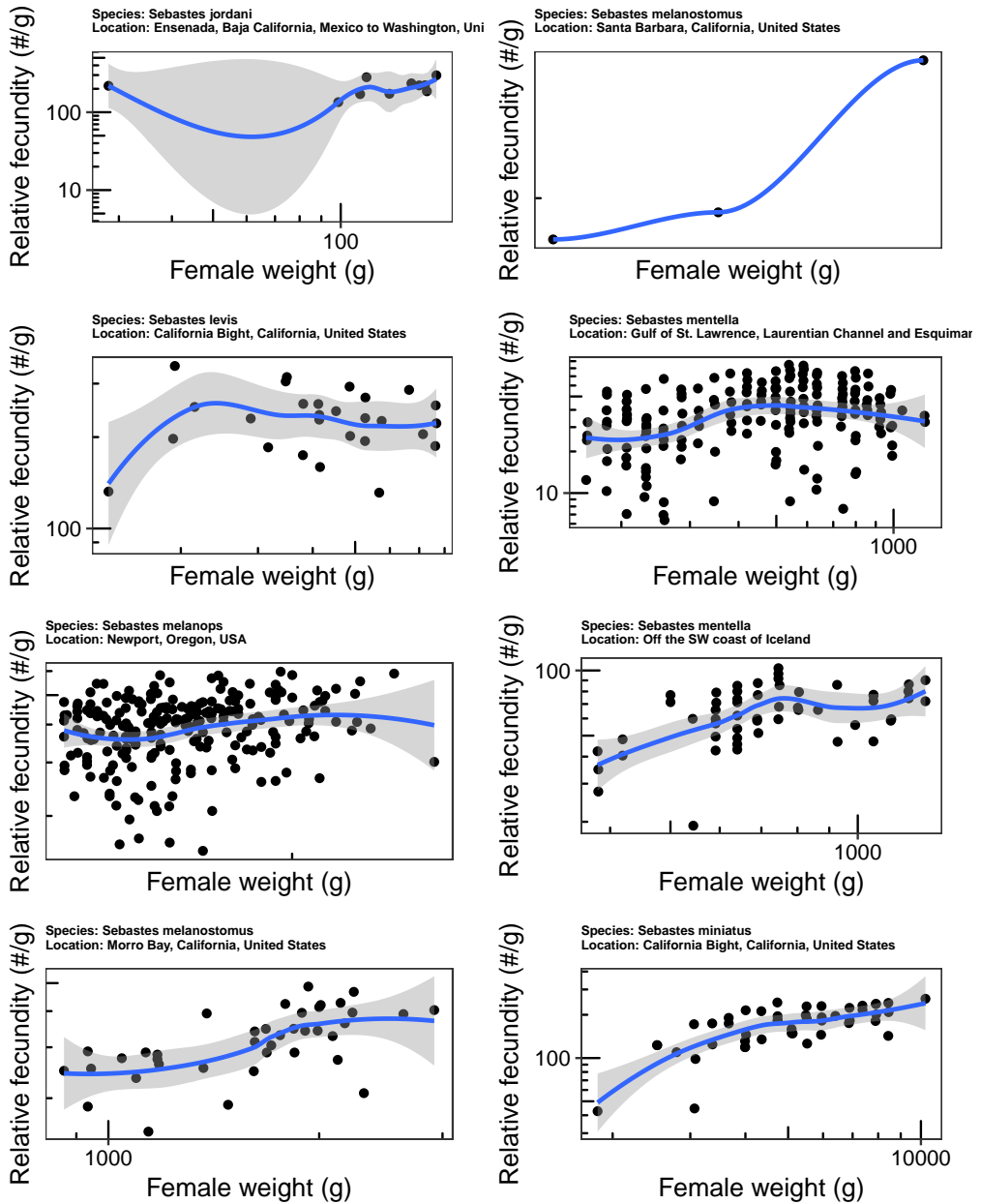


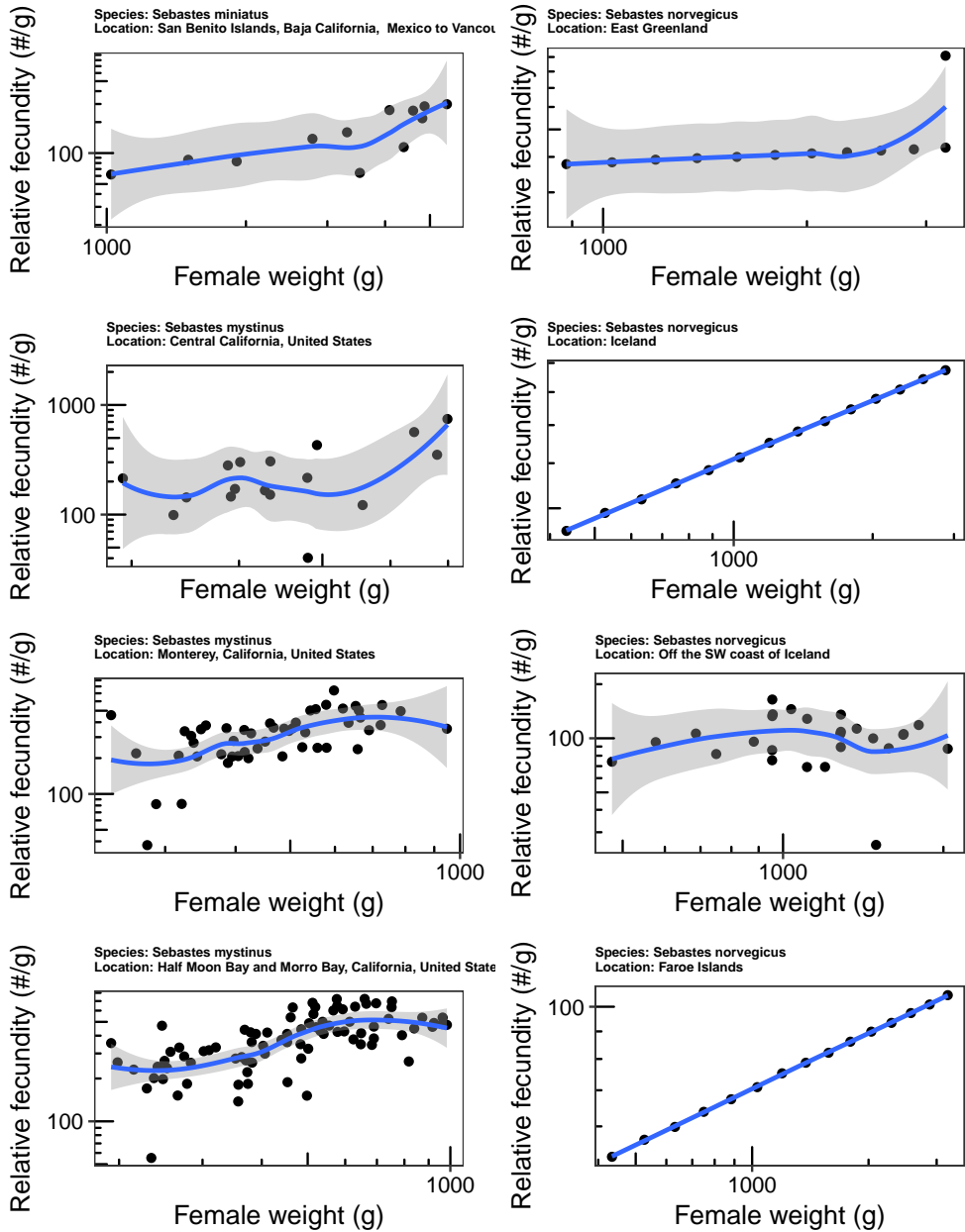


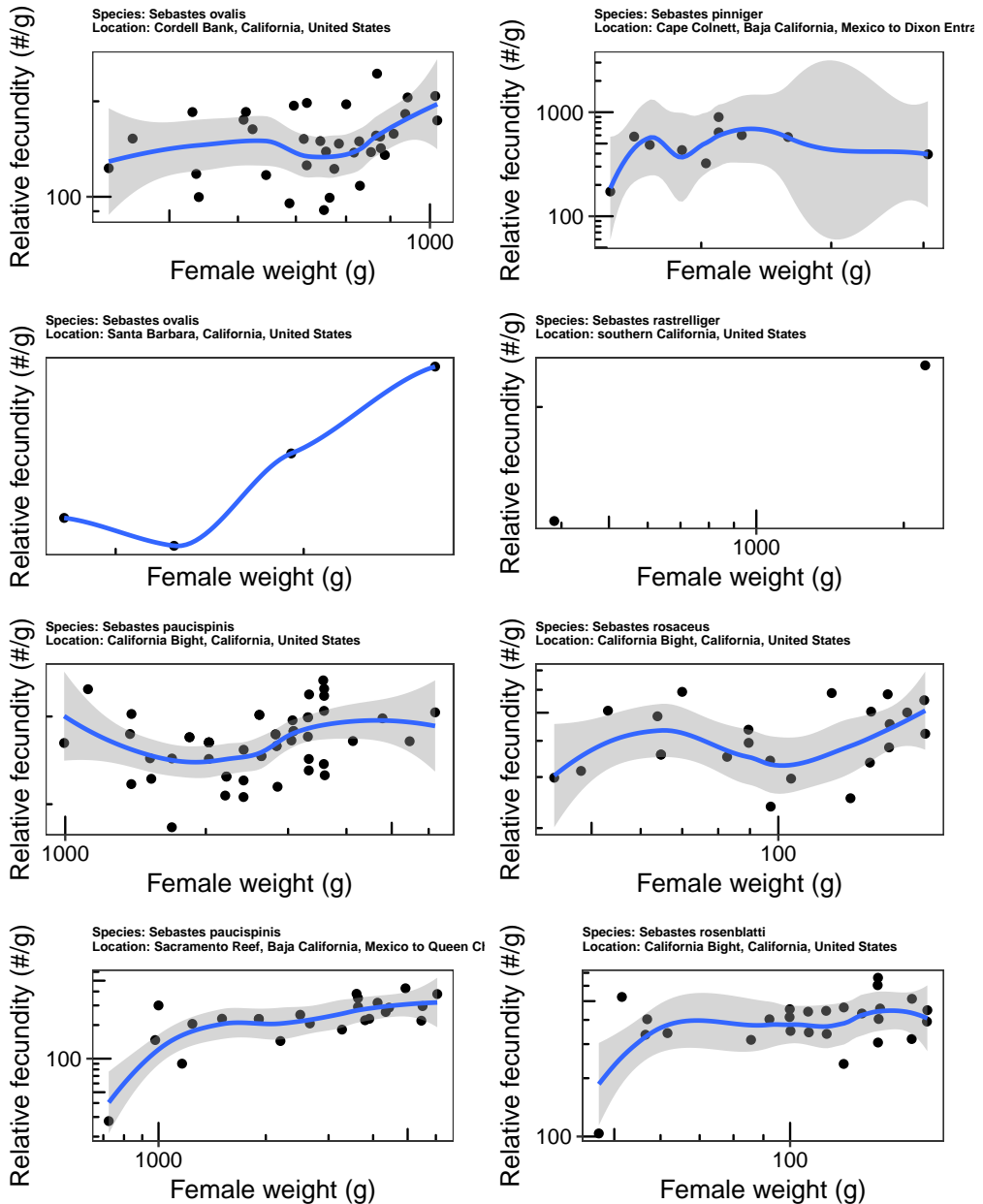


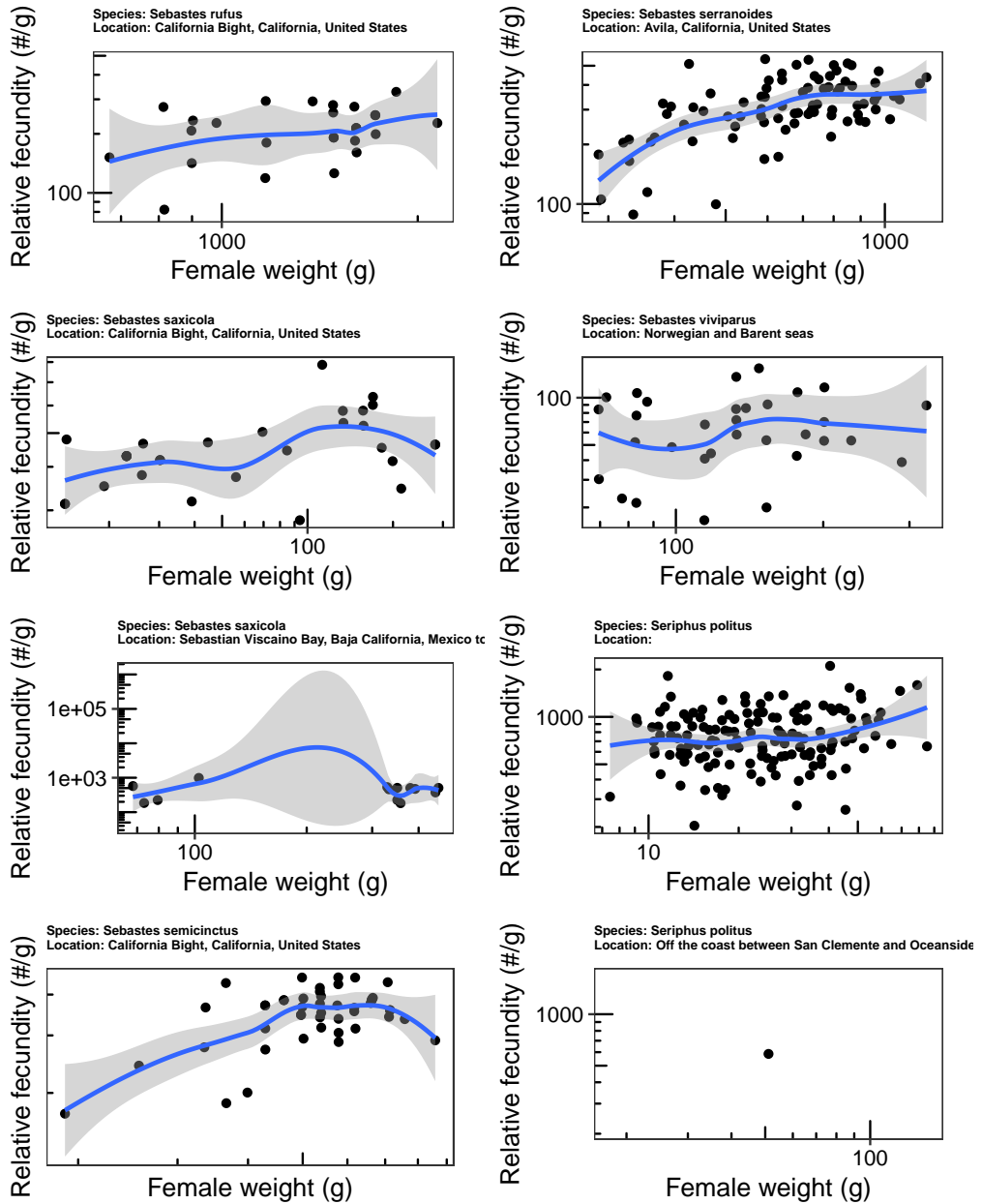


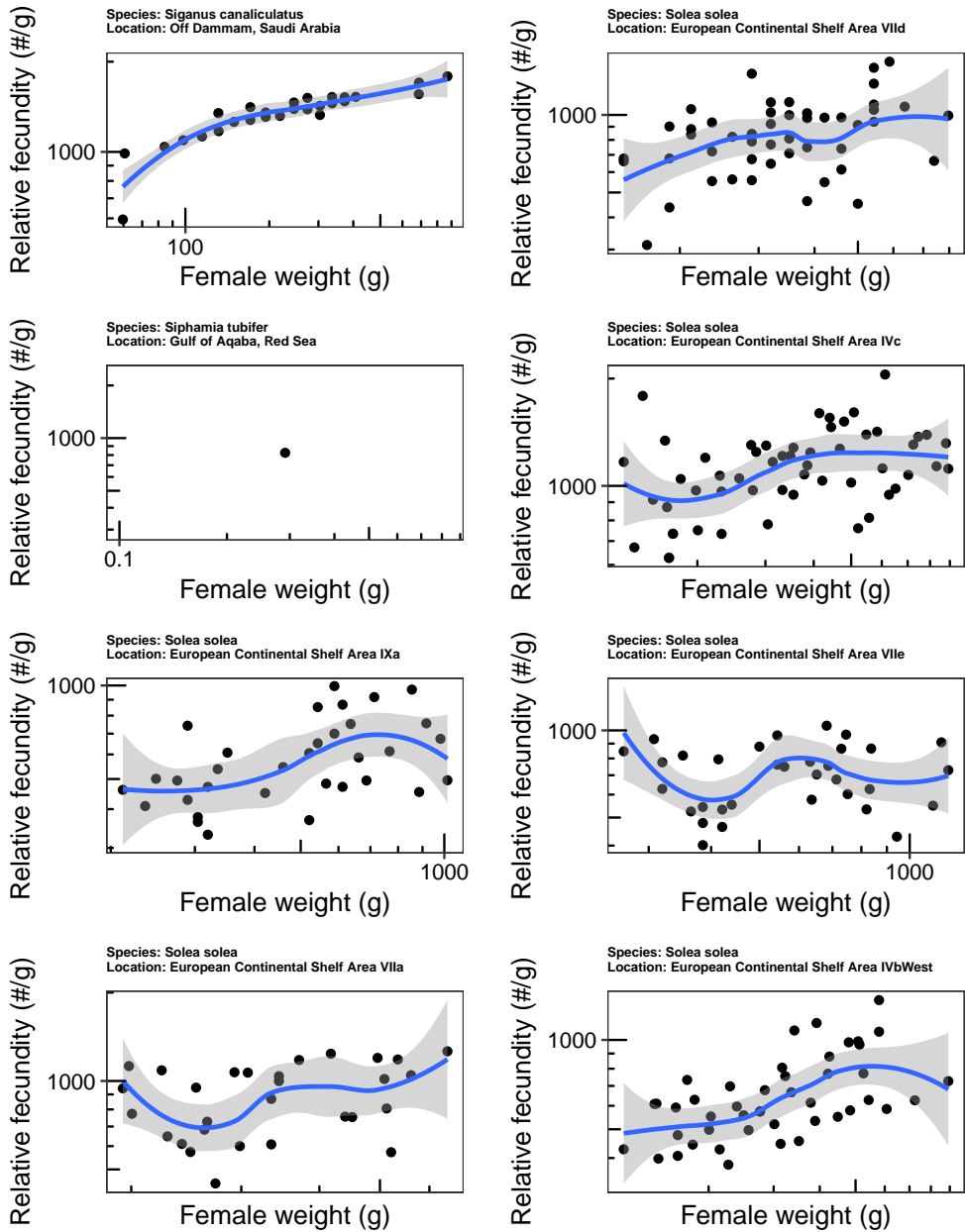


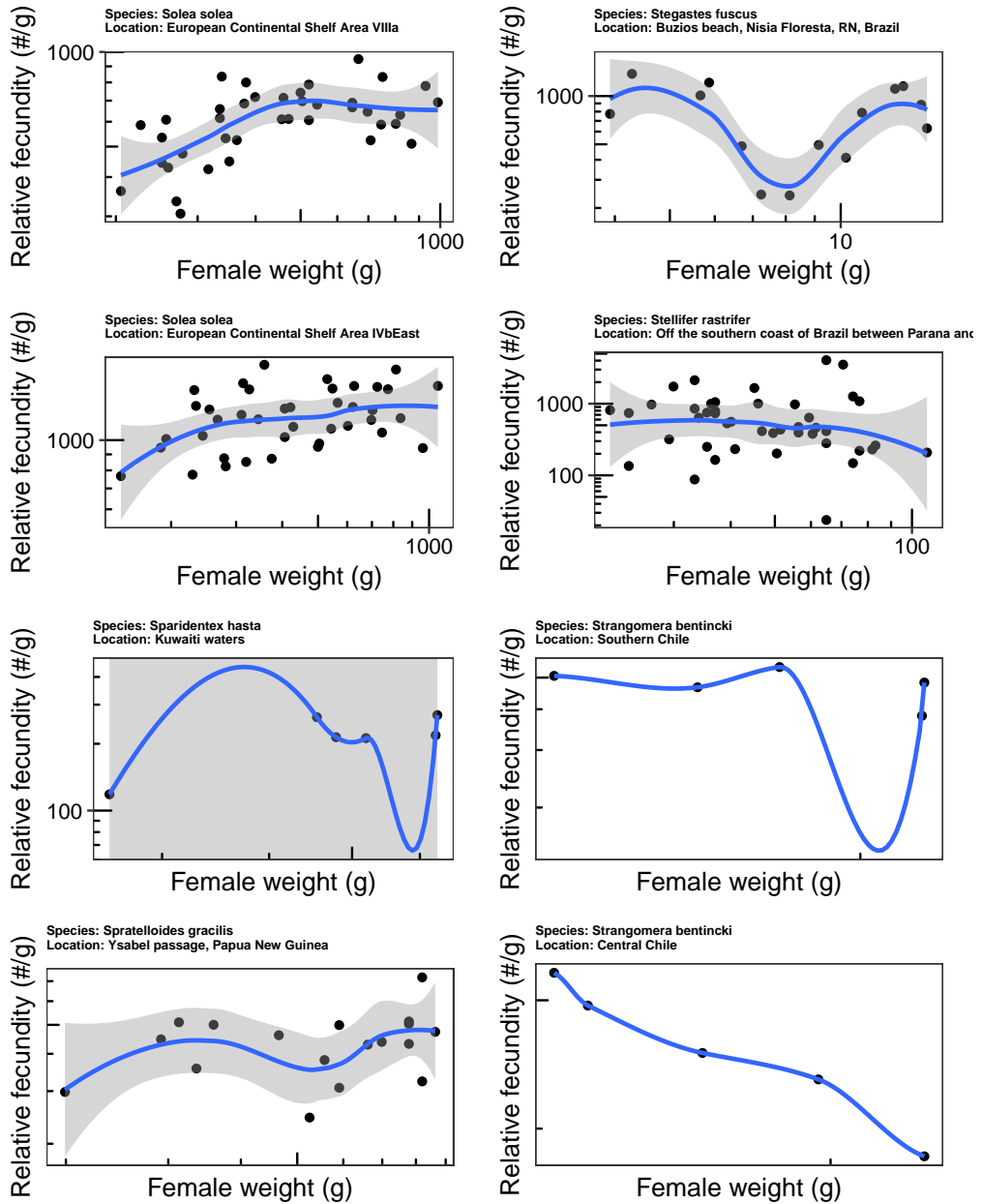


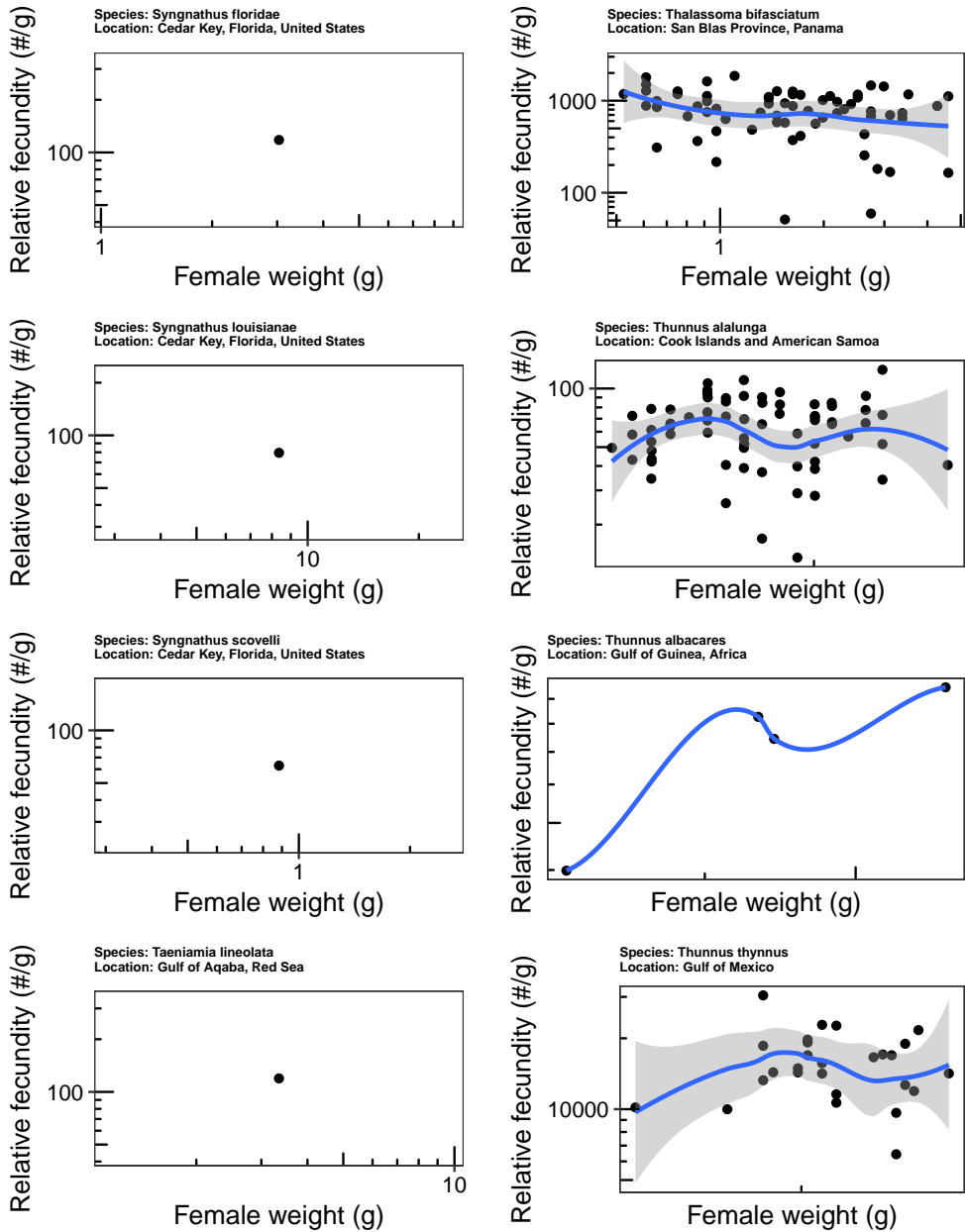


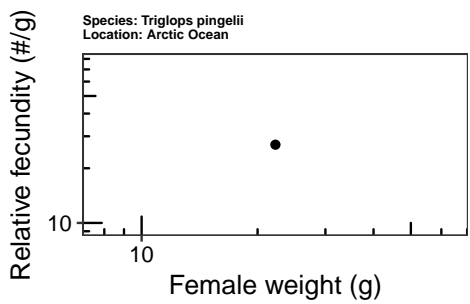
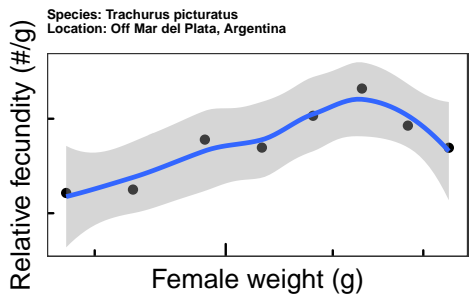












Appendix B Fits and Reproductive output

Table B.1: List of stocks where a power law and isometric relationship was fit to the data on w and R_w , including the results of the fits. Here, μ_{R_w} is calculated from $\mu_{\ln R_w}$ used in Equation 2, as $e^{\mu_{\ln R_w}}$.

Species	Stock	Isometric fit			Power law fit			p -value	RSS	AIC
		μ_{R_w}	RSS	AIC	α	β				
<i>Anhygaster stirm</i>	Parangipettai, SE coast of India	1.15e+03	8.82e+00	5.41e+01	1.22e+00	1.32e+00	6.85e-04	6.04e+00	4.36e+01	
<i>Archiviotella lepidotostole</i>	Near Rio Ribeira de Iguaque, SP, Brazil	1.62e+03	9.13e-01	-6.35e+00	2.67e+03	-1.90e-01	2.79e-01	8.64e-01	-5.66e+00	
<i>Archosargus rhomboidalis</i>	Terminos Lagoon, Mexico	8.28e+02	2.74e+00	2.03e+01	1.41e+03	-1.28e-01	2.70e-01	2.58e+00	2.10e+01	
<i>Atherinops presbyter</i>	Fowley power station Southampton, UK	6.38e+02	2.06e+00	6.16e+00	5.16e+02	1.19e-01	9.25e-02	1.88e+00	5.09e+00	
<i>Balistes capricus</i>	Gulf of Gabes, Tunisia	1.57e+03	1.17e+00	-2.05e+01	7.82e+02	1.17e-01	2.68e-01	1.13e+00	-1.99e+01	
<i>Balistes capricus</i>	Off Mobile Bay, Florida, USA	1.20e+03	2.71e+00	1.52e+01	9.22e+02	4.33e-02	7.84e-01	2.71e+00	1.71e+01	
<i>Balistes capricus</i>	Gulf waters offshore of Panama City, Florida, USA	2.20e+03	3.85e+00	5.75e+00	1.16e+03	1.07e-01	4.39e-01	3.81e+00	7.13e+00	
<i>Balistes capricus</i>	Off the coast of Senegal	4.48e+02	2.76e+01	9.81e+01	4.02e+04	2.35e+00	6.15e-08	1.18e+01	6.87e+01	
<i>Canthigaster valentini</i>	Lizard Island, GBR, Australia	2.17e+02	3.61e+00	-4.82e-01	2.40e+02	-8.41e-02	2.65e-01	3.54e+00	2.25e-01	
<i>Caulolatilis microps</i>	Onslow Bay, NC, USA	4.09e+02	2.11e+01	9.53e+01	6.13e+00	5.51e-01	4.20e-02	1.90e+01	9.30e+01	
<i>Cetengraulis mysticetus</i>	Gulf of Panama	7.97e+02	8.47e+00	4.87e+01	3.13e+02	2.56e-01	3.44e-02	8.03e+00	4.61e+01	
<i>Clupea harengus</i>	SW - S Coast of Iceland	3.86e+02	2.84e+01	6.55e+01	1.63e+01	5.54e-01	1.83e-48	1.70e+01	-1.48e+02	
<i>Cynoscion regalis</i>	from North Carolina to Gardiners Bay NY	3.88e+02	5.73e+00	3.93e+01	5.48e+00	5.65e-01	1.34e-04	3.31e+00	2.53e+01	
<i>Engraulis anchoita</i>	Off the coast of Mar del Plata	7.00e+02	1.69e+01	1.07e+02	3.23e+02	2.70e-01	5.79e-04	1.54e+01	9.68e+01	
<i>Engraulis anchoita</i>	Off the coast of Patagonia	7.73e+02	1.76e+00	8.65e+00	1.23e+02	5.61e-01	6.53e-02	1.52e+00	6.88e+00	
<i>Engraulis mordax</i>	Washington and Oregon, USA	1.02e+03	1.57e+00	9.17e+00	4.09e+02	3.34e-01	2.61e-01	1.47e+00	9.74e+00	
<i>Engraulis ringens</i>	Off the coast of Peru	5.64e+02	1.73e+01	1.11e+02	1.14e+02	4.90e-01	5.03e-04	1.57e+01	1.00e+02	
<i>Epinephelus aeneus</i>	Southeast Tunisian coast	6.69e+02	9.44e+00	5.23e+01	2.42e+02	1.30e-01	6.16e-01	9.35e+00	5.40e+01	
<i>Etmalosa fimbriata</i>	Elmina fishing harbour, Kakum River estuary	9.01e+01	1.30e+00	-7.78e+00	4.58e+02	-2.77e-01	1.13e-02	1.04e+00	-1.27e+01	
<i>Gradius morhua</i>	Off the eastern coast of Canada, between 42 and 54 degrees North	3.45e+02	2.18e+01	1.41e+02	1.19e+02	1.23e-01	4.93e-02	2.11e+01	1.39e+02	
<i>Gradius morhua</i>	Coastal Iceland	6.93e+02	1.00e+01	6.69e+01	2.02e+01	4.00e-01	1.49e-09	5.69e+00	3.09e+01	
<i>Gradius morhua</i>	Off northern Norway, between Vesteralen and Lofoten	3.97e+02	2.62e+01	1.61e+02	7.44e+01	1.97e-01	2.72e-11	2.13e+01	1.18e+02	
<i>Gasterosteus aculeatus</i>	River Rheidal near Aberystwyth, UK	1.10e+02	3.59e+00	-5.72e+01	1.14e+02	-8.10e-02	1.75e-02	3.40e+00	-6.09e+01	
<i>Genyonemus lineatus</i>	Between Palos Verdes and Huntington beach, CA, USA	4.58e+01	1.74e+01	8.81e+01	1.79e-01	1.04e+00	2.09e-07	9.11e+00	6.16e+01	
<i>Hippoglossoides platessoides</i>	off Mountstuart House on the east side of the Isle of Bute	9.52e+02	9.61e+00	1.39e+01	1.17e+03	-4.62e-02	3.03e-01	9.55e+00	1.48e+01	
<i>Hoplostethus atlanticus</i>	TAS, Australia	2.08e+01	5.47e+00	3.31e+01	8.48e-01	4.35e-01	7.76e-02	5.16e+00	3.19e+01	
<i>Hoplostethus atlanticus</i>	SA, Australia	2.28e+01	1.29e+01	8.40e+01	4.05e-01	5.42e-01	4.64e-02	1.21e+01	8.19e+01	
<i>Hoplostethus atlanticus</i>	NSW, Australia	2.65e+01	3.83e+00	2.31e+01	2.38e+01	1.51e-02	9.30e-01	3.83e+00	2.51e+01	
<i>Larimus fasciatus</i>	mouth of the Cape Fear River, NC, about 4-6 km off Oak Island	4.44e+03	1.40e+01	9.15e+01	3.77e+03	5.14e-02	6.13e-01	1.39e+01	9.32e+01	
<i>Lutjanus carponotatus</i>	Whitsunday Islands, Qld, Australia	4.85e+02	3.01e+01	1.27e+02	7.64e+00	8.13e-01	8.81e-05	2.25e+01	1.13e+02	
<i>Lutjanus synagris</i>	Off Iguaque, Aquiraz, CE, Brazil	1.12e+02	8.07e+00	5.32e+01	1.45e+03	-4.06e-01	1.40e-03	6.10e+00	4.43e+01	
<i>Macruronus antecedens</i>	Along the southern coast of Brazil below 29 degrees south	3.28e+02	1.95e+00	1.37e+01	6.90e+01	2.68e-01	1.50e-01	1.74e+00	1.34e+01	
<i>Mallotus villosus</i>	Barents Sea	4.80e+02	5.27e+01	-4.12e+01	5.90e+01	6.74e-01	2.25e-03	3.92e-01	-4.93e+01	

Table B.1: List of stocks where a power law and isometric relationship was fit to the data on w and R_w , including the results of the fits. Here, μ_{R_w} is calculated from $\mu_{\ln R_w}$ used in Equation 2, as $e^{\mu_{\ln R_w}}$.

Species	Stock	Isometric fit			Power law fit			p -value	RSS	AIC
		μ_{R_w}	RSS	AIC	α	β				
<i>Merlangius merlangus</i>	northern North Sea	1.30e+03	8.29e+00	-3.70e+01	1.12e+03	2.62e-02	4.44e-01	8.23e+00	-3.56e+01	
<i>Merluccius gayi gavi</i>	Off the coast of Chile between 34 and 38 degrees south	1.24e+02	2.76e+00	1.08e+00	3.03e+01	2.02e-01	5.53e-02	2.56e+00	-7.88e-01	
<i>Merluccius hubbsi</i>	Off the northern coast of Patagonia, Argentina, between 42 and 46 degrees south	3.67e+02	4.53e+01	2.86e+02	2.35e+02	6.22e-02	1.37e-01	4.49e+01	2.86e+02	
<i>Merluccius merluccius</i>	Off the coast of Galicia, Spain	1.21e+02	3.80e+01	2.41e+02	2.27e+02	-8.80e-02	3.77e-01	3.79e+01	2.42e+02	
<i>Micromesistius australis</i>	Mar Argentino	4.45e+01	1.45e+01	9.49e+01	1.09e+00	6.09e-01	9.84e-10	9.72e+00	5.85e+01	
<i>Microgonioides furnieri</i>	Along the southern coast of Brazil between 29 and 33 degrees south	3.29e+02	1.30e+01	8.01e+01	1.32e+03	-2.02e-01	2.50e-01	1.26e+01	8.08e+01	
<i>Microgonioides furnieri</i>	Off the mouth of Rio de La Plata between Uruguay and Argentina	2.22e+02	2.46e+00	1.35e+01	5.64e+01	1.96e-01	2.68e-02	2.07e+00	1.01e+01	
<i>Mugil cephalus</i>	Matanzas River Inlet south of St. Augustine, FL, USA	1.09e+03	2.17e+00	-4.22e+01	1.23e+03	-1.88e-02	7.36e-01	2.17e+00	-4.03e+01	
<i>Mugil cephalus</i>	Around the coast of Goa, India	1.03e+03	1.26e+00	3.53e+00	1.81e+03	-1.17e-01	2.01e-01	1.16e+00	3.68e+00	
<i>Ocyurus chrysurus</i>	Banco de Campeche, Mexico	1.01e+02	2.84e+00	2.16e+01	1.96e+01	2.77e-01	2.56e-01	2.65e+00	2.21e+01	
<i>Odontesthes argentinensis</i>	Lagoa dos Patos, RS, Brazil	9.70e+01	3.08e+00	2.28e+01	5.07e+01	1.40e-01	4.73e-01	3.01e+00	2.43e+01	
<i>Opisthonema libertate</i>	Punta Arenas, Costa Rica	4.10e+02	5.64e+00	3.34e+01	4.27e+02	-8.54e-03	9.72e-01	5.64e+00	3.54e+01	
<i>Opisthonema mediterraneum</i>	Punta Arenas, Costa Rica	3.78e+02	3.96e+00	2.18e+01	9.65e+01	2.80e-01	2.91e-01	3.86e+00	2.26e+01	
<i>Oxybelis pictus</i>	Monterey Bay California USA	3.82e+02	2.52e+01	-3.19e+01	4.87e+02	-6.32e-02	6.99e-01	2.50e+01	-3.01e+01	
<i>Paralichthys dentatus</i>	Middle Atlantic Bight (Cape Cod, Massachusetts to Cape Hatteras, North Carolina)	1.64e+02	7.35e+00	-4.79e+00	1.02e+02	5.25e-02	2.85e-01	7.28e+00	-3.95e+00	
<i>Paralichthys patagonicus</i>	Off the coast of Mar del Plata	6.86e+01	2.68e+00	1.95e+01	1.95e-01	8.38e-01	1.37e-02	2.02e+00	1.47e+01	
<i>Pleuronectes platessa</i>	North Sea	2.05e+02	4.31e+01	2.06e+02	9.92e+01	1.10e-01	1.51e-04	4.19e+01	1.94e+02	
<i>Pomacentrus coelestis</i>	Boohns (ML), Japan	1.80e+03	5.48e-01	-2.46e+01	2.00e+03	-1.33e-01	2.36e-01	5.17e-01	-2.42e+01	
<i>Pomacentrus coelestis</i>	Sesoko (LL), Japan	1.26e+03	5.06e-01	-2.67e+01	1.42e+03	-1.94e-01	1.44e-01	4.64e-01	-2.71e+01	
<i>Pomacentrus coelestis</i>	Kominato (HL), Japan	2.10e+03	6.35e-01	-2.06e+01	2.14e+03	-2.51e-02	8.86e-01	6.35e-01	-1.86e+01	
<i>Pomatomus minutus</i>	Ythan estuary, Aberdeenshire, Scotland	1.25e+03	1.30e+00	-2.54e+00	1.68e+03	-4.06e-01	1.16e-02	1.01e+00	-7.53e+00	
<i>Reinhardtius hippoglossoides</i>	Off the west coast of Bear Island, Northeast Arctic Sea	9.31e+00	9.21e+00	5.51e+01	4.42e-01	3.86e-01	3.33e-04	7.92e+00	4.39e+01	
<i>Rhomboptilus auronubens</i>	North and South Carolina, USA	2.50e+02	2.20e+01	9.49e+01	1.49e+01	4.00e-01	4.66e-03	1.79e+01	8.83e+01	
<i>Sardinops sagax</i>	Magdalena Bay, Baja California Sur, Mexico	2.36e+02	1.93e+01	1.11e+02	2.92e+02	-5.22e-02	3.98e-01	1.92e+01	1.12e+02	
<i>Scomber scombrus</i>	Great Sole Bank, eastern Atlantic	1.45e+03	1.96e+00	9.85e+00	9.20e+01	4.58e-01	3.61e-05	9.79e-01	-6.93e+00	
<i>Scomberomorus cavalla</i>	Louisiana	3.84e+02	8.36e+00	4.68e+01	6.40e+00	4.43e-01	3.24e-03	5.59e+00	3.91e+01	
<i>Sebastodes alutus</i>	Gulf of Alaska	4.59e+01	9.73e+00	6.21e+01	7.16e+00	2.99e-01	1.07e-01	9.12e+00	6.14e+01	
<i>Sebastodes auriculatus</i>	Port Orchard, Puget Sound, Washington, United States	2.13e+02	1.72e+00	-2.19e+00	1.90e+02	1.20e-02	1.20e-01	1.72e+00	-1.97e+01	
<i>Sebastodes caurinus</i>	Port Orchard, Puget Sound, Washington, United States	1.88e+02	1.04e+01	5.96e+01	8.80e-01	7.67e-01	1.25e-08	3.60e+00	2.66e+01	
<i>Sebastodes chlorostictus</i>	Bainbridge Island and Colvos Passage, Washington, United States	1.55e+02	6.15e+00	3.78e+01	1.55e-04	1.89e+00	3.53e-07	1.52e+00	1.05e+01	
<i>Sebastodes chlorostictus</i>	Monterey Bay, California, United States	2.80e+02	6.31e+00	4.28e+01	4.35e+00	6.65e-01	3.28e-08	3.23e+00	1.26e+01	

Table B.1: List of stocks where a power law and isometric relationship was fit to the data on w and R_w , including the results of the fits. Here, μ_{R_w} is calculated from $\mu_{\ln R_w}$ used in Equation 2, as $e^{\mu_{\ln R_w}}$.

Species	Stock	Isometric fit			Power law fit			RSS	p-value	AIC
		μ_{R_w}	RSS	AIC	α	β				
<i>Sebastodes constellatus</i>	California Bight, California, United States	2.91e+02	2.08e+00	1.51e+01	1.75e+01	4.70e-01	3.29e-02	1.63e+00	1.19e+01	
<i>Sebastodes dallii</i>	California Bight, California, United States	2.90e+02	1.53e+00	6.96e+00	1.22e+02	2.61e-01	3.08e-01	1.46e+00	7.79e+00	
<i>Sebastodes elongatus</i>	California Bight, California, United States	3.84e+02	2.54e+00	1.78e+01	6.37e+01	3.24e-01	2.37e-03	1.68e+00	9.50e+00	
<i>Sebastodes entomelas</i>	Newport, Oregon, USA	3.68e+02	6.30e+00	3.77e+01	1.84e+00	7.41e-01	2.10e-14	2.40e+00	-2.11e+01	
<i>Sebastodes entomelas</i>	California Bight, California, United States	3.60e+02	1.24e+00	-2.66e+00	1.53e+01	4.53e-01	6.84e-03	9.17e-01	-8.71e+00	
<i>Sebastodes entomelas</i>	San Diego, California, United States to southeastern Alaska, United States	2.66e+02	4.28e+00	2.99e+01	4.23e+00	5.94e-01	8.49e-03	2.88e+00	2.40e+01	
<i>Sebastodes fimbriatus</i>	California Bight, California, United States	3.15e+02	2.24e+00	7.98e+00	4.26e+00	5.80e-01	1.64e-04	1.43e+00	-5.34e+00	
<i>Sebastodes goodei</i>	California Bight, California, United States	3.88e+02	1.84e+00	-4.33e+00	1.38e+02	1.46e-01	1.06e-01	1.72e+00	-5.12e+00	
<i>Sebastodes goodei</i>	Magdalena Bay, Baja California, Mexico to Eureka, California, United States	1.41e+02	2.63e+00	1.94e+01	5.39e+00	4.61e-01	6.27e-06	9.73e-01	-1.47e+00	
<i>Sebastodes hopkinsi</i>	California Bight, California, United States	1.81e+02	1.51e+00	-1.22e+01	2.90e+02	-1.02e-01	4.13e-01	1.48e+00	-1.10e+01	
<i>Sebastodes levius</i>	California Bight, California, United States	2.24e+02	1.51e+00	2.70e+00	1.82e+02	2.53e-02	8.16e-01	1.50e+00	4.64e+00	
<i>Sebastodes melanops</i>	Newport, Oregon, USA	3.83e+02	1.52e+01	3.54e+01	3.70e+01	3.18e-01	7.18e-04	1.44e+01	2.58e+01	
<i>Sebastodes melanostomus</i>	Morro Bay, California, United States	3.10e+02	2.64e+00	9.63e+00	6.93e+00	5.15e-01	3.27e-05	1.65e+00	-6.79e+00	
<i>Sebastodes mentella</i>	Gulf of St. Lawrence, Laurentian Channel and Esquiman Channel	3.45e+01	5.61e+01	3.00e+02	4.85e+00	3.22e-01	5.17e-01	5.09e+01	2.85e+02	
<i>Sebastodes mentella</i>	Off the SW coast of Iceland	6.22e+01	5.38e+00	3.27e+01	2.52e+00	4.88e-01	1.81e-04	4.10e+00	2.00e+01	
<i>Sebastodes miniatus</i>	California Bight, California, United States	1.64e+02	6.38e+00	4.35e+01	5.29e+01	6.74e-01	5.93e-08	3.30e+00	1.45e+01	
<i>Sebastodes mystinus</i>	Monterey, California, United States	2.97e+02	1.36e+01	8.07e+01	7.90e-01	9.66e-01	1.91e-05	9.24e+00	6.35e+01	
<i>Sebastodes mystinus</i>	Half Moon Bay and Morro Bay, California, United States	3.62e+02	1.70e+01	1.11e+02	5.38e+00	6.87e-01	1.29e-10	1.06e+01	7.05e+01	
<i>Sebastodes mystinus</i>	Off the SW coast of Iceland	9.66e+01	3.17e+00	2.31e+01	1.30e+02	-4.27e-02	8.38e-01	3.16e+00	2.50e+01	
<i>Sebastodes norvegicus</i>	Cordell Bank, California, United States	1.48e+02	2.00e+00	3.13e+00	1.99e+01	3.03e-01	1.20e-01	1.86e+00	2.53e+00	
<i>Sebastodes ovalis</i>	California Bight, California, United States	2.65e+02	9.99e-01	-5.18e+01	1.20e+02	1.02e-01	4.98e-02	9.23e-01	-5.39e+01	
<i>Sebastodes paucispinis</i>	Sacramento Reef, Baja California, Mexico to Queen Charlotte Sound, British Columbia, Canada	2.20e+02	7.26e+00	4.34e+01	1.76e+00	6.13e-01	2.71e-04	3.92e+00	3.06e+01	
<i>Sebastodes rosaceus</i>	California Bight, California, United States	4.01e+02	1.58e+00	7.63e+00	1.97e+02	1.55e-01	2.52e-01	1.48e+00	8.16e+00	
<i>Sebastodes rosenblatti</i>	California Bight, California, United States	3.84e+02	3.01e+00	2.17e+01	6.65e+01	3.75e-01	3.50e-02	2.49e+00	1.88e+01	
<i>Sebastodes rufigilis</i>	California Bight, California, United States	2.04e+02	2.61e+00	1.75e+01	1.25e+01	3.89e-01	5.75e-02	2.25e+00	1.55e+01	
<i>Sebastodes saxicola</i>	California Bight, California, United States	4.43e+02	1.54e+00	-3.26e-02	2.88e+02	1.04e-01	1.20e-02	1.22e+00	-4.91e+00	
<i>Sebastodes seminudus</i>	California Bight, California, United States	3.43e+02	2.10e+00	-7.55e+00	6.80e+01	4.10e-01	1.12e-04	1.49e+00	-2.13e+01	
<i>Sebastodes serranoides</i>	Avila, California, United States	3.02e+02	1.15e+01	7.58e+01	5.50e+00	6.20e-01	1.15e-08	7.70e+00	4.42e+01	
<i>Sebastodes viviparus</i>	Norwegian and Barent seas	5.97e+01	9.95e+00	5.744e+01	2.28e+01	1.98e-01	4.31e-01	9.75e+00	5.88e+01	
<i>Seriplus politus</i>		7.41e+02	2.36e+01	1.526e+02	5.12e+02	1.17e-01	7.22e-02	2.31e+01	1.51e+02	

Table B.1: List of stocks where a power law and isometric relationship was fit to the data on w and R_w , including the results of the fits. Here, μ_{R_w} is calculated from $\mu_{\ln R_w}$ used in Equation 2, as $e^{\mu_{\ln R_w}}$.

Species	Stock	Isometric fit			Power law fit			RSS	p -value	RSS	AIC
		μ_{R_w}	RSS	AIC	α	β					
<i>Siganius canaliculatus</i>	Off Damnam, Saudi Arabia	1.32e+03	1.17e+00	-4.17e+00	3.16e+02	2.65e-01	8.97e-09	3.04e-01	-3.85e+01		
	European Continental Shelf Area IXa	5.64e+02	2.86e+00	1.70e+01	7.43e+01	3.28e-01	3.28e-03	2.16e+00	9.64e+00		
<i>Solea solea</i>	European Continental Shelf Area VIIa	8.58e+02	2.29e+00	1.27e+01	2.06e+02	2.45e-01	1.13e-01	2.08e+00	1.19e+01		
	European Continental Shelf Area VIIId	8.15e+02	5.23e+00	3.34e+01	1.32e+02	3.13e-01	5.68e-03	4.43e+00	2.73e+01		
<i>Solea solea</i>	European Continental Shelf Area IVC	1.10e+03	3.79e+00	1.29e+01	3.30e+02	2.06e-01	1.22e-03	3.10e+00	3.93e+00		
<i>Solea solea</i>	European Continental Shelf Area VIIe	6.83e+02	2.10e+00	6.82e+00	4.95e+02	5.09e-02	6.51e-01	2.09e+00	8.60e+00		
	European Continental Shelf Area IVbWest	6.33e+02	4.09e+00	2.37e+01	8.57e+01	3.50e-01	5.02e-05	2.78e+00	8.34e+00		
<i>Solea solea</i>	European Continental Shelf Area VIIa	5.94e+02	2.49e+00	7.39e+00	8.83e+01	3.13e-01	3.80e-04	1.76e+00	4.09e+00		
<i>Solea solea</i>	European Continental Shelf Area IVbEast	1.17e+03	1.83e+00	-5.36e+00	3.98e+02	1.78e-01	9.13e-03	1.55e+00	-1.06e+01		
<i>Stellifer brasiliensis</i>	Off the southern coast of Brazil between Parana and Santa Catarina	5.01e+02	4.04e+01	1.25e+02	2.08e+03	-3.70e-01	3.42e-01	3.95e+01	1.26e+02		
<i>Thalassoma bifasciatum</i>	San Blas Province, Panama	7.10e+02	3.32e+01	1.46e+02	8.08e+02	-2.98e-01	5.26e-02	3.13e+01	1.44e+02		
<i>Thunnus alalunga</i>	Cook Islands and American Samoa	5.95e+01	1.21e+01	7.96e+01	7.94e+01	-2.95e-02	9.39e-01	1.21e+01	8.16e+01		
<i>Thunnus thynnus</i>	Gulf of Mexico	1.50e+04	2.80e+00	1.94e+01	1.73e+04	-1.83e-02	9.63e-01	2.80e+00	2.14e+01		

Species: Amblygaster sirm
Location: Parangipettai, SE coast of India

Species: Amblygaster sirm
Location: Parangipettai, SE coast of India

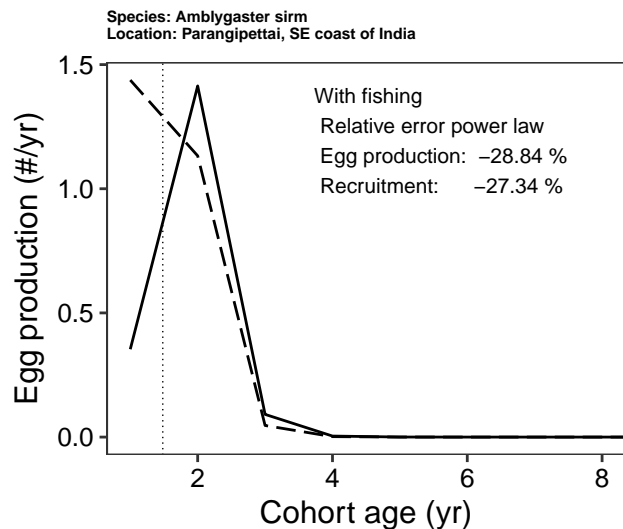
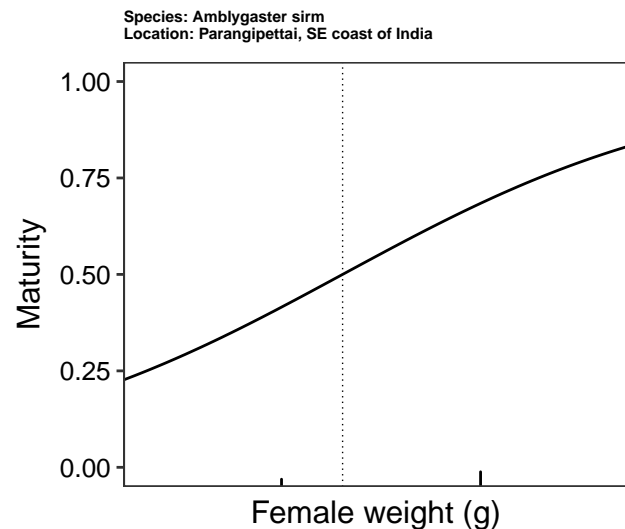
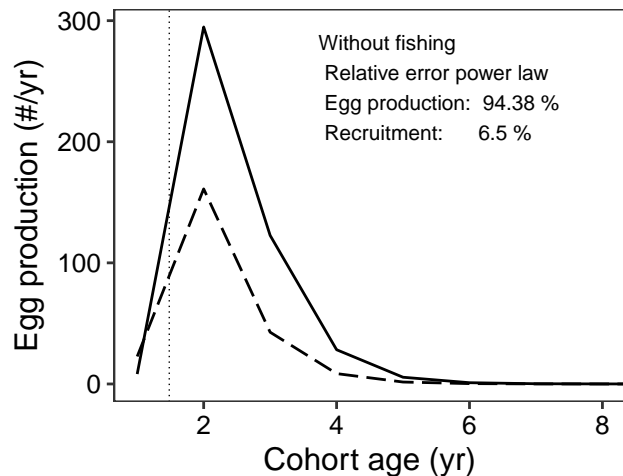
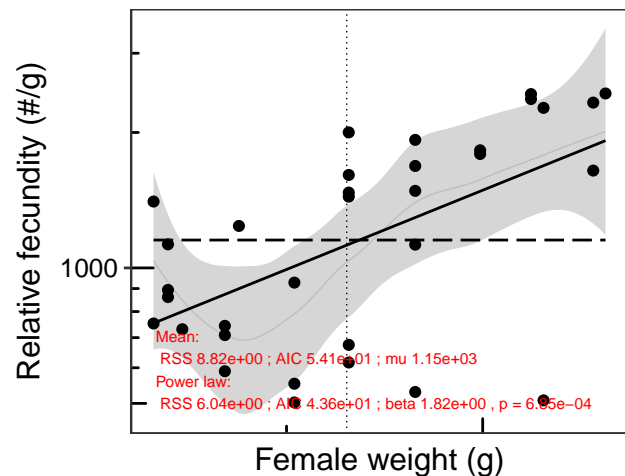
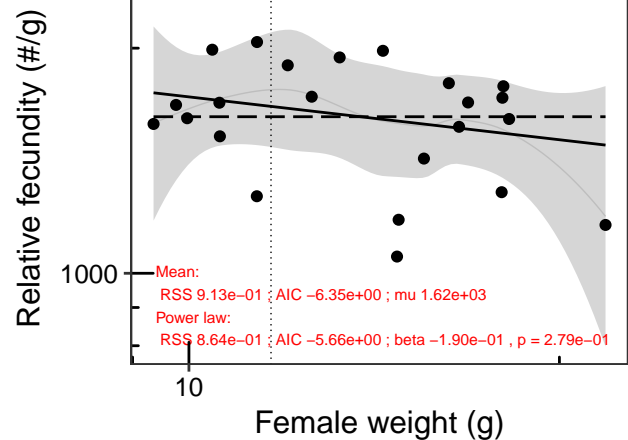
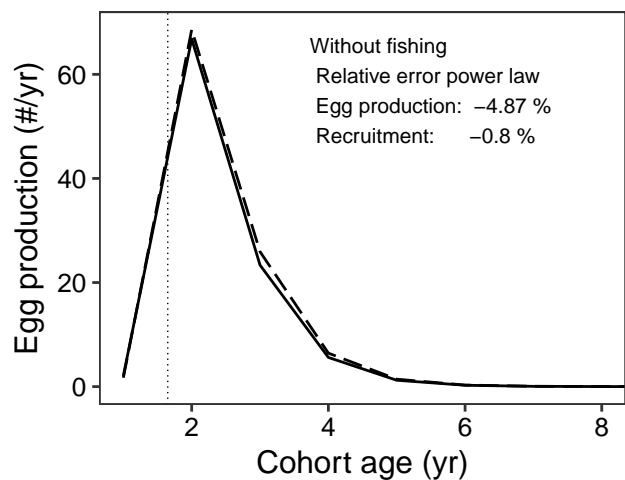


Figure B.1: Top-left: Overview of the isometric (dashed) and power law (solid) fit to the data on female size and relative fecundity. The red text show the fitted μ_R , RSS, and AIC values for the isometric fit, and the β (including p -value), RSS, and AIC values for the power law fit. The vertical dotted line shows size at 50% maturity, the grey line and grey area show the smoothed conditional mean of the data points with 95% confidence interval. Bottom-left: The maturity curve used in the population model, with the vertical dotted line showing size at 50% maturity. Top-right: Cohort egg production for $F = 0$, shown for the power law fit (solid) and isometric fit (dashed). The percentage relative error of the power law fit vs. isometric fit is shown both for total stock egg production and for total stock recruitment. The vertical dotted line shows size at 50% maturity. Bottom-right: Cohort egg production for $F = M$, shown for the power law fit (solid) and isometric fit (dashed). The percentage relative error of the power law fit vs. isometric fit is shown both for total stock egg production and for total stock recruitment. The vertical dotted line shows size at 50% maturity. Data from Barneche *et al.* (2018).

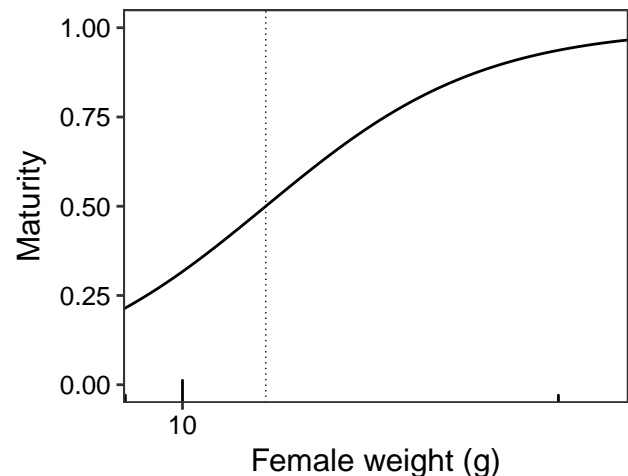
Species: *Anchoviella lepidentostole*
Location: Near Rio Ribeira de Iguape, SP, Brazil



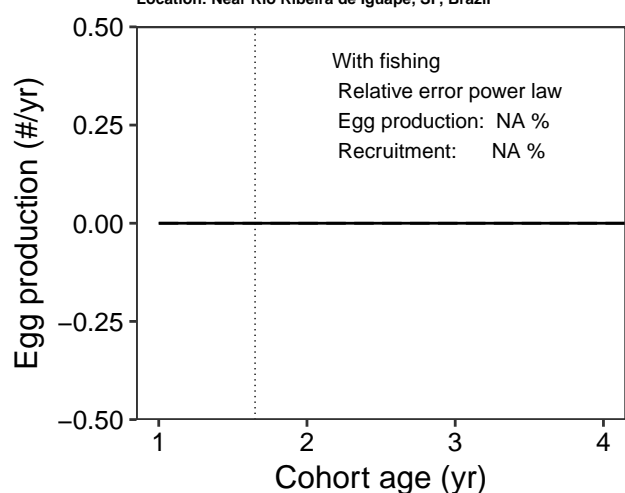
Species: *Anchoviella lepidentostole*
Location: Near Rio Ribeira de Iguape, SP, Brazil



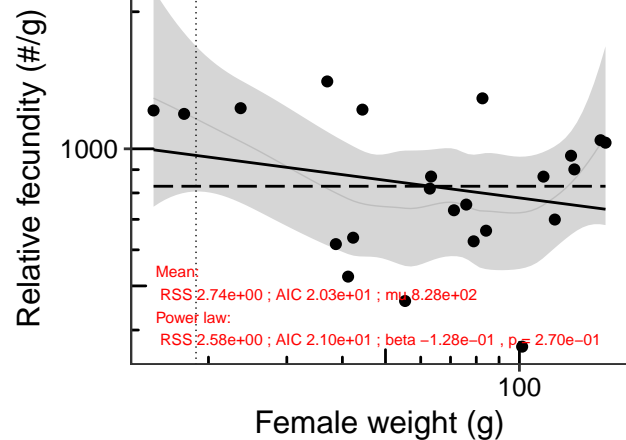
Species: *Anchoviella lepidentostole*
Location: Near Rio Ribeira de Iguape, SP, Brazil



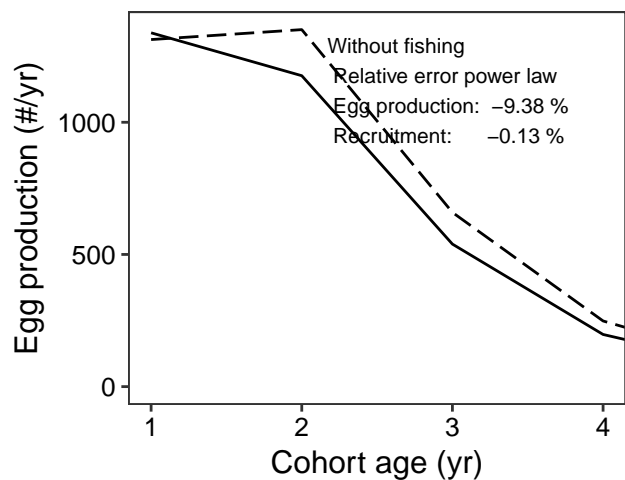
Species: *Anchoviella lepidentostole*
Location: Near Rio Ribeira de Iguape, SP, Brazil



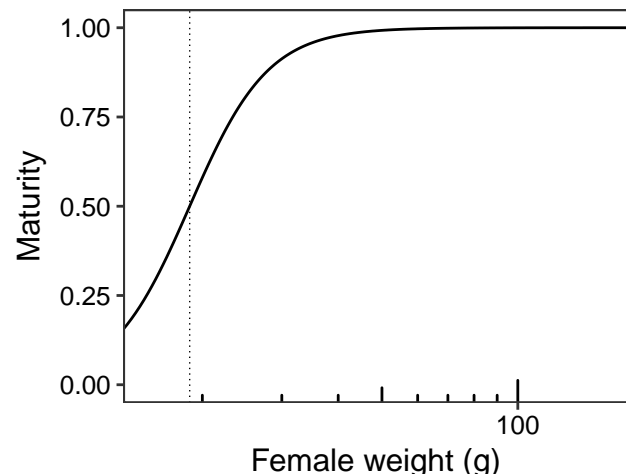
Species: *Archosargus rhomboidalis*
Location: Terminos Lagoon, Mexico



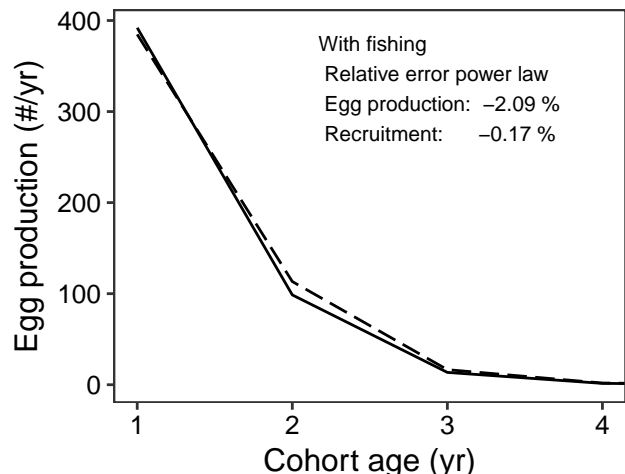
Species: *Archosargus rhomboidalis*
Location: Terminos Lagoon, Mexico



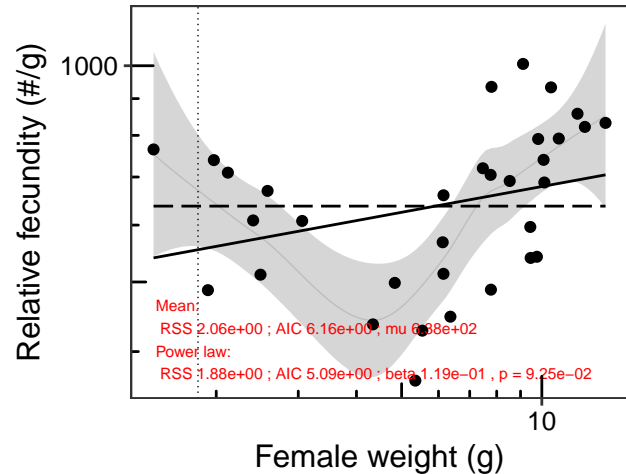
Species: *Archosargus rhomboidalis*
Location: Terminos Lagoon, Mexico



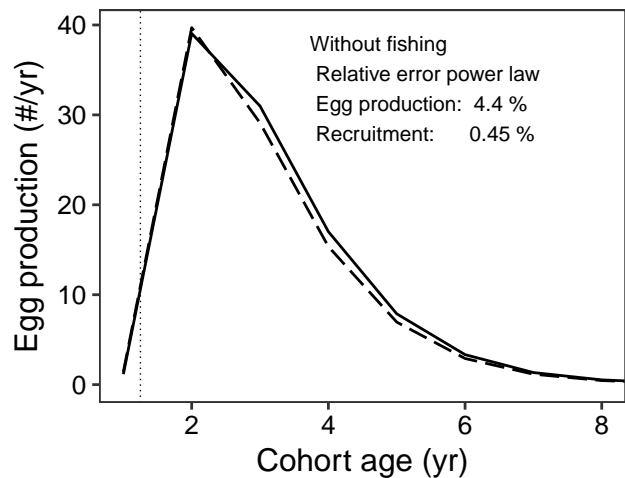
Species: *Archosargus rhomboidalis*
Location: Terminos Lagoon, Mexico



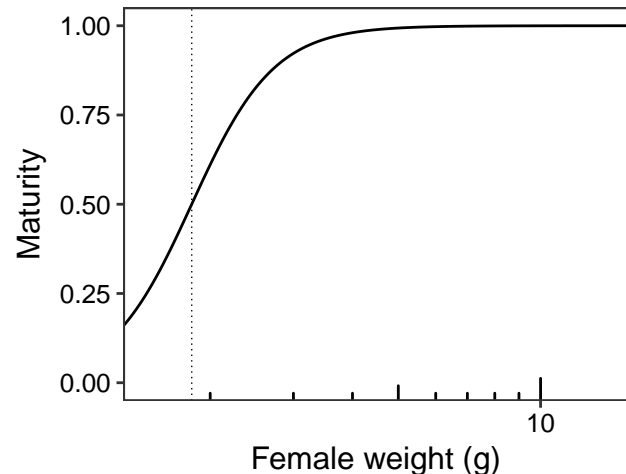
Species: *Atherina presbyter*
Location: Fowley power station Southampton, UK



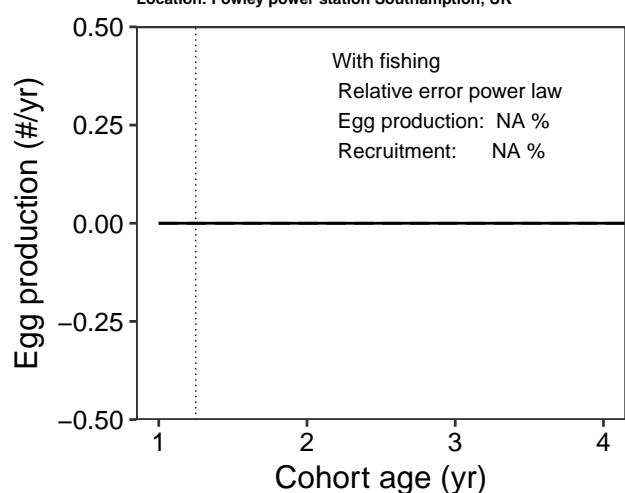
Species: *Atherina presbyter*
Location: Fowley power station Southampton, UK



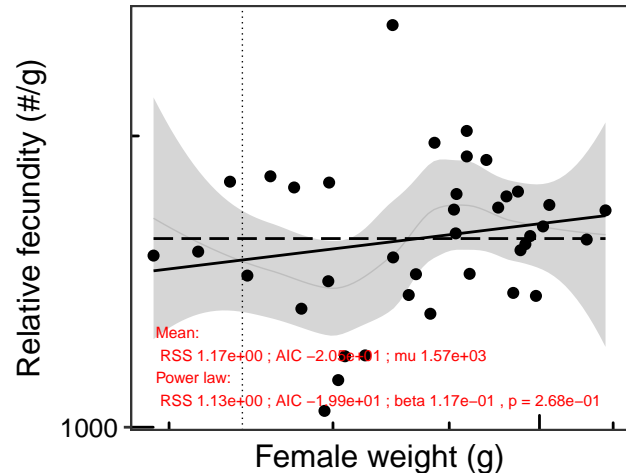
Species: *Atherina presbyter*
Location: Fowley power station Southampton, UK



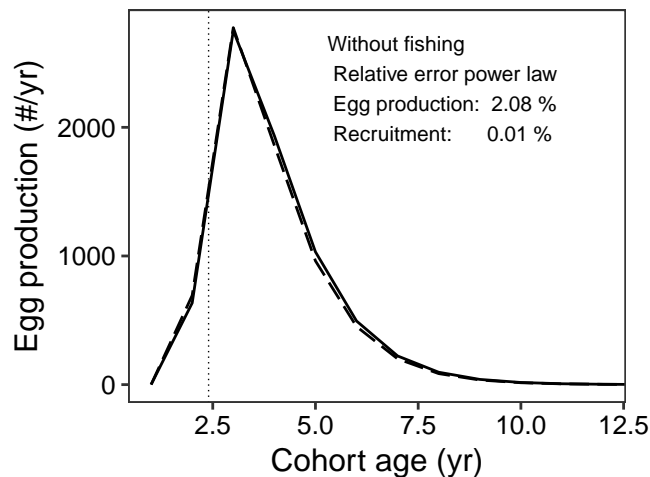
Species: *Atherina presbyter*
Location: Fowley power station Southampton, UK



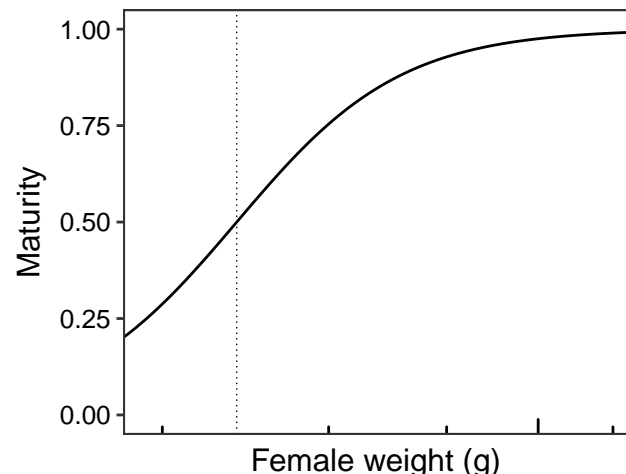
Species: *Balistes capriscus*
Location: Gulf of Gabes, Tunisia



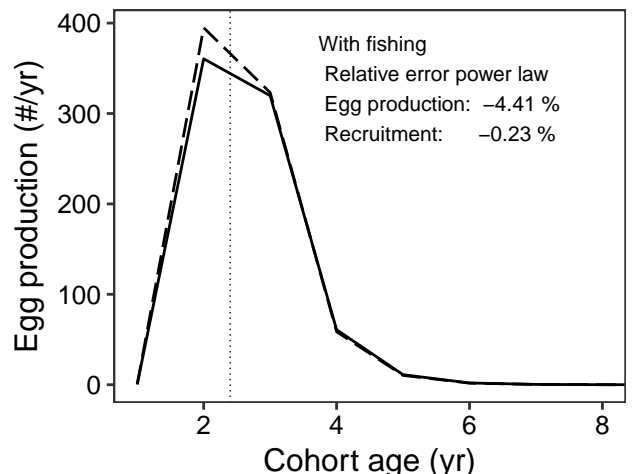
Species: *Balistes capriscus*
Location: Gulf of Gabes, Tunisia



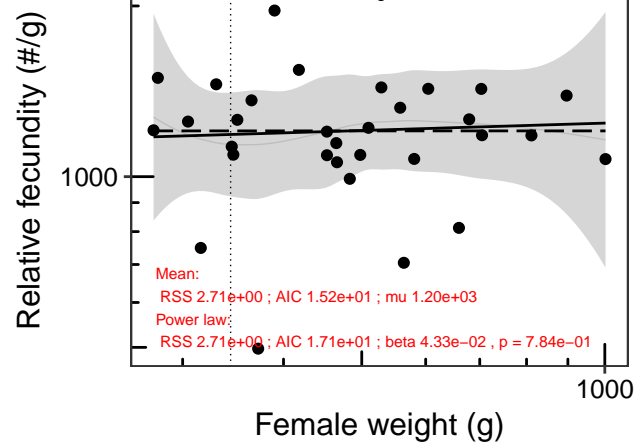
Species: *Balistes capriscus*
Location: Gulf of Gabes, Tunisia



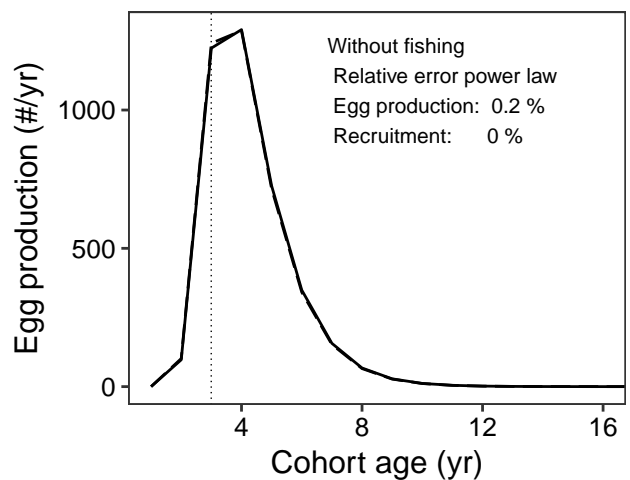
Species: *Balistes capriscus*
Location: Gulf of Gabes, Tunisia



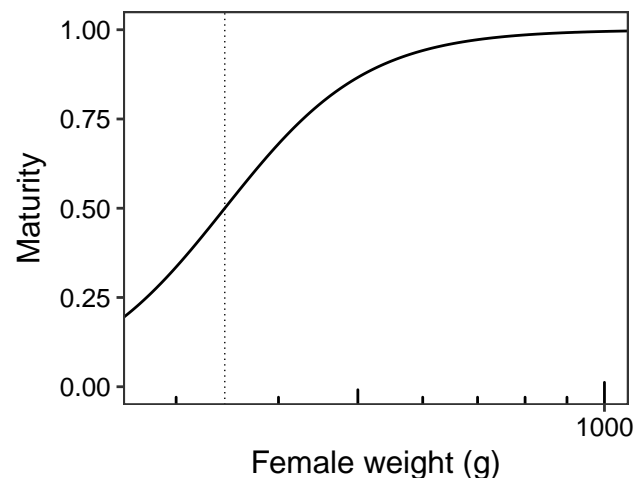
Species: *Balistes capriscus*
Location: Off Mobile Bay, Florida, USA



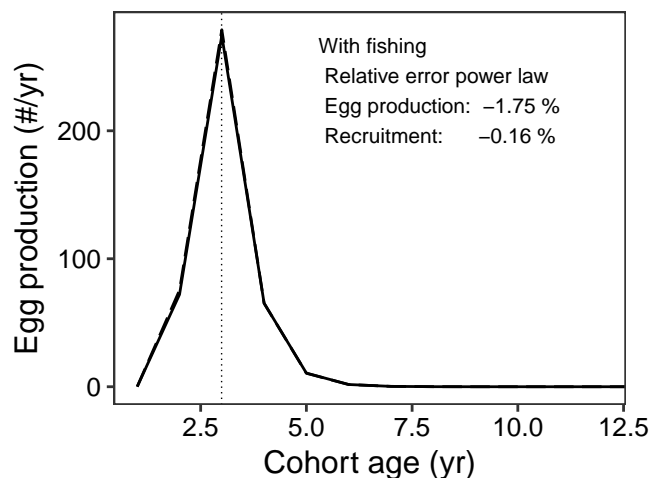
Species: *Balistes capriscus*
Location: Off Mobile Bay, Florida, USA



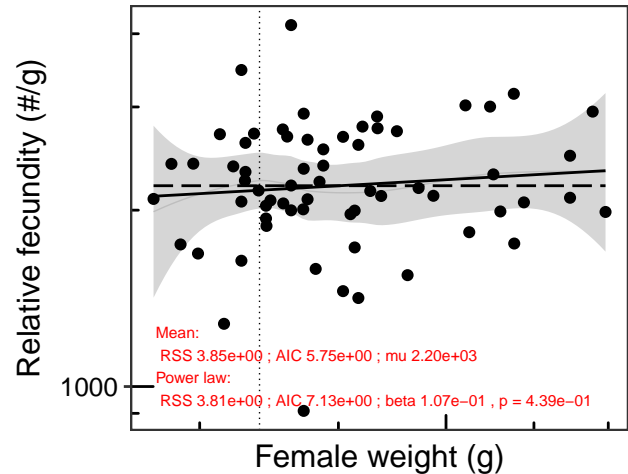
Species: *Balistes capriscus*
Location: Off Mobile Bay, Florida, USA



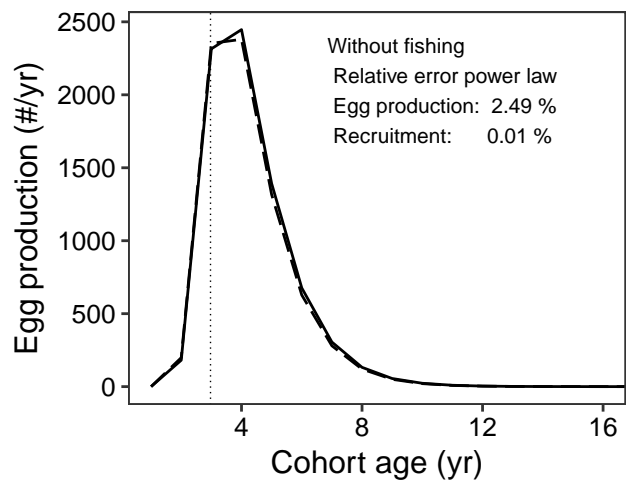
Species: *Balistes capriscus*
Location: Off Mobile Bay, Florida, USA



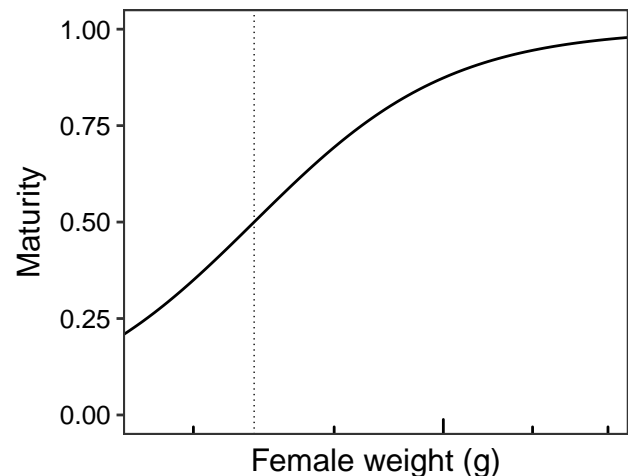
Species: *Balistes capriscus*
Location: Gulf waters offshore of Panama City, Florida, USA



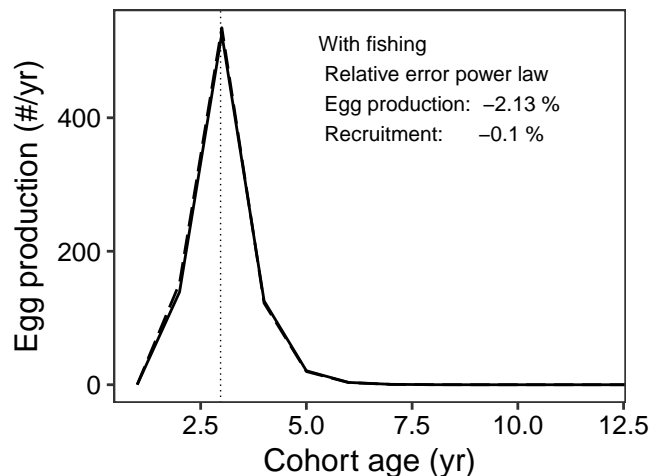
Species: *Balistes capriscus*
Location: Gulf waters offshore of Panama City, Florida, USA



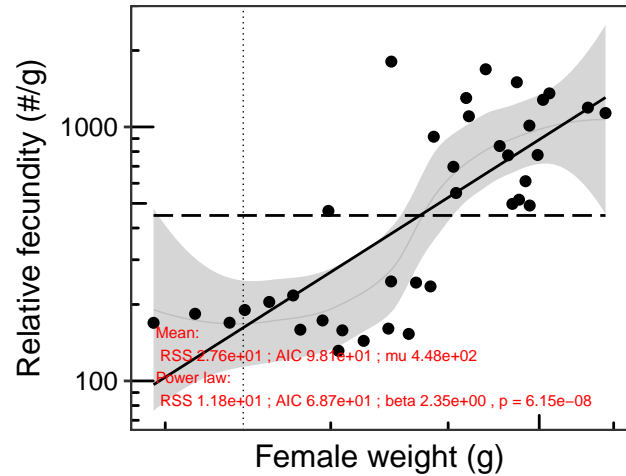
Species: *Balistes capriscus*
Location: Gulf waters offshore of Panama City, Florida, USA



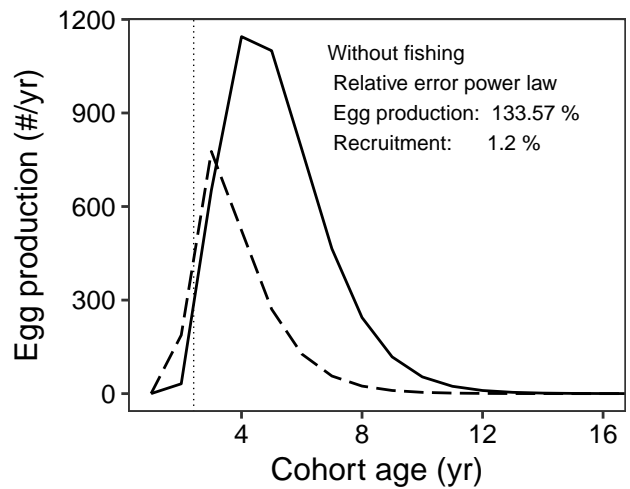
Species: *Balistes capriscus*
Location: Gulf waters offshore of Panama City, Florida, USA



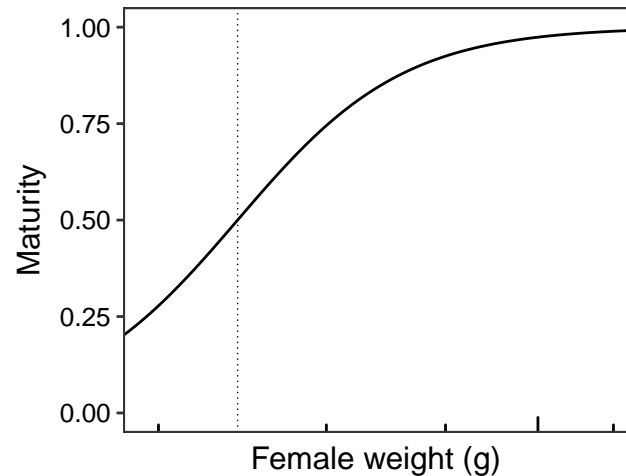
Species: *Balistes capriscus*
Location: Off the coast of Senegal



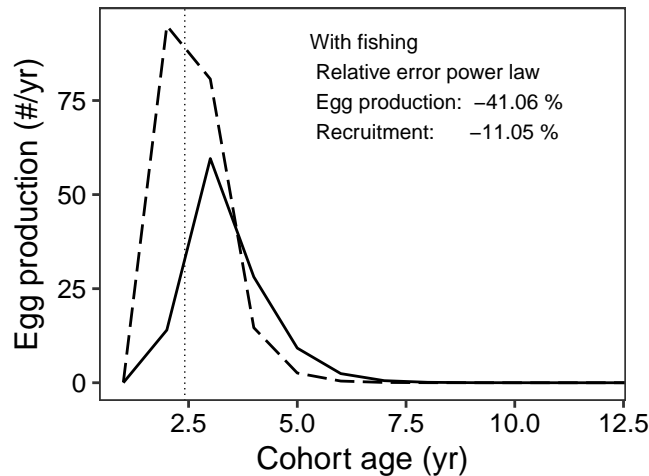
Species: *Balistes capriscus*
Location: Off the coast of Senegal



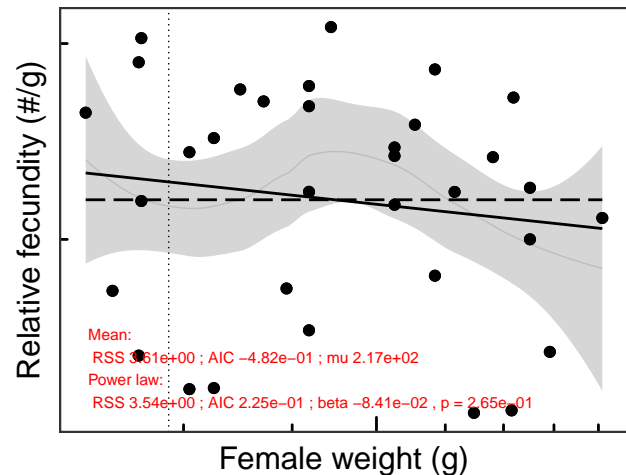
Species: *Balistes capriscus*
Location: Off the coast of Senegal



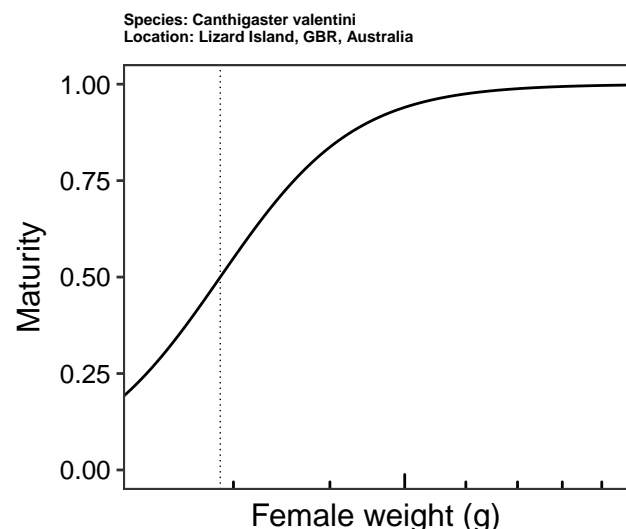
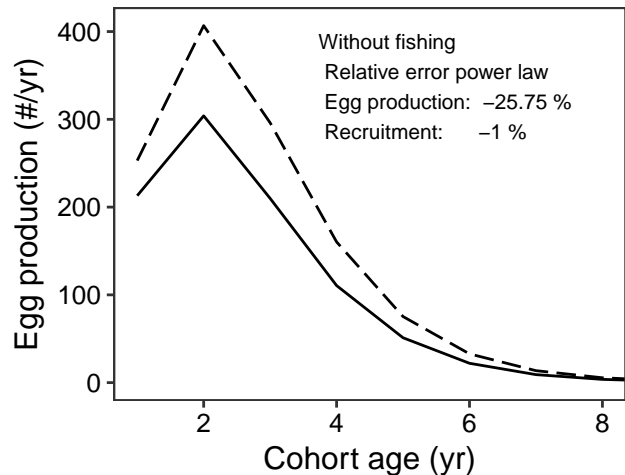
Species: *Balistes capriscus*
Location: Off the coast of Senegal



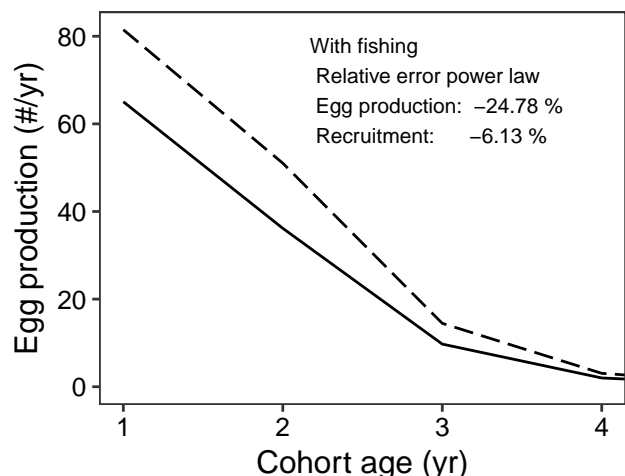
Species: *Canthigaster valentini*
Location: Lizard Island, GBR, Australia



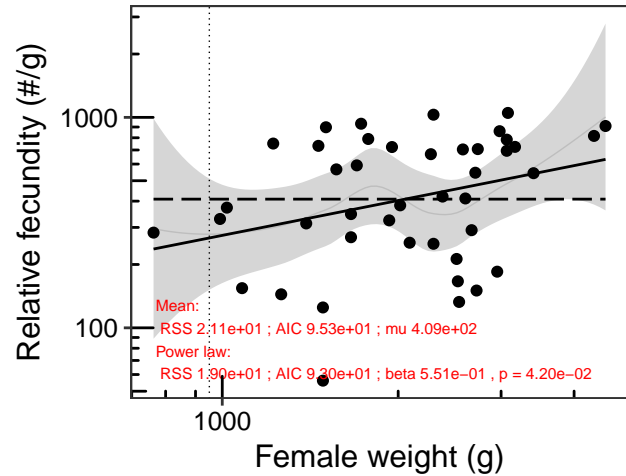
Species: *Canthigaster valentini*
Location: Lizard Island, GBR, Australia



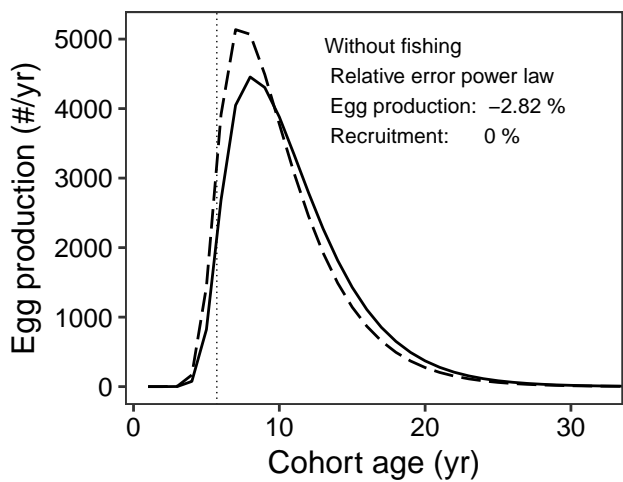
Species: *Canthigaster valentini*
Location: Lizard Island, GBR, Australia



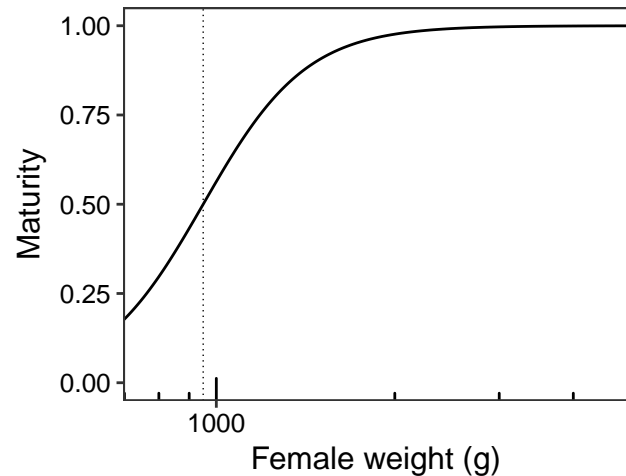
Species: *Caulolatilus microps*
Location: Onslow Bay, NC, USA



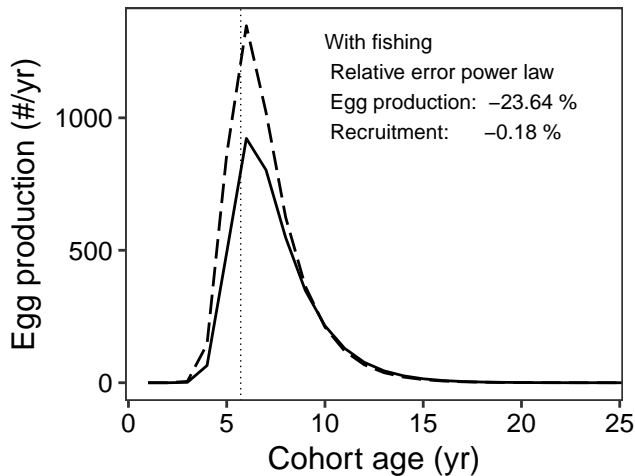
Species: *Caulolatilus microps*
Location: Onslow Bay, NC, USA



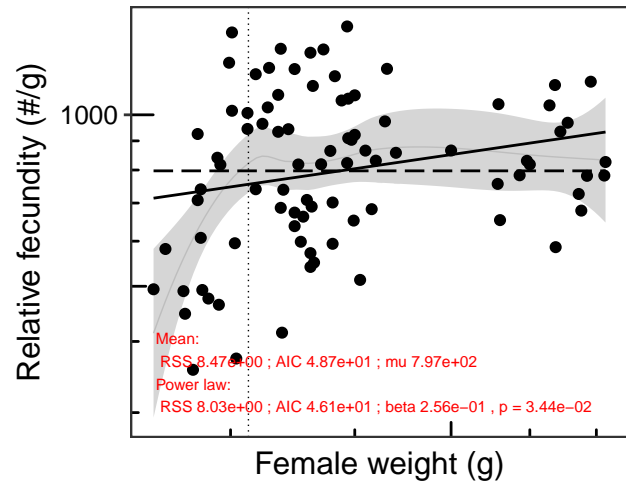
Species: *Caulolatilus microps*
Location: Onslow Bay, NC, USA



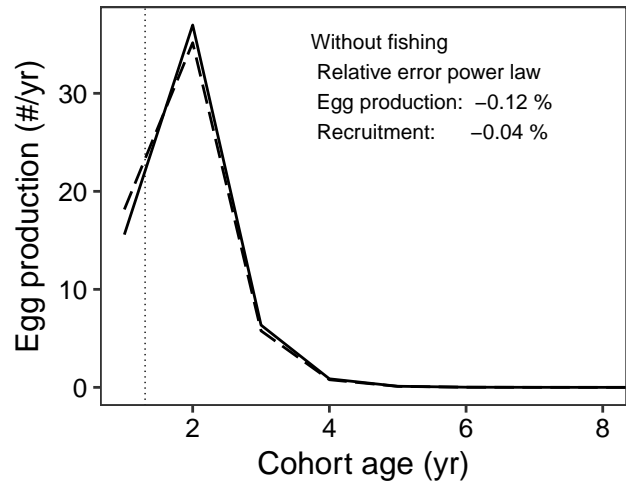
Species: *Caulolatilus microps*
Location: Onslow Bay, NC, USA



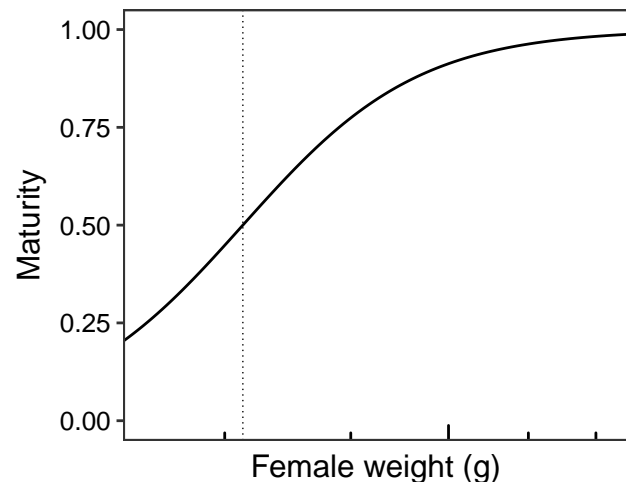
Species: *Cetengraulis mysticetus*
Location: Gulf of Panama



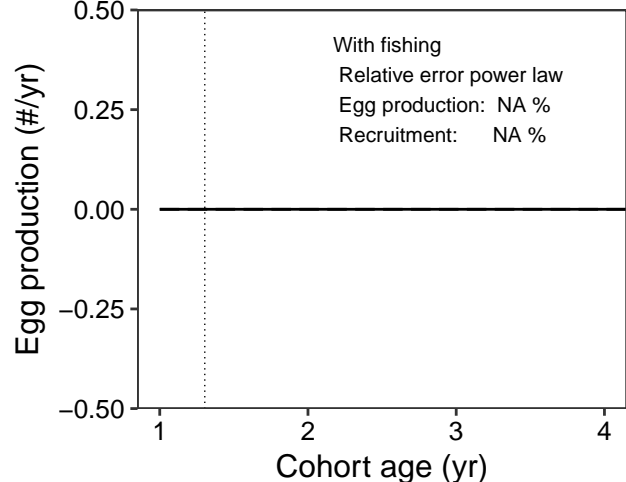
Species: *Cetengraulis mysticetus*
Location: Gulf of Panama



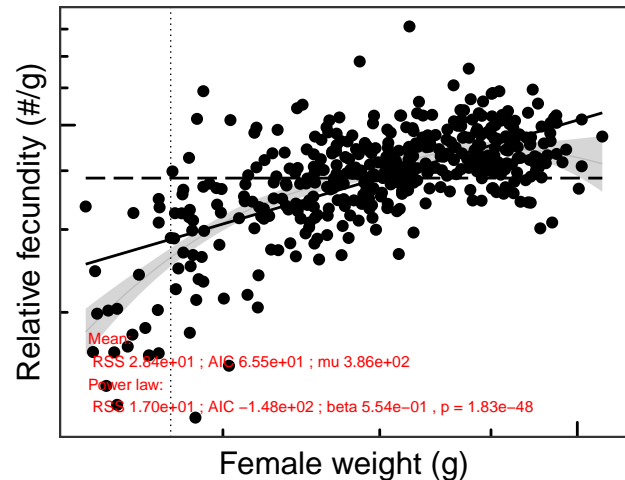
Species: *Cetengraulis mysticetus*
Location: Gulf of Panama



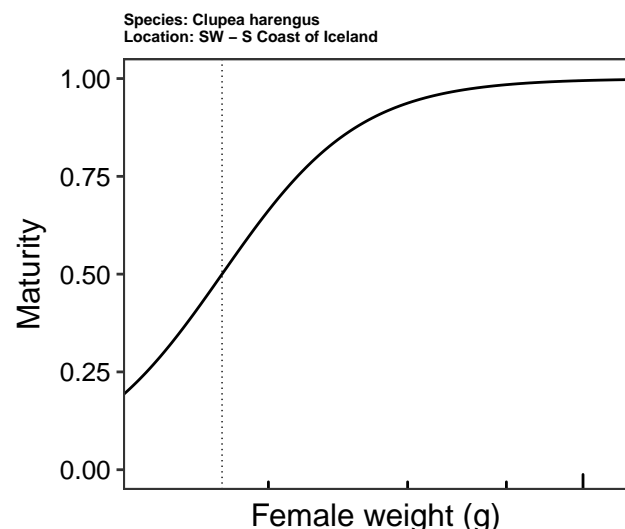
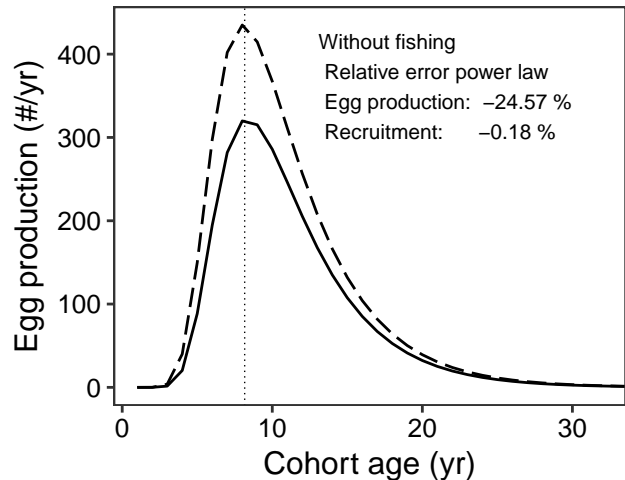
Species: *Cetengraulis mysticetus*
Location: Gulf of Panama



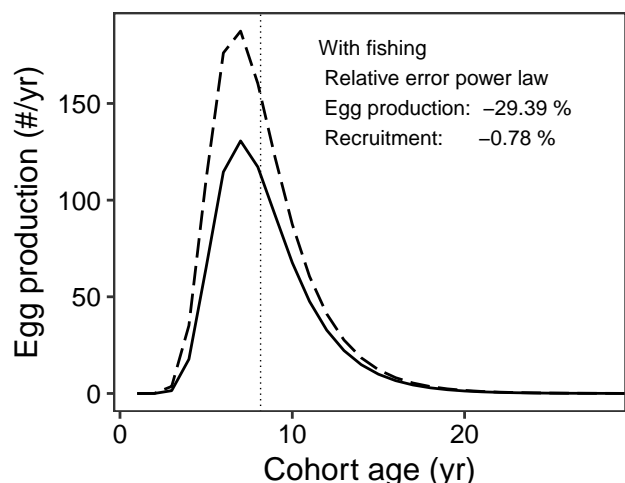
Species: *Clupea harengus*
Location: SW – S Coast of Iceland



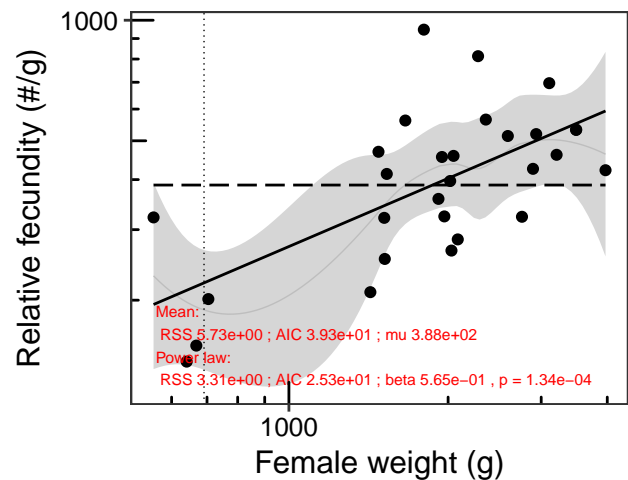
Species: *Clupea harengus*
Location: SW – S Coast of Iceland



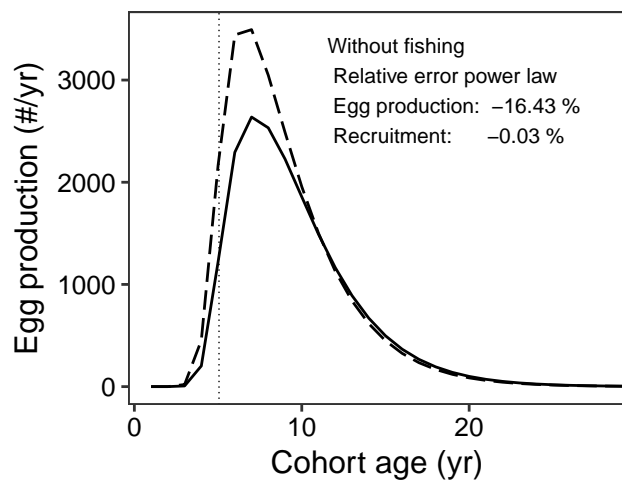
Species: *Clupea harengus*
Location: SW – S Coast of Iceland



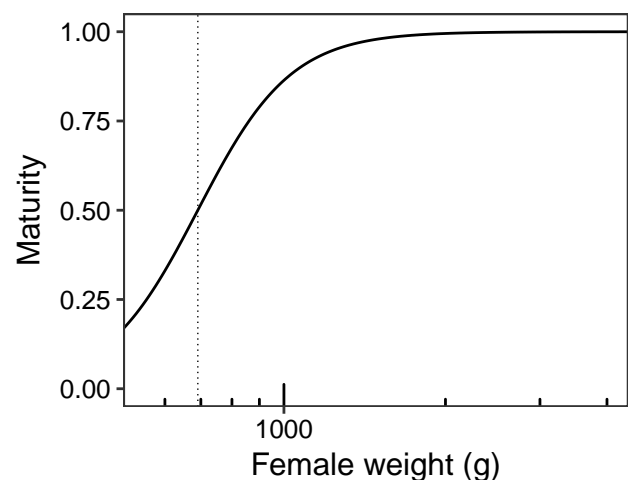
Species: *Cynoscion regalis*
Location: from North Carolina to Gardiners Bay NY



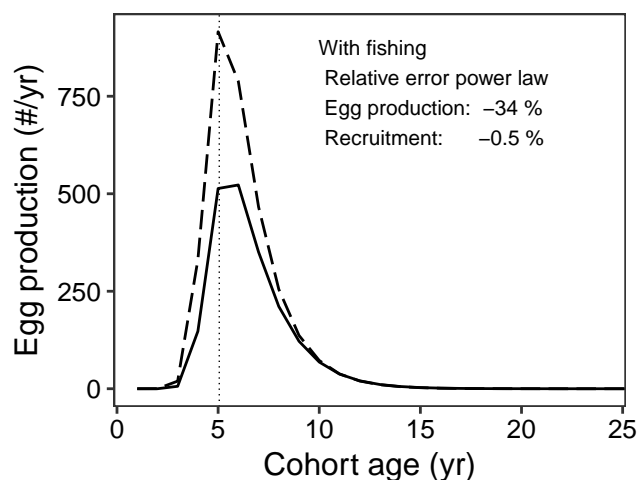
Species: *Cynoscion regalis*
Location: from North Carolina to Gardiners Bay NY



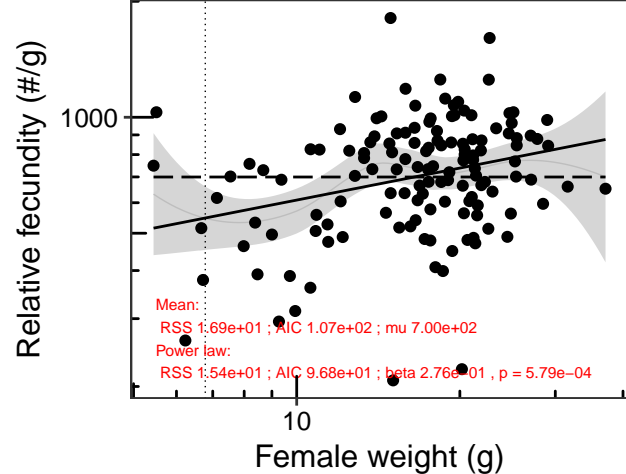
Species: *Cynoscion regalis*
Location: from North Carolina to Gardiners Bay NY



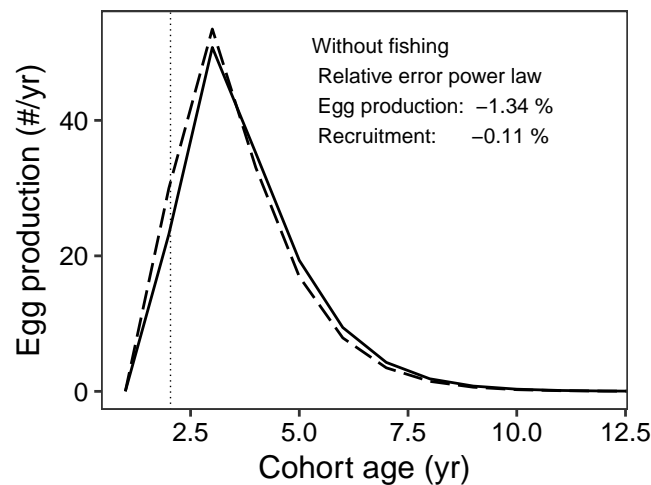
Species: *Cynoscion regalis*
Location: from North Carolina to Gardiners Bay NY



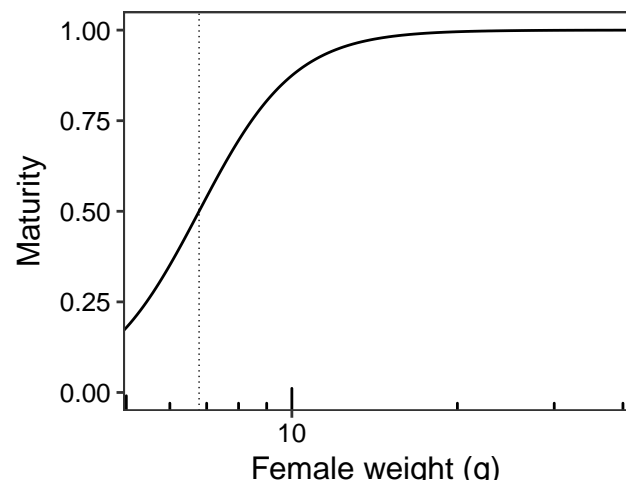
Species: *Engraulis anchoita*
Location: Off the coast of Mar del Plata



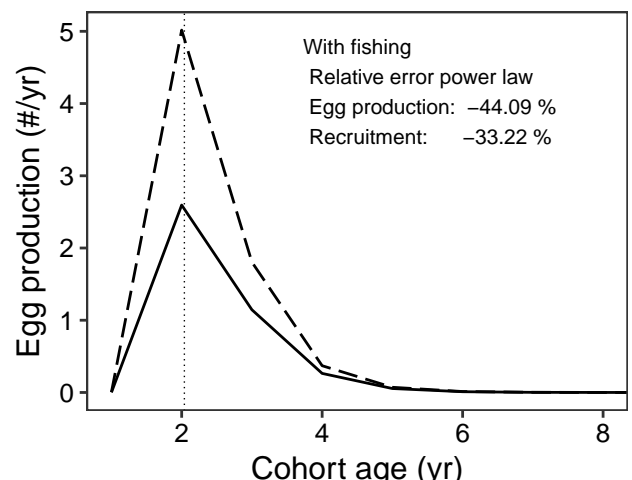
Species: *Engraulis anchoita*
Location: Off the coast of Mar del Plata



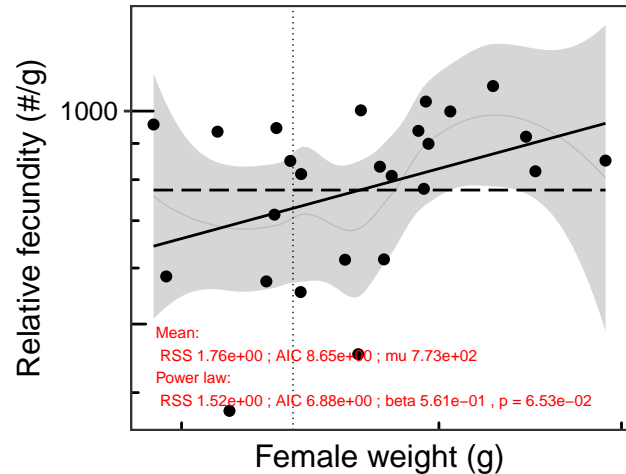
Species: *Engraulis anchoita*
Location: Off the coast of Mar del Plata



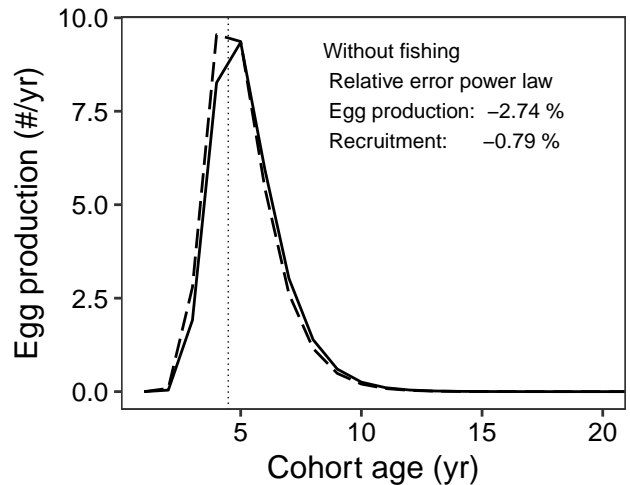
Species: *Engraulis anchoita*
Location: Off the coast of Mar del Plata



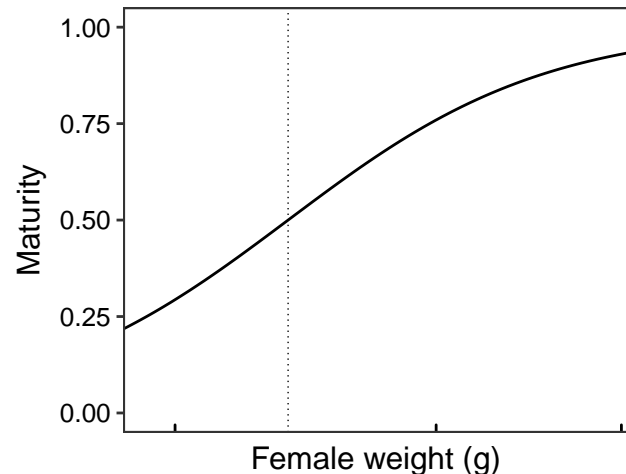
Species: *Engraulis anchoita*
Location: Off the coast of Patagonia



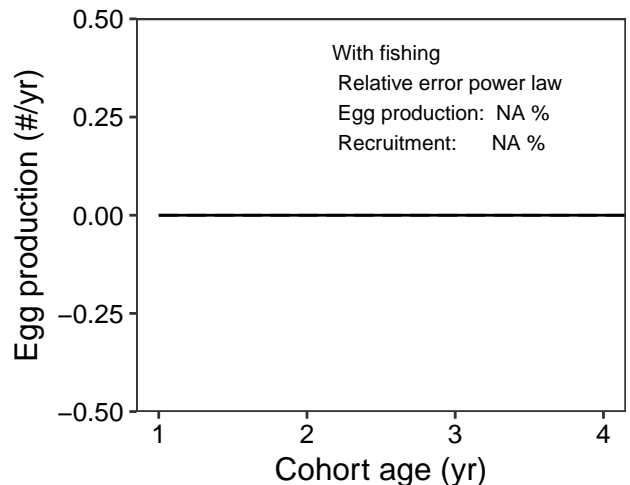
Species: *Engraulis anchoita*
Location: Off the coast of Patagonia



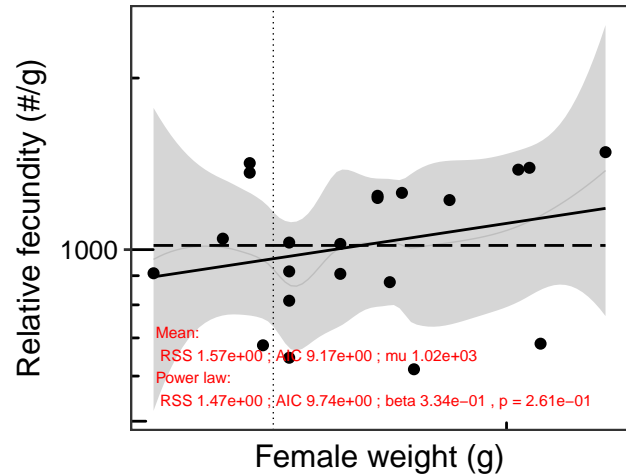
Species: *Engraulis anchoita*
Location: Off the coast of Patagonia



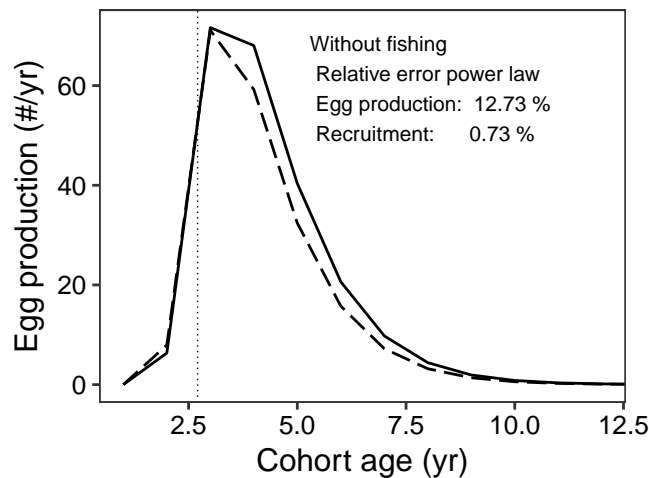
Species: *Engraulis anchoita*
Location: Off the coast of Patagonia



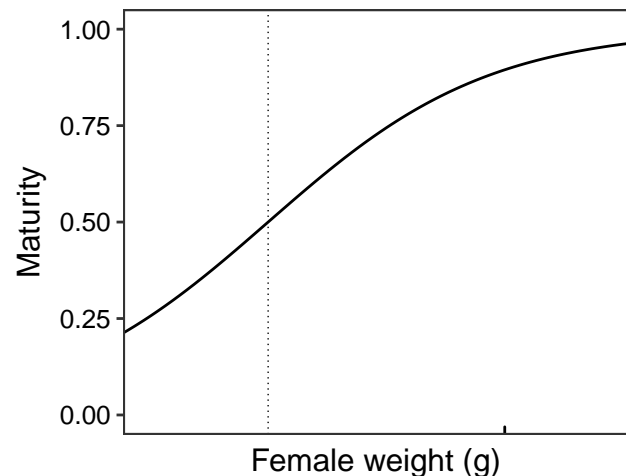
Species: *Engraulis mordax*
Location: Washington and Oregon, USA



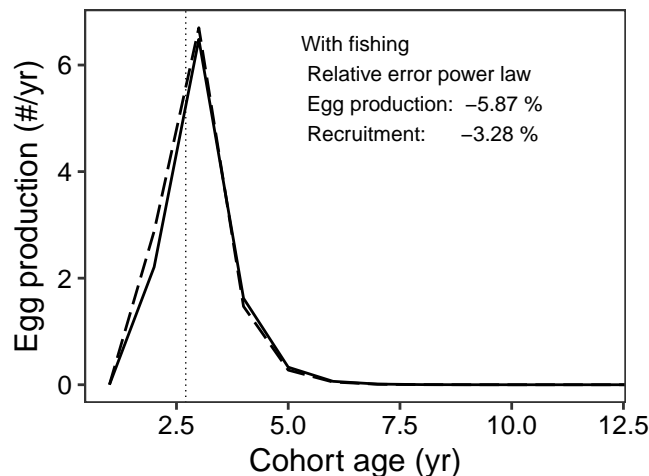
Species: *Engraulis mordax*
Location: Washington and Oregon, USA



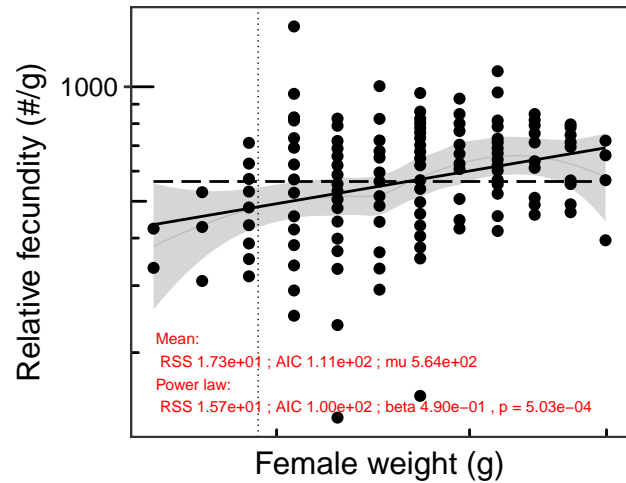
Species: *Engraulis mordax*
Location: Washington and Oregon, USA



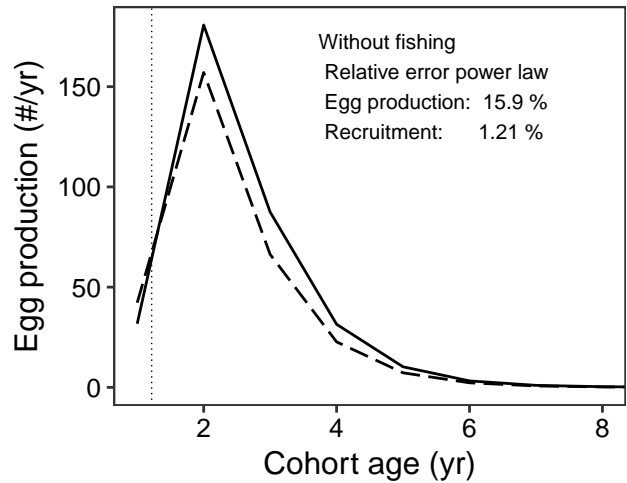
Species: *Engraulis mordax*
Location: Washington and Oregon, USA



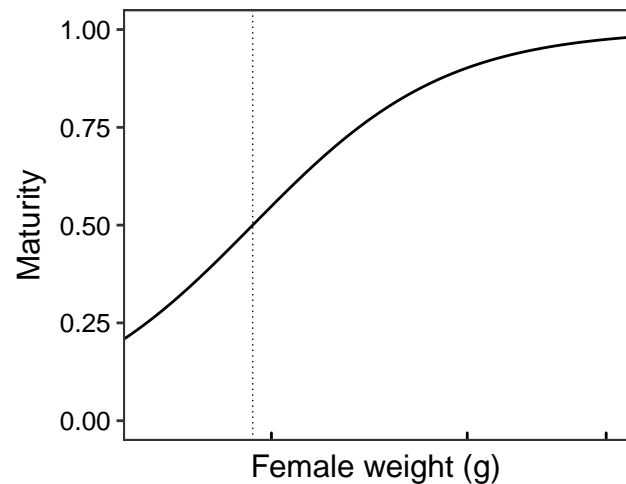
Species: *Engraulis ringens*
Location: Off the coast of Peru



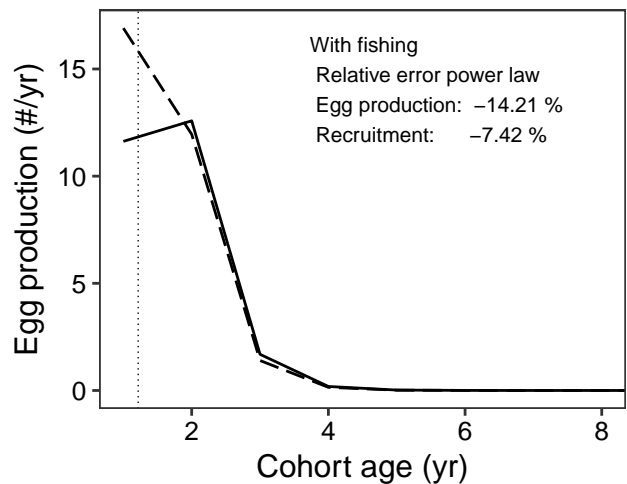
Species: *Engraulis ringens*
Location: Off the coast of Peru



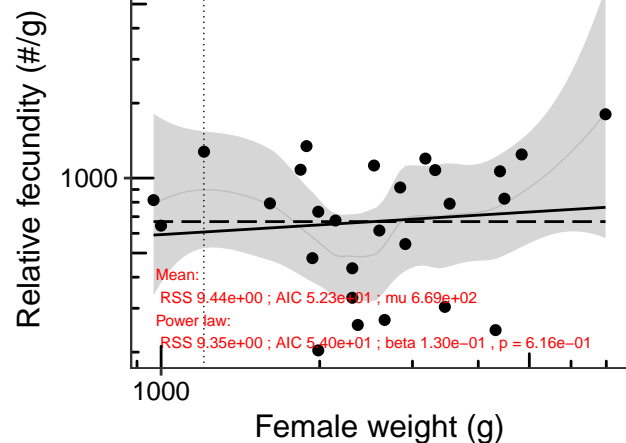
Species: *Engraulis ringens*
Location: Off the coast of Peru



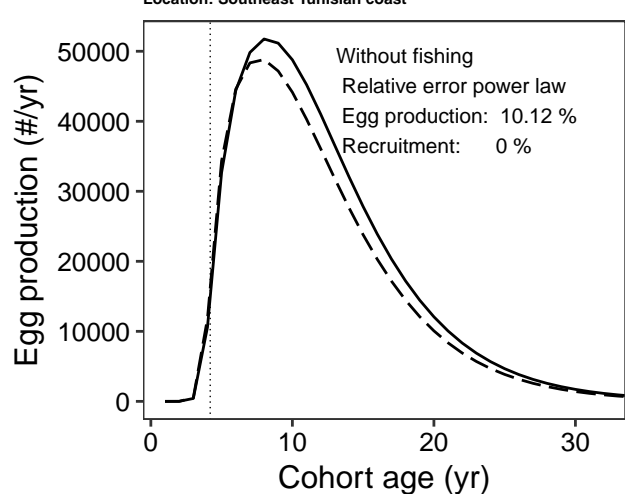
Species: *Engraulis ringens*
Location: Off the coast of Peru



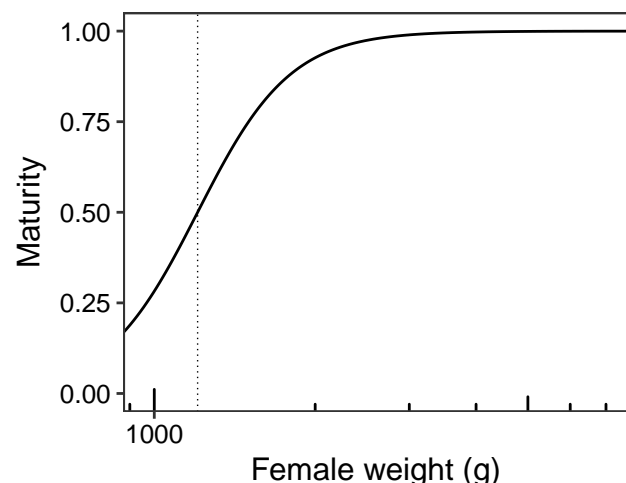
Species: *Epinephelus aeneus*
Location: Southeast Tunisian coast



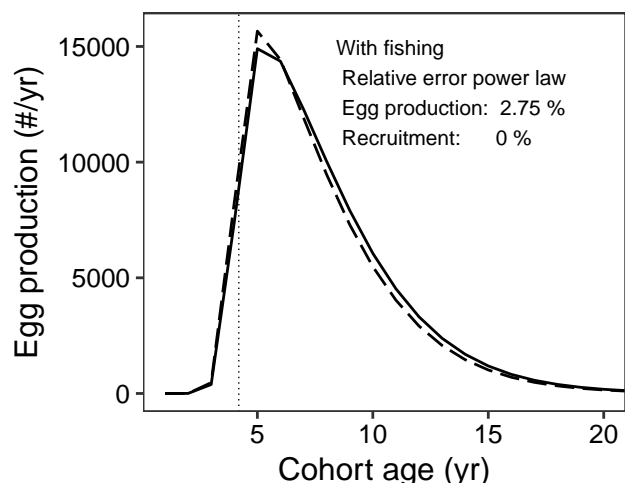
Species: *Epinephelus aeneus*
Location: Southeast Tunisian coast



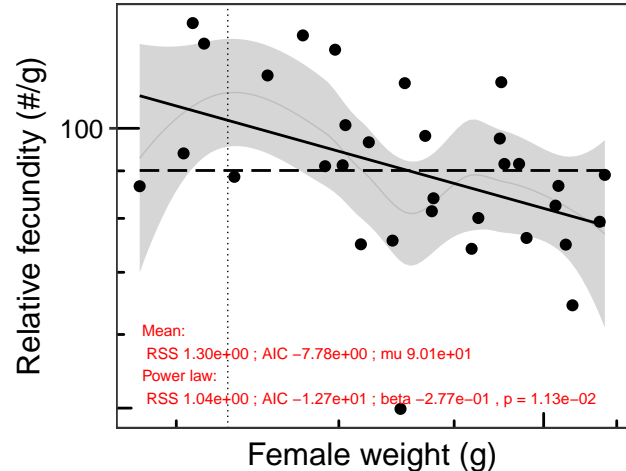
Species: *Epinephelus aeneus*
Location: Southeast Tunisian coast



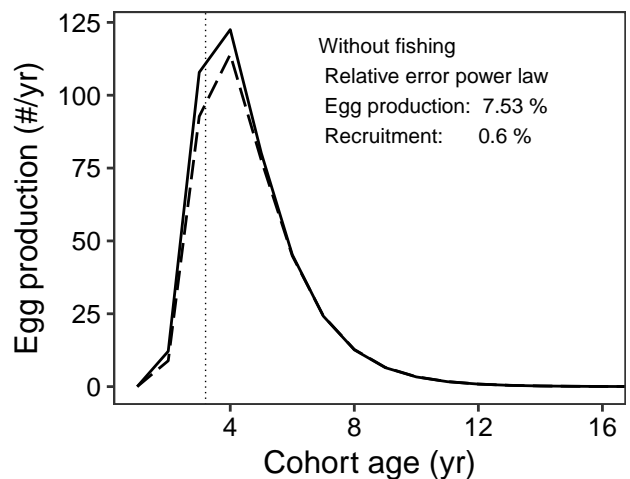
Species: *Epinephelus aeneus*
Location: Southeast Tunisian coast



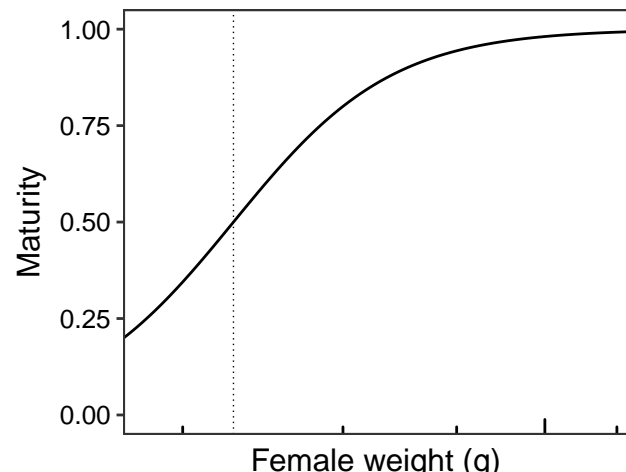
Species: *Ethmalosa fimbriata*
 Location: Elmina fishing harbour, Kakum River estuary



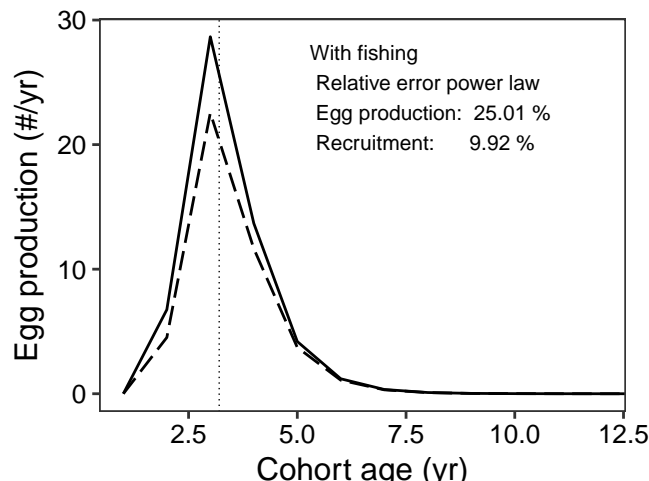
Species: *Ethmalosa fimbriata*
 Location: Elmina fishing harbour, Kakum River estuary



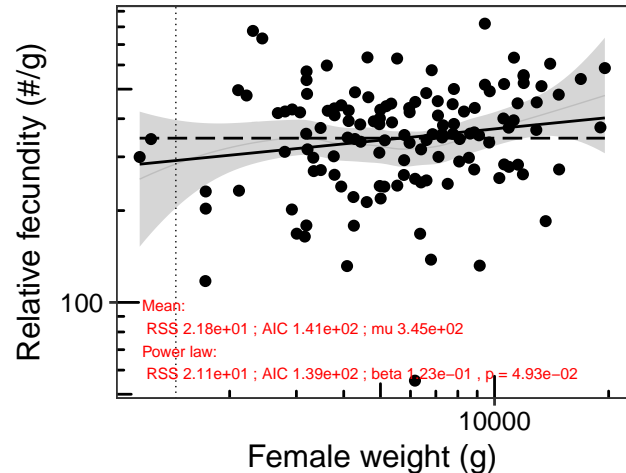
Species: *Ethmalosa fimbriata*
 Location: Elmina fishing harbour, Kakum River estuary



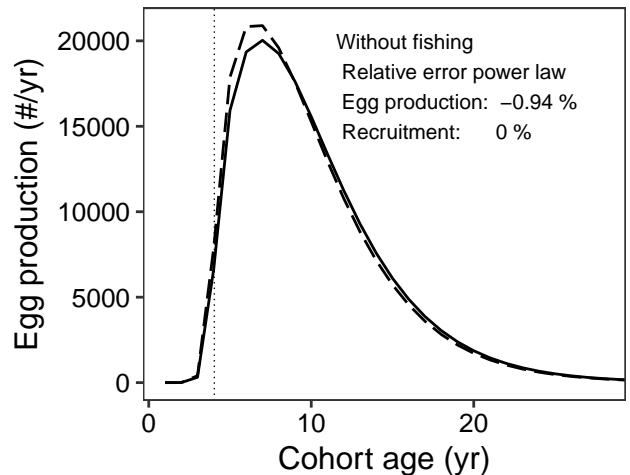
Species: *Ethmalosa fimbriata*
 Location: Elmina fishing harbour, Kakum River estuary



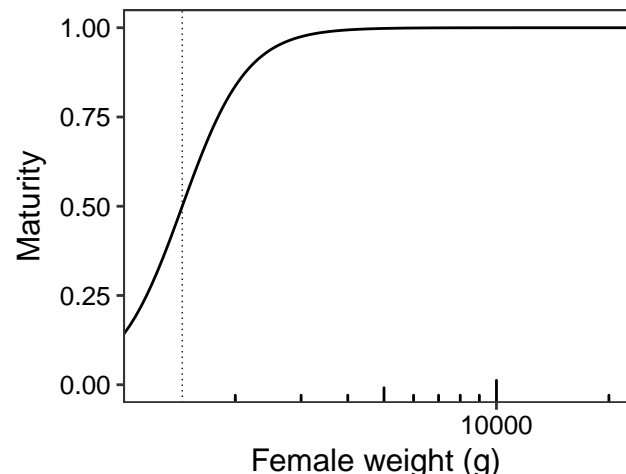
Species: *Gadus morhua*
 Location: Off the eastern coast of Canada, between 42 and 54 degrees No



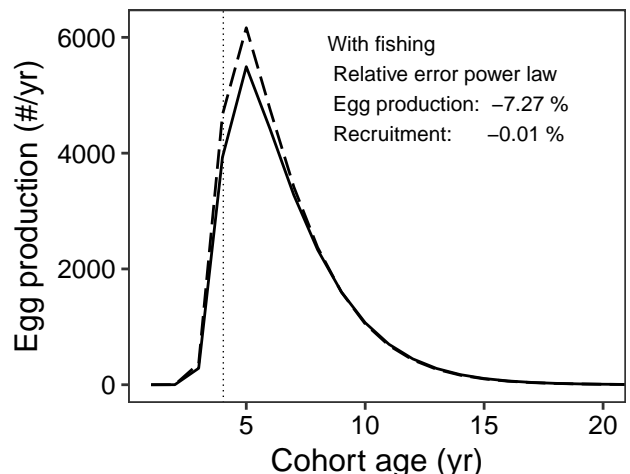
Species: *Gadus morhua*
 Location: Off the eastern coast of Canada, between 42 and 54 degrees N



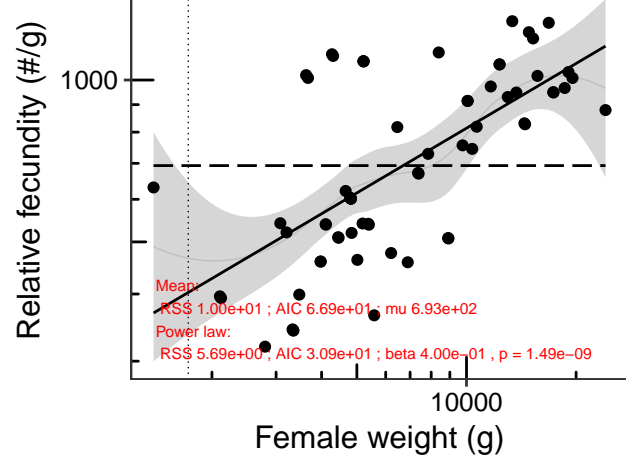
Species: *Gadus morhua*
 Location: Off the eastern coast of Canada, between 42 and 54 degrees N



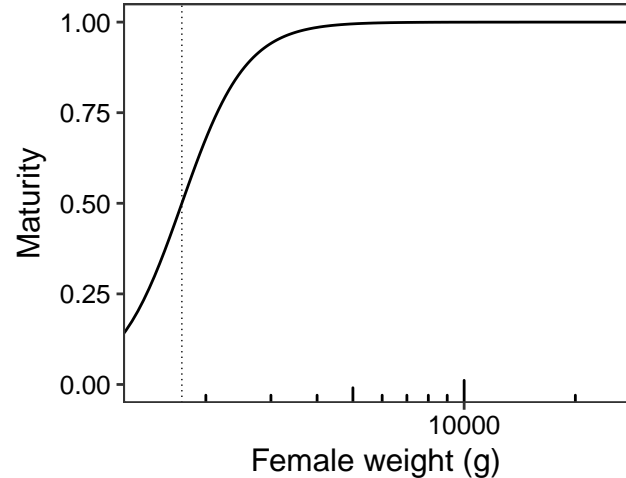
Species: *Gadus morhua*
 Location: Off the eastern coast of Canada, between 42 and 54 degrees N



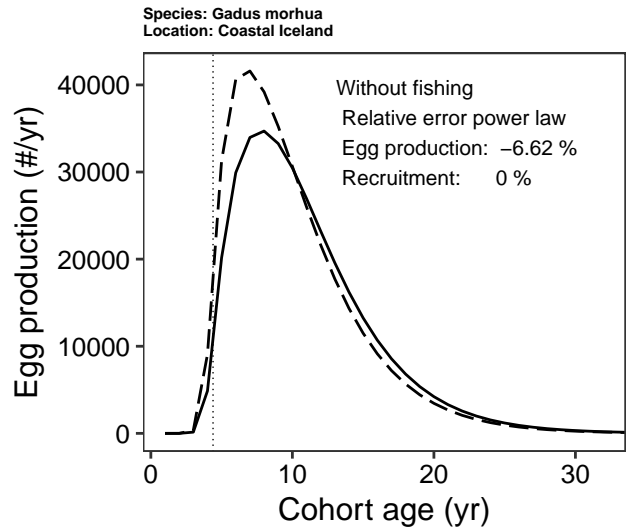
Species: *Gadus morhua*
Location: Coastal Iceland



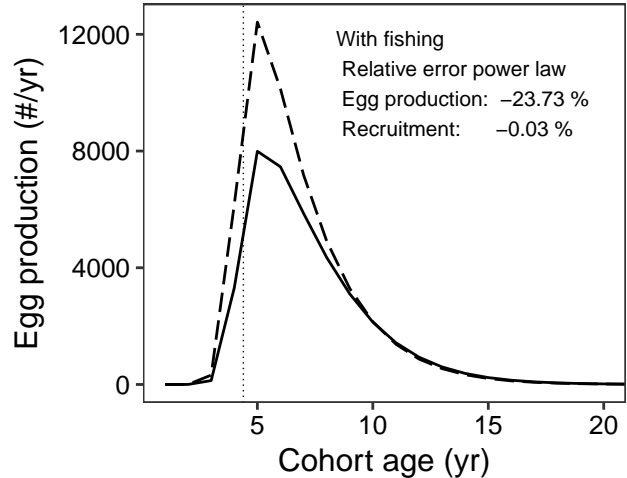
Species: *Gadus morhua*
Location: Coastal Iceland



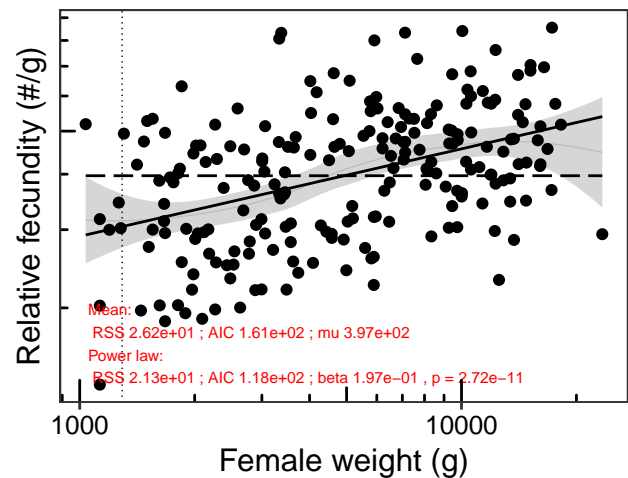
Species: *Gadus morhua*
Location: Coastal Iceland



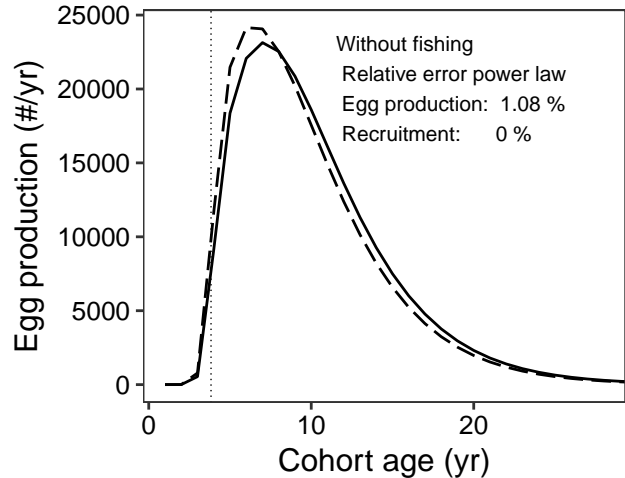
Species: *Gadus morhua*
Location: Coastal Iceland



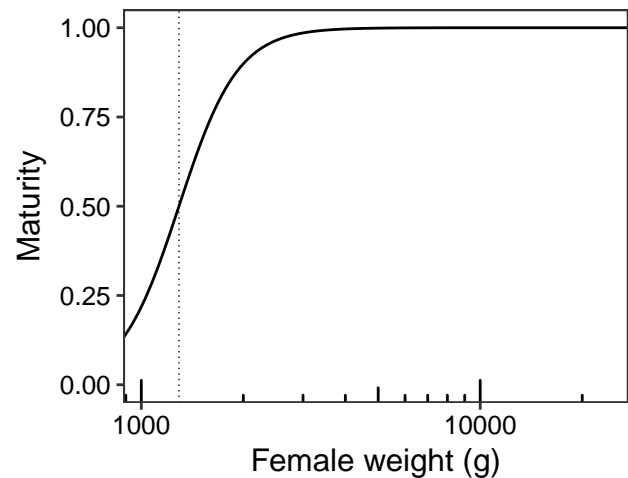
Species: *Gadus morhua*
Location: Off northern Norway, between Vesteralen and Lofoten



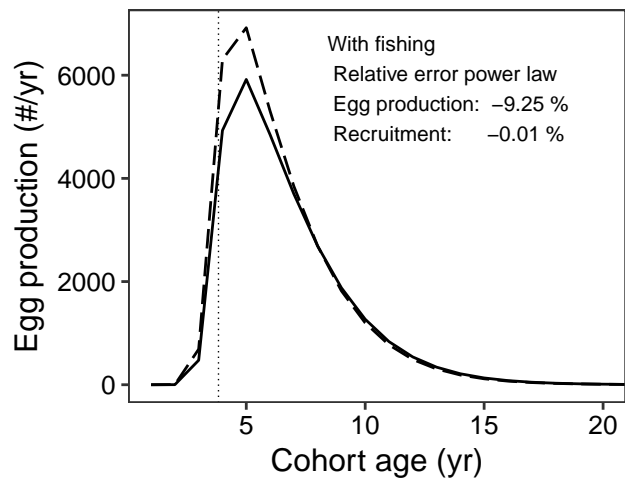
Species: *Gadus morhua*
Location: Off northern Norway, between Vesteralen and Lofoten



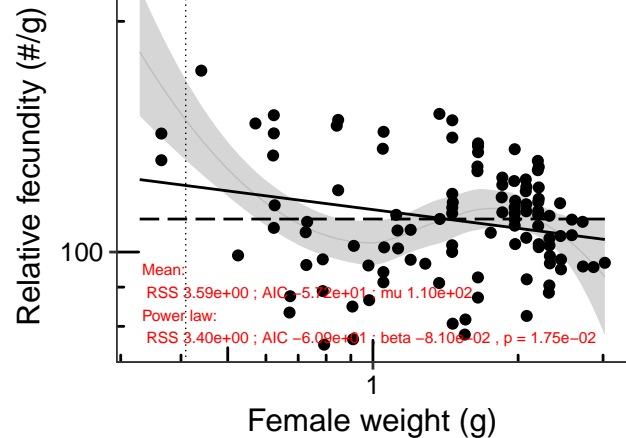
Species: *Gadus morhua*
Location: Off northern Norway, between Vesteralen and Lofoten



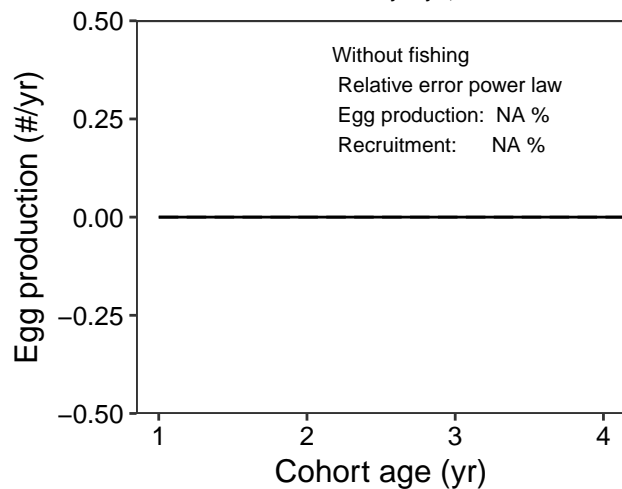
Species: *Gadus morhua*
Location: Off northern Norway, between Vesteralen and Lofoten



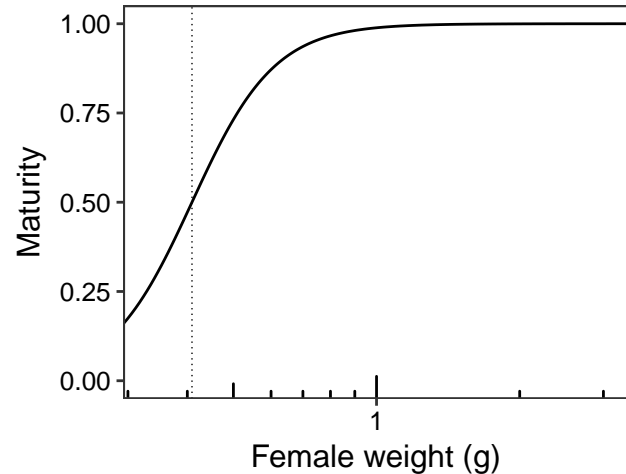
Species: *Gasterosteus aculeatus*
Location: River Rheidol near Aberystwyth, UK



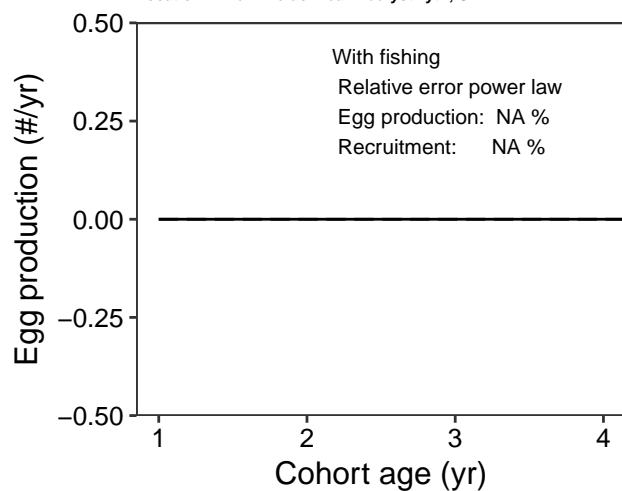
Species: *Gasterosteus aculeatus*
Location: River Rheidol near Aberystwyth, UK



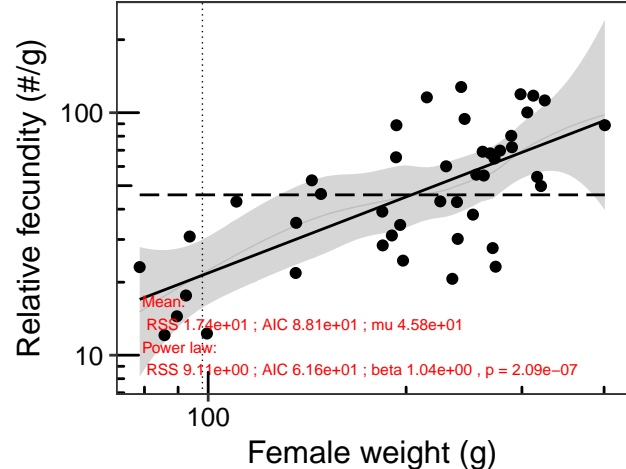
Species: *Gasterosteus aculeatus*
Location: River Rheidol near Aberystwyth, UK



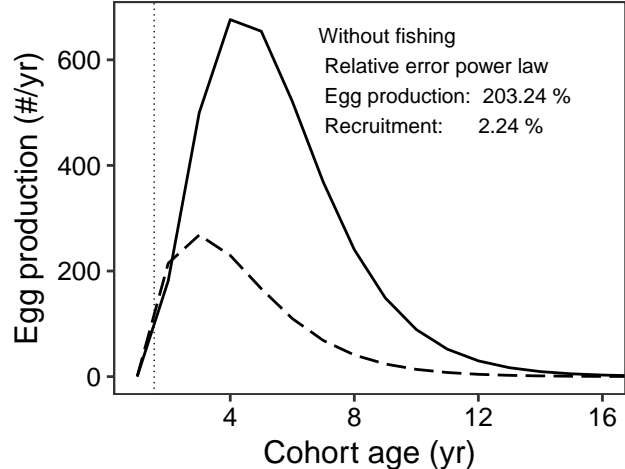
Species: *Gasterosteus aculeatus*
Location: River Rheidol near Aberystwyth, UK



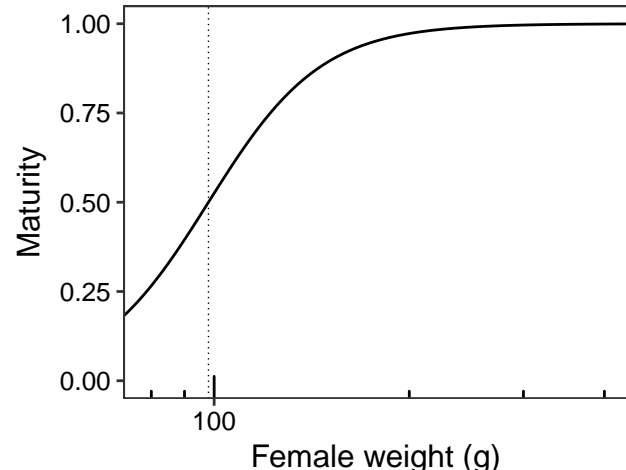
Species: *Genyonemus lineatus*
 Location: Between Palos Verdes and Huntington beach, CA, USA



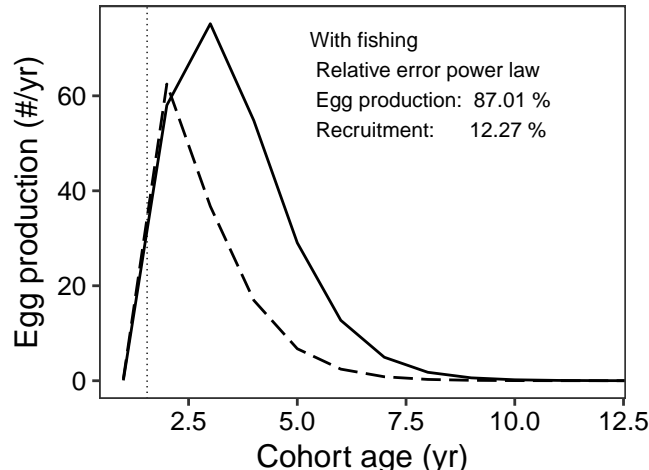
Species: *Genyonemus lineatus*
 Location: Between Palos Verdes and Huntington beach, CA, USA



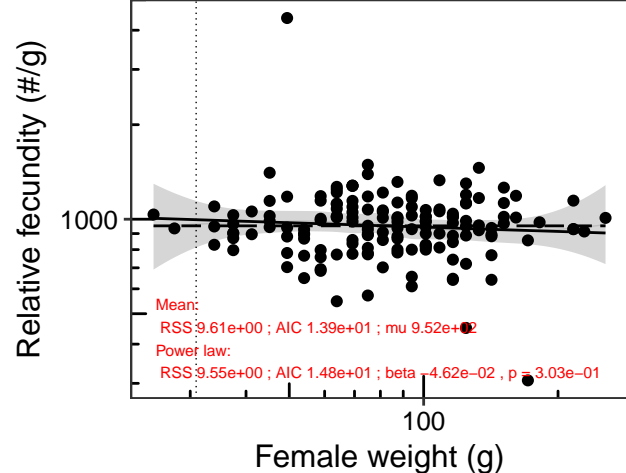
Species: *Genyonemus lineatus*
 Location: Between Palos Verdes and Huntington beach, CA, USA



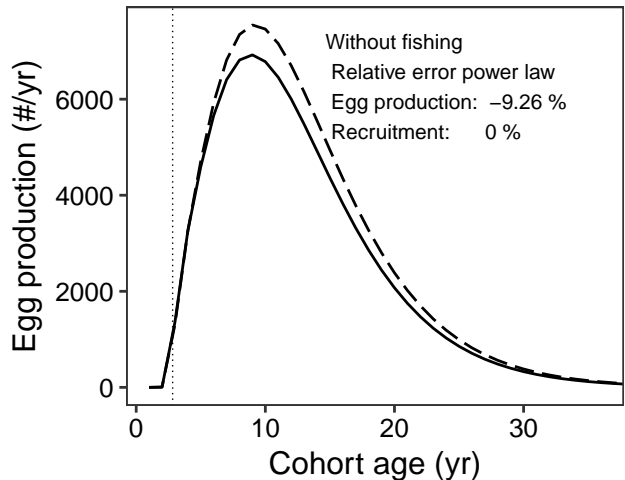
Species: *Genyonemus lineatus*
 Location: Between Palos Verdes and Huntington beach, CA, USA



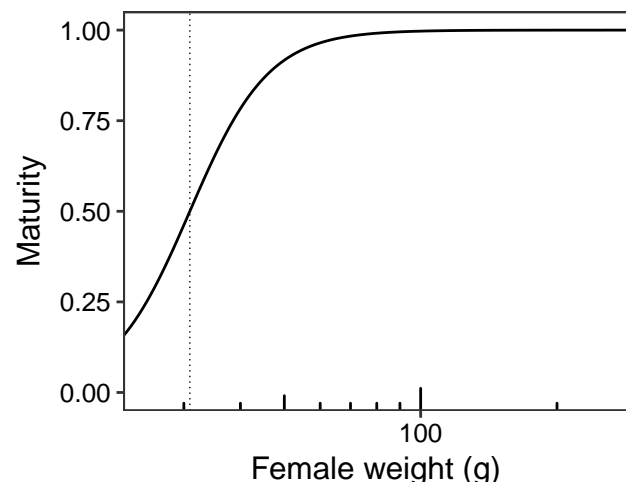
Species: *Hippoglossoides platessoides*
 Location: off Mountstuart House on the east side of the Isle of Bute



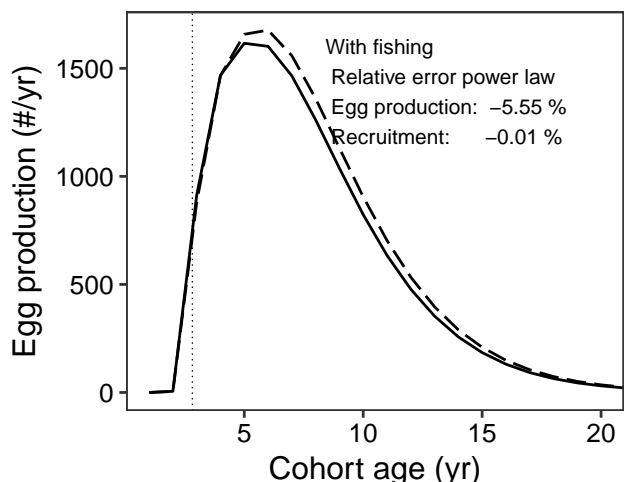
Species: *Hippoglossoides platessoides*
 Location: off Mountstuart House on the east side of the Isle of Bute



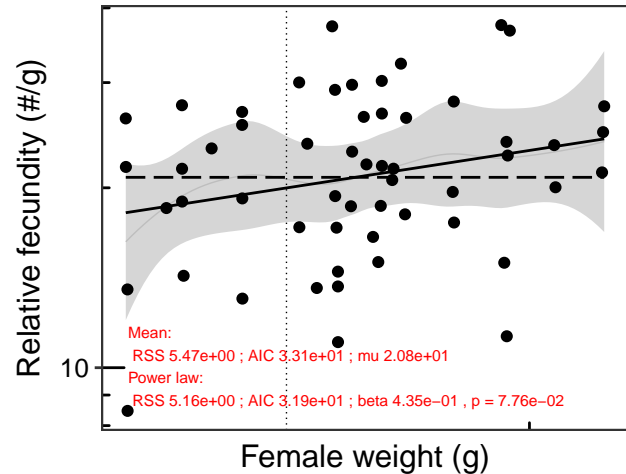
Species: *Hippoglossoides platessoides*
 Location: off Mountstuart House on the east side of the Isle of Bute



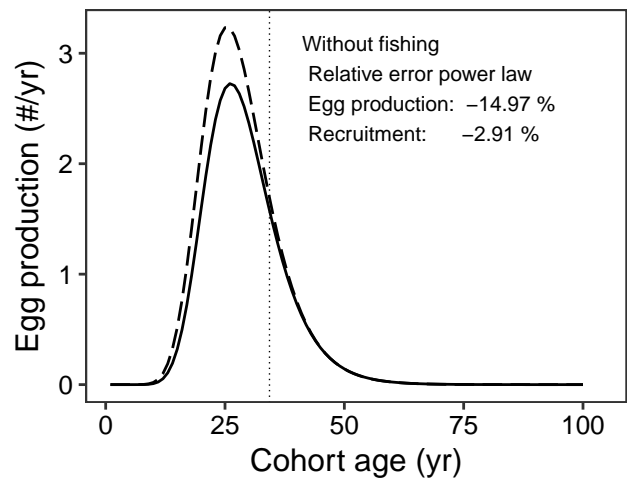
Species: *Hippoglossoides platessoides*
 Location: off Mountstuart House on the east side of the Isle of Bute



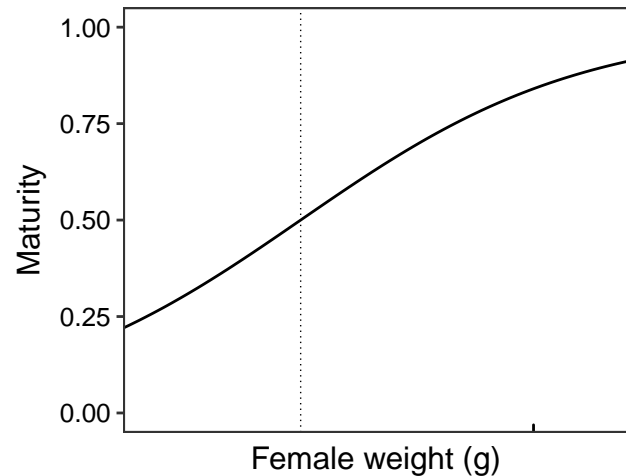
Species: *Hoplostethus atlanticus*
Location: TAS, Australia



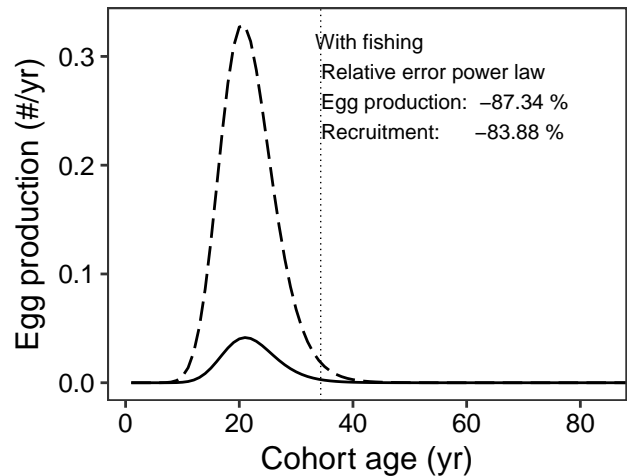
Species: *Hoplostethus atlanticus*
Location: TAS, Australia



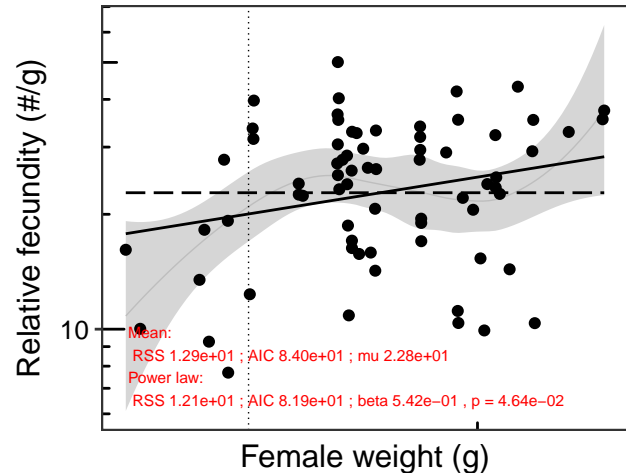
Species: *Hoplostethus atlanticus*
Location: TAS, Australia



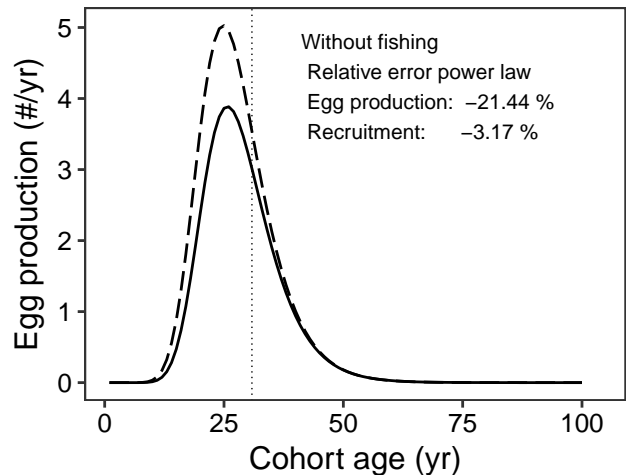
Species: *Hoplostethus atlanticus*
Location: TAS, Australia



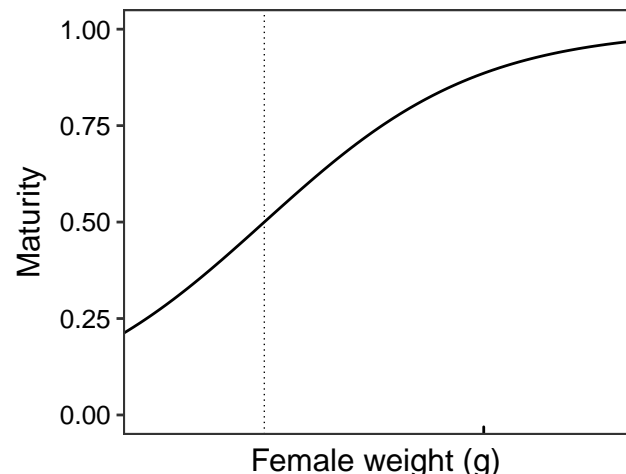
Species: Hoplostethus atlanticus
Location: SA, Australia



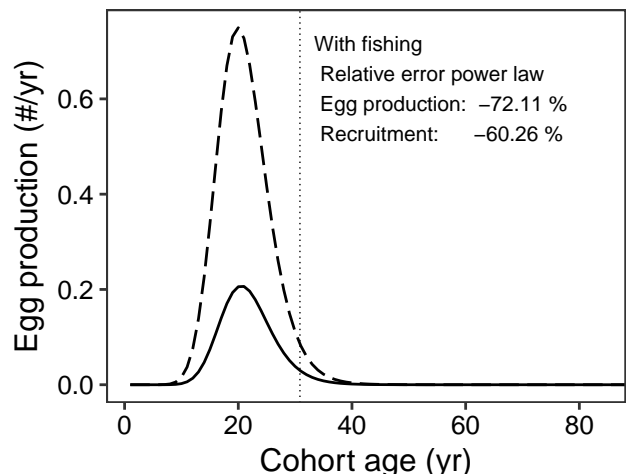
Species: Hoplostethus atlanticus
Location: SA, Australia



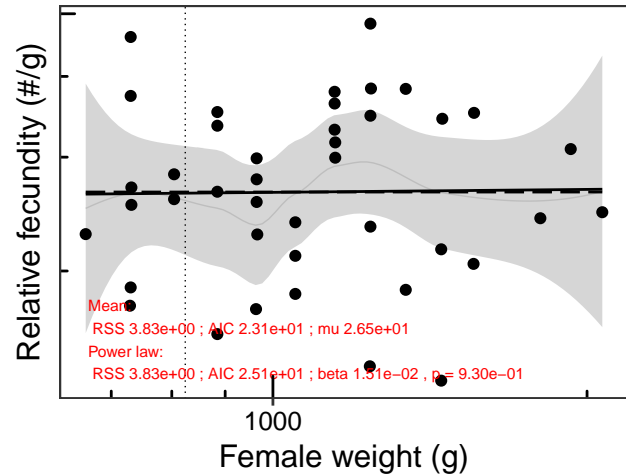
Species: Hoplostethus atlanticus
Location: SA, Australia



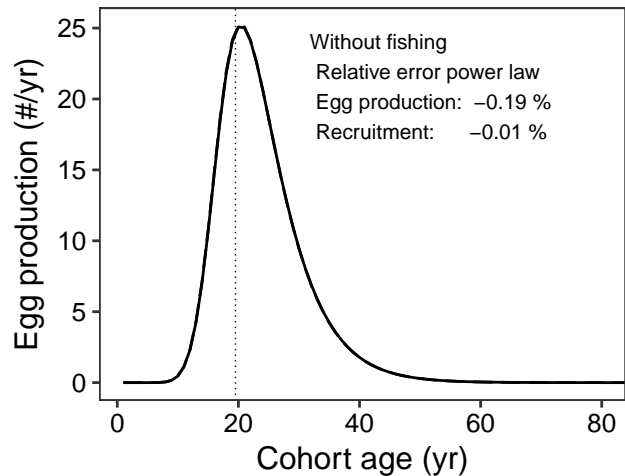
Species: Hoplostethus atlanticus
Location: SA, Australia



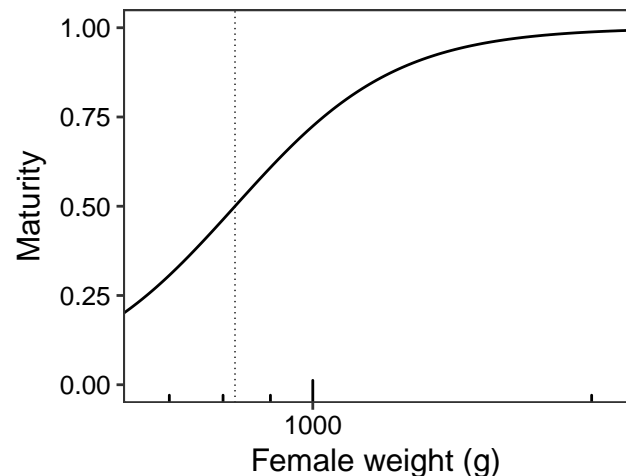
Species: Hoplostethus atlanticus
Location: NSW, Australia



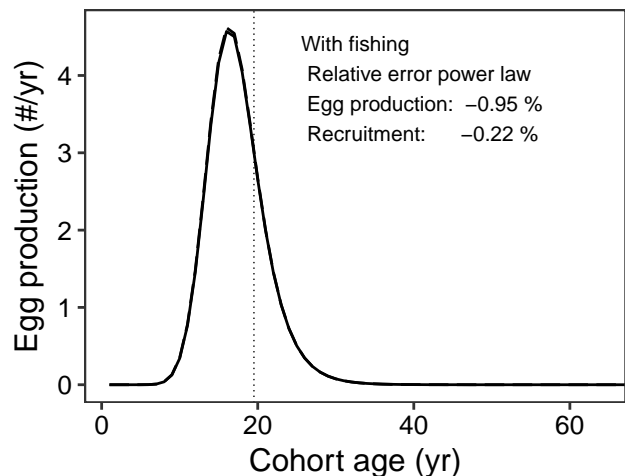
Species: Hoplostethus atlanticus
Location: NSW, Australia



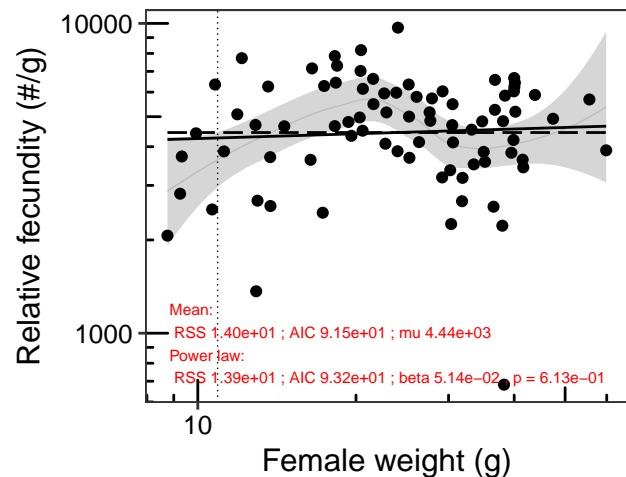
Species: Hoplostethus atlanticus
Location: NSW, Australia



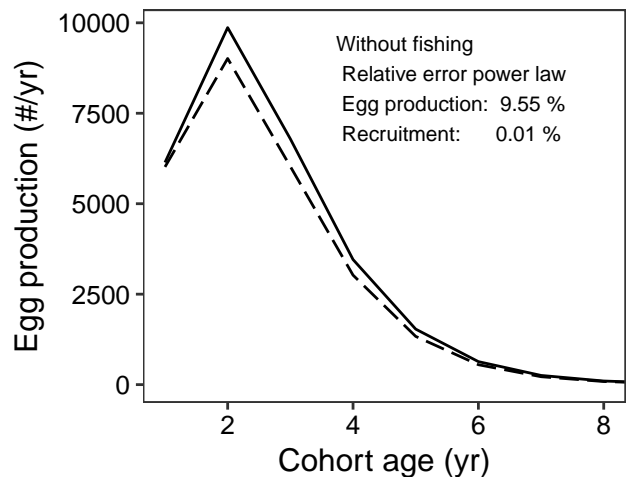
Species: Hoplostethus atlanticus
Location: NSW, Australia



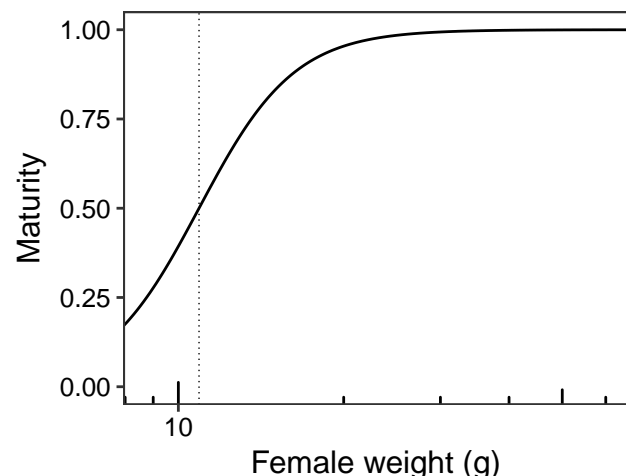
Species: *Larimus fasciatus*
 Location: mouth of the Cape Fear River, NC, about 4–6 km off Oak Island



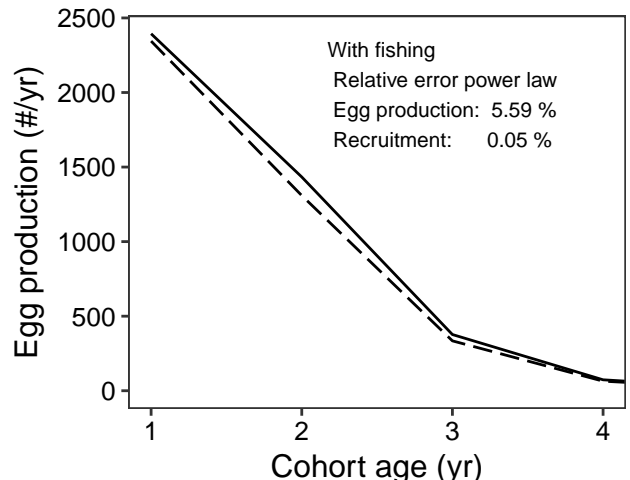
Species: *Larimus fasciatus*
 Location: mouth of the Cape Fear River, NC, about 4–6 km off Oak Island



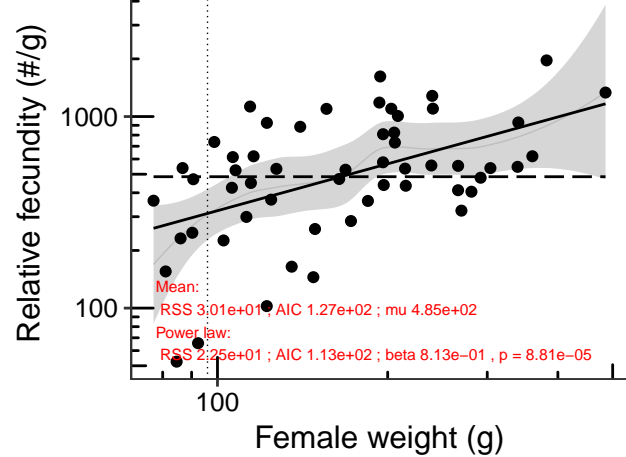
Species: *Larimus fasciatus*
 Location: mouth of the Cape Fear River, NC, about 4–6 km off Oak Island



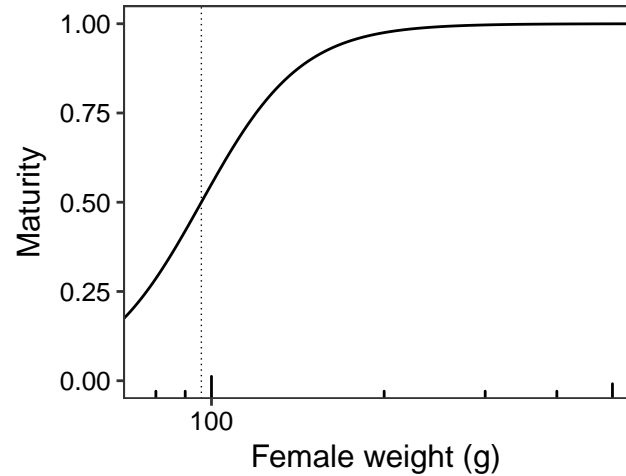
Species: *Larimus fasciatus*
 Location: mouth of the Cape Fear River, NC, about 4–6 km off Oak Island



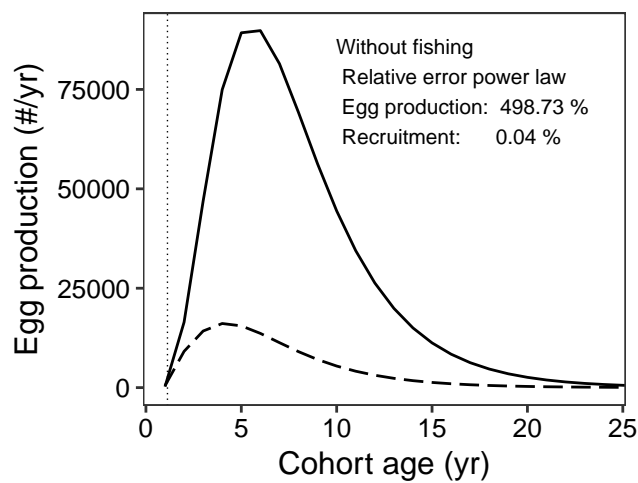
Species: *Lutjanus carponotatus*
Location: Whitsunday islands, Qld, Australia



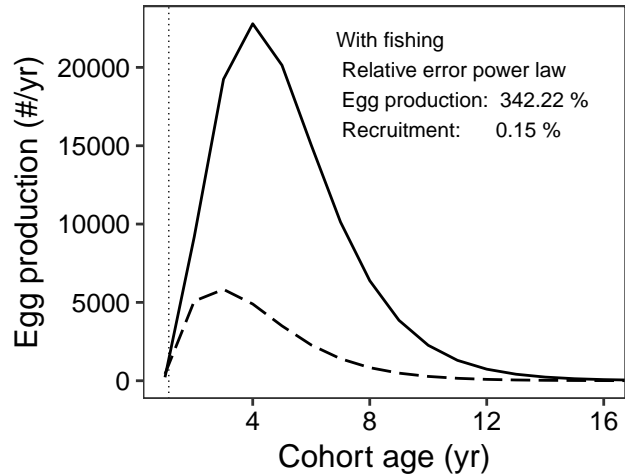
Species: *Lutjanus carponotatus*
Location: Whitsunday islands, Qld, Australia



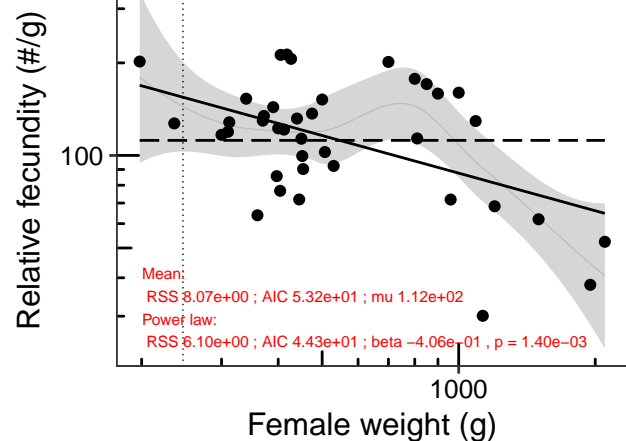
Species: *Lutjanus carponotatus*
Location: Whitsunday islands, Qld, Australia



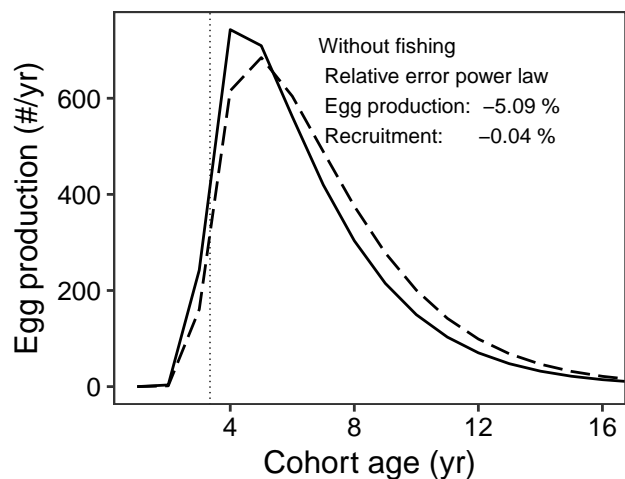
Species: *Lutjanus carponotatus*
Location: Whitsunday islands, Qld, Australia



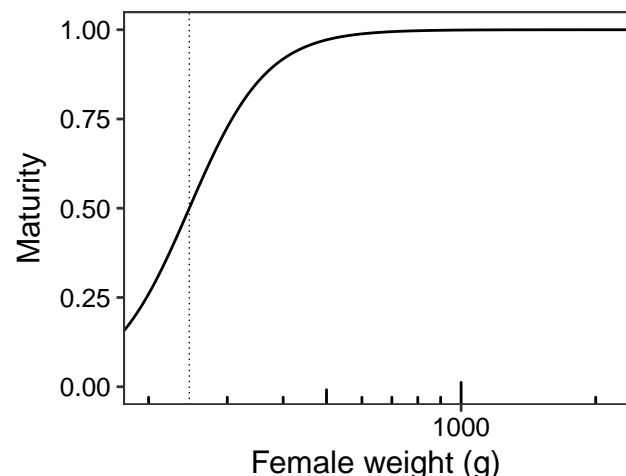
Species: *Lutjanus synagris*
Location: Off Iguape, Aquiraz, CE, Brazil



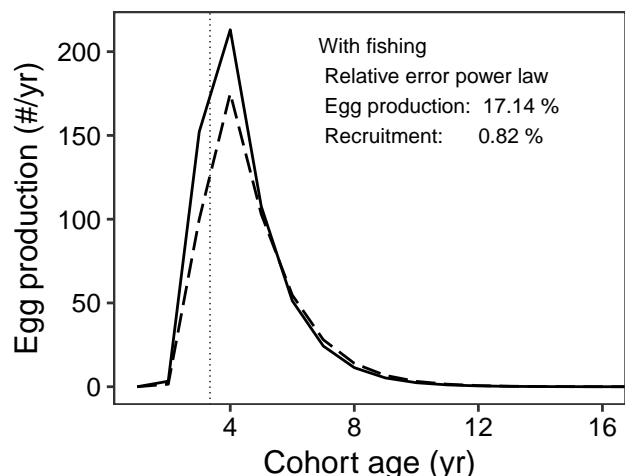
Species: *Lutjanus synagris*
Location: Off Iguape, Aquiraz, CE, Brazil



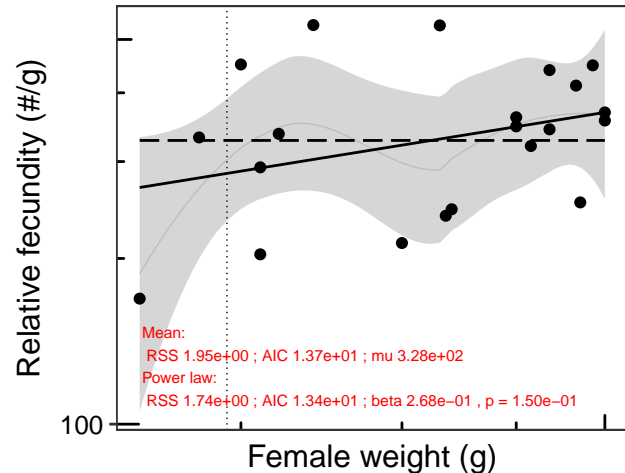
Species: *Lutjanus synagris*
Location: Off Iguape, Aquiraz, CE, Brazil



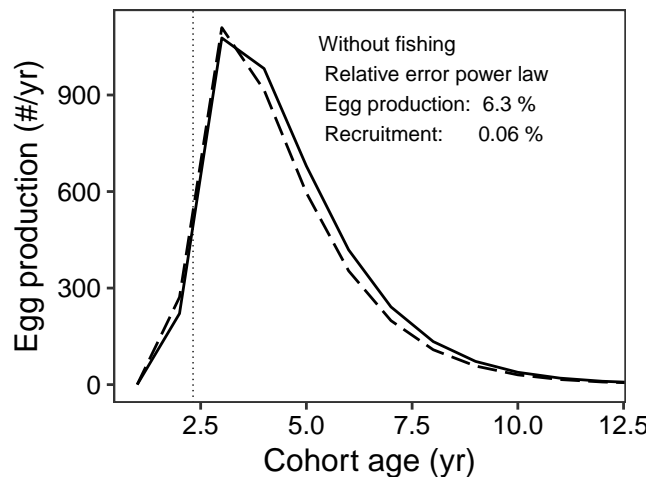
Species: *Lutjanus synagris*
Location: Off Iguape, Aquiraz, CE, Brazil



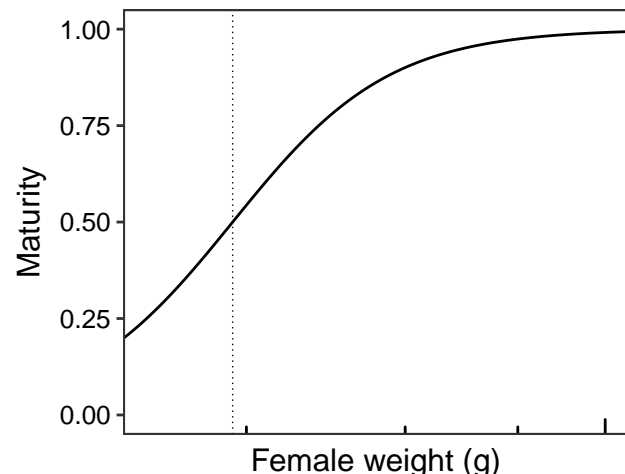
Species: *Macrodon ancylodon*
 Location: Along the southern coast of Brazil below 29 degrees south



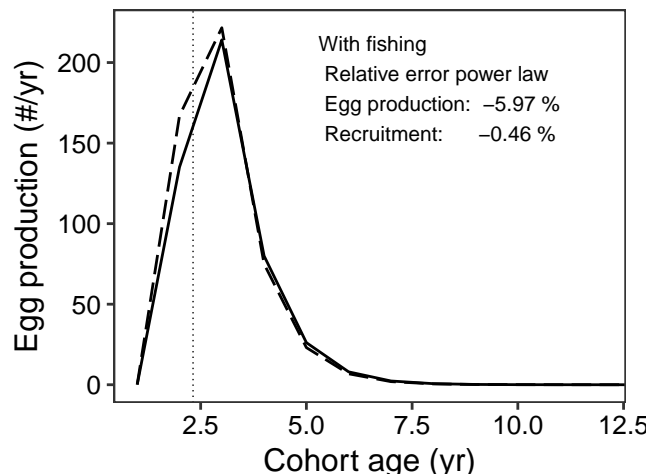
Species: *Macrodon ancylodon*
 Location: Along the southern coast of Brazil below 29 degrees south



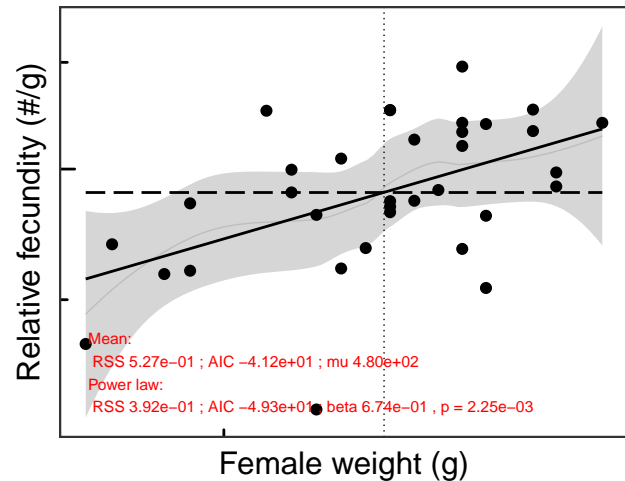
Species: *Macrodon ancylodon*
 Location: Along the southern coast of Brazil below 29 degrees south



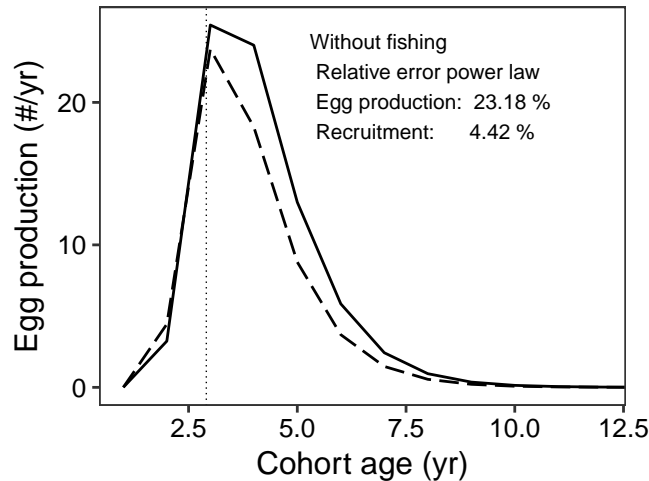
Species: *Macrodon ancylodon*
 Location: Along the southern coast of Brazil below 29 degrees south



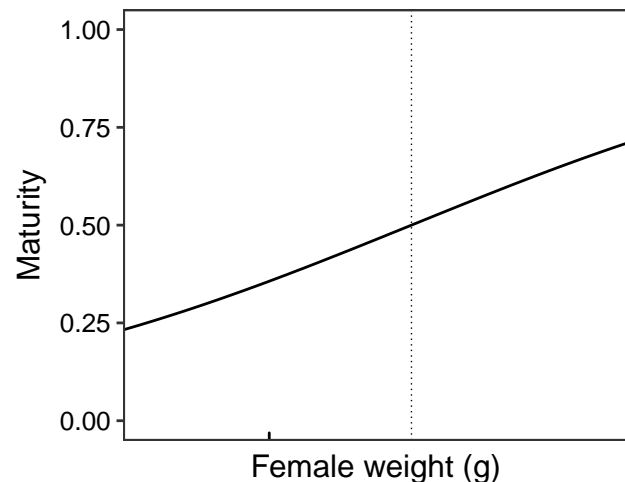
Species: *Mallotus villosus*
Location: Barents Sea



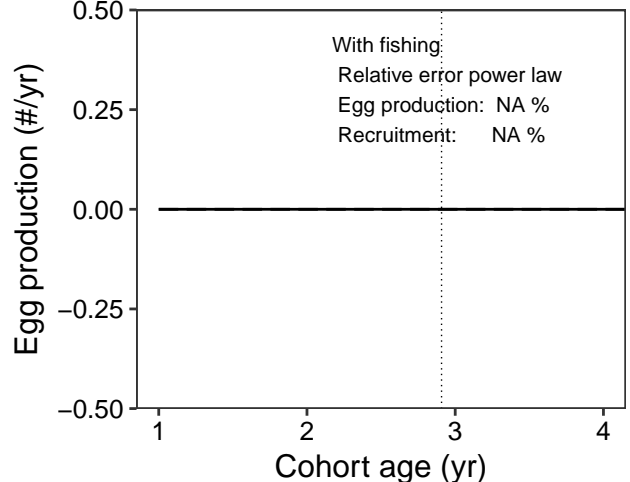
Species: *Mallotus villosus*
Location: Barents Sea



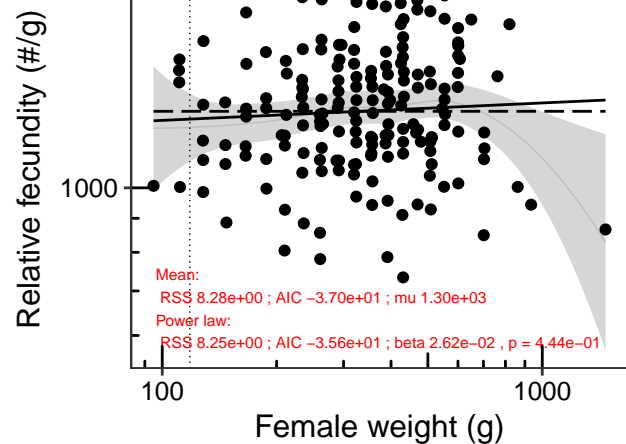
Species: *Mallotus villosus*
Location: Barents Sea



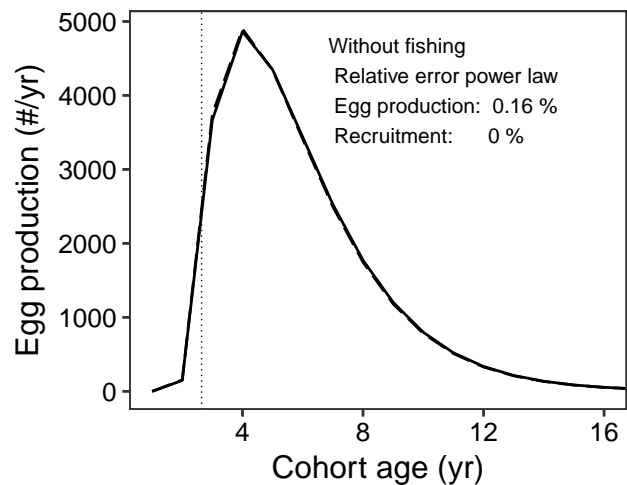
Species: *Mallotus villosus*
Location: Barents Sea



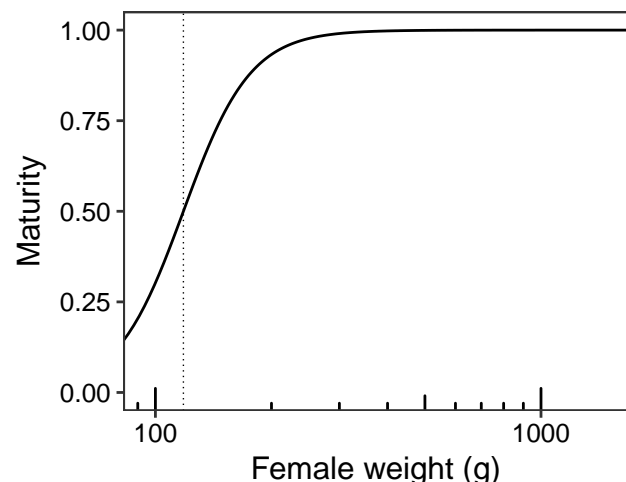
Species: *Merlangius merlangus*
Location: northern North Sea



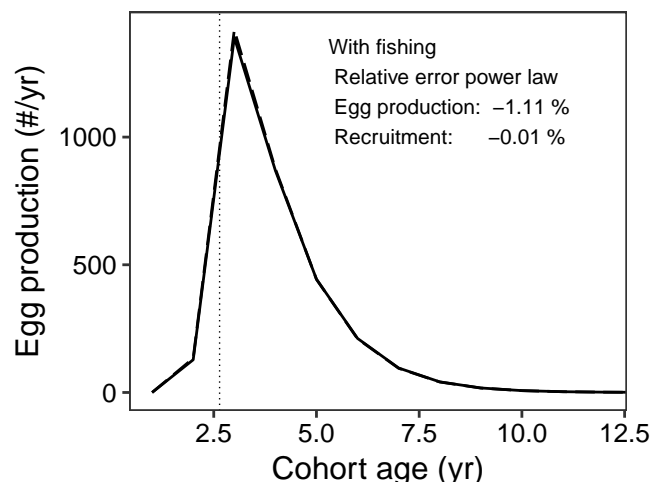
Species: *Merlangius merlangus*
Location: northern North Sea



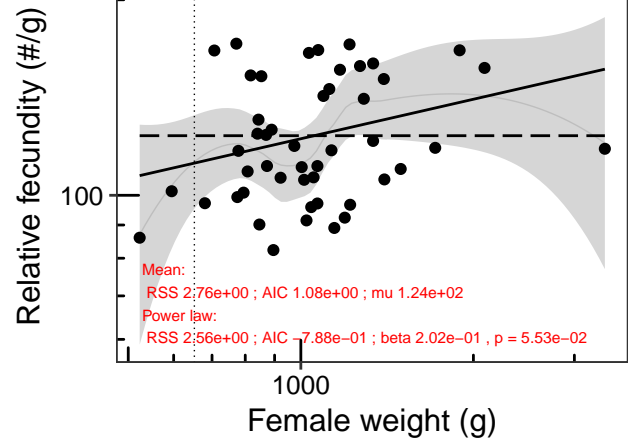
Species: *Merlangius merlangus*
Location: northern North Sea



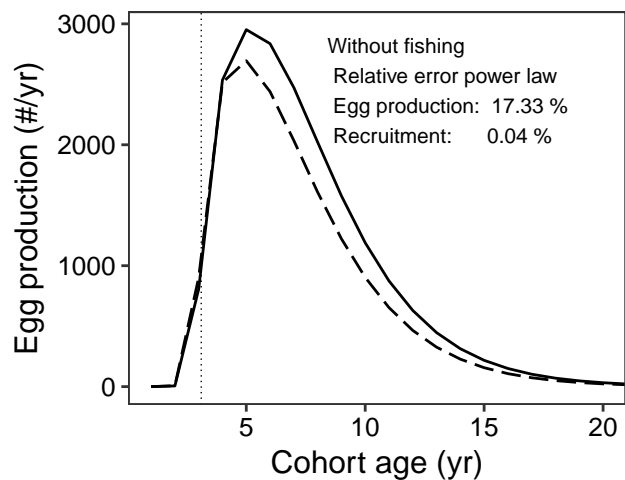
Species: *Merlangius merlangus*
Location: northern North Sea



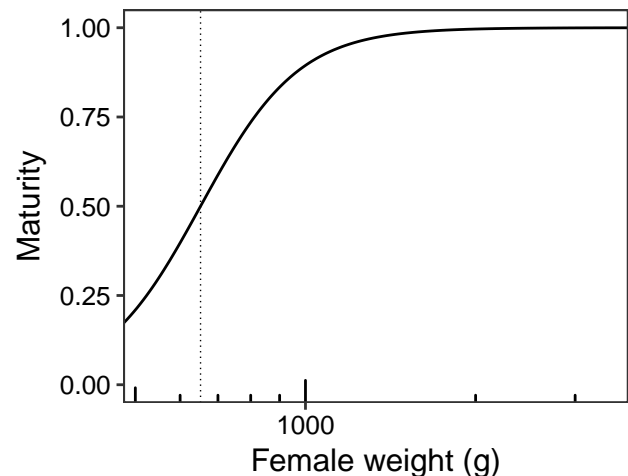
Species: *Merluccius gayi gayi*
 Location: Off the coast of Chile between 34 and 38 degrees south



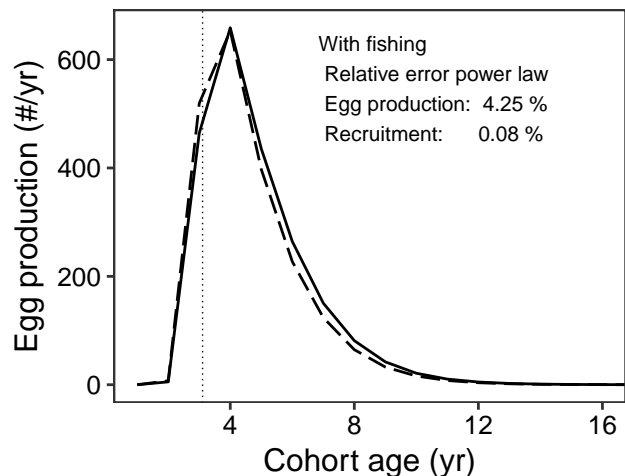
Species: *Merluccius gayi gayi*
 Location: Off the coast of Chile between 34 and 38 degrees south



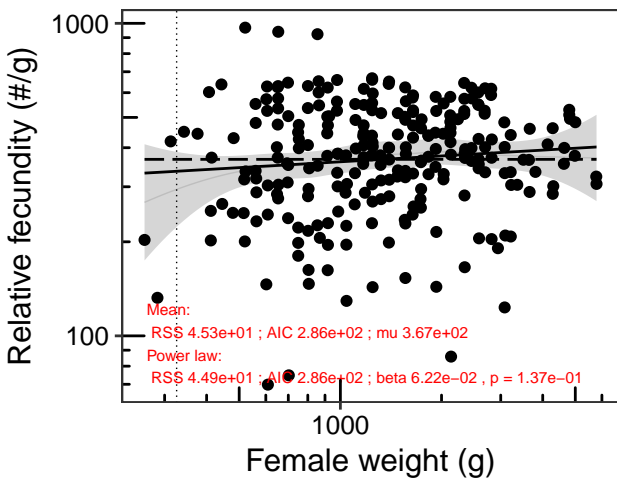
Species: *Merluccius gayi gayi*
 Location: Off the coast of Chile between 34 and 38 degrees south



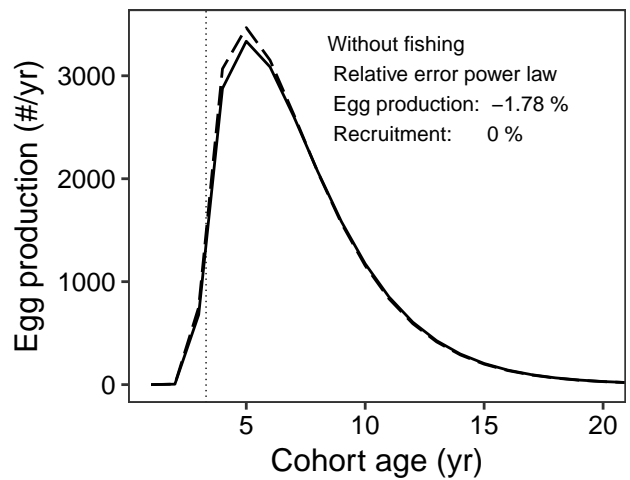
Species: *Merluccius gayi gayi*
 Location: Off the coast of Chile between 34 and 38 degrees south



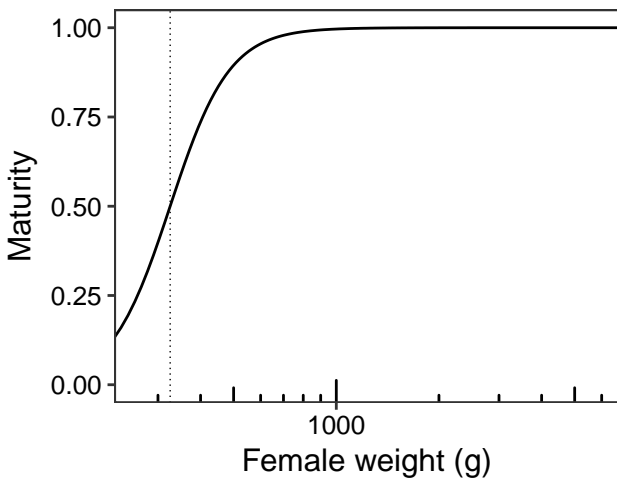
Species: *Merluccius hubbsi*
 Location: Off the northern coast of Patagonia, Argentina, between 42 an



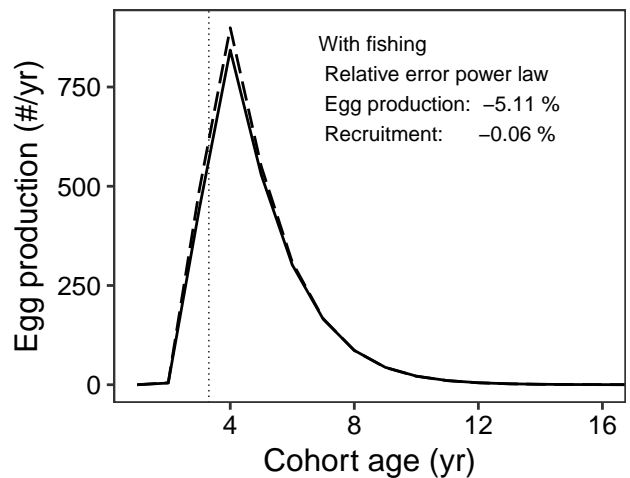
Species: *Merluccius hubbsi*
 Location: Off the northern coast of Patagonia, Argentina, between 42 an



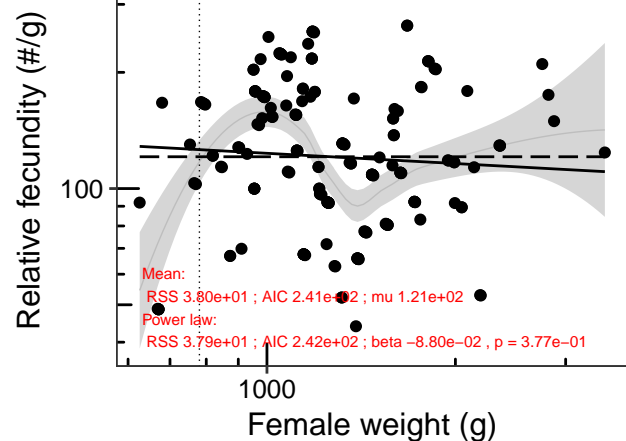
Species: *Merluccius hubbsi*
 Location: Off the northern coast of Patagonia, Argentina, between 42 an



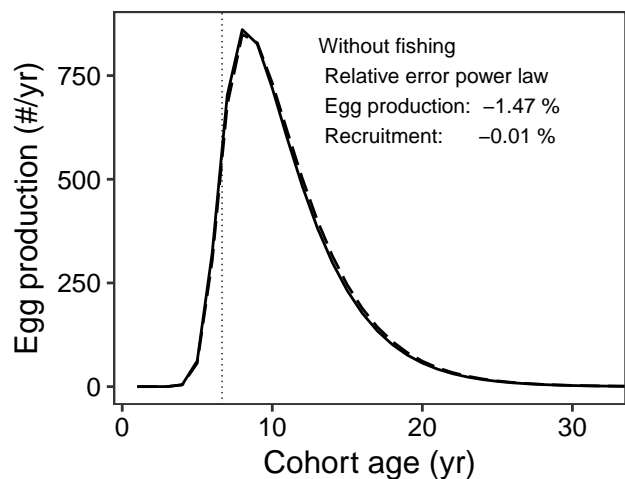
Species: *Merluccius hubbsi*
 Location: Off the northern coast of Patagonia, Argentina, between 42 and



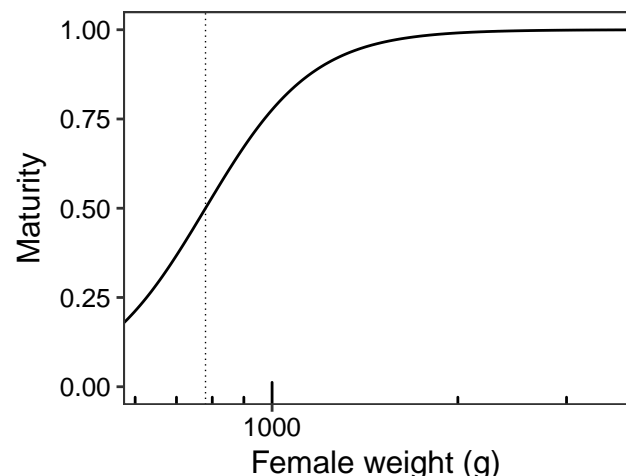
Species: *Merluccius merluccius*
Location: Off the coast of Galicia, Spain



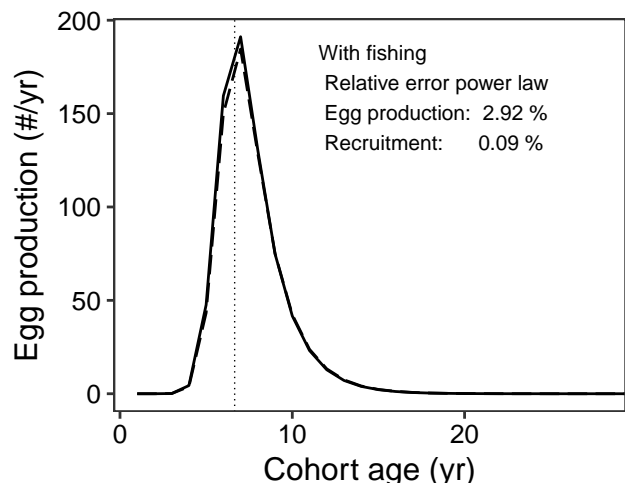
Species: *Merluccius merluccius*
Location: Off the coast of Galicia, Spain



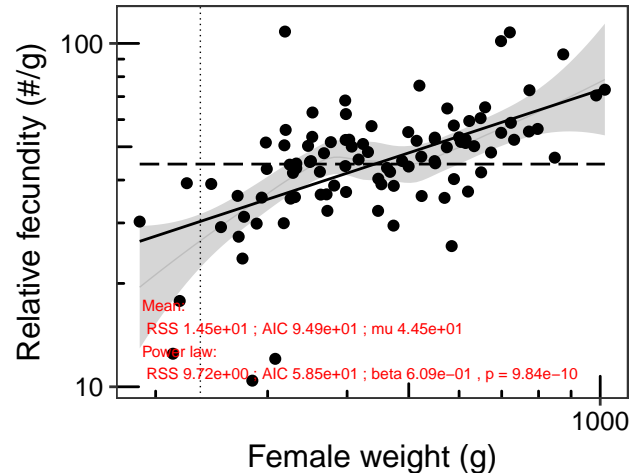
Species: *Merluccius merluccius*
Location: Off the coast of Galicia, Spain



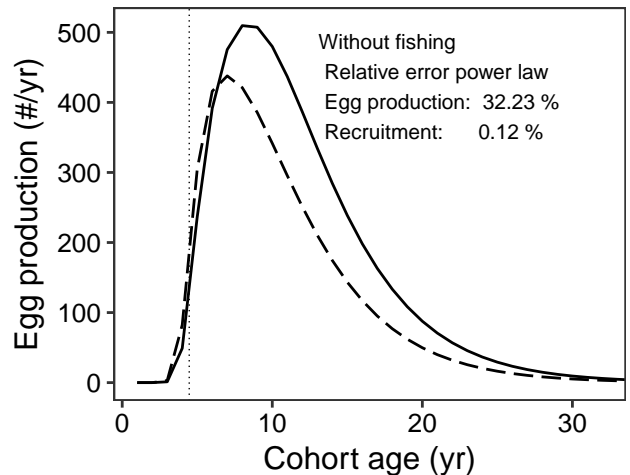
Species: *Merluccius merluccius*
Location: Off the coast of Galicia, Spain



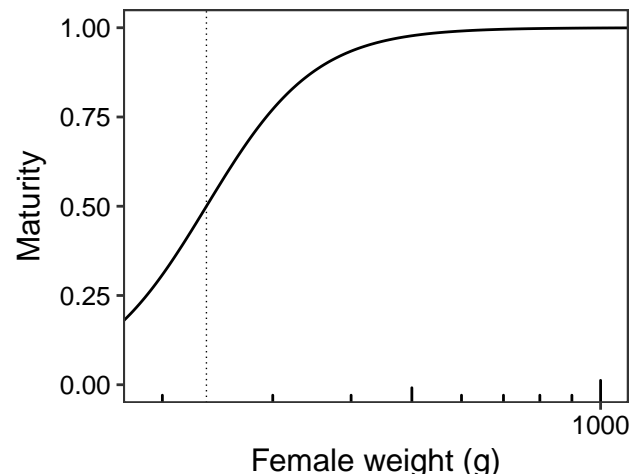
Species: *Micromesistius australis*
Location: Mar Argentino



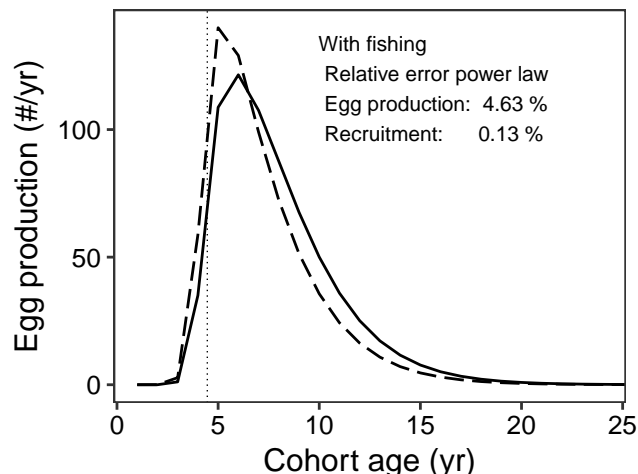
Species: *Micromesistius australis*
Location: Mar Argentino



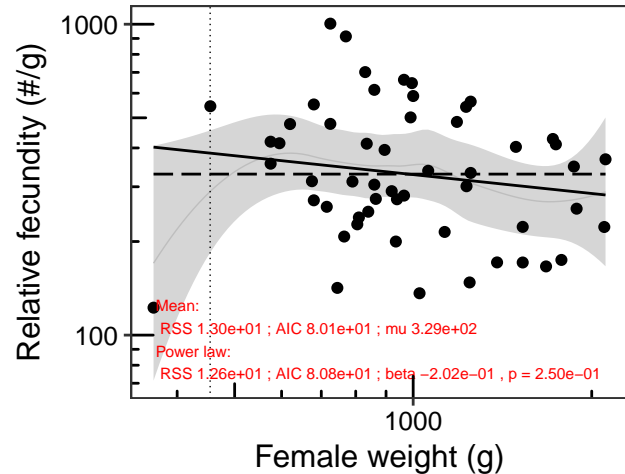
Species: *Micromesistius australis*
Location: Mar Argentino



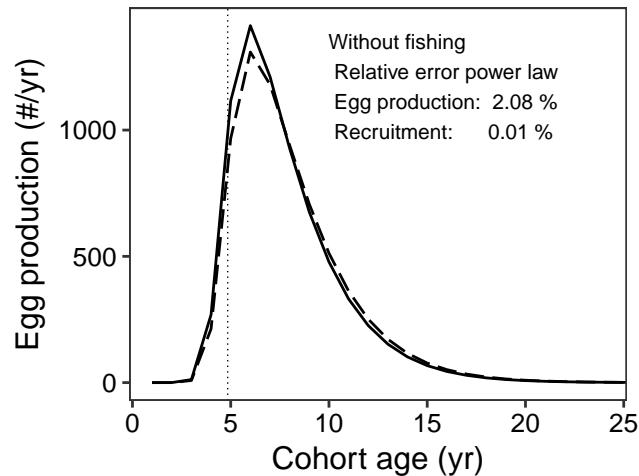
Species: *Micromesistius australis*
Location: Mar Argentino



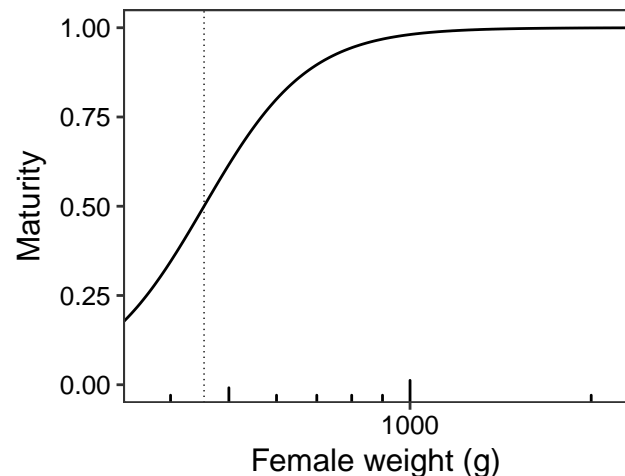
Species: *Micropogonias furnieri*
 Location: Along the southern coast of Brazil between 29 and 33 degrees



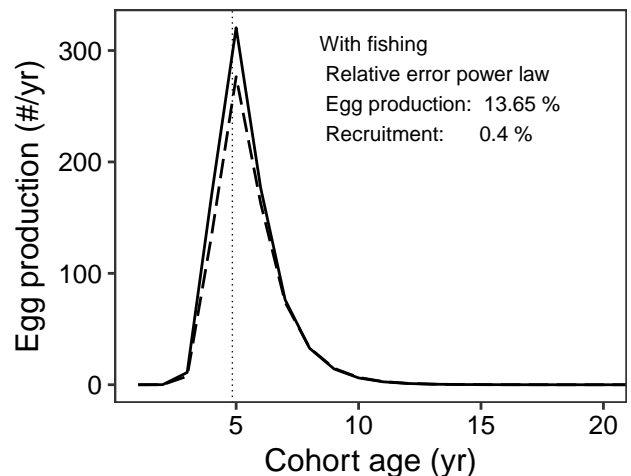
Species: *Micropogonias furnieri*
 Location: Along the southern coast of Brazil between 29 and 33 degrees



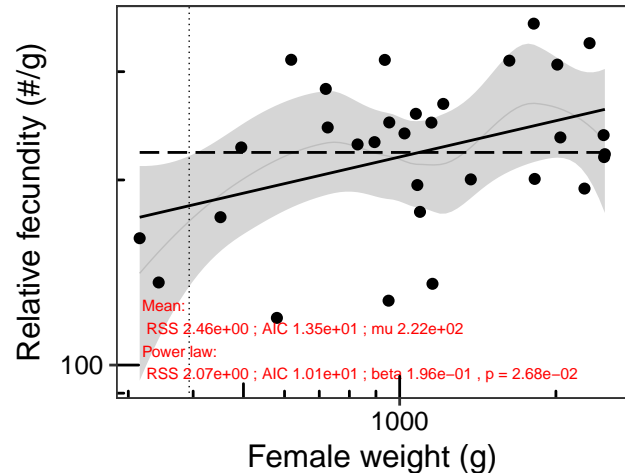
Species: *Micropogonias furnieri*
 Location: Along the southern coast of Brazil between 29 and 33 degrees



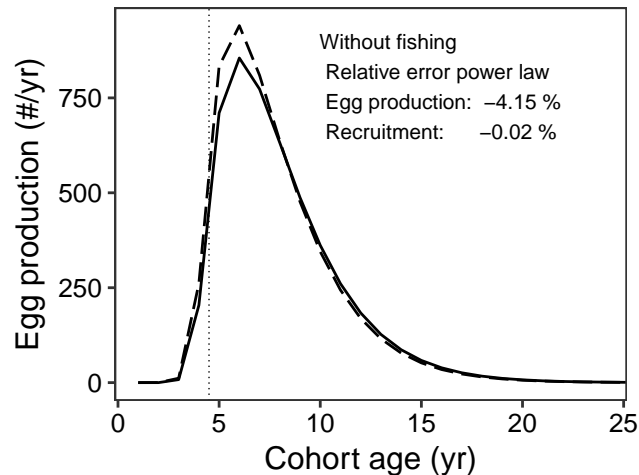
Species: *Micropogonias furnieri*
 Location: Along the southern coast of Brazil between 29 and 33 degrees



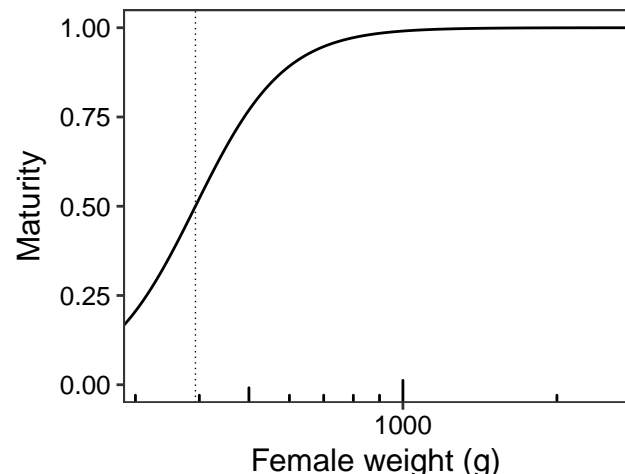
Species: *Micropogonias furnieri*
 Location: Off the mouth of Rio de La Plata between Uruguay and Argentina



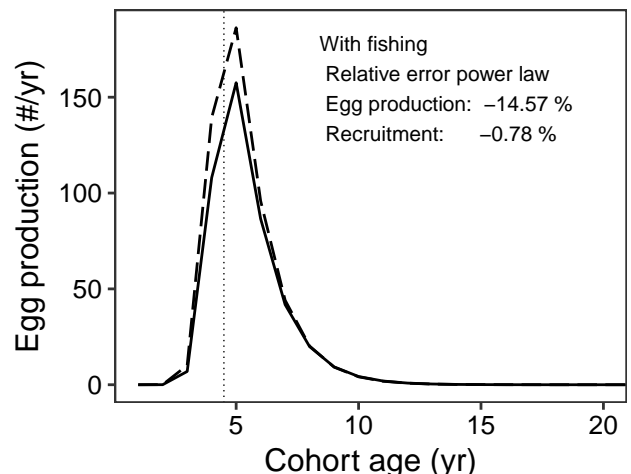
Species: *Micropogonias furnieri*
 Location: Off the mouth of Rio de La Plata between Uruguay and Argentina



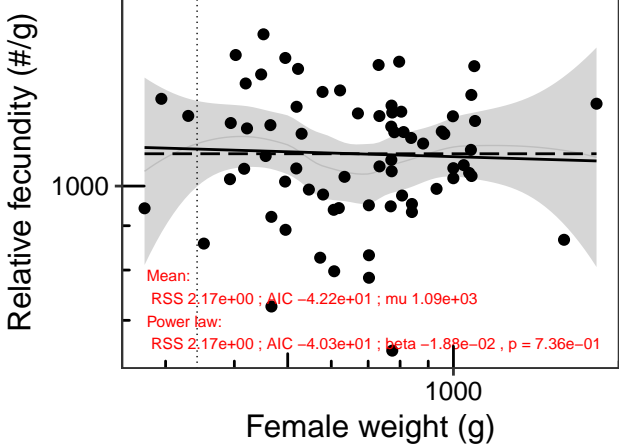
Species: *Micropogonias furnieri*
 Location: Off the mouth of Rio de La Plata between Uruguay and Argentina



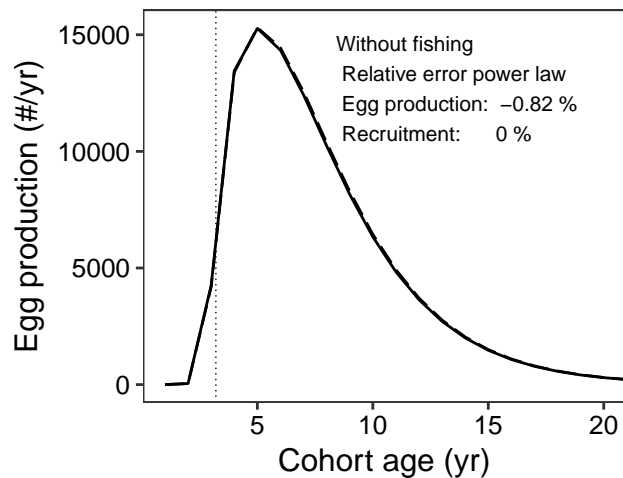
Species: *Micropogonias furnieri*
 Location: Off the mouth of Rio de La Plata between Uruguay and Argentina



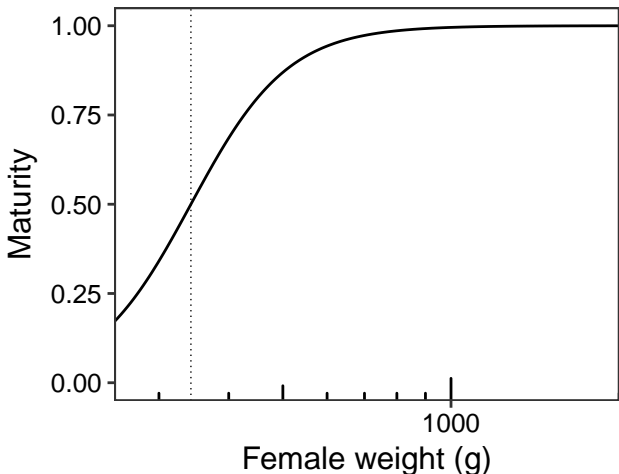
Species: *Mugil cephalus*
Location: Matanzas River Inlet south of St. Augustine, FL, USA



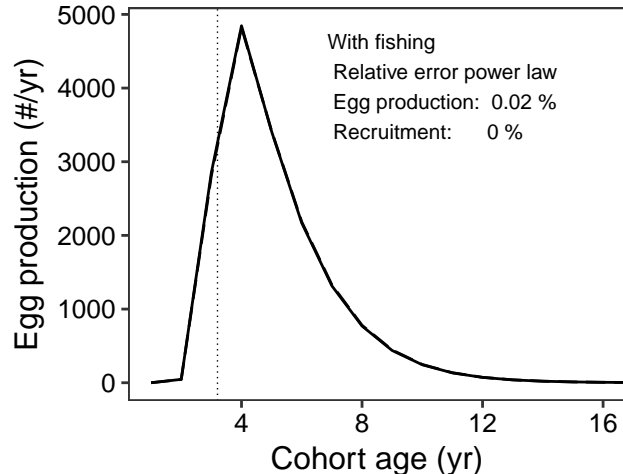
Species: *Mugil cephalus*
Location: Matanzas River Inlet south of St. Augustine, FL, USA



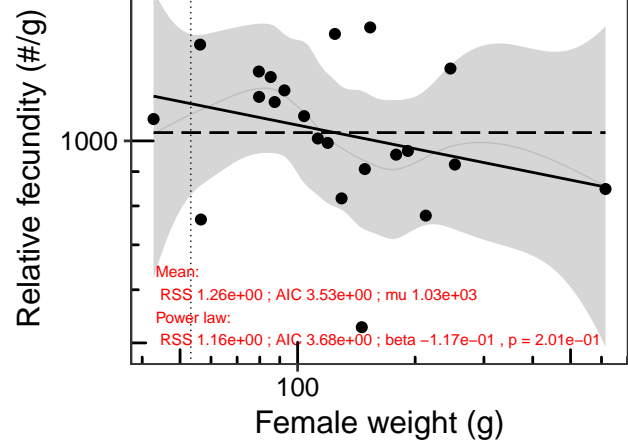
Species: *Mugil cephalus*
Location: Matanzas River Inlet south of St. Augustine, FL, USA



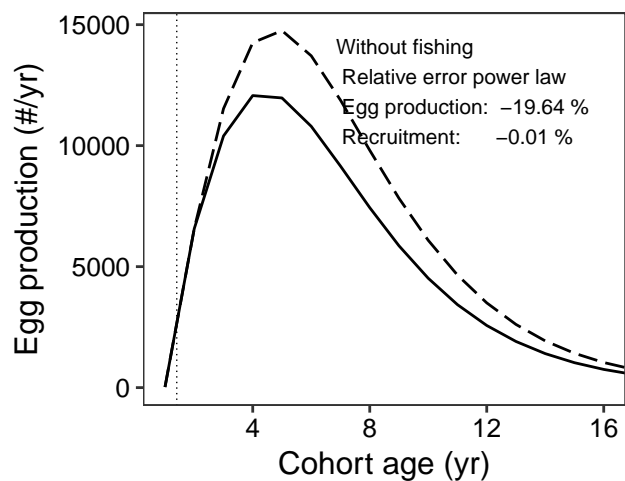
Species: *Mugil cephalus*
Location: Matanzas River Inlet south of St. Augustine, FL, USA



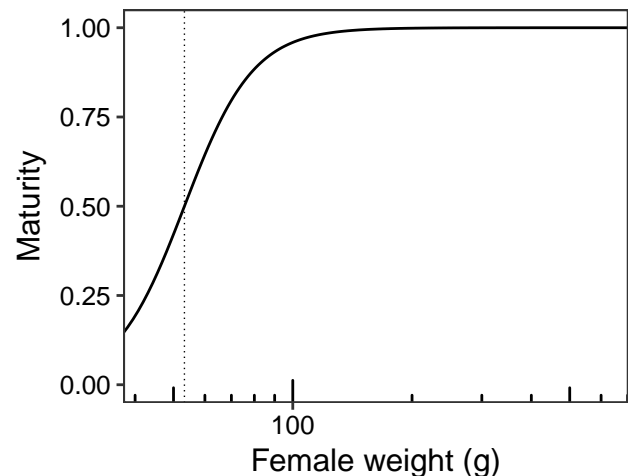
Species: *Mugil cephalus*
Location: Around the coast of Goa, India



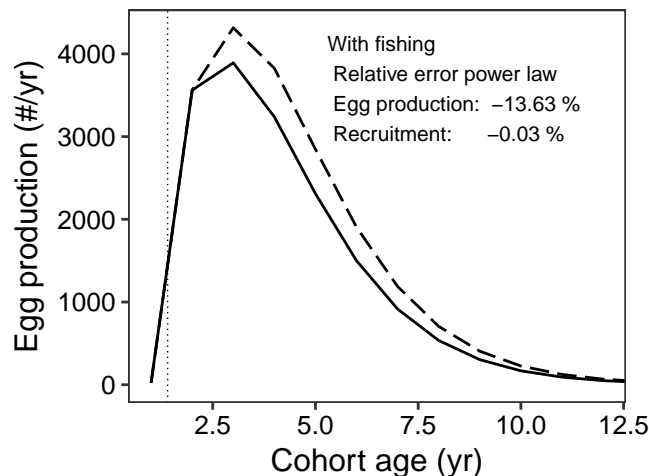
Species: *Mugil cephalus*
Location: Around the coast of Goa, India



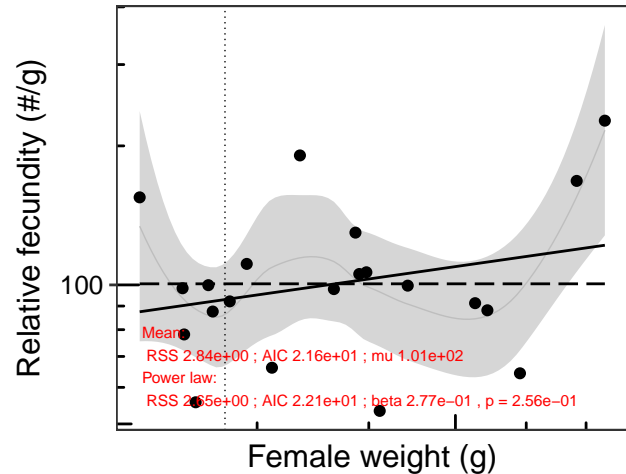
Species: *Mugil cephalus*
Location: Around the coast of Goa, India



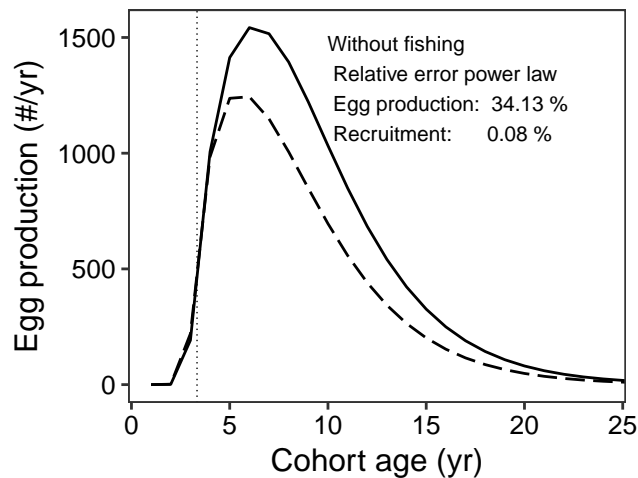
Species: *Mugil cephalus*
Location: Around the coast of Goa, India



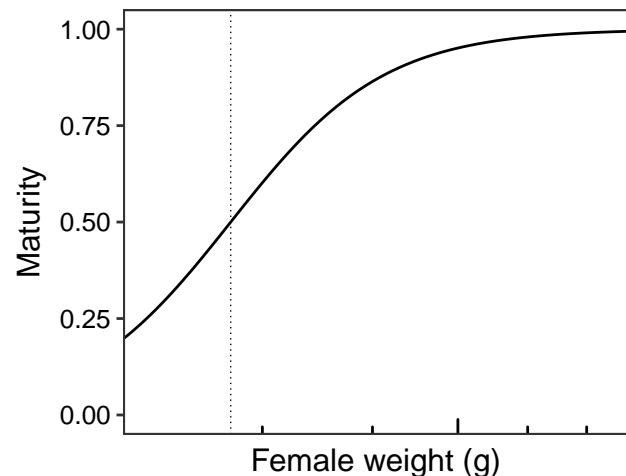
Species: *Ocyurus chrysurus*
Location: Banco de Campeche, Mexico



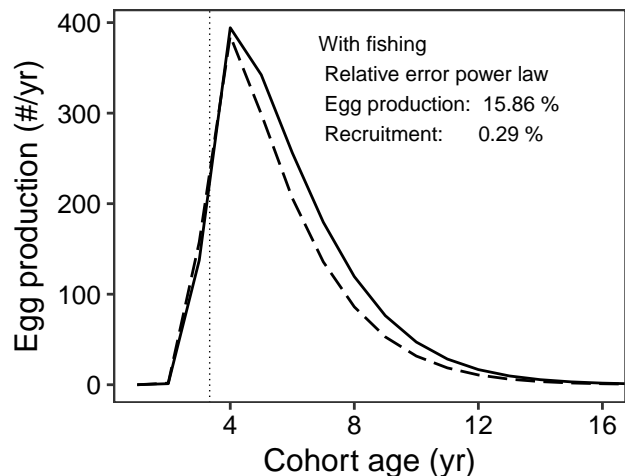
Species: *Ocyurus chrysurus*
Location: Banco de Campeche, Mexico



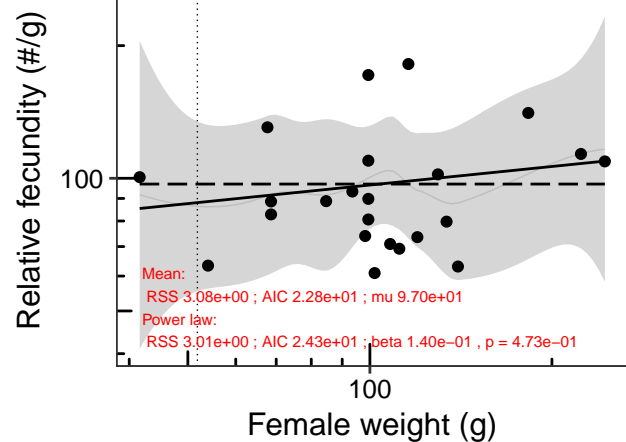
Species: *Ocyurus chrysurus*
Location: Banco de Campeche, Mexico



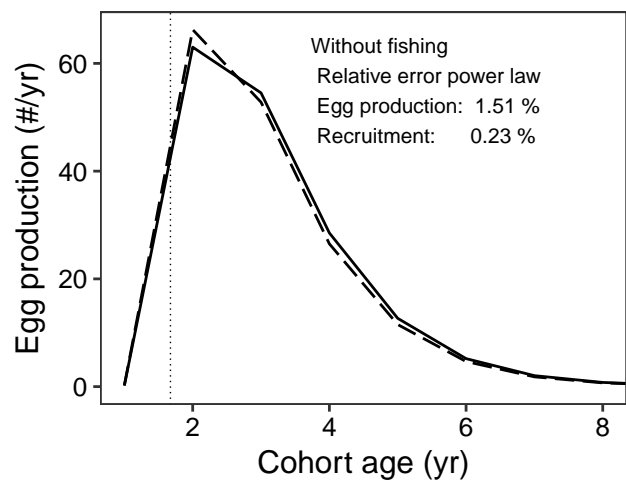
Species: *Ocyurus chrysurus*
Location: Banco de Campeche, Mexico



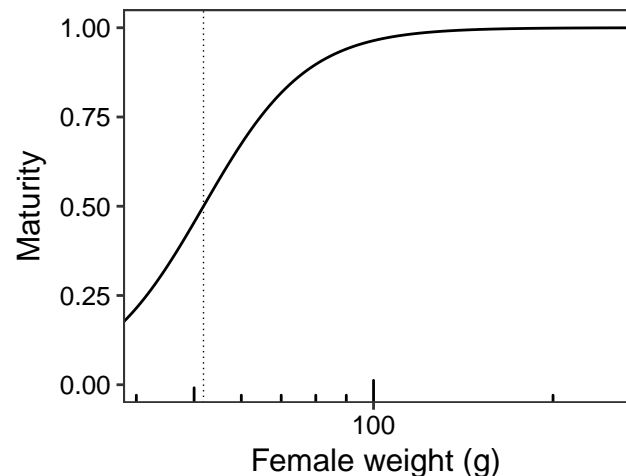
Species: *Odontesthes argentinensis*
Location: Lagoa dos Patos, RS, Brazil



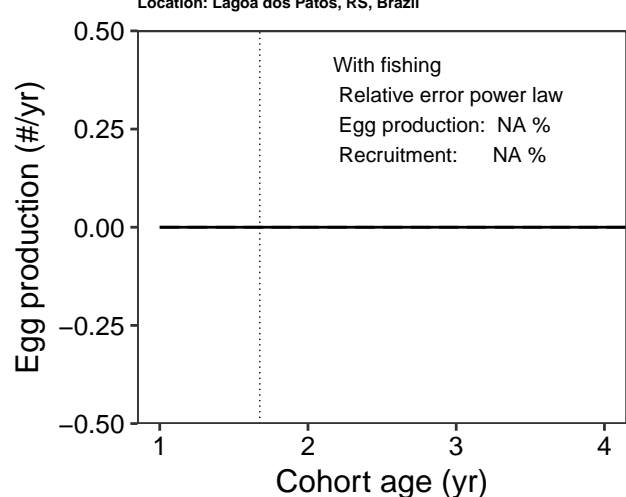
Species: *Odontesthes argentinensis*
Location: Lagoa dos Patos, RS, Brazil



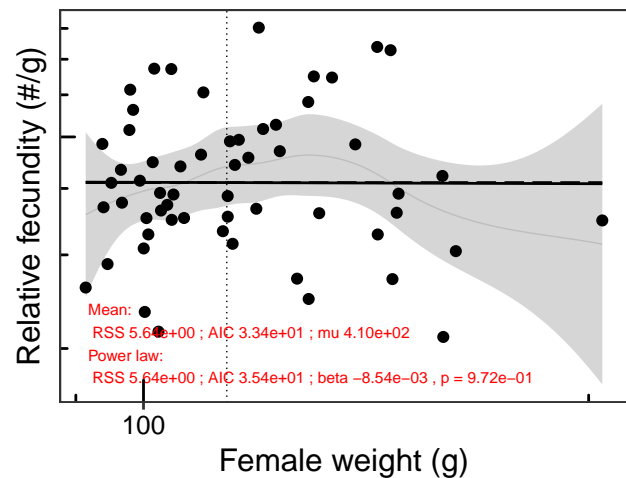
Species: *Odontesthes argentinensis*
Location: Lagoa dos Patos, RS, Brazil



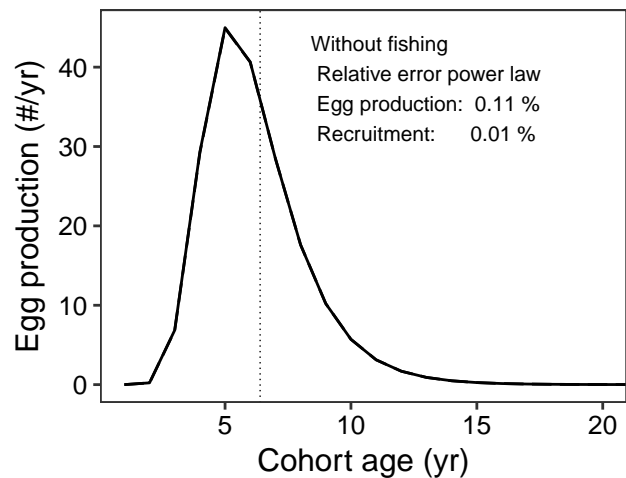
Species: *Odontesthes argentinensis*
Location: Lagoa dos Patos, RS, Brazil



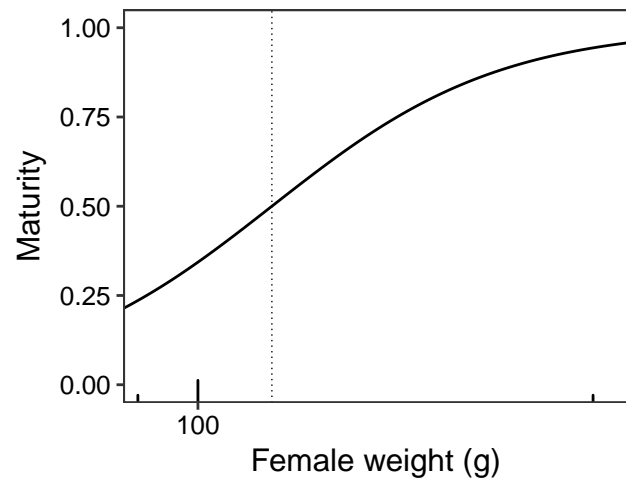
Species: *Opisthonema libertate*
Location: Punta Arenas, Costa Rica



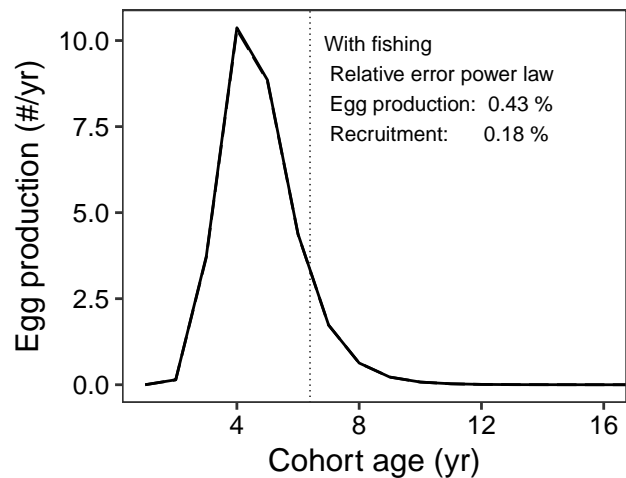
Species: *Opisthonema libertate*
Location: Punta Arenas, Costa Rica



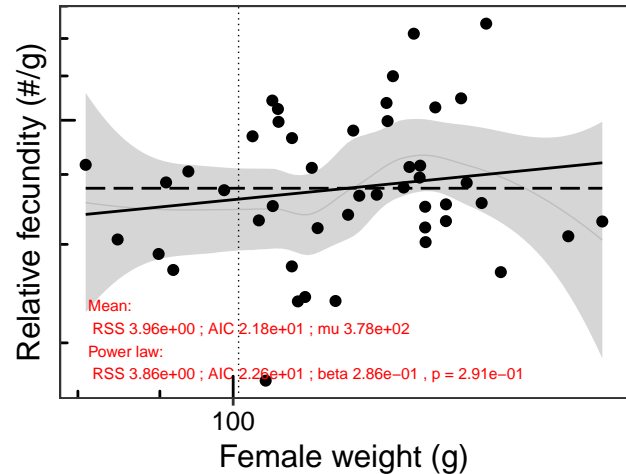
Species: *Opisthonema libertate*
Location: Punta Arenas, Costa Rica



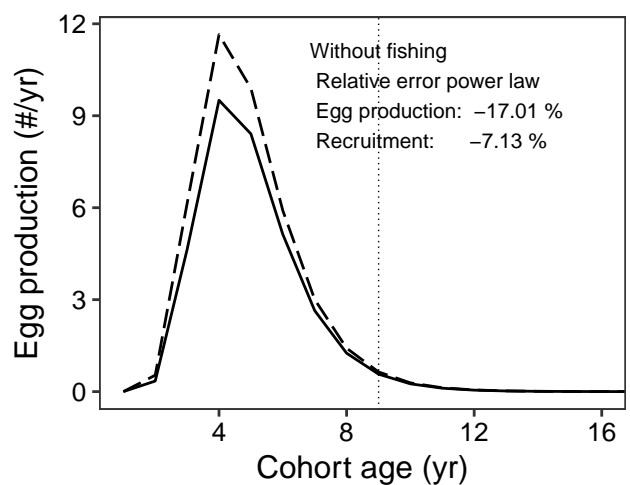
Species: *Opisthonema libertate*
Location: Punta Arenas, Costa Rica



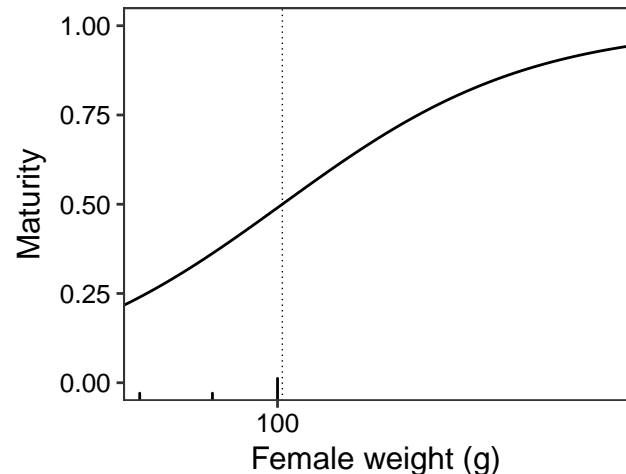
Species: *Opisthonema medirastre*
Location: Punta Arenas, Costa Rica



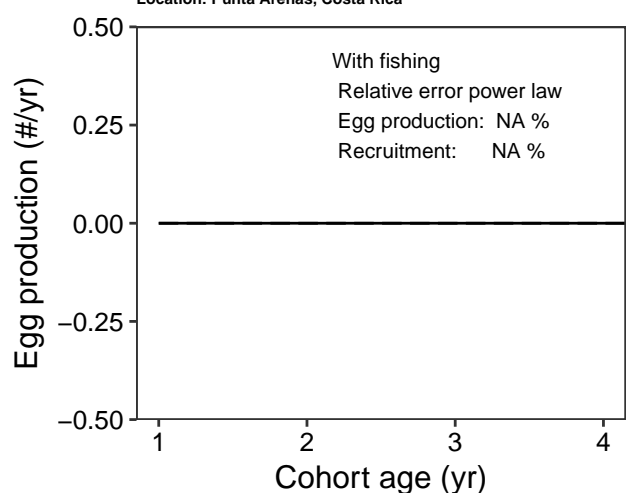
Species: *Opisthonema medirastre*
Location: Punta Arenas, Costa Rica



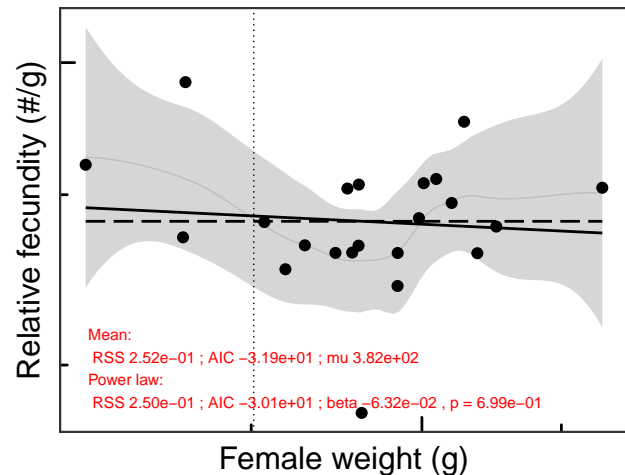
Species: *Opisthonema medirastre*
Location: Punta Arenas, Costa Rica



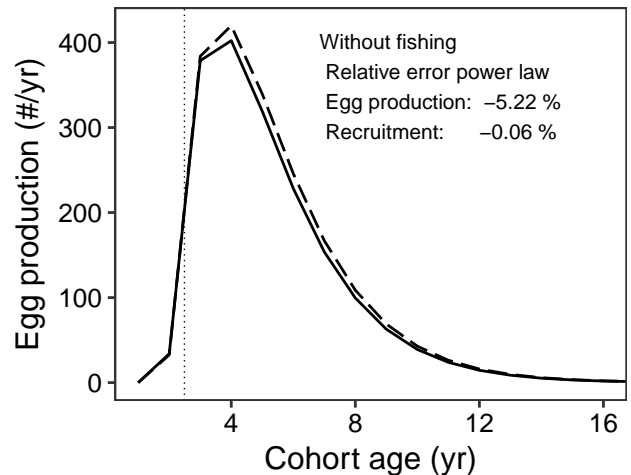
Species: *Opisthonema medirastre*
Location: Punta Arenas, Costa Rica



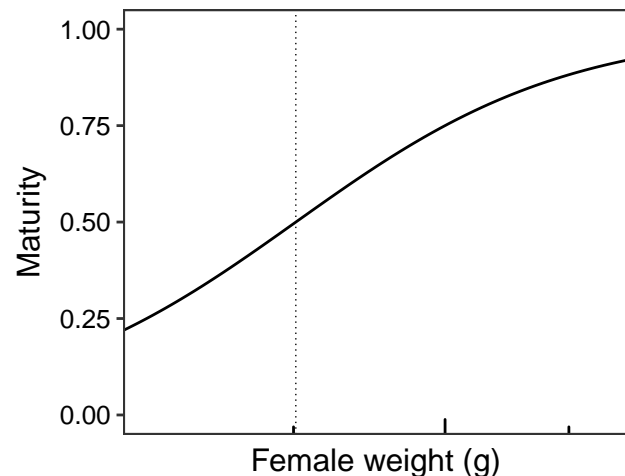
Species: *Oxylebius pictus*
Location: Monterey Bay California USA



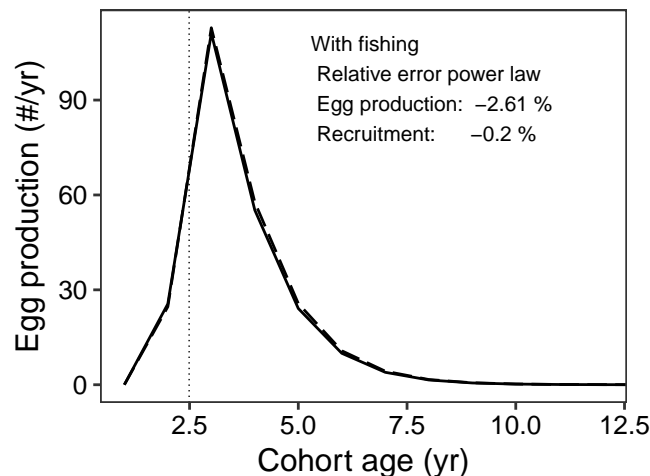
Species: *Oxylebius pictus*
Location: Monterey Bay California USA



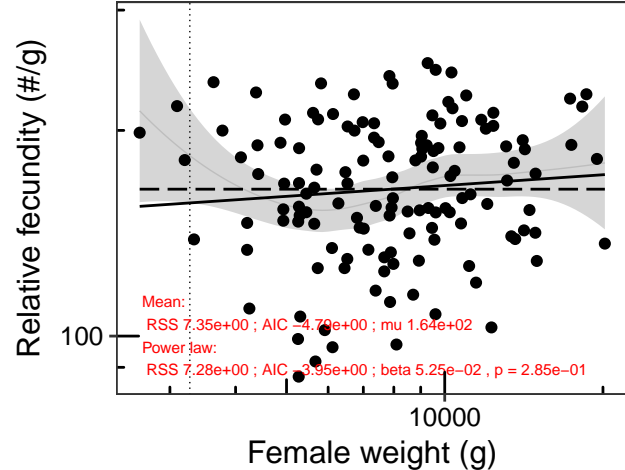
Species: *Oxylebius pictus*
Location: Monterey Bay California USA



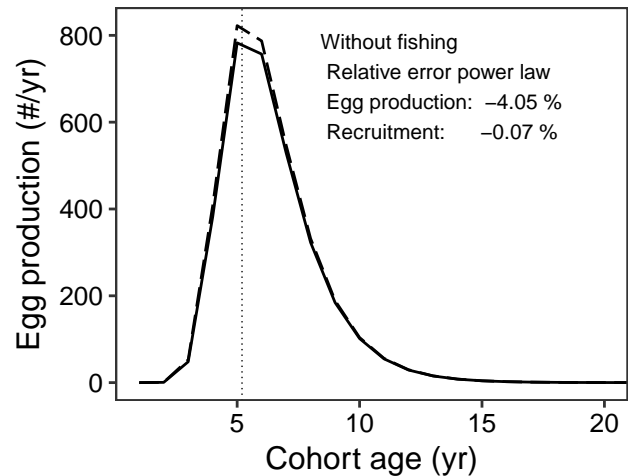
Species: *Oxylebius pictus*
Location: Monterey Bay California USA



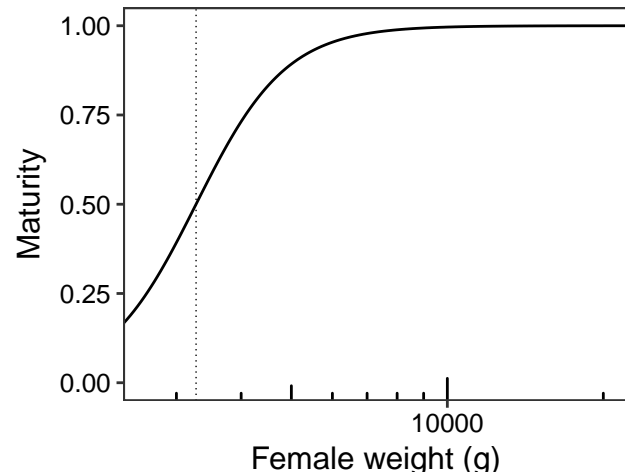
Species: *Paralichthys dentatus*
 Location: Middle Atlantic Bight (Cape Cod, Massachusetts to Cape Hatteras)



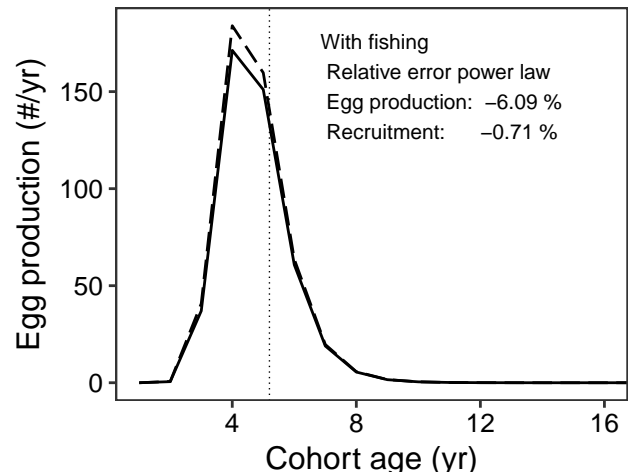
Species: *Paralichthys dentatus*
 Location: Middle Atlantic Bight (Cape Cod, Massachusetts to Cape Hatteras)



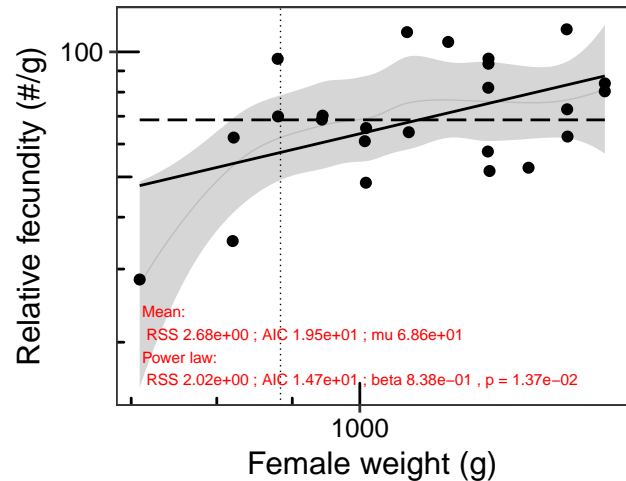
Species: *Paralichthys dentatus*
 Location: Middle Atlantic Bight (Cape Cod, Massachusetts to Cape Hatteras)



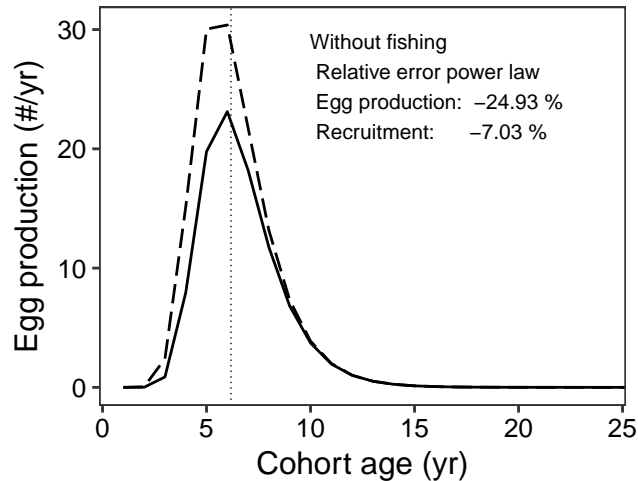
Species: *Paralichthys dentatus*
 Location: Middle Atlantic Bight (Cape Cod, Massachusetts to Cape Hatteras)



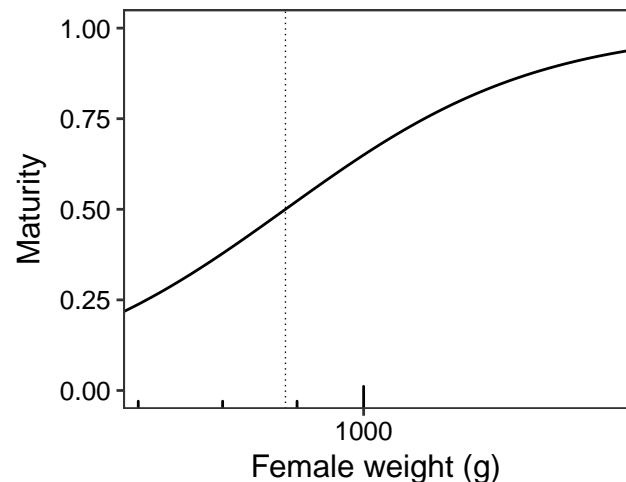
Species: *Paralichthys patagonicus*
Location: Off the coast of Mar del Plata



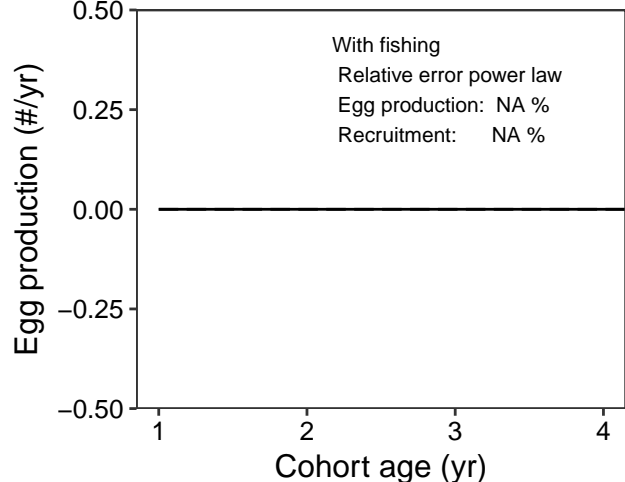
Species: *Paralichthys patagonicus*
Location: Off the coast of Mar del Plata



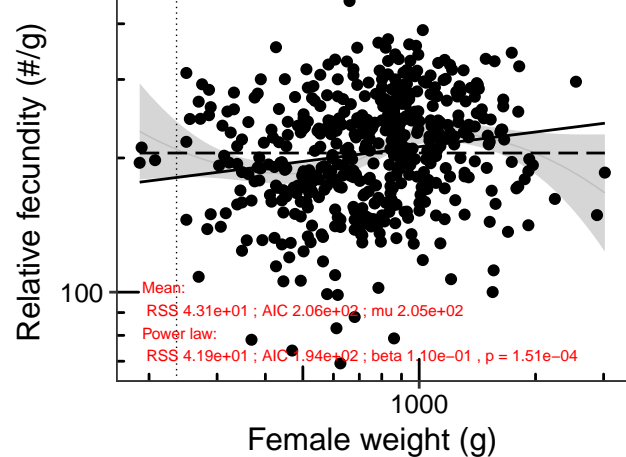
Species: *Paralichthys patagonicus*
Location: Off the coast of Mar del Plata



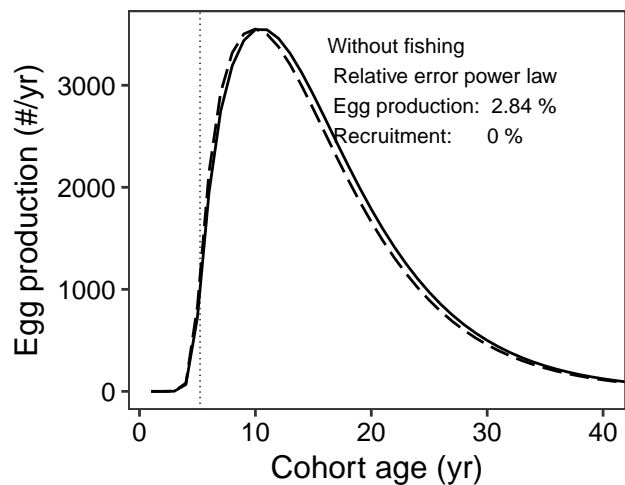
Species: *Paralichthys patagonicus*
Location: Off the coast of Mar del Plata



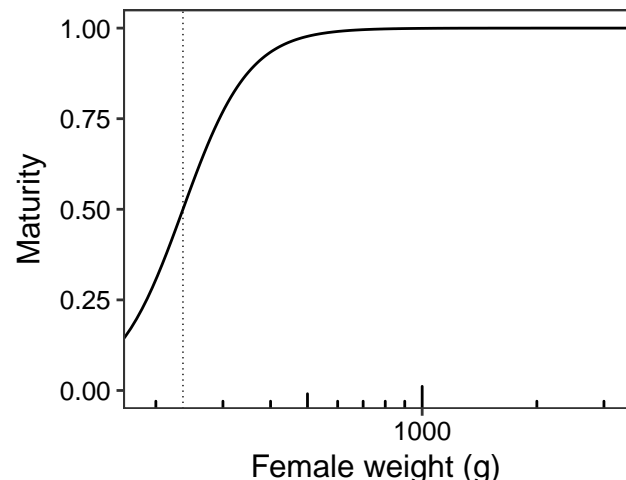
Species: *Pleuronectes platessa*
Location: North Sea



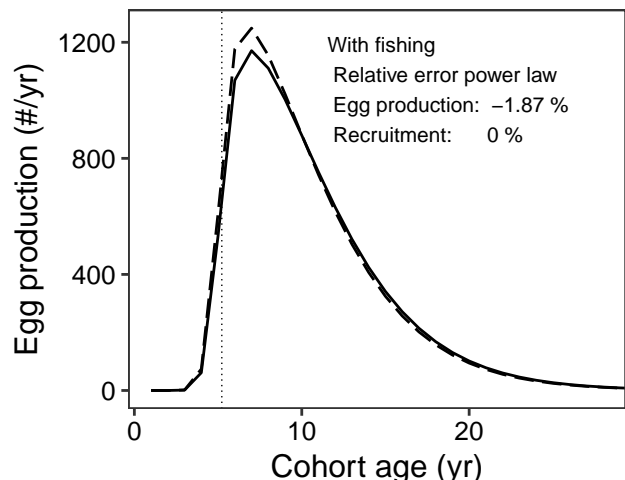
Species: *Pleuronectes platessa*
Location: North Sea



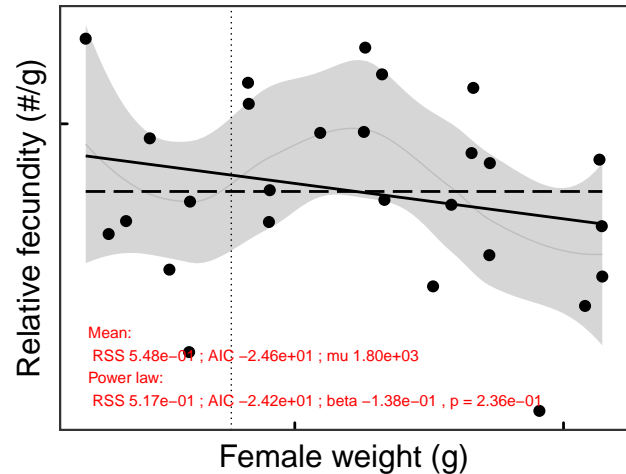
Species: *Pleuronectes platessa*
Location: North Sea



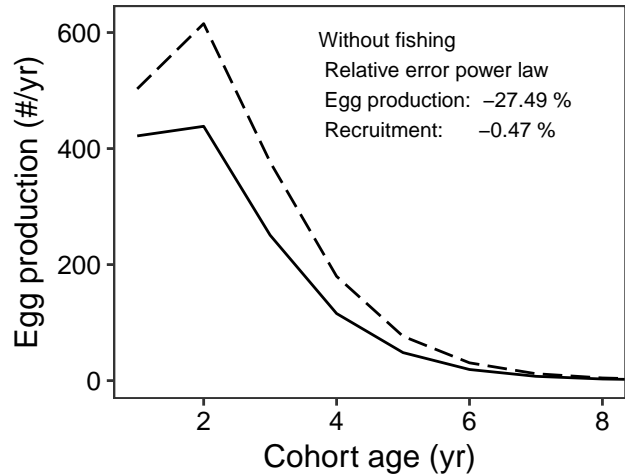
Species: *Pleuronectes platessa*
Location: North Sea



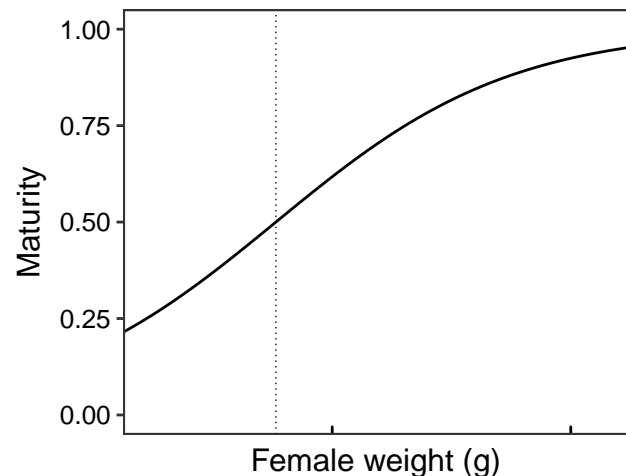
Species: *Pomacentrus coelestis*
Location: Bohnotsu (ML), Japan



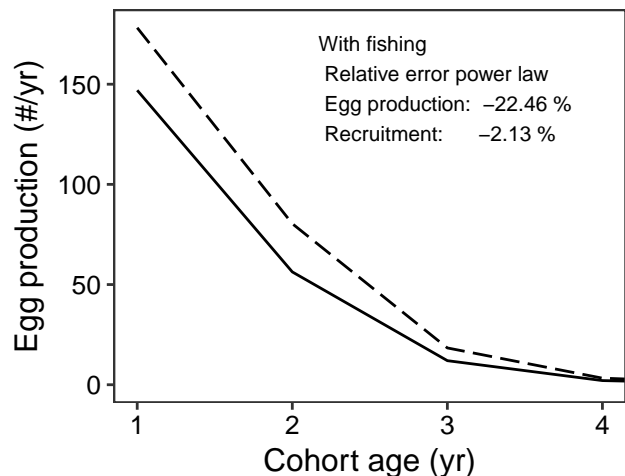
Species: *Pomacentrus coelestis*
Location: Bohnotsu (ML), Japan



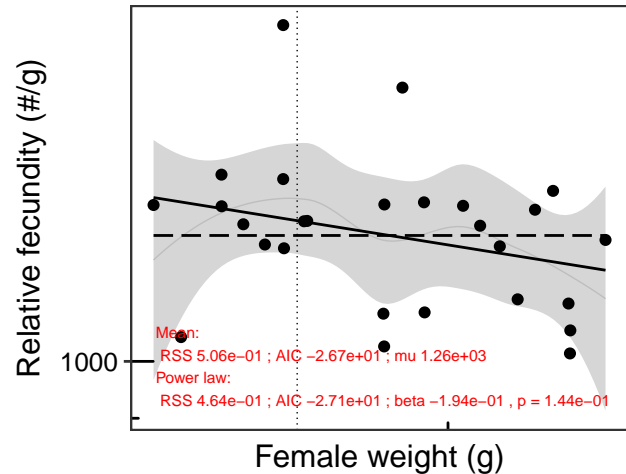
Species: *Pomacentrus coelestis*
Location: Bohnotsu (ML), Japan



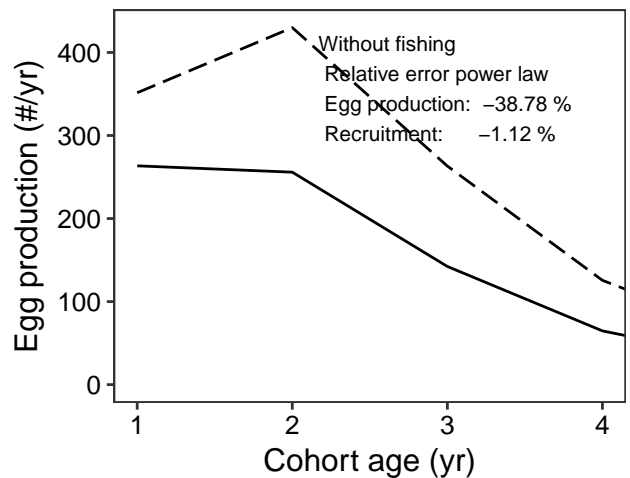
Species: *Pomacentrus coelestis*
Location: Bohnotsu (ML), Japan



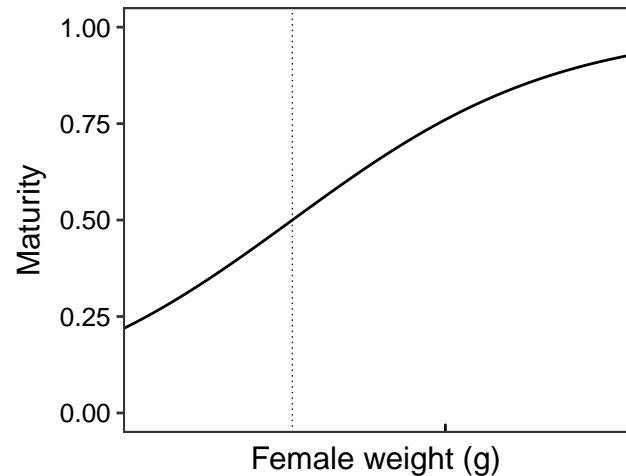
Species: *Pomacentrus coelestis*
Location: Sesoko (LL), Japan



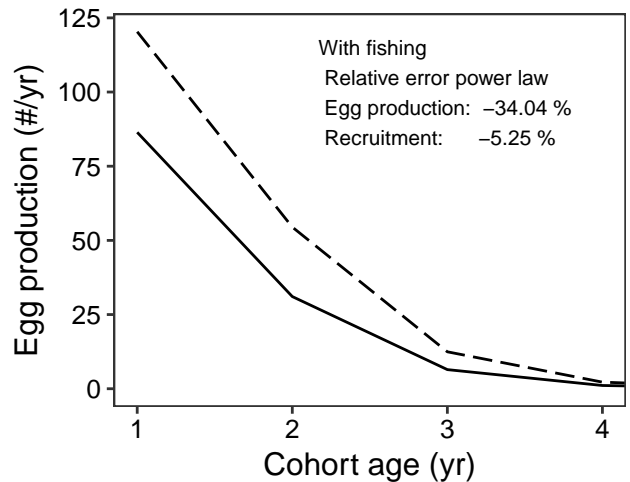
Species: *Pomacentrus coelestis*
Location: Sesoko (LL), Japan



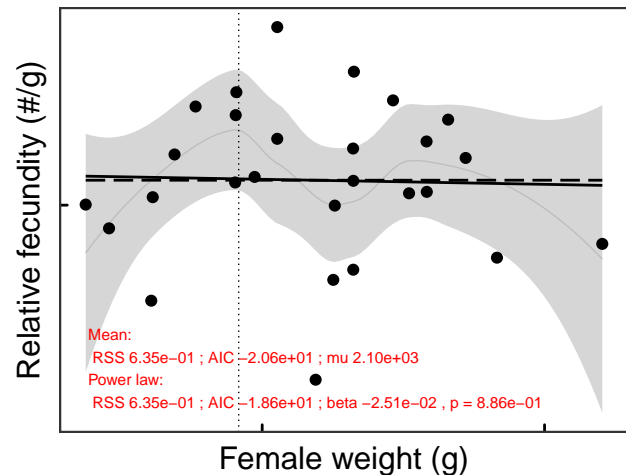
Species: *Pomacentrus coelestis*
Location: Sesoko (LL), Japan



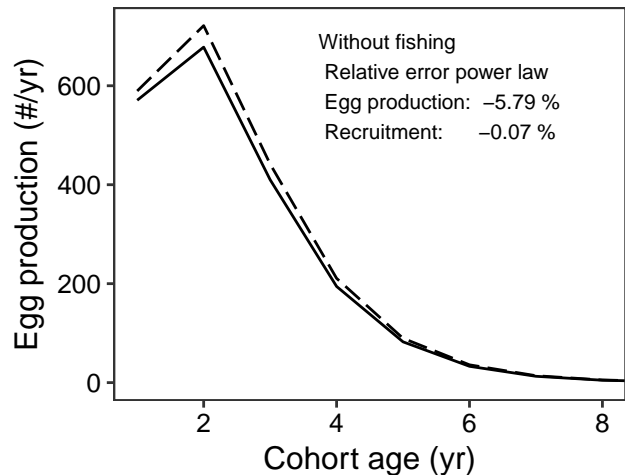
Species: *Pomacentrus coelestis*
Location: Sesoko (LL), Japan



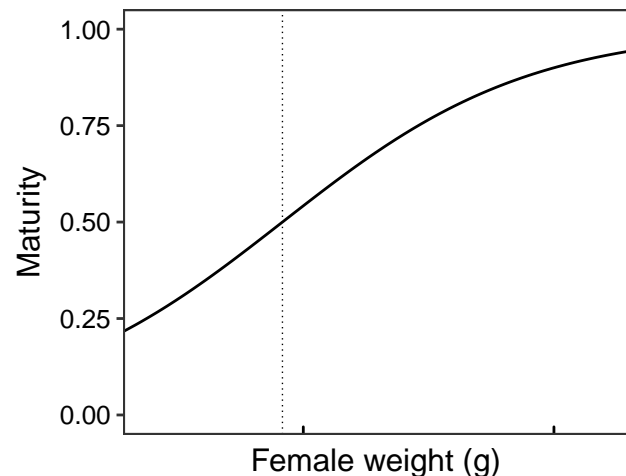
Species: *Pomacentrus coelestis*
Location: Kominato (HL), Japan



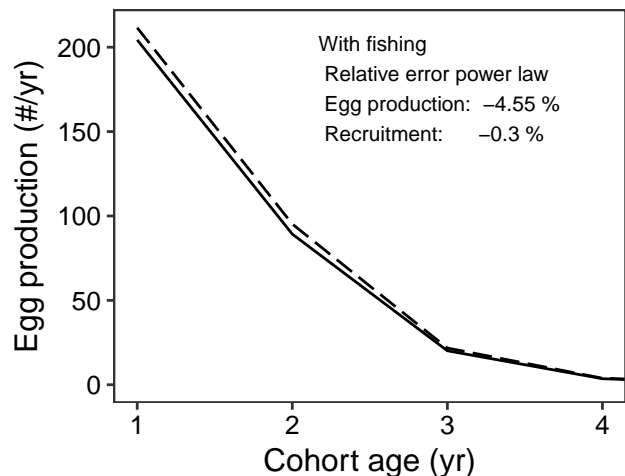
Species: *Pomacentrus coelestis*
Location: Kominato (HL), Japan



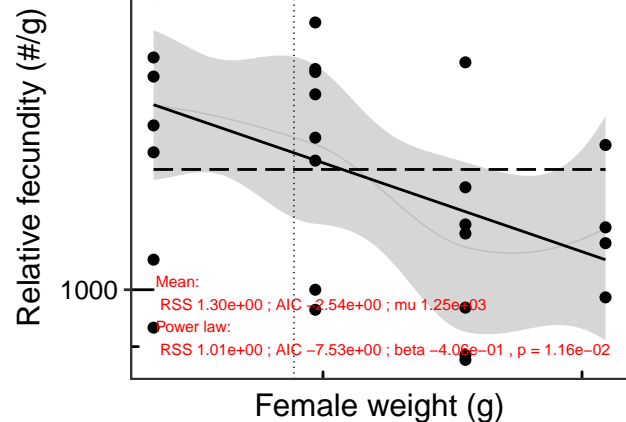
Species: *Pomacentrus coelestis*
Location: Kominato (HL), Japan



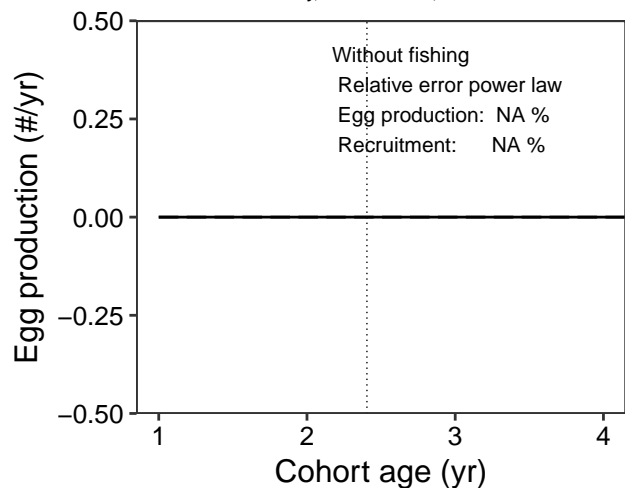
Species: *Pomacentrus coelestis*
Location: Kominato (HL), Japan



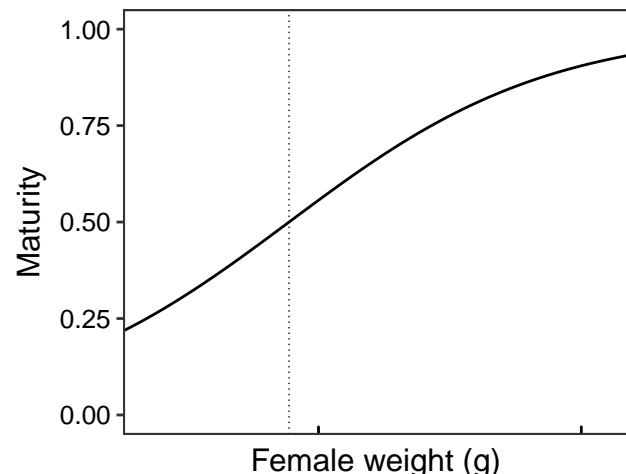
Species: *Pomatoschistus minutus*
Location: Ythan estuary, Aberdeenshire, Scotland



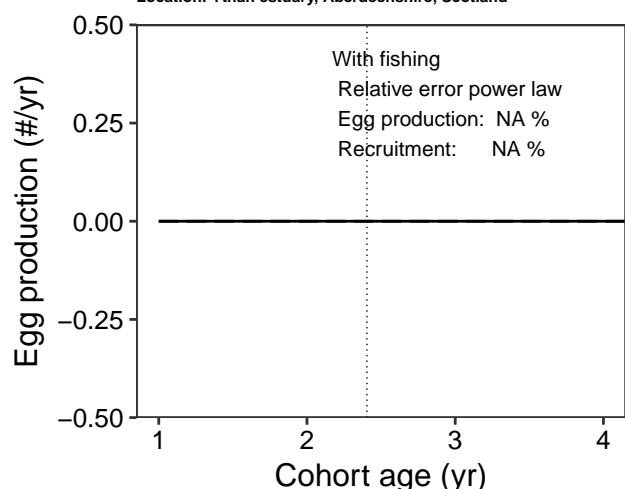
Species: *Pomatoschistus minutus*
Location: Ythan estuary, Aberdeenshire, Scotland



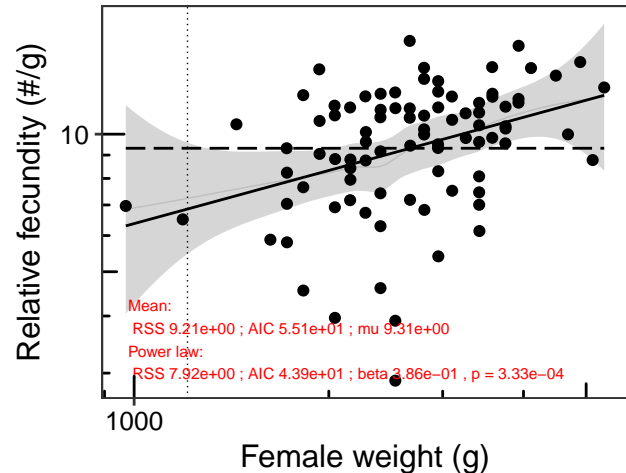
Species: *Pomatoschistus minutus*
Location: Ythan estuary, Aberdeenshire, Scotland



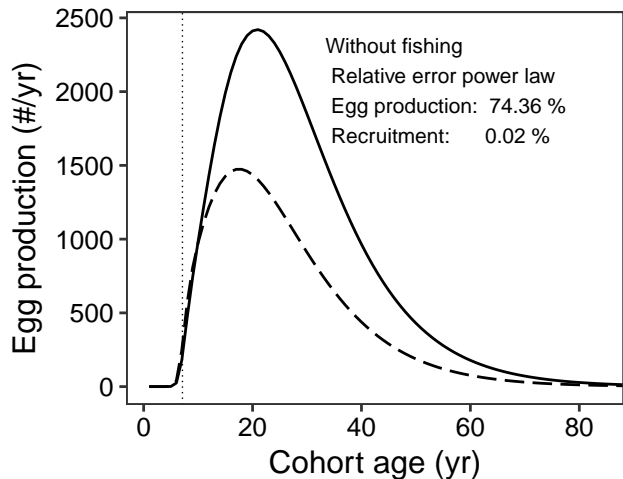
Species: *Pomatoschistus minutus*
Location: Ythan estuary, Aberdeenshire, Scotland



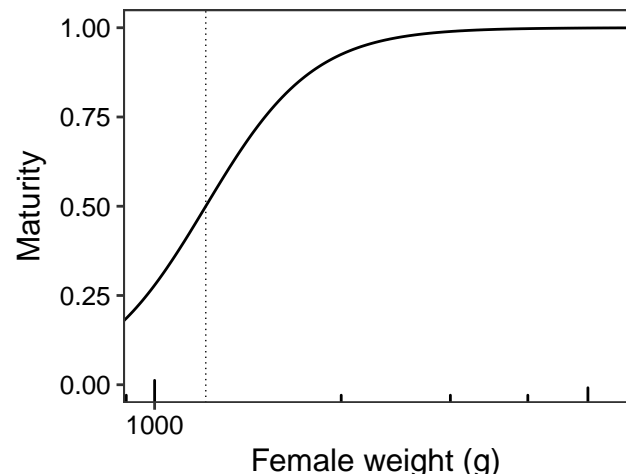
Species: *Reinhardtius hippoglossoides*
 Location: Off the west coast of Bear island, Northeast Arctic Sea



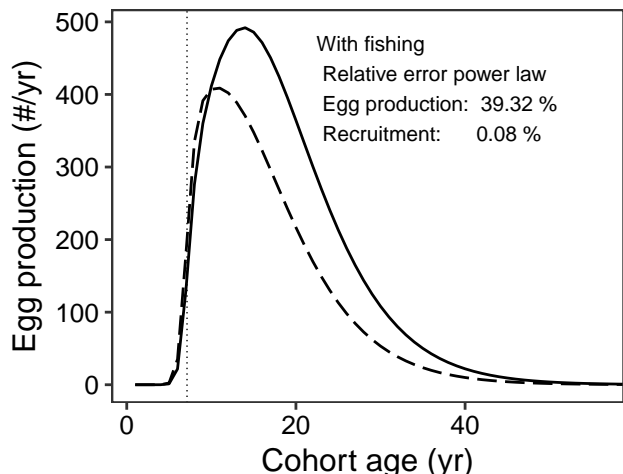
Species: *Reinhardtius hippoglossoides*
 Location: Off the west coast of Bear island, Northeast Arctic Sea



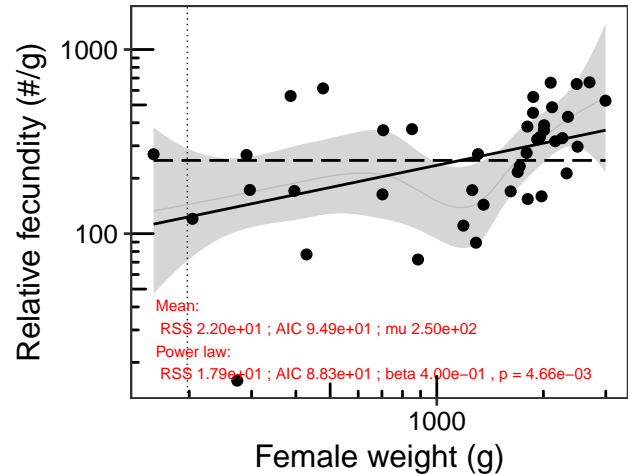
Species: *Reinhardtius hippoglossoides*
 Location: Off the west coast of Bear island, Northeast Arctic Sea



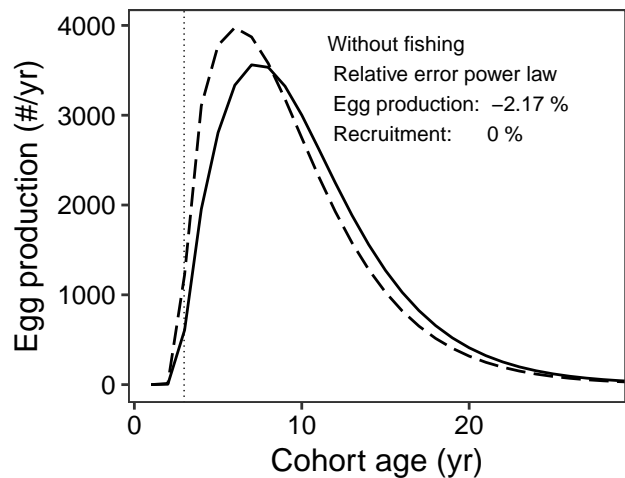
Species: *Reinhardtius hippoglossoides*
 Location: Off the west coast of Bear island, Northeast Arctic Sea



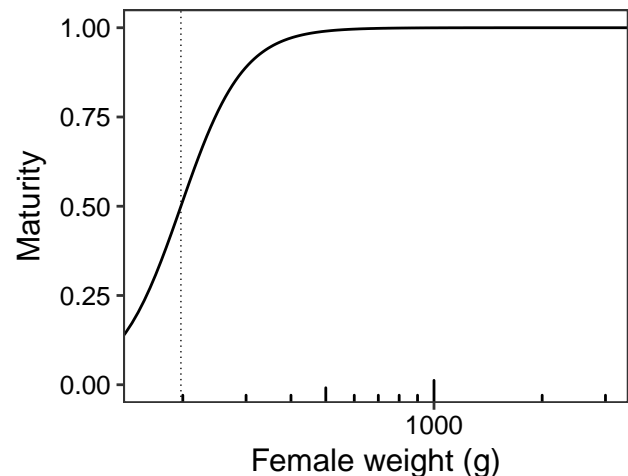
Species: *Rhomboptilus aurorubens*
Location: North and South Carolina, USA



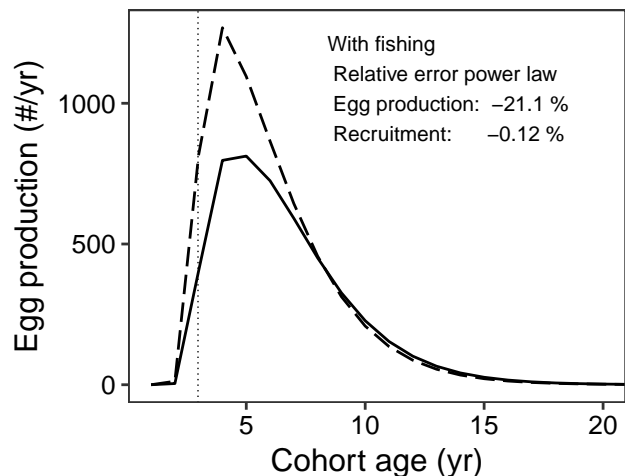
Species: *Rhomboptilus aurorubens*
Location: North and South Carolina, USA



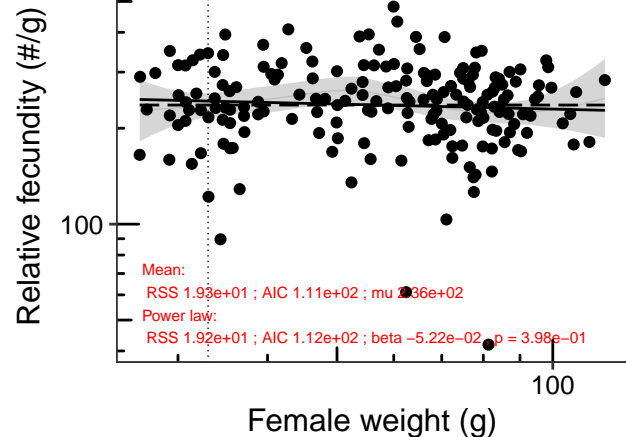
Species: *Rhomboptilus aurorubens*
Location: North and South Carolina, USA



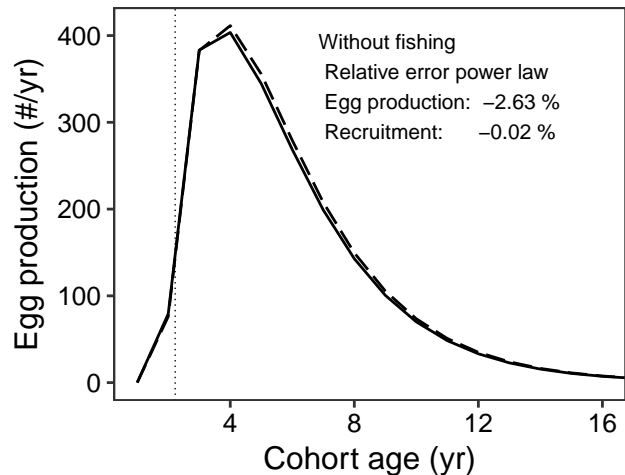
Species: *Rhomboptilus aurorubens*
Location: North and South Carolina, USA



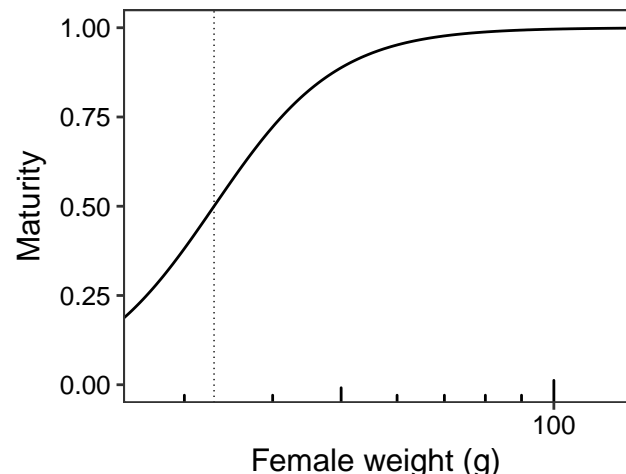
Species: *Sardinops sagax*
Location: Magdalena Bay, Baja California Sur, Mexico



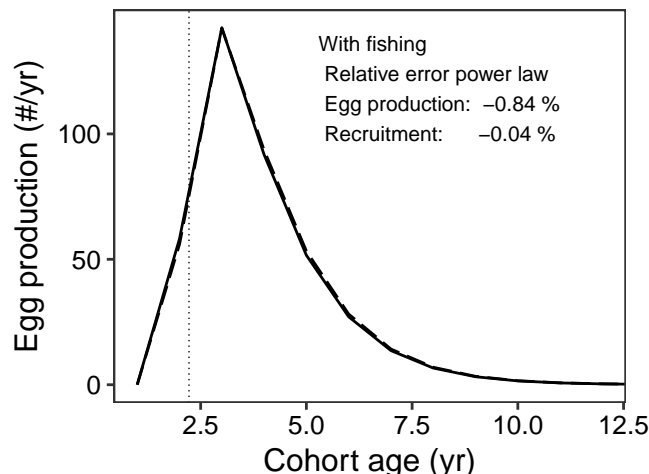
Species: *Sardinops sagax*
Location: Magdalena Bay, Baja California Sur, Mexico



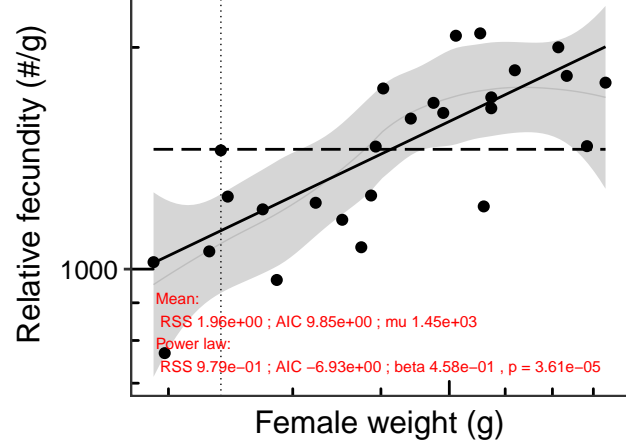
Species: *Sardinops sagax*
Location: Magdalena Bay, Baja California Sur, Mexico



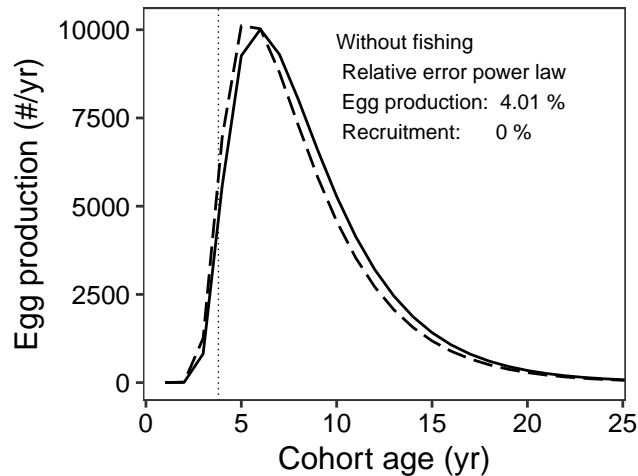
Species: *Sardinops sagax*
Location: Magdalena Bay, Baja California Sur, Mexico



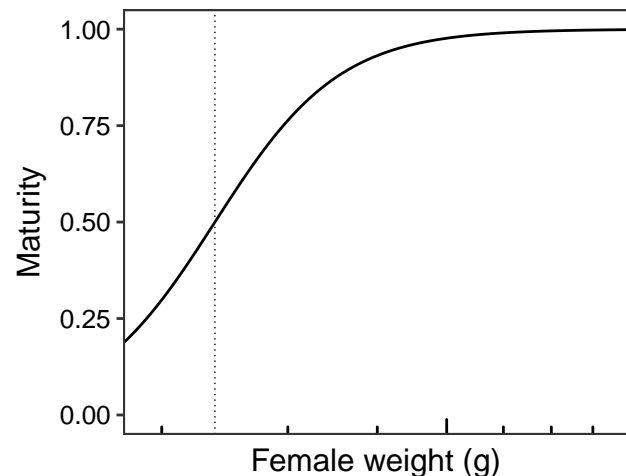
Species: *Scomber scombrus*
Location: Great Sole Bank, eastern Atlantic



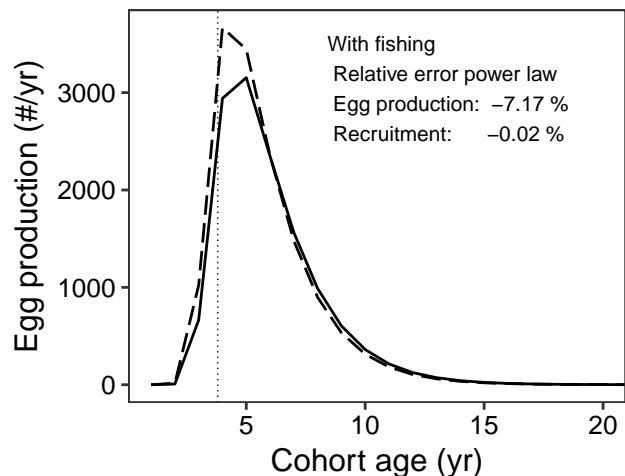
Species: *Scomber scombrus*
Location: Great Sole Bank, eastern Atlantic



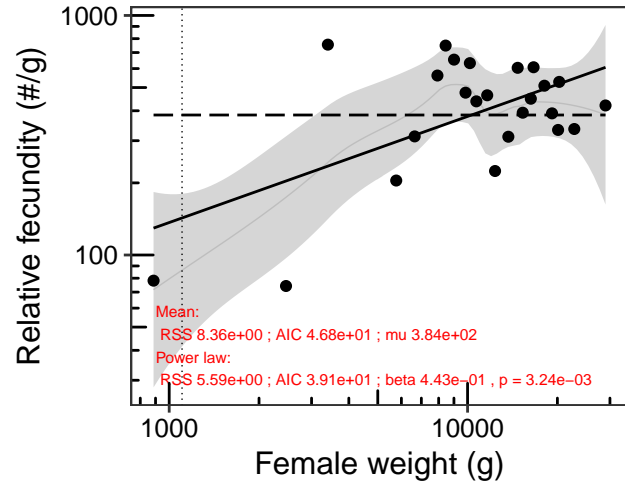
Species: *Scomber scombrus*
Location: Great Sole Bank, eastern Atlantic



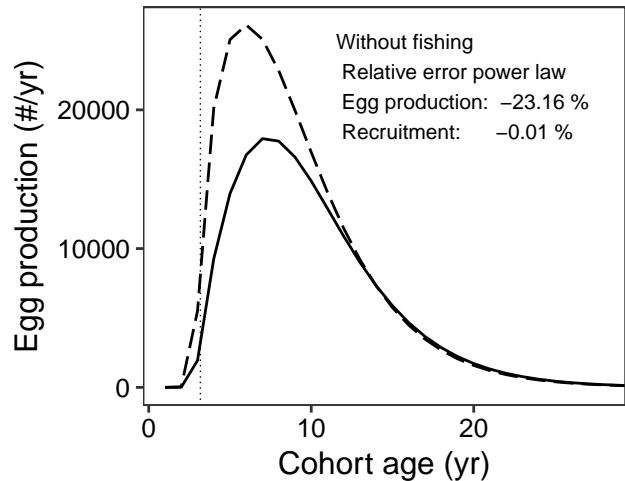
Species: *Scomber scombrus*
Location: Great Sole Bank, eastern Atlantic



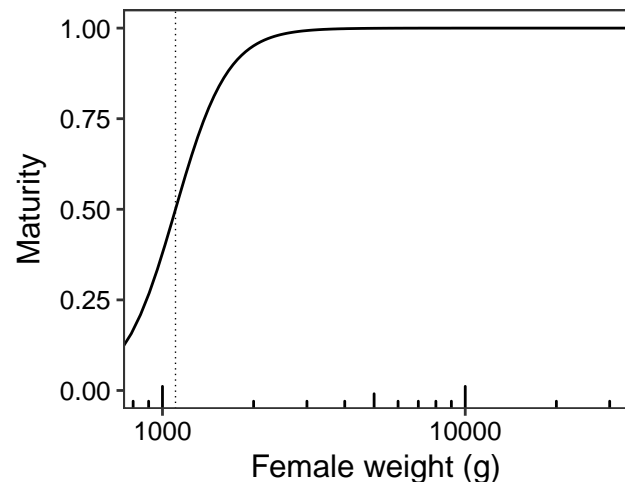
Species: *Scomberomorus cavalla*
Location: Louisiana



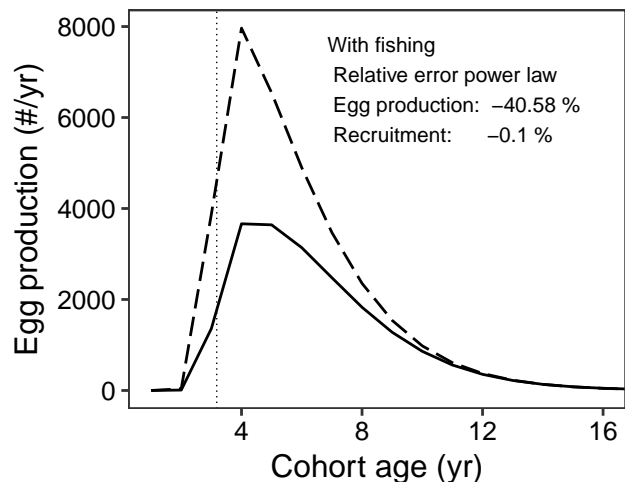
Species: *Scomberomorus cavalla*
Location: Louisiana

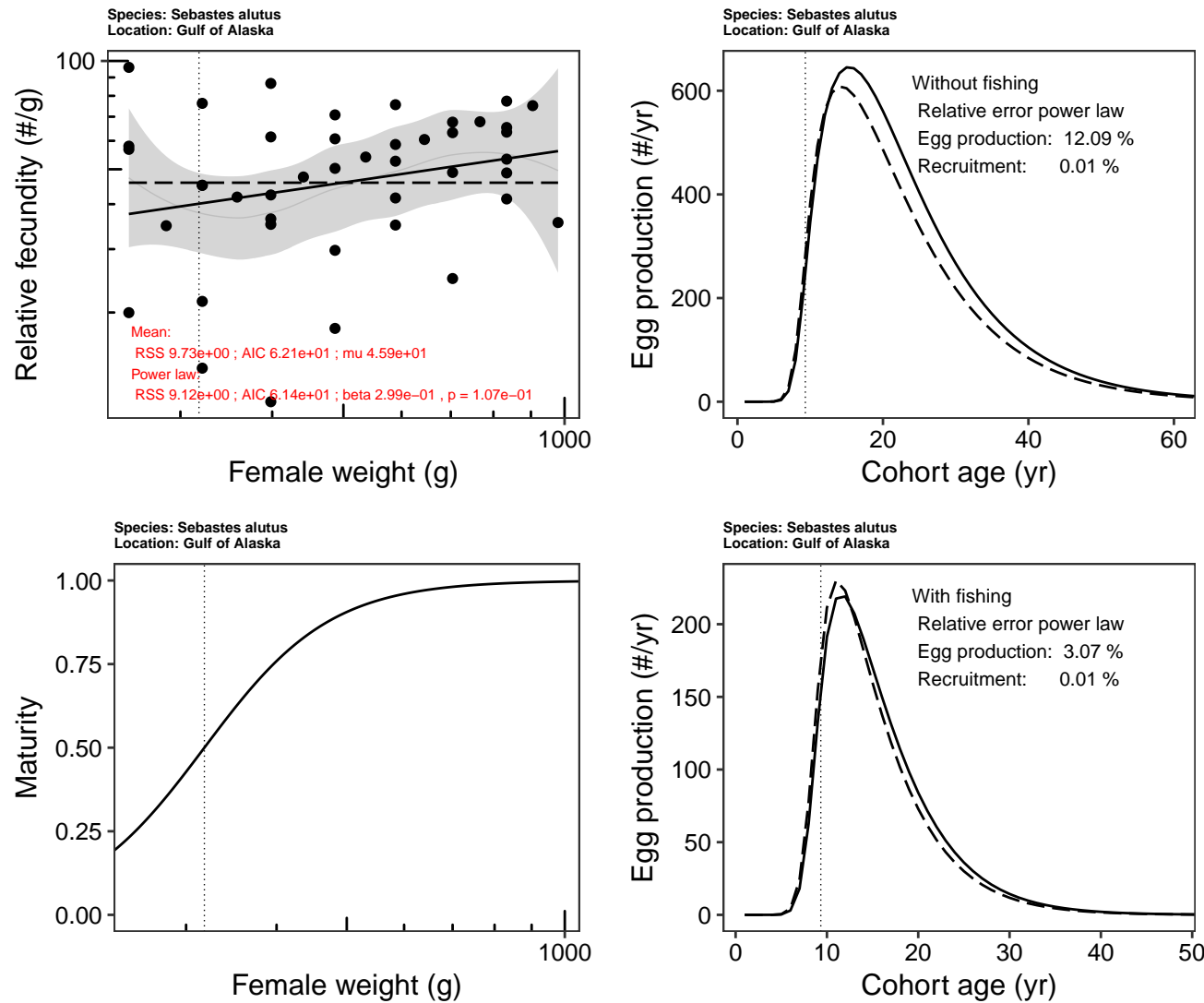


Species: *Scomberomorus cavalla*
Location: Louisiana

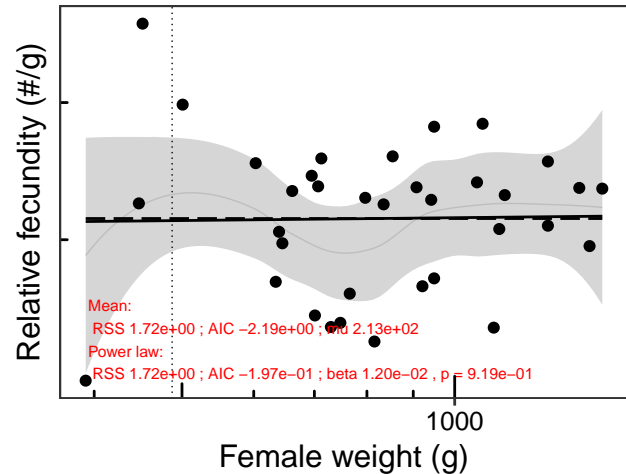


Species: *Scomberomorus cavalla*
Location: Louisiana

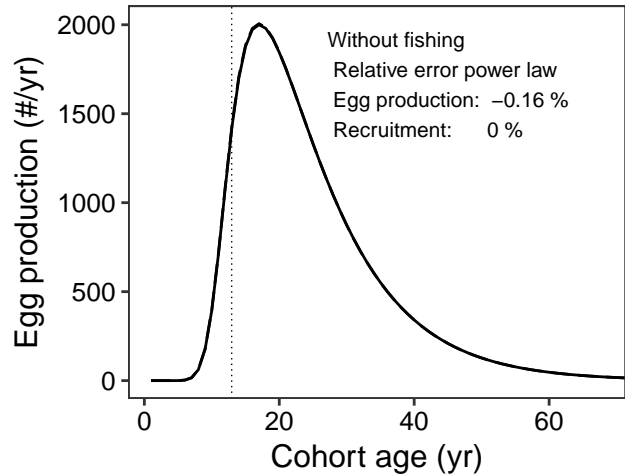




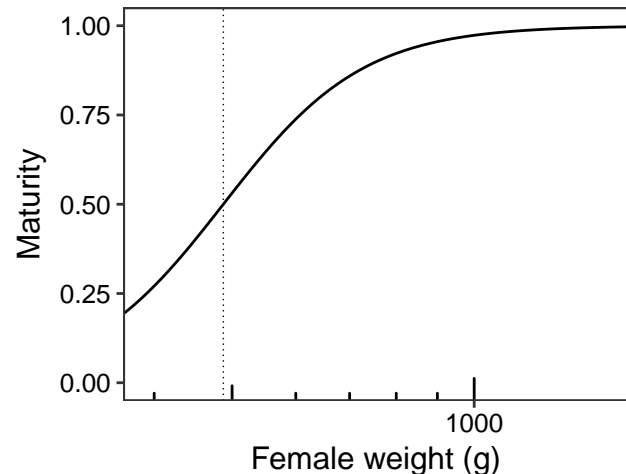
Species: *Sebastodes auriculatus*
Location: Port Orchard, Puget Sound, Washington, United States



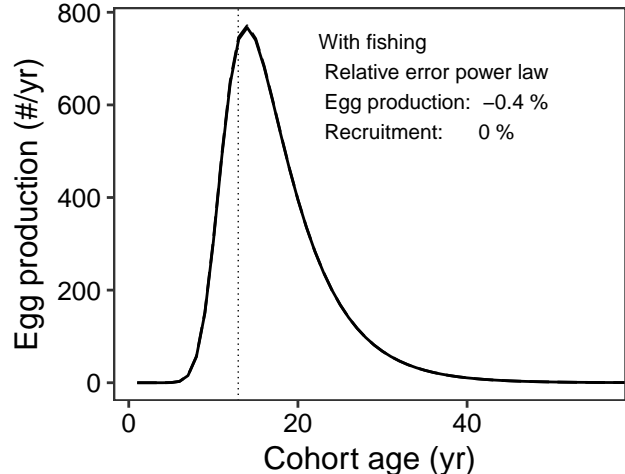
Species: *Sebastodes auriculatus*
Location: Port Orchard, Puget Sound, Washington, United States



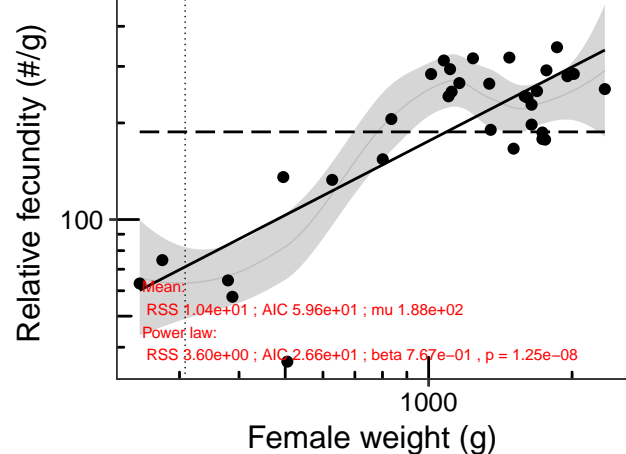
Species: *Sebastodes auriculatus*
Location: Port Orchard, Puget Sound, Washington, United States



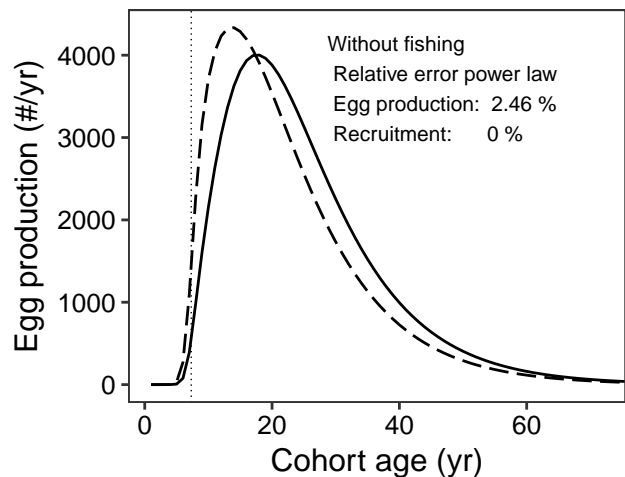
Species: *Sebastodes auriculatus*
Location: Port Orchard, Puget Sound, Washington, United States



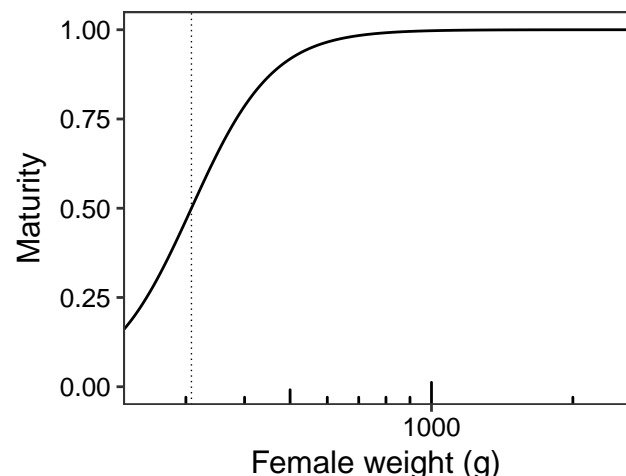
Species: *Sebastodes caurinus*
Location: Port Orchard, Puget Sound, Washington, United States



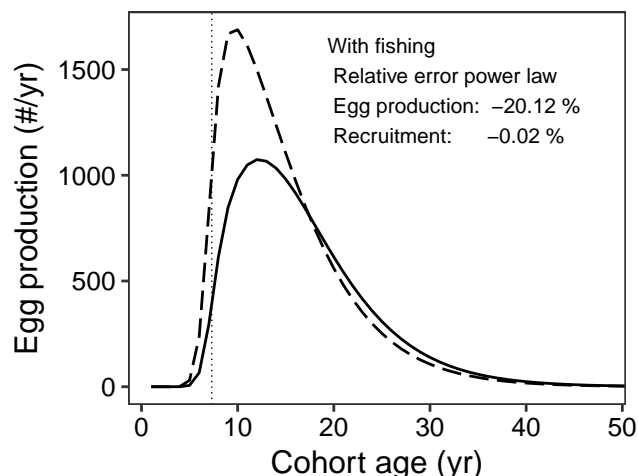
Species: *Sebastodes caurinus*
Location: Port Orchard, Puget Sound, Washington, United States



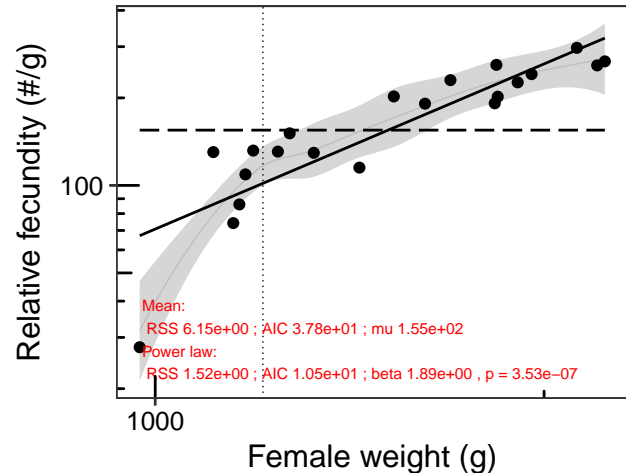
Species: *Sebastodes caurinus*
Location: Port Orchard, Puget Sound, Washington, United States



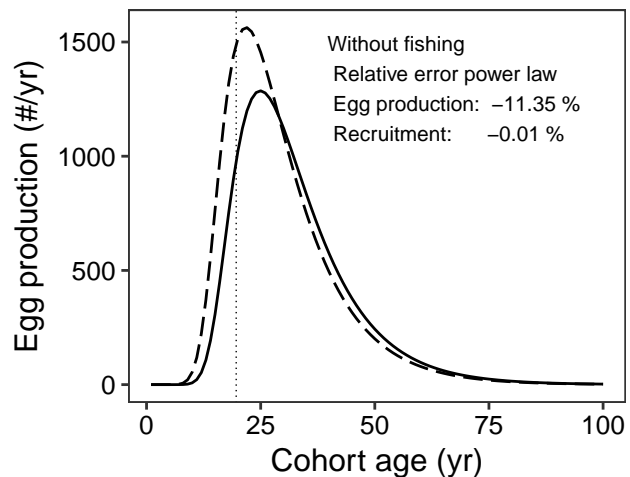
Species: *Sebastodes caurinus*
Location: Port Orchard, Puget Sound, Washington, United States



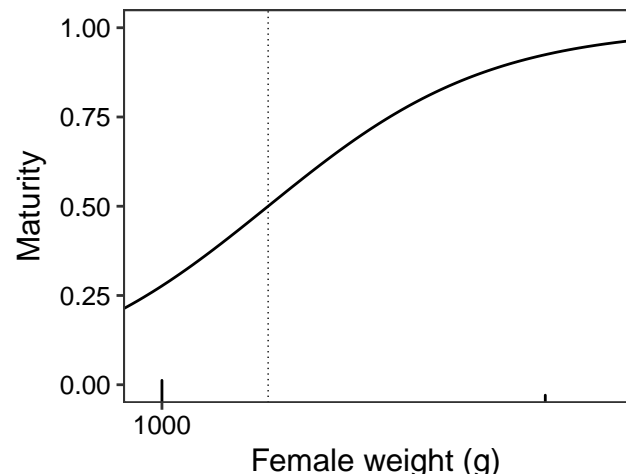
Species: *Sebastodes caurinus*
Location: Bainbridge Island and Colvos Passage, Washington, United States



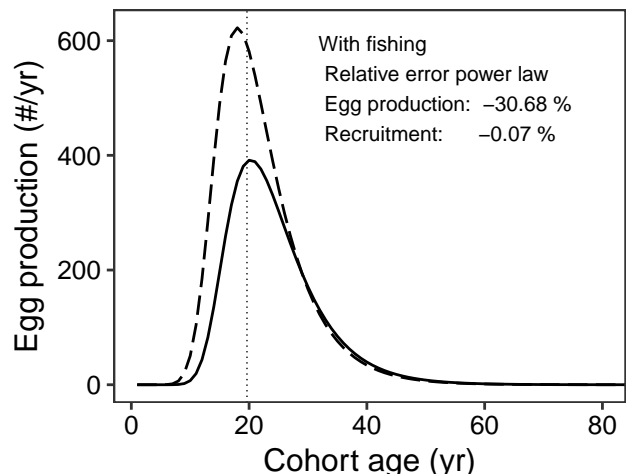
Species: *Sebastodes caurinus*
Location: Bainbridge Island and Colvos Passage, Washington, United States



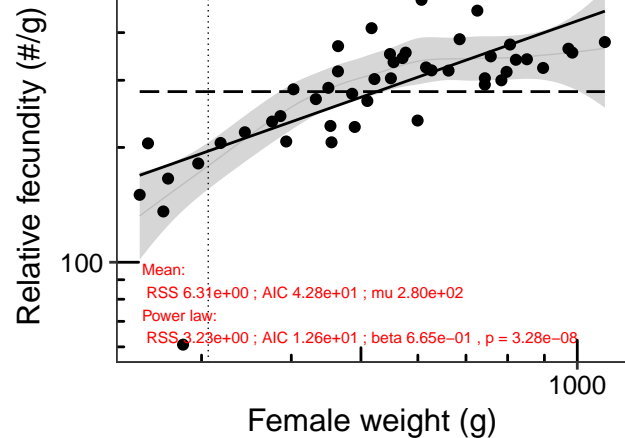
Species: *Sebastodes caurinus*
Location: Bainbridge Island and Colvos Passage, Washington, United States



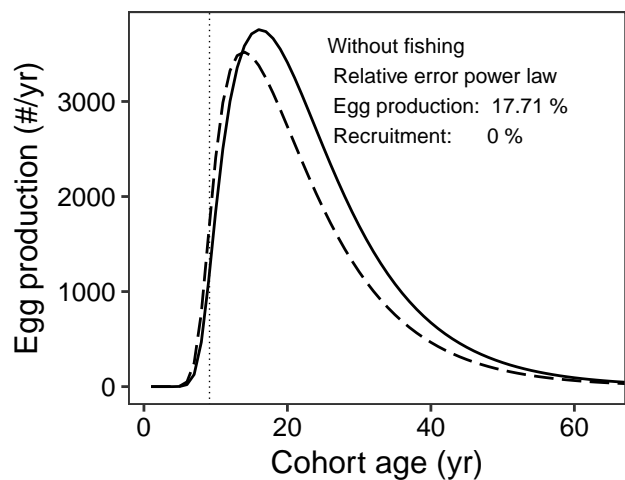
Species: *Sebastodes caurinus*
Location: Bainbridge Island and Colvos Passage, Washington, United States



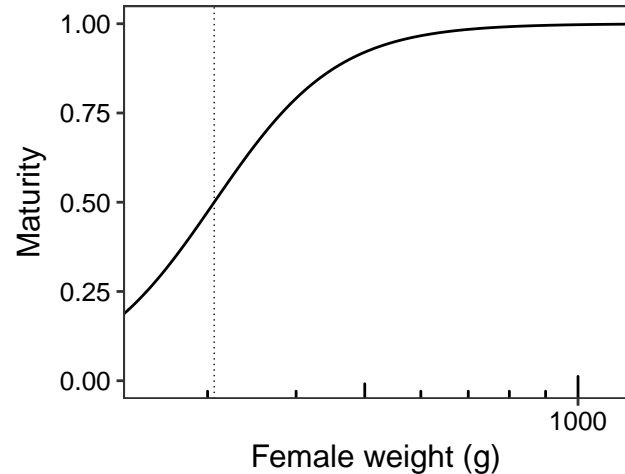
Species: *Sebastodes chlorostictus*
Location: Monterey Bay, California, United States



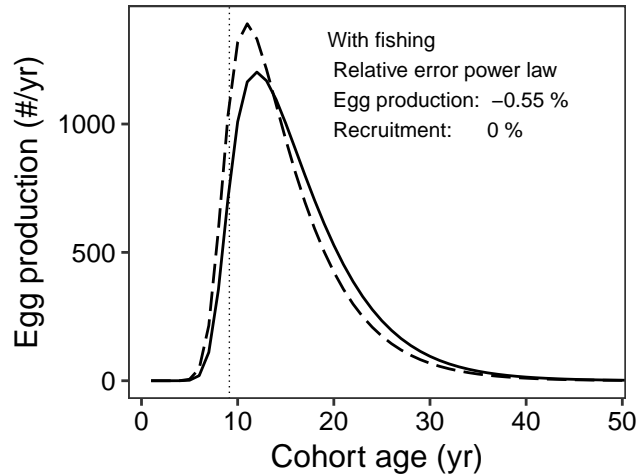
Species: *Sebastodes chlorostictus*
Location: Monterey Bay, California, United States



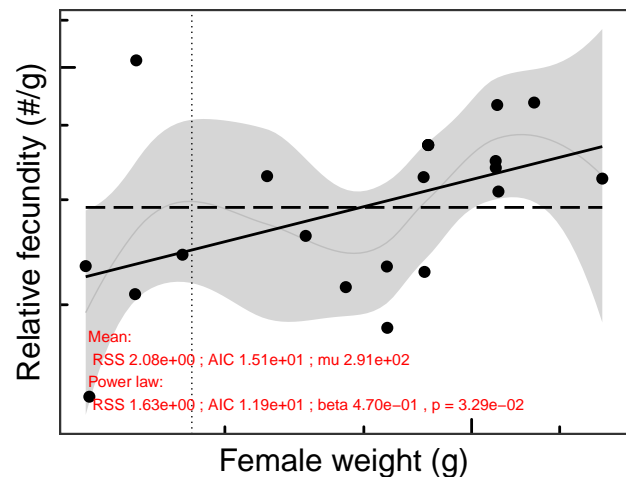
Species: *Sebastodes chlorostictus*
Location: Monterey Bay, California, United States



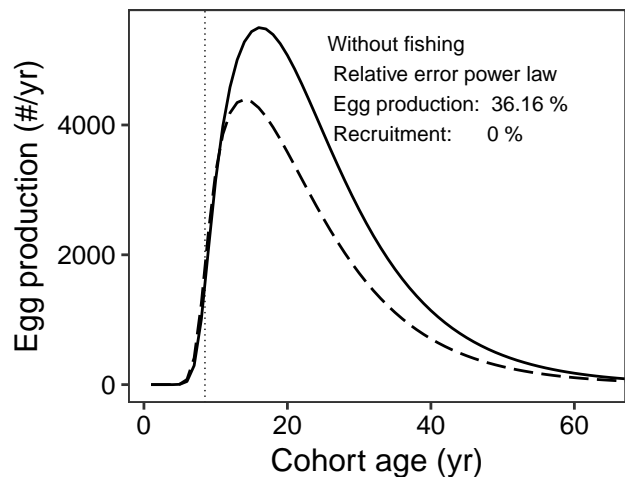
Species: *Sebastodes chlorostictus*
Location: Monterey Bay, California, United States



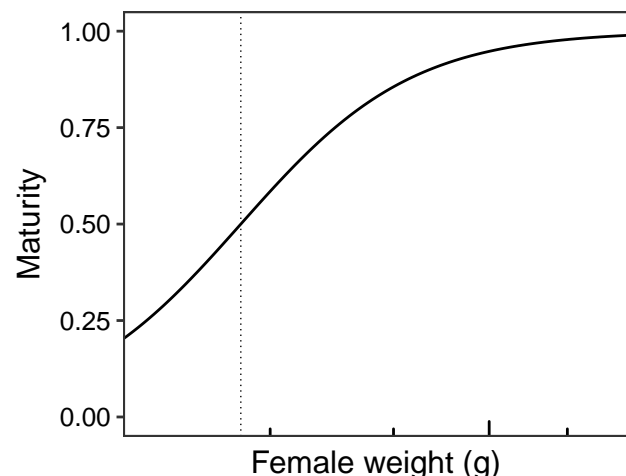
Species: *Sebastodes constellationis*
Location: California Bight, California, United States



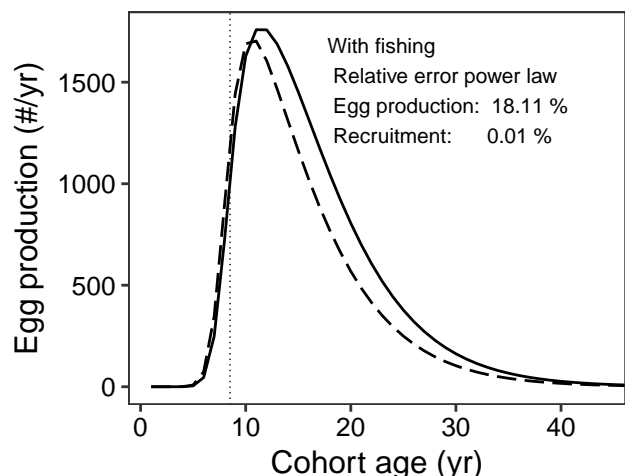
Species: *Sebastodes constellationis*
Location: California Bight, California, United States



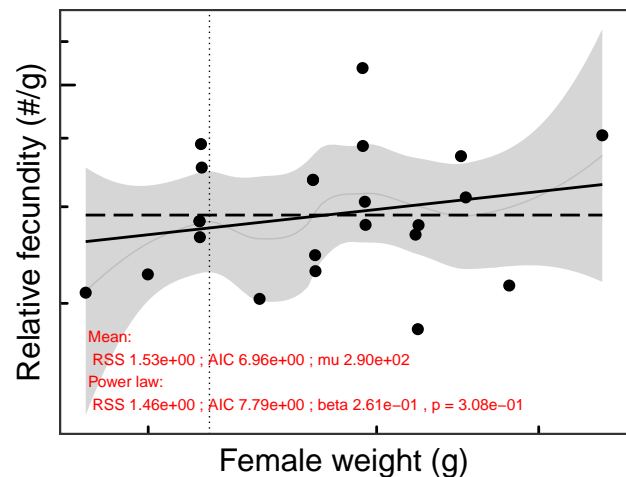
Species: *Sebastodes constellationis*
Location: California Bight, California, United States



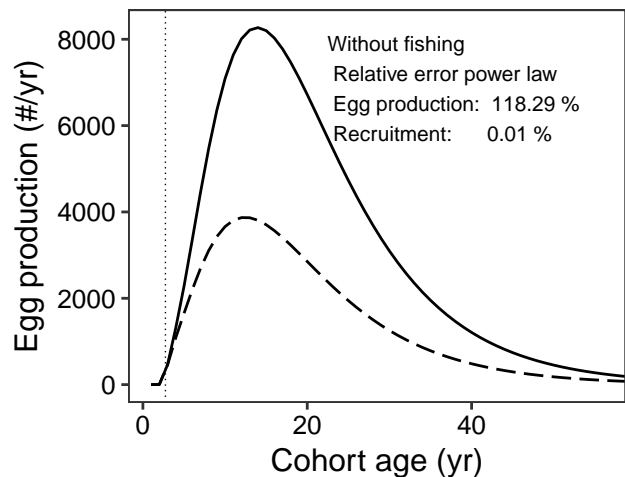
Species: *Sebastodes constellationis*
Location: California Bight, California, United States



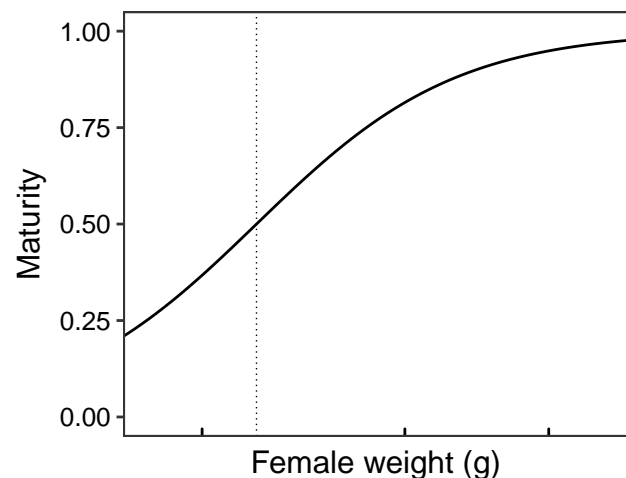
Species: *Sebastodes dallii*
Location: California Bight, California, United States



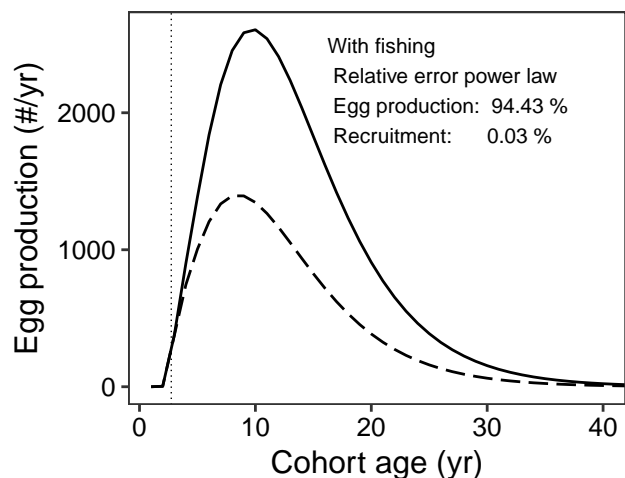
Species: *Sebastodes dallii*
Location: California Bight, California, United States



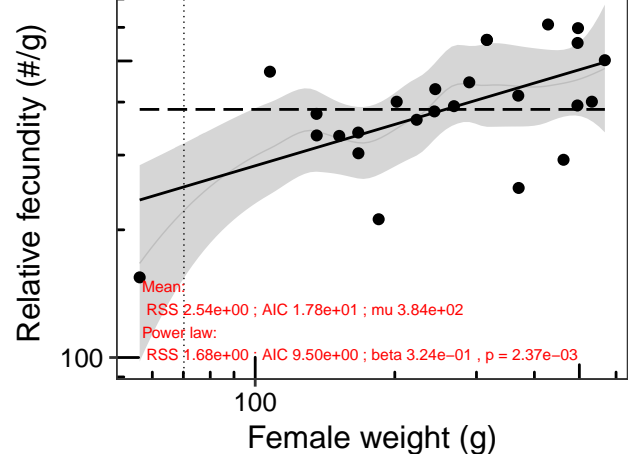
Species: *Sebastodes dallii*
Location: California Bight, California, United States



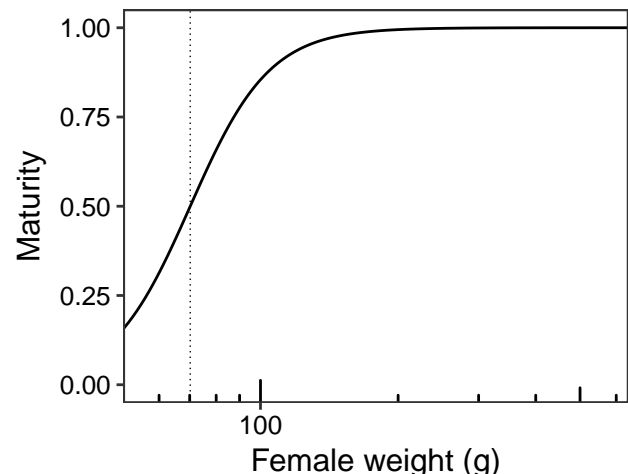
Species: *Sebastodes dallii*
Location: California Bight, California, United States



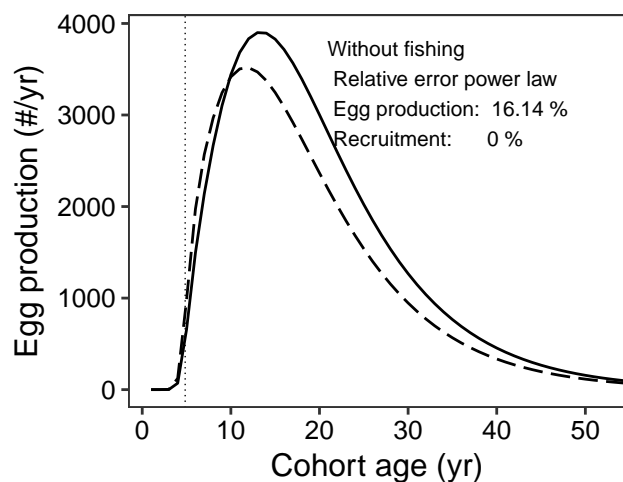
Species: *Sebastodes elongatus*
Location: California Bight, California, United States



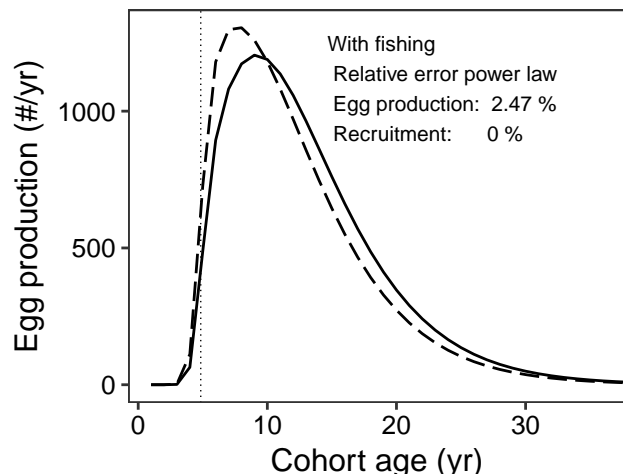
Species: *Sebastodes elongatus*
Location: California Bight, California, United States



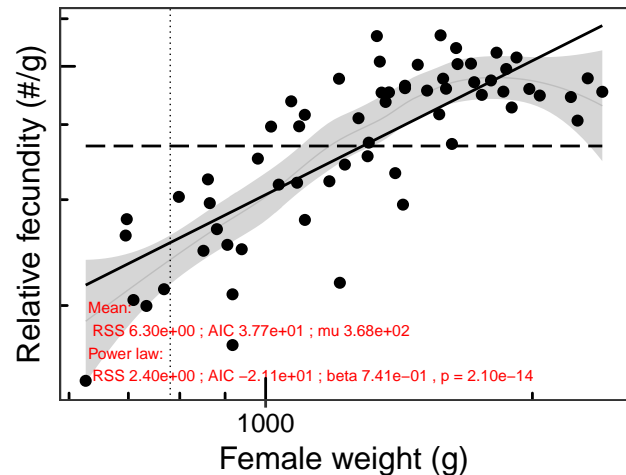
Species: *Sebastodes elongatus*
Location: California Bight, California, United States



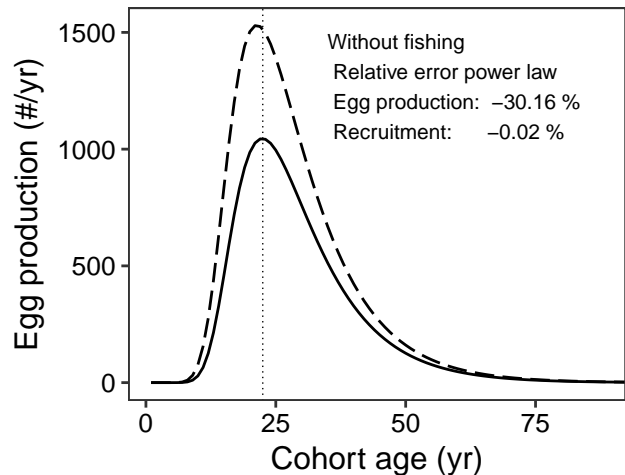
Species: *Sebastodes elongatus*
Location: California Bight, California, United States



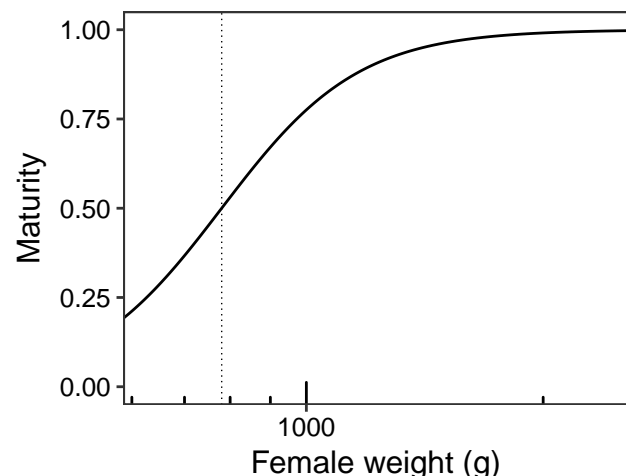
Species: *Sebastodes entomelas*
Location: Newport, Oregon, USA



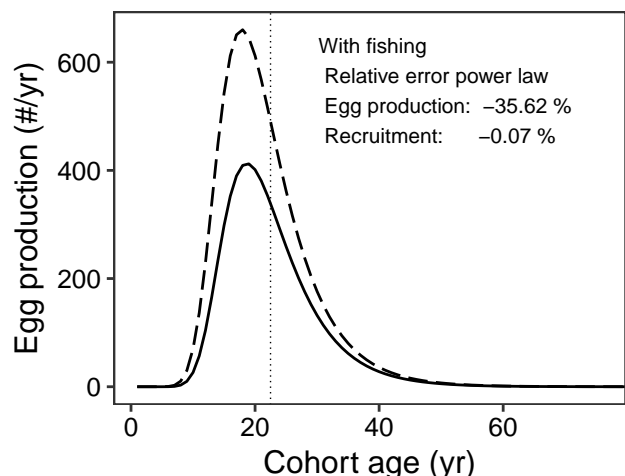
Species: *Sebastodes entomelas*
Location: Newport, Oregon, USA



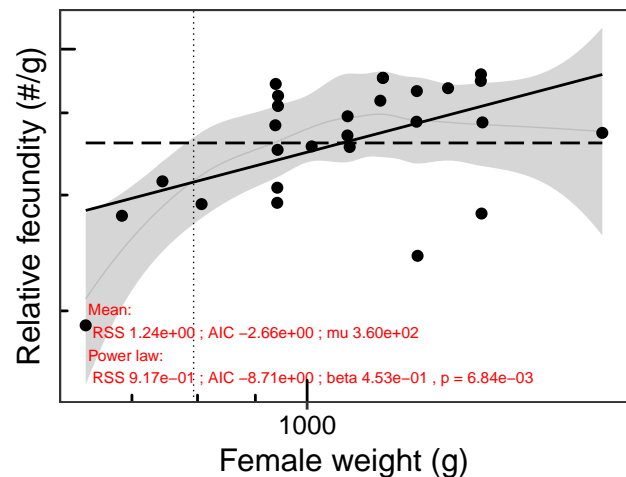
Species: *Sebastodes entomelas*
Location: Newport, Oregon, USA



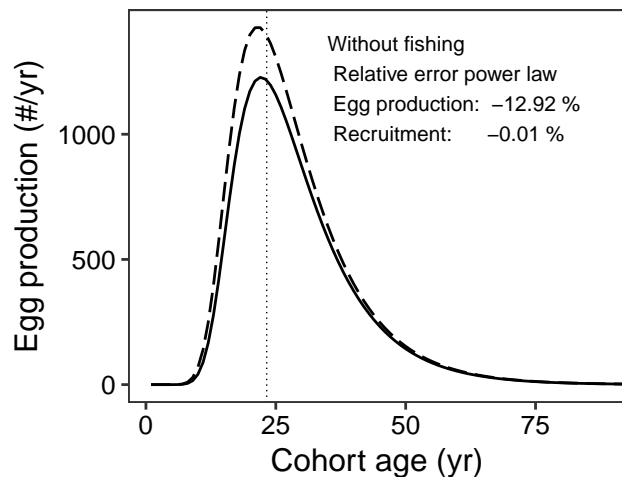
Species: *Sebastodes entomelas*
Location: Newport, Oregon, USA



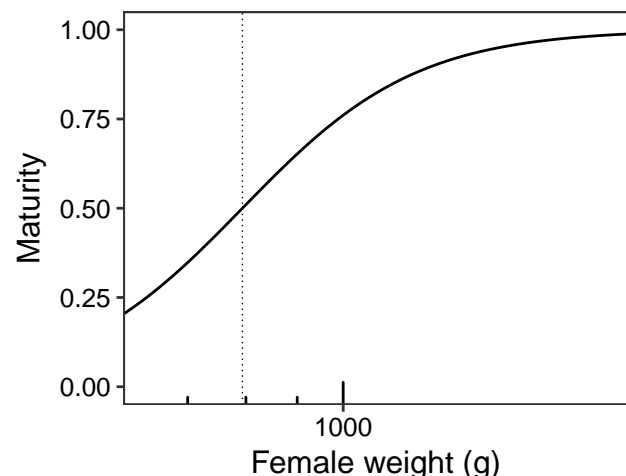
Species: *Sebastodes entomelas*
Location: California Bight, California, United States



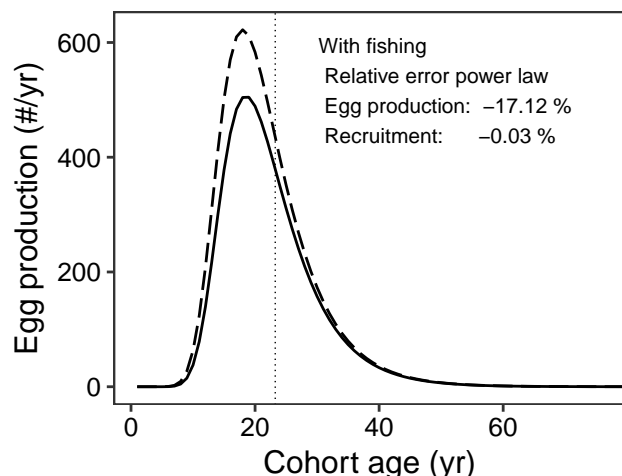
Species: *Sebastodes entomelas*
Location: California Bight, California, United States



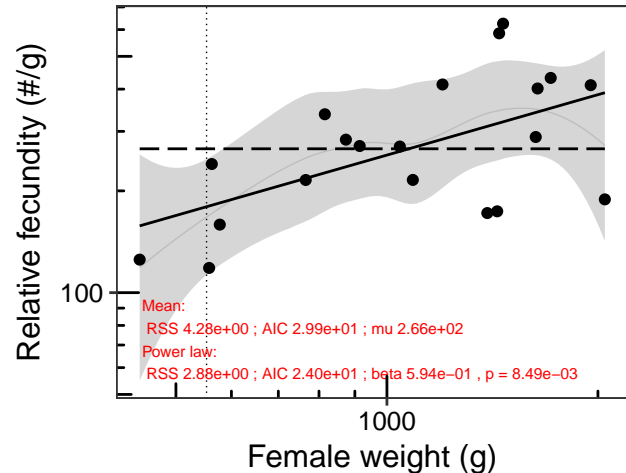
Species: *Sebastodes entomelas*
Location: California Bight, California, United States



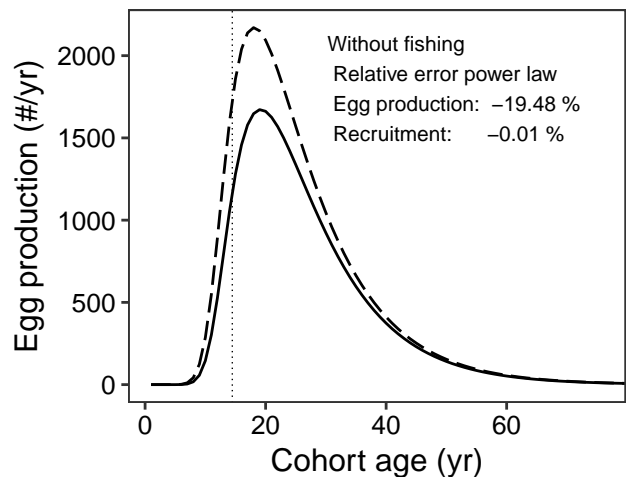
Species: *Sebastodes entomelas*
Location: California Bight, California, United States



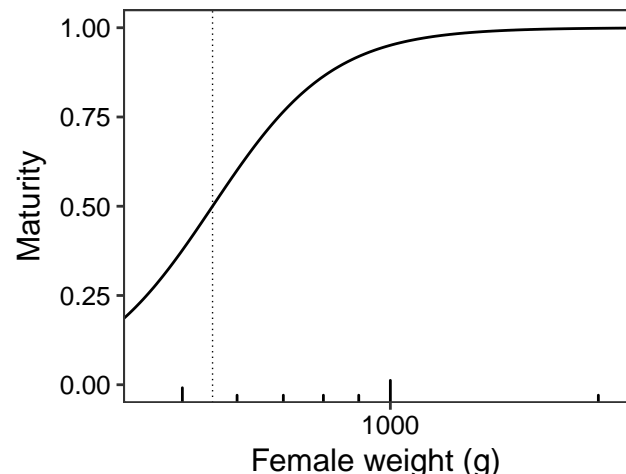
Species: *Sebastodes entomelas*
 Location: San Diego, California, United States to southeastern Alaska, Un



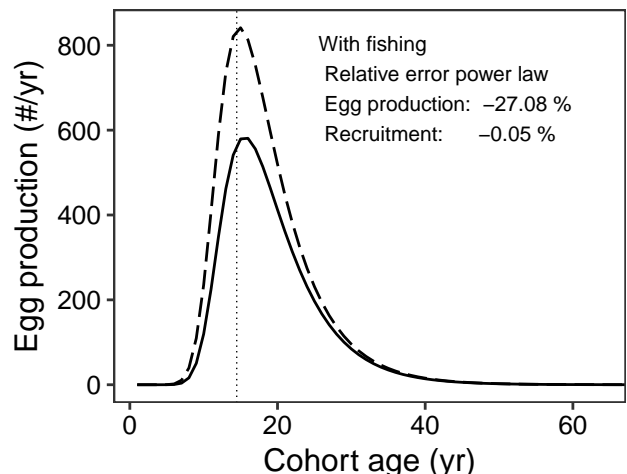
Species: *Sebastodes entomelas*
 Location: San Diego, California, United States to southeastern Alaska, Un



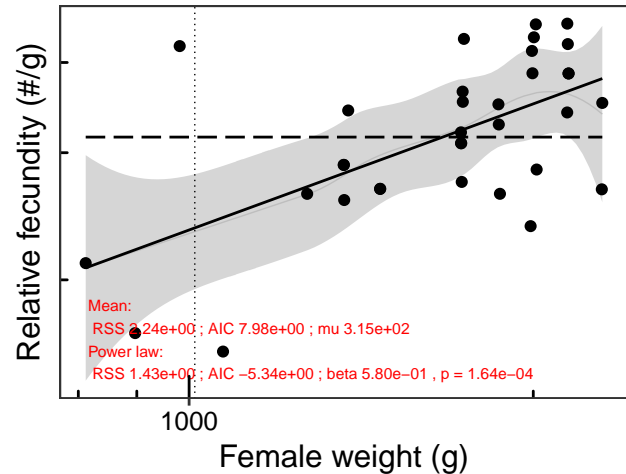
Species: *Sebastodes entomelas*
 Location: San Diego, California, United States to southeastern Alaska, Un



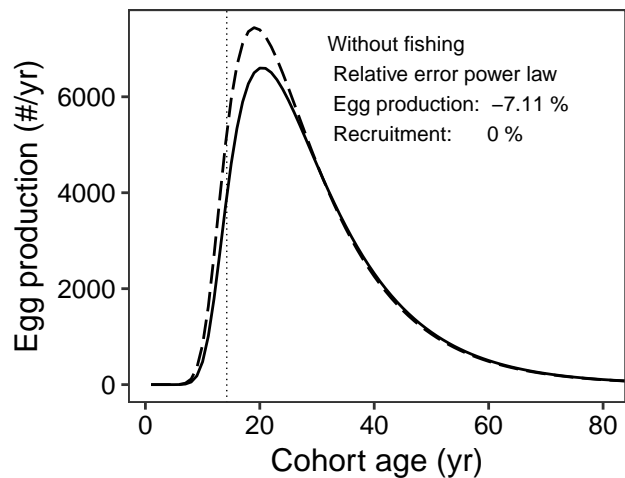
Species: *Sebastodes entomelas*
 Location: San Diego, California, United States to southeastern Alaska, Un



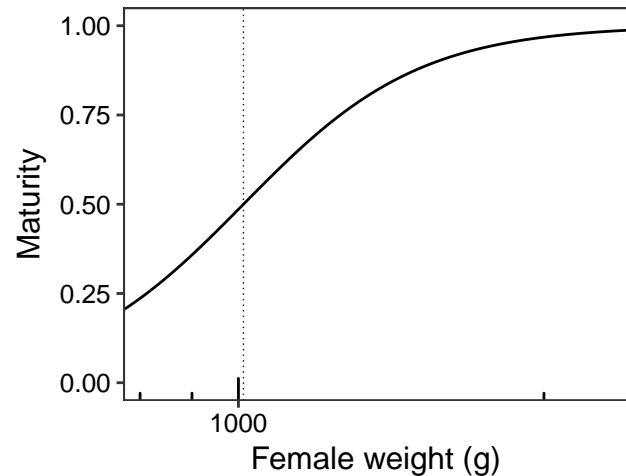
Species: *Sebastodes flavidus*
Location: California Bight, California, United States



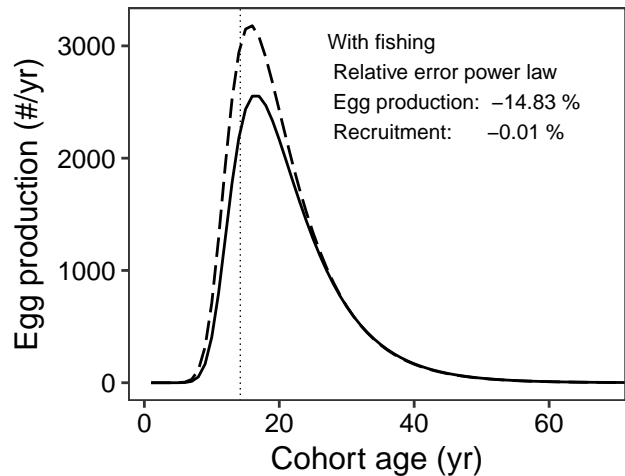
Species: *Sebastodes flavidus*
Location: California Bight, California, United States



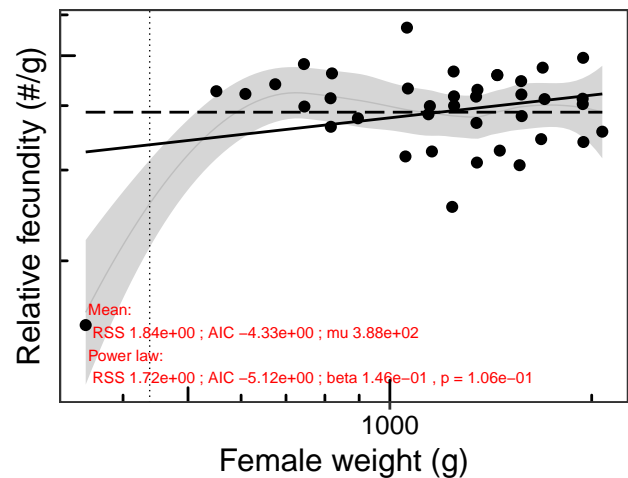
Species: *Sebastodes flavidus*
Location: California Bight, California, United States



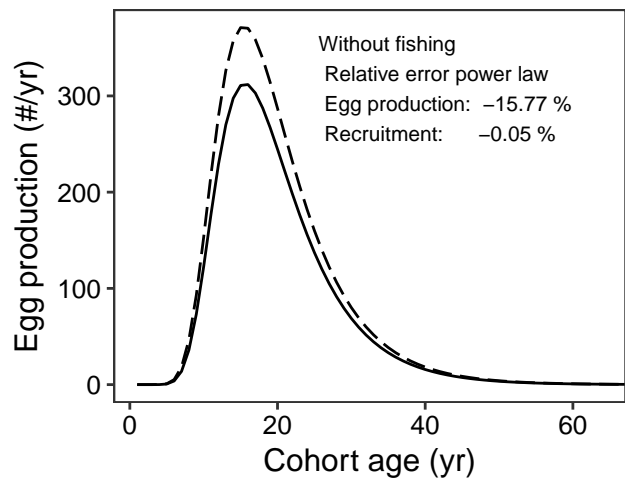
Species: *Sebastodes flavidus*
Location: California Bight, California, United States



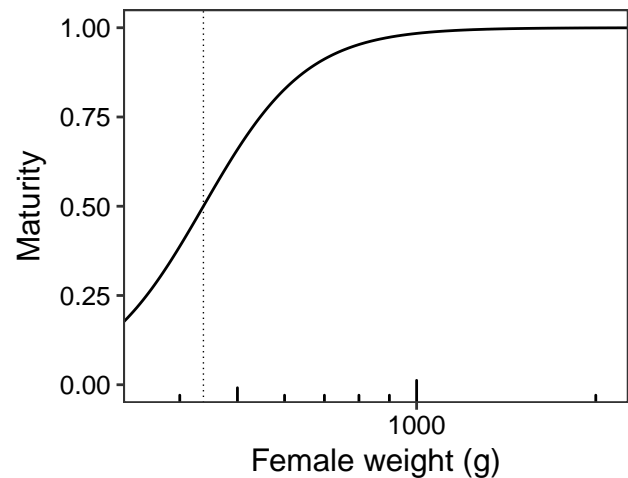
Species: *Sebastodes goodei*
Location: California Bight, California, United States



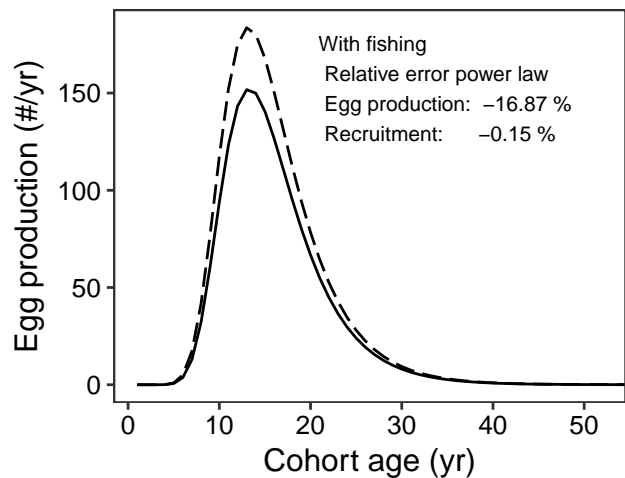
Species: *Sebastodes goodei*
Location: California Bight, California, United States



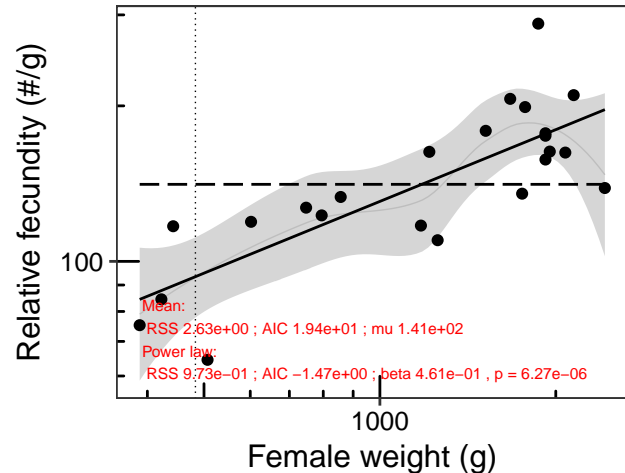
Species: *Sebastodes goodei*
Location: California Bight, California, United States



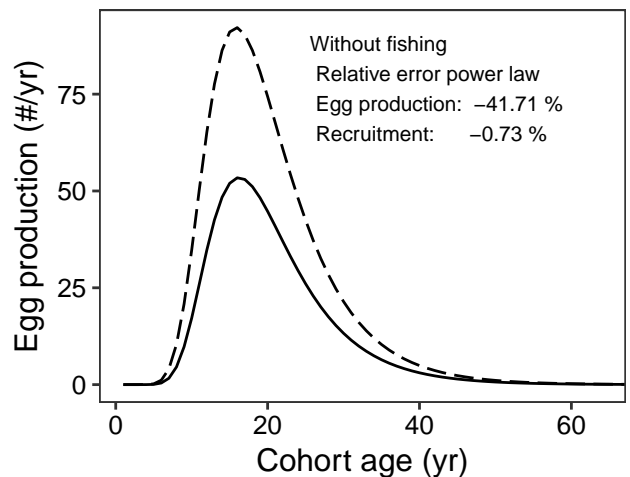
Species: *Sebastodes goodei*
Location: California Bight, California, United States



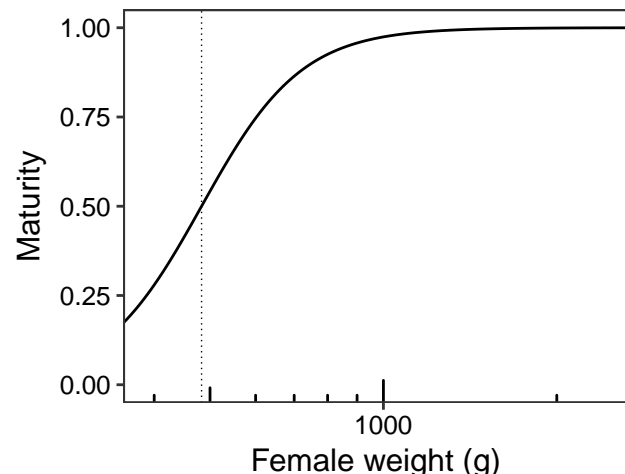
Species: *Sebastodes goodei*
 Location: Magdalena Bay, Baja California, Mexico to Eureka, California, U.S.A.



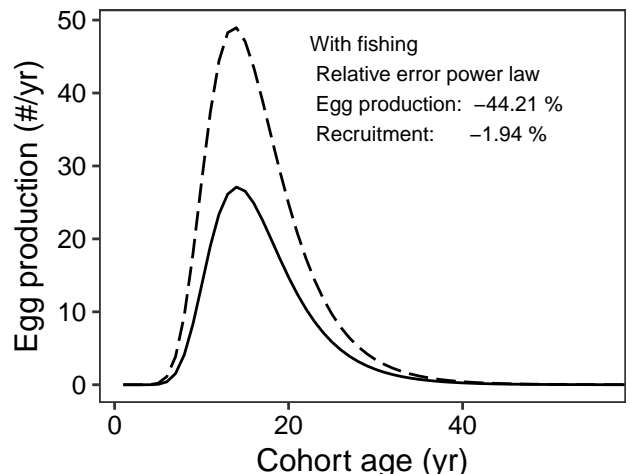
Species: *Sebastodes goodei*
 Location: Magdalena Bay, Baja California, Mexico to Eureka, California, U.S.A.



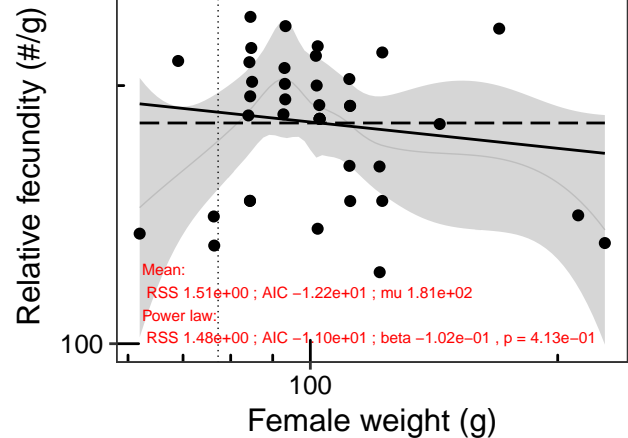
Species: *Sebastodes goodei*
 Location: Magdalena Bay, Baja California, Mexico to Eureka, California, U.S.A.



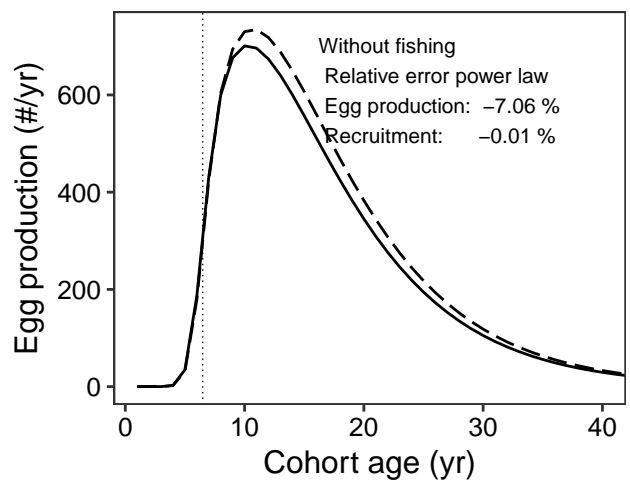
Species: *Sebastodes goodei*
 Location: Magdalena Bay, Baja California, Mexico to Eureka, California, U.S.A.



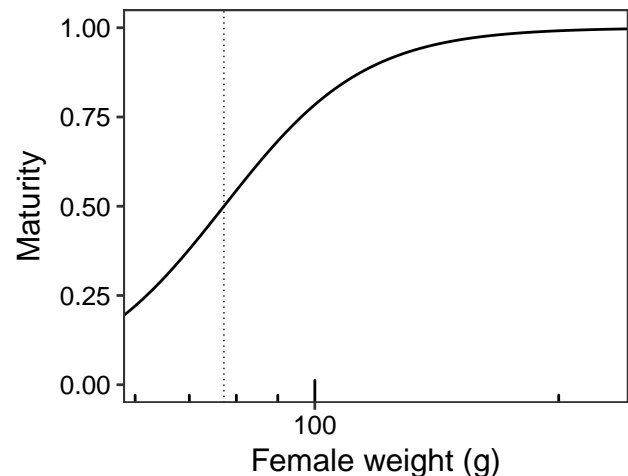
Species: *Sebastodes hopkinsi*
Location: California Bight, California, United States



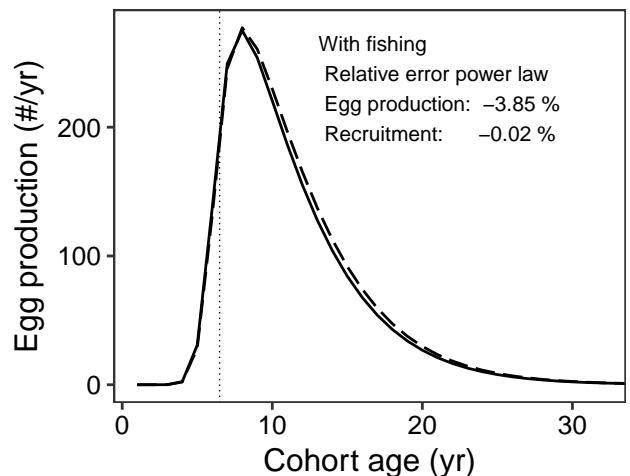
Species: *Sebastodes hopkinsi*
Location: California Bight, California, United States



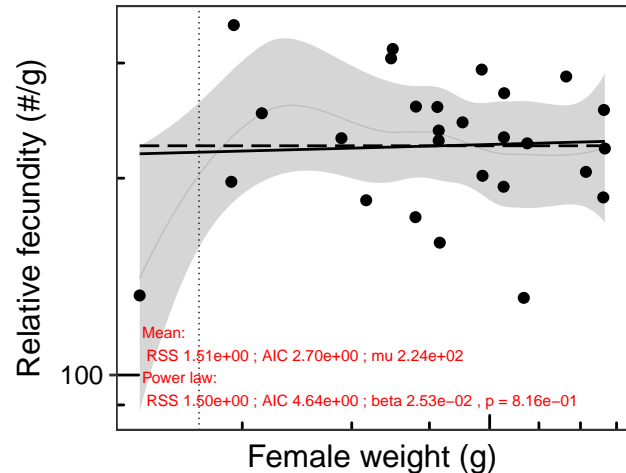
Species: *Sebastodes hopkinsi*
Location: California Bight, California, United States



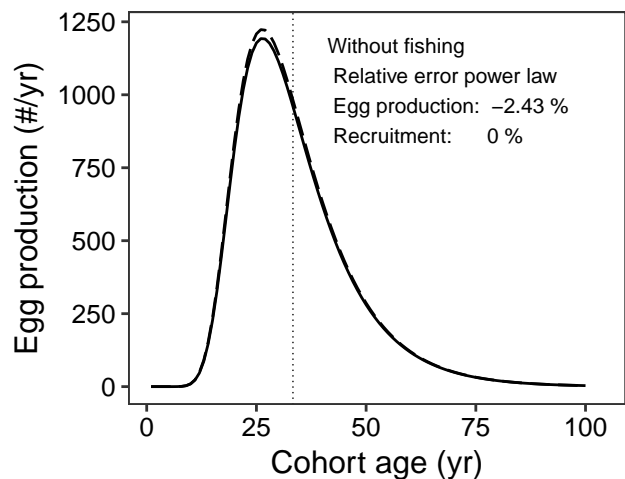
Species: *Sebastodes hopkinsi*
Location: California Bight, California, United States



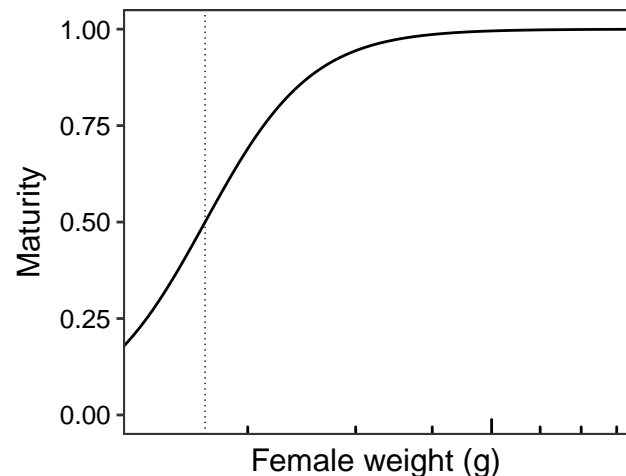
Species: *Sebastodes levis*
Location: California Bight, California, United States



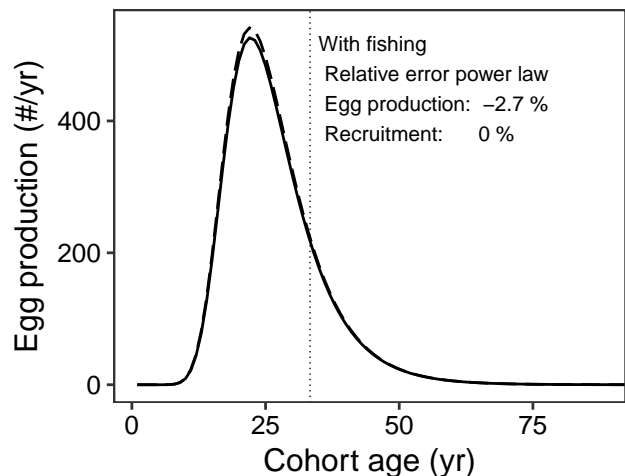
Species: *Sebastodes levis*
Location: California Bight, California, United States



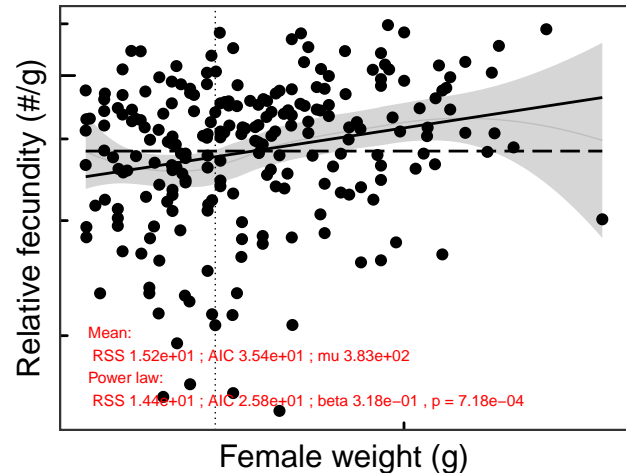
Species: *Sebastodes levis*
Location: California Bight, California, United States



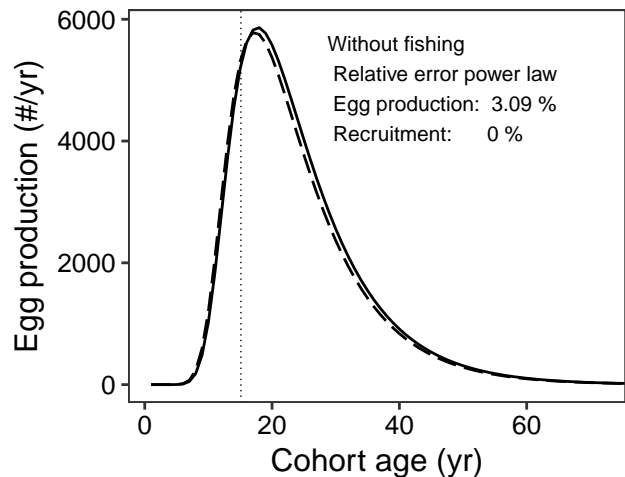
Species: *Sebastodes levis*
Location: California Bight, California, United States



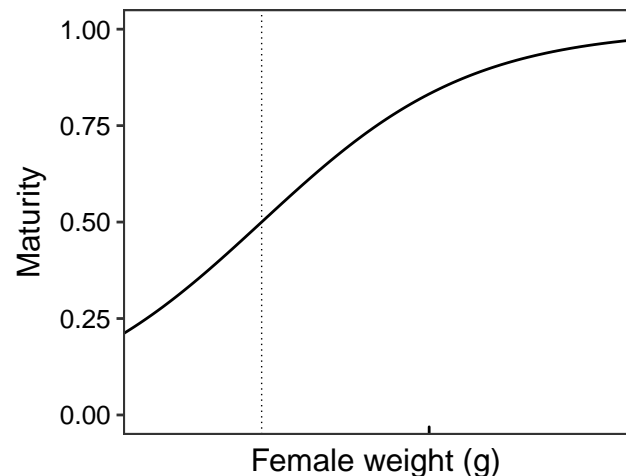
Species: *Sebastodes melanops*
Location: Newport, Oregon, USA



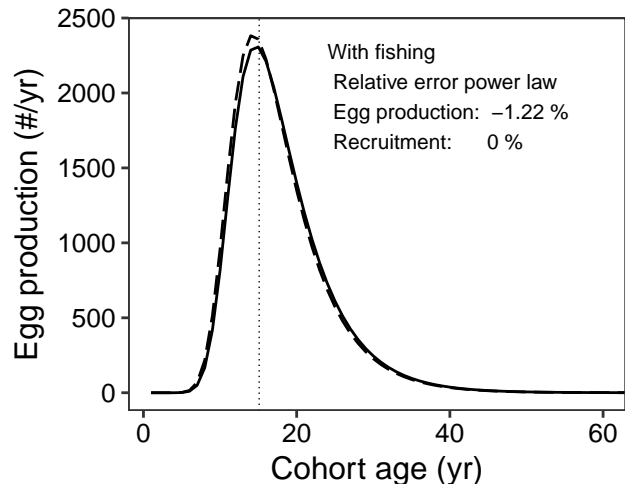
Species: *Sebastodes melanops*
Location: Newport, Oregon, USA



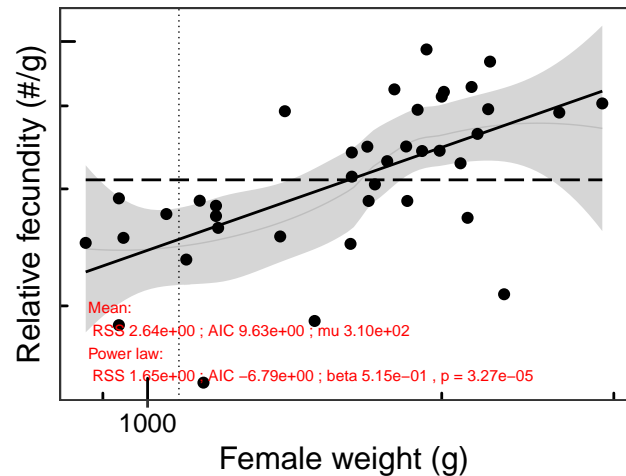
Species: *Sebastodes melanops*
Location: Newport, Oregon, USA



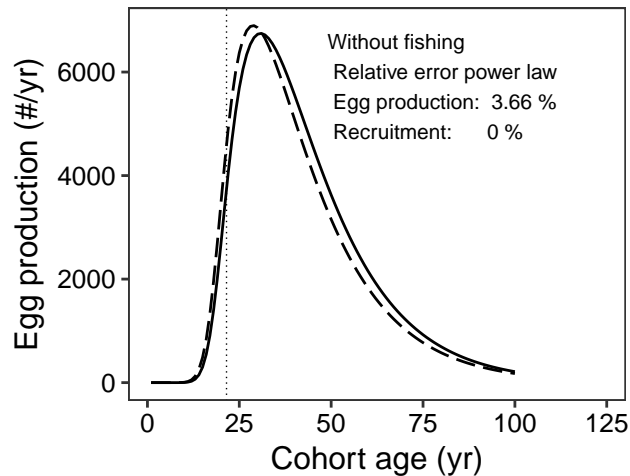
Species: *Sebastodes melanops*
Location: Newport, Oregon, USA



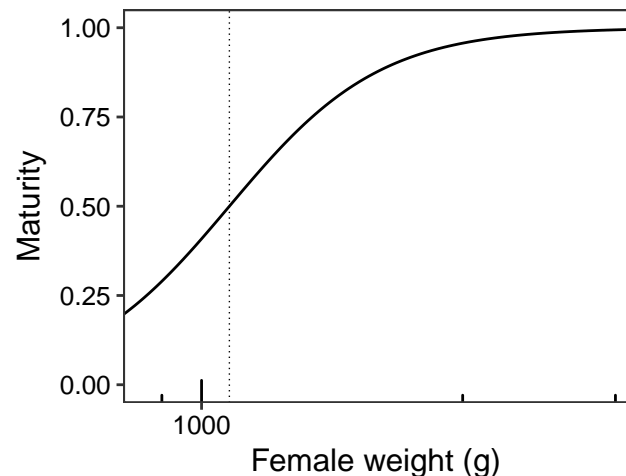
Species: *Sebastodes melanostomus*
Location: Morro Bay, California, United States



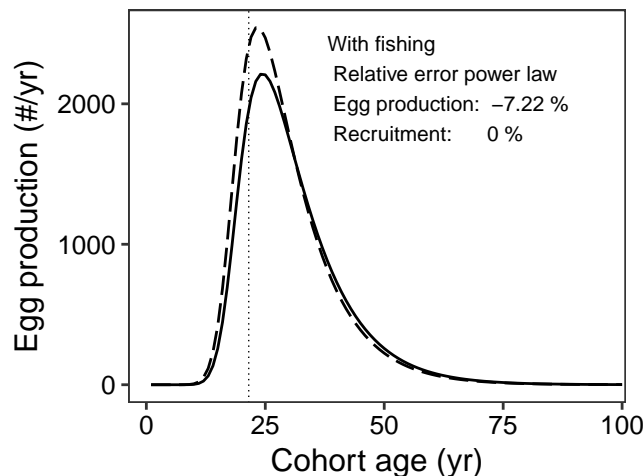
Species: *Sebastodes melanostomus*
Location: Morro Bay, California, United States



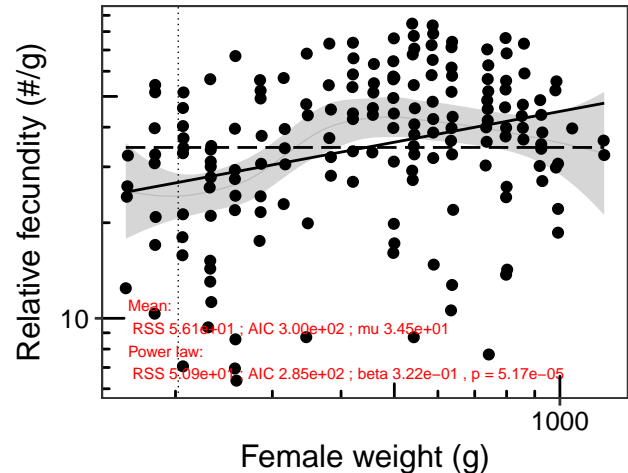
Species: *Sebastodes melanostomus*
Location: Morro Bay, California, United States



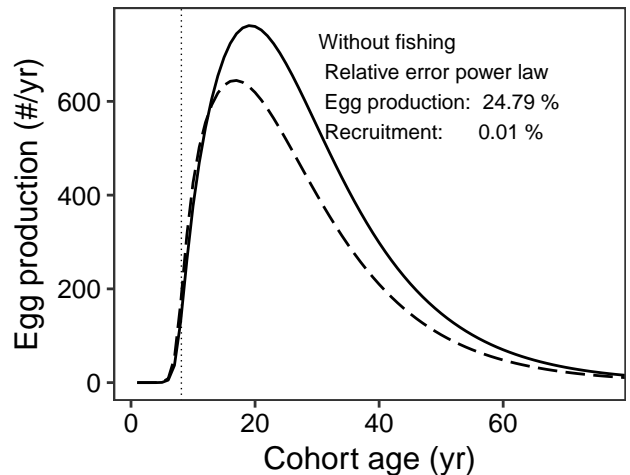
Species: *Sebastodes melanostomus*
Location: Morro Bay, California, United States



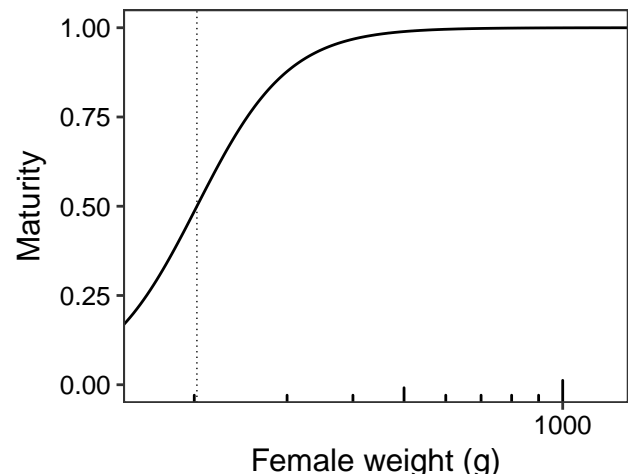
Species: *Sebastodes mentella*
 Location: Gulf of St. Lawrence, Laurentian Channel and Esquiman Channel



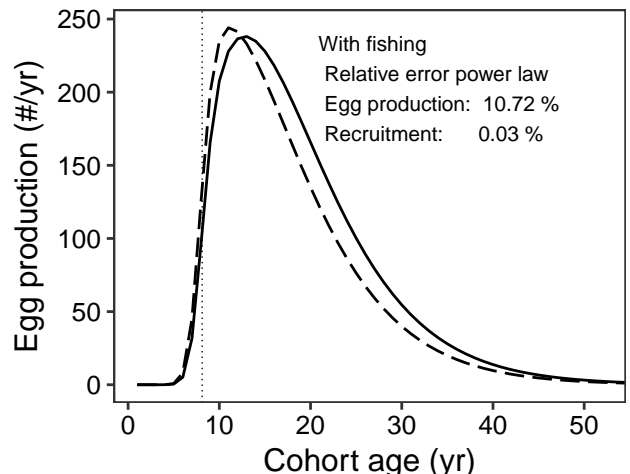
Species: *Sebastodes mentella*
 Location: Gulf of St. Lawrence, Laurentian Channel and Esquiman Chann



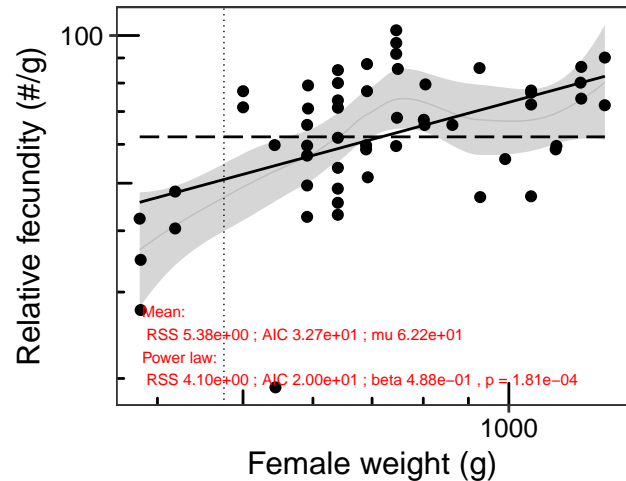
Species: *Sebastodes mentella*
 Location: Gulf of St. Lawrence, Laurentian Channel and Esquiman Chan



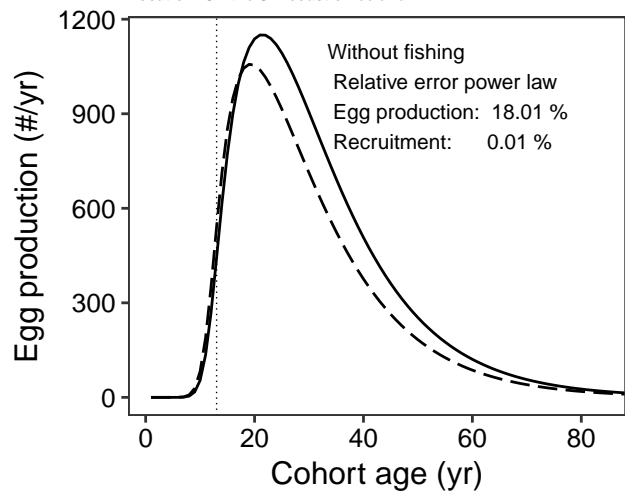
Species: *Sebastodes mentella*
 Location: Gulf of St. Lawrence, Laurentian Channel and Esquiman Chann



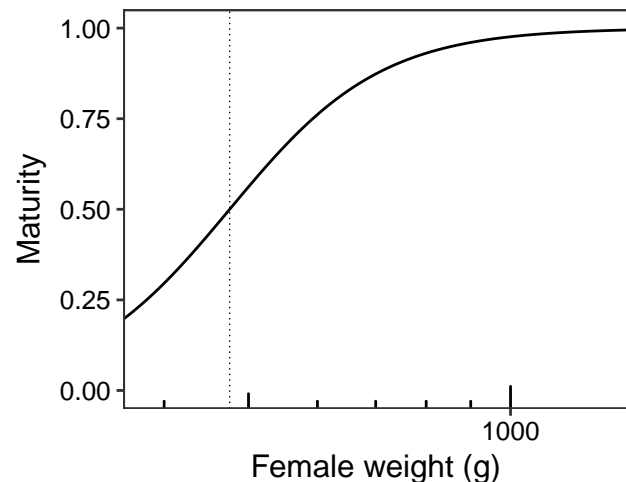
Species: *Sebastodes mentella*
Location: Off the SW coast of Iceland



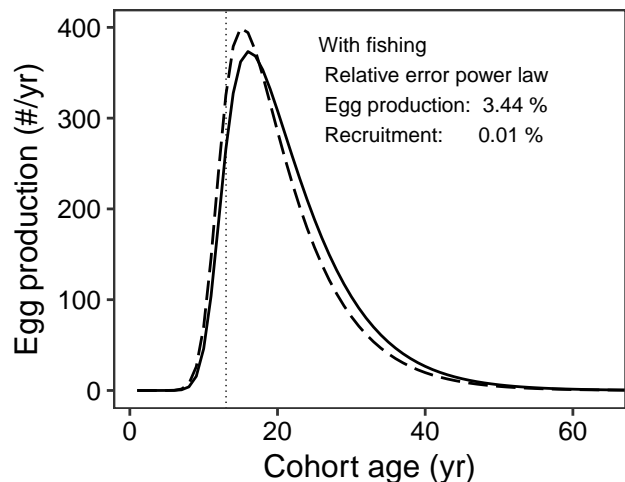
Species: *Sebastodes mentella*
Location: Off the SW coast of Iceland



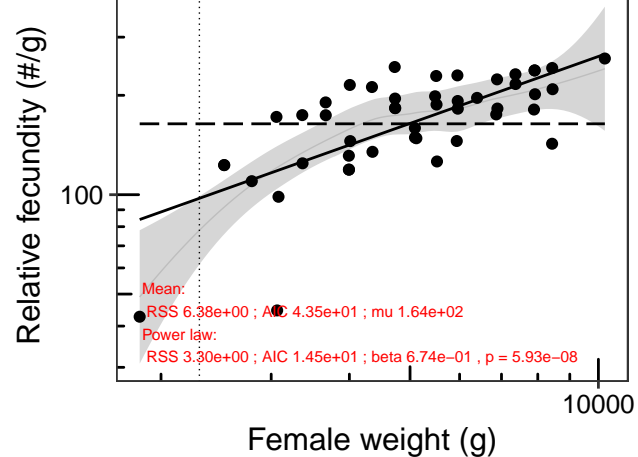
Species: *Sebastodes mentella*
Location: Off the SW coast of Iceland



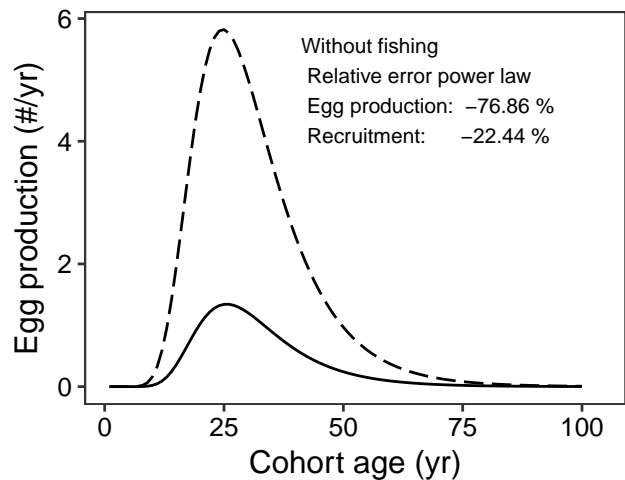
Species: *Sebastodes mentella*
Location: Off the SW coast of Iceland



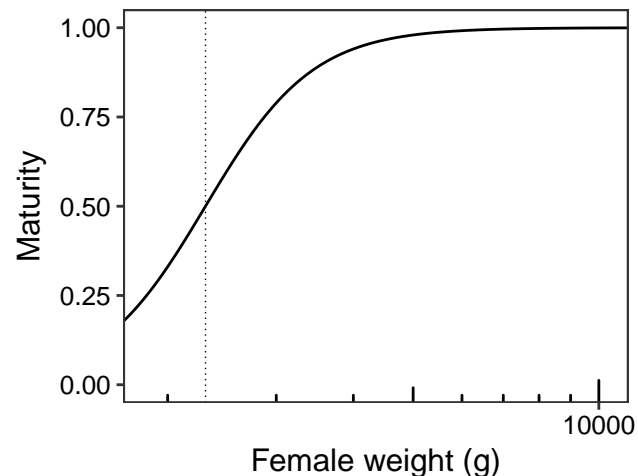
Species: *Sebastodes miniatus*
Location: California Bight, California, United States



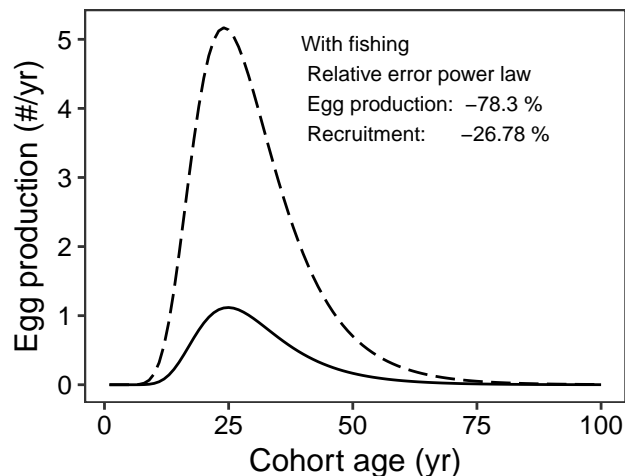
Species: *Sebastodes miniatus*
Location: California Bight, California, United States



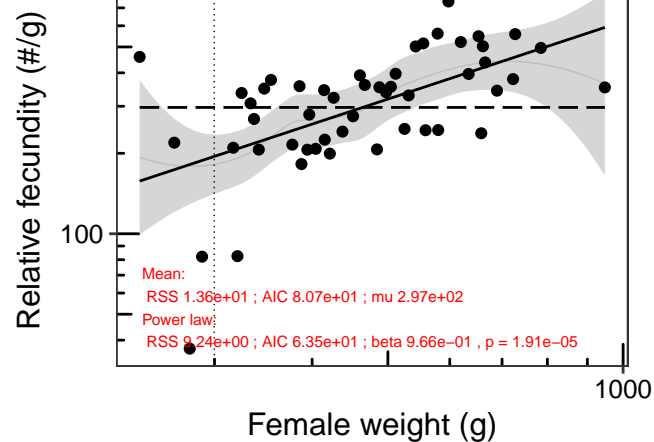
Species: *Sebastodes miniatus*
Location: California Bight, California, United States



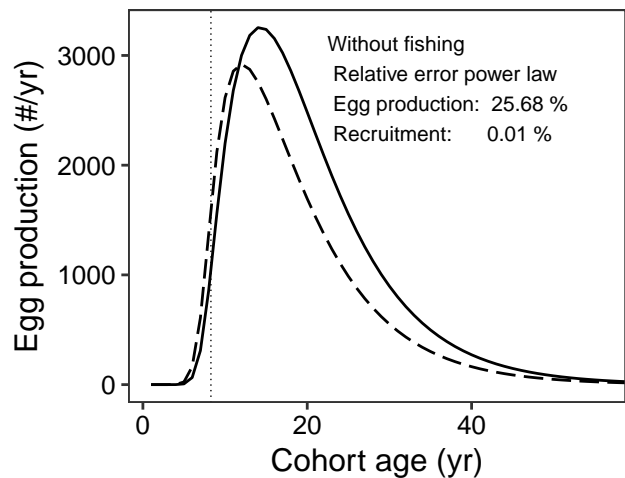
Species: *Sebastodes miniatus*
Location: California Bight, California, United States



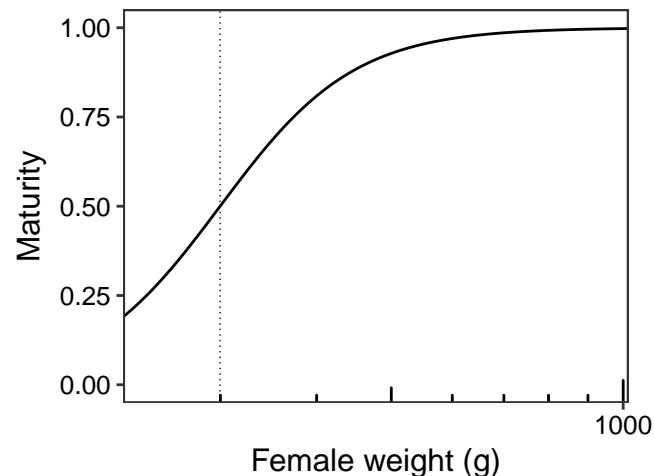
Species: *Sebastodes mystinus*
Location: Monterey, California, United States



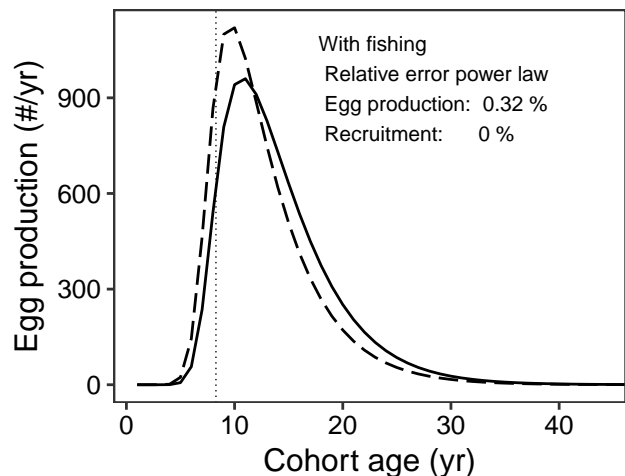
Species: *Sebastodes mystinus*
Location: Monterey, California, United States



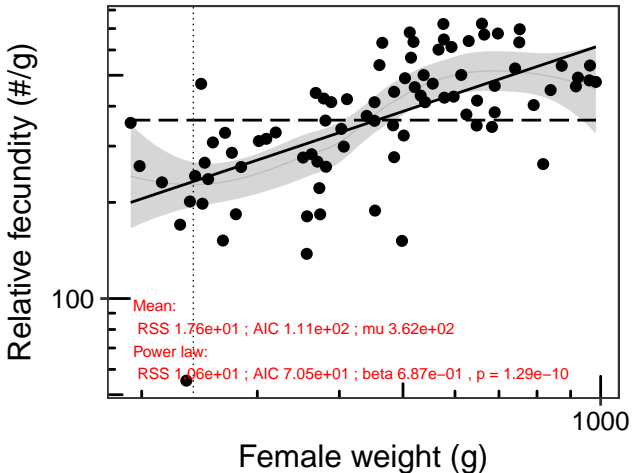
Species: *Sebastodes mystinus*
Location: Monterey, California, United States



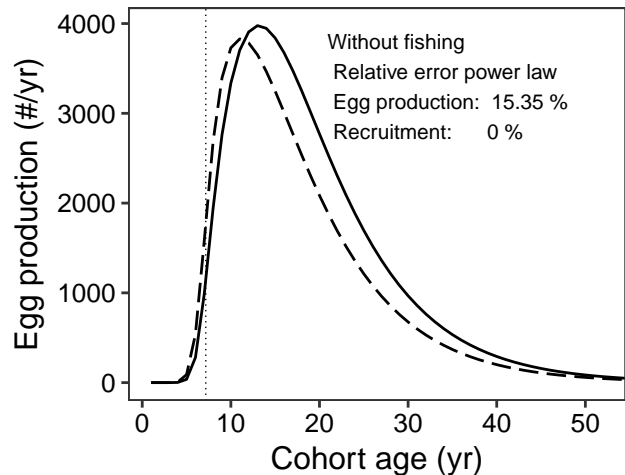
Species: *Sebastodes mystinus*
Location: Monterey, California, United States



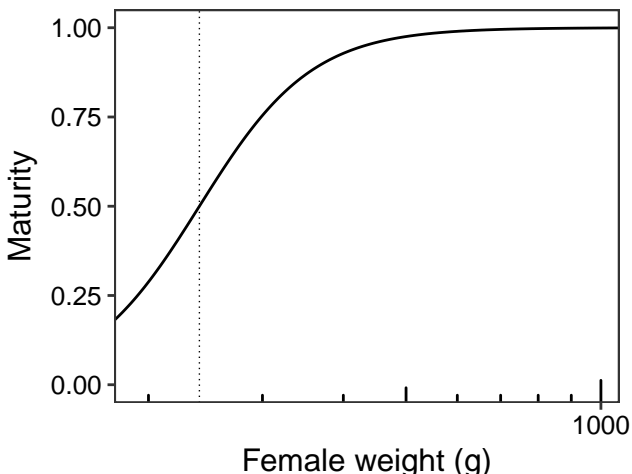
Species: *Sebastodes mystinus*
 Location: Half Moon Bay and Morro Bay, California, United States



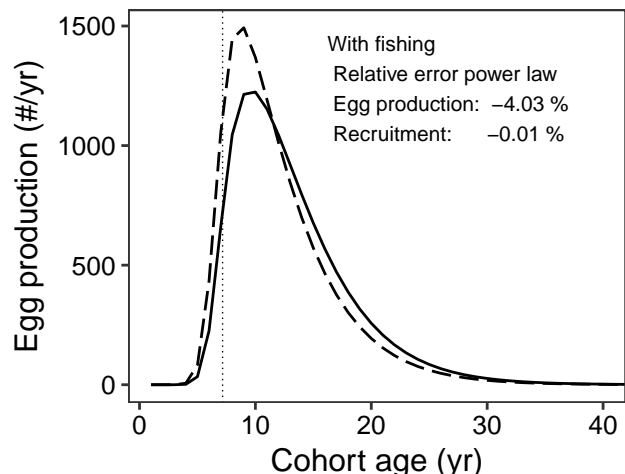
Species: *Sebastodes mystinus*
 Location: Half Moon Bay and Morro Bay, California, United States



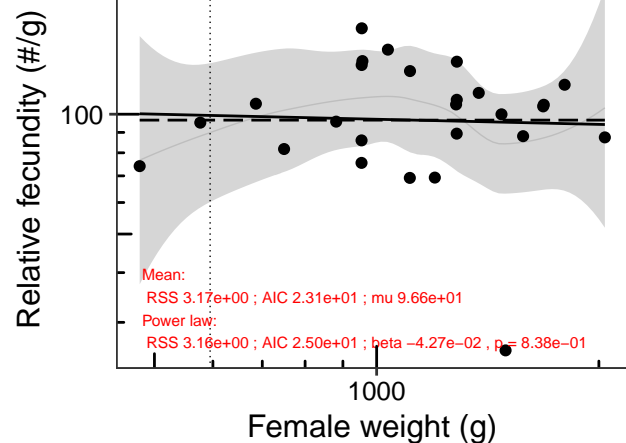
Species: *Sebastodes mystinus*
 Location: Half Moon Bay and Morro Bay, California, United States



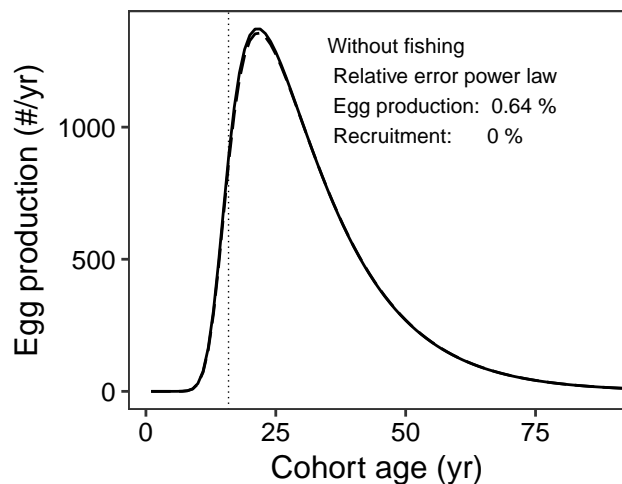
Species: *Sebastodes mystinus*
 Location: Half Moon Bay and Morro Bay, California, United States



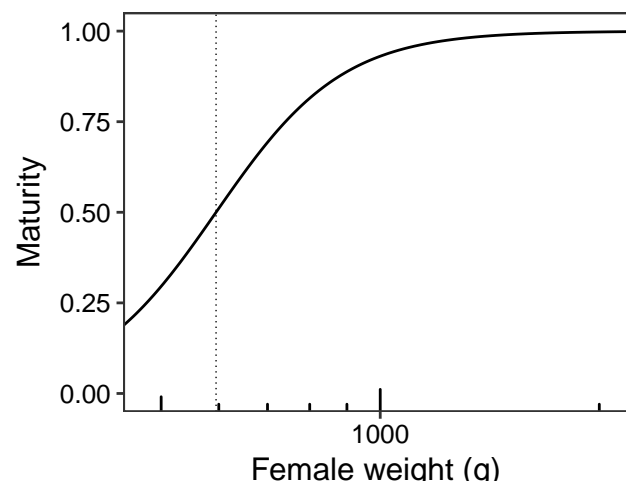
Species: *Sebastes norvegicus*
Location: Off the SW coast of Iceland



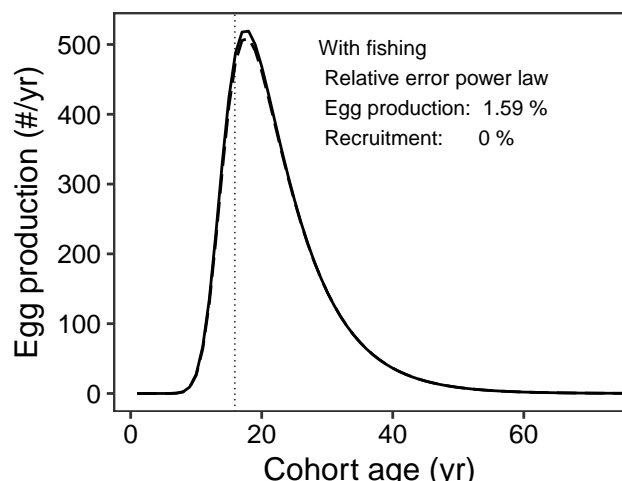
Species: *Sebastes norvegicus*
Location: Off the SW coast of Iceland



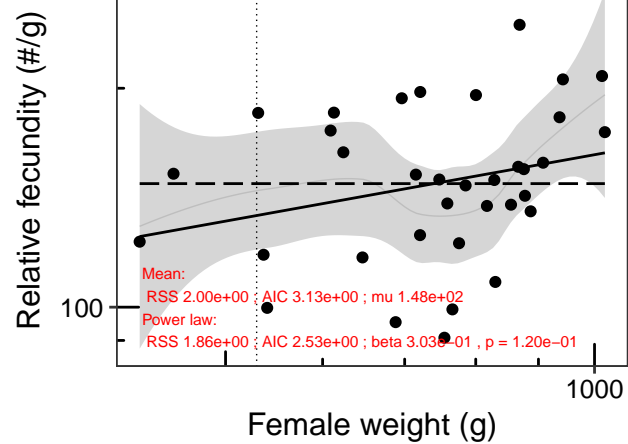
Species: *Sebastes norvegicus*
Location: Off the SW coast of Iceland



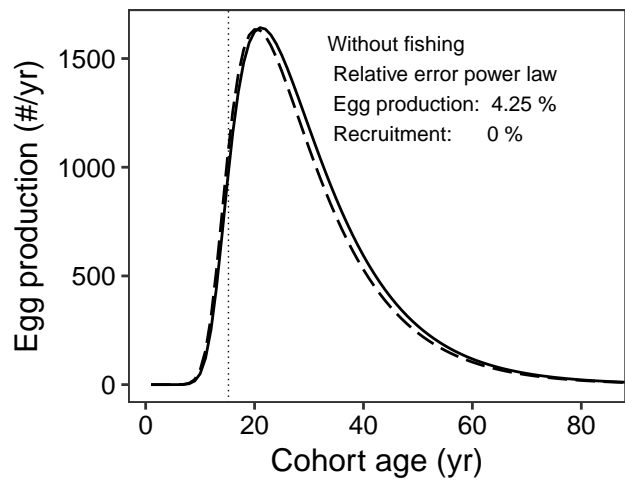
Species: *Sebastes norvegicus*
Location: Off the SW coast of Iceland



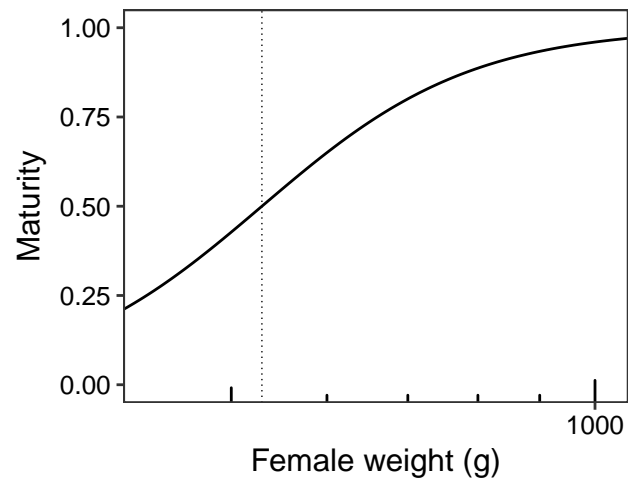
Species: *Sebastodes ovalis*
Location: Cordell Bank, California, United States



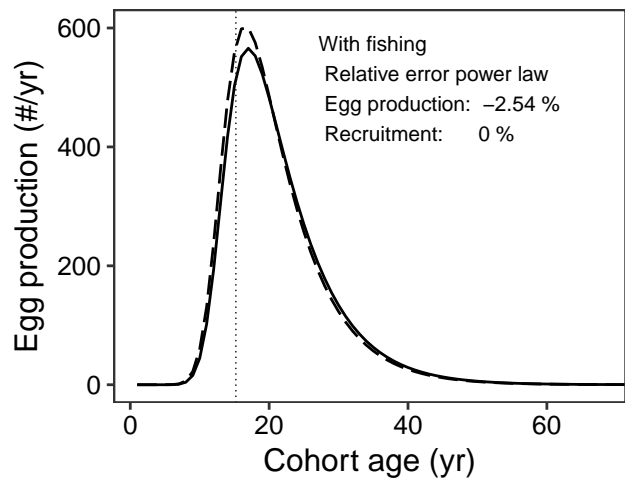
Species: *Sebastodes ovalis*
Location: Cordell Bank, California, United States



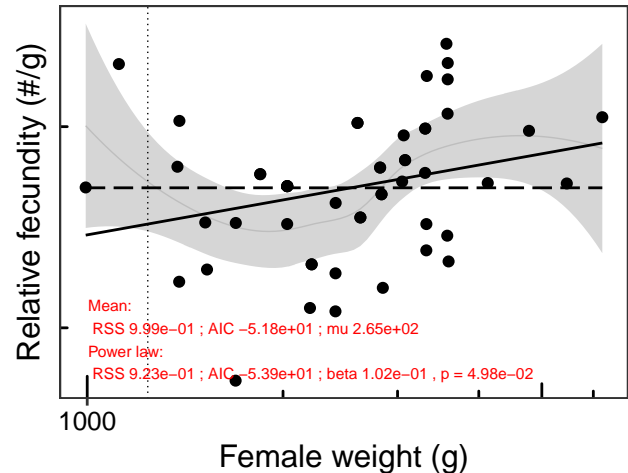
Species: *Sebastodes ovalis*
Location: Cordell Bank, California, United States



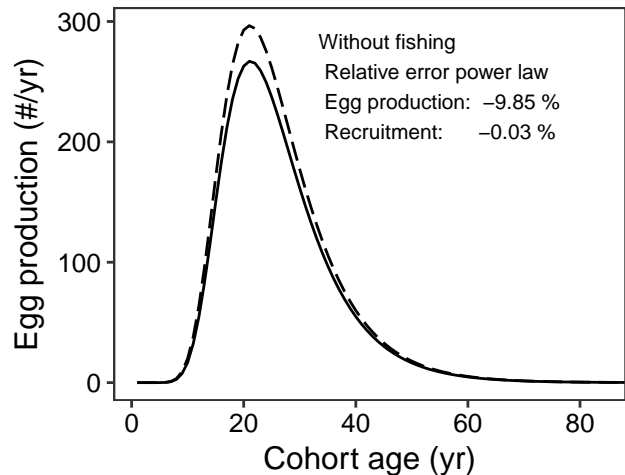
Species: *Sebastodes ovalis*
Location: Cordell Bank, California, United States



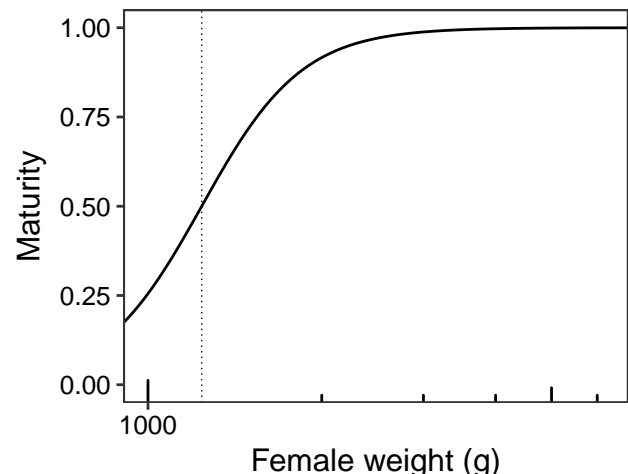
Species: *Sebastodes paucispinis*
Location: California Bight, California, United States



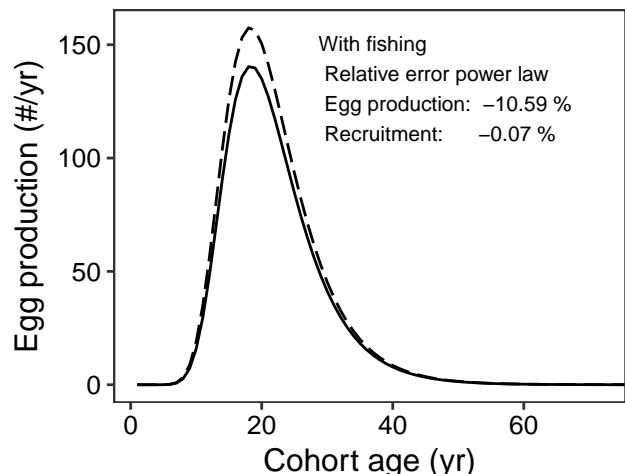
Species: *Sebastodes paucispinis*
Location: California Bight, California, United States



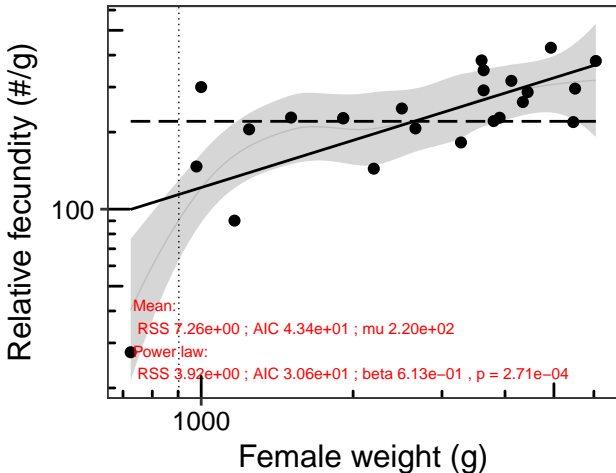
Species: *Sebastodes paucispinis*
Location: California Bight, California, United States



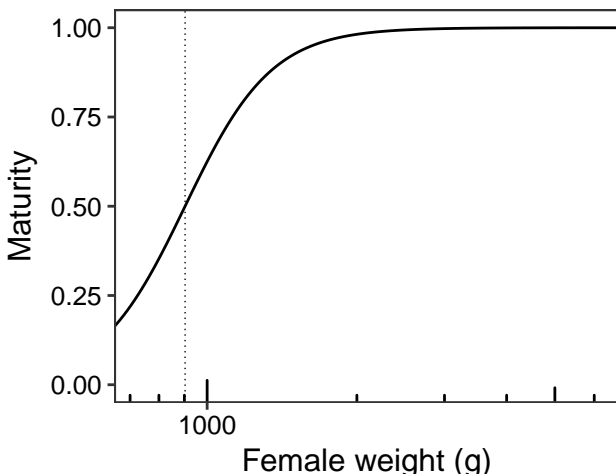
Species: *Sebastodes paucispinis*
Location: California Bight, California, United States



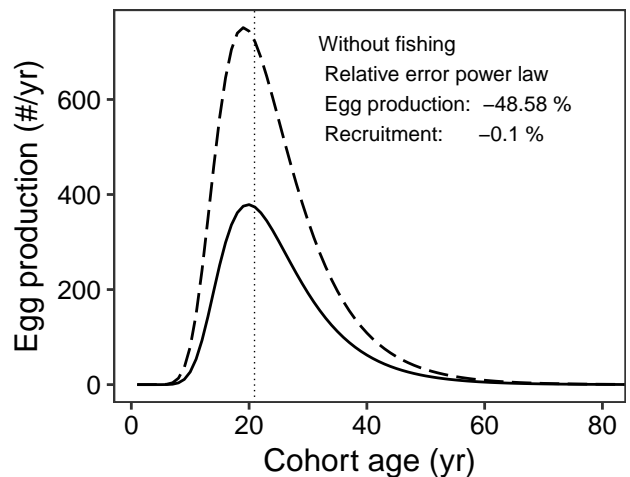
Species: *Sebastodes paucispinis*
Location: Sacramento Reef, Baja California, Mexico to Queen Charlotte S



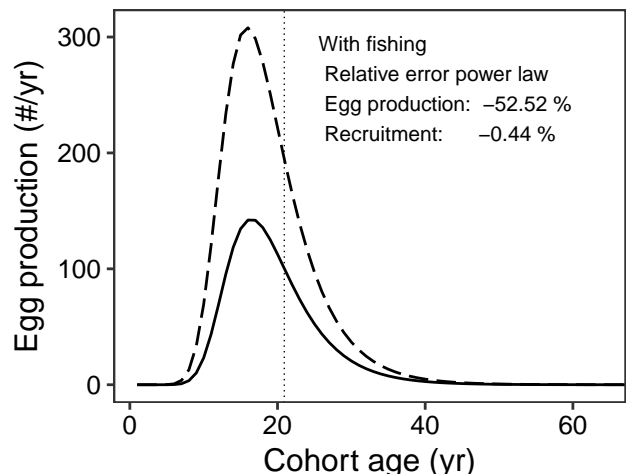
Species: *Sebastodes paucispinis*
Location: Sacramento Reef, Baja California, Mexico to Queen Charlotte S



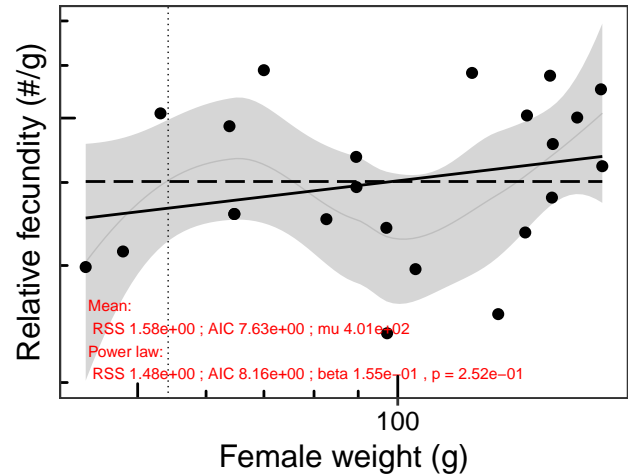
Species: *Sebastodes paucispinis*
Location: Sacramento Reef, Baja California, Mexico to Queen Charlotte S



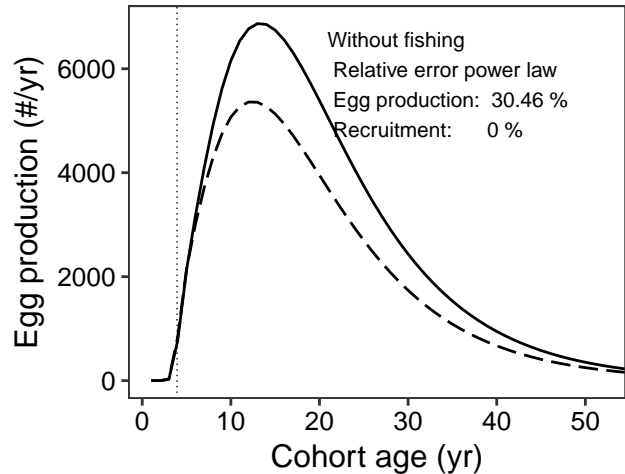
Species: *Sebastodes paucispinis*
Location: Sacramento Reef, Baja California, Mexico to Queen Charlotte S



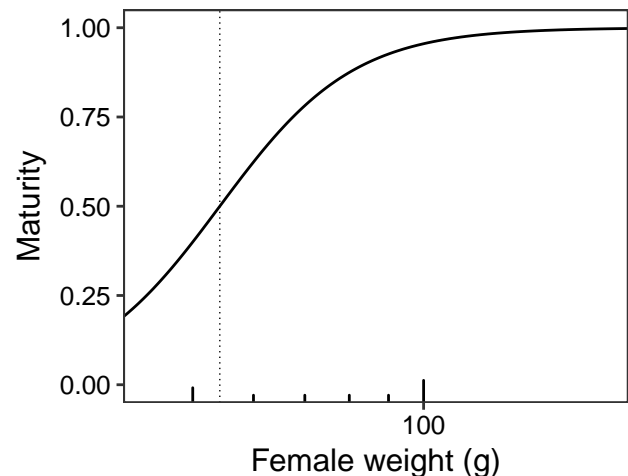
Species: *Sebastodes rosaceus*
Location: California Bight, California, United States



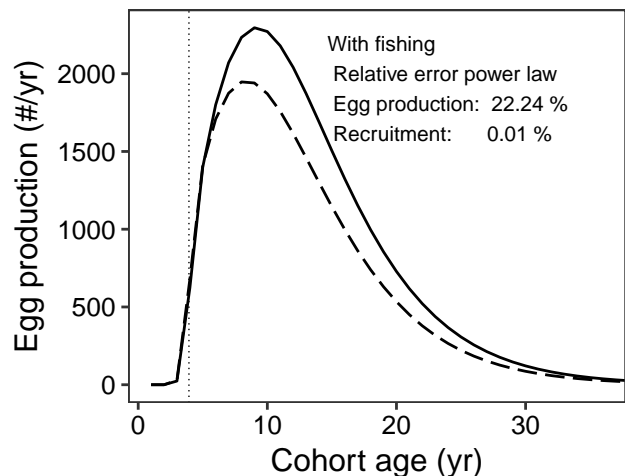
Species: *Sebastodes rosaceus*
Location: California Bight, California, United States



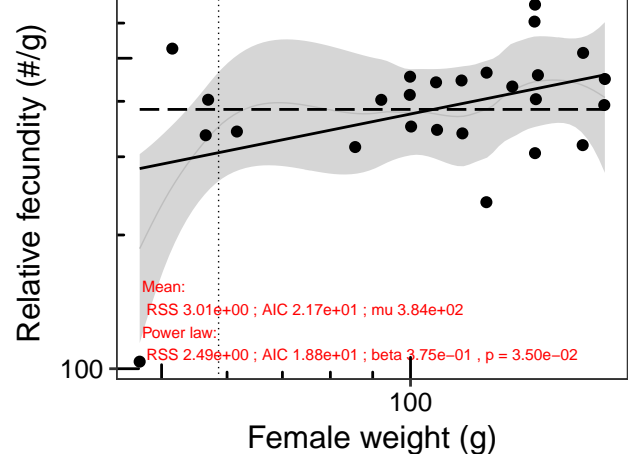
Species: *Sebastodes rosaceus*
Location: California Bight, California, United States



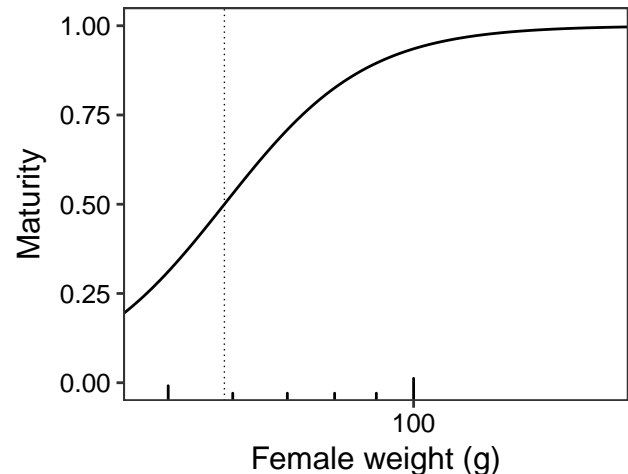
Species: *Sebastodes rosaceus*
Location: California Bight, California, United States



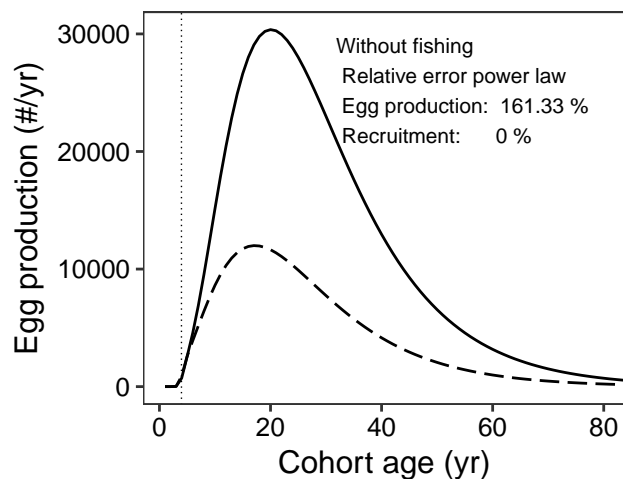
Species: *Sebastodes rosenblatti*
Location: California Bight, California, United States



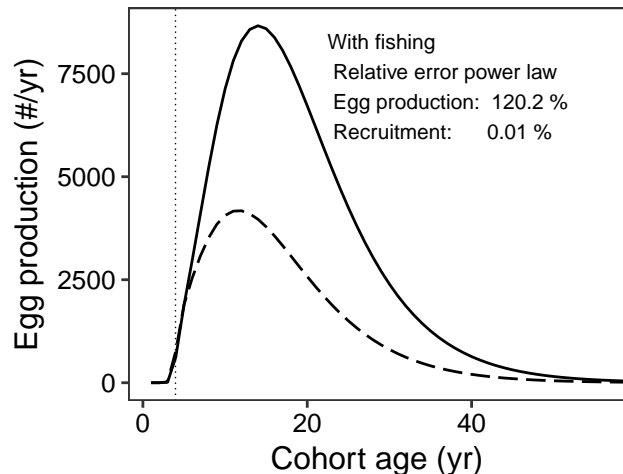
Species: *Sebastodes rosenblatti*
Location: California Bight, California, United States



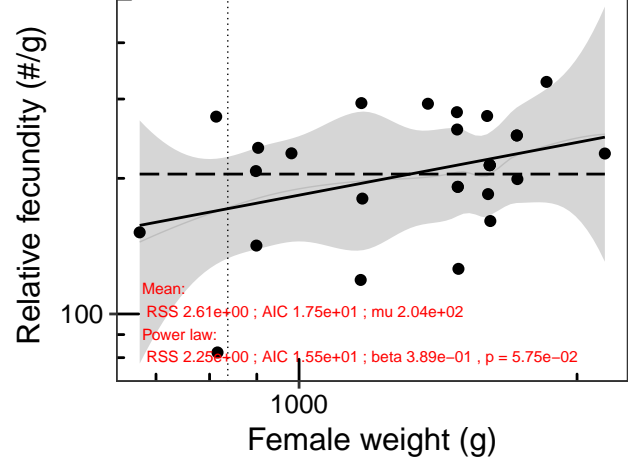
Species: *Sebastodes rosenblatti*
Location: California Bight, California, United States



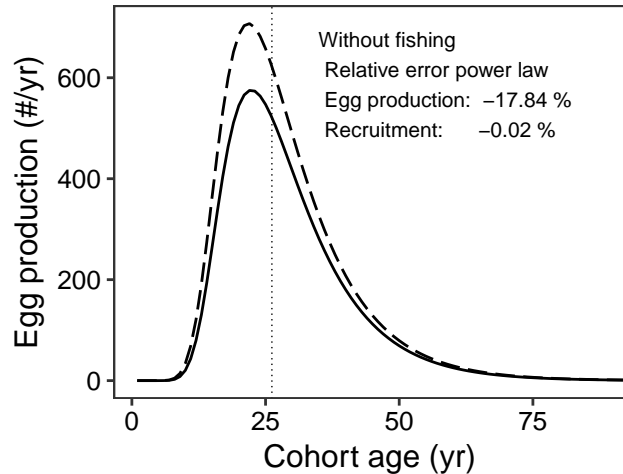
Species: *Sebastodes rosenblatti*
Location: California Bight, California, United States



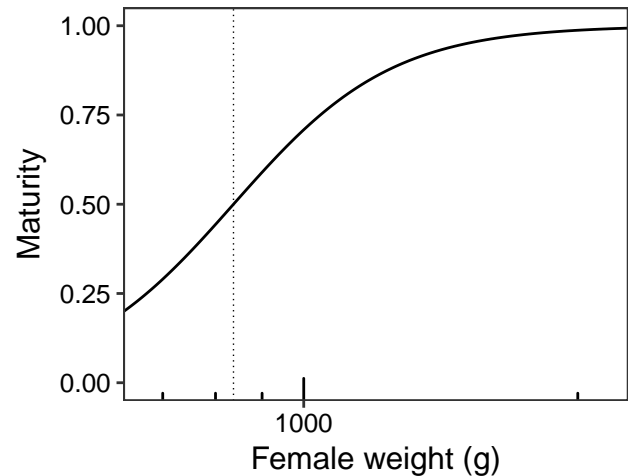
Species: *Sebastodes rufus*
Location: California Bight, California, United States



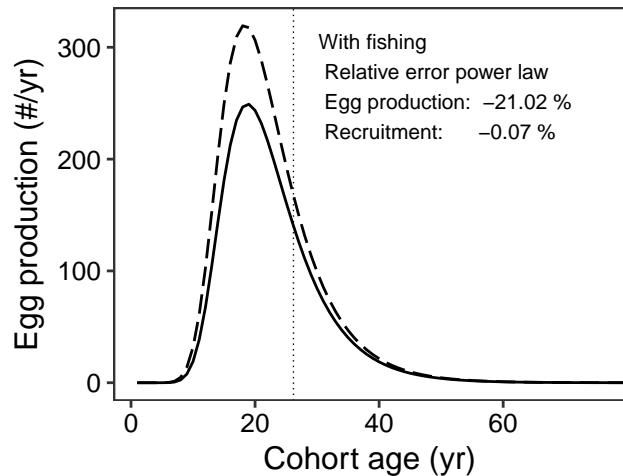
Species: *Sebastodes rufus*
Location: California Bight, California, United States



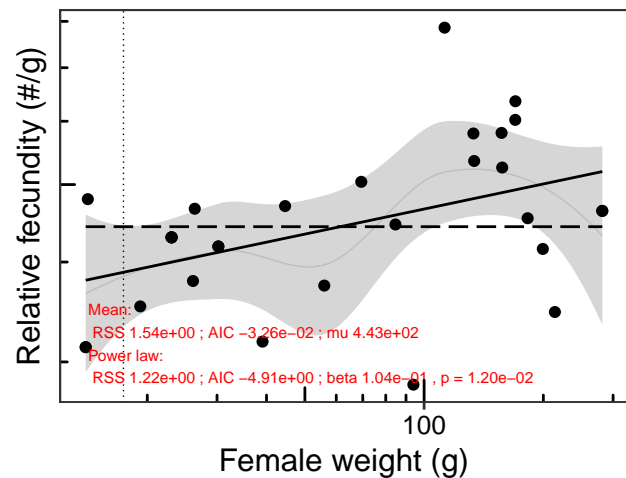
Species: *Sebastodes rufus*
Location: California Bight, California, United States



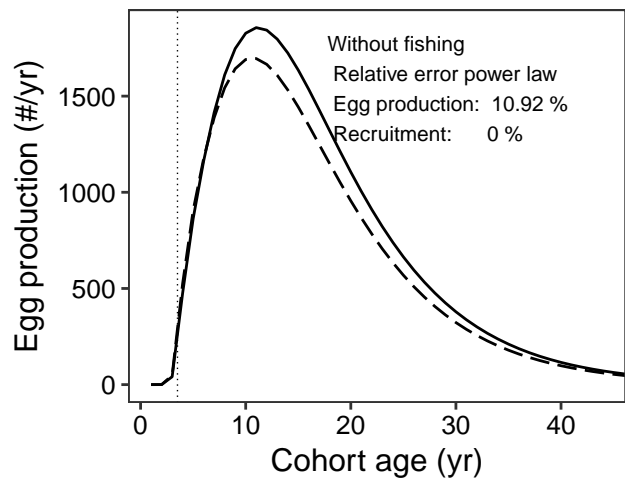
Species: *Sebastodes rufus*
Location: California Bight, California, United States



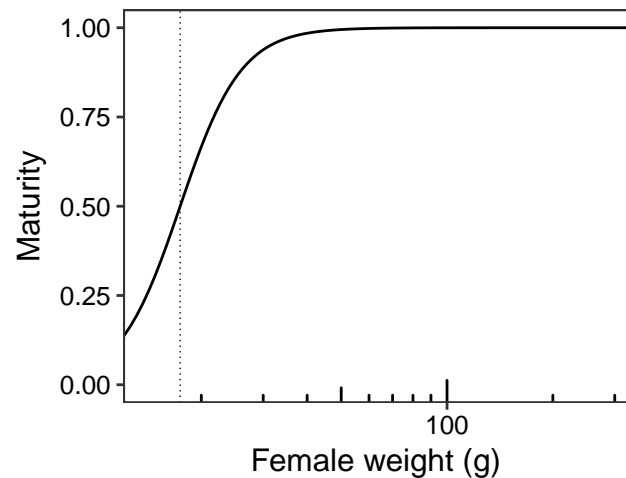
Species: *Sebastodes saxicola*
Location: California Bight, California, United States



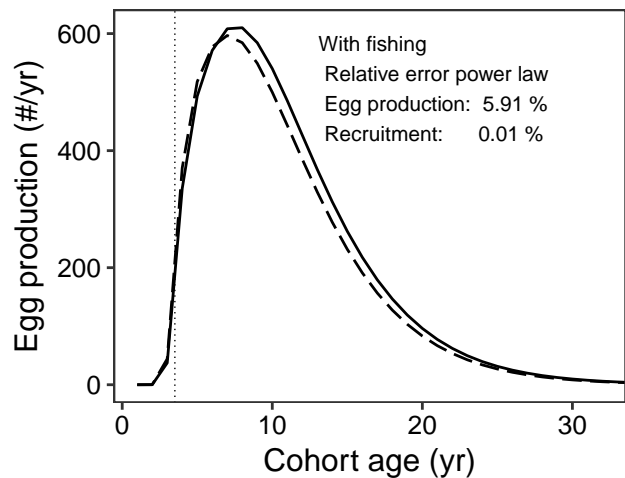
Species: *Sebastodes saxicola*
Location: California Bight, California, United States



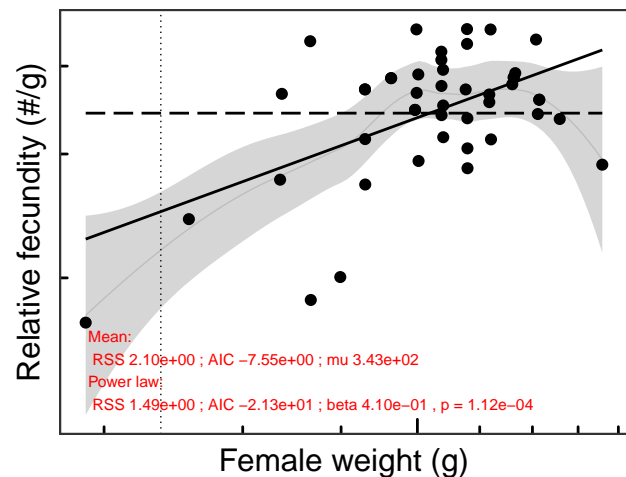
Species: *Sebastodes saxicola*
Location: California Bight, California, United States



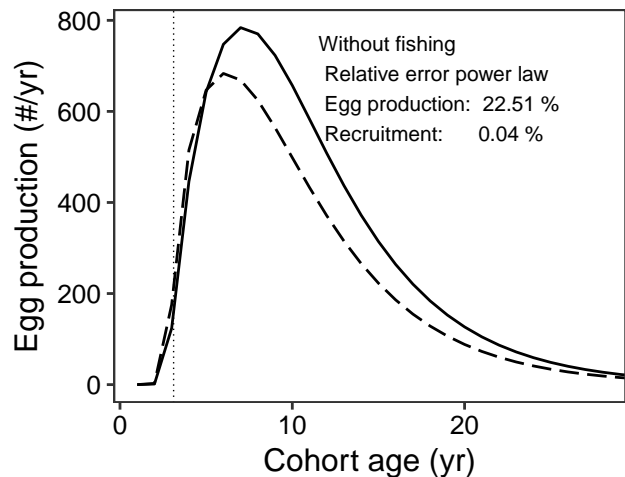
Species: *Sebastodes saxicola*
Location: California Bight, California, United States



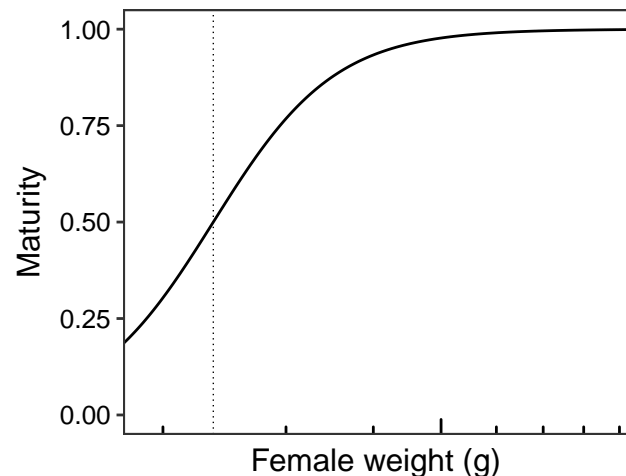
Species: *Sebastodes semicinctus*
Location: California Bight, California, United States



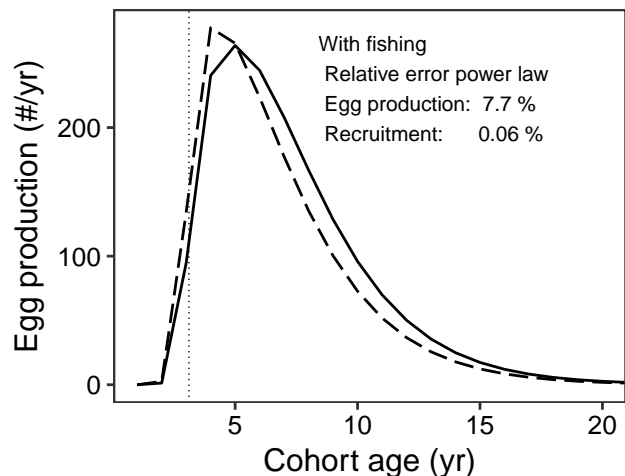
Species: *Sebastodes semicinctus*
Location: California Bight, California, United States



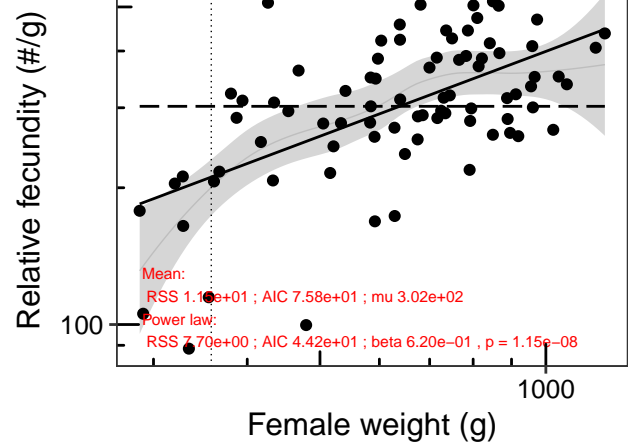
Species: *Sebastodes semicinctus*
Location: California Bight, California, United States



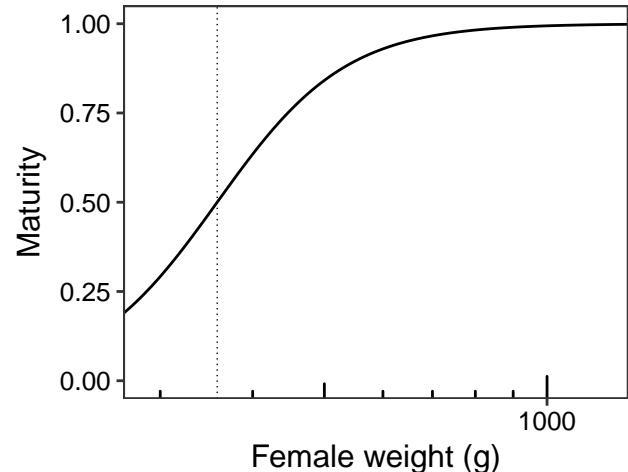
Species: *Sebastodes semicinctus*
Location: California Bight, California, United States



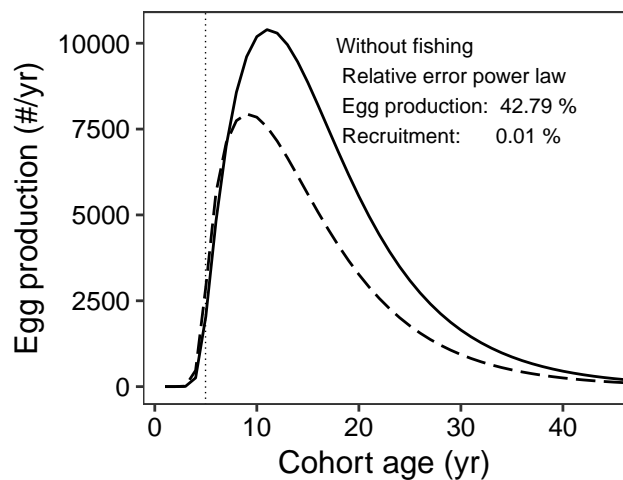
Species: *Sebastodes serranoides*
Location: Avila, California, United States



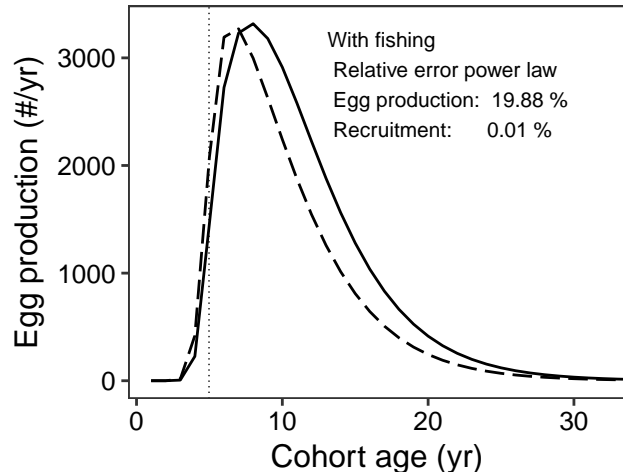
Species: *Sebastodes serranoides*
Location: Avila, California, United States



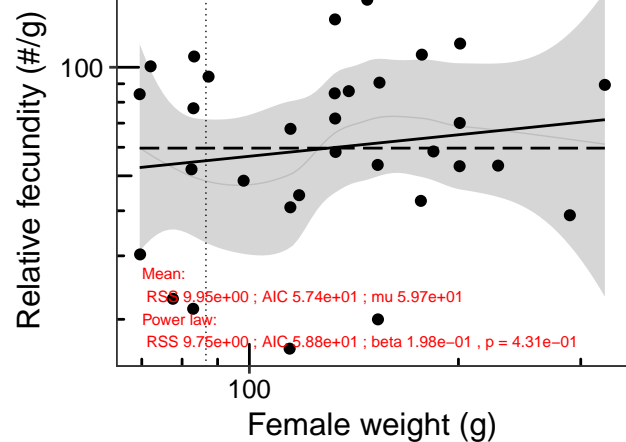
Species: *Sebastodes serranoides*
Location: Avila, California, United States



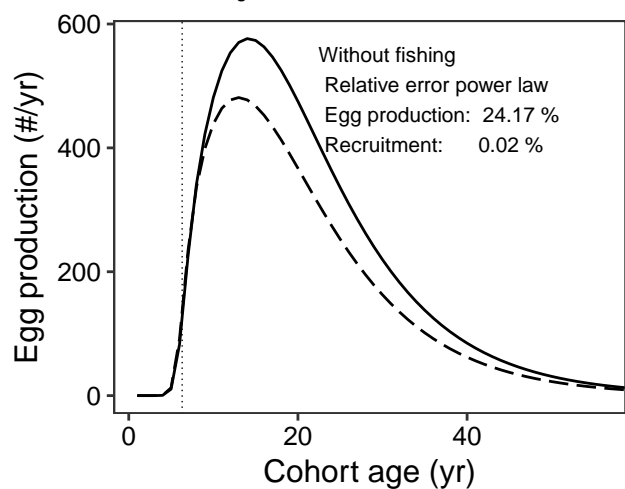
Species: *Sebastodes serranoides*
Location: Avila, California, United States



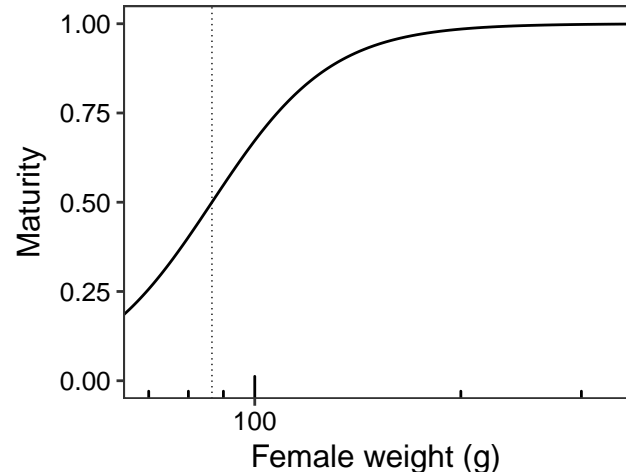
Species: *Sebastes viviparus*
Location: Norwegian and Barent seas



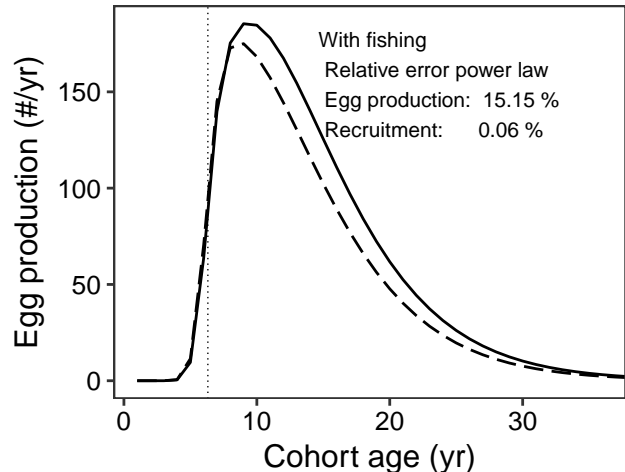
Species: *Sebastes viviparus*
Location: Norwegian and Barent seas

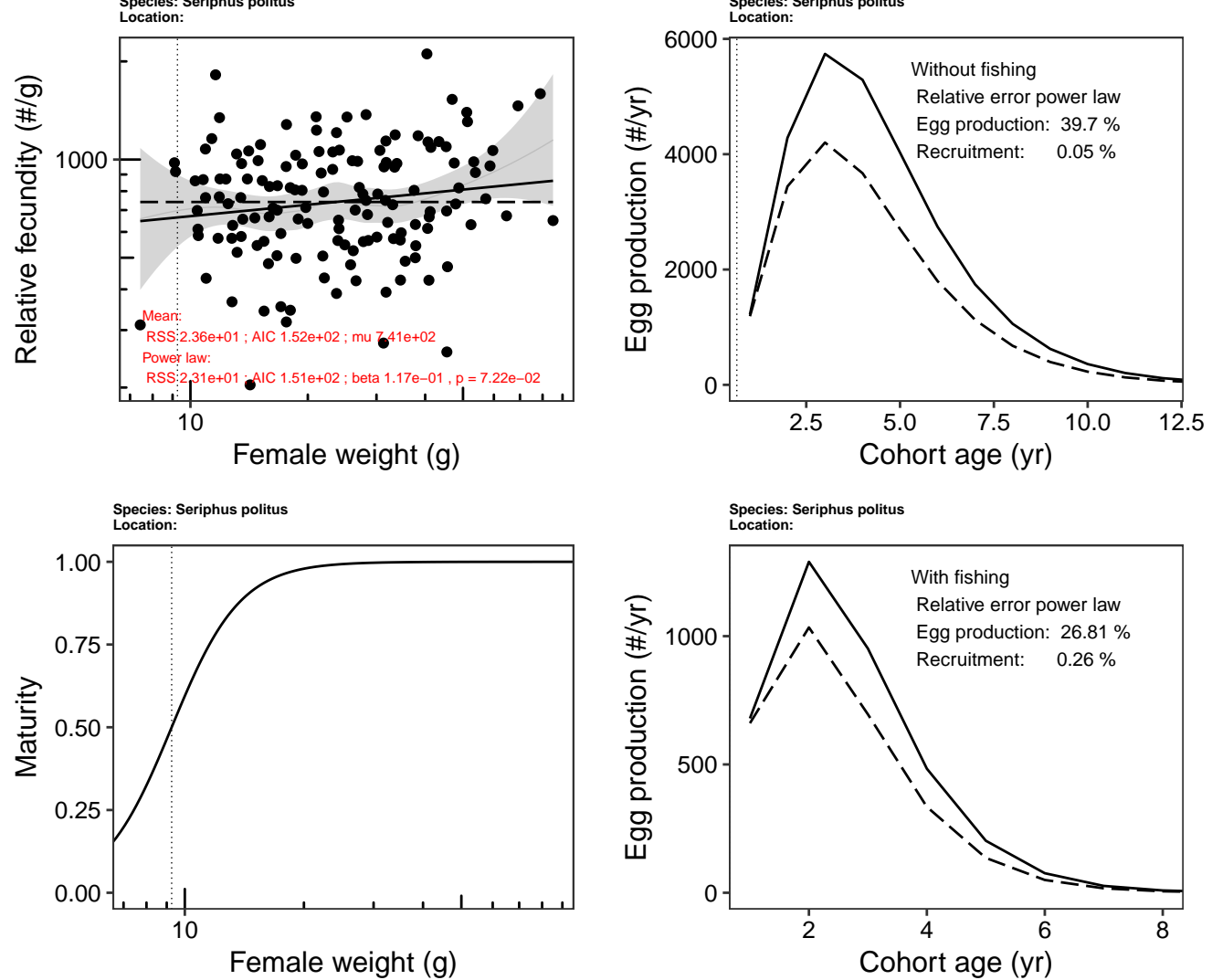


Species: *Sebastes viviparus*
Location: Norwegian and Barent seas

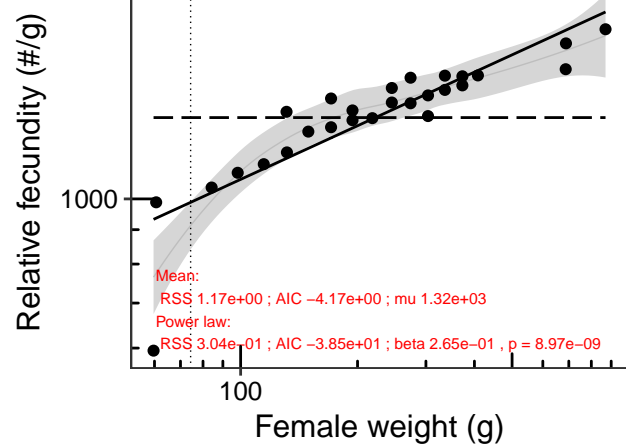


Species: *Sebastes viviparus*
Location: Norwegian and Barent seas

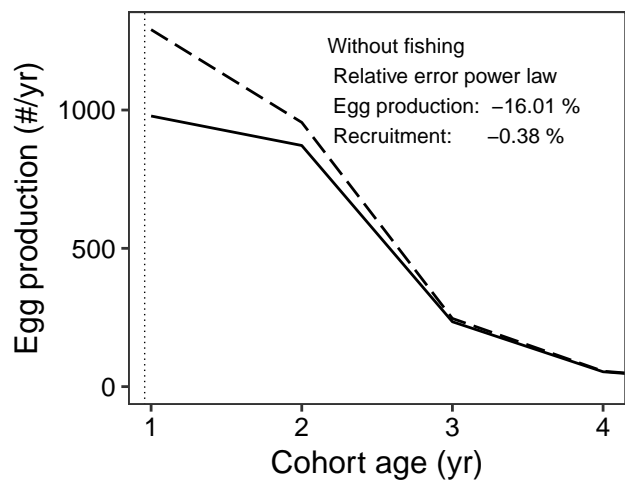




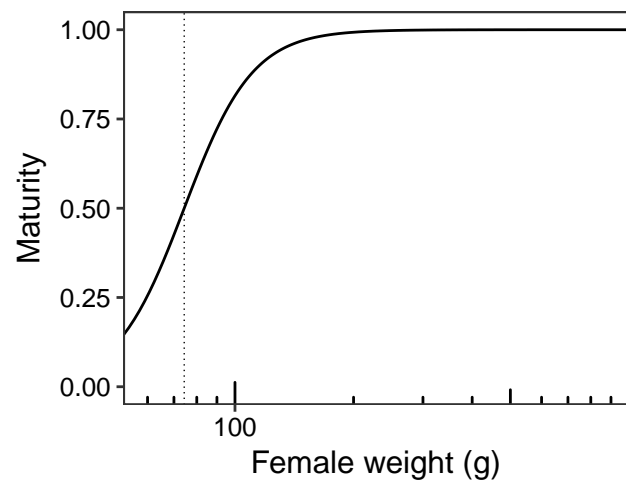
Species: *Siganus canaliculatus*
Location: Off Dammam, Saudi Arabia



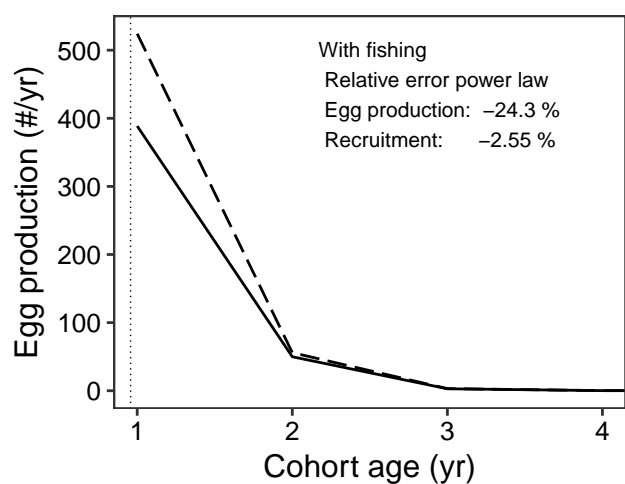
Species: *Siganus canaliculatus*
Location: Off Dammam, Saudi Arabia



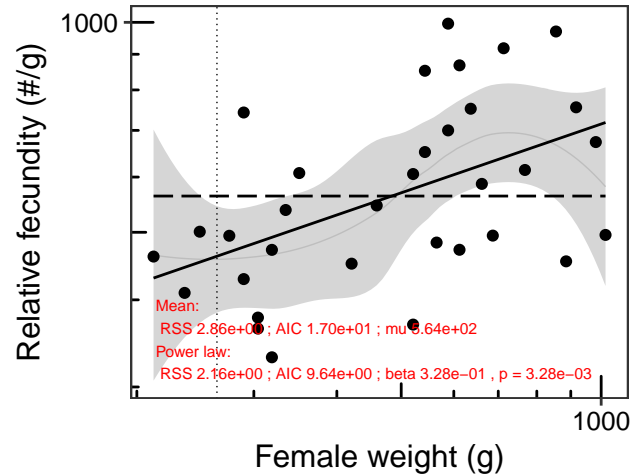
Species: *Siganus canaliculatus*
Location: Off Dammam, Saudi Arabia



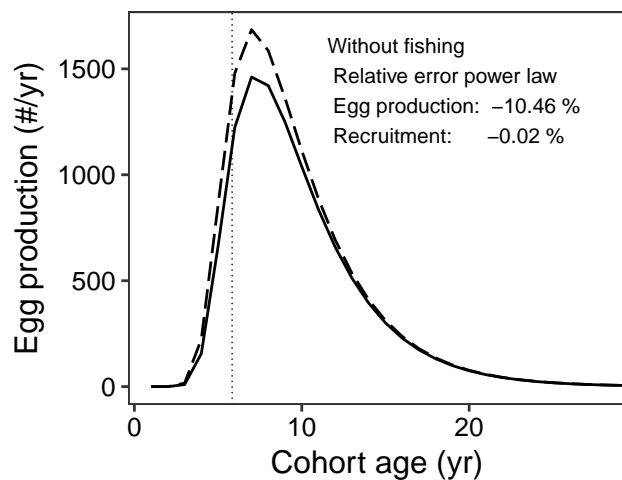
Species: *Siganus canaliculatus*
Location: Off Dammam, Saudi Arabia



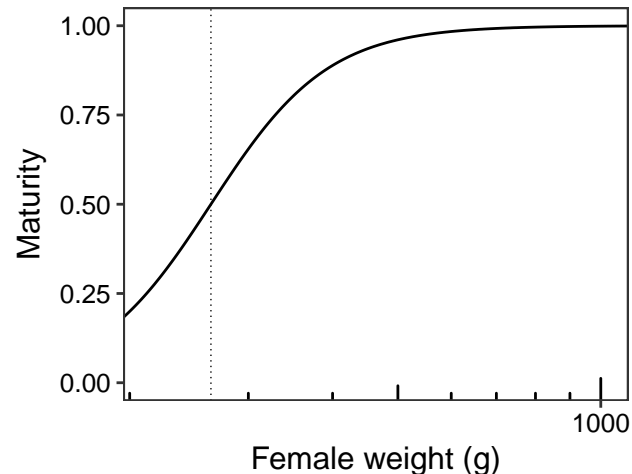
Species: *Solea solea*
Location: European Continental Shelf Area IXa



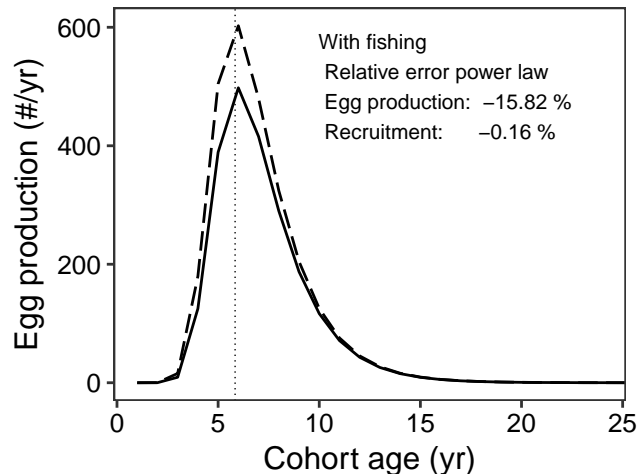
Species: *Solea solea*
Location: European Continental Shelf Area IXa



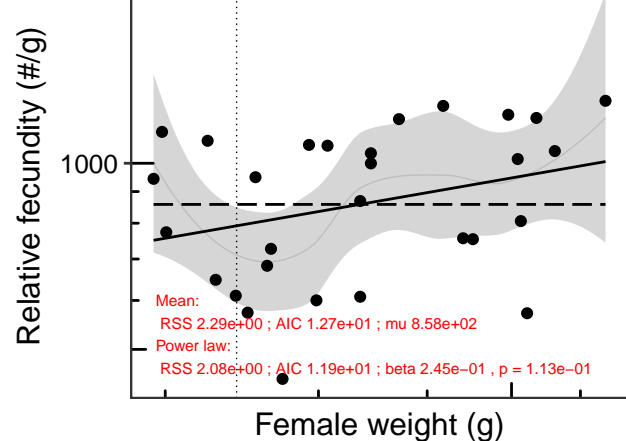
Species: *Solea solea*
Location: European Continental Shelf Area IXa



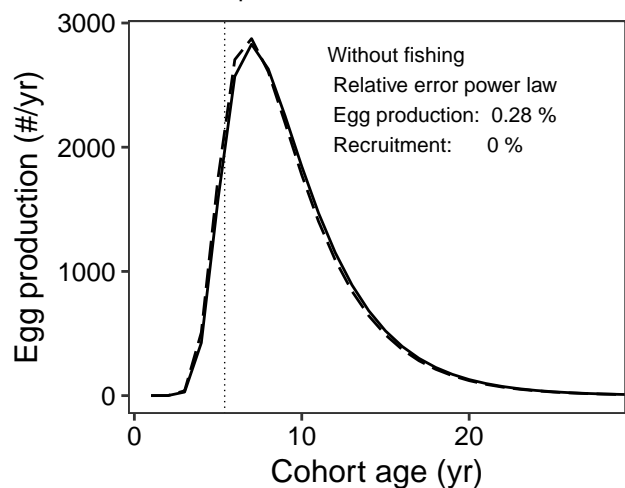
Species: *Solea solea*
Location: European Continental Shelf Area IXa



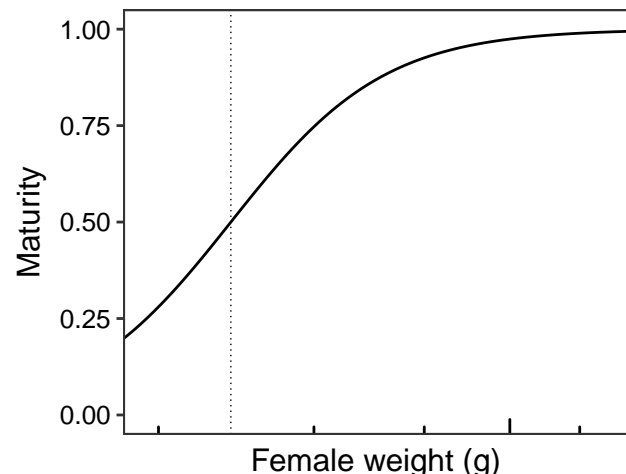
Species: *Solea solea*
Location: European Continental Shelf Area VIIa



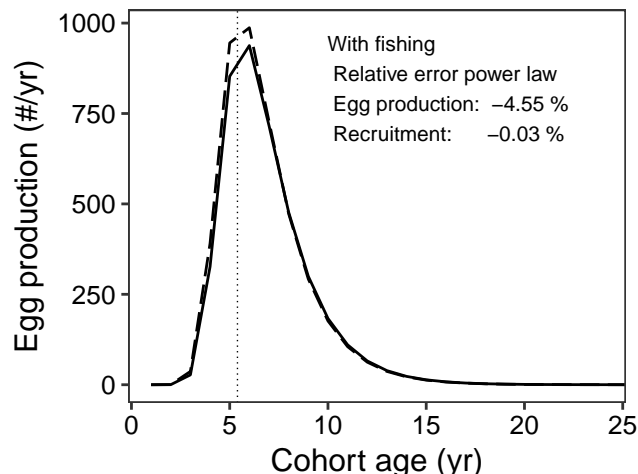
Species: *Solea solea*
Location: European Continental Shelf Area VIIa



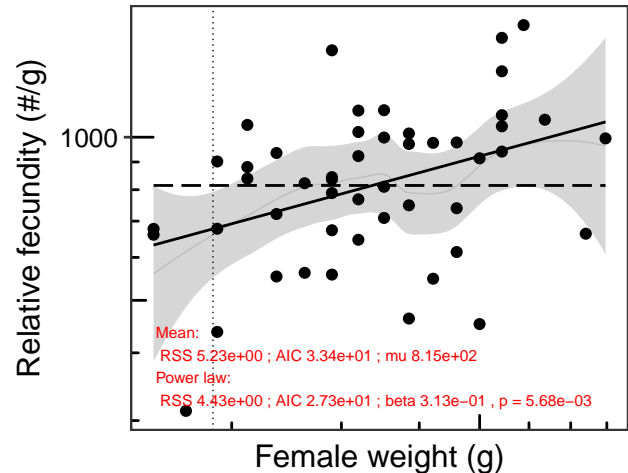
Species: *Solea solea*
Location: European Continental Shelf Area VIIa



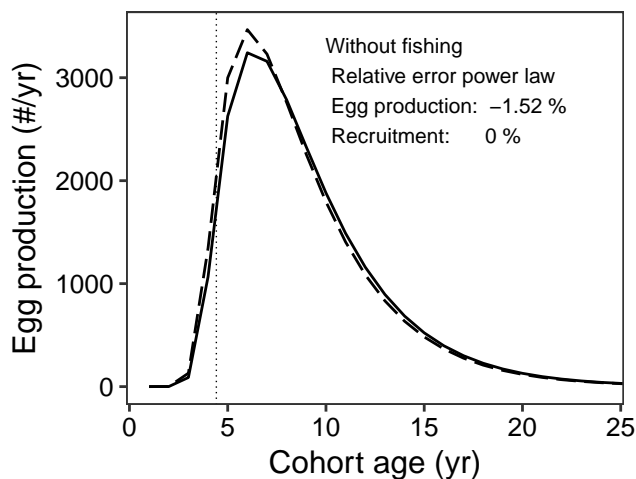
Species: *Solea solea*
Location: European Continental Shelf Area VIIa



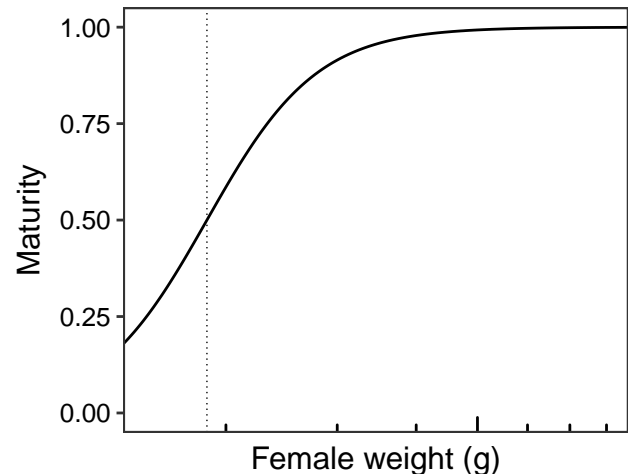
Species: *Solea solea*
Location: European Continental Shelf Area VIId



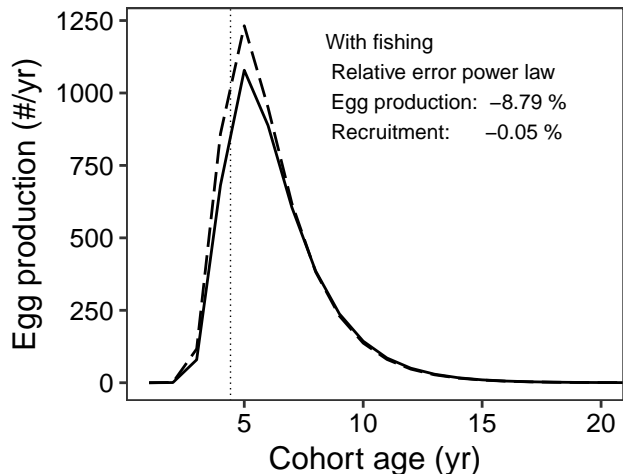
Species: *Solea solea*
Location: European Continental Shelf Area VIId



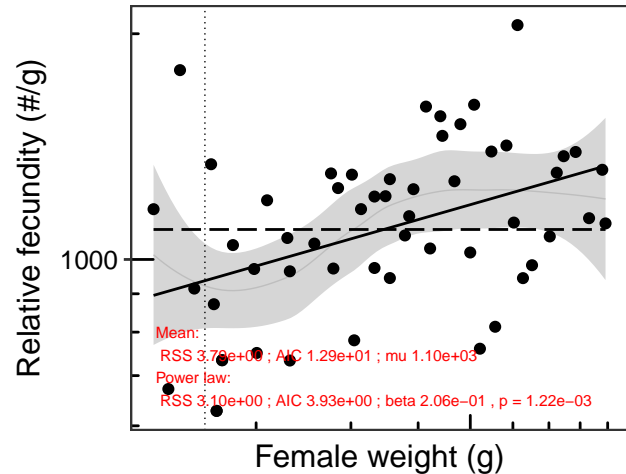
Species: *Solea solea*
Location: European Continental Shelf Area VIId



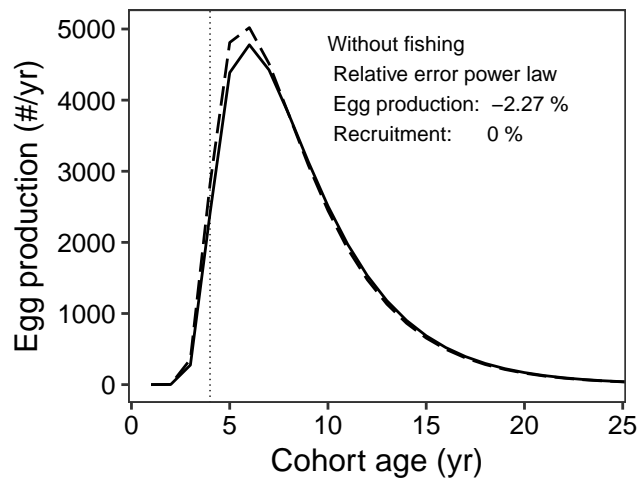
Species: *Solea solea*
Location: European Continental Shelf Area VIId



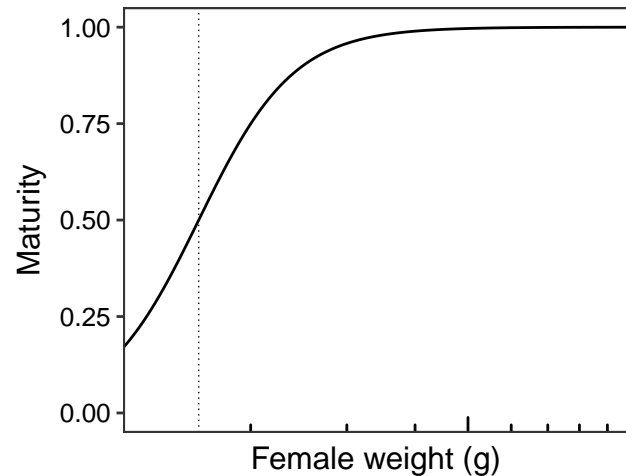
Species: *Solea solea*
Location: European Continental Shelf Area IVc



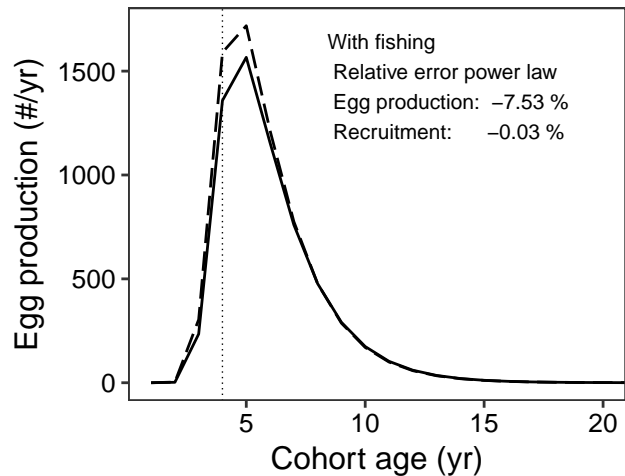
Species: *Solea solea*
Location: European Continental Shelf Area IVc



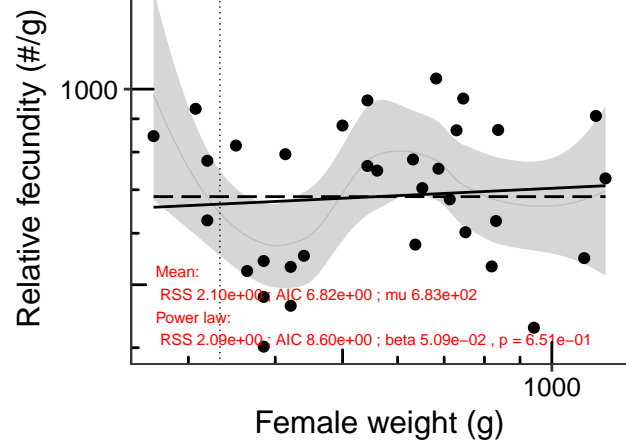
Species: *Solea solea*
Location: European Continental Shelf Area IVc



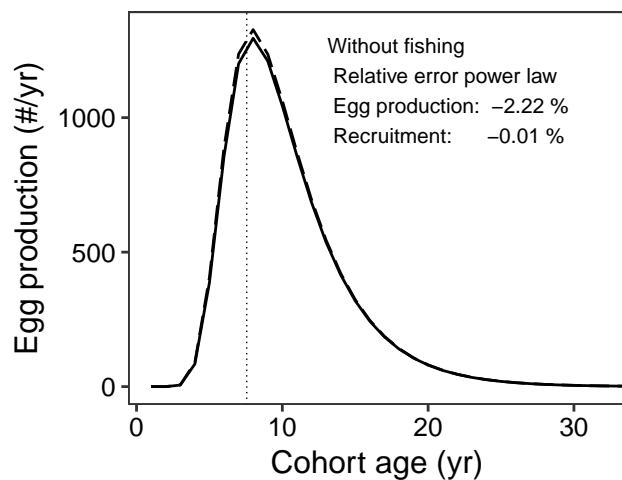
Species: *Solea solea*
Location: European Continental Shelf Area IVc



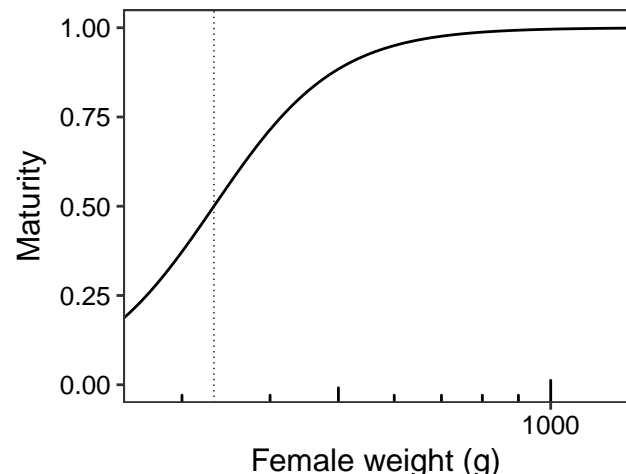
Species: *Solea solea*
Location: European Continental Shelf Area VIIe



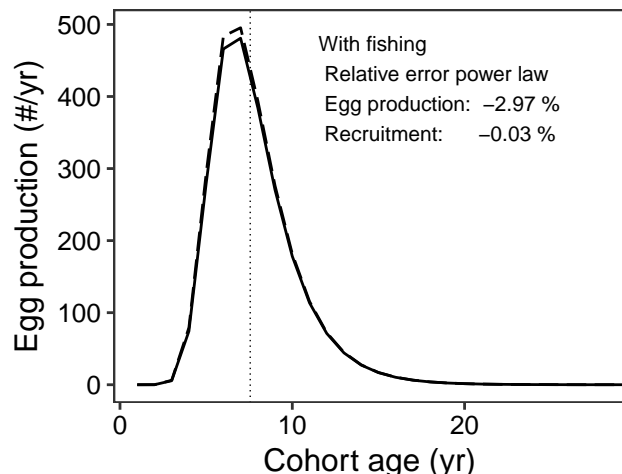
Species: *Solea solea*
Location: European Continental Shelf Area VIIe



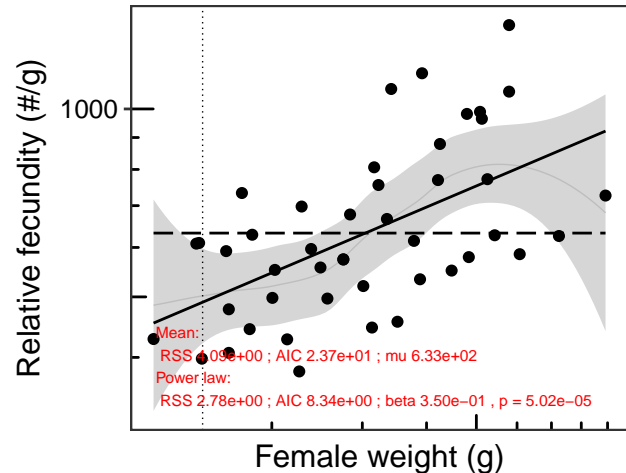
Species: *Solea solea*
Location: European Continental Shelf Area VIIe



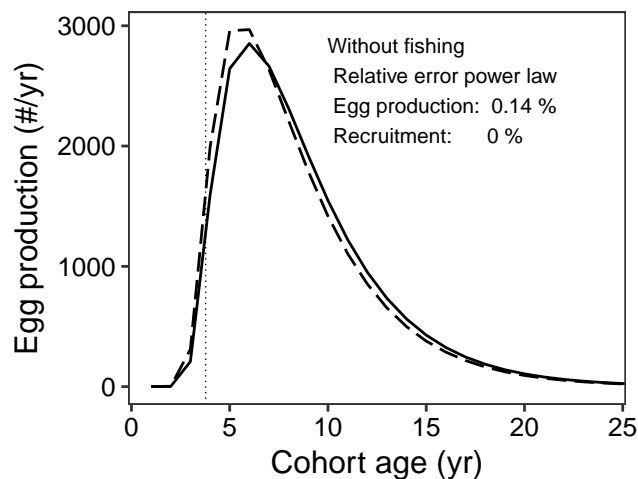
Species: *Solea solea*
Location: European Continental Shelf Area VIIe



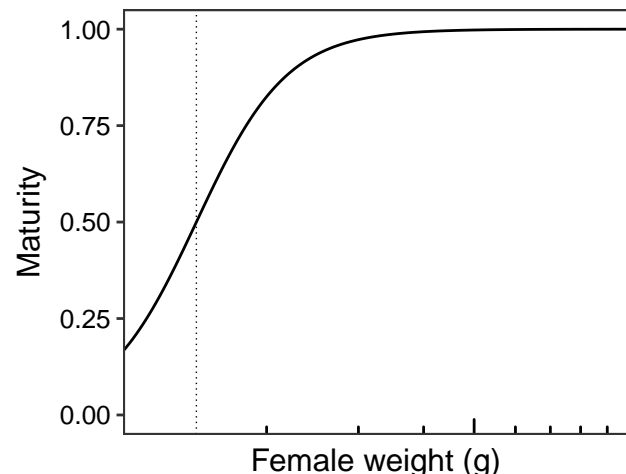
Species: *Solea solea*
Location: European Continental Shelf Area IVbWest



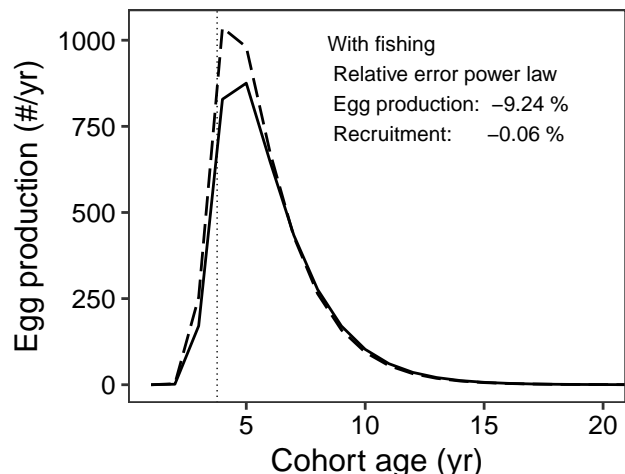
Species: *Solea solea*
Location: European Continental Shelf Area IVbWest



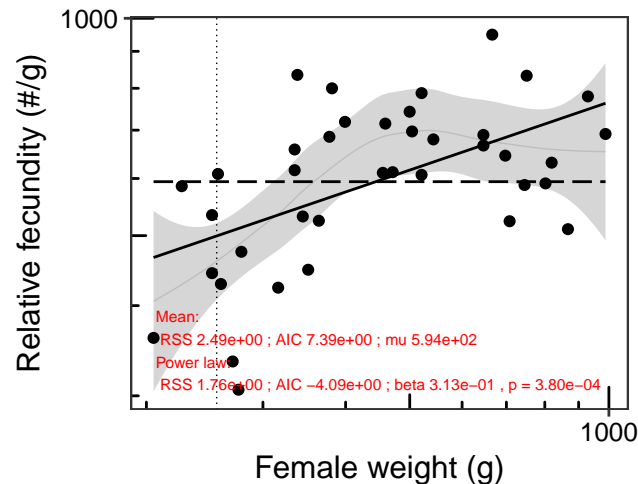
Species: *Solea solea*
Location: European Continental Shelf Area IVbWest



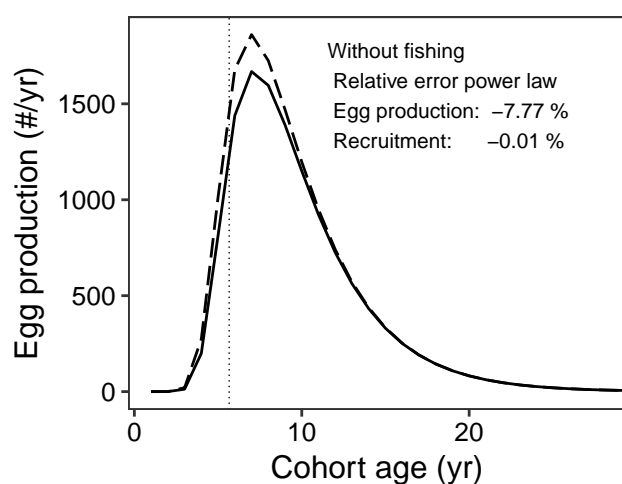
Species: *Solea solea*
Location: European Continental Shelf Area IVbWest



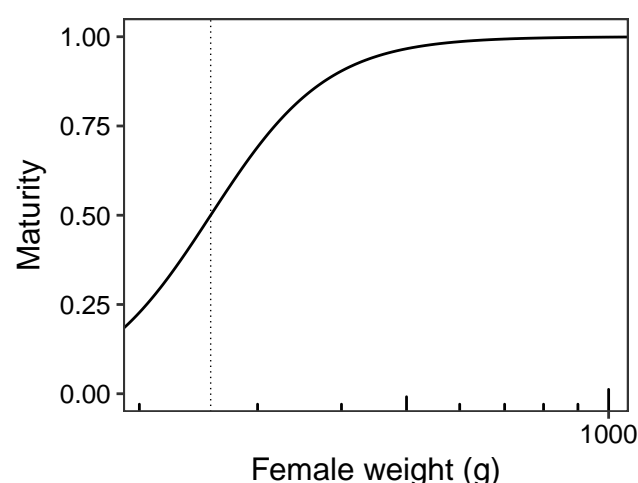
Species: *Solea solea*
Location: European Continental Shelf Area VIIa



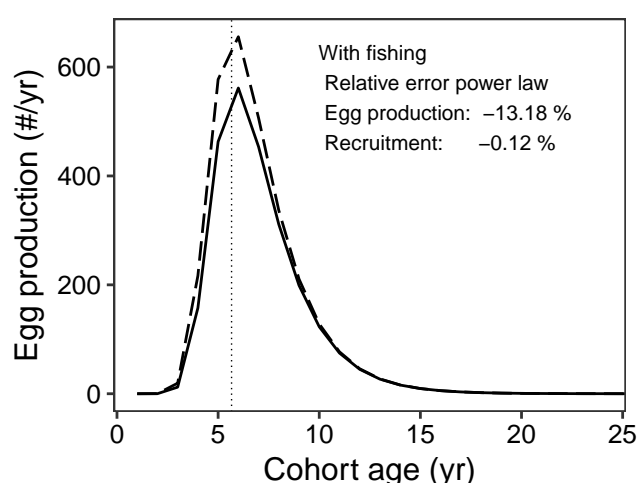
Species: *Solea solea*
Location: European Continental Shelf Area VIIa



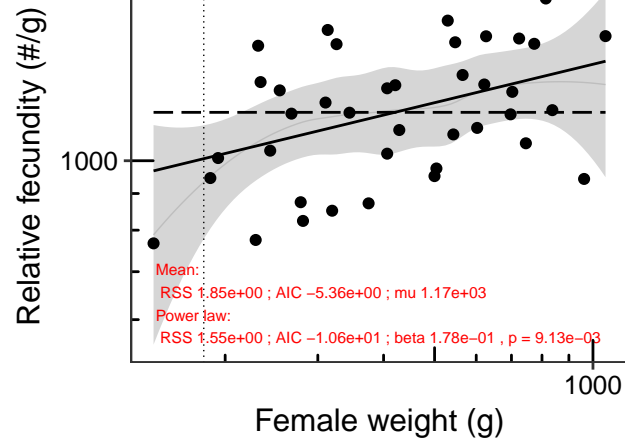
Species: *Solea solea*
Location: European Continental Shelf Area VIIa



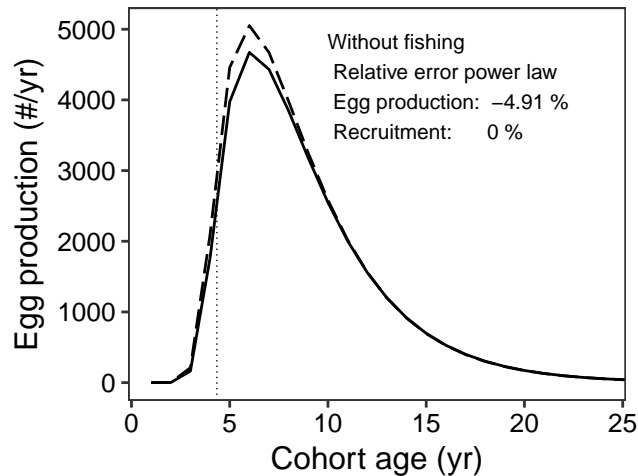
Species: *Solea solea*
Location: European Continental Shelf Area VIIa



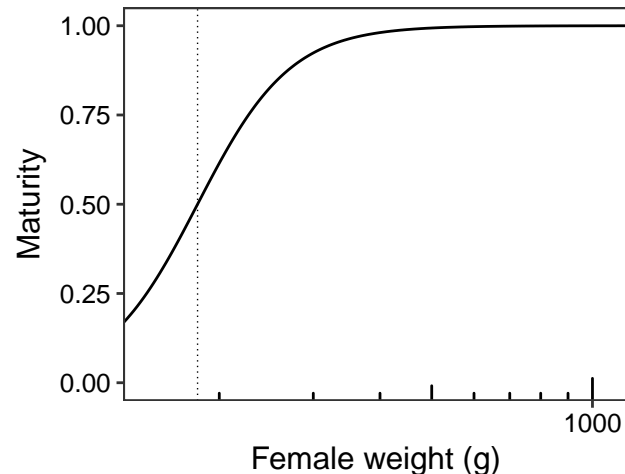
Species: *Solea solea*
Location: European Continental Shelf Area IVbEast



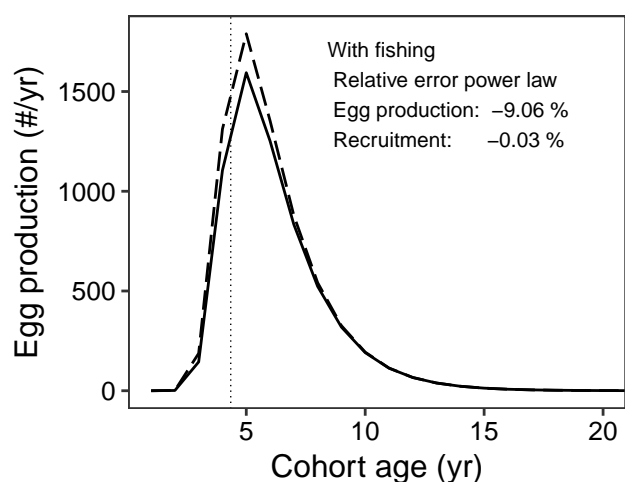
Species: *Solea solea*
Location: European Continental Shelf Area IVbEast



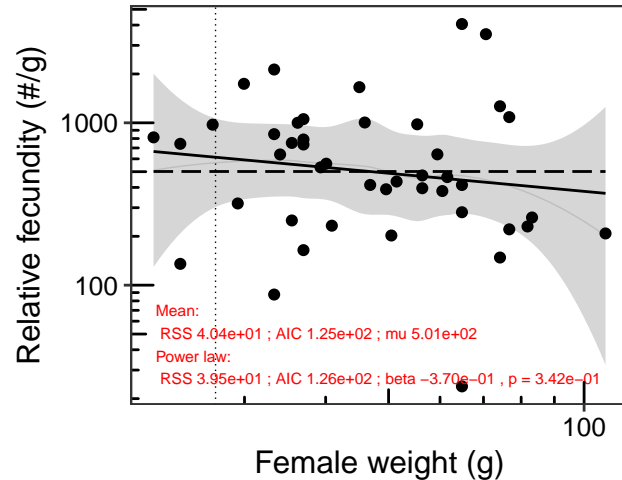
Species: *Solea solea*
Location: European Continental Shelf Area IVbEast



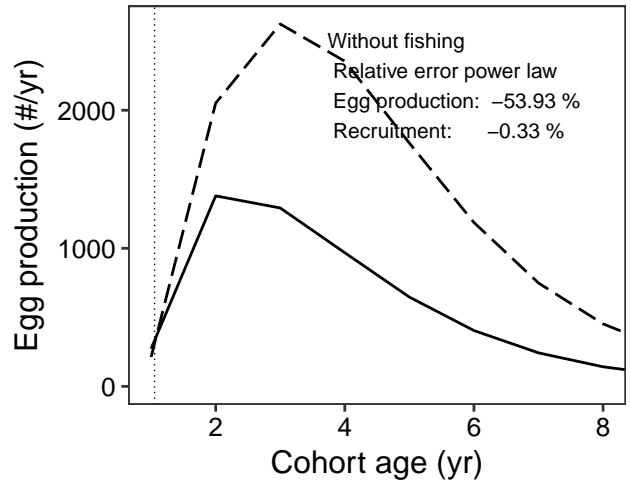
Species: *Solea solea*
Location: European Continental Shelf Area IVbEast



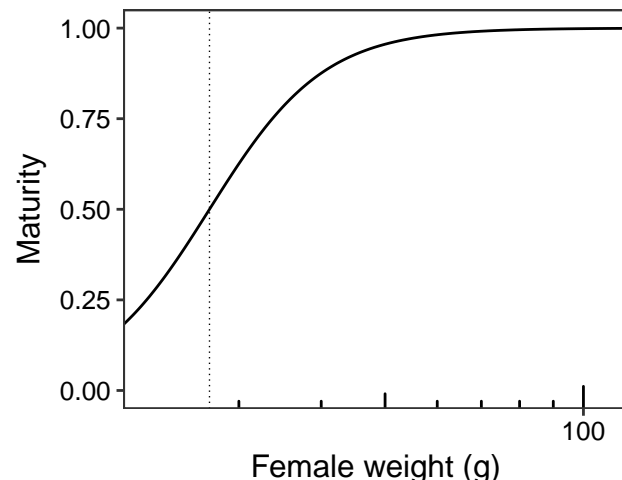
Species: *Stellifer rastrifer*
Location: Off the southern coast of Brazil between Parana and Santa Ca



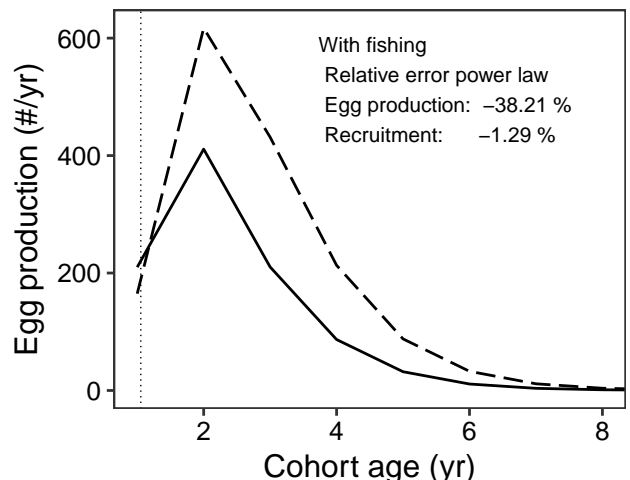
Species: *Stellifer rastrifer*
Location: Off the southern coast of Brazil between Parana and Santa Ca



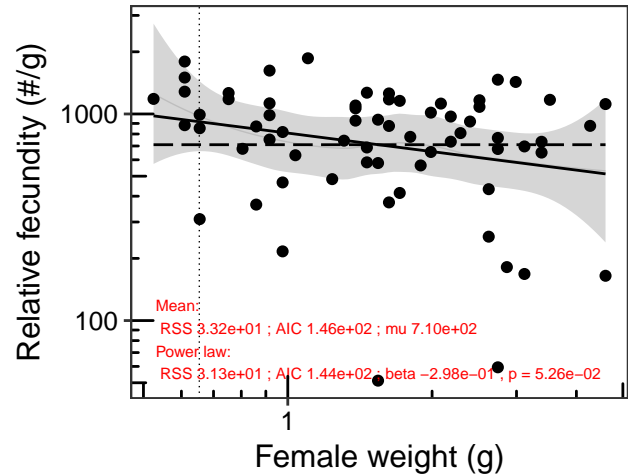
Species: *Stellifer rastrifer*
Location: Off the southern coast of Brazil between Parana and Santa Cat



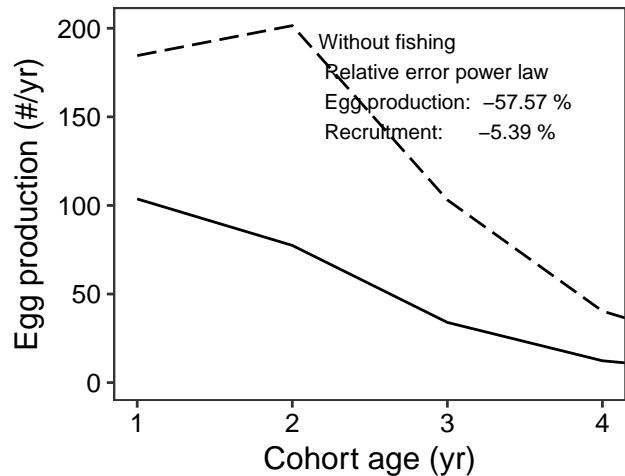
Species: *Stellifer rastrifer*
Location: Off the southern coast of Brazil between Parana and Santa Cata



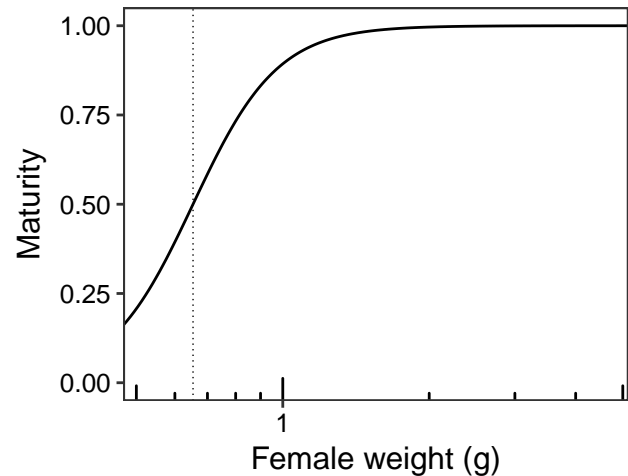
Species: *Thalassoma bifasciatum*
Location: San Blas Province, Panama



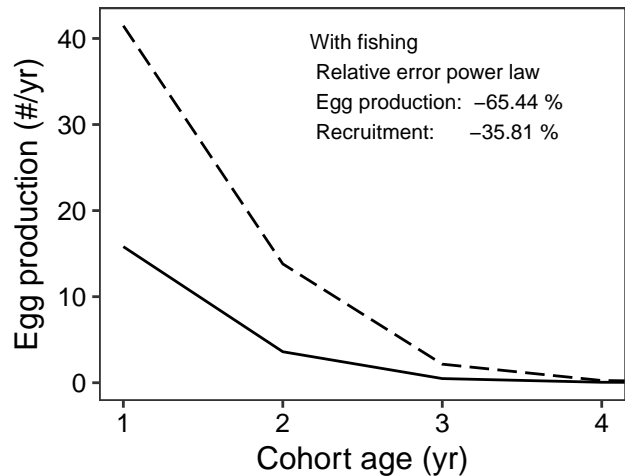
Species: *Thalassoma bifasciatum*
Location: San Blas Province, Panama



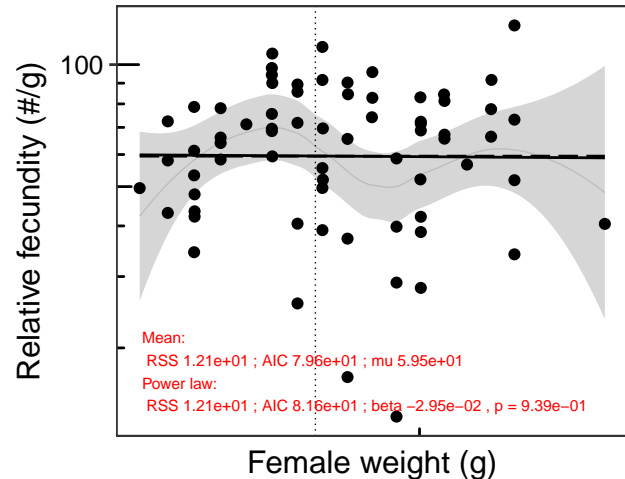
Species: *Thalassoma bifasciatum*
Location: San Blas Province, Panama



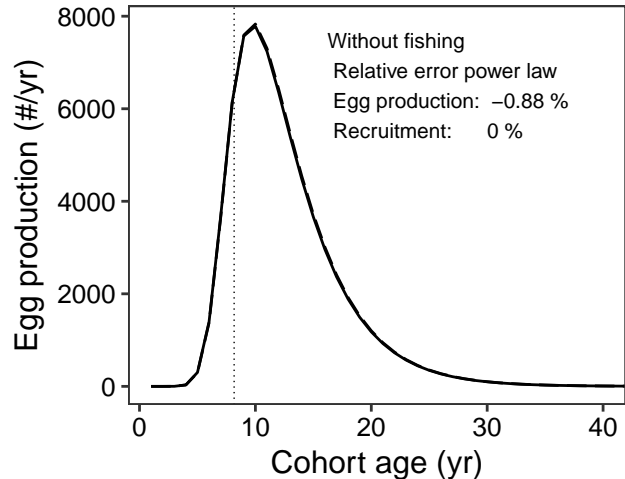
Species: *Thalassoma bifasciatum*
Location: San Blas Province, Panama



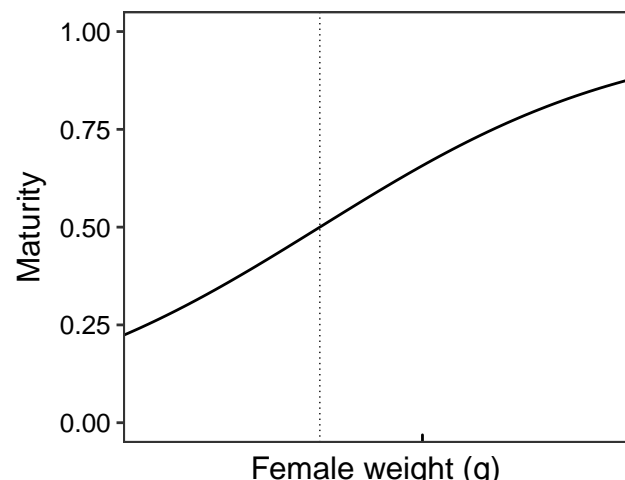
Species: *Thunnus alalunga*
Location: Cook Islands and American Samoa



Species: *Thunnus alalunga*
Location: Cook Islands and American Samoa



Species: *Thunnus alalunga*
Location: Cook Islands and American Samoa



Species: *Thunnus alalunga*
Location: Cook Islands and American Samoa

